Publication Date (Web): November 24, 2015 | doi: 10.1021/bk-2015-1203.fw001

Advances in Wine Research

In Advances in Wine Research; Ebeler, et al.;
ACS Symposium Series; American Chemical Society: Washington, DC, 2015.

Publication Date (Web): November 24, 2015 | doi: 10.1021/bk-2015-1203.fw001

ACS SYMPOSIUM SERIES **1203**

Advances in Wine Research

Susan B. Ebeler, Editor
University of California, Davis, Davis, California

Gavin Sacks, Editor
Cornell University, Ithaca, New York

Stéphane Vidal, Editor
Nomacorc, Rodilhan, France

Peter Winterhalter, Editor
Technische Universität Braunschweig, Braunschweig, Germany

Publication Date (Web): November 24, 2015 | doi: 10.1021/bk-2015-1203.fw001

Sponsored by the
ACS Division of Agriculture and Food Chemistry, Inc.

American Chemical Society, Washington, DC

Distributed in print by Oxford University Press

Library of Congress Cataloging-in-Publication Data

Names: Ebeler, Susan E., 1961- editor. | American Chemical Society. Division of Agricultural and Food Chemistry.
Title: Advances in wine research / Susan E. Ebeler, editor, University of California, Davis, Davis, California [and three others] ; sponsored by the ACS Division of Agriculture and Food Chemistry.
Description: Washington, DC : American Chemical Society, [2015] | Series: ACS symposium series ; 1203 | Includes bibliographical references and index.
Identifiers: LCCN 2015040661 (print) | LCCN 2015045452 (ebook) | ISBN 9780841230101 (alk. paper) | ISBN 9780841230118 ()
Subjects: LCSH: Wine and wine making--Chemistry. | Chemistry, Analytic.
Classification: LCC TP548 .A25 2015 (print) | LCC TP548 (ebook) | DDC 663/.2--dc23
LC record available at http://lccn.loc.gov/2015040661

The paper used in this publication meets the minimum requirements of American National Standard for Information Sciences—Permanence of Paper for Printed Library Materials, ANSI Z39.48n1984.

Distributed in print by Oxford University Press

PRINTED IN THE UNITED STATES OF AMERICA

Publication Date (Web): November 24, 2015 | doi: 10.1021/bk-2015-1203.fw001

Foreword

The ACS Symposium Series was first published in 1974 to provide a mechanism for publishing symposia quickly in book form. The purpose of the series is to publish timely, comprehensive books developed from the ACS sponsored symposia based on current scientific research. Occasionally, books are developed from symposia sponsored by other organizations when the topic is of keen interest to the chemistry audience.

Before agreeing to publish a book, the proposed table of contents is reviewed for appropriate and comprehensive coverage and for interest to the audience. Some papers may be excluded to better focus the book; others may be added to provide comprehensiveness. When appropriate, overview or introductory chapters are added. Drafts of chapters are peer-reviewed prior to final acceptance or rejection, and manuscripts are prepared in camera-ready format.

As a rule, only original research papers and original review papers are included in the volumes. Verbatim reproductions of previous published papers are not accepted.

ACS Books Department

Publication Date (Web): November 24, 2015 | doi: 10.1021/bk-2015-1203.fw001

Publication Date (Web): November 24, 2015 | doi: 10.1021/bk-2015-1203.pr001

Preface

The complexity of wine provides numerous avenues of discovery for food and analytical chemists. The American Chemical Society (ACS) has a long tradition of bringing together international experts to present the latest research findings focused on understanding the complexity of wine chemistry. This Proceedings, based on a symposium at the 248th ACS National Meeting 2014 in San Francisco, continues that tradition with a broad overview of recent advances in wine research from new analytical approaches, to flavor and oxidation chemistry, to sustainable grape and wine production practices. The San Francisco symposium generated numerous lively discussions and cross-disciplinary interactions and we hope that this Proceedings volume will also contribute to continued discussions and research in these areas.

This volume begins with an overview of advances in the analytical techniques used for grape and wine research, including chromatographic and mass spectrometric tools for understanding chemistry of volatiles, nonvolatiles and inorganic components of grapes and wines (Chapter 1). Non-targeted, high resolution mass spectrometry is a powerful approach for studying metabolite profiles in a variety of sample types and Chapters 2 and 3 describe applications for studying changes in wine chemistry during aging and storage. A simple approach for measuring sulfur dioxide in wine without disrupting key equilibria using colorimetric gas detection tubes is described in Chapter 4. The final two chapters in this section describe NMR techniques for monitoring diffusion of carbon dioxide bubbles in sparkling wines (Chapter 5) and for authentication of wine and alcoholic beverages (Chapter 6).

Recent advances in flavor chemistry are highlighted in the second section of this book. Regional differences in chemical and sensory profiles of Malbec and Cabernet Sauvignon wines are discussed in Chapter 7, followed by new studies on the key odorants in oak chips used in wine production (Chapter 8). Subsequent chapters consider the effects of the vineyard on grape and wine odorants, including the effects of site characteristics (i.e. *terroir,* Chapter 9) canopy management practices (Chapter 10) and under-vine management (Chapter 11). Finally, effects of the plant hormone, methyl jasmonate, on the biosynthesis of grape terpenoids are discussed in Chapter 12.

Oxidation chemistry during wine processing and storage provides the focus for the third section of this Proceedings. The effects of oxygen and antioxidants on aroma, color, and chemical composition of wine are described in Chapters 13, 14, 15, and16. This is followed by recent mechanistic insights into wine oxidation or reduction, including the roles of carbonyl-bisulfite adducts and copper-thiol complexes as precursors of off-aromas (Chapter 17), the potential reaction

In Advances in Wine Research; Ebeler, et al.;
ACS Symposium Series; American Chemical Society: Washington, DC, 2015.

pathways involving quinones (Chapter 18), and the fate of organic acids during photo-oxidation (Chapter 19). A novel approach for rapid monitoring of the extent of phenolic oxidation in wines using voltammetry and carbon electrodes is described in the final chapter of this section (Chapter 20).

The last section of this volume focuses on the intersection of grape and wine chemistry with sustainable production practices, reflecting the increasing scientific interest in byproduct utilization and global and environmental stewardship. Chapters 21 and 22 present studies on the isolation and characterization of high-value bioactive phenolics from pomace, grape seed extracts, and grapevine canes or cuttings. In Chapter 23, chemical measurements are described that can be used in an industrial viticulture and winemaking program to monitor and optimize effects of sustainable practices (e.g., deficit irrigation) on grape composition and quality. Finally, the section closes with an overview of green chemistry approaches for cleaning and sanitizing winery equipment (Chapter 24).

We thank the contributors, reviewers, and the following organizations that financially contributed to making the symposium and proceedings a success: Nomacorc, E. & J. Gallo Winery, Constellation Brands, ETS Laboratories, Symrise AG, and the ACS Division of Agricultural and Food Chemistry.

Susan E. Ebeler
Department of Viticulture & Enology, University of California, Davis
One Shields Avenue, Davis, California 95616

Gavin L. Sacks
Department of Food Science, Cornell University
Stocking Hall, Ithaca, New York 14853

Stéphane Vidal
Wine Quality Solutions Center, Nomacorc
Rodilhan, 30230, France

Peter Winterhalter
Institute of Food Chemistry, Technische Universität Braunschweig
Schleinitzstraße 20, DE 38106 Braunschweig, Germany

Publication Date (Web): November 24, 2015 | doi: 10.1021/bk-2015-1203.pr001

Publication Date (Web): November 24, 2015 | doi: 10.1021/bk-2015-1203.ot001

Editors' Biographies

Susan Ebeler

Susan Ebeler is a professor in the Department of Viticulture and Enology at the University of California, Davis. Her research is focused on development and application of analytical chemistry techniques to study flavor chemistry and the physic-chemical interactions of flavors with nonvolatile wine components. She also studies the chemical mechanisms for the observed health effects of food and wine components. At UC Davis, she teaches undergraduate and graduate classes on the analysis of grapes and wines as well as the flavor chemistry of foods and beverages. She is co-director of the UC Davis Food Safety and Measurement Facility, which seeks to advance the chemical understanding of foods and beverages for safety, authentication, and quality.

Gavin Sacks

Gavin Sacks is an Associate Professor in Food Science at Cornell University, where he has been a faculty member since 2007. He received his B.S. in Chemistry from the University of Virginia and his M.S. and Ph.D. in Chemistry from Cornell University. His research program uses both classic and modern analytical techniques in the studies of food flavor and color compounds, particularly in wines and grapes.

Stéphane Vidal

Stéphane Vidal joined Nomacorc in 2007 and is the global director of enology leading a team in charge of Nomacorc's initiatives on oxygen management support and solutions. His team is composed of wine scientists and wine specialists. Stéphane has been active in enological research for more than 20 years and worked with some of the world's most renowned research institutions including the Institut National de la Recherche Agronomique (INRA) in Montpellier, France and the Australian Wine Research Institute (AWRI) in Adelaide, Australia. Prior to Nomacorc, Stéphane managed Inter Rhone Laboratory and was responsible for the development of new analytical methods and several research programs including closure trials. Stéphane is a biochemist engineer from the Institut National des Sciences Appliquées in Lyon, France. He received his master's degree from Université Claude Bernard in Lyon, France and his Ph.D. from Université Joseph Fourier in Grenoble, France.

In Advances in Wine Research; Ebeler, et al.;
ACS Symposium Series; American Chemical Society: Washington, DC, 2015.

Peter Winterhalter

Peter Winterhalter is head of the Institute of Food Chemistry at the Technische Universität Braunschweig (TUBS), Germany. He graduated from the University of Karlsruhe and obtained his Ph.D. from Würzburg University in 1988. In 1989 he worked as a postdoctoral fellow at the Australian Wine Research Institute, Adelaide, before returning to Würzburg University as a Research Fellow. In 1995, he was appointed as Professor of Food Chemistry at the University of Erlangen-Nürnberg before finally moving to TUBS where he was dean of the Faculty of Chemistry and Pharmacy. His research activities focus on natural products/food chemistry and include aroma precursors, countercurrent chromatography, wine research, food authentication, and natural pigments.

Publication Date (Web): November 24, 2015 | doi: 10.1021/bk-2015-1203.ot001

Chapter 1

Analysis of Grapes and Wines: An Overview of New Approaches and Analytical Tools

Susan E. Ebeler*

Department of Viticulture and Enology,
University of California, Davis, California
***E-mail: seebeler@ucdavis.edu.**

Publication Date (Web): November 24, 2015 | doi: 10.1021/bk-2015-1203.ch001

A variety of new analytical tools are increasingly used to profile the volatile, nonvolatile, and elemental composition of grapes and wines in order to characterize components contributing to flavor (aroma, taste, color, mouthfeel) and for authentication purposes. Gas chromatography combined with tandem mass spectrometry (MS/MS) offers significant advantages for trace quantification of important aroma-active volatiles and taint compounds. Sorptive sample preparation techniques (*e.g.*, SPME, Headspace Sorptive Extraction and Stir-bar Sorptive Extraction) also can enhance throughput and/or sensitivity for GC-MS analyses. UHPLC-qTOF MS is a powerful approach for profiling nonvolatiles and when combined with multivariate statistical tools the compositional profiles may be used for varietal, geographic, and vintage authentication. ICP-MS can be used to comprehensively profile metals, including those that affect chemical stability and oxidative reactions. Finally, new approaches for gas chromatography combined with olfactometry (GC-O) can allow characterization of aroma qualities of complex mixtures. Each of these tools, alone and in combination are providing significant new insights into variables influencing grape and wine composition and flavor.

In Advances in Wine Research; Ebeler, et al.;
ACS Symposium Series; American Chemical Society: Washington, DC, 2015.

Publication Date (Web): November 24, 2015 | doi: 10.1021/bk-2015-1203.ch001

Introduction

Analytical tools for determining grape and wine composition are critical for a variety of experimental studies. Since the development of new chromatographic and spectrometric approaches at the beginning of the 20th century, commercial development of analytical instruments that are relatively cheap, easy to use and maintain, and that provide high levels of performance have made it easier to routinely identify and quantify components in complex mixtures such as grapes and wines. For example, improved separations using GC x GC and targeted trace analysis using tandem MS approaches have led to identification of new compounds and quantification of trace compounds in grapes and wines. Metabolomic approaches using both mass spectrometry (including high resolution mass spectrometry such as time-of-flight (TOF) and ion cyclotron resonance (ICR)) and nuclear magnetic resonance spectroscopy (NMR) have become increasingly popular for characterization and profiling of primary and secondary metabolites in a variety of biological systems. Finally, atomic spectroscopy, including Inductively Coupled Mass Spectrometry (ICP-MS) is a powerful tool for identifying the elemental composition of grapes and wines.

This Chapter will provide a brief overview of recent applications of these analytical tools for identifying and quantifying compounds and elements in grapes and wine samples. We will use examples that demonstrate how these tools have been used to understand the effects of viticulture and winemaking practices on grape and wine composition. We will further give examples of analytical approaches being used to understand how composition impacts 'quality' attributes, particularly assessment of sensory properties of individual components and complex mixtures. These examples are not intended to provide a comprehensive review, however, they provide an overview of techniques and applications that are increasingly used for characterization of grape and wine composition.

Targeted Analysis of Compounds

Selected ion monitoring and tandem mass spectrometric (MS/MS or MS^n) analyses are increasingly used for targeted analysis of trace analytes, particularly those compounds with important sensory properties (see also recent reviews (*1–3*)). In the tandem MS/MS experiment a series of mass filters in conjunction with a collision cell are used to filter specific target ions of interest, fragment the selected ions, and then filter the fragment ions in a final mass filter. As a result, background noise/ions are significantly reduced and trace level analytes can be detected and quantified.

Methods for analysis of 2,4,6-trichloroanisole (TCA) in wine provide a useful example of the role that advances in analytical instrumentation have played in improving sensitivity and overall throughput for trace analytes. TCA is the compound most widely associated with the musty off-aroma of wines described

Publication Date (Web): November 24, 2015 | doi: 10.1021/bk-2015-1203.ch001

as 'cork-taint', however other haloanisoles have also been implicated (*e.g.*, 2, 4-dichloranisole, 2,6-dichloroanisole, 2,3,4,6-tetrachloroanisole, pentachloranisole, and 2,4,6 tribromoanisole). TCA has a sensory threshold in wine of ~2-4 ng/L (see also review (*4*)) necessitating analytical methods with limits of detection and quantitation in this range. Early analyses for TCA required extensive and time-consuming solvent extraction and concentration steps combined with GC-MS or GC-Electron Capture Detectors to obtain the necessary sensitivity. However, in the late 1990's, GC-MS using a single quadrupole instrument in the selected ion monitoring mode and combined with sample preparation using solid phase microextraction (SPME) allowed for the trace analysis of TCA with a solvent-less extraction of ~ 25 min (TCA) (*5*, *6*). Using a deuterated TCA internal standard ($^2[H]_5$TCA), TCA in wines could be quantified with a limit of quantitation of 5 ng/L and relative standard deviation of 5-13% (measured at 10 and 250 ng/L) (*5*). Subsequently, with the development of ion-trap mass spectrometers and more recently the wide availability of linear quadrupole GC-MS/MS (tandem mass spectrometer) instruments, the analysis of TCA as well as a several related haloanisoles has been accomplished with a faster analysis time (10 min extraction, 11 min GC analysis time) and ~10 times lower limits of quantitation ((*7*); reviewed by (*4*)). The advantages of tandem MS instruments are that the sequential mass detectors (in the case of transmission quadrupole mass analyzers or in the case of ion traps manipulation of ions in time in the Paul ion traps) allow for the 'removal' of interfering ions so that the specific compounds of interest can be monitored with a high degree of selectivity and sensitivity (*1*, *3*).

HPLC-MS/MS has also proven to be a valuable tool for identification of nonvolatile grape and wine components with an elegant series of studies identifying the smoke-derived volatile phenols (*e.g.*, guaiacol and their glycoside precursors in grapes and wines) (*8–10*). Kennison and co-workers hypothesized that exposure of grapes to volatile phenols formed in bush fires resulted in formation of conjugated glycoside metabolites since acid and enzyme hydrolyzates of affected juices had higher concentrations of the free volatile phenols compared to the non-hydrolyzed juices. After synthesizing a β-D-glucopyranoside of guaiacol, the authors were able to identify the glycoside in smoke-affected grapes using LC-MS/MS where product ion spectra of the acetic acid adduct ion $[M\text{-}H+CH_3COOH]^-$ with *m/z* 345 were recorded and selected ion reaction mode (SRM) was used to monitor the mass transitions 345 → m/z 285, 161, 123, corresponding to $[M\text{-}H]^-$, dehydrated glucose, and deprotonated guaiacol, respectively.

In a subsequent experiment, the authors exposed grape berries and leaves to a mixture of unlabeled d_0-guaiacol and stable isotope labeled d_3-guaiacol (*11*). Using LC-MS/MS, the isotopic doublet pattern (separated by 3 Da) of seven different mono- and diglycosides and rutinosides of guaiacol were identified in the leaves and berries (Figure 1). Although isobaric conjugates could not be distinguished (*e.g.*, glucose and galactose conjugates), this study was the first to show that exogenous compounds in the atmosphere could be taken up by grape berries and leaves and biochemically converted to glycoside conjugates. Further, the study provided preliminary evidence that translocation of volatiles between leaf and berry occurred to a limited extent.

Publication Date (Web): November 24, 2015 | doi: 10.1021/bk-2015-1203.ch001

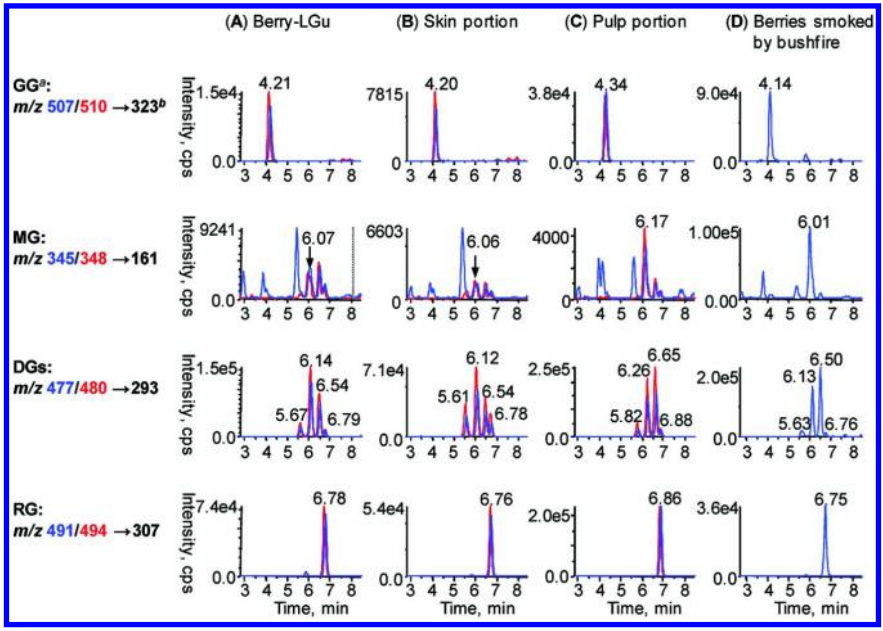

Figure 1. HPLC-Selected Reaction Monitoring (SRM) chromatograms of d_0- and d_3-guaiacol conjugates present in (A) the berry exposed to ~5 mg/L guaiacol sample (LGu), (B) skin and (C) pulp portions of the berry exposed to ~ 5 mg/L guaiacol sample, and (D) berries exposed to bushfire smoke. GG: Glucosylglucoside; MG: Glucoside; DG: 4 Diglycosides: RG: Rutinoside. Reproduced with permission from Ref. (11). (2010) (Elsevier).

Nontargeted Analysis and Profiling of Metabolites

Non-targeted profiling is becoming increasingly valuable for characterizing and classifying differences and similarities in the chemical composition of groups of samples. In many cases chromatographic separation is combined with mass spectrometry using high resolution mass spectrometers that allow for high mass accuracy measurements (*e.g.*, mass accuracy < 1 ppm). Time-of-flight (TOF) and ion cyclotron resonance (ICR) mass spectrometric instruments have been used in a range of studies for varietal and regional classification of wines. The high mass accuracy and the ability to do MS/MS experiments with some instruments allows for further identification of unknown compounds.

In a recent study, Vaclavik et al. (*12*) demonstrated that UHPLC combined with quadrupole time-of-flight mass spectrometry (qTOF) could be a powerful approach for varietal classification of wines. In this study, both positive and negative ion mode profiles were monitored, however, the positive ion data were most useful in characterizing the three wine varieties evaluated (Pinot noir, Cabernet Sauvignon, and Merlot). Using the accurate mass MS/MS capability of the instrument, selected marker compounds for the different varieties could be

identified. For example, the compound cyanidin 3-*O*-glucoside was identified based on accurate mass MS/MS and was found to be higher in Pinot noir wines compared to Cabernet and Merlot. These results point to the potential for UHPLC-qTOF-MS as a tool for metabolomics applications for authentication of wine varieties. Caution is required however, because while accurate mass and MS/MS information can reduce the number of potential molecular formulas and structures possible for a given entity, isomers and isobars are still possible and identification of unknown compounds is still difficult without confirmation using authentic standards (*13*).

Ion cyclotron resonance mass spectrometry (ICR-MS) may offer greater resolution and mass accuracy compared to the TOF instruments (particularly when samples are introduced by direct infusion with long sample averaging times), thereby increasing the number of putative entities detected and reducing even further the potential number of molecular formulas possible for a given entity (*3*). Gougeon and co-workers (*14*) used ICR-MS to characterize wines based on the oak used for barrel-aging and tentatively identified a unique compound associated with a specific lichen metabolite from oaks grown in the Bitche, France forest. More recently, ICR-MS has been used to characterize Pinot noir grapes and wines from four vineyards, two each in the Côte de Nuits and Côte de Beaune (Burgundy) region of France (*15*, *16*). The wines were studied across multiple vintages. The results showed that for grapes and wines analyzed immediately after fermentation the chemical composition of the villages could be differentiated within a vintage, but variability across vintages was significant (*15*). However, after bottle aging, wines from even closely spaced vineyards could be differentiated across the three vintages (*16*). More than 5000 chemical features were observed in this study and accurate identification and quantification of these putative compounds is limited in many cases by the lack of authentic standards. However, the ability to distinguish such large numbers of components combined with ability to putatively identify components based on unique masses that can be discerned as a result of the high mass accuracy of the ICR-MS method, makes this a particularly powerful approach for characterization of wine composition and discovery of unique compounds. An overview of this work is provided in a later chapter of this volume.

While high resolution mass spectrometers have increased the ability to identify thousands of compounds in grapes and wines based on the accurate mass of the analytes, multi-dimensional or comprehensive chromatographic approaches such as GC x GC, that allow hundreds of volatile compounds to be separated, quantified, and identified, have also been increasingly used to characterize wine composition (*1*, *3*). In GC x GC analysis, the column effluent from the first analytical column is cryo-trapped and quantitatively transferred to a second column for additional separation. As observed in the 2-D chromatogram (Figure 2), peaks that may appear to be composed of a single compound in the first separation dimension, often consist of multiple peaks when separated on a second column of differing polarity.

In a recent series of studies, Robinson et al. (*17–19*) used GC x GC combined with TOF-MS detection to tentatively identify over 350 volatile compounds in Australian Cabernet Sauvignon wines. Of these, 123 compounds

Publication Date (Web): November 24, 2015 | doi: 10.1021/bk-2015-1203.ch001

were statistically different among the samples and could be related to a range of sensory attributes. Chemical composition and sensory properties were different for two different Western Australia growing regions studied, indicating that environmental factors and viticultural practices (including canopy management), can impact both composition and sensory properties. Interestingly, the different vineyard site effects were greater than those for wines made from different yeasts. These studies provide one of the most comprehensive profiles of the volatile and semi-volatile composition of wines and while many relationships with sensory properties were observed, interactions among compounds and sensory effects that may occur at sub- and perithreshold levels make it difficult to fully predict sensory properties from composition alone. These interactions are discussed further in the section below. In addition, the work of Robinson et al. is further discussed in a later chapter of this volume.

Publication Date (Web): November 24, 2015 | doi: 10.1021/bk-2015-1203.ch001

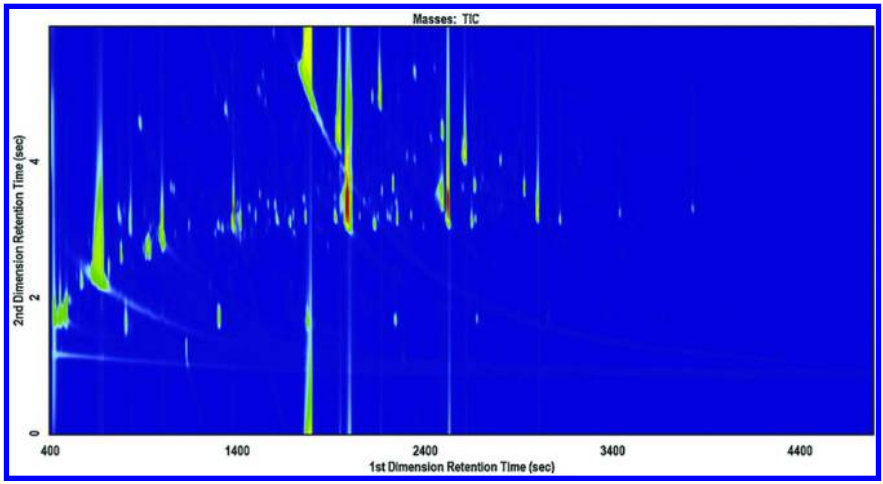

Figure 2. Typical contour plot of a HS-SPME/GC x GC-TOFMS chromatogram (TIC) demonstrating the separation of volatile compounds isolated from the headspace of a Cabernet Sauvignon wine. The color gradient reflects the intensity of the TOFMS signal (Z-axis) from low (blue) to high (red). Note that a substantial number of trace volatile compounds are not visible in this chromatogram due to the abundant esters dominating the Z-axis of the plot. Reproduced with permission from Ref. (17). (2011) (Elsevier).

Nuclear Magnetic Resonance (NMR) has also been used for rapid profiling grape and wine composition. For example, Skogerson et al. (*20*) used ^{1}H NMR metabolite profiles to relate composition to sensory perception of body and mouthfeel of white wines. Although only about half the number of metabolites that had been identified in the wines by GC-TOF-MS analysis could be identified by the ^{1}H NMR analysis, NMR profiling was still able to explain about 79% of the variation in sensory mouthfeel of the wines. Proline, lactate, and trigonelline

were correlated with the viscous mouthfeel. The NMR analysis was rapid with a total acquisition time of approximately 5 min and yielded valuable information on chemical factors influencing wine mouthfeel and viscosity. Additional applications of NMR profiling for grape and wine authentication studies are presented by Wittkowski in a later chapter of this volume.

Elemental Analysis

The trace element composition of grapes and wines can provide important information on the geographical origin of a food or beverage (*21*, *22*) as well as wine processing and storage conditions (*23*, *24*). Many trace elements are required for vine nutrition and growth and they may be taken up from the soil by the plant and/or used in agrochemicals. Elements such as copper and iron can influence the chemical stability of the wine (*e.g.*, see also chapters by Boulton, Ferriera, and others in this volume). The International Organization of Vine and Wine (OIV) has established maximum legal limits for many elements (*25*).

ICP-MS is rapidly gaining in popularity as a rapid and sensitive approach for simultaneous screening of a large number of elements and the principles and applications of ICP-MS have recently been reviewed (*26*). In a series of recent studies, Hopfer et al. (*21*, *24*) have shown that the elemental composition of wines can be related to the vineyard that the grapes were grown in, however, during winemaking and storage the elemental composition changes significantly and individual wineries can yield wines with unique elemental profiles (*24*). Changes in elemental composition of the wines can further occur during storage, for example, leaching of metals from stainless steel containers and from closures (*23*). These studies point to the need for much further work on the changes in elemental composition in grapes and wines as a result of vineyard and winemaking practices.

Relating Chemical Composition and Sensory Attributes

In the above sections, several studies were described where chemical composition was related to sensory properties. In the case of the haloanisole, TCA, the musty character of wine can frequently be directly correlated with the concentration of this single impact compound. However, masking effects of TCA on fruity perception of wines and interactions of other haloanisoles can also influence overall sensory properties (*27*).

In the case of metabolite profiles (volatiles and nonvolatiles), complex mixtures of compounds can be related to sensory properties using multivariate statistical approaches such as PCA and PLS. In these cases it is common to have one or more compounds that correlate with specific aroma or flavor attributes, however the compounds may not directly cause the perceived aromas. Examples of these types of correlations for relating chemical and sensory properties have been recently shown with US Cabernet Sauvignons and Malbecs from Argentina (*28*, *29*).

Publication Date (Web): November 24, 2015 | doi: 10.1021/bk-2015-1203.ch001

In an interesting example of the complex interactions that arise from mixtures of aroma compounds, Hopfer et al. (*30*) observed that monovarietal wines (Cabernet Sauvignon, Merlot, Cabernet franc) had unique sensory properties. However, when blended together, blends with similar sensory attributes could be obtained with a number of different blend mixtures. This is in contrast to the chemical composition, which represents the mathematical sum of the individual component wines in the blend. Additive, masking and synergistic effects all occur, while matrix interactions can also influence release and volatility of aroma compounds (*3*, *31*).

In an attempt to begin to develop analytical tools that can allow these perceptual interactions to be studied more fully, Johnson et al. (*32*) described a new approach called in-instrument GC-Recomposition Olfactometry that allows a chromatogram to be 'cut apart' and the components recombined in unique ways in order to evaluate their aroma qualities. This technique does not require that GC peaks be identified or quantified prior to the analysis of the aroma qualities of the recombination mixture. When used to evaluate components contributing to aroma of fresh lavender, unique additive, masking, and synergistic effects were observed. This work provides a valuable new analytic tool for developing a more holistic understanding of the way that aroma mixtures are perceived.

Publication Date (Web): November 24, 2015 | doi: 10.1021/bk-2015-1203.ch001

Summary

We have described selected applications to demonstrate the diversity and potential of new analytical tools for understanding the effects of viticultural and enological process on grape and wine composition and for relating composition to sensory properties. These tools can allow hundreds of volatile and nonvolatile compounds and trace elements in grapes and wines to be rapidly and sensitively quantified. However, to reach the full potential for throughput and discovery of novel components, the analytical instrument will require improved databases for compound identification as well as advanced data processing algorithms for rapidly and accurately deconvoluting and annotating complex chromatographic profiles. This work is further restricted by the limited availability of authentic standards, although promising new approaches for isolation of natural products, such as counter current chromatography, are improving the availability of novel polyphenol and other bioactives as described by Winterhalter et al. in this volume. As a result analytical advances will continue to provide new insights into grape and wine chemistry.

References

1. Ebeler, S. E. In *Gas Chromatography*; Poole, C. F., Ed.; Elsevier: New York; 2012; pp 689−710.
2. Robinson, A. L.; Boss, P. K.; Solomon, P. S.; Trengove, R. D.; Heymann, H.; Ebeler, S. E. *Am. J. Enol. Vitic.* **2014**, *65*, 1–24.
3. Robinson, A. L.; Boss, P. K.; Solomon, P. S.; Trengove, R. D.; Heymann, H.; Ebeler, S. E. *Am. J. Enol. Vitic.* **2014**, *65*, 25–42.

4. Collins, T. S.; Hjelmeland, A.; Ebeler, S. E. In *Recent Advances in the Analysis of Food and Flavors*; ACS Symposium Series 1098; Toth, S., Mussinan, C., Eds.; American Chemical Society: Washington, DC, 2012; pp 109−127.
5. Evans, T. J.; Butzke, C. E.; Ebeler, S. E. *J. Chromatogr.* **1997**, *786*, 293–298.
6. Fischer, C.; Fischer, U. *J. Agric. Food Chem.* **1997**, *45*, 1995–1997.
7. Hjelmeland, A. K.; Collins, T. S.; Miles, J. L.; Wylie, P. L.; Mitchell, A. E.; Ebeler, S. E. *Am. J. Enol. Vitic.* **2012**, *63*, 494–499.
8. Kennison, K. R.; Wilkinson, K. L.; Williams, H. G.; Smith, J. H.; Gibberd, M. R. *J. Agric. Food Chem.* **2007**, *55*, 10897–10901.
9. Kennison, K. R.; Gibberd, M. R.; Pollnitz, A. P.; Wilkinson, K. L. *J. Agric. Food Chem.* **2008**, *56*, 7379–7383.
10. Kennison, K. R.; Wilkinson, K. L.; Pollnitz, A. P.; Williams, H. G.; Gibberd, M. R. *Austr. J. Grape Wine Res.* **2009**, *15*, 228–2372009.
11. Hayasaka, Y.; Dungey, K. A.; Baldock, G. A.; Kennison, K. R.; Wilkinson, K. L. *Anal. Chim. Acta* **2010**, *660*, 143–148.
12. Vaclavik, L.; Lacina, O.; Hajslova, J.; Zweigenbaum, J. *Anal. Chim. Acta* **2011**, *685*, 45–51.
13. Flamini, R. *ISRN Spectroscopy Article ID 813563*; 2013, URL http://dx.doi.org/10.1155/2013/813563 (accessed on-line December 1, 2014).
14. Gougeon, R. D.; Lucio, M.; Frommberger, M.; Peyron, D.; Chassagne, D.; Alexandre, H.; Feuillat, F.; Voilley, A.; Cayot, P.; Gebefügi, I.; Hertkorn, N.; Schmitt-Kopplin, P. *Proc. Natl. Acad. Sci. U.S.A.* **2009**, *106*, 9174–9179.
15. Roullier-Gall, C.; Lucio, M.; Noret, L.; Schmitt-Kopplin, P.; Gougeon, R. D. *PLoS One* **2014**, *9*, e97615.
16. Roullier-Gall, C.; Boutegrabet, L.; Gougeon, R. D.; Schmitt-Kopplin, P. *Food Chem.* **2014**, *152*, 100–107.
17. Robinson, A. L.; Boss, P. K.; Heymann, H.; Solomon, P. S.; Trengove, R. D. *J. Chromatogr. A* **2011**, *1218*, 504–517.
18. Robinson, A. L.; Adams, D. O.; Boss, P. K.; Heymann, H.; Solomon, P. S.; Trengove, R. D. *Austr. J. Grape Wine Res.* **2011b**, *17*, 327–340.
19. Robinson, A. L.; Boss, P. K.; Heymann, H.; Solomon, P. S.; Trengove, R. D. *J. Agric. Food Chem.* **2011**, *59*, 3273–3284.
20. Skogerson, K.; Runnebaum, R.; Wohlgemuth, G.; de Ropp, J.; Heymann, H.; Fiehn, O. *J. Agric. Food Chem.* **2009**, *57*, 6899–6907.
21. Hopfer, H.; Nelson, J.; Collins, T. S.; Ebeler, S. E. *Spectroscopy* **2014**Sep.1, 34, 36, 39.
22. Versari, A.; Laurie, V. F.; Ricci, A.; Laghi, L.; Parpinello, G. P. *Food Res. Int.* **2014**, *60*, 2–18.
23. Hopfer, H.; Nelson, J.; Mitchell, A. E.; Heymann, H.; Ebeler, S. E. *J. Anal. At. Spectrom.* **2013**, *28*, 1288–1291Doi:10.1039/c3ja50098e.
24. Hopfer, H.; Nelson, J.; Collins, T. S.; Heymann, H.; Ebeler, S. E. *Food Chem.* **2015**, *172*, 486–496.
25. International Organization of Vine and Wine (OIV), OIV-MA-C1-01: R2011. *Maximum acceptable limits of various substances contained in wine*; 2011.
26. Ammann, A. *J. Mass Spectrom.* **2007**, *42*, 419–427.

Publication Date (Web): November 24, 2015 | doi: 10.1021/bk-2015-1203.ch001

27. Butzke, C. E.; Evans, T. J.; Ebeler, S. E. In *Chemistry of Wine Flavor*; ACS Symposium Series 714; Waterhouse, A. L., Ebeler, S. E., Eds.; American Chemical Society: Washington DC, 2009; pp 208−216.
28. Hjelmeland, A. K.; King, E. S.; Ebeler, S. E.; Heymann, H. *Am. J. Enol. Vitic.* **2013**, *64*, 169–179DOI:10.5344/ajev.2012.12107.
29. King, E. S.; Stoumen, M.; Buscema, F.; Hjelmeland, A. K.; Ebeler, S. E.; Heymann, H.; Boulton, R. B. *Food Chem.* **2014**, *143*, 256–267.
30. Hopfer, H.; Ebeler, S. E.; Heymann, H. *Am. J. Enol. Vitic.* **2012**, *63*, 313–324.
31. Polaskova, P.; Herszage, J.; Ebeler, S. E. *Chem. Soc. Rev.* **2008**, *37*, 2478–2489.
32. Johnson, A.; Hirson, G.; Ebeler, S. E. *PLoS One* **2012**, *7*, e42693.

Publication Date (Web): November 24, 2015 | doi: 10.1021/bk-2015-1203.ch001

Publication Date (Web): November 24, 2015 | doi: 10.1021/bk-2015-1203.ch002

Chapter 2

Combined Nontargeted Analytical Methodologies for the Characterization of the Chemical Evolution of Bottled Wines

C. Roullier-Gall,[1,2] M. Witting,[2] D. Tziotis,[2] A. Ruf,[2] M. Lucio,[2] P. Schmitt-Kopplin,[*,2,3] and R. D. Gougeon[*,1]

[1]UMR PAM Université de Bourgogne/AgroSup Dijon, Institut Universitaire de la Vigne et du Vin, Jules Guyot, 21000 Dijon, France
[2]Research Unit Analytical BioGeoChemistry, Department of Environmental Sciences, Helmholtz Zentrum München, 85764 Neuherberg, Germany
[3]Chair of Analytical Food Chemistry, Technische Universität München, 85354 Freising-Weihenstephan, Germany
[*]E-mail: regis.gougeon@u-bourgogne.fr.

Various non-targeted approaches have already shed light on the thousands of compounds that are present at various concentrations in grape and wine. Among them, direct injection Ion Cyclotron Resonance Fourier Transform Mass Spectrometry (FTICR-MS) undoubtedly provides the most comprehensive chemical fingerprints, based on unrivalled resolution on mass measurement, but limited to structural assumptions. Here, we show that the combination of FTICR-MS and Ultra-Performance Liquid Chromatography Mass Spectrometry (UPLC-QTOF-MS), which increases the scope of detectable unknown metabolites and allows the separation between isomers, provides an unprecedented synoptic characterization of the chemical complexity of wines, where results obtained with one platform can directly be validated with data from the other. To that respect, wine ageing appears to be particularly interesting when related to the oeno-diagenesis processes that operate in bottle, and which depend on the actual initial composition of the wine. Applied to Pinot noir red wines from three different appellations in

In Advances in Wine Research; Ebeler, et al.;
ACS Symposium Series; American Chemical Society: Washington, DC, 2015.

Burgundy, and over three vintages (1979, 1989, 1999), this approach revealed that the ageing chemistry is fundamentally driven by the metabolic baggage at bottling, characterized here by thousands of compounds from various chemical families including carbohydrates, amino acids, or polyphenols, but with a remarkably high distribution of nitrogen and sulfur-containing compounds.

Introduction

Publication Date (Web): November 24, 2015 | doi: 10.1021/bk-2015-1203.ch002

Because it addresses both scientists and non-scientists concerns, the diversity of knowledge about wine is valued by a range of audiences. Among these knowledges, wine chemical composition and its evolution throughout the entire winemaking process have become well-documented fields of chemistry, where the most advanced analytical tools can actually find numerous applications (*1–3*).

Among these tools, FTICR-MS with electrospray ionization (ESI) has now become a powerful technique for studying wine, in particular when employed in direct infusion experiments (*1*, *3*, *4*). However, if a chromatographic separation is not applied prior to the MS detection, a large number of molecules are subjected simultaneously to the ionization process, which can cause ion suppression for numerous analytes and the inability to separate isobaric and isomeric substances (*5*, *6*). Chromatographic separation prior to MS-analysis is therefore important for both targeted and non-targeted metabolomics, and it has already been used for untargeted metabolomics analysis of grape to differentiate grape berry ripening and post-harvest withering (*7*), for wine authentication (*8*), or for the understanding of the terroir impact in wine (*9*). The combination of UHPLC with time-of-fight mass spectrometry (TOF-MS) has preferentially been applied for many targeted wine studies such as the separation and detection of resveratrol (*10*), of phenolic compounds (*11–15*) or toxins (*16*). In contrast, so far very few studies have used such combination of highest chromatographic resolution, excellent sensitivity, fast data acquisition and high mass accuracy, for untargeted metabolomics analyses of grapes and wines (*17*, *18*).

A likely reason for this is that exact mass measurement can be obtained through the highest resolution achieved by FTICR-MS, which typically requires higher acquisition times by combining multiple narrow-range spectra into one wide range spectrum and thus do not fully exploit the potential of fast UPLC (*3*) or CE (*19*). Resolution of 400.000 around mass 400 and 800.000 around mass 200 in full scan mode (mass range 120 to 2000) are routinely obtained with the FT-ICR-MS, along with calibration with internal signals with 0.1 ppm precision. Neither this mass accuracy, nor this resolution can be obtained with QTOF systems. As a consequence, the combination of exact mass measurement by FTICR-MS, versatile UPLC-Q-ToF-MS and multivariate statistics appears to be at the forefront of non-targeted metabolomics of wines. Here, the versatility of LC-MS techniques definitely adds to the identification of unknowns through

the covering of the widest range of compounds, which can be separated either by reversed phase or hydrophilic interaction chromatography (*5*, *20*). Reversed-phase (RP) liquid chromatography has been highlighted as the mostly used separation mode for the metabolome analysis (*6*, *18*, *20*, *21*). RP separation covers a large part of the metabolome, and at the same time provides the most reliable and robust LC stationary phases. Hydrophilic interaction chromatography (HILIC) provides separations complementary to those obtained by RPLC–MS in that early eluting analytes in the RP mode are often well retained by HILIC (*5*, *6*, *22*).

In this paper, we show that such combination of FTICR-MS, UPLC-Q-ToF-MS and multivariate statistics can provide unprecedented chemical description of the chemistry associated with bottle ageing of Pinot noir red wines, during which the composition changes through a complex array of chemical reactions that are still only partly understood (*23–29*).

Publication Date (Web): November 24, 2015 | doi: 10.1021/bk-2015-1203.ch002

Materials and Methods

Chemicals

Methanol, acetonitrile and water (LC-MS grade) were purchased from Fluka Analytical (Sigma-Aldrich, St. Louis, USA). Low concentration ESI Tuning Mix for Q-ToF calibration was obtained from Agilent (Agilent, Waldbronn, Germany).

Wines

All measurements were done on Pinot noir wines from three different appellations in Burgundy (Richebourg (R), Grand Echezeaux (GE) and Beaune (B)) and from three vintages (1979, 1989 and 1999), sampled directly from the bottles in 2 ml vials under argon to protect them from oxygen. 50 µl of wine were diluted into 950µl methanol for FTICR-MS analysis and 40 µl of acetonitrile was added to 960 µl of wine with for both RP and HILIC LC-MS analysis.

Fourier Transform Ion Cyclotron Resonance Mass Spectrometry Analysis (FTICR-MS)

Ultra high-resolution mass spectra were acquired using a FTICR-MS instrument (solariX, Bruker Daltonik, Bremen, Germany) equipped with a 12 Tesla superconducting magnet and an Apollo II electrospray ionization source operated in the negative ionization mode. Samples were introduced at a flow rate of 120 $\mu L.h^{-1}$ using a syringe pump. The MS was externally calibrated on clusters of arginine (10 $mg.L^{-1}$) in methanol. Spectra were acquired with a time domain of

4 mega-words per second with a mass range from m/z 100 to 1000 to guarantee a high accuracy in elemental formula assignments in this proof-of-principle study. Up to 500 scans per sample were accumulated. A resolving power (R), greater than 500,000 at mass 400 was achieved. Fourier Transform Ion Cyclotron Resonance (FTICR) spectra were internally recalibrated on a list composed by fatty acids and recurrent compounds in wine, linear up to m/z 600, with mass errors below 0.05 ppm (expressed using the formula (mass error/exact mass).10^6 where mass error is the difference between the exact mass and the measured mass) and peak with a signal-to-noise ratio (S/N) of 4 and higher were exported to peak lists. In conjunction with an automated theoretical isotope pattern comparison, the generated formulas were validated by setting sensible chemical constraints (n rule; O/C ratio ≤ 1; H/C ratio ≤ 2n+2; element counts: C ≤ 100, H ≤ 200, O ≤ 80, N ≤ 3, S ≤ 3 and P ≤ 1).

Publication Date (Web): November 24, 2015 | doi: 10.1021/bk-2015-1203.ch002

Ultraperformance Liquid Chromatography Coupled to Quadrupole Time of Flight Mass Spectrometry Analysis (UPLC/Q-ToF-MS)

Analyses were performed on a Waters Acquity UPLC (Waters, Milford, USA) coupled to a maXis™ UHR-ToF-MS (Bruker Daltonik, Bremen, Germany) system using reversed phase (RP) and hydrophilic interaction liquid chromatography (HILIC) separation (*3*). Sample analyses were carried out in (-) ESI.

RP separation was performed using a Waters ACQUITY UPLC BEH C18 column (1.7 µm; 1.0x150 mm) using gradient elution with an initial isocratic hold of 100% A for 0.5 min, followed by a linear increase to 100% solvent B in 4.9 min, isocratic conditions for 3 min and return to initial conditions in 1.6 min (solvent A: 10% ACN, 1 mM ammonium formate; solvent B: 100% ACN).

HILIC separations were performed on a Waters ACQUITY UPLC BEH Amide column (1.7 µm; 2.1x150 mm) using a two-step gradient elution program from 100% A to 100% solvent B (solvent A: 95% ACN, 5% water, 1 mM ammonium formate; solvent B: 50% ACN, 50% water, 1 mM ammonium formate).

The flow rate for both separation modes was set to 0.25 ml/min with a column temperature of 40 °C and a full loop injection of 10 µl.

UHR-ToF-MS acquisitions were carried out in profile spectra mode with 1 Hz accumulation time. Instrument tuning focused on detection and resolution of molecular weight compounds in the mass range of 50-2000 Da. Mass calibration was carried with Low Concentration ESI Tuning Mix (Agilent, Waldbronn, Germany) (Table 1).

Publication Date (Web): November 24, 2015 | doi: 10.1021/bk-2015-1203.ch002

Table 1. Composition of the Low Concentration ESI Tuning Mix Used for the Mass Calibration of Ultraperformance Liquid Chromatography Coupled to Quadrupole Time of Flight Mass Spectrometry

Name	*CAS*	*Formula*	*Molecular weight*
Trifluoroqcetic acid ammonium salt	3336-58-1	$C_2H_4NO_3F_3$	131.05
Betaine	107-43-7	$C_5H_{12}NO_2$	151.61
Tris(trifluoromethyl)-1, 3, 5-triazine	368-66-1	$C_6F_9N_3$	285.07
Hexamethoxyphosphazine	957-13-1	$C_6H_{18}N_3O_6P_3$	321.14
Tris(heptafluoropropyl)-1, 3, 5-triazine	915-76-4	$C_{12}F_{21}N_3$	585.11
Hexakis(2,2-difluoroethoxy)phosphazine	186817-57-2	$C_{12}H_{18}F_{12}N_3O_6P_3$	621.19
Hexakis(1H, 1H, 3H-tetrafluoropropoxy)phosphazine	58943-98-9	$C_{18}H_{18}F_{24}N_3O_6P_3$	921.23

Network Analysis

To obtain chemical formulas for subsequent use in querying chemical databases, exact masses were subjected to mass difference network analysis using the Netcalc algorithm and in-house software tool (*30*). In a mass difference network, nodes represent m/z values (metabolite candidates) and edges represent chemical reactions. Netcalc enables network reconstruction by comparing the mass differences of all experimental masses of a mass spectrum to a list of user-defined theoretical mass differences (selected according to atomic units, e.g. C, H, N, O, S, P, or common functionality groups, e.g. homologous series of CH_2, H_2, or OH. The mass difference list used in this example was optimized to detect chemical differences between all annotatable nodes in the experimental data in order to reveal patterns in compositional or functional chemical spaces. The purpose of mass difference network analysis is the visualization of the sample's compositional structure and the calculation of elemental formulae of experimental masses. In such a scale-free network, highly inter-connected nodes tend to cluster together while sparsely connected ones are peripherally dispersed. Netcalc increases the percentage of m/z peaks, which can be assigned to a preliminary formula up to a 40-60% per dataset including isotope peaks ^{13}C (*5*). The goal of this model is the visual and mathematical evaluation of organic molecular complexity in terms of elemental composition, an approach that permits explicitly defined relationships between different samples (*30*).

Statistical Analysis

Filtering of masses was performed in MS Excel 2010 (Microsoft, Redmond, USA). All further statistical analyses were performed with Genedata Expressionist for MS 8.0 (Genedata, Basel, Switzerland) and Simca-P 9.0 software (Umetrics, Sweden) (*3*).

Results and Discussion

FTICR-MS

Samples were analyzed by direct injection ESI (-) FTICR-MS (*1*, *4*, *31*). Negative ionization was used as it provides a higher number of different resolved ion signals in the selected mass range than the positive ionization mode (*32*). As illustrated for the 1999 wine, the ultra-high resolution power of FTICR-MS spectra enabled the detection of more than 18000 distinct mass signals with a signal-to-noise ratio ≥ 4 in the negative-ion mode in the 100-1000 Da mass range (Figure 1). Only singly charged peaks were detected as shown in the enlargement (Figure 1A-C).

In Advances in Wine Research; Ebeler, et al.;
ACS Symposium Series; American Chemical Society: Washington, DC, 2015.

Publication Date (Web): November 24, 2015 | doi: 10.1021/bk-2015-1203.ch002

Publication Date (Web): November 24, 2015 | doi: 10.1021/bk-2015-1203.ch002

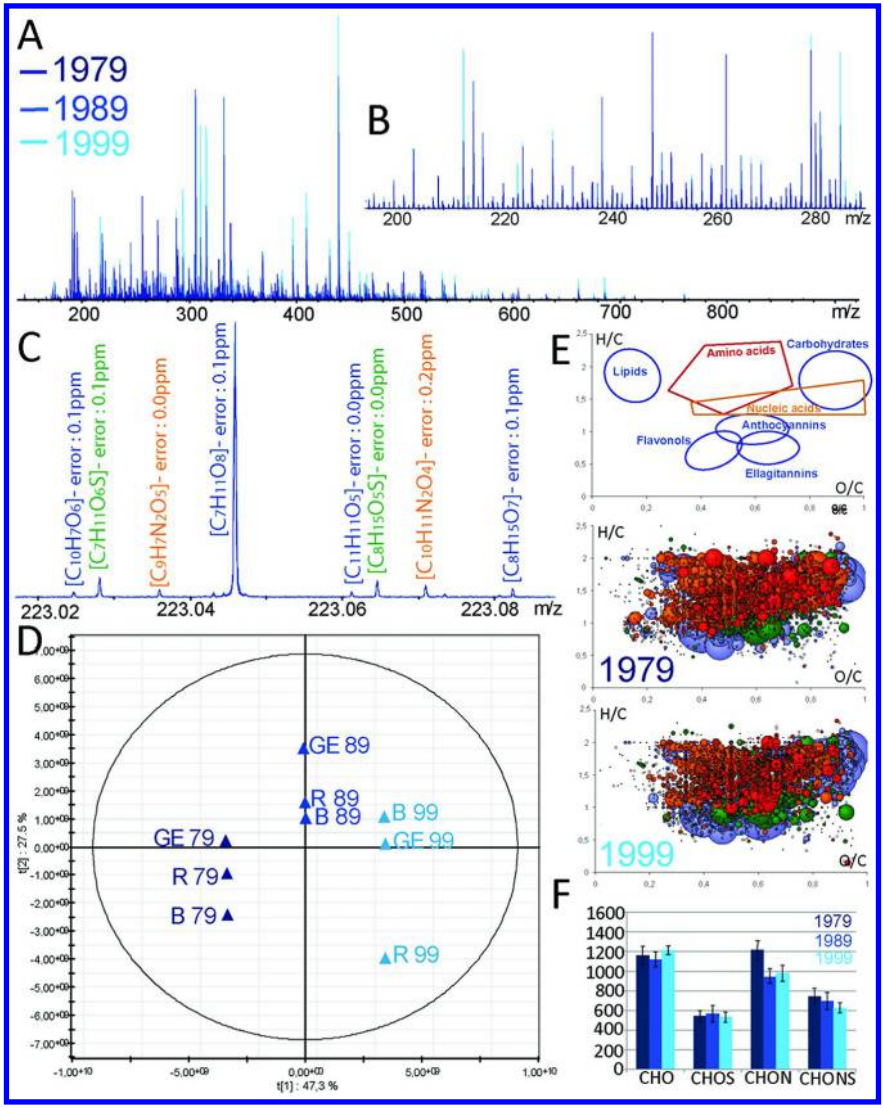

Figure 1. Progressive detailed visualization of the ESI(-) FTICR/MS spectra of the three red wines in the 100-1000Da mass range (A), 200-230Da (B) and 223.00-223.10Da with credible elemental formula assignments (C). OPLS score plot analysis of the three wines from the three vintages. Q^2(cum)=0.995 and R^2(Y)=0.967(D). Visualisation of the regions specific to chemical families and the FTICR/MS data of 1979 and 1999 wines as van Krevelen diagrams, (H/C vs. O/C atomic ratios) (E). Relative frequency histograms of average elemental compositions for the three wines (GE, R and B) for each vintages (F). Color code for van Krevelen diagrams and formula: CHO (blue), CHOS (green), CHON (yellow), CHONS (red.) The bubble sizes correspond to the relative intensity of peaks annotated with elemental formulas associated with these O/C and H/C ratio. (see color insert)

In Advances in Wine Research; Ebeler, et al.;
ACS Symposium Series; American Chemical Society: Washington, DC, 2015.

Publication Date (Web): November 24, 2015 | doi: 10.1021/bk-2015-1203.ch002

An OPLS supervised statistical analysis satisafactorily discriminated wines according to vintages along the first axis, regardless of the appellation, consistently with many previous reports on FTICR-MS analyses of wines (*31*, *33*). van Krevelen diagrams provided a striking representation of the chemical diversity of these red wines, with abundance of carbohydrates, polyphenols and amino acids in particular (Figure 1E). Furthermore, as illustrated by the counts of CHONS formulas averaged over the three appellations for a given vintage, these wines exhibited only low variability in terms of composition, and appeard to be relatively rich in nitrogen and sulfur-containing compounds, compared to recent wines (*31*) (Figure 1F). Sulfur-containing compounds were significantly associated with polyphenols (region centered around O/C=0.6 and H/C=1) in agreement with the sulfites/polyphenols chemistry, and the more than 400 CHOS elemental formulas provided a snapshot of the extent of the yet-unknown sulfur-related chemistry associated with bottle ageing of wines. Most interestingly, the counts in Figure 1F also revealed that over the 20 years period investigated here the overall chemical diversity did not decrease with ageing, and the older 1979 wines could still exhibit the highest number of CHON compounds, thus providing an unsual representation of the acknowledged ageing ability of great red wines.

Mass difference network analyses were set to determine elementary compositions and thus faciltate metabolite annotations as well as visualize functional connectivities within the data (Figure 2). Using common structural functional-group (Figure 2), which may be seen in highly complex data, a mass difference network was created. For these wine samples, several regions showed a local high density of masses with mostly CHO compounds. Sulphur-containing compounds (CHOS and CHONS corresponding to green and red links, respectively) seemed to be distributed over the entire network showing an unspecific reactivity of sulphur within the structural domain. As an illustration, the enlargement of a small portion of the network around m/z 458.22566 ($[C_{19}H_{32}N_5O_8]^-$) showed a functional connectivity to m/z 490.19778 ($[C_{19}H_{32}N_5O_8S]^-$) by an accurate 31.97212 mass difference, which corresponds to a S functional difference. Such network-based approach theoretically enables the calculation of the elemental formulas of multiple metabolites in a sample, starting from a small number of known metabolites. Some sub networks appeared to be disconnected from the main graph, showing that the functional mass differences list may be incomplete; ongoing work implies the mass difference networking based on more than hundred biological transformations derived from databases and literature to set up a more comprehensive metabolic picture (*3*). Frequencies of some individual modifications can be observed (Figure 2), with highest frequencies found for H_2, H_2O, CO, CO_2 and CH_2O functional differences. Here again, no clear age-related trend could be observed, and it is actually the older wine which exhibited the highest number of functional differences (including differences involving N and S), whereas the intermediate 1989 wine showed the lowest number. Remebering that all of these wines were analysed at the same time, thus with the 1989 and the 1979 wines being 10 and 20 years older, respectively, than the 1999 wine, this non-regular distribution of functional differences remarkably illustrated the predominant vintage-related

chemistry, which actually drives the evolution of the chemical diversity over ageing in bottle. In other words, at bottling, wines were not equipped with the same metabolic baggage, which could be the result of distinct initial compositions of grapes, and our non-targeted FTICR-MS analyses are able to provide snapshots of the corresponding instantaneous chemical signatures, which could still appear independent of the appellation, even after more than 30 years of bottle ageing (which is the case of the 1979 wines).

Publication Date (Web): November 24, 2015 | doi: 10.1021/bk-2015-1203.ch002

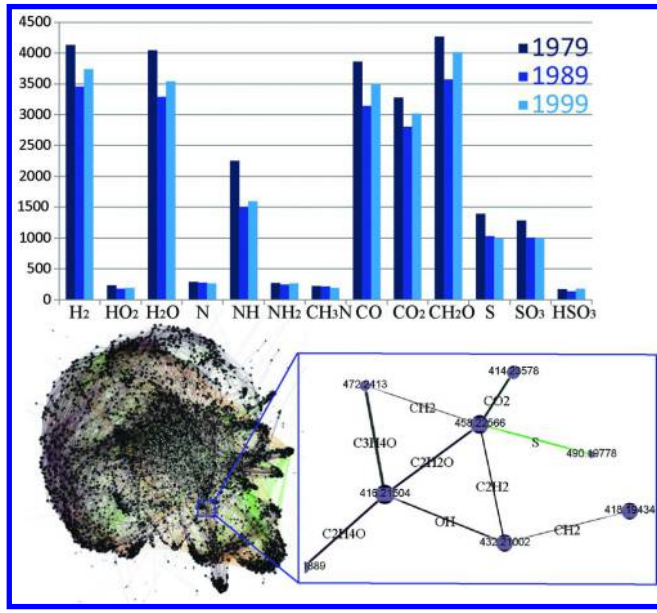

Figure 2. Overview on Netcalc networks drawn from R wines data. Counts of selected mass differences observed in the main network (Top) and main network from negative ionization mode (bottom left), and enlargement of this network centered on few masses (bottom right). Color code: CHO (blue), CHOS (green), CHON (yellow), CHONS (red) of red wine and an older red wine (grey). (see color insert)

Combination of FTICR-MS, Reverse Phase, and HILIC UPLC/Q-ToF MS

To increase the scope of detectable metabolites and get structural information, in particular through the separation of isobaric and isomeric compounds, data obtained by direct infusion FTICR-MS can be combined with data obtained by

on-line UPLC/Q-ToF-MS techniques. Since FTICR-MS combines excellent mass accuracy and ultra-high resolution, it offers high sensitivity and dynamic range, which allows the detection of analytes on a wide range of concentrations (*34*). The combination with two orthogonal UPLC/Q-ToF-MS methods increases the scope of detectable metabolites, decreases putative ion suppression effects and achieves a separation between isobaric substances (*5*, *22*). To enable good sensitivity in FTICR-MS an accumulation of several hundreds of scans (>3s per scan) is needed in the instrumental setup leading to the highest resolution in full scan. As a consequence, coupling of FTICR-MS to liquid chromatography, with a necessary reduction of the acquisition time, is definitely detrimental to both sensitivity and spectral resolution (*5*). As a consequence, our combined approach definitely provide the best of both chromatography and mass spectrometry worlds.

This approach, which depends both on column characteristics and chromatographic methods, thus brings two additional criteria for the structure determination. Reversed phase (RP) chromatography mostly separates mid- to non-polar metabolites and molecules elute according to their hydrophobicities, starting with the most hydrophilic substance in the mixture while HILIC is used for polar metabolites like amino acids. The coupling of a chromatographic technique and mass spectrometry extends the investigation of the widest range of compound classes and helps in the characterization of important compounds. Limitations of MS-based separation such as the inability to differentiate isobars or isomers and the suppression effect caused by the molecules competing for ionization, can be overcome by UPLC separation prior to MS injection (*5*, *22*). As examples, Table 2 reports the possible number of isomers (retention times) that could be detected by RP UPLC/Q-ToF-MS for 8 mass peaks observed in FTICR-MS throughout the observed mass range. For instance, m/z 149.00916 ($[C_4H_5O_6]^-$) actually corresponded to three different isomers with retention times of 3.4, 4.9 and 16.1 min, whereas m/z 153.05585 ($[C_8H_7NO_2]^-$) could be related to one isomer with a retention time of 2.7 min (Table 2). The former example clearly illustrated the input of our combined approach, where based on FTICR-MS alone, a pertinent metabolite structure can be hypothetically associated with an elemental formula – here tartaric acid – and where chromatographic dimensions – here only RP – reveal that at least two other metabolites may actually contribute to the FTICR-MS peak, but not consistently over vintages. However, Table 2 also shows that many FTICR-MS features can have unique correspondances in LC-MS features. Altogether, these examples show that there are situations where multiple FT-ICR peaks exist within the envelope of a single QTOF peak, and alternatively, there are situations where only one FT-ICR peak exist within the envelope of a single QTOF peak. Furthermore, as shown below there are also situations where masses detected by FT/MS are not detected by LC-MS, because of ion selection by LC.

Although the mass resolution of the Q-ToF instrument is clearly not sufficient to separate all the m/z features observed in FTICR-MS, mass profiles exhibited similarities among the techniques (Figure 3A). An enlargement of the m/z 227.00-227.20 region of the mass spectrum illustrates the limitation of the resolving power of the ToF. The mass error for the 227.07136 peak, corresponding to the $[C_{14}H_{11}O_3]^-$ $[M-H]^-$ ion which can tentatively be assigned to resveratrol

Publication Date (Web): November 24, 2015 | doi: 10.1021/bk-2015-1203.ch002

isomers, was 0.04 ppm for FTICR-MS, whereas the error was higher by a factor of about 100 for RP UPLC/Q-ToF-MS (3.03 ppm). No peaks were detected at that mass using HILIC/Q-ToF-MS. Similarly, the mass error of the 227.10335 peak (corresponding to the [M-H]- ion $[C_{10}H_{13}N_2O_4]^-$) was 1.62 ppm for FTICR-MS and approximately ten times higher for HILIC/Q-ToF-MS (19.8 ppm) (Figure 3A). Five major peaks were present in the FTICR-MS for this mass range, and two of them could also be found using RP UPLC/Q-ToF-MS, while a third metabolite was confirmed with HILIC/Q-ToF-MS. The Venn diagram (Figure 3B) showed the overlap of masses found by the three applied techniques, when all 9 wine samples were considered. A total of 14,405 masses were detected using (-) FTICR-MS, including 10,476 specific to this method and 1,553 common to RP UPLC/Q-ToF-MS (but not to HILIC/Q-ToF-MS); 5,920 were detected by (-) RP UPLC/Q-ToF-MS, with only 2,230 specific to this method, whereas only 4,915 were detected with (-) HILIC/Q-ToF-MS with 1,518 specific to this separation. Up to 15 percent of all of the annotations were detected in at least two analytical procedures and masses common to all instruments (1,116) represented only 3.4 percent of the detected masses. It must be noted that the apparent lower number for both LC-based methods compared to FTICR-MS is due to the fact that only m/z features were considered in Figure 3B. As mentioned before through Table 2, the consideration of retention times (thus isomers) associated with each of LC-based m/z features would clearly increase the actual number of detected compounds. Therefore, as shown by the survey view, which corresponds to the two-dimensional chromatogram plot (Figure 3C), the advantage of the UPLC separation prior to MS injection is that it allows for the separation and identification of isomeric compounds, for example, the detection of two different isomers, at two close though distinct retention times (4.1 and 4.3 min), for the m/z 227.07136. Within an error of 0.1 ppm, the corresponding [M-H]- ions with mass formula $[C_{14}H_{11}O_3]^-$ could be associated with up to 2011 substances (from the SciFinder search facility: https://scifinder.cas.org) but only two of them, *i.e.* resveratrol (*1*) and benzilic acid (*35*), actually appeared to be consistent with compounds that are known to be present in red wine. Conversely, only one isomer was detected for the 227.09921 mass using HILIC/Q-ToF-MS (Figure 3). Consequently, our results show that both methods are working orthogonal and complementary, rather than being redundant. Although being out of the scope of this study, it should be noted that some of the LC-based detected peaks may still be composite peaks resulting from the coalescence of isobaric ions, which would not be distinguished with the achievable Q-ToF-MS resolution. If hyphenated LC separations would be ideally suited to handle such question, the search for isotopologues within LC- Q-ToF specra also provides a validation of the unicity of the LC peak. The complementarity of FTICR-MS is again illustrated here, because only its mass accuracy allows for an accurate isotopologues search.

Publication Date (Web): November 24, 2015 | doi: 10.1021/bk-2015-1203.ch002

Publication Date (Web): November 24, 2015 | doi: 10.1021/bk-2015-1203.ch002

Table 2. Example of Isomers, Which Were Detected by RP UPLC-MS for the Individual Masses Measured by FTICR-MS

		Retention time (min) RP UPLC-MS		
m/z FTICR-MS	***Molecular ion formula***	***1979***	***1989***	***1999***
149.00968	$[C_4H_5O_6]$-	-	-	3.4
		4.9	4.9	4.9
		16.1	-	-
153.01931	$[C_7H_6O_4]$-	2.9	2.9	2.9
		5.1	5.1	-
153.05585	$[C_8H_7NO_2]$-	2.7	2.7	2.7
215.00199	$[C_8H_6O_5S]$-	5.2	5.2	-
341.03334	$[C_{14}H_{12}O_8S]$-	1.8	1.8	1.8
451.17443	$[C_{26}H_{28}O_7]$-	16.7	16.7	-
		-	-	17.6
528.18239	$[C_{20}H_{34}NO_{15}]$-	17.1	17.1	-
		-	-	17.8
533.17633	$[C_{19}H_{34}O_{17}]$-	18.3	18.3	-

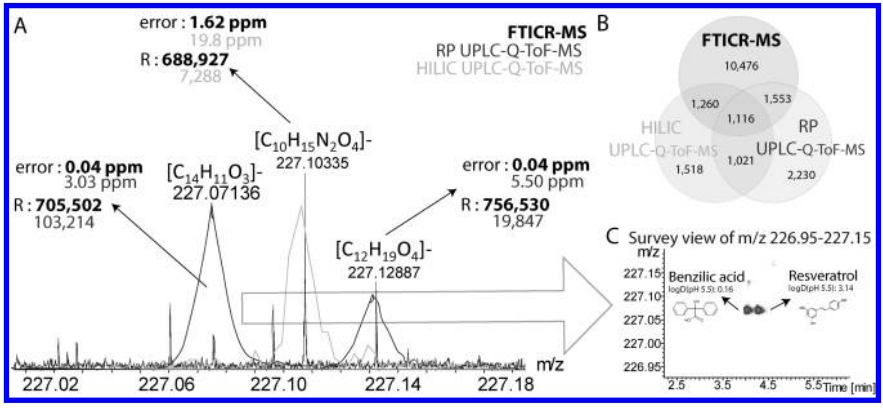

Figure 3. Enlargement of combined visualizations of the ESI(-) FTICR-MS spectrum, (-) RP UPLC- and HILIC- MS spectra in the 227.00-227.20Da mass range (A). Venn diagram showing the comparison of masses recovery according to applied techniques (B) Given numbers represent the count of unique or common detected masses. Zoom into the survey view of m/z 226.90-227.20 in RP LC-MS (C).

Publication Date (Web): November 24, 2015 | doi: 10.1021/bk-2015-1203.ch002

Identification and Annotation

Although 14,405 masses (10,476 + 1,260 + 1,116 + 1,153) were detected using FTICR-MS (Figure 3), only 1,421 masses could be detected and annotated using MassTRIX, a webserver for direct annotation of FTICR-MS data to metabolic pathways (*36*, *37*) questioning different databases and especially the KEGG (*38*) and HMDB (*39*) databases. MassTRIX provides hypothetical structural identifications and enables the visualization of compounds annotation on pathways of a chosen organism, *Vitis vinifera* in case of wines samples. MassTRIX also enabled the assignment of 816 masses from the 5,920 masses provided by the RP UPLC/Q-ToF-MS data and 855 from the 4,915 masses provided by the HILIC/Q-ToF-MS data of which 563 annotations were found in both FTICR-MS and RP UPLC/Q-ToF-MS for example. Thus, our results also showed that whatever the method used, a considerable part of the chemical composition of wines remains unknown from actual accessible databases. One also has to be bear in mind that the number of UPLC/Q-ToF-MS detected metabolites might tend to be over-represented due to the different tolerated mass errors used for the annotation (*3*).

Conclusion

A methodology based on the combination of ultra-high resolution FTICR-MS and both RP UPLC/Q-ToF-MS and HILIC UPLC/Q-ToF- MS for non-targeted metabolomics has been adapted for the analysis of wines. A major problem in metabolomics using mass spectrometry is the structural identification of the detected masses. The attribution of correct elemental compositions needs high accuracy in the mass calculation, which requires to consider all of the elements which might be present, not only carbon, hydrogen, oxygen, nitrogen, sulphur and phosphorous, but also isotopes. There are thus several advantages in combining different non-targeted approaches: FTICR-MS data allow for the precise determination of exact masses and their correlation with UPLC/Q-ToF-MS signals obtained at lower resolution, while UPLC/Q-ToF-MS when based on multiple separation criteria, enables the validation of annotations of important compounds, along with distinguishing between isomers. The current capacity to describe complex samples, in this case wine samples, by means of FTICR-MS and UPLC/Q-ToF-MS is thus greatly expanded and our results indicated that up to 10,000 accurate masses could be detected by FTICR-MS for wines from three different appellations and over three vintages. Considering a low average value of only two possible isomers, as detected by UPLC/Q-ToF-MS per exact masses measured by FTICR-MS, the latter method would extend the current count of chemical compounds in wine far beyond the known and identified volatile and non-volatile metabolites in wine so far (about 3,000 altogether). When applied to the comparison of three wines from the same grape variety but from three different vintages, the methodology presented here revealed that, even after more than thirty years of ageing, Pinot noir red wines from Burgundy could still exhibit

remarkable chemical diversity compared to younger wines, and thus provide an unprecedented picture of the oenodiagenesis operating in the bottle during the ageing of great wines.

Acknowledgments

We warmly thank the Domaine de la Velle in Meursault, and the Domaine de la Romanée Conti in Vosne Romanée. This work was financially supported by the Région Bourgogne, the Bureau Interprofessionnel des Vins de Bourgogne (BIVB) and the Comité Interprofessionnel des Vins de Champagne (CIVC).

Publication Date (Web): November 24, 2015 | doi: 10.1021/bk-2015-1203.ch002

References

1. Gougeon, R. D.; Lucio, M.; Frommberger, M.; Peyron, D.; Chassagne, D.; Alexandre, H.; Feuillat, F.; Voilley, A.; Cayot, P.; Gebefügi, I.; Hertkorn, N.; Schmitt-Kopplin, P. *Proc. Natl. Acad. Sci. U.S.A.* **2009**, *106*, 9174–9179.
2. Skogerson, K. *Nature* **2008**, *455*, 699–699.
3. Roullier-Gall, C.; Witting, M.; Gougeon, R. D.; Schmitt-Kopplin, P. *Front. Chem.* **2014**, *2*, 102.
4. Liger-Belair, G.; Cilindre, C.; Gougeon, R. D.; Lucio, M.; Gebefügi, I.; Jeandet, P.; Schmitt-Kopplin, P. *Proc. Natl. Acad. Sci. U.S.A.* **2009**, *106*, 16545–16549.
5. Forcisi, S.; Moritz, F.; Kanawati, B.; Tziotis, D.; Lehmann, R.; Schmitt-Kopplin, P. *J. Chromatogr. A* **2013**, *1292*, 51–65.
6. Gika, H. G.; Theodoridis, G. A.; Plumb, R. S.; Wilson, I. D. *J. Pharm. Biomed. Anal.* **2014**, *87*, 12–25.
7. Toffali, K.; Zamboni, A.; Anesi, A.; Stocchero, M.; Pezzotti, M.; Levi, M.; Guzzo, F. *Metabolomics* **2011**, *7*, 424–436.
8. Rubert, J.; Lacina, O.; Fauhl-Hassek, C.; Hajslova, J. *Anal. Bioanal. Chem.* **2014**, *406*, 6791–6803.
9. Tarr, P. T.; Dreyer, M. L.; Athanas, M.; Shahgholi, M.; Saarloos, K.; Second, T. P. *Metabolomics* **2013**, *9*, 170–177.
10. Wang, Y.; Catana, F.; Yang, Y.; Roderick, R.; van Breemen, R. B. *J. Agric. Food Chem.* **2002**, *50*, 431–435.
11. Gruz, J.; Novák, O.; Strnad, M. *Food Chem.* **2008**, *111*, 789–794.
12. Jaitz, L.; Siegl, K.; Eder, R.; Rak, G.; Abranko, L.; Koellensperger, G.; Hann, S. *Food Chem.* **2010**, *122*, 366–372.
13. Prosen, H.; Strlic, M.; Kocar, D.; Rusjan, D. *LC-GC EUR* **2007**, *20*, 617–621.
14. Püssa, T.; Floren, J.; Kuldkepp, P.; Raal, A. *J. Agric. Food Chem.* **2006**, *54*, 7488–7494.
15. Sun, B.; Leandro, M. C.; de Freitas, V.; Spranger, M. I. *J. Chromatogr. A* **2006**, *1128*, 27–38.
16. Zöllner, P.; Leitner, A.; Lubda, D.; Cabrera, K.; Lidner, W. *Chromatographia* **2000**, *52*, 818–820.
17. Arapitsas, P.; Scholz, M.; Vrhovsek, U.; Di Blasi, S.; Biondi Bartolini, A.; Masuero, D.; Perenzoni, D.; Rigo, A.; Mattivi, F. *PLoS One* **2012**, *7*, e37783.

18. Vaclavik, L.; Lacina, O.; Hajslova, J.; Zweigenbaum, J. *Anal. Chim. Acta* **2011**, *685*, 45–51.
19. He, Y.; Harir, M.; Chen, G.; Gougeon, R. D.; Zhang, L.; Huang, X.; Schmitt-Kopplin, P. *Electrophoresis* **2014**, *35*, 1965–1975.
20. Theodoridis, G. A.; Gika, H. G.; Want, E. J.; Wilson, I. D. *Anal. Chim. Acta* **2012**, *711*, 7–16.
21. Theodoridis, G.; Gika, H.; Franceschi, P.; Caputi, L.; Arapitsas, P.; Scholz, M.; Masuero, D.; Wehrens, R.; Vrhovsek, U.; Mattivi, F. *Metabolomics* **2012**, *8*, 175–185.
22. Müller, C.; Dietz, I.; Tziotis, D.; Moritz, F.; Rupp, J.; Schmitt-Kopplin, P. *Anal. Bioanal. Chem.* **2013**, *405*, 5119–5121.
23. Chira, K.; Pacella, N.; Jourdes, M.; Teissedre, P.-L. *Food Chem.* **2011**, *126*, 1971–1977.
24. Marquez, A.; Serratosa, M. P.; Merida, J. *Food Chem.* **2014**, *146*, 507–514.
25. McRae, J. M.; Dambergs, R. G.; Kassara, S.; Parker, M.; Jeffery, D. W.; Herderich, M. J.; Smith, P. A. *J. Agric. Food Chem.* **2012**, *60*, 10093–10102.
26. Monagas, M.; Martín-Álvarez, P. J.; Bartolomé, B.; Gómez-Cordovés, C. *Eur. Food Res. Technol.* **2006**, *222*, 702–709.
27. Puškaš, V.; Miljić, U. *Food Control* **2012**, *28*, 362–367.
28. Recamales, Á. F.; Sayago, A.; González-Miret, M. L.; Hernanz, D. *Food Res. Int.* **2006**, *39*, 220–229.
29. Ugliano, M. *J. Agric. Food Chem.* **2013**, *61*, 6125–6136.
30. Tziotis, D.; N, H.; P, S.-K. *Eur. J. Mass Spectrom.* **2010**, *17*, 415–421.
31. Roullier-Gall, C.; Boutegrabet, L.; Gougeon, R. D.; Schmitt-Kopplin, P. *Food Chem.* **2014**, *152*, 100–107.
32. Hertkorn, N.; Frommberger, M.; Witt, M.; Koch, B. P.; Schmitt-Kopplin, P.; Perdue, E. M. *Anal. Chem.* **2008**, *80*, 8908–8919.
33. Roullier-Gall, C.; Lucio, M.; Noret, L.; Schmitt-Kopplin, P.; Gougeon, R. D. *PLoS One* **2014**, *9*, e97615.
34. Brown, S. C.; Kruppa, G.; Dasseux, J.-L. *Mass Spectrom. Rev.* **2005**, *24*, 223–231.
35. Dugo, G.; Salvo, F.; Bambara, G.; Picciolo, F.; Mondello, L.; Dugo, P. *Vignevini* **2000**, 120–124.
36. Suhre, K.; Schmitt-Kopplin, P. *Nucleic Acids Res.* **2008**, *36*, 481–484.
37. Wägele, B.; Witting, M.; Schmitt-Kopplin, P.; Suhre, K. *PLoS One* **2012**, *7*, e39860.
38. Kanehisa, M.; Goto, S.; Sato, Y.; Furumichi, M.; Tanabe, M. *Nucleic Acids Res.* **2011**, *40*, 109–114.
39. Wishart, D. S.; Jewison, T.; Guo, A. C.; Wilson, M.; Knox, C.; Liu, Y.; Djoumbou, Y.; Mandal, R.; Aziat, F.; Dong, E.; Bouatra, S.; Sinelnikov, I.; Arndt, D.; Xia, J.; Liu, P.; Yallou, F.; Bjorndahl, T.; Perez-Pineiro, R.; Eisner, R.; Allen, F.; Neveu, V.; Greiner, R.; Scalbert, A. *Nucleic Acids Res.* **2012**, *41*, 801–807.

Publication Date (Web): November 24, 2015 | doi: 10.1021/bk-2015-1203.ch002

Publication Date (Web): November 24, 2015 | doi: 10.1021/bk-2015-1203.ch003

Chapter 3

Influence of Storage Conditions on the Composition of Red Wines

Fulvio Mattivi,[*,1] Panagiotis Arapitsas,[1] Daniele Perenzoni,[1] and Graziano Guella[2]

[1]Department of Food Quality and Nutrition, Research and Innovation Centre, Fondazione Edmund Mach, via E. Mach 1, San Michele all'Adige, Italy
[2]Department of Physics, University of Trento, Via Sommarive 14, Povo, Italy
[*]E-mail: fulvio.mattivi@fmach.it.

Knowledge of the influence of temperature on the chemical composition of red wines should be useful, given that inappropriate storage is likely to shorten shelf life while decreasing wine quality. Putative markers of ageing for red wines stored for two years at two different storage temperatures (cellar vs. domestic) were investigated using MS-based untargeted metabolomics, and further confirmed by additional metabolite profiling. Of the 10k features extracted from the metabolomic dataset, those significant in terms of their ability to distinguish between the two storage conditions were mostly pigments and other phenolics, several of which were annotated with 1st level identification. Tentative identification of the remaining chromatographic peaks was made by using spectral features, literature information about chromatographic properties and mass spectra records from databases and an internal database for the wine metabolome based on the bibliography. The results of multivariate analysis clearly showed that wines stored in the cellar changed little even after two years of storage, while wines stored in typical domestic conditions developed approximately 3-4 times faster. Ageing

In Advances in Wine Research; Ebeler, et al.;
ACS Symposium Series; American Chemical Society: Washington, DC, 2015.

in domestic conditions appeared to induce an accelerated decrease in native anthocyanins, while specifically promoting the formation of pinotin A-like pigments. Interestingly, we observed a temperature-dependent pathway involving the addition of bisulfite to the flavanols and leading to the formation of several catechin and proanthocyanidin sulfonates, along with hydrolysis reactions involving various phenolics, including flavonols. The temperature-dependent sulfonation process of flavanols was reproduced in a model wine system, making it possible to isolate the main reaction products. Two main metabolites were structurally elucidated using NMR measurements and confirmed to correspond to the products found in wines aged in domestic conditions. Epicatechin 4β-sulfonate and procyanidin B2 4β-sulfonate are suggested as promising markers present in wines stored at elevated temperature.

Publication Date (Web): November 24, 2015 | doi: 10.1021/bk-2015-1203.ch003

Introduction

The quality of any wine produced by a winery should fulfil certain legal requirements and comply with winemakers' standards. From the winery to the consumer many factors can influence wine quality, especially storage conditions and duration. Exposure to high temperature during transport is not uncommon, damaging the quality of wine, given that wines are distributed from the production area to destinations all over the world (*1*). Heat shock can last up to several days when wines are distributed via unrefrigerated trucks in warm weather, and even weeks when wines are transported by ship across the equator. Billions of bottles are indeed sent between the Southern and Northern Hemispheres every year. It has been observed that most wines are shipped in worse conditions than a pint of ice cream or a head of lettuce, for various reasons including producers', shippers' and consumers' ignorance of the issue (*1*). This is, incidentally, a long-standing issue, considering that the depreciation of wine during transport from France to England led Louis Pasteur to carry out investigations for several years, resulting in the discovery of some of the most severe cases of microbial wine instability (*2*).

Once wines reach their final destination, they are expected to have a different shelf life. Cheap wines are usually consumed within a short time, while premium quality wines are expected to last and even improve with age, and are frequently stored for up to several years. Consumers consider ageing as a positive characteristic for wine, and not without reason. Many high quality red wines are aggressive and difficult to drink when young, but with ageing their quality improves, meaning that consumers prefer them and pay more to purchase them. Unfortunately, ageing is not a one-way route for high quality wines. Optimum temperature and humidity conditions may improve wine quality through ageing, while incorrect or excessively long storage leads to negative results. The metabolic changes which improve wine quality are slow, and accelerated ageing

does not lead to the same positive results. High temperatures,which increase the rate of chemical processes, can facilitate and accelerate unwanted reactions thus leading to a decay of the wine sensorial quality.

During wine tasting, the oenologist analyses each sample holistically without focusing on only one specific characteristic. This unconventional 'analytical method' is fast, practical and functional, but not so robust, difficult to generalise and requires extensive experience. On the basis of wine tasting it is widely accepted that fine wines are at risk of depreciation during prolonged storage at elevated temperatures. Nevertheless, there is a limited knowledge about which temperature-induced chemical changes are produced during prolonged storage. It is expected that improved mechanistic knowledge of this process would provide essential information to wine producers, wine professionals and consumers, leading to better awareness.

Targeted analytical methods have helped to tackle this problem by providing selectivity, sensitivity, robustness, velocity and a common language, but they lack the holistic view. Chemists use many different analytical methods to cover a small part of the metabolic space of a sample. According to some calculations, the plant metabolome is estimated to cover 200K metabolites, most of them unknown. Wine is definitely one of the most complex foods as far as the metabolomic profile is concerned, since grapes, yeasts, bacteria, fungi, exogenous antioxidants, fining agents and other oenological materials and ageing are involved in its preparation. Over the last few years, with the advent of untargeted techniques, analytical chemists have tried to approach various biological and chemical studies in a holistic manner.

Untargeted metabolomics deals with the study of changes in the metabolic content (organic molecules with a molecular mass smaller than 2000 Daltons) of a biological sample in response to a stimulus or modification. The idea works and offers very interesting results, mainly in the medical and pharmaceutical sectors but less commonly in food research, since it is an expensive technique and requires the collaboration of scientists from different fields.

In the last few years, different metabolomics approaches have also appeared in literature focusing on wine, providing interesting information about various oenological issues and offering new hypotheses for further experiments (*3–11*).

In general, analytical chemistry studies dealing with wine storage use targeted methods for the analysis of volatiles, amino acids, amines, organic acids and phenolics. Most of these studies were carried out using accelerated storage conditions and for short time periods, trying to predict the results of real storage conditions (*12–24*).

The object of this study was to evaluate the effect of storage on 20 red wines, comparing optimum storage with typical domestic conditions for a period of 24 months. With the further scope of obtaining the clearest possible chemical image of the non-volatile fraction and finding new tentative markers for sub-optimal storage, untargeted metabolomics was used as the key analytical approach.

Publication Date (Web): November 24, 2015 | doi: 10.1021/bk-2015-1203.ch003

Materials and Methods

Wine Storage Experiment

Experimental Design

The wine storage project focused on the analysis of 400 bottles of 20 different red Sangiovese wines. The bottles of each wine were divided and stored for 24 months in the following conditions: a) half were stored in optimum storage conditions 15–17 °C (59-63°F), 70% humidity, horizontally and inside wine boxes, while the other half b) were stored in such a way as to mimic typical modern apartment storage, with a temperature of 20–27 °C (68-81°F), fluctuating with the seasons, and variable humidity during the year, away from any heating systems or bad smells, horizontally and inside boxes. Every 6 months 2 bottles from each wine/storage system were sampled up to the 24 month time point (*3*).

Publication Date (Web): November 24, 2015 | doi: 10.1021/bk-2015-1203.ch003

LC-MS Analysis

Sample preparation and UPLC-QTOF MS untargeted analysis were performed within two months of the end of the ageing experiment and during this period the wines were kept at 4 °C to slow down possible reactions. Wines were uncorked under nitrogen atmosphere and an aliquot was transferred into a 15 mL amber vial (filled to capacity). 1 mL of each wine was then diluted with 1 mL Milli-Q water (1:1 dilution) and 20 µL of the internal standard mix was then added. Finally, each sample was filtrated with 0.2 µm PTFE filters into a 2 mL amber vial (MS certificated) prior to LC/MS analysis. The internal standard mix was 10 mg 3-indol propionic acid and 17 mg 2,6-dihydroxy benzoic acid in 10 mL of MeOH:H_2O (1:1) (*3*).

A Waters Acquity UPLC was used, coupled via an electrospray ionization (ESI) interface to a Synapt HDMS QTOF MS (Waters, Manchester, U.K.) operating in W-mode and controlled by MassLynx 4.1. All samples were analyzed on a reversed phase (RP) ACQUITY UPLC 1.8 µm 2.1 x 150 mm HSS T3 column (Waters) protected with an Acquity UPLC® BEH HSS T3 1.8 µm, 2.1 x 5 mm precolumn (Waters), at 40 °C and under a mobile phase flow rate of 0.28 mL/min. Water was used as weak eluting solvent (A) and methanol as strong eluting solvent (B); formic acid 0.1% v/v was used as the additive in both eluents. The multistep linear gradient used was as follows: 0-1 min, 100% A isocratic; 1-3 min, 100-90% A; 3-18 min, 90-60 % A; 18-21 min, 60-0% A; 21-25.5 min, 0% A isocratic; 25.5-25.6 min, 0-100% A; 25.6-28 min 100% isocratic. Injection volume was 10 µL, unless otherwise stated, and the samples were kept at 4 ºC throughout the analysis. Mass spectrometric data were collected by separate runs in positive and negative ESI mode over a mass range of 50 to 2000 amu, with scan duration of 0.3 s in centroid mode. The transfer collision energy and trap collision energy were set at 6 V and 4 V. The source parameters were set as follows:

capillary 3 kV for positive scan and 2.5 kV for negative scan, sampling cone 25 V, extraction cone 3V, source temperature 150 ºC, desolvation temperature 500 ºC, desolvation gas flow 1000 L/h and nebulizer gas 50 L/h. External calibration of the instrument was performed at the beginning of each batch of analysis by direct infusion of a sodium formate solution (10% formic acid/0.1 M NaOH/Acetonitrile at a ratio of 1/1/8), controlling the mass accuracy from 40 to 2000 *m/z* (less than 5 ppm) and mass resolution (over 14000 FWHM). LockMass calibration was applied using a solution of leucine encephalin (0.5 mg/L, *m/z* 556.2771 for positive and 554.2620 for negative ion mode) at 0.1 mL/min[3].

Publication Date (Web): November 24, 2015 | doi: 10.1021/bk-2015-1203.ch003

Tannins Reaction with Bisulfite

Reactions

60 g of a commercial apple tannin with title in polyphenols 75% (PFANNEN SCHMIDT, Hamburg, Germany. Art-Nr: 11278112; Batch: 1005013-21) and 20 g of $Na_2S_2O_5$ were dissolved in 6 L of a model wine solution (10% ethanol, 5 g of tartaric acid, pH 3.6) and then divided in 250 ml dark glass bottles: a) 2 bottles were stored at 20 °C, b) 10 bottles at 40 °C and c) 10 bottles at 60 °C. After 22, 27, 35, 43, 51, 63, 95 and 182 days, 1 mL of each reaction was sampled, diluted with water (1/10) and analyzed using LC-MS/MS. Assuming an average molecular weight of 290 g/mol and taking into account the titles, the SO_2 was in slight molar excess, (ca. 1.25). The concentration of the compounds of interest in the apple extract were 12 mg/g of catechin, 29 mg/g of epicatechin, 53 mg/g of type B procyanidins (evaluated by UHPLC-MS/MS) plus ca. 600 mg/g of oligomeric procyanidins (evaluated by phloroglucinolysis).

LC-MS Analysis

All LC–MS/MS analyses were performed with an ACQUITY Ultra Performance Liquid Chromatographic System (Waters, MA, U.S.A.) coupled to a Xevo TQ MS System (Waters, U.K.) operating using MassLynxTM Software. The column was an Acquity UPLC HSS T3 1.7 µm, 2.1 x 150 mm column (Waters) and pure commercial compounds or the pure standard isolated in this experiment were used for quantification, with the external standard method. The injection volume was 2 µL. For the TQMS, capillary voltage was 3.5 kV in positive mode and −2.5 kV in negative mode; the source was kept at 150 °C; desolvation temperature was 500 °C; cone gas flow, 50 L/h; and desolvation gas flow, 800 L/h. Unit resolution was applied to each quadrupole. The detailed LC-MS parameters for the commercial chemical references are reported in Ehrhardt et al.; the sulfonated derivatives were analyzed under selected ion monitoring (SIM) ESI- scanning mode (*25*). The retention times of the sulfonated epicatechin **3** (SIR 369 *m/z*), the open sulfonated forms **1**-**2** (SIR 371 *m/z*) and sulfonated procyanidin B2 **4** (SIR 371 *m/z*) were 1.74, 2.19 and 2.17 min respectively (Figures 1 and 2).

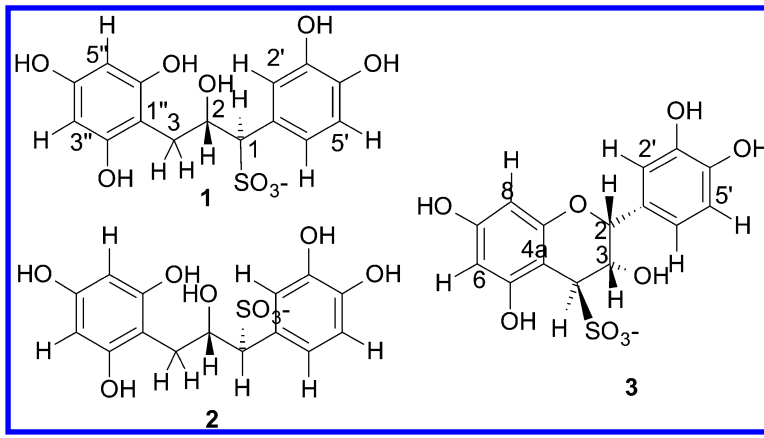

*Figure 1. Structures of the open sulfonated flavanols **1-2** and sulfonated epicatechin **3**.*

Sulfonated Flavanols Isolation

Isolation of sulfonated epicatechin and sulfonated procyanidin B was achieved with a Waters 2695 HPLC equipped with a Waters 996 DAD detector (Waters Corp., Milford, MA, U.S.A.). The column used was Supelco Discovery C18, 5 μm, 4.6 × 250 mm, the flow rate was 1.5 mL/min, the eluents were water (A) and methanol (B), the injection volume was 20 μL, and the column oven temperature was 40 °C. The gradient was isocratic (100% A) for the first 6 min, from 6 to 11 min isocratic with 100% B, and finally isocratic again with 100% A from 11 to 16 min. Automatic fractionation was carried out using a Fraction Collector III (Waters).

With this set up, two major peaks were isolated and later categorised as epicatechin 4β-sulfonate **3** and procyanidin B2 4β-sulfonate **4** (Figures 1 and 2). A similar procedure was used for the isolation of the open structures produced by monomeric flavanols at high temperature (90 °C). The purity of each isolated standard was established by ^{1}H-NMR.

For the calculation the average experimental molar absorptivity (ε) of each pure sulfonated compound, two methanolic solutions were prepared, one twice the other, ca. 25 and 50 mg/L, to obtain an absorbance value in the range of 0.3-0.7 UA. The spectral characteristics of the known solutions were recorded on a Hitachi U-2000 UV−vis spectrophotometer using quartz cells with a 10 mm optical path.

Sulfonated Flavanols Identification

^{1}H (400 MHz), ^{13}C (100 MHz) and 2D-NMR spectra were recorded in CD_3COCD_3 (99.90%) or in CD_3OD (99.9%) or in D_2O (99.5%) at 300 K on a Bruker-Avance 400 MHz NMR spectrometer, by using a 5 mm BBI probe

equipped with pulsed-gradient field utility. The chemical shift scale (δ) was calibrated on the residual proton signal of deuterated acetone (δ_H 2.050 ppm and δ_C 29.80 ppm), or tetradeuterated methanol (δ_H 3.310 ppm and δ_C 49.00 ppm) or deuterated water (δ_H 4.75 ppm). Molecular mechanics (MM) calculations were carried out using the MM2 force fields as implemented in PCMODEL 8.5 (Serena Software, Bloomington, U.S.A.). The LC-MS instrument used for the extact mass was the Synapt HDMS QTOF MS (Waters, Manchester, U.K.) described in the earlier section.

1-R-(3,4-dihydroxyphenyl)-2S-hydroxy-3-(2,4,6-trihydroxyphenyl)-propane-1-sulfonate (**1** in Figure 1):

This was by far the most significant product of the reaction performed either in methanol or in the model wine at 90 °C.

^{1}H-NMR (D_2O, 300K): 6.89 (d, J=1.5, H-2′); 6.83 (dd, 8.1Hz, H-5′); 6.79 (brd, J=8.1 Hz, H5′); 5.94 (s, H-3″ and H-5″); 4.64 (ddd, 4.4, 8.8, 9.5 Hz, H-2); 3.94 (d, 9.5 Hz, H-1); 2.56 (dd, J 4.4, 14.8, Ha-C(3)); 2.61 (dd, J 8.8, 14.8, Hb-C(3)).

^{13}C-NMR (CD_3OD, 300 K): 156.6 (C-2″ and C-6″); 155.8 (C-4″); 144.5 (C-3′ or C-4′); 144.1 (C-4′ or C-3′); 127.2 (C-1′); 123.1 (C-6′), 117.8 (C-5′); 116.4 (C-2′); 105.2 (C-1″); 95.9 (C-3″ and C-5″); 72.0 (C-2); 71.3 (C-1); 29.9 (C-3).

HRMS (ESI) calcd for $C_{15}H_{16}O_9S$ $[M–H]^-$ 371.0442, found 371.0435.

1-S-(3,4-dihydroxyphenyl)-2S-hydroxy-3-(2,4,6-trihydroxyphenyl)-propane-1-sulfonate (**2** in Figure 1):

This was a minor product of the reaction performed either in methanol or in the model wine at 90 °C.

Only signals different to those attributed to the main epimer are reported here.

^{1}H-NMR (D_2O, 300K): 7.09 (d, J=1.5, H-2′); 6.93 (d, J=8.5, H6′); 6.87 (brd, J=8.5, H5′); 6.01 (s, H-3 and H-5); 4.31 (br s, H-1); 2.80 (dd, J 5.5, 14.3, Ha-C(3)); 2.62 (dd, J =7.2, 14.3, Hb-C(3)).

HRMS (ESI) calcd for $C_{15}H_{16}O_9S$ $[M–H]^-$ 371.0442, found 371.0435.

Epicatechin-4β-sulfonate (**3** in Figure 1)

^{1}H-NMR (CD_3COCD_3, 300K): 7.04 (d, J=1.9, 1H, H-2’); 6.89 (dd, J=1.9,8.1Hz, 1H, H-6′); 6.77 (d, J=8.1 Hz, 1H, H5′); 5.98 (m. 2H, H-6+H-8); 5.48 (br s, W1/2 =3 Hz, 1H, H-2); 4.54 (br s, W1/2 =4.5 Hz, 1H, H-3); 4.03 (br s, W1/2 =3Hz, 1H, H-4).

^{1}H-NMR (CD_3OD, 300K): 7.02 (brs, 1H, H-2′); 6.87 (brd, J=8.1Hz, 1H, H-6′); 6.80 (d, J=8.1 Hz, 1H, H5′); 6.05 (m. 2H, H-6+H-8); 5.45 (br s, W1/2 =3.5 Hz, 1H, H-2); 4.54 (br s, W1/2 =4.3 Hz, 1H, H-3); 4.17 (br s, W1/2 =4.0 Hz, 1H, H-4).

^{13}C-NMR (CD_3OD, 300 K): 159.5 (C-8a); 159.0 (C-5 or C-7); 157.9 (C-7 or C-5); 145.7 (C-3′ + C-4′); 145.6 (C-4′ or C-3′); 131.8 (C-1′); 119.5 (C-6′); 116.0 (C-5′); 115.4 (C-2′); 97.7 (C-4a); 97.4 (C-6 or C-8); 97.3 (C-8 or C-6), 76.4 (C-2); 67.4 (C-3); 61.4 (C-4).

HRMS (ESI) calcd for $C_{15}H_{14}O_9S$ $[M–H]^-$ 369.0285, found 369.0278. The experimental molar absorptivity in methanol ε was 4070 (278 nm).

In Advances in Wine Research; Ebeler, et al.;
ACS Symposium Series; American Chemical Society: Washington, DC, 2015.

Publication Date (Web): November 24, 2015 | doi: 10.1021/bk-2015-1203.ch003

Procyanidin B2-4β-sulfonate (**4** in Figure 2):

^{1}H-NMR (CD_3COCD_3, 300K, t = terminal unit) : 7.04 (brs, 2H, H-2′+H2′t); 6.84 (brd, J=8.1Hz, 2H, H-6′+H6′t); 6.79 (d, J=8.1 Hz, 2H, H5+H5′t′); 6.02 and 5.99 (m, 3H, H-6+H-8+H6t); 5.45 (br s, 1H, H-2t); 5.10 (m, 1H, H-2); 4.68 (brs, 1H, H-4), 4.53 (br s, 1H, H-3t); 4.23 (br s, 1H, H-4t); 4.01 (br s, 1H, H-3). ^{13}C-NMR (CD_3COCD_3, 300 K, t = terminal unit): 159.5-157.0 (C-5+C-5t,C-7+C-7t,C-8a+C-8at); 145.7-145.2 (C-3′+C3′t, C-4′+C-4′t); 131.7 (C-1′); 119.5-115.4 (C-2′+C-2′t, C-5′+C-5′t, C-6′+C-6′t);107.8 (C-4); 98.4-96.5 (C-4at, C-6 +C-6t, C-8+C-8t)); 76.6 (C-2); 76.4 (C-2t); 72.9 (C-3); 67.4 (C-3); 67.1 (C-3t); 62.1 (C-4t); 37.1 (C-4).

HRMS (ESI) calcd for $C_{30}H_{26}O_{15}S$ $[M–H]^-$ 657.0920, found 657.0927. The experimental molar absorptivity in methanol ε was 6732 (278 nm).

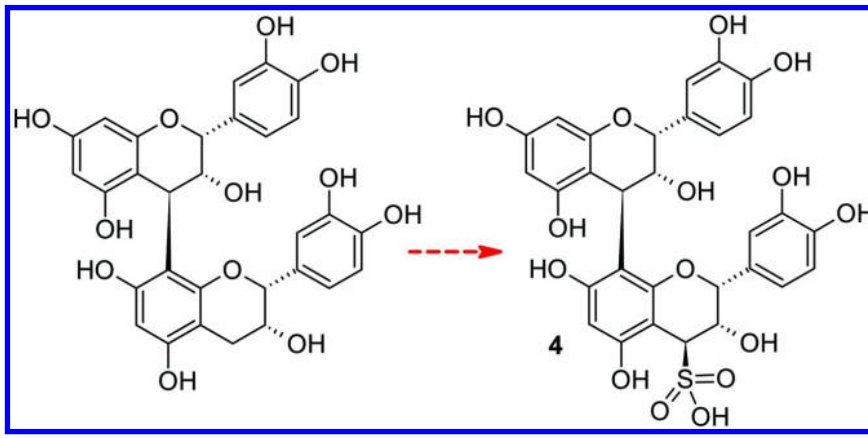

Figure 2. Sulfonation of wine procyanidins occurring in wine stored in temperatures higher than the optimum.

Publication Date (Web): November 24, 2015 | doi: 10.1021/bk-2015-1203.ch003

Wine Precipitate

Two bottles of defective Sangiovese wine of the year 2011 were provided by a commercial winery in Tuscany. The wine belonging to this lot number was considered unmarketable since after bottling it developed floating flakes in all their volume of unknown cause. Each bottle was filtrated with a 0.22 μm filter and the filtrate was dried under vacuum for 24 hours. The flakes formed were weighted, then solubilised in methanol and directly analyzed without preliminary hydrolysis (*25*). The images of the dry precipitate were obtained with a Nikon Digital Sight DS-Fi1 camera mounted on a stereomicroscope Nikon SMZ800 with zoom range from 1x to 6.3x.

Publication Date (Web): November 24, 2015 | doi: 10.1021/bk-2015-1203.ch003

Results and Discussion

Wine Storage Experiment

Metabolomics follows a similar workflow to targeted analysis, but is definitely more complicated. In Figure 3 we try to show a simplified workflow for a metabolomics experiment. In metabolomics method development is usually minimal and requires little time; method validation does not typically take place, but the data analysis step requires a very long time (several months if not a few years). In contrast, in targeted analysis method development and validation are very important steps and typically need long investigation periods, while data analysis is definitely much faster. Other essential steps requiring attention in metabolomics are experimental design, the various quality controls (during and after analysis) and marker discovery, identification and validation (which are part of the data analysis step). Since a metabolomics sequence can last from days to weeks, the first quality control (Figure 3) step is fast, but essential to evaluate instrument performance during the analysis, the second is more detailed and carried out at the end of analysis to ensure the quality of the dataset, while the last focuses more on tentative bio-markers in order to avoid false positives (Figure 3). For example, a fast and visual evaluation of the data quality is the strong clustering of the QC (a pooled sample) injections in the PCA plot (Figure 4). The last step, hypothesis validation, refers to additional analysis that could be carried out with a targeted method for the measurement of a specific tentative marker or group of tentatives markers, or using a different sample set analyzed with the same untargeted method.

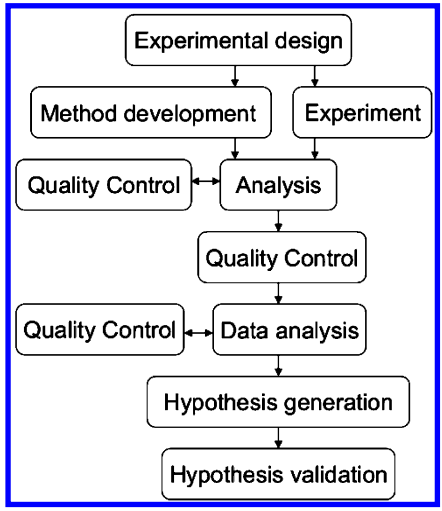

Figure 3. General metabolomics workflow.

Publication Date (Web): November 24, 2015 | doi: 10.1021/bk-2015-1203.ch003

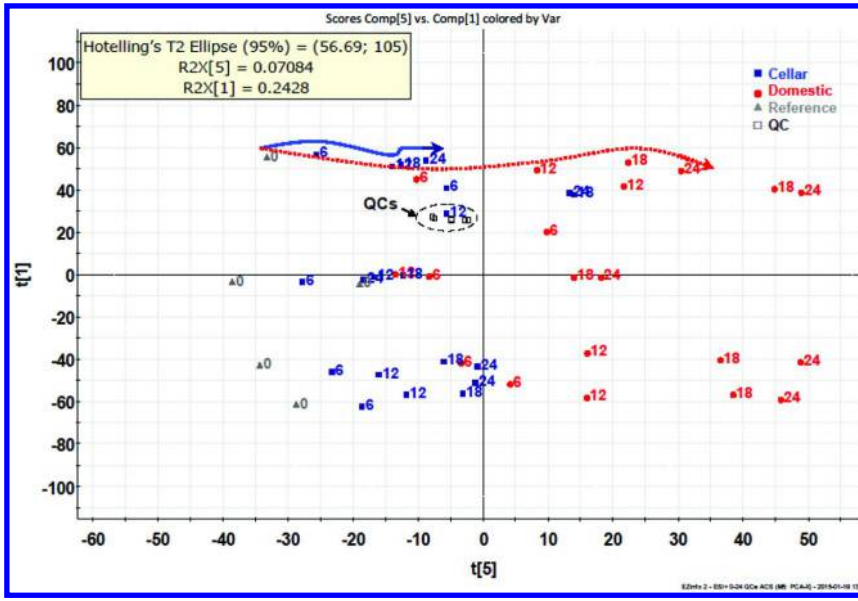

Figure 4. PCA plot of the LC-MS in ESI+ experiment, comparing the evolution of 5 different red wines stored under cellar and domestic conditions for 24 months. The numbers indicate the storage duration in months. In the upper part are shown the trajectories indicating how the metabolic fingerprint of one of the wines was changing under the two conditions from time zero to 24 months. It is apparent that the direction of the change is the same for all wines (from left to right) and that the distance from the reference increases greatly under domestic conditions.

Researchers in metabolomics are used to working with a large amount of data. A typical LC-MS dataset can easily have 2-20K variables, the so-called features which are molecular entities with a unique *m/z* and retention time. Each metabolite can have more than one feature, such as isotopes, adducts or fragments. Most of the time, only a small number of these features make a significant difference in a metabolomics experiment and supervised multivariate statistical analysis is often applied to find significant differences, while unsupervised PCA plots are used mainly to judge the quality of the data. We observed (data not shown) that most of these features were not affected during this storage experiment. Wine is after all considered to be a stable commodity, and this relative stability was expected. However, hundreds of the measured compositional features still showed variations during storage. Despite the high number of features (~10.000) (*3*) and the biological variability, from the PCA plot (Figure 4) it was already possible to arrive at some considerations, not only as regards the quality of the data but also about the effect of storage on different wines. The wine samples all develop in the same direction, suggesting that most of the reactions are qualitatively much the same for the different lots of wine and different storage conditions. However, the path clearly has a different length. The metabolic profile of bottles of wine stored under optimum conditions remained more stable as compared to samples

Publication Date (Web): November 24, 2015 | doi: 10.1021/bk-2015-1203.ch003

stored in domestic conditions. This is not surprising given that these condition were within the range suggested by HKQAA certification for optimal storage of fine wines (*26*). Wines stored for 6 months in optimal conditions had a metabolic fingerprint similar to wines stored in domestic conditions for 18/24 months, so we can observe that the average speed of the overall metabolic changes was much faster in domestic conditions. It is worth emphasising that such a big difference was not observed by comparing optimum conditions with extreme or accelerated conditions, but rather with domestic storage parameters which could be perceived as a viable possibility. In detail, in domestic conditions wines were kept in amber glass bottles, horizontally, in the dark, away from any heating systems or bad smells, at a temperature varying over the seasons and typical for human wellbeing (*3*). It can be assumed that the parameters chosen were both realistic and common since most consumers live in houses without an underground cellar or any specialised climate-controlled environment, such as a wine-fridge.

The situation is not expected to be any better also in several professional conditions, if we consider that HKQAA certification for commercial wine storage (*26*) can be awarded for storage temperature of 22 °C with allowed a daily and annual fluctuation range of, respectively, 5 and 10% (*27*). These conditions nicely overlap with the domestic conditions in our experiment.

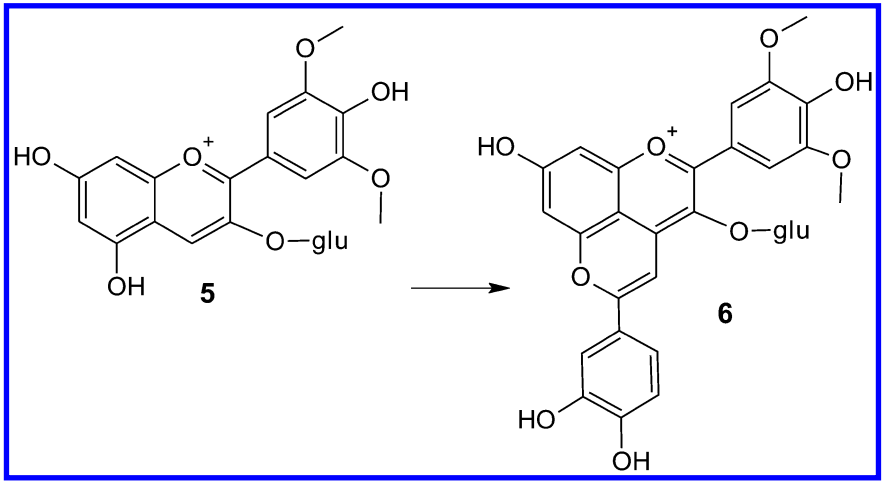

*Figure 5. Typical domestic conditions of wine storage favored the production of vinylphenol-pyranoanthocyanins (e.g. Pinotin A **6**) from the grape anthocyanins (e.g. malvidin 3-glucoside **5**).*

The first practical indication which can be deduced from this figure is that the "chemical age" of a red wine stored in domestic conditions could differ from the age written on the label of the bottle: home storage leads to a sort of unwanted "accelerated ageing".

The experiment started in spring 2010 and finished in spring 2012, so the 12th and 24th month sampling points were after a winter period, whereas the 6th and 18th month sampling points were after a summer period. In Figure 2 it is also

possible to see the result of this fluctuation, showing how the summer/hot period increases the distance between domestic sampling conditions by accelerating metabolic profile changes.

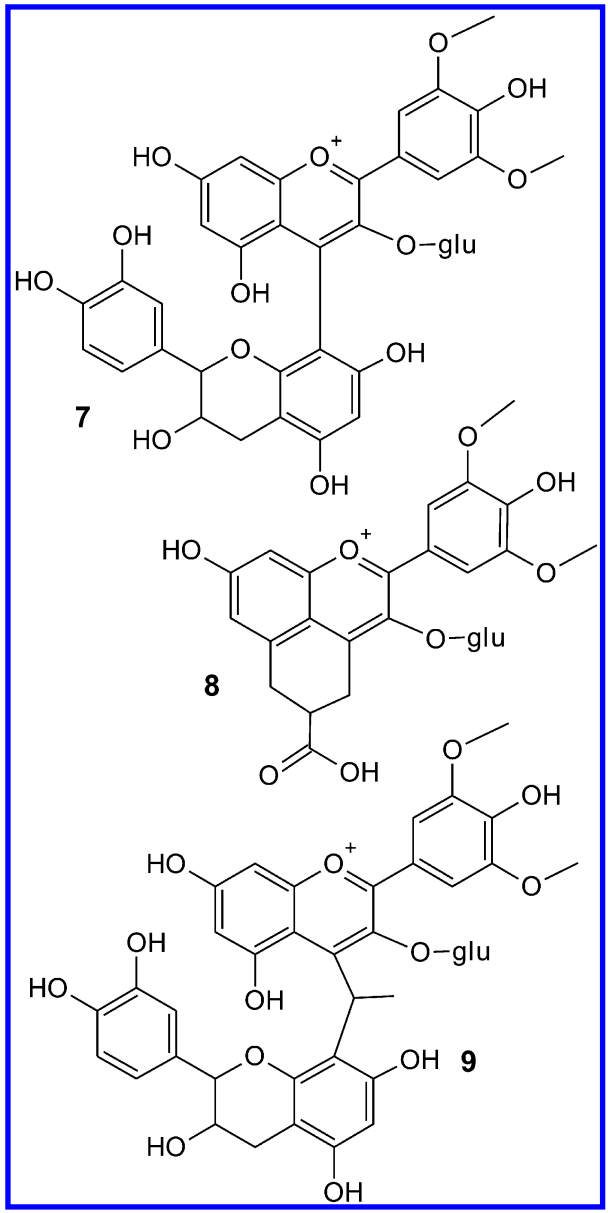

*Figure 6. Pigments (directed linked flavanol-anthocyanins **7**, pyranoanthocyanins **8** and ethyl bridge flavanol-anthocyanins **9**) which formation was favored by the optimum wine storage.*

In Advances in Wine Research; Ebeler, et al.;
ACS Symposium Series; American Chemical Society: Washington, DC, 2015.

Publication Date (Web): November 24, 2015 | doi: 10.1021/bk-2015-1203.ch003

Publication Date (Web): November 24, 2015 | doi: 10.1021/bk-2015-1203.ch003

Supervised multivariate analysis in both the ESI- and ESI+ LC-MS experiments, showed various metabolites with a significant concentration difference between the two storage conditions (*3*). The significance of these tentative markers for red wine storage increased over time, as can already be seen in the PCA plot of Figure 4. As expected, a group of markers for this experiment (which we suggest as tentative markers for high temperature wine storage), was the group of pigments. Grape pigments (i.e. glucosides of malvidin, peonidin, petunidin, cyanidin and delphinidin and their corresponding acetyl, p-coumaroyl and caffeoyl esters) decreased much faster in domestic conditions, while the group of vinylphenol-pyranoanthocyanins (e.g. pinotin A **6** in Figure 5) were the only pigments showing a positive correlation with domestic storage over time, since their concentration increased much faster in domestic conditions (*3*). Vinylphenol-pyranoanthocyanins are known for their orange colour (*28*), whereas red pigments formed during wine ageing, such as pyranoanthocyanins and flavanol-anthocyanins (Figure 6), had a higher concentration in the wines stored in optimum conditions. As a result, the wines stored in the cellar maintained their red colour, an important quality parameter, while the home-stored wines shifted from red towards orange tones, which are a negative characteristic associated with the browning of red wines (*3*). This is not the first time that vinylphenol-pyranoanthocyanins have been correlated with the length of ageing and oxygen management enological practices (*4*, *29–32*).

The second group of tentative markers for wine storage was made up of various hydrolysis products of phenolic metabolites (*3*). Prolonged and sub-optimal wine storage induced substantial hydrolysis of flavonols from their glucosides, and hydroxycinnamic acids from their tartaric acid esters (Figure 7).

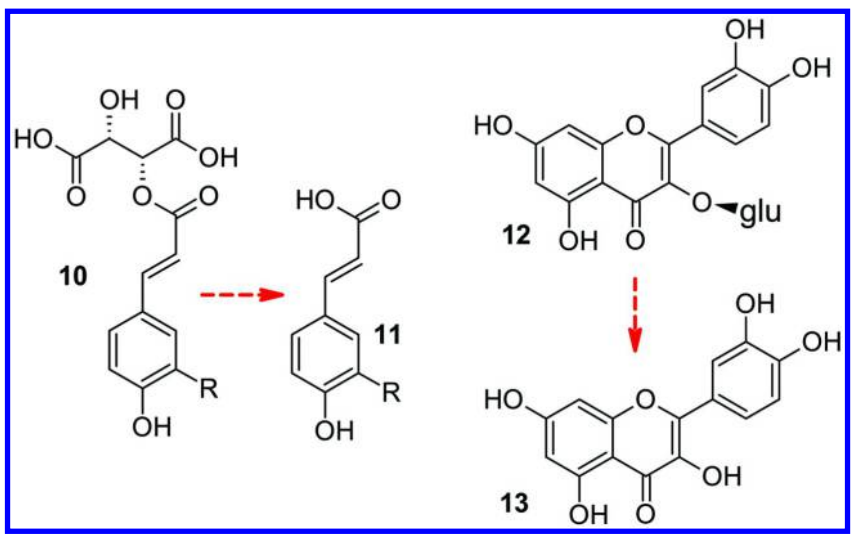

*Figure 7. Two major hydrolysis reaction favored by the domestic storage conditions. The first one refers to the hydrolysis of hydroxycinnamic acid esters with tartaric acid (**10** to **11**); and the second to the hydrolysis of glycosidic flavonoids to their aglycons (**12** to **13**).*

In Advances in Wine Research; Ebeler, et al.;
ACS Symposium Series; American Chemical Society: Washington, DC, 2015.

Publication Date (Web): November 24, 2015 | doi: 10.1021/bk-2015-1203.ch003

The increase in free flavonols during the storage of Sangiovese wines should be considered as a serious negative trait, given that the formation of precipitates rich in quercetin during the storage of Sangiovese wines in the bottle is reported relatively frequently by producers. These unwanted, floating precipitates, to date not described in the literature, are a serious concern for producers, since their formation makes the wine unmarketable (Figure 8). In defective wine we observed that the flakes, shown in Figure 8, consisted mainly of quercetin (c. 57% of dry weight) and also contained other flavonols (kaempferol, myricetin and isorhamnetin) in minor amounts. No evidences that this precipitate could be associated with any metal were found. So probably these disk-shaped, floating flakes appear to be mainly made up of flavonol aglycones, compounds naturally present in wine but at insufficient concentrations to adversely affect it, which could cause wine defects in the case of an excessive concentration. This could be the case with quercetin, which as we observed increased its concentration in wine by >300% during the 24 months of storage, with a faster trend in wines stored in domestic conditions (*3*).

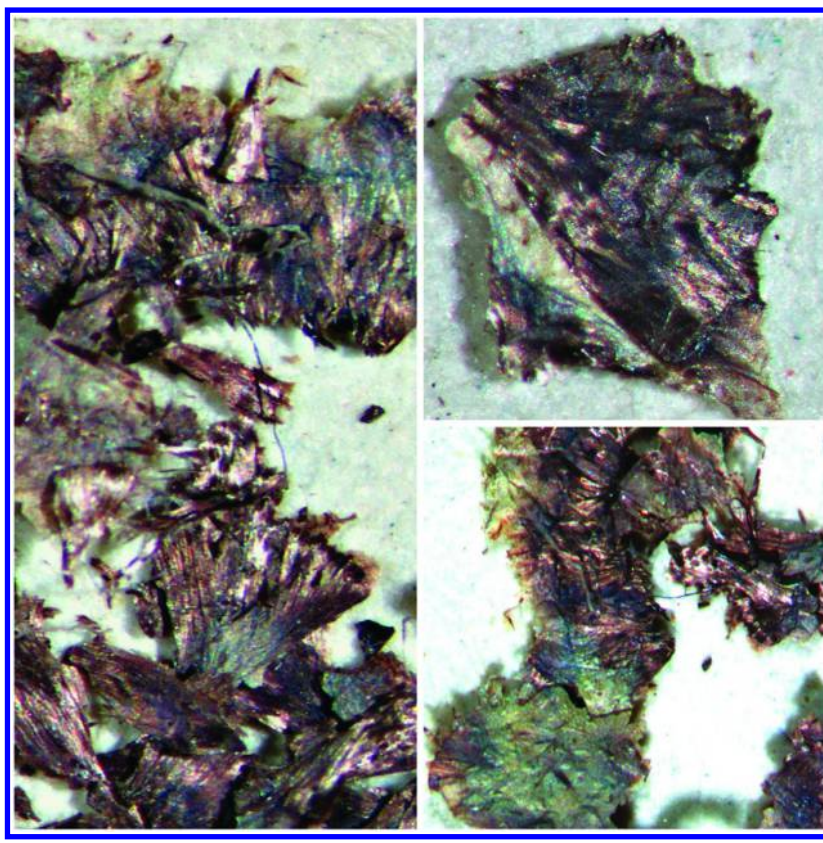

Figure 8. Floating flakes isolated from a Sangiovese wine, and consisted mainly of quercetin and other flavonols in minor amounts. (see color insert)

In Advances in Wine Research; Ebeler, et al.;
ACS Symposium Series; American Chemical Society: Washington, DC, 2015.

A third group of markers was made up of flavanols. The concentration of dimeric B type procyanidins was more stable in cellar conditions, while their sulfonated derivatives were strong markers in our study, positively correlated with domestic storage (Figure 2). This is the first experiment in which sulfonate flavanols have been reported in wine, pointing out the power of untargeted metabolomics, capable of measuring the presence of unexpected compounds. According to the literature, since these metabolites are not commercially available, sulfonation could occur at C-6′ of the B-ring or at C-4′ of the C-ring of the flavanic (*33*, *34*),. In order to identify the structure of these high temperature storage markers, we tried to reproduce the sulfonation reaction in the laboratory.

Publication Date (Web): November 24, 2015 | doi: 10.1021/bk-2015-1203.ch003

Tannins Reaction with Bisulfite

*1-(3,4-Dihydroxyphenyl)-2-hydroxy-3-(2,4,6-trihydroxyphenyl)-propane-1-sulfonates (**1 and 2**)*

Preliminary synthesis starting from pure monomeric flavanols either in methanol or in model wine, under reflux and at 90 °C for 24 hours, under molar ratio 1:1, resulted in a single main peak in reversed-phase chromatography from both epicatechin and catechin, which was easily isolated using preparative chromatography. In particular, the NMR spectra of the peak obtained by sulfonation of catechin showed the presence of two distinct sets of signals in a molar ratio of 5:1. Both compounds showed that the aromatic carbon atoms and corresponding protons at C(6) and C(8) on ring A gave single NMR resonances (δ_H 5.94 ppm and δ_C 95.9 ppm for 1R,2S whilst δ_H ppm for the 1S, 2R epimer), thus indicating their symmetrical relationship as compared to the alkyl-chain at C4a; this implies that we are dealing with structures where the pyran C cycle is open, affording 1-(3,4-dihydroxyphenyl)-2-hydroxy-3-(2,4,6-trihydroxyphenyl)-propane-1-sulfonates. This skeleton was also confirmed by long range ^{1}H-^{13}C NMR spectra. Since racemization at C-2(worth of note this is C-3 in the catechin numbering system) can be ruled out in the mild working conditions of our sulfonation process, and the coupling pattern of NMR proton resonance on ring B is conserved, we can safely conclude that the two sets of resonances should belong to the expected C(1) epimers, due to sulfite attack on the opposite side. According to our MM calculations, carried out on 1R,2S (compound **1** in Figure 1) and 1S,2R (compound **2** in Figure 1) epimeric sulfonates, in the most stable conformation of the 1R,2S epimer, H-1 and H-2 have an almost *trans*-relationship, whilst in the minimum conformation of the 1S,2S epimer these protons have a *gauche*-relationship. In both cases, these conformations were found to be significantly more stable than other conformers deriving from rotations around C(1)-C(2)-C(3) single bonds. These conformational preferences are imposed by the need to maintain an overall *trans*-relationship in the C(1′)-C(1)-C(2)-C(3)-C(1″) propane-diaryl system. Since the vicinal coupling constant J(1,2) was found to be 9.4 Hz in the main epimer, the average H(1)-H(2) torsional angle can be expected to be almost 180°, in agreement with 1R, 2S absolute stereochemistry. On the other hand, the signal attributable to

H-C(1) in the 1S,2R stereoisomer was found to be a broad singlet at δ_H 4.31 ppm, thus suggesting that the average H(1)-H(2) torsional angle can be expected to be around 90°, in turn in agreement with the extensive prevalence of *gauche* rotamers. These structures are produced by opening the pyran C ring of catechins and sulfonation at C-2, as already discussed by Foo et al. (*35*) No trace of the compounds **1** and **2** were found in our wine samples, leading to the conclusion that this is not the sulfonation mechanism relevant for wine storage. We therefore decided to reproduce the reaction in the temperature range relevant for wine storage.

Publication Date (Web): November 24, 2015 | doi: 10.1021/bk-2015-1203.ch003

*Epicatechin-4β-sulfonate (**3**) and Procyanidin B2-4β-sulfonate (**4**)*

In a successful experiment described in this study, the slow reaction of a mixture of monomeric and polymeric apple flavanols with sulfonic acid and temperature in the range 20- 60 °C proved that the reaction is favoured by temperature and takes place in the C ring, specifically at the C-4 position of the epicatechin flavanic structure. Two peaks, corresponding to the mono-sulfonated epicatechin (**3** in Figure 1) and the main epicatechin-dimer sulfonated **4**, were purified and subjected to NMR characterisation.

The ^{1}H-NMR spectrum of our epicatechin-sulfonate showed that the $-SO_3H$ group should be attached to C-4, since the diastereotopics protons at δ_H around 2.8 ppm (2H-C4) were lacking and substituted by a broad singlet signal at δ_H 4.03 in acetone d_6 (δ_H 4.18 in CD_3OD). HSQC and HMBC-measurements and reference to literature data (*35*) allowed us to firmly establish that this sulfonyl group was attached to C-4. Finally, molecular mechanics calculations indicated that only a *cis-trans* relationship between substituents at C(2)-C(3)-C(4) was compatible with the J coupling patterns of the corresponding protons linked to these Carbon atoms. As further support, only a β-substituent at C(4) would be able to impose a strong shielding γ-gauche effect (about 5 ppm) on the C(2) of epicatechin (δ_C of C-2 is in fact 81.1 ppm with respect to δ_C 76.4 ppm in **3**) .

It is interesting to observe that while both epicatechin and catechin were present in the apple extract, in a molar ratio of c. 4:1, both of which were expected to react with bisulfite, only the product corresponding to epicatechin 4β-sulfonate was produced. This highlights the importance of sterical constraint of the *cis*-configuration at the C2-C3 position of flavanols for the reaction mechanism.

The main dimeric compound produced by the same apple polyphenol reaction was found to be procyanidin B2 4β-sulfonate (**4**), with sulfonation on the terminal unit, thus retaining the same β stereochemistry as in **3**.

The structure of **4** (Figure 2) was established by NMR measurements, in particular by ^{1}H-^{13}C multiple bonds correlation (HMBC). The analysis of the ^{1}H-NMR spectrum of **4** is strongly hindered by the presence of a slow conformational process due to restricted rotation around the C4(extending unit)-C8 (terminal unit) interflavanol bond. This process implies that several ^{1}H resonances appear in the spectrum as very broad peaks in particular protons bonded to both pyran rings. This difficulty is partially overcome in HSQC and

HMBC experiments which allow to establish the overall atoms connectivity. Our data are in good agreement with partial ^{13}C-NMR assignments of **4** as reported by Foo et al. (*35*) and allow to establish the relative stereochemistry of all its chiral centers.

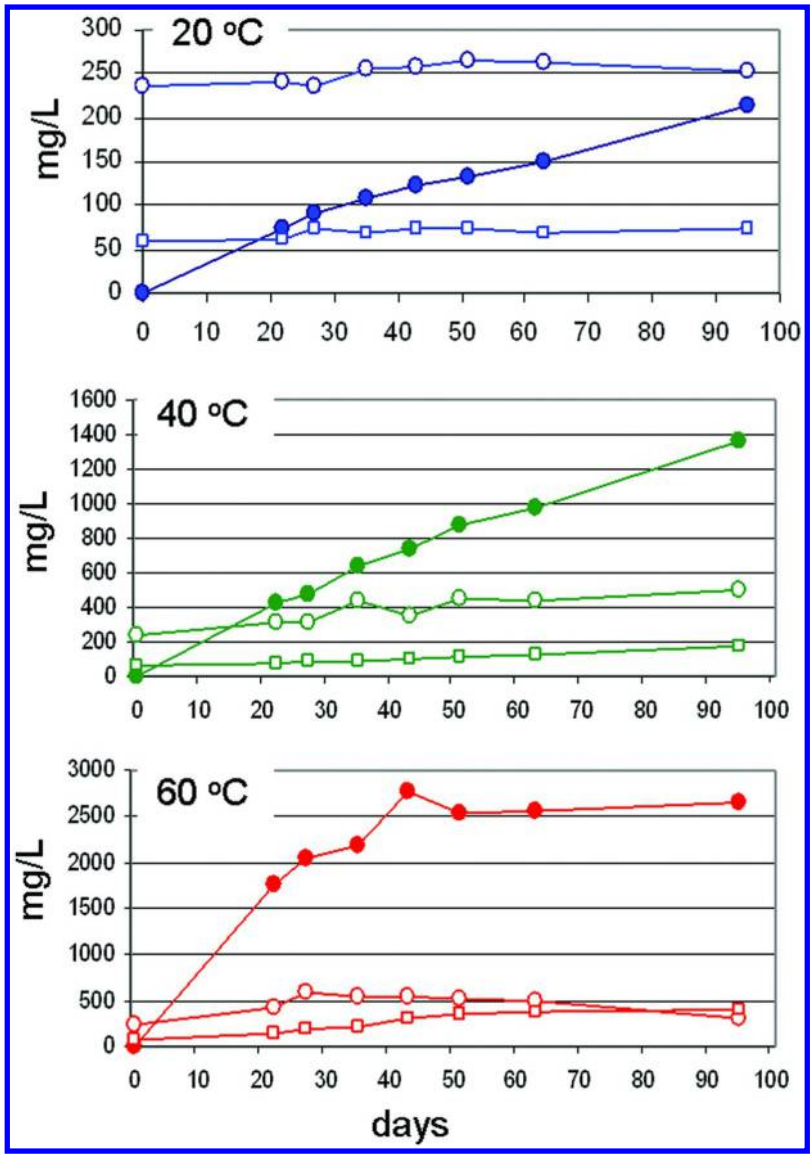

Figure 9. Evolution of the concentration of epicatechin (○), epicatechin 4-sulfonate (●) and catechin (□), of a commercial apple extract in the presence of SO_2, in model wine solution (10% ethanol, 5 g of tartaric acid, pH 3.6) and at 3 temperatures (20, 40 and 60 °C).

Publication Date (Web): November 24, 2015 | doi: 10.1021/bk-2015-1203.ch003

By spiking the wines aged under domestic conditions with the isolated standard, it was finally confirmed that these structures are the main sulfonated flavanols formed in wine.

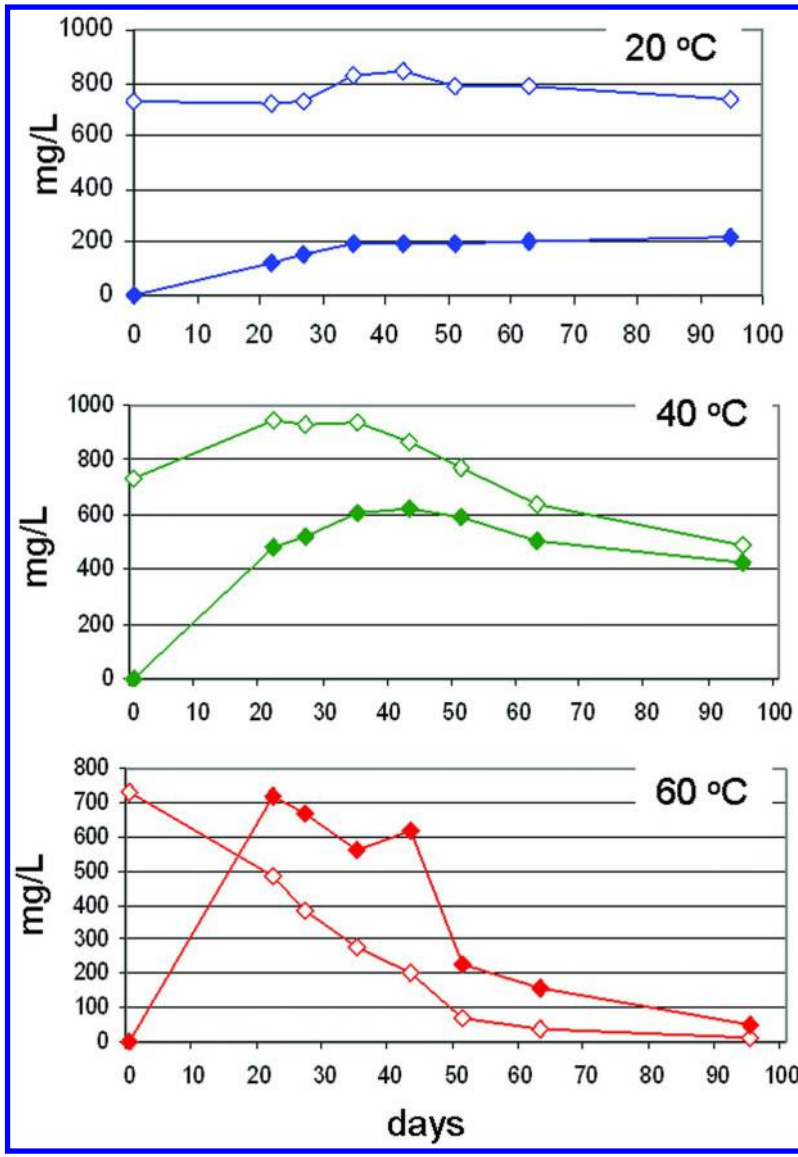

*Figure 10. Evolution of the concentration of procyanidin type B sum (◊) and sulfonated procyanidin B2 **4** of a commercial apple extract in the presence of SO_2, in model wine solution (10% ethanol, 5 g of tartaric acid, pH 3.6) and at 3 temperatures (20, 40 and 60 °C).*

Publication Date (Web): November 24, 2015 | doi: 10.1021/bk-2015-1203.ch003

The reaction of the apple extract in a model wine solution gave some interesting results in terms of the behaviour of flavanol sulfonation. The use of a polyphenolic mixture containing catechin, epicatechin, B type procyanidins and other polymeric flavanols made it possible to evaluate the reactivity of more than one compound at the same time. The model wine with the addition of a mixture of apple tannins provided conditions more similar to wine composition. Catechin and epicatechin concentrations were relatively stable at 20 °C and increased at 40 °C and 60 °C during the 95 days of the experiment (except for epicatechin at 60 °C, which started to decrease after 60 days). At 40 °C, and even more clearly at 60°C, there was clear evidence of new formation of epicatechin, via depolymerization of apple procyanidins. In these conditions, where the availability of bisulfite was not a limiting factor (in contrast to wine), the amount of epicatechin 4β-sulfonate **3** produced was greatly enhanced by temperature, and at 40-60 °C, the absolute amount produced was considerably higher as compared to the amount of epicatechin present at the beginning of the experiment. This leads to the conclusion that condensed tannins are the main precursors (Figure 9).

The sum of B type procyanidins was stable at 20 °C, increased for the first days and then decreased at 40 °C, continuing to decrease throughout the whole experiment at 60 °C. The main B type sulfonated procyanidin, which was also isolated and identified by MS and NMR, was the procyanidin B2. Absolute quantification of the two isolated sulfonated derivatives in the reaction mixture showed that epicatechin 4β-sulfonate concentration increased at all temperatures during the 95 days (at 60 °C its concentration was stable after 43 days), and sulfonated procyanidin increased for the first ~30 days at all three temperatures and then stabilised (20 °C) or decreased (40 and 60 °C) (Figure 10). In conclusion, the features of this reaction can be summarised as i) a fast initial reaction rate at 40-60 °C; ii) max reaction yield at 40-60 °C, iii) evidence of new formation of procyanidins at 40 °C, further enhanced at 60 °C, when the sulfonated product was also rapidly consumed.

Conclusions

Wine sulfonated flavanols are hydrophilic compounds with increased solubility as compared to free flavanols. They can be produced in part via cleavage of larger oligomers. These sulfonated products cannot be involved in inter-flavanic linkages at their C4 terminal, possibly leading to reduced mDP of wine tannins if this reaction occurs. Most importantly, both from the scientific and practical point of view, they can be considered as new markers of inappropriate storage, induced by storage at elevated temperature. Their formation reaction is relatively slow, and on the basis of our experiments we can suggest that their presence in wine could be induced either by long storage at a moderately high temperature or by relatively short storage at extreme temperatures. Further studies are required to validate their use, but we expect that in the future they could be used to prove the inappropriate storage of wine, an important objective

Publication Date (Web): November 24, 2015 | doi: 10.1021/bk-2015-1203.ch003

(*1*), thus providing wine producers with information on post-winery handling of their wines and giving them a new analytical tool to check whether the wine is reaching the consumer as they intended.

Acknowledgments

The authors would like to acknowledge the project QUALIFU – Qualità' alimentare e funzionale, D.M. 2087/7303/09 of 28/01/2009, for financial support; the Consortium del Brunello di Montalcino for providing the grapes, Tomas Roman for small scale winemaking, Mario Malacarne for oenological analysis, Cristina Salvadori for the images of the dry precipitate in Figure 8, Kajetan Trost for characterizing the apple tannins extract and the winery of the Fondazione Edmund Mach for the cellar storage experiment.

Publication Date (Web): November 24, 2015 | doi: 10.1021/bk-2015-1203.ch003

References

1. Butzke, C. E.; Vogt, E. E.; Chacón-Rodríguez, L. *J. Wine Res.* **2012**, *23*, 15–25.
2. Pauster, L. In *Etudes sur le Vin*; Librairie F. Savy: Paris, 1873; p 344.
3. Arapitsas, P.; Speri, G.; Angeli, A.; Perenzoni, D.; Mattivi, F. *Metabolomics* **2014**, *10*, 816–832.
4. Arapitsas, P.; Scholz, M.; Vrhovsek, U.; Di Blasi, S.; Biondi Bartolini, A.; Masuero, D.; Perenzoni, D.; Rigo, A.; Mattivi, F. *PLoS ONE* **2012**, *7*, e37783.
5. Cuadros-Inostroza, A.; Giavalisco, P.; Hummel, J.; Eckardt, A.; Willmitzer, L.; Peña-Cortés, H. *Anal. Chem.* **2010**, *82*, 3573–3580.
6. Fulcrand, H.; Mané, C.; Preys, S.; Mazerolles, G.; Bouchut, C.; Mazauric, J.-P.; Souquet, J.-M.; Meudec, E.; Li, Y.; Cole, R. B.; et al. *Phytochemistry* **2008**, *69*, 3131–3138.
7. Gougeon, R. D.; Lucio, M.; Frommberger, M.; Peyron, D.; Chassagne, D.; Alexandre, H.; Feuillat, F.; Voilley, A.; Cayot, P.; Gebefügi, I.; et al. *Proc. Natl. Acad. Sci. U.S.A.* **2009**, *106*, 9174–9179.
8. Hong, Y.-S.; Cilindre, C.; Liger-Belair, G.; Jeandet, P.; Hertkorn, N.; Schmitt-Kopplin, P. *J. Agric. Food Chem.* **2011**, *59*, 7237–7245.
9. Son, H.-S.; Hwang, G.-S.; Kim, K. M.; Ahn, H.-J.; Park, W.-M.; Van Den Berg, F.; Hong, Y.-S.; Lee, C.-H. *J. Agric. Food Chem.* **2009**, *57*, 1481–1490.
10. Vaclavik, L.; Lacina, O.; Hajslova, J.; Zweigenbaum, J. *Anal. Chim. Acta* **2011**, *685*, 45–51.
11. Villagra, E.; Santos, L. S.; Vaz, B. G.; Eberlin, M. N.; Felipe Laurie, V. *Food Chem.* **2012**, *131*, 692–697.
12. Burin, V. M.; Freitas Costa, L. L.; Rosier, J. P.; Bordignon-Luiz, M. T. *LWT - Food Sci.Technol.* **2011**, *44*, 1931–1938.
13. Cejudo-Bastante, M. J.; Hermosín-Gutiérrez, I.; Pérez-Coello, M. S. *J. Food Sci.* **2013**, *78*, C507–13.
14. Ghidossi, R.; Poupot, C.; Thibon, C.; Pons, A.; Darriet, P.; Riquier, L.; De Revel, G.; Mietton Peuchot, M. *Food Control* **2012**, *23*, 302–311.
15. González Marco, A.; Ancín Azpilicueta, C. *Food Chem.* **2006**, *99*, 680–685.

16. Hernanz, D.; Gallo, V.; Recamales, Á. F.; Meléndez-Martínez, A. J.; González-Miret, M. L.; Heredia, F. J. *Food Chem.* **2009**, *113*, 530–537.
17. Hopfer, H.; Ebeler, S. E.; Heymann, H. *J. Agric. Food Chem.* **2012**, *60*, 10743–10754.
18. Kallithraka, S.; Salacha, M. I.; Tzourou, I. *Food Chem.* **2009**, *113*, 500–505.
19. Loscos, N.; Hernández-Orte, P.; Cacho, J.; Ferreira, V. *Food Chem.* **2010**, *120*, 205–216.
20. Makhotkina, O.; Pineau, B.; Kilmartin, P. A. *Aust. J. Grape Wine Res.* **2012**, *18*, 91–99.
21. Maury, C.; Clark, A. C.; Scollary, G. R. *Anal. Chim. Acta* **2010**, *660*, 81–86.
22. Monagas, M.; Bartolomè, B.; Gomez-Cordovès, C. *Eur. Food Res. Technol.* **2005**, *220*, 331–340.
23. Ugliano, M. *J. Agric. Food Chem.* **2013**, *61*, 6125–6136.
24. Wirth, J.; Morel-Salmi, C.; Souquet, J. M.; Dieval, J. B.; Aagaard, O.; Vidal, S.; Fulcrand, H.; Cheynier, V. *Food Chem.* **2010**, *123*, 107–116.
25. Ehrhardt, C.; Arapitsas, P.; Stefanini, M.; Flick, G.; Mattivi, F. *J. Mass Spectrom.* **2014**, *49*, 860–869.
26. Press release of HKQAA: World's First Wine Storage Management Systems for Wine Retailers Certification Scheme. http://www.hkqaa.org/cmsimg/1303277590WSMS%20Press%20Release%20Eng%20v3%20web.pdf (October 2014 accessed).
27. Lam, H. Y.; Choy, K. L.; Ho, G. T. S.; Kwong, C. K.; Lee, C. K. M. *Expert Syst. Appl.* **2013**, *40*, 3665–3678.
28. Mateus, N.; Oliveira, J.; Santos-Buelga, C.; Silva, A. M. S.; De Freitas, V. *Tetrahedron Lett.* **2004**, *45*, 3455–3457.
29. Arapitsas, P.; Perenzoni, D.; Nicolini, G.; Mattivi, F. *J. Agric. Food Chem.* **2012**, *60*, 10461–10471.
30. Håkansson, A. E.; Pardon, K.; Hayasaka, Y.; De Sa, M.; Herderich, M. *Tetrahedron Lett.* **2003**, *44*, 4887–4891.
31. Leopoldini, M.; Rondinelli, F.; Russo, N.; Toscano, M. *J. Agric. Food Chem.* **2010**, *58*, 8862–8871.
32. Rentzsch, M.; Schwarz, M.; Winterhalter, P.; Blanco-Vega, D.; Hermosín-Gutiérrez, I. *Food Chem.* **2010**, *119*, 1426–1434.
33. Laurie, V. F.; Zúñiga, M. C.; Carrasco-Sánchez, V.; Santos, L. S.; Cañete, Á.; Olea-Azar, C.; Ugliano, M.; Agosin, E. *Food Chem.* **2012**, *131*, 1510–1516.
34. Bae, Y. Douglas-fir Inner Bark Procyanidins: Sulfonation, Isolation and Characterization. Ph.D. Thesis, Oregon State University, Oregon, 1989
35. Foo, L. Y.; McGraw, G. W.; Hemingway, R. W. *J. Chem. Soc., Chem. Commun.* **1983**, 672–673.

Publication Date (Web): November 24, 2015 | doi: 10.1021/bk-2015-1203.ch003

Publication Date (Web): November 24, 2015 | doi: 10.1021/bk-2015-1203.ch004

Chapter 4

Gas Detection Tubes for Measurement of Molecular and Free SO_2 in Wine

Patricia A. Howe,[1] Jussara M. Coelho,[2] and Gavin L. Sacks*,[1]

[1]Department of Food Science, Cornell University, Ithaca, New York, U.S.A.
[2]Department of Food Technology, Federal University of Viçosa, Viçosa, MG, Brazil
***E-mail: gls9@cornell.edu.**

curate measurements of the major active sulfur dioxide species in wine (HSO_3^- and SO_2) are important to studies of wine oxidation chemistry and microbial stability. These so-called "free SO_2" forms are traditionally measured by iodometric titration, aeration-oxidation (A-O) or by comparable modern variants. These standard approaches require sample dilution and/or pH shifts. We describe a simple headspace method for quantifying either molecular or free SO_2 in wine utilizing colorimetric gas detection tubes (HS-GDT) that avoids perturbation of equilibria. Henry's coefficients were constant over ethanol concentrations of 0-17% v/v. The HS-GDT method limit of detection in a model wine (pH 3.56, 12% v/v ethanol) was 0.21 mg/L molecular SO_2, and was linear over 0.29-1.13 mg/L. Good agreement was observed between HS-GDT and A-O for white and blush wines, but molecular SO_2 in red wines averaged 2-fold lower by HS-GDT, likely because the standard A-O approach results in dissolution of weakly bound bisulfite-anthocyanin adducts.

In Advances in Wine Research; Ebeler, et al.;
ACS Symposium Series; American Chemical Society: Washington, DC, 2015.

Publication Date (Web): November 24, 2015 | doi: 10.1021/bk-2015-1203.ch004

Introduction

The first written description of using sulfur dioxide (SO_2) as a wine preservative dates to 1670 (*1*), in which it is suggested to add wine or other alcoholic beverages to a container filled with fumes from burnt sulfur. In modern winemaking, SO_2 is a near ubiquitous addition for prevention of wine oxidation and microbial spoilage (*2*). While low levels of SO_2 are formed endogenously by yeast metabolism during fermentation, typically <10 mg/L (*3*), larger amounts of SO_2 are typically added following alcoholic and/or malolactic fermentation and then at regular intervals throughout storage, in the form of compressed SO_2 gas, liquid SO_2 solutions, or potassium metabisulfite (*2*).

SO_2 Species in Solution

In wine and other food systems, SO_2 exists as multiple species with different activities, sensory effects, and regulatory requirements. The roles and typical targets or constraints for these species are summarized in Table 1.

Table 1. Properties of Different Species of SO_2 in Wine

SO_2 Fraction	*Major Role*	*Typical target or constraint (as SO_2 equivalents)*
Molecular SO_2 (free acid form)	Antimicrobial	Microbial stability: typically, 0.5-0.8 mg/L. Irritation threshold: 2 mg/L
Bisulfite (HSO_3^-)	Antioxidant, accounts for >95% of free SO_2 (see below)	
Sulfite (SO_3^{2-})	Negligible (<0.01% of bisulfite at wine pH)	
Free SO_2: Sum of Molecular, HSO_3^-, SO_3^{2-}	Antioxidant	Preventing wine oxidation: typically, 20-40 mg/L
Bound Bisulfite Adducts	Contribute to total SO_2. May have minor antimicrobial activity. Weakly bound adducts can dissociate and add to free SO_2 pool following loss of free bisulfite	
Total: Free + Bound SO_2	Regulatory	Regulated in most countries: In US, must be < 350 mg/L for all wines

Because SO_2 is a weak acid (pK_{a1} in water at 20 °C = 1.81), the predominant species at wine pH (3-4) is bisulfite (HSO_3^-), with minor concentrations of the free acid SO_2 species (<5%) and negligible concentrations of sulfite (SO_3^{2-}, pK_{a2} = 7.2) (Figure 1). The sum of these species (molecular, bisulfite, sulfite) is referred to as "free SO_2", and as described later, free SO_2 (mostly bisulfite) is the primary species involved in wine redox chemistry.

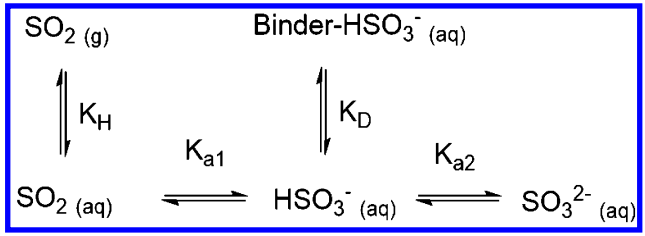

Figure 1. Equilibrium relationships among SO_2 species in wine. K_{a1}, K_{a2}: First and second acid-dissociation constants; K_H: Henry's Coefficient; K_D: Dissociation constant of a sulfonate adduct ("bound SO_2" species).

Publication Date (Web): November 24, 2015 | doi: 10.1021/bk-2015-1203.ch004

HSO_3^- may covalently bind with electrophiles to form the fraction referred to as "bound SO_2". In most wines, the major contributor to bound SO_2 is acetaldehyde, which will form a *strongly bound* α-hydroxysulfonic acid adduct with bisulfite. Because of the low dissociation constant ($K_d = 1\times10^{-6}$) of the acetaldehyde-bisulfite adduct, >99% of acetaldehyde will be bound in a wine with a typical free SO_2 concentrations of 20-40 mg/L (*2*). Other carbonyl species, particularly α-keto acids from fermentation (e.g. pyruvate, α-ketoglutarate) or oxo-acids from spoilage organisms (e.g. glucuronic acid) may form *weakly bound* adducts, ($K_d > 1\times10^{-5}$) (*4*). In sweet wines, binding by glucose may represent a significant pool of bound SO_2, in spite of its relatively low affinity for bisulfite ($K_d = 0.6$) (*4*). In red wines, anthocyanins can also represent a major sink of bound SO_2 due to their relatively high binding constants ($K_d = 1\times10^{-5}$) (*5*). Over a range of free SO_2 concentrations (30 - 90 mg/L – on the high end for commercial wines) and pH values (3.0-3.8) approximately 70-85% of monomeric anthocyanins are reported to be bound (*6*). Finally, total SO_2, refers to the sum of free and bound forms of SO_2 species and is regulated in many countries due to health concerns (*7*).

Activity of SO_2 Species - Antimicrobial and Antioxidant

SO_2 may be added to grapes or must prior to fermentation to inhibit spoilage micro-organism activity, favor *S. cerevesiae* growth, or inhibit polyphenol oxidase and slow enzymatic browning (*2*). However, SO_2 is more widely used as an antimicrobial and antioxidant after fermentation. In spite of its low concentration (<1% of free SO_2), the molecular SO_2 species has been demonstrated to be the species responsible for antimicrobial activity in juices and wine (*8*). The mechanism of action is believed to involve the passive diffusion of neutral molecular SO_2 across the cell membrane, followed by formation of HSO_3^- at intracellular pH (*9*). Several mechanisms for toxicity are then available to HSO_3^-, including nucleophilic addition to key metabolites, damage to DNA, and reduction of protein disulfide bridges. Typical recommendations for preventing microbial spoilage are in the range of 0.5-0.8 mg/L molecular SO_2 for dry wines, with higher concentrations sometimes recommended for sweet wines (*2*, *10*).

As mentioned previously, free HSO_3^- is the major species involved in redox reactions. The primary pathway by which O_2 is consumed in wine under abiotic conditions involves initial activation of triplet O_2 to a reactive oxygen species (ROS, singlet O_2) by transition metal catalysts (particularly Fe^{2+}) (*11*). The ROS can then react with 1,2-diphenol moieties in wine to yield 1,2-quinones and H_2O_2, which can participate in further oxidative reactions with wine components, e.g. by coupling with nucleophiles or oxidizing alcohols to aldehydes (*12*). HSO_3^- can exert its antioxidant influence by rapidly reacting with 1,2-quinones and H_2O_2 (*12*), although it may also accelerate the rate of O_2 consumption by facilitating regeneration of transition metal catalysts and reacting with quinones (*13*). The many potential roles of HSO_3^- in wine oxidation are summarized in Figure 2.

Publication Date (Web): November 24, 2015 | doi: 10.1021/bk-2015-1203.ch004

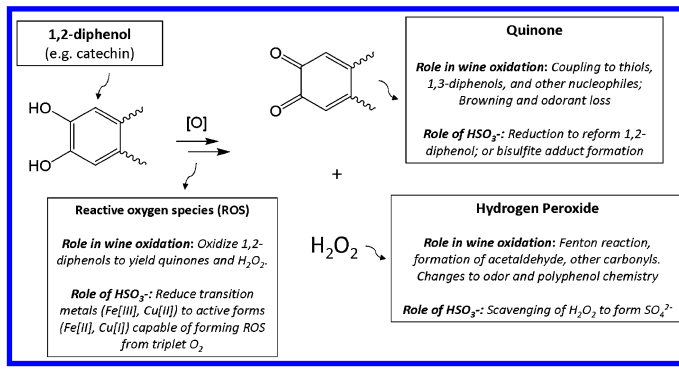

Figure 2. Overview of role of HSO_3^- during wine oxidation.

The bound SO_2 fraction is thought to have weaker anti-microbial and anti-oxidant activity than free SO_2, but some forms (particularly acetaldehyde-bisulfite adducts) appear to have a weak inhibitory effect against lactic acid bacteria (*14*). Weakly bound bisulfite adducts do not appear to directly participate in oxidation reactions, but may dissociate to partially replenish free SO_2 following loss of the latter.

Current Methods for Measurement of Molecular and Free SO_2

As compared to other SO_2 species, winemakers are generally most concerned with measurement of free and molecular SO_2 (*10*), as bisulfite is the major species responsible for preventing wine oxidation and molecular SO_2 is the main species responsible for preventing microbial growth. If the pH is known, the free SO_2 can be used to calculate the molecular SO_2 concentration via the Henderson-Hasselbalch equation (*2*). Common methods for measuring free SO_2 in wines can be classified into two categories:

Approach 1. Direct Colorimetric or Titrimetric Measurement

These methods utilize an oxidizing reagent, e.g. iodine in the "Ripper" titration of an acidified wine sample (*15*) and *p*-rosaniline in the "fuschin" colorimetric assay (*16*). While these assays are relatively straightforward to perform, the absence of a separation step results in interferences from other reducing compounds and suspect interlaboratory reproducibility (*16–18*).

Approach 2. Isolation of Molecular SO_2 Following Sample Acidification and Prior to Quantification

Improved selectivity and reproducibility for free SO_2 measurements can be achieved by initially acidifying the sample and then separating molecular SO_2. In many wineries, a modified version of the classic Monier-Williams method is used, often referred to as 'aeration-oxidation' or A-O (*19*, *20*). Using an aspirator, SO_2 is swept from the acidified sample by a gas stream into a receiving flask containing H_2O_2. Reaction of H_2O_2 and SO_2 yields H_2SO_4 which can then be titrated to calculate the original concentration of SO_2. A similar but more readily automated approach to distillation is to use a gas-permeable membrane to separate SO_2 from the acidified wine sample prior to quantification of SO_2 by some means, e.g. colorimetric (*21*) or electrochemical (*22*). More recently, the use of colorimetric gas detection tubes for quantification of SO_2 has been described, and is reported to yield near-identical results with lesser requirements in time and cost (*23*).

Publication Date (Web): November 24, 2015 | doi: 10.1021/bk-2015-1203.ch004

Problems with Classic Approaches and Alternate Approaches to Artifact-Free Measurements of Free and Molecular SO_2

As has been pointed out by multiple authors, the acidification and dilution steps inherent to the approaches described above can result in the dissolution of sulfonate adducts and overestimation of free and molecular SO_2 (*2*, *19*, *24*). This is less of a concern for more stable sulfonate adducts like acetaldehyde-bisulfite, but is of greater concern for less stable bound forms such as anthocyanin-bisulfite adducts with dissociation rate constants on the order of a 0.2 min^{-1} under acidic conditions (*25*) and thus may dissociate over the time frame of classical SO_2 analyses. The degree to which the standard approaches overestimate HSO_3^- is not well established, but has been reported to be up to an order of magnitude too high for red wines (*26*).

Despite this recognized shortcoming of classic approaches, few papers report using techniques which would avoid disturbance of SO_2 wine equilibria. Capillary electrophoresis (CE) can be used to measure bisulfite without artifactual dissolution of bound SO_2 forms (*26*), but this approach has not been widely adopted, likely due to the technical complexity of the analysis. Ion chromatography (IC) has been used for measurement of total SO_2 in wine following pH adjustment to 7.5 or greater (*27*), but it is unclear if this approach would be appropriate for free SO_2, i.e. measurement of HSO_3^- without pH adjustment. Alternatively, the molecular SO_2 concentration can be calculated

from the headspace SO_2 concentration of an equilibrated sample, assuming the Henry's coefficient is known (see Figure 1). HSO_3^- and free SO_2 can then be calculated from molecular SO_2 via the Henderson-Hasselbalch equation. Good agreement was observed between A-O and a headspace gas chromatography (HS-GC) method for white wines (*28*) but A-O yielded two-fold higher values for a red wine, presumably due to less dissolution of weak anthocyanin-bisulfite adducts. Infrared spectroscopy (*29*), inductively-coupled plasma optical-emission spectrometry (ICP-OES) (*30*) and flame molecular absorption spectrometry (*31*) can also be used for measurement of vapor-phase SO_2 from wine. However, to our knowledge, artifact-free approaches to measurement of SO_2 (e.g. headspace methods, CE) have not been widely adopted in either wineries or research labs, possibly due to the cost and complexity of the techniques. This will be a constraint on future studies intending to define minimal SO_2 concentrations necessary to inhibit microbial spoilage in real wines, or in understanding wine oxidation mechanisms.

Gas detection tubes (GDT) were originally developed for the mining industry and consist of a glass tube packed with color-sensitive reagent that stains following exposure to a target analyte. GDT have been used for several wine applications including quantification of H_2S during fermentation (*32*) and more recently for measurement of free SO_2 in a modified A-O protocol (*23*). This latter application involved initial acidification and dilution of the sample, and thus would be expected to suffer from similar artifacts as reported for other standard approaches. We chose here to evaluate the use of GDT for quantifying headspace SO_2 above an unaltered wine sample, and using this information to calculate molecular and free SO_2 in the wine.

Materials and Methods

Chemicals

Potassium metabisulfite (97% w/w) and ethanol (95% v/v) were obtained from Acros Organics (Geel, Germany). Potassium bitartrate (99% w/v), hydrogen peroxide (30% w/v), sodium hydroxide (0.01 N) and *o*-phosphoric acid (85% w/w) were obtained from Fisher Scientific (Waltham, MA). A nominally 25% phosphoric acid solution was prepared as a 2.38:1 dilution of 294 mL phosphoric acid (85%) with 700 mL DI water. Hydrochloric acid (36.5% w/w) was obtained from BDH Merck (Poole Dorset, United Kingdom).

SO_2 Working Standards

SO_2 stock solutions at nominal concentrations of 1000 and 10000 mg/L as SO_2 were prepared weekly by dissolution of potassium metabisulfite in a solution of methanol in water (10% v/v) to avoid SO_2 auto-oxidation. Working standards for analysis were prepared as needed by addition of an appropriate volume of a stock solution to 100 mL of a saturated potassium bitartrate buffer (pH 3.56). Iodometric titrations of the Ripper method were used to determine the actual SO_2 concentration of the stock and working solutions.

Publication Date (Web): November 24, 2015 | doi: 10.1021/bk-2015-1203.ch004

Publication Date (Web): November 24, 2015 | doi: 10.1021/bk-2015-1203.ch004

SO_2 Measurements by Aeration-Oxidation (A-O)

A-O was performed according to established protocols to determine free SO_2 (*15*). Molecular SO_2 concentration was then determined by rearrangement of the Henderson-Hasselbalch equation (Equation 1) using ethanol-, ionic strength-, and temperature- corrected pK_{a1} values from the literature (*33*). Ionic strength was estimated to be constant at 0.50M based on typical literature values (*34*).

Equation 1: $[\text{Molecular } SO_2] = [\text{Free } SO_2] / (1+10^{pH-pKa})$

Protocol for SO_2 Measurement by Headspace Gas Detection Tube (HS GDT)

The HS-GDT protocol is summarized in Figure 3. The apparatus consists of a 60 mL Becton Dickinson polypropylene syringe with a Luer tip, and a polypropylene plunger with a polyisoprene latex-free plunger tip. A customized dispensing stop was constructed from an additional syringe body. The Luer tip was fitting to a two- way polycarbonate male Luer stopcock, and a short piece of silicone tubing connected the other end of the stopcock to a Gastec 5Lb GDT (Gastec Corporation; Fukayanaka, Japan). If the GDT had been previously used, the "start" point of color transition was marked on the tube with a fine point permanent marker. If the tube had not been used, the beginning of the packing material indicated the run "start".

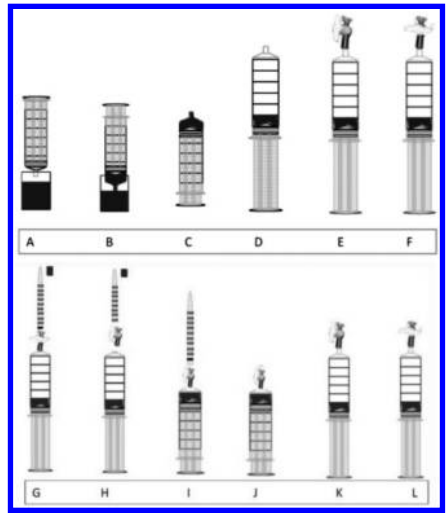

Figure 3. Schematic of HS-GDT measurement. Step A: Prepare syringe and sample; B: Sample 10 mL of wine into syringe; C: Invert syringe; D: Create 50 mL of headspace; E: Place valve on syringe; F: Close valve and equilibrate syringe for 5 min; G: Connect Gas Detection Tube (GDT) with stain location marked; H: Open valve; I: Quickly (10 sec) depress syringe to expel headspace; J: Remove GDT, mark new stain location; K, L: Repeat starting with Step D.

For each analysis, the syringe was used to sample 10 mL of a wine or working standard and the syringe barrel then withdrawn further to create an additional 50 mL of headspace. Once the stopcock was closed and the syringe stop set at 10 mL, the syringe was placed nose-up and allowed to equilibrate for 5 min. A GDT was then connected, the stopcock was opened, and the syringe was depressed at a constant rate to the stop over a 10 sec period. Following expulsion of headspace through the GDT, the colorimetric reaction was allowed to stabilize for 1 min. This action was performed four times, such that a total volume of 200 mL was sampled through the tube. The distance from the stain startpoint to endpoint were measured in millimeters using a ruler.

Publication Date (Web): November 24, 2015 | doi: 10.1021/bk-2015-1203.ch004

Determination of P_{SO2}, Molecular SO_2, and Free SO_2 from Raw GDT Measurements

The commercial GDT have printed scales in units of SO_2 partial pressure (P_{SO2}) in ppm (μL/L). To overcome the poor resolution of the scale, a best fit cubic interpolation function, f(x) was determined for each lot of tubes. To achieve this, the distance from the origin (in mm) of each printed P_{SO2} value (in μL/L) was recorded, and the best fit function, f(x), was calculated using Microsoft Excel 2010 (Redmond, WA).

Following a sample analysis, P_{SO2} was calculated from the locations of the startpoint (x_{start}) and the endpoint (x_{end}) measurements in mm using the aforementioned cubic interpolation function, f(x).

Equation 2: $P_{SO2} = f(x_{end}) - f(x_{start})$

The molar concentration of molecular SO_2 can then be calculated by dividing P_{SO2} by either an experimentally determined or literature Henry's coefficient. In practice, we achieved better results by utilizing calibration curves to relate P_{SO2} to molecular SO_2, due to a consistent non-zero intercept associated with the HS-GDT.

Ethanol Dependence of Henry's Coefficient for SO_2

SO_2 solutions (1 mg/L) were prepared from a 100 mg/L SO_2 stock solution in 10 mL of 1M HCl (pH 0) to favor the molecular SO_2 form and isolate the effect of ethanol on SO_2 volatility. These solutions were prepared with varying ethanol concentration (0, 8, 11, 14 and 17% v/v) by addition of the stock solution directly to syringes containing the hydroalcoholic solutions to minimize losses due to volatization. The samples were analyzed by the HS-GDT method (n=8 for each ethanol concentration). The Henry's coefficient (K_H) of SO_2 was determined from P_{SO2} and the molecular SO_2 concentration.

Equation 3: $K_H = P_{SO2} / [\text{Molecular } SO_2]$

In Advances in Wine Research; Ebeler, et al.;
ACS Symposium Series; American Chemical Society: Washington, DC, 2015.

Publication Date (Web): November 24, 2015 | doi: 10.1021/bk-2015-1203.ch004

Calibration Curve and Figures of Merit for HS-GDT Method

Standards solutions at nominal concentrations of 5, 10, 15, 20, 30 and 40 mg/L as free SO_2 were made in a potassium bitartrate buffer with ethanol 12% v/v. Molecular SO_2 concentration was then determined from the Henderson-Hasselbalch equation using ethanol-, ionic strength-, and temperature-corrected pK_{a1} values from the literature (*33*).

Standards were then analyzed by the HS-GDT method in replicate (n=12 per standard, total of 72 analyses). The coefficient of variation for each standard concentration was calculated as the standard deviation divided by the mean. Linearity was evaluated by linear regression of measured P_{SO2} vs. expected P_{SO2}. The concentration independent noise (σ) was estimated by Pallesen's method (*35*), and the detection limit (LOD) was calculated as $3 \times \sigma$.

pK_a of SO_2 as a Function of Ethanol Concentration:

SO_2 solutions (50 mg/L) were prepared in a potassium bitartate buffer with varying ethanol concentrations (0, 7, 14 or 20% v/v) and pH values (3.1, 3.3, 3.5, and 3.7). The HS-GDT protocol was then used to determine P_{SO2} which was then converted to molecular SO_2. The apparent pK_a for each solution was calculated from the measured molecular SO_2 and known free SO_2 concentration using the Henderson-Hasselbalch equation. The room temperature at the time of the experiment was 21.9°C.

A-O versus HS-GDT: Comparison with Commercial Wines

Commercial wines (10 red, 12 white, 5 blush) from the 2009-2013 vintages and representing multiple countries of origin (US, Australia, Argentina) were purchased at local stores. Molecular SO_2 was determined for each wine by both A-O and HS-GDT approaches. Additional wine parameters were analyzed by ETS Laboratories (St Helena, CA): pH (by meter), alcohol (FTIR), volatile acidity (as acetic acid, measured by enzymatic assay), malic acid (enzymatic) and glucose plus fructose (enzymatic) were measured by accredited methods; quercetin glucosides, catechin, tannins, polymeric anthocyanins and total anthocyanins were measured by HPLC (*36*). Monomeric anthocyanins were calculated as the difference in concentration between total and polymeric anthocyanins.

Statistical Analyses

SAS 9.0 was used for statistical analysis.

Results and Discussion

Effects of Ethanol on Henry's Coefficient (K_H) of SO_2

Using the HS-GDT assay, P_{SO2} was measured for 1 mg/L SO_2 solutions (pH 0, 21 °C) over a range of ethanol concentrations. Samples were acidified to well below the pK_{a1} of SO_2 to eliminate any confounding effects from ethanol-induced changes to pK_{a1}. The mean value for P_{SO2} based on the manufacturer markings was 5.92 µL/L, which equates to a K_H = 0.38 Atm/M at 21 °C. This is highly comparable to a recent previous report of 0.28 Atm/M for SO_2 in water at 25 °C (*37*). Furthermore, P_{SO2} (and thus K_H) were ethanol independent over the range 0-17% v/v ethanol (Table 2).

Publication Date (Web): November 24, 2015 | doi: 10.1021/bk-2015-1203.ch004

Table 2. Effects of Ethanol on SO_2 Partial Pressures (P_{SO2}) in a pH 0 Matrix (>95% Molecular SO_2 form). Lack of Significant Differences Indicates That Henry's Coefficient Is Ethanol-Independent over the Range 0-17% Abv.

Ethanol (%v/v)	*P_{SO2} (µL/L)*	*Standard error*
0	5.98	0.19
8	5.99	0.18
11	5.91	0.14
14	5.75	0.17
17	5.96	0.27

The independence of K_H from ethanol concentration is somewhat surprising, since the volatility of wine components such as esters and higher alcohols are well known to decrease in real or model wines as compared to 100% aqueous systems (*38*). This lesser effect may arise from the greater polarity of SO_2 as compared to other wine volatiles, which diminishes its ability to participate in hydrophobic interactions with ethanol.

Effects of Ethanol Concentration on pK_{a1} of SO_2

P_{SO2} was determined by HS-GDT for standard solutions containing a range of ethanol and SO_2. pK_a values were then calculated for each ethanol concentration, and these values then used to determine a best-fit line (r^2 = 0.97) for pK_a as a function of ethanol concentration

Equation 4 $$pK_a = 0.0137 \times (\text{Ethanol \%v/v}) + 1.83$$

Eq 4 yields predicted acid-dissociation constants of pK_a = 1.83 at 0% ethanol and pK_a = 1.96 at 10% alcohol, comparable to pK_a values determined elsewhere by titrimetry: 1.81 and 2.00, respectively (*33*). Some wine texts recommend using the pK_a of SO_2 in water at 20 °C (1.81) for calculations of molecular SO_2 from free SO_2 in wine regardless of the ethanol concentration (*7*, *39*), which would lead to

a non-trivial underestimation of the actual molecular SO2 concentration in typical wines: A wine with an alcohol content of 14.6% v/v and analyzed at 23.5 °C, as was done in our experiments, has a predicted pK_a value of 2.15, which would lead to over a 2-fold error in calculated molecular SO_2. In any case, our ability to match values observed with other methods suggests that HS-GDT is an appropriate method for measurement of molecular SO_2 and further estimates of molecular SO_2 in this paper are based on ethanol-, temperature-, and ionic strength- corrected pK_a values.

Figures of Merit for the HS-GDT Method

Figures of merit were determined for the HS-GDT method using SO_2 standards (0.14 to 1.13 mg/L molecular SO_2) in a model wine containing 12% v/v ethanol. Results are shown below in Table 3. Linearity ($r^2 = .97$) was satisfactory, and reproducibility was good (coefficient of variation < 10%) for concentrations at or above typical target values for molecular SO_2 in wine, 0.5 mg/L. The limit of detection was determined to be $P_{SO2} = 0.74$ µL/L, which equates to a molecular SO_2 of 0.21 mg/L at pH 3.56. Predicted molecular SO_2 concentrations were within ±0.06 mg/L of the expected values. Since the pK_{a1} of SO_2 in wine is typically around 2.1 following corrections for temperature, ionic strength, and ethanol (*33*), this equates to free SO_2 within ±2 mg/L of expected values – comparable to the reproducibility expected for conventional methods like A-O (*23*).

Table 3. SO_2 Partial Pressures, (P_{SO2}), Calculated Molecular SO_2, and Coefficients of Variation (%CV) for Calibration Standards in Model Wine Using the HS-GDT Approach

Molecular So_2 Of Standard (Mg/L) [a]	*P_{So2} By Hs-Gdt (µL/L)*	*Molecular So_2 By Hs-Gdt (Mg/L)* [b]	*Molecular So_2 By Hs-Gdt, Cv (%)*
0.14	0.45	<Lod	<Lod
0.29	0.84	0.23	30%
0.46	1.91	0.41	14%
0.55	2.94	0.58	6%
0.84	4.85	0.90	8%
1.13	6.15	1.12	3%

[a] Standards prepared in potassium bitartrate buffer, 12% ethanol, pH = 3.56, T = 21 °C. Molecular SO_2 calculated from Henderson-Hasselbalch equation using $pK_a = 1.99$. [b] Molecular SO_2 concentration predicted from P_{SO2} by inversion of calibration curve, $P_{SO2} = 5.99$ [Molecular SO_2] + 0.55. [c] Abbreviations: CV = coefficient of variance, LOD = Limit of detection.

Publication Date (Web): November 24, 2015 | doi: 10.1021/bk-2015-1203.ch004

Interestingly, the y-intercept was negative, and negligible signal could be observed for standards with $P_{SO2} < 0.25$ µL/L (~.07 mg/L molecular SO_2 for the system tested). This reason for this effect is unknown, but higher vapor-phase concentrations yielded a linear response, and the method is still useful.

The detection limit of the HS-GDT method in model wine (0.21 mg/L as molecular SO_2) is above what is typically reported for the A-O method. However, it is below typical target molecular SO_2 levels for wine. These targets vary among source and wine type, but typical values recommended to inhibit microbial spoilage range from 0.5 to 0.8 mg/L molecular SO_2 (*2*).

A-O versus HS-GDT: Comparison with Commercial Wines

Twenty seven commercial wines were evaluated for molecular SO_2 by both HS-GDT and A-O methods. The wines covered a wide range of styles as well as free SO_2 concentrations (4-51 mg/L by A-O). A good correlation was observed between the two methods in white and blush wines ($r^2 = 0.89$, plot not shown), and on average HS-GDT values were 85% that of A-O values. However, a much weaker correlation was observed for red wines ($r^2 = 0.46$, plot not shown), and HS-GDT values averaged 50% lower than A-O values (Figure 4).

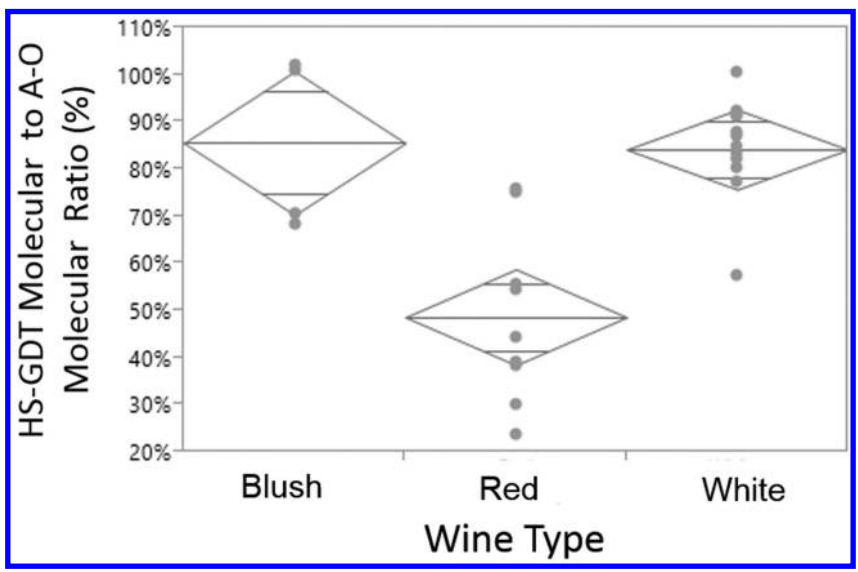

Figure 4. Ratio of 'Molecular SO_2 measured by HS-GDT' to 'Molecular SO_2 by A-O', grouped by wine type. Plots depict individual wine values (circles), mean values (center lines), overlap regions among wine types ($p<0.05$), and 95% confidence intervals (diamond tips).

Publication Date (Web): November 24, 2015 | doi: 10.1021/bk-2015-1203.ch004

Publication Date (Web): November 24, 2015 | doi: 10.1021/bk-2015-1203.ch004

Regression analysis was then performed to determine which wine components were correlated with a lower ratio of HS-GDT / A-O measurements. As shown in Table 4, most wine components were uncorrelated with this ratio, with the exception of total anthocyanins (range = 36-221 mg/L; median = 146), and to lesser extent monomeric anthocyanins. Thus, the large discrepancy between the two methods for red wines is likely due to artifactual dissolution of weakly bound anthocyanin-bisulfite adducts during A-O sample preparation steps (acidification, dilution) and the long subsequent sampling time (15 minutes) (*19*). A similar overestimation would be expected with other "standard" approaches such as the Ripper iodometric titration. A limited number of previous studies that have used non-perturbing methods to quantify SO_2 in red wines, and have observed similar results. A group using a non-perturbing headspace GC method reported a 45% higher free SO_2 value in a single red wine as compared to A-O (*28*). Thesis work by Bogren reported free SO_2 values up to an order of magnitude higher by Ripper and A-O as compared to the non-perturbing CE method (*26*), and another report using a colorimetric method observed similar degree of over-estimation (*24*). Interestingly, in our work, polymeric anthocyanins (defined by HPLC elution time) did not correlate with the HS-GDT / A-O ratio, likely because components of this late eluting peak are known to be less susceptible to SO_2 bleaching (*40*).

Table 4. Correlation Coefficients between Wine GDT/AO Ratios and Wine Chemical Parameters

Correlation	*Correlation coeff., R*	*P value*
GDT/AO Ratio . . . × Ethanol (red or white wines) × Malic acid (red or white) × residual sugars (red or white) × volatile acidity (red or white) × catechin (red) × quercetin glycosides (red) × tannin (red) × polymeric anthocyanins (red)	n.s.[a]	n.s.
GDT/AO Ratio × monomeric anthocyanins (red)	0.67	0.047
GDT/AO Ratio × total anthocyanins (red)	0.80	0.011

[a] n.s. = not significant.

The slightly lower values (85%) in white and blush wines by HS-GDT as compared to A-O are likely due to dissolution of other weakly bound adducts, such as those formed by pyruvate, diacetyl, or α-ketoglutarate (*4*). Several sweet wines were included in the study (up to 220 g/L fructose + glucose; median for all wines = 19 g/L). The lack of correlation of between methodological differences and residual sugars was somewhat surprising, since glucose can act as important sink

of bound SO_2 in sweet wines and the dissolution of glucose-bisulfite complexes has been suggested as a potential cause of free SO_2 overestimation (*2*). However, the first order rate constant for the dissolution of the glucose-bisulfite complex is reportedly 3.7×10^{-4} min^{-1} at pH~1 (*41*), and thus this complex is expected to be stable during the time of an A-O analysis. By comparison, the first order rate constant for the dissolution of anthocyanin-bisulfite adducts is approximately 2×10^{-1} min^{-1} (*25*).

While additional validation of the HS-GDT method would be desirable, traditional approaches to method validation, e.g. standard addition, are not appropriate for free and molecular SO_2 in wine matrices. SO_2 additions result in variable increases in free or molecular SO_2 because of varying concentrations of SO_2 binders across wines. Further validation of the HS-GDT method could be done by comparison with free (or molecular) SO_2 values determined by other techniques that preserve equilibria, such as headspace GC or CE.

These preliminary results appear to confirm the occasionally noted (and often overlooked) observation that standard approaches for measurement of free and molecular SO_2 result in overestimation of both due to dissolution of weakly bound bisulfite adducts. This issue is of particular concern in red wines due to the high concentration of labile anthocyanin-bisulfite adducts. Additionally, common estimates for pK_a used in wine analysis are often incorrectly low because of the significant and frequently overlooked effects of temperature, ionic strength, and ethanol on this value. However, accurate measurements of both molecular and free SO_2 are expected to be critical for future work on the mechanisms of wine oxidation or detailed investigations of microbiological tolerance to SO_2. The HS-GDT approach described here may be a useful, inexpensive tool for these investigations, by providing a rapid measurement of the accurate molecular and free SO_2 concentration of a wine.

References

1. McGovern, P. E. *Ancient Wine: the Search for the Origins of Viniculture*; Princeton University Press: Princeton, 2003.
2. Boulton, R. B.; Singleton, V. L.; Bisson, L. F.; Kunkee, R. E. *Principles and Practices of Winemaking*; Kluwer Academic/Plenum Publishers: New York, 1999.
3. Suzzi, G.; Romano, P.; Zambonelli, C. Saccharomyces strain selection in minimizing SO_2 requirement during vinification. *Am. J. Enol. Vitic.* **1985**, *36*, 199–202.
4. Burroughs, L. F.; Sparks, A. H. Sulphite-binding power of wines and ciders. I. Equilibrium constants for the dissociation of carbonyl bisulphite compounds. *J. Sci. Food Agric.* **1973**, *24*, 187–198.
5. Brouillard, R.; El Hage Chahine, J. M. Chemistry of Anthocyanin Pigments. 6. Kinetic and Thermodynamic Study of Hydrogen Sulfite Addition to Cyanin - Formation of a Highly Stable Meisenheimer-Type Adduct Derived from a 2-Phenylbenzopyrylium Salt. *J. Am. Chem. Soc.* **1980**, *102*, 5375–5378.

Publication Date (Web): November 24, 2015 | doi: 10.1021/bk-2015-1203.ch004

6. Usseglio-Tomasset, L.; Ciolfi, G.; di Stefano, R. The influence of the presence of anthocyanins on the antiseptic activity of sulfur dioxide towards yeasts. *Vini Ital.* **1982**, *24*, 86–94.
7. Margalit, Y.; Crum, J. D. *Concepts in Wine Chemistry*; Wine Appreciation Guild: San Francisco, CA, 2004.
8. Macris, B. J.; Markakis, P. Transport and toxicity of sulphur dioxide in Saccharomyces cerevisiae var ellipsoideus. *J. Sci. Food Agric.* **1974**, *25*, 21.
9. Divol, B.; du Toit, M.; Duckitt, E. Surviving in the presence of sulphur dioxide: strategies developed by wine yeasts. *Appl. Microbiol. Biotechnol.* **2012**, *95*, 601–613.
10. Zoecklein, B. W.; Fugelsang, K. C.; Gump, B. H.; Nury, F. S. *Wine Analysis and Production*; Kluwer Academic/Plenum Publishers: New York, 1999.
11. Danilewicz, J. C. Interaction of sulfur dioxide, polyphenols, and oxygen in a wine-model system: central role of iron and copper. *Am. J. Enol. Vitic.* **2007**, *58*, 53–60.
12. Ugliano, M. Oxygen Contribution to Wine Aroma Evolution during Bottle Aging. *J. Agric. Food Chem.* **2013**, *61*, 6125–6136.
13. Danilewicz, J. C. Review of oxidative processes in wine and value of reduction potentials in enology. *Am. J. Enol. Vitic.* **2012**, *63*, 1–10.
14. Wells, A.; Osborne, J. P. Impact of acetaldehyde- and pyruvic acid-bound sulphur dioxide on wine lactic acid bacteria. *Lett. Appl. Microbiol.* **2012**, *54*, 187–194.
15. Iland, P. *Chemical Analysis of Grapes and Wine: Techniques and Concepts*; Patrick Iland Wine Promotions PTYLTD: Campbelltown, SA, Australia, 2004.
16. Joslyn, M. A. Sulfur dioxide content of wine. II. Acid-bleached fuchsin-formaldehyde colormetric method. *Am. J. Enol. Vitic.* **1955**, *6*, 1–11.
17. Vahl, J. M.; Converse, J. E. Ripper procedure for determining sulfur dioxide in wine: collaborative study. *J. - Assoc. Off. Anal. Chem.* **1980**, *63*, 194–9.
18. Joslyn, M. A. Sulfur dioxide content of wine I. Iodometric titration. *Am. J. Enol. Vitic.* **1955**, *6*, 1–10.
19. Rankine, B. C.; Pocock, K. F. Alkalimetric determination of sulphur dioxide in wine. *Aust. Wine Brew. Spirit Rev.* **1970**, *88*.
20. Buechsenstein, J. W.; Ough, C. S. SO_2 determination by aeration-oxidation: a comparison with Ripper. *Am. J. Enol. Vitic.* **1978**, *29*, 161–164.
21. Bartroli, J.; Escalada, M.; Jorquera, C. J.; Alonso, J. Determination of total and free sulfur-dioxide in wine by flow-injection analysis and gas-diffusion using para-aminoazobenzene as the colorimetric-reagent. *Anal. Chem.* **1991**, *63*, 2532–2535.
22. Ruiz-Capillas, C.; Jiménez-Colmenero, F. Application of flow injection analysis for determining sulphites in food and beverages: A review. *Food Chem.* **2009**, *112*, 487–493.
23. Pegram, Z.; Kwasniewski, M. T.; Sacks, G. L. Simplified method for free SO_2 measurement using gas detection tubes. *Am. J. Enol. Vitic.* **2013**, *64*, 405–410.

24. Burroughs, L. F. Determining Free Sulfur Dioxide in Red Wine. *Am. J. Enol. Vitic.* **1975**, *26*, 25–29.
25. Brouillard, R.; El Hage Chahine, J. M. Chemistry of Anthocyanin Pigments. 6. Kinetic and Thermodynamic Study of Hydrogen Sulfite Addition to Cyanin. Formation of a Highly Stable Meisenheimer-Type Adduct Derived from a 2-Phenylbenzopyrylium Salt. *J. Am. Chem. Soc.* **1980**, *102*, 5375–5378.
26. Bogren, L. N. H. *The Effect of Sulfur Dioxide on Saccharaomyces Cereviseae*; University of California - Davis: Davis, CA, 1996.
27. Kim, H. J. Determination of sulfite in foods and beverages by ion exclusion chromatography with electrochemical detection: collaborative study. *J. - Assoc. Off. Anal. Chem.* **1990**, *73*, 216–222.
28. Davis, E. G.; Barnett, D.; Moy, P. M. Determination of molecular and free sulphur dioxide in foods by headspace gas chromatography. *Int. J. Food Sci. Technol.* **1983**, *18*, 233–240.
29. Henningsen, J. Measurement of free SO_2 in wine with 7.4-μm difference frequency spectrometer. *Appl. Phys. B* **2003**, *76*, 451–456.
30. Cmelik, J.; Machat, J.; Niedobova, E.; Otruba, V.; Kanicky, V. Determination of free and total sulfur dioxide in wine samples by vapour-generation inductively coupled plasma-optical-emission spectrometry. *Anal. Bioanal. Chem.* **2005**, *383*, 483–488.
31. Huang, M. D.; Becker-Ross, H.; Florek, S.; Heitmann, U.; Okruss, M.; Patz, C. D. Determination of sulfur forms in wine including free and total sulfur dioxide based on molecular absorption of carbon monosulfide in the air-acetylene flame. *Anal Bioanal Chem* **2008**, *390*, 361–367.
32. Park, S. K. Development of a method to measure hydrogen sulfide in wine fermentation. *J. Microbiol. Biotechnol.* **2008**, *18*, 1550–1554.
33. Usseglio Tomasset, L.; Bosia, P. La prima costante di dissociazione dell'acido solforoso [nei vini]. *Vini Ital.* **1984**, *26*, 7–14.
34. Prenesti, E.; Toso, S.; Daniele, P. G.; Zelano, V.; Ginepro, M. Acid–base chemistry of red wine: analytical multi-technique characterisation and equilibrium-based chemical modelling. *Anal. Chim. Acta* **2004**, *507*, 263–273.
35. Mac Berthouex, P.; Brown, L. C. *Statistics for Environmental Engineers*, 2nd ed.; CRC Press: Boca Raton, 2002.
36. Waterhouse, A. L.; Price, S. F.; McCord, J. D. Reversed-phase high-performance liquid chromatography methods for analysis of wine polyphenols. *Methods Enzymol.* **1999**, *299*, 113–121.
37. Zhang, N.; Zhang, J.; Zhang, Y.; Bai, J.; Wei, X. Solubility and Henry's law constant of sulfur dioxide in aqueous polyethylene glycol 300 solution at different temperatures and pressures. *Fluid Phase Equilib.* **2013**, *348*, 9–16.
38. Mouret, J. R.; Morakul, S.; Nicolle, P.; Athes, V.; Sablayrolles, J. M. Gas–liquid transfer of aroma compounds during winemaking fermentations. *LWT - Food Sci. Technol.* **2012**, *49*, 238–244.
39. Jacobson, J. L. *Introduction to Wine Laboratory Practices and Procedures*. Springer: New York, 2006.

Publication Date (Web): November 24, 2015 | doi: 10.1021/bk-2015-1203.ch004

40. Versari, A.; Boulton, R. B.; Parpinello, G. P. A comparison of analytical methods for measuring the color components of red wines. *Food Chem.* **2008**, *106*, 397–402.
41. Vas, K. The equilibrium between glucose and sulphurous acid. *J. Soc. Chem. Ind.* **1949**, *68*, 340–343.

Publication Date (Web): November 24, 2015 | doi: 10.1021/bk-2015-1203.ch004

Publication Date (Web): November 24, 2015 | doi: 10.1021/bk-2015-1203.ch005

Chapter 5

Temperature Dependence of CO_2 and Ethanol Diffusion in Champagne Wines: A Joint Molecular Dynamics and ^{13}C NMR Study

David A. Bonhommeau,*[,1] Alexandre Perret,[1] Jean-Marc Nuzillard,[2] Clara Cilindre,[1] Thibaud Cours,[1] Alexander Alijah, and Gérard Liger-Belair[1]

[1]GSMA, UMR CNRS 7331, Université de Reims Champagne-Ardenne, Campus Moulin de la Housse BP 1039, 51687 Reims Cedex 2, France
[2]ICMR, UMR CNRS 7312, Université de Reims Champagne-Ardenne, Campus Moulin de la Housse BP 1039, 51687 Reims Cedex 2, France
***E-mail: david.bonhommeau@univ-reims.fr.**

The diffusion of carbon dioxide (CO_2) is the main physical process responsible for the formation and growth of CO_2 bubbles in sparkling beverages and thus contributes to account for CO_2 outgassing that may affect tasting sensations. An extensive comparison of CO_2 diffusion coefficients deduced from classical molecular dynamics simulations and measured by ^{13}C NMR spectroscopy in carbonated hydroalcoholic solutions and in common brut champagnes reveals that ethanol is probably the main species, apart from water, responsible for the value of the CO_2 diffusion coefficient in these beverages. Bulk viscosities deduced from ethanol or CO_2 diffusion coefficients are also found to be properly estimated by applying the Stokes–Einstein relationship.

How Molecular Diffusion Impacts Champagne Tasting

Since the end of the 17th century, champagne has been a world-renowned French sparkling wine. Nevertheless, only since the past decade has much research been devoted to depict each and every parameter involved in its bubbling process (the highly sought-after and so-called *effervescence* process) (*1*, *2*). From a strictly chemical point of view, champagne wines are multicomponent hydroalcoholic

In Advances in Wine Research; Ebeler, et al.;
ACS Symposium Series; American Chemical Society: Washington, DC, 2015.

systems, with a density close to unity, a surface tension $\gamma \approx 50$ mN/m, and a viscosity about 50 % larger than that of pure water, partly due to the presence of 12.5 % v/v ethanol. Champagne wines are supersaturated with dissolved CO_2, formed together with ethanol during a second fermentation process, called *prise de mousse* (promoted by adding yeasts and sugar inside bottles filled with a base wine and sealed with a cap). Champagnes, or sparkling wines elaborated through the same traditional method, therefore hold a concentration of dissolved CO_2 proportional to the level of sugar added to promote this second fermentation. Actually, a standard 75 centiliters champagne bottle typically holds about 9 grams of dissolved CO_2, which correspond to a volume close to 5 liters of gaseous CO_2 under standard conditions for temperature and pressure (*3*).

When champagne is poured into a glass, there are indeed two pathways for progressive CO_2 and volatile organic compounds (VOC) losses. CO_2 and VOCs escape (i) into the form of heterogeneously nucleated bubbles (through effervescence), and (ii) by "invisible" diffusion through the free surface of the glass (*3*). Generally speaking, a link has been recently evidenced between carbonation and the release of some aroma compounds in carbonated waters (*4*, *5*). Sensory analysis results indeed revealed for example that the presence of CO_2 increased aroma perception in mint-flavored carbonated beverages (*5*). More recently, experiments conducted under standard tasting conditions revealed that the concentration of gaseous ethanol above champagne glasses was highly enhanced if the glass showed effervescence, thus pointing out the crucial role of bursting bubbles in champagne tasting (*6*). Moreover, by use of ultrahigh resolution mass spectrometry, it was demonstrated that ascending bubbles radiate a cloud of tiny champagne droplets overconcentrated (compared to their concentration in the bulk liquid) with compounds known to be aromatic or the precursors of aromas (*7*).

Molecular diffusion is actually the mechanism behind the progressive desorption of dissolved gas species or VOCs from the free surface area of a supersaturated liquid medium. Generally speaking, the mobility of species in a liquid phase is ruled by molecular diffusion (Brownian motion driven by thermal agitation). It mainly depends on the size of the diffusing molecules, and on the viscosity of the liquid phase itself. The higher the mobility of a given molecular species in a liquid phase, the better it diffuses to reach a gas phase (as dissolved CO_2 and ethanol continuously do from the free air/champagne interface, once the bottle is uncorked). The parameter which reflects the mobility of species in a liquid phase is the so-called diffusion coefficient. Under standard tasting conditions, the growth rate of ascending bubbles, and the rate at which VOCs progressively invade bubbles are therefore definitely under the influence of the diffusion coefficients of molecules in play (namely the dissolved CO_2 and the various VOCs typically found in Champagne wines). Among all the numerous VOCs found in wines, ethanol is obviously the most concentrated one. Ethanol is an effective gustatory, olfactory and trigeminal stimulus (*8*). In recent studies, it has also been shown that variation of wine ethanol content significantly contributes to the partitioning of odorants molecules in the wine headspace, by modification of their solubility (*9–11*).

Publication Date (Web): November 24, 2015 | doi: 10.1021/bk-2015-1203.ch005

Following these recent highlights, no wonder a very strong coupling finally exists in champagne and sparkling wines tasting, between dissolved CO_2, the presence of ascending CO_2 bubbles, CO_2 discharge and VOCs release. Moreover, the diffusion coefficient of molecules dispersed in a liquid phase is indeed strongly temperature-dependent, which therefore directly impacts the rate at which species escape the liquid phase through molecular diffusion. This chapter reports a thorough temperature dependence study of CO_2 and ethanol (EtOH) diffusion coefficients in a carbonated water/EtOH mixture, and in a standard Champagne wine, through classical force field molecular dynamics and ^{13}C NMR spectroscopy measurements.

Publication Date (Web): November 24, 2015 | doi: 10.1021/bk-2015-1203.ch005

Molecular Diffusion in Champagnes

Theoretical Evaluation Based on Classical Molecular Dynamics Simulations

Molecular Model for Champagne Wines

As emphasized in the previous section, Champagne wines are multicomponent systems composed of a number of species, from monoatomic ions to macromolecules such as proteins. Although most of the champagne ingredients may have an influence on tasting sensations, CO_2 diffusion should mainly depend on the more abundant species, namely water (H_2O) and ethanol (EtOH) molecules. Sugars might also play a non-negligible role in sweet champagnes ($c \approx 50$ g/L) but, nowadays, brut champagnes ($c \approx 10$ g/L) are the most common commercial sparkling wines and we will focus our discussion on these beverages, for which sugars should have minor effects on CO_2 diffusion. Brut champagnes will therefore be modeled, in first approximation, as a ternary mixture composed of H_2O, EtOH, and CO_2. However, a typical flute poured with 100 mL of champagne contains more than N_A molecules (N_A is the Avogadro number) which makes the exact modeling of this system impossible. We then consider a subunit of the real system that reflects the molecular proportions of H_2O, EtOH, and CO_2 in standard brut champagnes. The simulation container in our molecular dynamics simulations will thus contain 50 CO_2, 440 EtOH, and 10^4 H_2O, as illustrated in Figure 1 (*12*).

In our simulations, water molecules are described within two models, the three-site SPC/E model (*13*) and the five-site TIP5P model (*14*). In the SPC/E model, a positive charge $q_H = +04238e$ is assigned to each hydrogen atom and a negative charge $q_O = -0.8476e$ is assigned to the oxygen atom. The OH distance is fixed to $r_{OH} = 0.1$ nm and the HOH angle to $\theta_{HOH} = 109.47°$. In the TIP5P model, charges are distributed over 4 sites, the two hydrogen atoms with $q_H = +0.241e$ and two virtual atoms with $q_L = -0.241e$. The virtual atoms, commonly denoted L, represent water lone pairs. The oxygen atom does not carry any charge in this model where $r_{OH} = 0.09572$ nm, $\theta_{HOH} = 104.52°$, $r_{OL} = 0.070$ nm, and $\theta_{LOL} = 109.47°$.

Publication Date (Web): November 24, 2015 | doi: 10.1021/bk-2015-1203.ch005

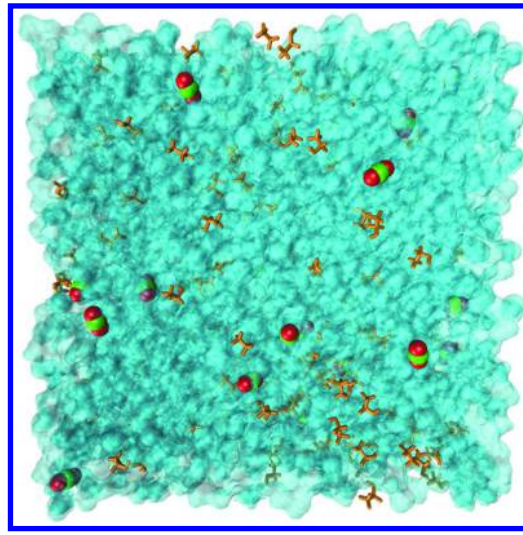

Figure 1. Simulation box containing 50 CO_2 (oxygen atoms in red and carbon atoms in green), 440 EtOH molecules (orange), and 10^4 H_2O molecules (fluid colored in cyan). (Adapted with permission from Ref. (12). Copyright 2014 American Chemical Society). (see color insert)

Classical Molecular Dynamics Simulations

Transport properties such as diffusion cannot be properly evaluated in finite-sized containers (eg, V ≈ 350 nm^3 in our simulations) because of possible molecule bounces at the container walls. The addition of periodic boundary conditions is required to avoid these artifacts by mimicking the existence of an infinite-sized system. The CHARMM27 force field (*15*), a set of parameters (atomic distances, bond angles, dihedrals, partial charges, Lennard-Jones pair diameter and well depth, etc.) to model chemical bonding in a number of species (alcohols, acids, peptides, etc.), is used to model the intermolecular and intramolecular interactions of ethanol and partial charges on the carbon, and oxygen atoms of CO_2 are taken from the literature (*16*). Initial structures for independent trajectories at five temperatures of interest, namely 277 K (fridge temperature), 281 K and 285 K (cellar temperature), 289 K, and 293 K (room temperature), are produced by replica exchange molecular dynamics (REMD) and subsequent standard MD (non-REMD) simulations in the isothermal-isobaric (*NPT*) ensemble. Ten trajectories are then run for 2 ns at each temperature (1 ns for equilibration and 1 ns for accumulation) in the *NPT* ensemble. The final data are collected and used for evaluating CO_2 and EtOH diffusion coefficients as well as the mixture viscosity (*12*).

Publication Date (Web): November 24, 2015 | doi: 10.1021/bk-2015-1203.ch005

Molecular diffusion is an irreversible phenomenon that makes species highly concentrated in some regions of a liquid to migrate toward lower concentration regions. This transport property was rationalized on binary mixtures as early as 1855 by Adolf Fick (*17*) who considered that the flux $\mathbf{J_1}$ of species of type 1 was proportional to the gradient of its mole fraction x_1 in solution as

$$\mathbf{J}_1 = -c_t D_{12} \nabla x_1 \tag{1}$$

where D_{12} is the diffusion coefficient of species 1 in the mixture (D_{12} = D_{21}), and c_t is the total molar concentration. In multicomponent systems composed of n species, the law expressed in Equation (1), also called the Fick's first law of diffusion, can be generalized to a system of n-1 equations providing $\mathbf{J_i}$ fluxes of species i.

$$\mathbf{J_i} = -c_t \sum_{j=1}^{n-1} D_{ij} \nabla x_j \tag{2}$$

The flux $\mathbf{J_n}$ of species n (the solvent) is deduced from the n-1 other fluxes by noting that the sum of fluxes vanishes. It is also worth noting that $D_{ij} \neq D_{ji}$ since D_{ij} are not representative of i-j interactions as in Fick's first law of diffusion.

In the case of Champagne wines, we already pointed out that a carbonated hydroalcoholic solution could be used, in first approximation, as model mixture in MD simulations. This solution is a ternary mixture and the generalized Fick's equation then writes

$$\mathbf{J_1} = -c_t D_{11} \nabla x_1 - c_t D_{12} \nabla x_2 \tag{3a}$$
$$\mathbf{J_2} = -c_t D_{21} \nabla x_1 - c_t D_{22} \nabla x_2 \tag{3b}$$
$$\mathbf{J_3} = -\mathbf{J_1} - \mathbf{J_2} \tag{3c}$$

where indices 1, 2, and 3 refer to CO_2, EtOH, and H_2O molecules, respectively. Evaluating the diffusion coefficients from this set of equations remains challenging and we might need to simplify it. The crudest approximation would consist in assuming that EtOH and CO_2 are infinitely diluted in water. Although water roughly represents 90 % of the mass and 95 % of the quantity of matter in this mixture, this approximation is not valid since it is well known that a small fraction of ethanol in water increases the mixture viscosity. However, we will show that the theory behind this approximation may prove useful.

Within the infinite dilution approximation all the species other than solvent molecules are considered to be present in trace amounts and concentration gradients of side species j do not influence the diffusion of species i (ie, D_{12}=0 and D_{21}=0 in the ternary system considered here). After simplifying Equations (3a) and (3b) and discarding useless indices, the typical flux of CO_2 molecules in a water-ethanol mixture and that of EtOH molecules in carbonated water would become

In Advances in Wine Research; Ebeler, et al.;
ACS Symposium Series; American Chemical Society: Washington, DC, 2015.

$$\mathbf{J} = -c_t D \nabla x \tag{4}$$

where the respective diffusion coefficients would take obviously different values. Equation (4) looks like the expression of the flux of particles self-diffusing in simple fluids such as liquid argon or, equivalently, the flux of one species in a binary mixture. In other words, although the infinite dilution is not valid in champagnes, we can use Equation (4) with an effective diffusion coefficient different from D_{ii} (i = 1 or 2) provided that we check that the subsequent probability density of diffusing particle positions is in agreement with experimental findings. The suitability of the effective diffusion coefficient is therefore hard to predict in advance without any theoretical or experimental reference data. However, we can expect that this approach will remain reliable when the standard requirements of simple fluids are fulfilled on average, namely homogeneity (that ensures spatial translation and rotational invariance), absence of chemical reaction (that prevents drastic composition changes in the mixture that would alter molar factions), and presence of one prevailing molecule (solvent).

When using Equation (4) for fluxes, the time-dependent evolution of CO_2 (or EtOH) concentrations should follow the same kind of equation as binary mixtures (*18*)

$$\frac{\partial c}{\partial t} + \nabla \cdot (\mathbf{N_t} x) = \nabla \cdot (c_t D \nabla x) \tag{5}$$

where $\mathbf{N_t} = c_t \mathbf{u}$ is the total molar flux and $\mathbf{u}$ is the molar average velocity. In MD simulations on champagnes, the total concentration c_t can be considered constant since no chemical reaction occurs between the mixture components and no loss of matter is allowed when imposing periodic boundary conditions. Champagne can also be regarded as a stationary liquid ($\mathbf{u} = \mathbf{0}$) whose properties are invariant by spatial translation (on average any molecule can occupy any position in the simulation box which should make the system globally homogeneous). Under these conditions Equation (5) becomes

$$\frac{\partial c}{\partial t} = D \nabla^2 c \tag{6}$$

whose solution $c(\mathbf{r}\text{-}\mathbf{r_0},t)$ is proportional to a Gaussian probability density $G(\mathbf{r}\text{-}\mathbf{r_0},t)$.

$$G(\mathbf{r} - \mathbf{r}_0, t) = \frac{1}{(4\pi D t)^{3/2}} \exp\left[-\frac{(\mathbf{r} - \mathbf{r}_0)^2}{4Dt}\right] \tag{7}$$

The diffusion coefficient D of CO_2 (or EtOH) can then be evaluated by pointing out that it is related to the mean-squared displacement (MSD) of diffusing molecules.

$$MSD(t) = \langle [\mathbf{r}(t) - \mathbf{r}(0)]^2 \rangle = \int_{-\infty}^{+\infty} G(\mathbf{r} - \mathbf{r}_0, t)(\mathbf{r} - \mathbf{r}_0)^2 d^3 r = 6Dt \tag{8}$$

In Advances in Wine Research; Ebeler, et al.;
ACS Symposium Series; American Chemical Society: Washington, DC, 2015.

Publication Date (Web): November 24, 2015 | doi: 10.1021/bk-2015-1203.ch005

Practically speaking, the MSD can be calculated by averaging the squared displacements of each atom belonging to the diffusing molecule, or by simply taking into account the motion of the molecule center of mass, which removes the vibrational noise. However, some statistical noise, due to the small number of trajectories and the short MD simulations length of time, may persist and $MSD(t)$ curves are therefore replaced by $MSD(\Delta t)$ curves where Δt is the time between two printed out steps of the dynamics (*12*, *19*). The reliability of MSD values at short time is therefore increased since, for instance, $MSD(\Delta t = 1\ ps)$ is averaged over 1000 values in the case of a 1 ns dynamics where data are printed out every picosecond.

The diffusion coefficients obtained for ethanol can also be compared to empirical formulae such as the correlations proposed by Siddiqi and coworkers (*20*) to represent the infinite dilution of a liquid labelled 1 (eg, EtOH), in another liquid labelled 2 (eg, water).

$$D_{12}^{\circ} = 2.98 \times 10^{-7} \eta_2^{-1.026} V_1^{-0.5473} T \qquad (9)$$

The presence of CO_2 in our model mixture combined to the fact that EtOH cannot be considered as infinitely diluted in water, should yield some deviations compared to Equation (9) but it can be interesting to evaluate the magnitude of these deviations.

Experimental Evaluation Based on ^{13}C NMR Spectroscopy Measurements

Although the CO_2 diffusion coefficients in champagnes might be evaluated by focusing on CO_2 diffusion in carbonated hydroalcoholic solutions due to the molecular composition of these beverages, comparisons with experimental diffusion coefficients would remove all doubt on the validity of the model.

Translational diffusion coefficients measurements by ^{13}C NMR spectroscopy have thus been achieved in a model hydroalcoholic mixture (87.5:12.5 (v/v) H_2O:EtOH) and in a standard brut Champagne wine sample. The amount of dissolved CO_2 and the low natural abundance of ^{13}C in the mixture do not allow the recording of useful data within a reasonable amount of time. Therefore, solutions (600 µL) were supplemented with 2 mg of 99% ^{13}C $NaHCO_3$. NMR spectrometer field stabilization by the deuterium lock required the addition of 60 µL of a 87.5:12.5 (v/v) D_2O:EtOH mixture to the solutions and NMR sample tubes were closed by a standard plastic stopper tightened with a stretchable polymer film. Diffusion coefficients were measured using the BPPLED (BiPolar Pulses, Longitudinal Eddy Currents) pulse sequence (*21*). Basically, the sample is submitted to two identical static field gradient pulses of intensity G during a preparatory stimulated echo period; the efficiency of the magnetization refocusing at the end of the echo is the lowest for the most rapidly moving molecules, thus leading to the lowest signal intensity. The signal $I(G)$ is scaled according to the Stejskal-Tanner equation, in which D, the gradient intensity G, the pulse duration δ, the delay between the field gradient pulses Δ and the gyromagnetic ratio γ of nuclei intervene.

In Advances in Wine Research; Ebeler, et al.;
ACS Symposium Series; American Chemical Society: Washington, DC, 2015.

Publication Date (Web): November 24, 2015 | doi: 10.1021/bk-2015-1203.ch005

$$I(G) = I_0 \exp\left[-\gamma^2 G^2 \delta^2 D \left(\Delta - \frac{\delta}{3}\right)\right] \quad (10)$$

Diffusion coefficients can be determined from a series of signal intensities obtained from various values of G, keeping all other parameters constant. The recording of two singlet signals for EtOH, one for each NMR ^{13}C chemical shift required the application of a decoupling ^{1}H radio-frequency field during signal acquisition.

Semiempirical Evaluation Based on the Stokes−Einstein Relationship

Beside theoretical and experimental evaluation of diffusion coefficients, some simple semiempirical relationships, chief among which is the Stokes−Einstein formula, remain valuable. The Stokes−Einstein formula relates the viscosity η (Pa.s) of a fluid at temperature T (K) to the diffusion coefficient D (m^2/s) and the hydrodynamic radius R (m) of diffusing particles assumed spherical.

$$\eta = \frac{k_B T}{6\pi D R} \quad (11)$$

This relationship could therefore be used to evaluate theoretically the viscosity of a fluid from the knowledge of the diffusion coefficient and of the hydrodynamic radius of any diffusing particle. Reciprocally, diffusion coefficients can be evaluated if an expression for the viscosity of the fluid is known. As an example, the viscosity of typical brut champagnes is sometimes considered to follow an Arrhenius-like law (*2*).

$$\eta \approx 1.08 \times 10^{-4} e^{2806/T} \quad (12)$$

Comparison between Results from MD Simulations and ^{13}C NMR Spectroscopy Measurements

Influence of Ethanol on CO_2 Diffusion

Diffusion coefficients can be safely evaluated from Eq. (8) by standard fitting procedures based on general least-squares solvers, provided that MSD curves derived from MD simulations are linear with respect to time. As illustrated in Figure 2a for CO_2 diffusion coefficients, MSD curves obtained at temperatures ranging from 277 K to 293 K with different water models (ie, the three-site SPC/E model and the five-site TIP5P model) are indeed perfectly linear and the evaluation of CO_2 diffusion coefficients is thus straightforward.

In Advances in Wine Research; Ebeler, et al.;
ACS Symposium Series; American Chemical Society: Washington, DC, 2015.

Publication Date (Web): November 24, 2015 | doi: 10.1021/bk-2015-1203.ch005

Publication Date (Web): November 24, 2015 | doi: 10.1021/bk-2015-1203.ch005

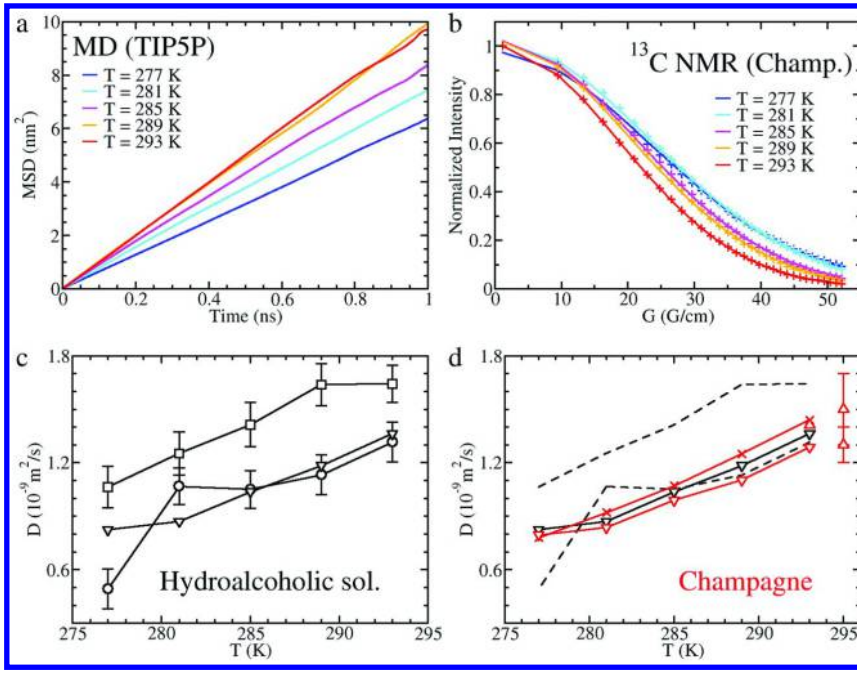

Figure 2. (a) Mean squared displacements (MSDs) of CO_2 centers of mass in a carbonated TIP5P water/ethanol mixture at different temperatures. (b) ^{13}C NMR spectra of CO_2 measured in a champagne sample. Experimental data points are reported as crosses, the curves represent the non-linear fit of the 32 data points. (c) CO_2 diffusion coefficients in carbonated hydroalcoholic solutions deduced from TIP5P MD runs (black squares), SPC/E MD runs (black circles), and ^{13}C NMR spectroscopy measurements (black downward triangles). (d) CO_2 diffusion coefficients in common Champagne wines deduced from ^{13}C NMR spectroscopy measurements (red downward triangles), NMR spectroscopy measurements from the literature (22, 23) (red upward triangles), and the Stokes-Einstein relationship of Eq. (1) (red crosses). The dashed curves refer to the TIP5P and SPC/E diffusion coefficients plotted in (c). (Adapted with permission from Ref. (24). Copyright 2014 American Chemical Society). (see color insert)

The comparative diffusion coefficients deduced from ^{13}C NMR spectroscopy measurements come from an average over the results from two independent experiments performed on different samples of carbonated hydroalcoholic solutions and Champagne wines at five temperatures (see Figure 2b), where diffusion coefficients of each sample at a given temperature are obtained by fitting the intensity of a set of 32 $^{13}CO_2$ peaks (see Figure 2b). For carbonated hydroalcoholic solutions (see Figure 2c), the CO_2 diffusion coefficients are superimposed with theoretical coefficients based on the SPC/E water model at temperatures above 285 K. The poor agreement obtained at 277 K is not

surprising since the SPC/E model is a reparameterization of the older SPC model (*13*) at temperatures around 300-310 K. It is therefore not expected to perfectly reproduce water properties at much lower temperatures, such as the peak of water density at 277 K. In contrast, the TIP5P water model yields a slight overestimation of CO_2 diffusion coefficients although the increase of these coefficients is qualitatively closer to the experimental trend. The comparison with CO_2 diffusion coefficients in champagnes reported in Figure 2d reveals that the other molecules present in champagne have little effect on the value of CO_2 diffusion coefficients although their influence on tasting sensations is essential. The diffusion coefficients obtained for carbonated hydroalcoholic solutions, both theoretically and experimentally, are indeed very close to CO_2 diffusion coefficients deduced from NMR measurements on typical brut champagnes or estimated from the Arrhenius–like law in Equation (12). This emphasizes the fact that ethanol is the main molecule, apart from water, responsible for the value of the CO_2 diffusion coefficient in typical Champagne wines; a result that can probably be extended to most sparkling wines with similar concentrations of ethanol. To the best of our knowledge, the only additional molecules that might have a significant effect on CO_2 diffusion in sparkling wines, and especially sweet ones, are sugars. In brut champagnes, the concentration of sugars is about 10 g/L (that would correspond to roughly adding 5 saccharose molecules in our simulation box) but it can rise to 50 g/L for sweet champagnes. Despite the lesser commercial relevance of sweet champagnes, the investigation of CO_2 diffusion in these liquids could confirm whether some ingredients of Champagne wines have a direct effect on both the value CO_2 diffusion coefficients and tasting sensations.

The underlying question behind the prevailing role of EtOH in explaining the value of CO_2 diffusion coefficients in champagnes concerns the origin of the interplay between CO_2 and EtOH molecules. According to generalized Fick's equations (see Equations (3a) and (3b) for instance), the flux of EtOH should depend on the gradient of concentrations of EtOH and CO_2 even if CO_2 molecules represent less than 0.5 % of the total number of molecules and might have a limited influence on the diffusion of EtOH molecules. The diffusion coefficients deduced from the fitting of EtOH MSD curves (see Figure 3a) and those derived from ^{13}C NMR spectroscopy measurements of the CH_3- or -CH_2- EtOH groups (see Figure 3b), increase steadily with temperature and lie 0.1-0.2$\times 0^{-9}$ m^2/s below the upper limit obtained for the infinite dilution of EtOH in water (see Equation (9) and Figure 3c).

The reduced diffusivity of EtOH molecules, compared with nonpolar CO_2 molecules (factor of 1.5-2 over the whole temperature range investigated here), can be attributed to its larger size and the H-bonding network they form with water molecules (*24*). The diffusion coefficients of EtOH in typical champagne wines and carbonated hydroalcoholic solutions (see Figure 3d) only differ by about 0.5 $\times$ 10^{-10} m^2/s which suggests that glycerol, sugars, and other macromolecules are probably too rare to have any significant effect on the value of EtOH diffusion coefficients.

On the contrary, nonpolar CO_2 molecules can be mostly considered as spectator in the water-ethanol mixture since the number of H bonds formed with water molecules (based on a purely geometric criterion (*25*)) is negligible

Publication Date (Web): November 24, 2015 | doi: 10.1021/bk-2015-1203.ch005

(*24*). This different interplay between EtOH, CO_2, and water molecules can also certainly account for the greater similarity between TIP5P and SPC/E results when evaluating EtOH diffusion coefficients (see Figures 2c and 3c).

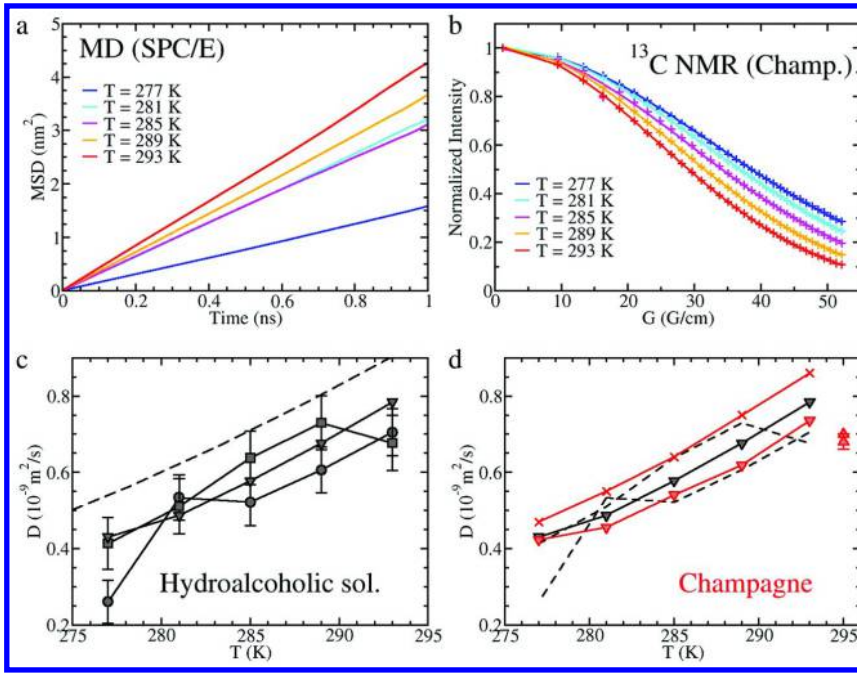

Figure 3. (a) Mean squared displacements (MSDs) of EtOH centers of mass in a carbonated SPC/E water/ethanol mixture at different temperatures. (b) ^{13}C NMR spectra of the EtOH methylene group (CH_2) measured in a champagne sample. Experimental data points are reported as crosses, the curves represent the non-linear fit of the 32 data points. (c) EtOH diffusion coefficients in carbonated hydroalcoholic solutions deduced from TIP5P MD runs (black squares), SPC/E MD runs (black circles), and ^{13}C NMR spectroscopy measurements (black downward triangles). (d) EtOH diffusion coefficients in common Champagne wines deduced from ^{13}C NMR spectroscopy measurements (red downward triangles), NMR spectroscopy measurements from the literature (23) (red upward triangles), and the Stokes-Einstein relationship of Eq. (1) (red crosses). The dashed curves refer to the TIP5P and SPC/E diffusion coefficients plotted in (c). (Adapted with permission from Ref. (24). Copyright 2014 American Chemical Society). (see color insert)

Viscosities from the Stokes-Einstein Relationship

According to the Stokes-Einstein formula presented in Equation (11), an estimation of viscosity at a given temperature can be obtained from the hydrodynamic radius and diffusion coefficient of diffusing molecules. In the

In Advances in Wine Research; Ebeler, et al.;
ACS Symposium Series; American Chemical Society: Washington, DC, 2015.

Publication Date (Web): November 24, 2015 | doi: 10.1021/bk-2015-1203.ch005

previous section we presented CO_2 and EtOH diffusion coefficients in carbonated hydroalcoholic solutions and brut champagnes as a function of temperature. In MD simulations, the hydrodynamic radius of a molecule can be identified roughly with the root-mean-squared distance of its atoms to the center of mass of the molecule. This definition might not be perfectly suitable for any molecule but it has the significant advantage to be simple and universal (*12*), and its deviation to more sophisticated theoretical or experimental definitions does not exceed 20 % for CO_2 and EtOH molecules (*24*). The hydrodynamic radii of CO_2 and EtOH would be worth ~0.95 Å and ~1.6 Å, respectively.

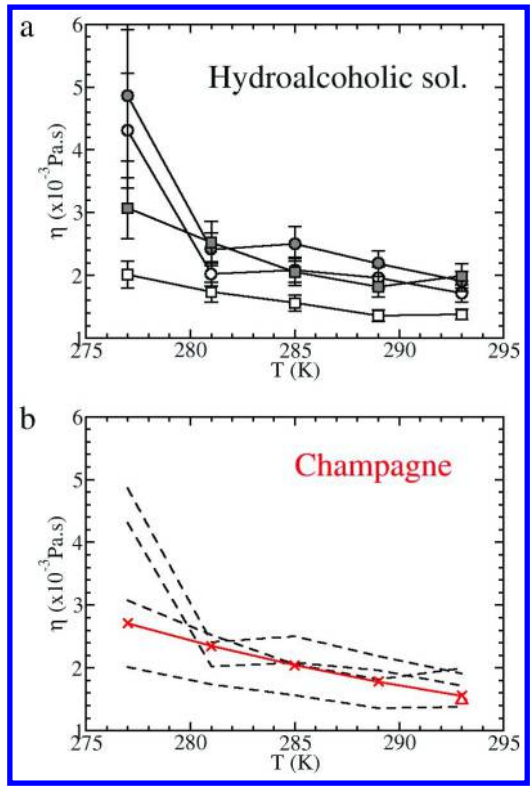

Figure 4. (a) Theoretical viscosities derived from the Stokes-Einstein relationship in Equation (1) by using MD-based CO_2 diffusion coefficients (open black symbols) and MD-based EtOH diffusion coefficients (filled black symbols) with TIP5P water molecules (squares) and SPC/E water molecules (circles). (b) Viscosities of Champagne wines based on an Arrhenius-like law (red crosses) and deduced from viscometry measurements (23) (red upward triangle). Dashed curves refer to theoretical viscosities plotted in (a). (see color insert)

Viscosities of model carbonated hydroalcoholic solutions and Champagne wines are reported in Figures 4a and 4b. The overall trend of the curve, namely a decrease when temperature increases, is well reproduced by TIP5P and SPC/E

Publication Date (Web): November 24, 2015 | doi: 10.1021/bk-2015-1203.ch005

water models despite an expected glitch at T = 277 K with the SPC/E model, that only reflects the relatively poor reliability of this model at low temperature in our MD simulations (see also Figures 2c and 3c). The Stokes-Einstein relationship can therefore be regarded as a valuable formula for evaluating viscosities, at least in first approximation.

Conclusion

In this chapter, we discussed the close interplay between CO_2 and EtOH molecules in standard brut champagnes. To achieve this goal, classical MD simulations were performed on a model carbonated hydroalcoholic solution in the *NPT* ensemble and the CO_2 diffusion coefficients were compared to results deduced from ^{13}C NMR spectroscopy measurements of carbonated hydroalcoholic solution and champagne samples. The very close agreement between theoretical and experimental CO_2 diffusion coefficients suggested that macromolecules commonly present in brut champagnes (eg, sugars, peptides, etc.) should have a much smaller effect on CO_2 diffusion coefficients than EtOH and water molecules, although they may affect tasting sensations. Even if this conclusion should hold for most sparkling wines with alike ethanol and sugar concentrations, it raises several questions on the relevance of sugars to account for CO_2 diffusion in sweet beverages, a problem that could be tackled by similar approaches as those developed in the present chapter, and on the possible use of such method to model CO_2 diffusion through the walls of cellulose fibers, nucleation sites of bubbles. In particular, unraveling the mysteries behind the latter issue would enable a precise evaluation of the frequency of bubble formation, and therefore shed some light on the whole mechanism responsible for CO_2 outgassing. It is also worth noting that some indirect experimental approaches are currently under development to evaluate the CO_2 diffusion coefficient in champagnes by measuring the increase of bubble radii (and therefore the bubble growth rate) as a function of time in the bulk. This promising method is expected to provide results compatible with MD simulations and NMR spectroscopy measurements, provided that the proper model is considered to describe the dynamics of bubbles.

Publication Date (Web): November 24, 2015 | doi: 10.1021/bk-2015-1203.ch005

References

1. Liger-Belair, G. The Physics behind the Fizz in Champagne and Sparkling Wines. *Eur. Phys. J.: Spec. Top.* **2012**, *201*, 1–88.
2. Liger-Belair, G.; Parmentier, M.; Jeandet, P. Modeling the Kinetics of Bubble Nucleation in Champagne and Carbonated Beverages. *J. Phys. Chem. B.* **2006**, *110*, 21145–21151.
3. Liger-Belair, G.; Villaume, S.; Cilindre, C.; Polidori, G.; Jeandet, P. CO_2 Volume Fluxes Outgassing from Champagne Glasses in Tasting Conditions: Flute vs Coupe. *J. Agric. Food Chem.* **2009**, *57*, 4939–4947.
4. Pozo-Bayon, M. A.; Santos, M.; Martin-Alvarez, P. J.; Reineccius, G. Influence of Carbonation on Aroma Release from Liquid Systems Using

an Artificial Throat and a Proton Transfer Reaction-mass Spectrometric Technique (PTR-MS). *Flavour Fragrance J.* **2009**, *24*, 226–233.
5. Saint-Eve, A.; Déléris, I.; Aubin, E.; Semon, E.; Feron, G.; Rabillier, J.-M.; Ibarra, D.; Guichard, E.; Souchon, I. Influence of Composition (CO_2 and Sugar) on Aroma Release and Perception of Mint-Flavored Carbonated Beverages. *J. Agric. Food Chem.* **2009**, *57*, 5891–5898.
6. Cilindre, C.; Conreux, A.; Liger-Belair, G. Simultaneous Monitoring of Gaseous CO_2 and Ethanol Above Champagne Glasses via Micro-Gas Chromatography (μGC). *J. Agric. Food Chem.* **2011**, *59*, 7317–7323.
7. Liger-Belair, G.; Cilindre, C.; Gougeon, R.; Lucio, M.; Gebefügi, I.; Jeandet, P.; Schmitt-Kopplin, P. Unraveling Different Chemical Fingerprints Between a Champagne Wine and its Aerosols. *Proc. Natl. Acad. Sci. U.S.A.* **2009**, *106*, 16545–16549.
8. Mattes, R. D.; DiMeglio, D. Ethanol Perception and Ingestion. *Physiol. Behav.* **2001**, *72*, 217–229.
9. Ryan, D.; Prenzler, P. D.; Saliba, A. J.; Scollary, G. R. The Significance of Low Impact Odorants in Global Odour Perception. *Trends Food Sci. Technol.* **2008**, *19*, 383–389.
10. Robinson, A. L.; Ebeler, S. E.; Heymann, H.; Boss, P. K.; Solomon, P. S.; Trengove, R. D. Interactions Between Wine Volatile Compounds and Grape and Wine Matrix Components Influence Aroma Compound Headspace Partitioning. *J. Agric. Food Chem.* **2009**, *57*, 10313–10322.
11. Goldner, M. C.; Zamora, M. C.; Lira, P. L.; Gianninoto, H.; Bandoni, A. Effect of Ethanol Level in the Perception of Aroma Attributes and the Detection of Volatile Compounds in Red Wine. *J. Sens. Stud.* **2009**, *24*, 243–257.
12. Perret, A.; Bonhommeau, D. A.; Liger-Belair, G.; Cours, T.; Alijah, A. CO_2 Diffusion in Champagne Wines: A Molecular Dynamics Study. *J. Phys. Chem. B.* **2014**, *118*, 1839–1847.
13. Berendsen, H. J. C.; Grigera, J. R.; Straatsma, T. P. The Missing Term in Effective Pair Potentials. *J. Phys. Chem.* **1987**, *91*, 6269–6271.
14. Mahoney, M. W.; Jorgensen, W. L. A Five-Site Model for Liquid Water and the Reproduction of the Density Anomaly by Rigid, Nonpolarizable Potential Functions. *J. Chem. Phys.* **2000**, *112*, 8910–8922.
15. Brooks, B. R.; Brooks, C. L., III; MacKerell, A. D., Jr; Nilsson, L.; Petrella, R. J.; Roux, B.; Won, Y.; Archontis, G.; Bartels, C.; Boresch, S.; Caflisch, A.; Caves, L; Cui, Q.; Dinner, A. R.; Feig, M.; Fischer, S; Gao, J.; Hodoscek, M.; Im, W.; Kuczera, K; Lazaridis, T.; Ma, J.; Ovchinnikov, V.; Paci, E.; Pastor, R. W.; Post, C. B.; Pu, J. Z.; Schaefer, M.; Tidor, B.; Venable, R. M.; Woodcock, H. L.; Wu, X.; Yang, W.; York, D. M.; Karplus, M. CHARMM: the Biomolecular Simulation Program. *J. Comput. Chem.* **2009**, *30*, 1545–1614.
16. Garcia-Ratés, M.; de Hemptinne, J.-C.; Bonet Avalos, J.; Nieto-Draghi, C. Molecular Modeling of Diffusion Coefficient and Ionic Conductivity of CO_2 in Aqueous Ionic Solutions. *J. Phys. Chem. B.* **2012**, *116*, 2787–2800.
17. Fick, A. On Liquid Diffusion. *Philos. Mag.* **1855**, *10*, 30–39.

Publication Date (Web): November 24, 2015 | doi: 10.1021/bk-2015-1203.ch005

18. Taylor, R. ; Krishna, R. In *Multicomponent Mass Transfer*; Wiley Series in Chemical Engineering; Wiley: New York, NY, 1993; pp 95−96.
19. Frenkel, D.; Smit, B. In *Understanding Molecular Simulation: from Algorithms to Applications*; Academic Press: San Diego, CA, 2002; pp 87−97.
20. Siddiqi, M. A.; Lucas, K. Correlations for Prediction of Diffusion in Liquids. *Can. J. Chem. Eng.* **1986**, *64*, 839–843.
21. Wu, D. H.; Chen, A. D.; Johnson, C. S. An Improved Diffusion-Ordered Spectroscopy Experiment Incorporating Bipolar-Gradient Pulses. *J. Magn. Reson.* **1995**, *115*, 260–264.
22. Liger-Belair, G.; Prost, E.; Parmentier, M.; Jeandet, P.; Nuzillard, J.-M. Diffusion Coefficient of CO_2 Molecules as Determined by ^{13}C NMR in Various Carbonated Beverages. *J. Agric. Food Chem.* **2003**, *51*, 7560–7563.
23. Autret, G.; Liger-Belair, G.; Nuzillard, J.-M.; Parmentier, M.; Dubois de Montreynaud, A.; Jeandet, P.; Doan, B.-T.; Beloeil, J.-C. Use of Magnetic Resonance Spectroscopy for the Investigation of the CO_2 Dissolved in Champagne and Sparkling Wines: a Nondestructive and Unintrusive Method. *Anal Chim. Acta*. **2005**, *535*, 73–78.
24. Bonhommeau, D. A.; Perret, A.; Nuzillard, J.-M.; Cours, T.; Alijah, A.; Liger-Belair, G. Unveiling the Interplay Between Diffusing CO_2 and Ethanol Molecules in Champagne Wines by Classical Molecular Dynamics and ^{13}C NMR Spectroscopy. *J. Phys. Chem. Lett.* **2014**, *5*, 4232–4237.
25. Chandler, D. Interfaces and the Driving Force of Hydrophobic Assembly. *Nature*. **2005**, *437*, 640–647.

Publication Date (Web): November 24, 2015 | doi: 10.1021/bk-2015-1203.ch005

Publication Date (Web): November 24, 2015 | doi: 10.1021/bk-2015-1203.ch006

Chapter 6

Authentication of Wine by ^{1}H-NMR Spectroscopy: Opportunities and Challenges

Susanne Esslinger, Carsten Fauhl-Hassek, and Reiner Wittkowski*

BfR Federal Institute for Risk Assessment, Department of Safety in the Food Chain - Max-Dohrn-Str. 8-10, D-10589 Berlin, Germany
***E-mail: reiner.wittkowski@bfr.bund.de. Phone: +493018412-3376.**

The verification of wine identity and authenticity is of urgent importance in the current context of a growing market globalization. As a result, wine authentication is an indispensable as well as essential aspect in today's consumer protection. Regarding its chemical analysis the matrix wine is challenging, whereas its valuable characteristics are based on different factors, such as different types of tastes, the geographical origin associated with the growing conditions, vintage and grape variety. Accordingly, the range of analytical methods to enable a comprehensive characterization of these products is highly diversified. In this context, ^{1}H-NMR spectroscopy is currently employed to characterize wine in terms of targeted as well as nontargeted analysis in only a few minutes and therefore allows the simultaneous investigation of diverse parameters. As the targeted approach enables an identification and quantification of different key ingredients in wine, the nontargeted, also called fingerprinting analysis, with subsequent statistical data evaluation investigates the whole spectrum of the matrix. Therefore, the capability to detect known adulterants, but also the ability to detect further abnormalities, and the assessment of challenging authentication parameters (grape variety, origin, vintage) appoint this technique of utmost interest for quality control, research and control institutions. Particularly concerning the nontargeted approaches, current relevant scientific literature is typically based on feasibility, demonstration or research studies within one laboratory on one instrument exclusively, which

In Advances in Wine Research; Ebeler, et al.;
ACS Symposium Series; American Chemical Society: Washington, DC, 2015.

restricts validation possibilities and degrees. Validation of the whole analytical procedure including statistical data evaluation and consistency of the measurement over time, instruments and laboratories is, however, essential for routine application and in official control. Therefore, the use of nontargeted fingerprinting approaches is due to actual missing validation strategies still restricted for official control purposes, thereby offering complex challenges for the scientific community.

Introduction

Publication Date (Web): November 24, 2015 | doi: 10.1021/bk-2015-1203.ch006

Usually, appearance, aroma, taste and mouth feeling are attributes, defining the value of a wine or respective products and effecting the consumer's acceptance, even if only unconsciously. In addition to these sensory properties, there are other product criteria, including brand, labeling of ingredients and their quantitative data, as well as the geographical origin, which are crucial in terms of the consumer's decision to buy. Not at least because of the increasing globalization of supply chains, the consumers are aware on the authenticity of a product in an increasing degree. Therefore, the requirements on food, the appropriate ingredients and their labeling are strictly regulated in the European Union (EU). In this context, the term *authentication* describes the confirmation of all requirements regarding the legal product description or the detection of the fraudulent statements (*1*, *2*) particularly in view of:

(i) the substitution by cheaper but similar ingredients,
(ii) extension of food using adulterants (e.g. water, starch including exogenous material) or blending and/or undeclared processes (e.g. irradiation, extraction),
(iii) the origin, e.g. geographic, species or method of production.

The increasing requirements on wine authentication (not at least because of the complex composition of such products), result in the need for reliable strategies in the wine control.

Actually official wine control in Europe consists of the:

- control of wine quality/fair merchantable quality: sensory and "off-flavors",
- control of statements on the label, e.g. alcohol content, quality, grape variety (blending), geographical origin, vintage,
- chemical adulterations, e.g. illegal acidification, addition of water, glycerol, alcohol, sugar, dyes, sweeteners, preservatives, flavors.

In view of these aims, the classical authenticity assessment of wine is usually based on the analysis of specific marker compounds, which are indicative for a certain property of the product. Wine authentication is therefore performed routinely (in official food control) by targeted analysis using the classic

wet-chemical approaches, e.g. stable isotope analysis by isotope ratio mass spectrometry (IRMS), site-specific natural isotopic fractionation (SNIF)- NMR® spectroscopy, Fourier-transform infrared spectroscopy (FT-IR, e.g. (*3*)), high performance liquid chromatography as well as gas chromatography (*4*).

In the last few years the nontargeted analysis, also called food fingerprinting, obtained increasingly importance (*5*), but is not yet established in official wine control. These applications are usually based on spectroscopic and spectrometric data providing the capability for a comprehensive characterization of the investigated matrices, the differentiation of the samples due to their botanical or geographical origin, the production process (e.g. organic versus conventional), the identification of adulterations etc. This strategy is based on the principle of metabonomics, describing the scientific study of small molecules, the metabolites, of a biological system based on comprehensive chemical analysis (omics technologies) with the aim to detect as many substances as possible (*6*). Because of its up-coming importance in wine authentication the general steps of nontargeted analysis are highlighted in Figure 1.

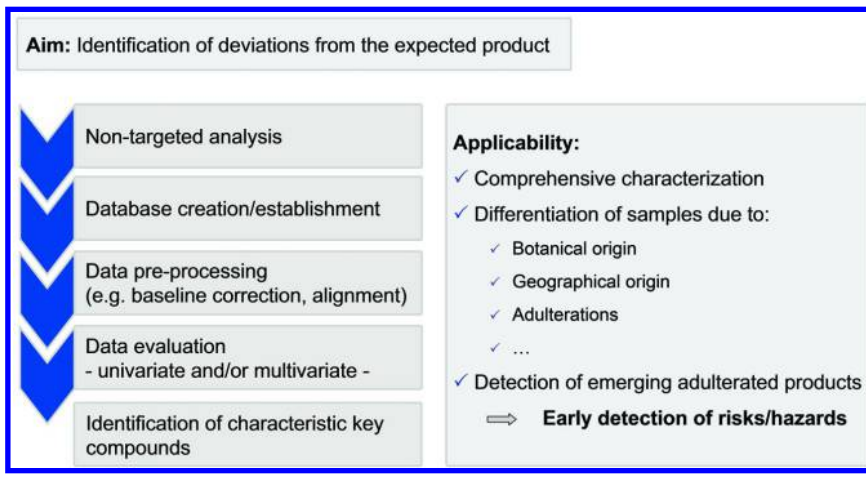

Figure 1. Schematic overview on the general steps and their applicability of nontargeted analysis.

In principle, this approach in food and wine analysis is characterized by a nontargeted, fast and easy spectroscopic or spectrometric analysis, acquiring sample specific fingerprints. These profiles are compared to a large database of authentic or typical samples using a univariate and/or multivariate statistical approach. Essential part of the statistical evaluation procedure is the data pre-processing, whereby data are often prepared, in order to transform them into a suitable form for statistical analysis. Generally, the choice for the different possibilities in data pre-processing depends strongly on the used analytical technique as well as the objective (*1*). The objectives which are pursued in the subsequent multivariate data analysis divide the respective applications in three main categories (*7*):

Publication Date (Web): November 24, 2015 | doi: 10.1021/bk-2015-1203.ch006

- data description (explorative data structure modeling),
- discrimination and classification,
- regression and prediction.

Afterwards, in dependence of the used analytical method and the statistical evaluation, it might be possible to identify compounds responsible e.g. for the differentiation or classification. Therefore, the nontargeted approach is also called a *bottom-up strategy*.

Within a comprehensive literature review by Esslinger *et al.*, where food fingerprinting studies of the last five years were analyzed, it was stated that the spectroscopic methods Near Infrared (NIR), Fourier-transform (Mid) Infrared (FT-(M)IR) and Nuclear Magnetic Resonance (NMR) spectroscopy were the most common techniques used in food fingerprinting (*1*). Compared to this, mass spectrometry (MS)-based methods were less often used, thereby applying various kinds of techniques such as direct MS (Fourier-transform ion cyclotron resonance, time-of-flight, secondary electrospray ionization and proton-transfer-reaction mass spectrometry) or MS coupled to different chromatographic separation techniques (Gas Chromatography (GC), Liquid Chromatography (LC)) as well as the direct injection (*1*).

As the following article focuses on the authentication of wine using ^{1}H-NMR spectroscopy, the topic will be discussed accordingly and from the perspective of the official wine control, illustrating the possibilities and challenges of the technique.

Publication Date (Web): November 24, 2015 | doi: 10.1021/bk-2015-1203.ch006

NMR Spectroscopy

Typically, NMR spectroscopy is used as tool for structure elucidation in organic chemistry. Super conducting magnets with very stable high magnetic fields are indispensable tools in structure elucidation since decades. The strength of the magnetic field is either expressed in Tesla (T) or by the corresponding resonance frequency of the protons in Megahertz (MHz). Apart from its function as structural elucidator NMR spectroscopy became and becomes a more and more interesting tool in metabolomics (e.g. (*8*, *9*)), nutritional (e.g. (*10*, *11*)) and food science (e.g. (*12*)) also due to its unique quantitative properties.

In relation to wine analysis the so-called SNIF-NMR® spectroscopy is well established for the detection of illegal sugar addition to must and wine (chaptalization) for more than 25 years. In fact this measurement consists in the site-specific quantification of deuterium (D) in ethanol, which is indicative for the type of the initially fermented sugar (*13*, *14*). ^{13}C-NMR spectroscopy was used by the working group of Professor A. Rapp in Germany for the quantification of wine ingredients by NMR in the 1980's (*15–17*). However, this methodology never found application in the routine analysis of wine.

Recently - during the last 10 years – quantitative ^{1}H-NMR spectroscopy for fruit juice and even more recently for wine became of interest in research but also in routine applications. Instrumental developments enable the fast and reliable quantification in combination with easy to handle NMR spectrometers

("push button") of wine ingredients as well as authentication of wine by the application of chemometrics/statistics to ^{1}H-NMR data. ^{1}H-NMR spectroscopy has a number of advantages in comparison to ^{13}C-NMR spectroscopy and other techniques but also some limitations. ^{1}H-NMR is more sensitive – based on its higher gyromagnetic ratio, higher natural abundance, compared to ^{13}C-NMR (*18*). However, due to its low spectral resolution, signal overlap occurs in ^{1}H-NMR spectroscopy and needs to be considered carefully in the spectra evaluation. In addition, it must be clearly noted as general remark that ^{1}H-NMR is not and will not be a tool for trace analysis, but the limits of detection for quantification go down to the low mg/L range for routinely used NMR instruments of the newest generation. The sensitivity depends of course on the field strength and the type of probe used (*19*). Typically in case of food and wine analysis instruments of 400 MHz up to 600 MHz are established (*20–22*). NMR spectroscopy is characterized by an excellent linearity; the generated signals are proportional to the underlying concentrations over orders of magnitudes (*19*). NMR data contain also structural information as it is used for structure elucidation, meaning that unknown signals for example might be assigned to certain compounds. Data acquisition is done in a few minutes with a reasonable signal to noise ratio including the detection of minor components. As general drawback the costs of instrumentation needs to be mentioned.

Publication Date (Web): November 24, 2015 | doi: 10.1021/bk-2015-1203.ch006

Wine Authentication by ^{1}H-NMR – Status Quo

Sample Preparation

As result of the mentioned advantages and technical progress a lot of scientific literature was published investigating the applicability of ^{1}H-NMR spectroscopy for wine authentication (*23–26*). Starting with the sample preparation of the wine matrix, several approaches have been described. Most studies investigating this topic, take typically a certain amount of the wine sample as it is (e.g. (*24*)), eventually filtration was performed. Apart from the simple addition of deuterium oxide (D_2O), which is necessary as "lock substance", buffer systems containing D_2O and often phosphate have been used for the ^{1}H-NMR analysis of wine, resulting in more stable and reproducible spectra. This application of phosphate buffer systems is already known and common practice in the metabolite profiling analysis of biofluids, e.g. urine (*19*) aiming the reduction of the pH-dependent chemical shift variation in ^{1}H-NMR spectroscopy. Son *et al.* report lyophilization as sample preparation with the benefit of getting rid of the water and ethanol signals but on the expense of a more laborious sample preparation (*26*). In order to adjust the chemical shift scale the addition of trimethylsilyl propionic acid (TSP), the water soluble correspondent to tetramethylsilane, is very often used. For quantification purposes – this is a different aim than the chemical shift adjustment – also other internal standards, e.g. anthracene (*27*, *28*) or nicotinamide (*29*) have been described.

Furthermore, a practical application using ^{1}H-NMR spectroscopy (400 MHz) in the field of wine analysis and authentication was developed and is commercially available. Joint efforts of Bruker BioSpin GmbH and SGF International e.V.

resulted in a NMR-based screening method, so-called FoodScreener™ for wine (WineScreener™) as well as for fruit juices (JuiceScreener™), combined with the Profiling™ technique (*30–33*). Within this concept, it is possible to compare actual nontargeted spectral ^{1}H-NMR data with the corresponding group of reference spectra (e.g. database of several thousands of reference juices, obtained from production sites all over the world) using verification models. The aim of the classification or verification analysis in the case of the WineScreener™ is the determination of the grape variety, geographical origin and vintage. Furthermore, the models enable the detection of any deviation from authentic reference data in the nontargeted approach. Besides a nontargeted analysis of matrix, this screening method also provides targeted results in a single measurement. Especially in wine analysis, the targeted evaluation for varieties and origins provides automatic quantification of about 30 parameters per sample. By the way for fruit juice (JuiceScreener™), currently the quantification of about 60 parameters is offered in the commercial tool.

In case of the analysis of wine, the sample preparation of the Bruker WineScreener™ protocol consists of the addition of special buffer solution containing D_2O and afterwards the pH of the wine buffer solution is carefully and very precisely adjusted by the addition of hydrochloric acid (HCl) or sodium hydroxide solution (NaOH) against a reference solution (Bruker). After the adjustment an aliquot of the solution is transferred into a NMR tube and submitted to the ^{1}H-NMR data acquisition.

A general aspect of the sophisticated NMR application (WineScreener™) is that this system shows a very high sensitivity, so that e.g. the filling height of the solution in the tube as well as the quality of the tubes play an important role. Here, e.g. the wall thickness is affecting the amount of sample in the NMR measurement coil. On the deuterium channel of the NMR instrument the magnetic field is locked and homogenized ("shimmed"). The proton channel is used for data acquisition.

^{1}H-NMR Measurement

The next step in the analysis of wine by ^{1}H-NMR spectroscopy is the actual acquisition of the NMR spectrum. Due to the composition of wine its ^{1}H-NMR spectrum is predominated by the water signal (~4.8 ppm) followed by the ethanol signals, the quartet of the methylene group and the triplet of the methyl group at 3.6 ppm and 1.2 ppm, whereas further signals are not visible at first glance in a simple ^{1}H-NMR spectrum. In NMR spectroscopy water suppression is applied in routine and in an excellent reproducible matter but in wine apart from water the ethanol is present. Thus multiple signal suppression was introduced in which the water signal plus the ethanol methylene and methyl group signals are suppressed by a so-called eightfold suppression ((*34*, *35*), Figure 2).

This routine has been perfectly integrated into the automation of spectra acquisition and results in the significant signal enhancement of the minor components. This development has been also integrated in the WineScreener™ measurement procedure. The distortion of the spectrum sections, close to the suppressed areas, remains minimal, thus signals very close to the suppressed range can be evaluated and quantified as well.

Publication Date (Web): November 24, 2015 | doi: 10.1021/bk-2015-1203.ch006

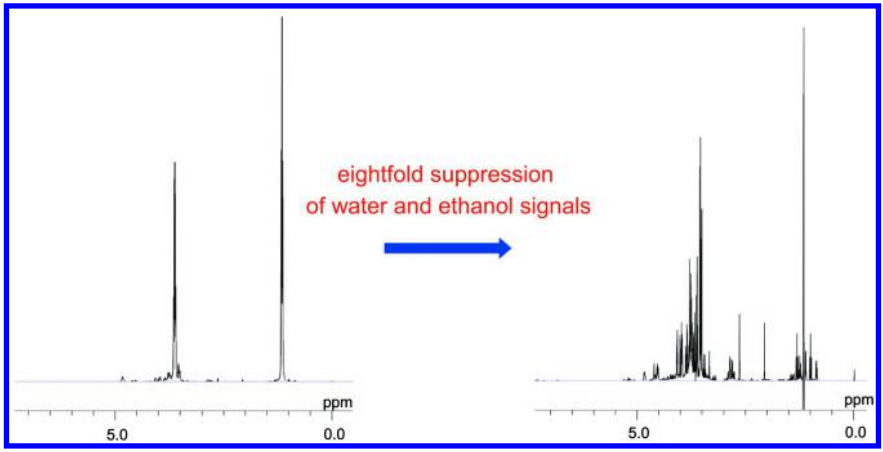

Figure 2. Presentation of the effect of eightfold suppression of water and ethanol signals in a wine sample (according to (34)), showing that the signal intensities of remaining minor wine ingredients are increased.

Particularly, in case of ^{1}H-NMR analysis of wine, pH effects for some signals, mainly for organic acids but also for other signals, were observed. As already mentioned in the previous chapter "Sample preparation", the chemical shift of certain signals varies with the pH value of the wine sample, but this phenomenon is unpredictable so far. The pH value of wine typically varies between 2.8 and 3.4 and in fact wine itself must be considered as buffer system, due to its high content of minerals and acids.

These described signal shifts cause difficulties in the subsequently performed statistical spectrum analysis, either in quantification or in multivariate statistics. For quantification particularly in automation the integration routine is often fixed to particular limits of the signal and any shift could cause miss-integration. Multivariate statistics also depend on stable chemical shifts in the NMR data, otherwise these evaluations might end up in erroneous classifications led by the wine's pH value instead of the actual considered attribute for example. The physical pH adjustment by adding acid or base is not the only way to accommodate these shifts; it can also be done mathematically by application of certain algorithms, e.g. Interval-Correlation-Shifting (ICOSHIFT (*36*);).

A further major breakthrough in NMR analysis of food and here wine was the improvement of the repeatability/reproducibility of the acquisition. In Figure 3 the overlay of 21 spectra of different preparations of one "quality control sample" (white wine) is shown.

Developments in the hardware, such as improved stability control of temperature, improvements in the phase and baseline stability and their adjustments in automation contributed to such a prominent repeatability achievable on modern NMR instruments. This data consistency and stability – in longer term view – is "the prerequisite" for further developments in the field of authentication e.g. for the creation of one common spectral database which goes behind the requirements of typical "metabonomics" application. In metabonomics

Publication Date (Web): November 24, 2015 | doi: 10.1021/bk-2015-1203.ch006

studies usually differences in the metabolites composition between samples are considered at a certain stage of time – when the measurement is performed – whereas authentication requires essentially data consistency and measurements over longer periods of time. As recently shown by Minoja and Napoli excellent reproducibility is achieved with the Bruker WineScreener™ also at different sites employing different instruments of the same type and vendor (*37*).

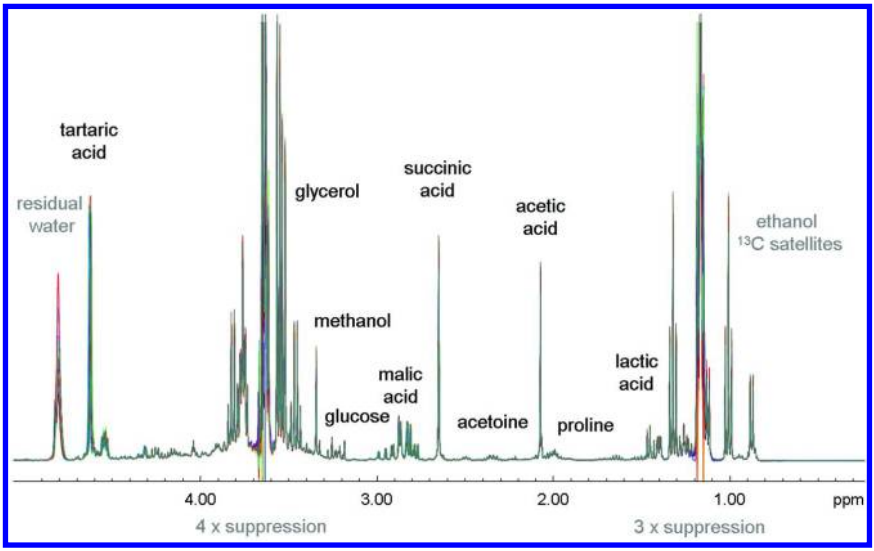

Figure 3. Overlaid [1]H-NMR spectra of 21 replicates of a "quality control sample" (white wine), showing the good reproducibility of the technique.

Targeted Data Evaluation

Subsequent to the sample preparation and analysis by [1]H-NMR, the evaluation of the acquired data takes place, whereas the quantification of ingredients is the next step, in case of targeted analysis. Very different procedures are applied for the quantification of wine ingredients by [1]H-NMR spectroscopy: use of internal standards, external/matrix calibration and standard addition are known and established quantification methodologies in classical analytical chemistry.

Further, multivariate regression models, e.g. partial least square analysis (PLS) with reference data can be used. Herein, an external matrix or parameter – typically the concentration of the wine ingredient in question – which has been determined by an external procedure, e.g. the reference method, is correlated with the NMR spectra. Signals or areas of signals which correlate will be identified and used to calibrate the multivariate model.

There are also further and more NMR specific quantification procedures described, for example the so-called PULCON (pulse length based concentration determination) method (*38*). Due to the excellent measurement stability of

Publication Date (Web): November 24, 2015 | doi: 10.1021/bk-2015-1203.ch006

modern NMR instrumentation, it is possible to determine the area per µmol proton using externally measured chemical standards (in an extra tube). A quantification of the analytes in the actual sample is then conducted by using this constant response factor and enables even the quantification of wine ingredients without any respective standard available.

However, quantification of wine ingredients by ^{1}H-NMR spectroscopy requires deep understanding of the underlying molecular structure and great care during the integration. Therefore,

1) relevant signals need to be assigned properly,
2) integration of the signal areas needs to be done with great care including the reflection of possibly overlapping signals, which might require a curve fitting procedure (e.g. deconvolution) for integration, and finally,
3) over- or underestimation effects by e.g. pulsation transfer or incomplete relaxation of certain signals of particular analytes need to be proven by extensive spiking experiments.

Publication Date (Web): November 24, 2015 | doi: 10.1021/bk-2015-1203.ch006

Nontargeted Data Evaluation

The nontargeted evaluation of the acquired spectral data needs, in most cases, dedicated statistical data pre-processing to compensate differences, e.g. slight signal shifts, unequal baselines etc.. The most widely used mathematical approach to reduce the acquired data size and to minimize peak shift effects in NMR spectroscopy for multivariate statistics is the so-called bucketing (or binning) (*1*). Bucketing is based on segmenting a spectrum into small areas (buckets/bins) and taking the area of the spectrum for each segment for further evaluation. This procedure results in a new spectrum, containing a significantly reduced number of data points. Experiments investigating the authenticity of international wines (Esslinger, Strassberger, Blaas, Fauhl-Hassek, 2013, *unpublished,* data not shown) showed that a major drawback of bucketing might be the loss of a considerable amount of information compared to the original spectra. Additionally, in some cases, the borders of the buckets are fixed and applied rigorously in automation, irrespective of potential deviations. By that, a non-correct alignment can lead to erroneous bucket loads. Larger signal shifts between different spectra, e.g. due to instrumental variations in the analysis, pH value dependent variations or changes of the salt concentration in the matrix, may lead to a larger variation in the resulting data set/matrix and obscure the identification of patterns in the data set.

Subsequent to the sample pre-processing, e.g. bucketing, statistical data evaluation is performed. For sample verification within the commercial application WineScreener™ the whole NMR profile of a specific sample is compared with the corresponding group of reference spectra (database (*39*),) at first hand explorative and univariate. For this, quantile plots are generated to visualize the respective results. By visual and/or mathematical inspection of the "fitting", this approach enables to determine deviations from the "reference data".

The inspection of the quantile plot, an example is given in Figure 4, is similar to the classical authentication process considering single parameters transposed to the whole spectral information.

Publication Date (Web): November 24, 2015 | doi: 10.1021/bk-2015-1203.ch006

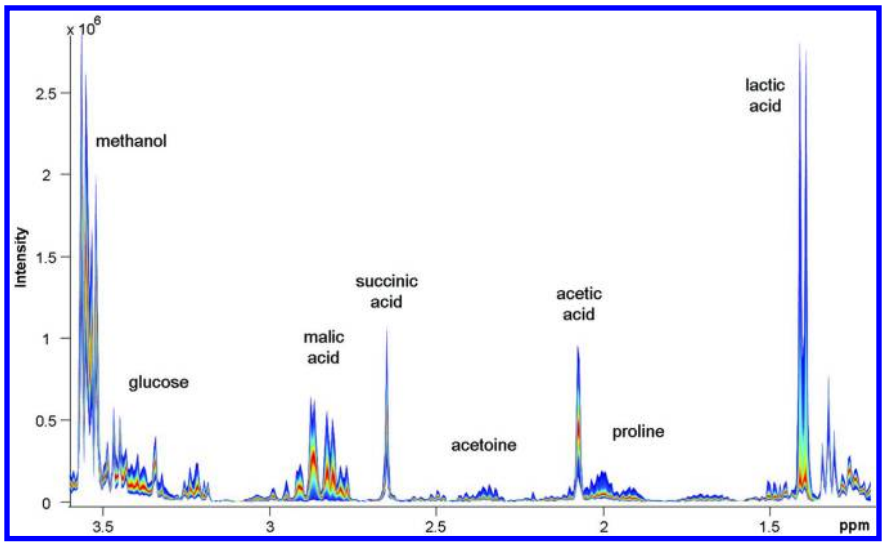

Figure 4. Quantile plot of 353 white wine samples (presented in Table 1), analyzed by ^{1}H-NMR (1.2 - 3.7 ppm); red line represents the median value; further colors are the distribution of the sample's variation. Quantile plot was generated using a MATLAB (MathWorks®) code.

In case of classical single parameter assessment, the approach consists in determining the concentration of selected natural components which are characteristic for the specific type of wine. The comparison of the data obtained with the previously established normal concentration ranges of the substance is the particular decisive factor of this assessment. The point to start with is the collection of data of authentic or unsuspicious samples. Here, authentication data of "unsuspicious samples" are collected. From these data a calculation of the authenticity range is performed usually by employing the student factor, which is a tabulated value for a certain probability and number of observations (*40*). This factor is multiplied by the standard deviation observed giving a so-called confidence interval which represents the "authenticity range". This authenticity range for single parameters is in principle similar to the quantile limits in the spectral evaluation. The next step is the comparison of the actual measurement value with the authenticity ranges. If the value fits into this range, it is unsuspicious and the sample or at least the parameter investigated is assessed to be compliant. On the other hand if the value lies outside, it is a clear indication for fraud and further investigations or actions should be carried out (*41*).

After the NMR measurement, followed by the statistical data pre-processing, the resulting data matrices comprise partially (in dependence of the chosen data pre-processing procedure) of several thousands of variables including analytical results as well as meta data (e.g. variety, geographical origin, vintage). Figure 5 shows a respective example of a data matrix after the analysis of wine by ^{1}H-NMR spectroscopy.

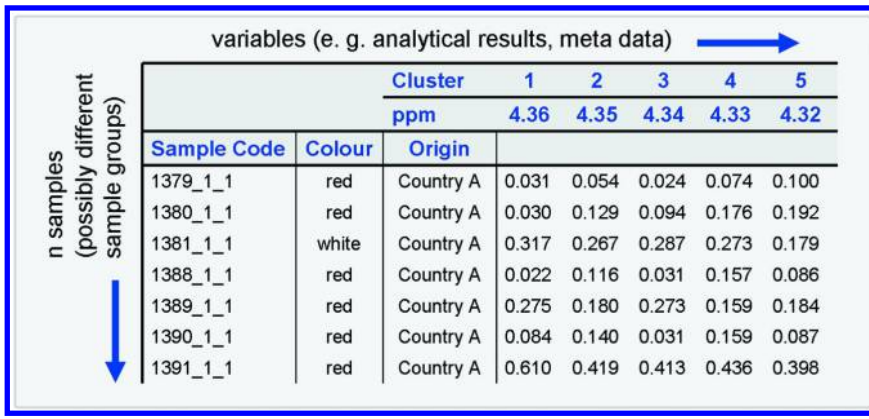

		Cluster	1	2	3	4	5
		ppm	4.36	4.35	4.34	4.33	4.32
Sample Code	Colour	Origin					
1379_1_1	red	Country A	0.031	0.054	0.024	0.074	0.100
1380_1_1	red	Country A	0.030	0.129	0.094	0.176	0.192
1381_1_1	white	Country A	0.317	0.267	0.287	0.273	0.179
1388_1_1	red	Country A	0.022	0.116	0.031	0.157	0.086
1389_1_1	red	Country A	0.275	0.180	0.273	0.159	0.184
1390_1_1	red	Country A	0.084	0.140	0.031	0.159	0.087
1391_1_1	red	Country A	0.610	0.419	0.413	0.436	0.398

Figure 5. The exemplary presentation of a data matrix after NMR analysis, including metadata, where the samples are listed line-by-line and the variables (analytical results and meta data) are mentioned column-wise.

In this case, the observations (samples) are listed line-by-line. The first columns on the left side of the table describe the respective metadata, followed by the columns including the analytical results. This matrix is fundamental for the subsequently performed multivariate data evaluation. Multivariate statistics can generally be divided in unsupervised and supervised classification methods as well as in regression methods (for quantification).

Unsupervised methods aim to identify patterns in the data that could not be derived from a *priori* available knowledge of the data. Several tools for exploring the data are available. Principal component analysis (PCA), factor analysis (FA) and hierarchical cluster analysis (HCA) are variable reduction techniques defining a number of latent variables by making linear combinations of the original variables following a given criterion. For all methods, the projections of the n objects from the original data space on a latent variable are called the scores on this latent variable (*42*).

In contrast, supervised methods use calibration or training sets with a *priori* known information (e.g. about variety or vintage) to build a classification model. Then, the model is tested using an independent sample set also with a *priori* known information to validate the predictive properties of the model before using it on unknown samples (*43*).

The most popular supervised techniques for the classification include linear discriminant analysis (LDA), soft independent modeling of class analogy (SIMCA), partial least squares–discriminant analysis (PLS-DA) and orthogonal projections to latent structures–discriminant analysis (OPLS-DA). As already mentioned, regression methods are used for multivariate calibration to quantify/predict properties of interest such as total flavonoid content, anti-oxidant activity, etc.

Publication Date (Web): November 24, 2015 | doi: 10.1021/bk-2015-1203.ch006

Excellent and very promising results have been reported by applying ^{1}H-NMR spectroscopy for some of the classical challenges in wine analysis: the proof of the grape variety and vintage. Apart from the assignment of the geographical origin these attributes are still of utmost interest in the official control of wines. Excellent differentiation between different white wine varieties was achieved by ^{1}H-NMR analysis (*31*).

Referring to the variety authentication, two examples of targeted approaches to demonstrate what currently is done and possible in official wine control should be mentioned.

a) Anthocyanin pattern
   Although similar types of anthocyanins are found in different grape varieties, the relative amounts of the individual compounds differ. For example, it has been noted that Pinot Noir grapes contain no acylated anthocyanins. These compounds have proven to be particularly characteristic for certain grape varieties, with considerable practical significance (*44*, *45*). This feature of Pinot noir wines is successfully applied for their variety control in Germany, and the differentiation of Merlot wine would be straight forward.
b) Content of shikimic acid
   In addition, for some questions the shikimic acid gives interesting information on the authenticity of the wine variety, here again the Burgundy wines including the white wine varieties show specific concentrations. For example Riesling wines are characterized by a high content in contrast to the Burgundy wines, which show a low concentration of shikimic acid. Therefore, shikimic acid is an indicator for certain varieties and can also be indicative for some others. According to the information of the German wine control the number of objections dropped down drastically after the consideration of the confidence limits for the Burgundy wines.

However, these are the only forensic applications in the targeted variety authentication of wine. Certainly there are many further open questions – concerning this topic – including red wine varieties, differentiation of Merlot/Cabernet Sauvignon, Syrah etc. and white wine varieties, e.g. Sauvignon Blanc/Chardonnay/Riesling/Silvaner/Müller-Thurgau. These questions regarding the variety proof actually can not be answered by targeted analysis.

In addition, the indication of the vintage, of very specific geographic origins and a single variety was demonstrated by using ^{1}H-NMR spectroscopy by Godelmann *et al.* (*31*). It should be noted that there is no forensic methodology for the proof of the vintage, and therefore these results are very interesting for official wine control.

It may be mentioned in this context that the measurement of the ^{14}C in ethanol has a resolution of about five years only and the activity after the extended nuclear tests in the mid sixties dropped down to the original natural level, which means that no effect can be measured nowadays. Particular the “reserva” attributes - with different obligations of storage - are of interest. Sometimes doubts about the

Publication Date (Web): November 24, 2015 | doi: 10.1021/bk-2015-1203.ch006

history of certain wines occur, by suspicious sensory analysis and/or anthocyanins pattern analysis (decreasing with ageing, polymerization), but no forensic method of analysis for vintage verification could be established in routine/control so far (*46*).

Further Research Using ^{1}H-NMR Spectroscopy for the Variety Authentication of Wine

Experimental Design

In order to tackle the variety authentication, further research was conducted (Esslinger, Strassberger, Blaas, Fauhl-Hassek, 2013, *unpublished*). The aim of this study was the development of a ^{1}H-NMR based method for a nontargeted analysis of wine to investigate the matrices with regard to authenticity. For this a set of 495 commercial wine samples was investigated. Four different red wine varieties and four different white wine varieties were considered: Merlot, Tempranillo, Pinot Noir and Syrah for the red wines and Riesling, Chardonnay, Sauvignon Blanc and Silvaner for the white wines (Table 1). The study was conducted intentionally with commercial wines.

Publication Date (Web): November 24, 2015 | doi: 10.1021/bk-2015-1203.ch006

Table 1. Overview on the Investigated Wine Samples and Respective Number of Samples (n) within the Presented Study Investigating the Variety Authentication of Wine by ^{1}H-NMR Spectroscopy and Multivariate Statistics

Red wine variety	*n*	*White wine variety*	*n*
Merlot	46	Riesling	206
Tempranillo	45	Chardonnay	49
Pinot Noir	22	Sauvignon Blanc	48
Syrah	29	Silvaner	50

In this context, it should be mentioned, that one of the main criticism of authenticity testing in general is that the data used as reference are not covering the natural diversity and that possibly some effects – biological or oenological – on the parameter in question have not been adequately investigated. Authentic samples or experimental samples (e.g. from the stable isotope databank according to Regulation (EC) 555/2008; European Union, 2008 (*13*)) of which the authenticity is "guaranteed" provide the risk that their production might differ – even only slightly – from commercial samples, and therefore may not reflect the reality sufficiently. A strong argument for using commercial samples is that all possible effects and variations are covered already and the data are therefore

fairly robust. One the other hand natural differences may be caused by authorized oenological practices, which may result in variances in the acquired spectral data, that make the statistical evaluation more difficult.

However, within the presented study, commercial wine samples were used to establish a respective sample preparation including a pre-processing of the acquired data. The samples were analyzed using a NMR spectrometer (400 MHz). The sample preparation was performed according to the WineScreener™ protocol but with slight deviations (*47*, *48*): The set of samples was prepared after the addition of a laboratory internally developed phosphate buffer including the additional pH adjustment to a value of 3.00 ± 0.04. The achieved data set was used to investigate different pre-processing methods:

- → bucketing (including different techniques as well as different bucket widths),
- → identification and elimination of outliers using PCA,
- → classification according to grape variety using PLS-DA.

Publication Date (Web): November 24, 2015 | doi: 10.1021/bk-2015-1203.ch006

Outlier Identification

Since the multivariate data analysis is based on the variance in the data space, a check with respect to the identification of outliers must be carried out in a first step. The visual inspection of all acquired spectra was performed, but only hard outliers can be detected easily as shown in Figure 6A. All spectra are overlaid (black lines), whereas the red line spectrum deviates. In this case the water suppression during the acquisition did not perform perfectly, thus this sample was re-measured. Other reasons for outlying spectra have been identified, e.g. erroneous pH adjustment or the spoilage of a sample. These types of outliers are also easily detected by applying PCA, which is typically performed to obtain an overview on the acquired data as exploratory analysis. In Figure 6B a PCA scores plot is shown, visualizing the observed outliers (red dot).

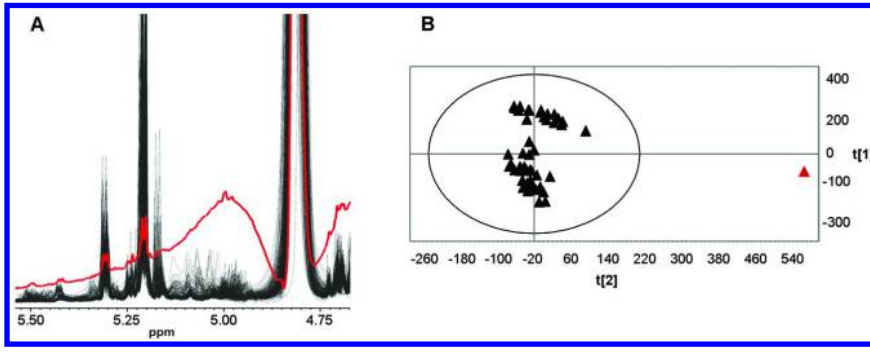

*Figure 6. Two examples of determining outliers after NMR analysis. **A**: Overlaid ^{1}H-NMR spectra, indicating one outlier (red line). **B**: Outlier identification by the use of exploratory PCA analysis. The outlier is highlighted in red.*

In Advances in Wine Research; Ebeler, et al.;
ACS Symposium Series; American Chemical Society: Washington, DC, 2015.

Publication Date (Web): November 24, 2015 | doi: 10.1021/bk-2015-1203.ch006

Quality Assurance

Quality assurance measures e.g. the inclusion of quality control samples are very important also in nontargeted analysis and should become standard. The implementation of quality control samples serves as control of the whole performance of the approach (including the sample preparation and NMR measurement) with regard to its repeatability and variance.

Moreover, the quality control (QC) sample should have a certain shelf life and thus be stable over the observation period. Compared to targeted analysis, where only the analyte or a group of compounds of interest has to be free of decomposition or degradation, in nontargeted analysis, the stability of the matrix itself has to be ensured. This is difficult because most foods are subject to alteration and spoilage over a certain period of time (*1*).

In general, it must be noted that the basic prerequisite for any reliable mathematical model is that the variance of the QC sample replicates (sample preparation and measurement) must be smaller than the natural variance of the "authentic" samples, as demonstrated in this PCA scores plot in Figure 7.

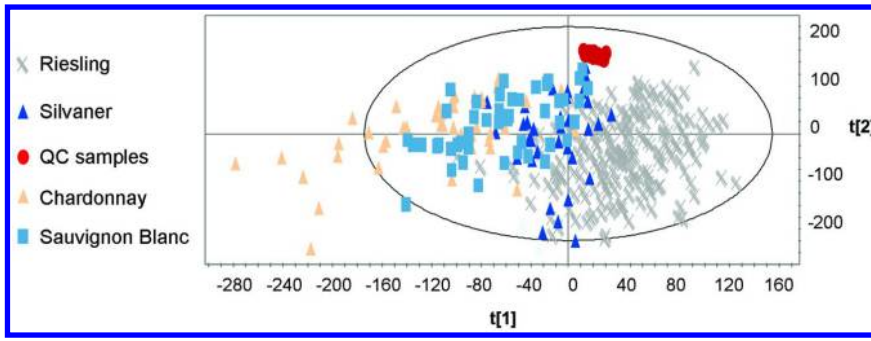

Figure 7. Exemplary presentation of a PCA scores plot of investigated wine samples, including the quality control (QC) samples, showing their small variance compared to the other "authentic" samples.

Furthermore, using a QC sample, which should be of a similar composition as the investigated authentic samples, and exploratory analysis (e.g. PCA) a possible time dependent drift might also be detectable. As an example, Nietner *et al.* investigated feed material using nontargeted FT-IR spectroscopy and used starch, which is a main component of the investigated matrix, as QC sample (*49*).

Within the presented investigations of wine samples, a commercial white wine was used as QC sample, which was prepared and analyzed twice a day. The subsequent evaluation of the acquired spectral data focused on the performance of the technical equipment (NMR), e.g. with regard to the performed water suppression and the used shim quality as well as the sample preparation, e.g. imprecise pH value adjustment. For this, several parameters (integral of malic acid and glucose signal, chemical shift of tartaric acid and TSP, as well as the peak width at half-height of the TSP signal) were used to create Shewhart control

charts. As an example the "Upper Control Limit - Lower Control Limit"-range of the chemical shift of tartaric acid was calculated at 4.625 ppm ± 0.008 ppm. In case of exceeding these ranges, the causes have to be found and removed. In a second step, the multivariate evaluation of the analyzed control samples (as mentioned in this chapter) took place.

Data Evaluation

After identification of outliers and monitoring the QC sample, a further PCA was performed to get an overview on the present data set. The respective scores plot (Figure 8) representing the explained variance of the data, shows the entire data set in multivariate space.

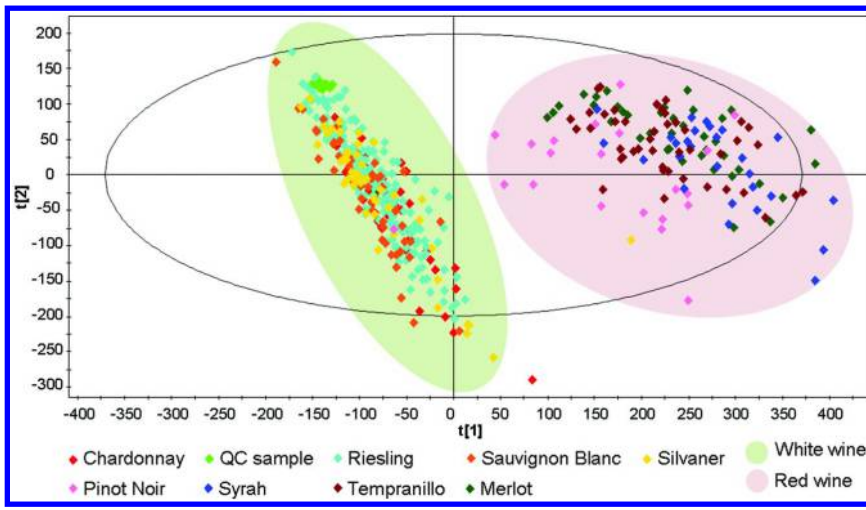

Figure 8. PCA scores plot (over the first two principal components), calculated with all analyzed wine samples, colored by variety, showing a grouping of red wines (right side) and white wine (left side).

Within this model, the data points have been colored according to the variety of the respective wine samples showing a clear separation of red wine (right group) varieties and white wine varieties (left group). Therefore, the main variance of the data set is based on the differences between red and white wine. The differentiation between these two groups is already of high interest due to notifications about the illegal addition of white wine to red wine as well as decolorized red wine to white wine in dependence to the market/consumer preference. Particularly, the addition of small proportions of white wines to red wine is challenging for the analytical chemist. Perceptively, the development of a decision cascade/tree might be of interest, e.g. the differentiation between red and white wine, followed by the possibility to distinguish between several varieties. Thereafter, objectives like geographical origin and vintage might be of interest.

Publication Date (Web): November 24, 2015 | doi: 10.1021/bk-2015-1203.ch006

Subsequent to the exploratory analysis of the data set (by PCA), in many cases, a classification/regression model was developed. In order to avoid over-fitted models, the appropriate validation of the mathematical models is essential in the application of multivariate statistics. Only the validation enables the reliable and sustainable development of models to be used in control. One fair option for doing so is the creation of two data sets, one training set, comprising of e.g. 2/3 of the analyzed samples which is used to generate the classification model and one independent test set of e.g. 1/3 of the data to proof the prediction ability of the model. This approach is called "external validation". Within the presented study, the total data set, consisting of about 500 wine samples, was divided into two separate models of white wine varieties and red wine varieties, respectively. Afterwards, PLS-DA was applied as classification method to the training data set. Due to the fact, that PLS-DA is a supervised method, different classes were generated in each model, each for one variety. The application of these models to the test set resulted in correct classification rates between about 70% and 98%. Although the commercial application WineScreenerTM reports better classification results on the similar varieties, our results appear encouraging for further investigations.

Publication Date (Web): November 24, 2015 | doi: 10.1021/bk-2015-1203.ch006

Future Challenges

Validation Procedures

The validation of an analytical method serves the "confirmation by examination and the provision of objective evidence that the particular requirements for a specific intended use are fulfilled" (European Standard EN ISO / IEC 17025: 2005; International Organization for Standardization, 2005 (*50*)). This allows preparing the operational readiness of the developed method in routine analysis as well as its ensuring by statistically based quality assurance measures.

With regard to the preventive consumer protection, it is necessary/essential for laboratories of official food control that non-standardized or in-house developed analytical methods are validated to confirm that the methods are suitable for the intended use. The validation of these methods comprises the complete analytical procedure from e.g. the sampling or sample extraction to statistical evaluation of acquired data. Its extend should be set according to the need to fulfill the requirements of the intended use or the relevant application area. Common validation parameters are e.g. the determination of the linearity range, the limits of detection and quantification, accuracy, precision, trueness, robustness as well as the calculation of the measurement uncertainty. In few areas, e.g. pesticides or pharmacological drugs, requirements and parameters to validate respective analytical methods are precisely defined.

Validation of nontargeted approaches is neither defined nor scientifically agreed, classical terms such as: limit of detection, limit of quantification, accuracy, trueness, precision, measurement uncertainty do not fit. Therefore, new validation strategies are needed for nontargeted fingerprinting, completely new

concepts required, including the definition of the relevant questions. So-called "good practice" procedures for the model validation of nontargeted methods are needed, on the conduction itself but also for the publication of such studies. With special regard to this latter point, parameters and indicators need to be determined and stated when published, e.g. the principal mention of the analyzed number of samples, the used validation procedure or the size of the final matrix, which was used for the development of the mathematical model. The scientific community has realized these needs and certain activities e.g. in the similar field of metabolomics started (*51*, *52*).

Publication Date (Web): November 24, 2015 | doi: 10.1021/bk-2015-1203.ch006

Detection of the Unknown

A general point of discussion is the ability to detect known but also unknown adulterations using the respectively established mathematical model. Typical multivariate statistics (e.g. DA, LDA, PLS-DA, SIMCA) perform better with a previous training (by internal or external validation) of the adulteration of interest. That implies that the respective deviation from the product is already known. Using these trained models to detect currently unknown adulterations that have not been trained, one may run into danger to get false-positive or false-negative results. Further investigations are needed to identify and establish mathematical models which enable the reliable detection of known and unknown deviations from a typical food product.

Some approaches try to resolve this particular problem – detecting the unknown – by univariate data evaluation, e.g. quantile plot, z-score, or by single parameters derived from the multivariate statistical process control, e.g. Mahalanobis distance, Distance to the model of X-space (DModX). Zhang and Nie exclusively used the Mahalanobis distance to classify the adulterated samples of *Radix Astragali* (Chinese medicine) as acceptable or unacceptable for the known data set (*53*). This tool is similar to the Euclidean distance, but takes into account that some variables may be correlated and therefore, measure more or less the same properties (*54*).

A further technique to detect adulterations (moderate outliers) is by consideration of the model residuals (DModX). DModX describes the distance of the observation to the X model plane ore hyper plane and is also known as the residual error or the residual standard deviation (*7*, *55*). The evaluation of the results is similar to the Mahalanobis distance approaches. For this, evaluation criteria are to be defined, e.g. the maximum value of DModX for the unadulterated/authentic samples is to be considered as threshold above which a test sample could be considered as suspect. The investigations of chemical contaminations in carbonated soft drinks (by NMR spectroscopy (*55*);) as well as of melamine adulterations of soya bean meal (by NIR (*56*);) showed that the identification of moderate outliers using DModX parameter from a SIMCA model is particularly suitable for the detection of contaminations without previous knowledge of their identity.

In general, multivariate data analysis of fingerprints has some advantages compared to univariate statistics of e.g. single components of the fingerprints (*57*, *58*). Advantageous in first instance is the fact that the whole spectra information detected with the nontargeted approach is used. Nonetheless, also univariate statistical approaches were used to evaluate the data sets.

Despite these alternatives, further investigations are needed to identify and establish mathematical models which enable the reliable detection of known and unknown deviations from a typical food product including wine.

Data Consistency and Exchangeability

Publication Date (Web): November 24, 2015 | doi: 10.1021/bk-2015-1203.ch006

Data consistency is a very important issue in nontargeted authenticity studies, including NMR methodologies. The typical procedure in case of nontargeted NMR studies as well as in other nontargeted studies consists of several steps: the method development (including sample preparation, measurement protocol, standardized data processing) and evaluation takes place in one laboratory (the usual situation is that only one high-tech e.g. NMR instrument is present), ending up in a "measurement procedure". By this kind of procedure a defined set of samples is analyzed and evaluated. As mentioned earlier the validation of the procedure should be conducted according to the "good practice" which is to be defined. In this relation only in some studies quality control samples are analyzed with the set of samples and considered in the process to monitor the consistency and stability of the whole procedure over the measurement period. Also only in some occasions the model is extended by the later measurement of further samples (e.g. in a second batch at different point of time), sometimes this important fact in view of data consistency is simply not stated.

Considering the "one laboratory" approach, from a more global point of view it should be mentioned that many research studies and publications end with the measurement of one series of samples, often obtained within a project. Although very interesting results are obtained, only a few studies include the measurement of more batches.

However, what was introduced with Bruker WineScreener™, is a proprietary measurement procedure, what means that a second laboratory and also further laboratories, equipped with the same instrument, can use the data together. This fact must be acknowledged and according to the author's present knowledge this is very unique in the area of nontargeted analysis.

Although considerable efforts and results in this field, this theme needs to be further strengthened and further investigations should be conducted, especially in view of the application of the nontargeted analysis and its comparability after using analytical instruments e.g. from different vendors. Especially with regard to the establishment of these approaches in the official wine control, it is to be considered that standard setting organizations such as Codex Alimentarius and the International Organisation of Vine and Wine (OIV) adapt proprietary methods only, if specified prerequisites are given.

Publication Date (Web): November 24, 2015 | doi: 10.1021/bk-2015-1203.ch006

Conclusion

^{1}H-NMR has a lot of very interesting capabilities. It is fast, the quantification of many wine ingredients is possible within one analytical run resulting in a cost efficient analysis, substituting other methods of analysis (HPLC/GC etc.). These advantages are overshadowed by the high investment costs for the analytical instrumentation.

Besides the high linearity range of this method, it should be mentioned that the NMR spectroscopy is not able to detect compounds in lower concentrations (trace analysis). But the classical wine analysis/control is focused only partially on trace compounds. In addition, the quantitative NMR analysis is a so-called primary reference measurement procedure, enabling the quantification of compounds without relation to (similar) standards.

The nontargeted analysis by ^{1}H-NMR can potentially serve the authentication of wine samples with regard to the discrimination between e.g. varieties, vintages or geographical origin, in complementation of established targeted methods. Furthermore, there are indications that the NMR analysis may allow the accomplishment of so far open challenges in wine control, e.g. the investigation of the labeled vintage.

Nevertheless, the forensic application in official control requires the appropriate validation of such a nontargeted methodology. Standard procedures have to be identified and agreed scientifically as discussed in this contribution. In addition, further concepts for the use of common data bases need to be developed. Particularly the data sharing/ownership/maintenance between different users, including official control, requires further discussions.

References

1. Esslinger, S.; Riedl, J.; Fauhl-Hassek, C. Potential and limitations of non-targeted fingerprinting for authentication of food in official control. *Food Res. Int.* **2014**, *60*, 189–204.
2. MoniQA. *Food Authenticity - General considerations*; 2013; URL http://www.moniqa.eu/authenticity (date accessed: June 2014).
3. Patz, C. D.; Blieke, A.; Ristow, R.; Dietrich, H. Application of FT-MIR spectrometry in wine analysis. *Anal. Chim. Acta* **2004**, *513*, 81–89.
4. Schlesier, K.; Fauhl-Hassek, C.; Forina, M.; Cotea, V.; Kocsi, E.; Schoula, R.; van Jaarsveld, F.; Wittkowski, R. Characterisation and determination of the geographical origin of wines. Part I: overview. *Eur. Food Res. Technol.* **2009**, *230*, 1–13.
5. Esslinger, S.; Lahrssen-Wiederholt, M.; Fauhl-Hassek, C. Fingerprinting: An innovative approach in the wine analysis [Fingerprinting: Ein innovativer Ansatz in der Weinanalytik]. *Dtsch. Lebensm.-Rundsch.* **2012**, *108*, 457–462.
6. Roessner, U.; Nahid, A.; Chapman, B.; Hunter, A.; Bellgrad, M. Metabolomics - The Combination of Analytical Biochemistry, Biology, and Informatics. In *Comprehensive Biotechnology*; Scientific Fundamentals of

Biotechnology; Murray, M.-Y., Ed.; Elsevier: Amsterdam, 2011; Vol. 1, pp 447−459.
7. Eriksson, L.; Johansson, E.; Kettaneh-Wold, N.; Trygg, J.; Wikström, C.; Wold, S. *Multi- and Megavariate Data Analysis Part I Basic Principles and Applications*; Umetrics AB: Umeå, SW 2006.
8. Emwas, A.-H.; Salek, R.; Griffin, J.; Merzaban, J. NMR-based metabolomics in human disease diagnosis: applications, limitations, and recommendations. *Metabolomics* **2013**, *9*, 1048–1072.
9. Duarte, I. F.; Diaz, S. O.; Gil, A. M. NMR metabolomics of human blood and urine in disease research. *J. Pharm. Biomed. Anal.* **2014**, *93*, 17–26.
10. Fischman, A. J.; Tompkins, R. G. Perspective on the applications of NMR in nutrition. *Trends Food Sci. Technol.* **1992**, *3*, 220–225.
11. Rezzi, S.; Ramadan, Z.; Fay, L. B.; Kochhar, S. Nutritional Metabonomics: Applications and Perspectives. *J. Proteome Res.* **2007**, *6*, 513–525.
12. Spyros, A.; Dais, P. *NMR Spectroscopy in Food Analysis*; RSC Food Analysis Monographs No. 10; Royal Society of Chemistry: Cambridge, U.K., 2013; pp 1−329.
13. European Union. Commission Regulation (EC) No. 555/2008 laying down detailed rules for implementing Council Regulation (EC) No. 479/2008 on the common organisation of the market in wine as regards support programmes, trade with third countries, production potential and on controls in the wine sector. *Off. J. Eur. Union L* **2008**, *170*, 1–80.
14. OIV. *International Organisation of Vine and Wine. Compendium of International Methods of Analysis of Wines and Musts*; 2013; URL http://www.oiv.int/oiv/info/enmethodesinternationalesvin (date accessed: June 2014).
15. Rapp, A.; Markowetz, A.; Spraul, M.; Humpfer, E. Application of ^{13}C-NMR-Spectroscopy in wine analysis [Anwendung der ^{13}C-NMR-Spektroskopie in der Weinanalytik]. *Fresenius' Z. Anal. Chem.* **1988**, *330*, 462–463.
16. Rapp, A.; Markowetz, A.; Spraul, M.; Humpfer, E. Detection and quantitative determination of sugar, sugar alcohols and sugar acids in wine by ^{13}C-NMR-spectroscopy [Nachweis und quantitative Bestimmung von Zuckern, Zuckeralkoholen und Zuckersäuren im Wein mit ^{13}C-NMR-Spektroskopie]. *Z. Lebens.-Unters. Forsch.* **1989**, *188*, 138–143.
17. Rapp, A.; Spraul, M.; Humpfer, E. Determination of diethylene glycol in wine with ^{13}C NMR-spectroscopy [^{13}C NMR-spektroskopische Bestimmung von Diethylenglykol im Wein]. *Z. Lebens.-Unters. Forsch.* **1986**, *182*, 419–421.
18. Fauhl, C.; Wittkowski, R. Hochauflösende Kernresonanz-Spektroskopie (NMR). In *Schnellmethoden zur Beurteilung von Lebensmitteln und ihren Rohstoffen*; Baltes, W., Kroh, L. W., Eds.; Behr's Verlag: Hamburg, 2004; pp 229−250.
19. Ross, A.; Schlotterbeck, G.; Dieterle, F.; Senn, H. NMR Spectroscopy Techniques for Application to Metabonomics. In *The Handbook of Metabonomics and Metabolomics*; Lindon, J. C., Nicholson, J. K., Holmes, E., Eds.; Elsevier Science B.V.: Amsterdam, 2007; Chapter 3, pp 55−112.

Publication Date (Web): November 24, 2015 | doi: 10.1021/bk-2015-1203.ch006

20. Monakhova, Y.; Schütz, B.; Schäfer, H.; Spraul, M.; Kuballa, T.; Hahn, H.; Lachenmeier, D. Validation studies for multicomponent quantitative NMR analysis: the example of apple fruit juice. *Accredit. Qual. Assur.* **2014**, *19*, 17–29.
21. Monakhova, Y. B.; Kuballa, T.; Lachenmeier, D. W. Chemometric methods in NMR spectroscopic analysis of food products. *J. Anal. Chem.* **2013**, *68*, 755–766.
22. Lachenmeier, D. W.; Humpfer, E.; Fang, F.; Schütz, B.; Dvortsak, P.; Sproll, C.; Spraul, M. NMR-Spectroscopy for Nontargeted Screening and Simultaneous Quantification of Health-Relevant Compounds in Foods: The Example of Melamine. *J. Agric. Food Chem.* **2009**, *57*, 7194–7199.
23. Koda, M.; Furihata, K.; Wei, F.; Miyakawa, T.; Tanokura, M. NMR-Based Metabolic Profiling of Rice Wines by F 2-Selective Total Correlation Spectra. *J. Agric. Food Chem.* **2012**, *60*, 4818–4825.
24. Larsen, F. H.; van den Berg, F.; Engelsen, S. B. An exploratory chemometric study of ^{1}H NMR spectra of table wines. *J. Chemom.* **2006**, *20*, 198–208.
25. Papotti, G.; Bertelli, D.; Graziosi, R.; Silvestri, M.; Bertacchini, L.; Durante, C.; Plessi, M. Application of One- and Two-Dimensional NMR Spectroscopy for the Characterization of Protected Designation of Origin Lambrusco Wines of Modena. *J. Agric. Food Chem.* **2013**, *61*, 1741–1746.
26. Son, H. S.; Hwang, G. S.; Ahn, H. J.; Park, W. M.; Lee, C. H.; Hong, Y. S. Characterization of wines from grape varieties through multivariate statistical analysis of ^{1}H NMR spectroscopic data. *Food Res. Int.* **2009**, *42*, 1483–1491.
27. Choi, Y. H.; Choi, H.-K.; Peltenburg-Looman, A. M. G.; Lefeber, A. W. M.; Verpoorte, R. Quantitative analysis of ginkgolic acids from Ginkgo leaves and products using ^{1}H-NMR. *Phytochem. Anal.* **2004**, *15*, 325–330.
28. Kim, H. K.; Choi, Y. H.; Chang, W.-T.; Verpoorte, R. Quantitative analysis of ephedrine analogues from *Ephedra* species using ^{1}H-NMR. *Chem. Pharm. Bull.* **2003**, *51*, 1382–1385.
29. Jiao, P.; Jia, Q.; Randel, G.; Diehl, B.; Weaver, S.; Milligan, G. Quantitative ^{1}H-NMR spectrometry method for quality control of *Aloe vera* products. *J. AOAC Int.* **2010**, *93*, 842–848.
30. BioSpin, B. *JuiceScreener - Enabling SGF Profiling*™; 2012; URL http://www.bruker-biospin.com/juicescreener-dir.html (date accessed: June 2014).
31. Godelmann, R.; Fang, F.; Humpfer, E.; Schütz, B.; Bansbach, M.; Schäfer, H.; Spraul, M. Targeted and Nontargeted Wine Analysis by ^{1}H NMR Spectroscopy Combined with Multivariate Statistical Analysis. Differentiation of Important Parameters: Grape Variety, Geographical Origin, Year of Vintage. *J. Agric. Food Chem.* **2013**, *61*, 5610–5619.
32. Spraul, M.; Schütz, B.; Rinke, P.; Koswig, S.; Humpfer, E.; Schäfer, H.; Mörtter, M.; Fang, F.; Marx, U.; Minoja, A. NMR-based multi parametric quality control of fruit juices: SGF profiling. *Nutrients* **2009**, *1*, 148–155.
33. SGF. *SGF International e.V. SGF Profiling*; (2012; URL http://www.sgf.org/en/home/forschung-und-projekte/profiling/ (date accessed: June 2014).
34. Monakhova, Y. B.; Schäfer, H.; Humpfer, E.; Spraul, M.; Kuballa, T.; Lachenmeier, D. W. Application of automated eightfold suppression of

water and ethanol signals in ^{1}H NMR to provide sensitivity for analyzing alcoholic beverages. *Magn. Reson. Chem.* **2011**, *49*, 734–739.
35. Monakhova, Y. B.; Mushtakova, S. P.; Kuballa, T.; Lachenmeier, D. W. Investigation into the structural composition of hydroalcoholic solutions as basis for the development of multiple suppression pulse sequences for NMR measurement of alcoholic beverages. *Magn. Reson. Chem.* **2014** DOI:10.1002/mrc.4129.
36. Savorani, F.; Tomasi, G.; Engelsen, S. B. icoshift: A versatile tool for the rapid alignment of 1D NMR spectra. *J. Magn. Reson.* **2010**, *202*, 190–202.
37. Minoja, A. P.; Napoli, C. NMR screening in the quality control of food and nutraceuticals. *Food Res. Int.* **2014**, *63* (Part B), 126–131.
38. Wider, G.; Dreier, L. Measuring Protein Concentrations by NMR Spectroscopy. *J. Am. Chem. Soc.* **2006**, *128*, 2571–2576.
39. Bruker. *Non-Targeted Analysis/Verification*; 2014; URL http://www.bruker.com/products/mr/nmr/food-screener/winescreener/applications.html (date accessed: October 2014).
40. Miller, J. N.; Miller, J. C. *Statistics and Chemometrics for Analytical Chemistry*, 4th ed.; Prentice Hall: Harlow, U.K., 2000; pp 1−271.
41. Fauhl, C. Measurement uncertainty in wine appreciation. *Mitt. Klosterneuburg* **2006**, *56*, 3–13.
42. Esbensen, K. H.; Guyot, D.; Westad, F.; Houmøller, L. P. *Multivariate Data Analysis - in Practice : an Introduction to Multivariate Data Analysis and Experimental Design*; CAMO: Oslo, 2002; pp 1−598.
43. Massart, D. L.; Vandeginste, B. G. M.; Deming, S. N.; Michotte, Y.; Kaufman, L. *Chemometrics: A Textbook*; Elsevier: Amsterdam, 1988; pp 1−488.
44. Revilla, E.; García-Beneytez, E.; Cabello, F.; Martín-Ortega, G.; Ryan, J.-M. Value of high-performance liquid chromatographic analysis of anthocyanins in the differentiation of red grape cultivars and red wines made from them. *J. Chromatogr. A* **2001**, *915*, 53–60.
45. Holbach, B.; Marx, R.; Zimmer, M. Bedeutung der Shikimisäure und des Anthocyanspektrums für die Charakterisierung von Rebsorten. *Lebensmittelchemie* **2001**, *55*, 32–34.
46. Asenstorfer, R. E.; Jones, G. P.; Laurence, G.; Zoppi, U. Authentication of Red Wine Vintage Using Bomb-Pulse ^{14}C. In *Progress in Authentication of Food and Wine*; Ebeler, S. E., Takeoka, G. R., Winterhalter, P., Eds.; ACS Symposium Series 1081; American Chemical Society: Washington, DC, 2011; Chapter 6, pp 89−99.
47. Spraul, M. Uncovering the truth: wine analysis with next generation NMR screening. *The Resonance*; 2014; URL http://www.theresonance.com/ (date accessed: June 2014).
48. Heintz, L.; Godelmann, R.; Cannet, C.; Fang, F.; Humpfer, E.; Schuetz, B.; Schäfer, H.; Spraul, M. Differentiation of Wine Grape Varieties Using 1H-NMR Profiling. *The Resonance*; 2013; URL http://www.theresonance.com/ (date accessed: June 2014).
49. Nietner, T.; Pfister, M.; Glomb, M. A.; Fauhl-Hassek, C. Authentication of the Botanical and Geographical Origin of Distillers Dried Grains and

Publication Date (Web): November 24, 2015 | doi: 10.1021/bk-2015-1203.ch006

Solubles (DDGS) by FT-IR Spectroscopy. *J. Agric. Food Chem.* **2013**, *61*, 7225–7233.
50. ISO International Organization for Standardization. *ISO/IEC 17025:2005 General requirements for the competence of testing and calibration laboratories*; 2005.
51. MSI. *The Metabolomics Standards Initiative (MSI)*; 2014; URL http://msi-workgroups.sourceforge.net/ (date accessed: October 2014).
52. Naz, S.; Vallejo, M.; García, A.; Barbas, C. Method validation strategies involved in non-targeted metabolomics. *J. Chromatogr. A* **2014**, *1353*, 99–105.
53. Zhang, L.; Nie, L. Discrimination of geographical origin and adulteration of radix astragali using fourier transform infrared spectroscopy and chemometric methods. *Phytochem. Anal.* **2010**, *21*, 609–615.
54. Brereton, R. G. *Chemometrics: Data Analysis for the Laboratory and Chemical Plant*, John Wiley & Sons Ltd: Chichester, U.K., 2003; pp 1−489.
55. Charlton, A. J.; Robb, P.; Donarski, J. A.; Godward, J. Non-targeted detection of chemical contamination in carbonated soft drinks using NMR spectroscopy, variable selection and chemometrics. *Anal. Chim. Acta* **2008**, *618*, 196–203.
56. Haughey, S. A.; Graham, S. F.; Cancouët, E.; Elliott, C. T. The application of Near-Infrared Reflectance Spectroscopy (NIRS) to detect melamine adulteration of soya bean meal. *Food Chem.* **2013**, *136*, 1557–1561.
57. Olivieri, A. C. Analytical Advantages of Multivariate Data Processing. One, Two, Three, Infinity? *Anal. Chem.* **2008**, *80*, 5713–5720.
58. Trygg, J.; Gullberg, J.; Johansson, A. I.; Jonsson, P.; Moritz, T. Chemometrics in Metabolomics - An Introduction. In *Plant Metabolomics*; Saito, K., Dixon, R., Willmitzer, L., Eds.; Springer: Berlin, 2006; pp 117−128.

Publication Date (Web): November 24, 2015 | doi: 10.1021/bk-2015-1203.ch006

Publication Date (Web): November 24, 2015 | doi: 10.1021/bk-2015-1203.ch007

Chapter 7

Effect of Region on the Volatile Composition and Sensory Profiles of Malbec and Cabernet Sauvignon Wines

H. Heymann,* A. L. Robinson, F. Buscema, M. E. Stoumen, E. S. King, H. Hopfer, R. B. Boulton, and S. E. Ebeler

Department of Viticulture and Enology, University of California-Davis, One Shields Avenue, Davis, California 95616
***E-mail: hheymann@ucdavis.edu.**

Regionality, frequently called *terroir*, is often used as a way to market wines from different locations. In this chapter we will discuss the chemical and sensory effects of regionality using thirty commercially made Australian Cabernet Sauvignon wines as well as forty one research lots of Californian and Argentinean Malbec wines. In both studies the volatile profiles of the wines separated the regions from one another. The separations based solely on sensory descriptive analysis data was less clear cut for the Cabernet wines and more so for the Malbec wines. When the volatile chemical and sensory data were combined separating regions was possible for both sets of wines. These studies showed that for both very well controlled research fermentations and for less controlled commercial fermentations it is possible to determine sensory and chemical regional differences for wines.

In Advances in Wine Research; Ebeler, et al.;
ACS Symposium Series; American Chemical Society: Washington, DC, 2015.

Publication Date (Web): November 24, 2015 | doi: 10.1021/bk-2015-1203.ch007

The effect of region on the quality of wine is a very old concept as seen by the writings of Pliny and Columella (*1*). Around 1825 James Busby stated "… we sometimes see, under the same climate, very different qualities of wine, because the differences of soil, exposure, or culture, modify the immediate influence of this grand agent" (*2*). In the more modern era the concept of terroir has received a great deal of popular press and there are numerous scientific publications on terroir. The listed references are a selection of recent publications (*3–6*). We prefer the word 'regionality' to the more emotionally charged 'terroir' and will use that in this manuscript. We include growing conditions, microbial differences in vineyrads and wineries as well as common regional winemaking practices in our concept of regionality. We also believe that distinguishing regions by sensory and/or chemical means are useful in the elucidation of regionailty. We will describe the sensory descriptive analysis and volatile profile analyses used to describe the differences among Cabernet Sauvignon wines from different regions in Australia and among Malbec wines from different regions in Argentina and California.

Australian Cabernet Sauvignon Wines

Australian wine regions are divided into Geographical Indications (GIs) and in this study thirty 2009 Australian Cabernet Sauvignon wines were selected (*7*, *8*). Three wines were selected from each of the following ten GIs: Western Australia: Margaret River (MR), Frankland River (FR) and Mount Barker (MB); South Australia: Clare Valley (CV), Barossa Valley (BV), McLaren Vale (MV), Langhorne Creek (LC), Padthaway (PA), Coonawarra (CW) and Wrattonbully (WR). We asked the winemakers from each GI to select a wine (after 3 to 4 months) that in the winemaker's opinion represented the best regional reflection of Cabernet Sauvignon from that specific GI. The wines were then immediately racked, and bottled (without fining or filtration) in 750 ml screw cap bottles. The volatile profile analyses were performed within four months of bottling and the sensory descriptive analyses were performed approximately ten months after the 2009 harvest. In this study we had no control over the viticultural practices and except for asking for a 'best representation of the GI' essentially no control over the winemaking.

A sensory panel (18 subjects) was trained using the consensus method (*9*) and they used sixteen aroma terms (bell pepper, black berry, black pepper, butter, canned vegetable, chocolate, dried fruit, earthy, eucalyptus, floral, leather, mint, oak, red berry, smoky and vanilla) and four taste and mouthfeel terms (alcohol, astringent, bitter and sour) to describe the wines. See Robinson et al. (*7*) for the composition of the reference standards. The wines were evaluated in individual sensory booths (temperature 20 °C) equipped with a computer screen and mouse for data collection using FIZZ (Biosystèmes, Couternon, France) and a continuous unstructured line scale (10 cm). Clear glasses (ISO 3591:1977), containing twenty five mL aliquots of wine, covered with a plastic lid were labelled with three-digit random codes. Wines were served in triplicate over eighteen sessions with five wines per session using a modified Williams Latin Square design. All samples were expectorated and panelists had an enforced 30 sec break between samples

during which time they rinsed their mouths with water and an unsalted water cracker.

The volatile profiles of the wines were analyzed using a sensitive non-targeted HS-SPME GCxGC-TOFMS methodology previously described in Robinson et al. (*10*). Briefly, a CTC CombiPAL autosampler (CTC Analytics, Zwingen, Switzerland) with an agitator and SPME fiber conditioning station was coupled to a LECO Pegasus™ 4D GCxGC-TOFMS (LECO, St Joseph, MI, U.S.A.) was used for volatile aroma compound analysis. Samples were prepared in 20 mL amber glass headspace vials with 300 g/L sodium chloride added to 10 mL wine. Methyl nonanoate (an internal standard) and retention index probes were loaded onto the SPME fiber coating (Setkova et al, 2007a, 2007b). The sample headspace was sampled using a 2 cm DVB/CAR/PDMS 50/30 µm SPME fiber (Supelco, Bellefonte, PA, U.S.A.) for 120 min at 30 °C and desorbed in the GC inlet at 260 °C for 1 min. The primary column was a 30 m Varian FactorFour VF-5MS capillary column, 0.25 mm i.d. and 0.25 µm film thickness, with a 10 m EZ-guard column (Varian, Walnut Creek, CA, U.S.A.). This column was joined to the second column (in a secondary oven) by a SilTite mini-union (SGE, Ringwood, Vic., Australia). The second column was a 1.65 m Varian FactorFour VF-17MS capillary column, 0.10 mm i.d. and 0.20 µm film thickness of which 1.44 m was coiled in the secondary oven. TOFMS data was acquired at 100 scans/s and the TOFMS detector collected masses between 35 and 350 amu at 1800 V. ChromaTOF™ (LECO, St Joseph, MI, U.S.A.) optimized for the Pegasus™ 4D software Version 4.24 was used for interrogation and spectral deconvolution. Compound mass spectral data were compared against the NIST 2008 and Wiley 9th edition Mass Spectral Libraries. The retention index (RI) for each identified compound was compared to published RI for 5% phenyl polysilphenylene-siloxane capillary GC columns or equivalent (*11*, *12*). The minimum similarity match was set at 600 and the first and second dimension RI deviation was set at 6 and 0.25, respectively. Peak areas were normalized against the in-fiber internal standard and exported for statistical analyses.

Unless otherwise indicated all analyses were conducted using JMP (ver. 8.0.2, SAS Institute, Cary, NC, USA). Some multivariate analyses were conducted in either XLSTAT (Addinsoft, New York, NY, U.S.A.) or R-Studio ver. 0.98.507 (http://www.rstudio.com/). One-way (main effect: Product) analysis of variance (ANOVA) of the normalized peak areas was used to analyze the standard wine analyses and the volatile profile data. Significant volatile compounds were used as dependent variables in a PCA with panellipse (SensomineR, R-Studio) to determine the locations of the 10 GIs in multivariate space. A three-way ANOVA (Product, Judge and Replication) with all two-way interactions was performed for the sensory attributes using REML and a pseudo-mixed model with the mean square for Judge by Product as the denominator. An overall canonical variate analysis (CVA) was conducted using all 10 GI as the categorical factor and all significant sensory attributes from the analyses above. Additional CVAs were conducted for subsets of GIs. For these subsets the number of significant sensory attributes were determined via three-way ANOVA suing only products from the specified GIs in the subset. Multifactor analysis (MFA) using XLSTAT was used to compare the sensory and chemical data.

Publication Date (Web): November 24, 2015 | doi: 10.1021/bk-2015-1203.ch007

Publication Date (Web): November 24, 2015 | doi: 10.1021/bk-2015-1203.ch007

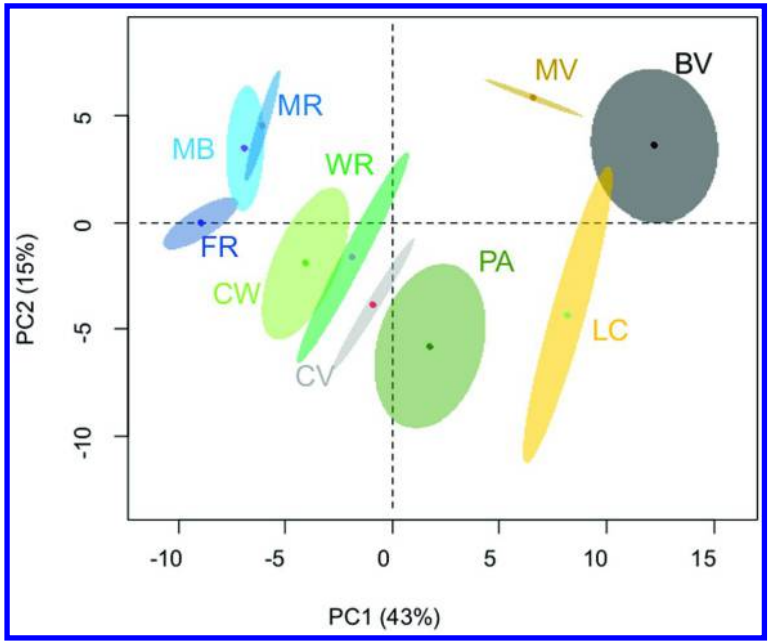

Figure 1. Principal component analysis score plot for PC1 and PC2 of the volatile compounds for the Cabernet Sauvignon wines from the ten Geographical Indications. Ellipses indicate 95% confidence intervals. MR=Margeret River, FR=Frankland River, MB=Mount Barker, CV=Clare Valley, BV=Barossa Valley, MV=MacLaren Vale, LC=Langhorne Creek, PA=Padthaway, CW=Coonawarra, Wrattonbully=WR.

The one-way ANOVA showed that 303 of the 420 volatile compounds differed significantly ($p<0.05$) across the products. These significant compounds were used to create the PCA score plot with 95% confidence intervals shown in Figure 1. The loadings plot with 303 compounds was cluttered and is not shown. The first two dimensions of the PCA explained 68% of the variance in the data set. The score plot shows that the Western Australian GIs (MR, MB and FR) were clearly separated from all South Australian GIs. The South Australian GIs are apparently divided into two groupings with CW, WR, CV and PA in one group and BV, MV and LC in a second. However, CV is closer geographically to the BV, MC and LC group but based on its volatile profile the wines are more similar to the GIs from further south-east.

Publication Date (Web): November 24, 2015 | doi: 10.1021/bk-2015-1203.ch007

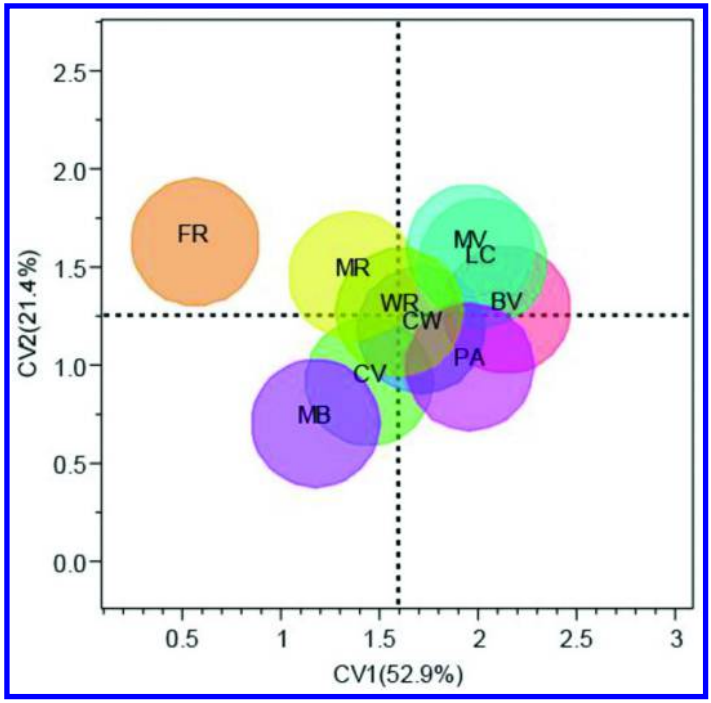

Figure 2. Canonical variate analysis score plot for CV1 and CV2 of the sensory attributes for the Cabernet Sauvignon wines from the 10 Geographical Indications. Circles indicate 95% confidence intervals. MR=Margeret River, FR=Frankland River, MB=Mount Barker, CV=Clare Valley, BV=Barossa Valley, MV=MacLaren Vale, LC=Langhorne Creek, PA=Padthaway, CW=Coonawarra, Wrattonbully=WR. (Modified, with permission from Reference (8). AJEV, 2012)

The three-way ANOVA showed that fifteen of the sensory attributes significantly discriminated among the GIs namely bell pepper, butter, canned vegetable, dried fruit, earthy, eucalyptus, floral, leather, mint, oak, red berry, smoky, vanilla, alcohol, astringent and sour. The CVA of the significant sensory terms using all ten GIs as the grouping factor is shown in Figure 2. The first two dimensions of this CVA explained 74.3% of the variance ratio. In this plot 95% confidence circles indicate that FR is separated from all the other GIs. The CV, MB and MR GIs are separated from the BV, LC, and MV GIs. Additionally the WR, CW, PA and MR GIs differed significantly from the MB GI. However, the differences were not huge (unlike the separations due to the volatile data) and we were interested in determining whether subsets of GIs would be better

separated. We therefore performed CVA analyses on the sensory data of the GIs as they were clustered by the volatile data in Figure 1. The CVA of the Western Australian subset was based on ten significant sensory attributes and the first two dimensions, as expected, explain 100% of the variance ratio (Figure 3). Despite the relatively close proximity of the three GIs there was no overlap among these GIs. The MR wines were more floral and astringent than the wines from the other two GIs, while the FR wines were higher in canned vegetable, smoky and earthy characteristics. The MB wines were more sour and had more bell pepper aromas than the FR and MR wines. As shown in Figure 4 the first two dimensions CVA of the BV, LC and MV GIs again explains 100% of the variance ratio and the three regions are well separated with the BV GI wines higher in red berry and dried fruit aromas, the MV wines higher in oak aromas and more bitter, and the LC GI wines had more eucalyptus and mint aromas than the wines from the other two GIs. The first two dimensions of the last subset of GIs (Figure 5) explained 79% of the variance ratio and here, despite in some cases being further apart, the separation among the GIs were not as clear. The wines from the CW GI overlapped those of the other three GIs but those three GIs were well separated from one another. In this subset the wines from Wrattonbully were highest in eucalyptus, smoky and butter aromas while those from CV were earthier, higher in bell pepper and mintier. Wines from the PA GI had more red berry and oak aromas and were more sour and astringent. The wines from CW were balanced in terms of their sensory attributes.

Publication Date (Web): November 24, 2015 | doi: 10.1021/bk-2015-1203.ch007

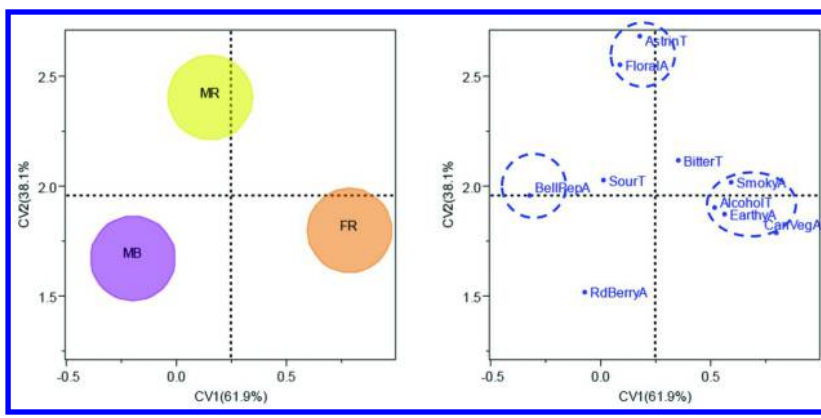

Figure 3. Canonical variate analysis score and loadings plots for CV1 and CV2 of the sensory attributes for the Cabernet Sauvignon wines from the three Western Australian Geographical Indications (Margaret River, Frankland River and Mount Barker). Circles indicate 95% confidence intervals.

Publication Date (Web): November 24, 2015 | doi: 10.1021/bk-2015-1203.ch007

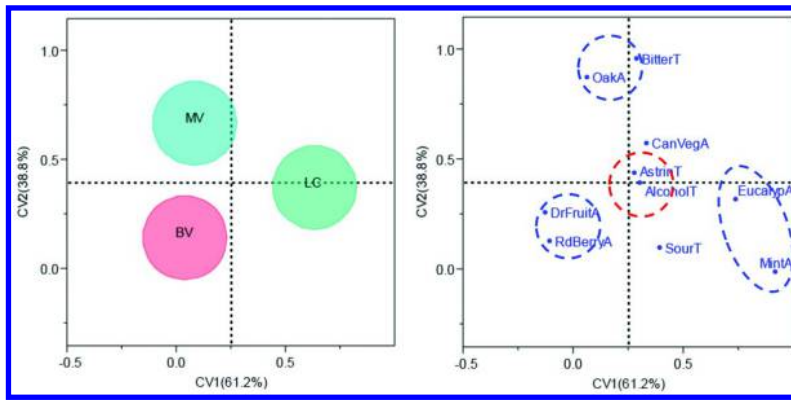

Figure 4. Canonical variate analysis score and loadings plots for CV1 and CV2 of the sensory attributes for the Cabernet Sauvignon wines from the three South Australian Geographical Indications clustered together based on the volatile data in Figure 1. Circles indicate 95% confidence intervals.

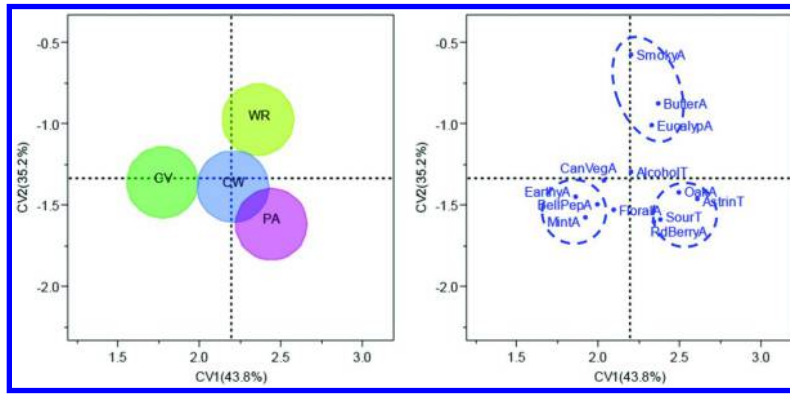

Figure 5. Canonical variate analysis score and loadings plots for CV1 and CV2 of the sensory attributes for the Cabernet Sauvignon wines from the four South Australian Geographical Indications clustered together based on the volatile data in Figure 1. Circles indicate 95% confidence intervals.

Figure 6 shows the MFA score plot for the ten GIs and is based on the 303 volatile compounds and the fifteen sensory attributes that significantly differed across the products. The RV coefficient shows similarities between the two configurations and can be viewed as a 'goodness of fit' measure (*13*). The RV coefficient of the relationship between the chemical and sensory data was 0.795. An RV coefficient of 0.700 is generally viewed as a good level of agreement (*14*, *15*) but one should keep in mind that the value is also dependent on the number of products and variables in the data set as well as the underlying structure of the data (*16*). The first two dimensions of the MFA explained 47% of the variance

with the third dimension added an additional 12% (data not shown). The partial axes for each GI shows the discrepancy between the two data sets relative to the consensus position. For example in the first two dimensions the two data sets were somewhat different for FR and BV but the data sets were very similar for CV and WB. In a plot (data not shown) of the 1st and 3rd dimensions all of the partial axes were small – of a similar length to the partial axes of PA and MB in Figure 5. Similar to Figure 1 the Western Australian GIs are separated from the other GIs on the right side of the graph while BV, MV, and LC are grouped together on the left side.

Publication Date (Web): November 24, 2015 | doi: 10.1021/bk-2015-1203.ch007

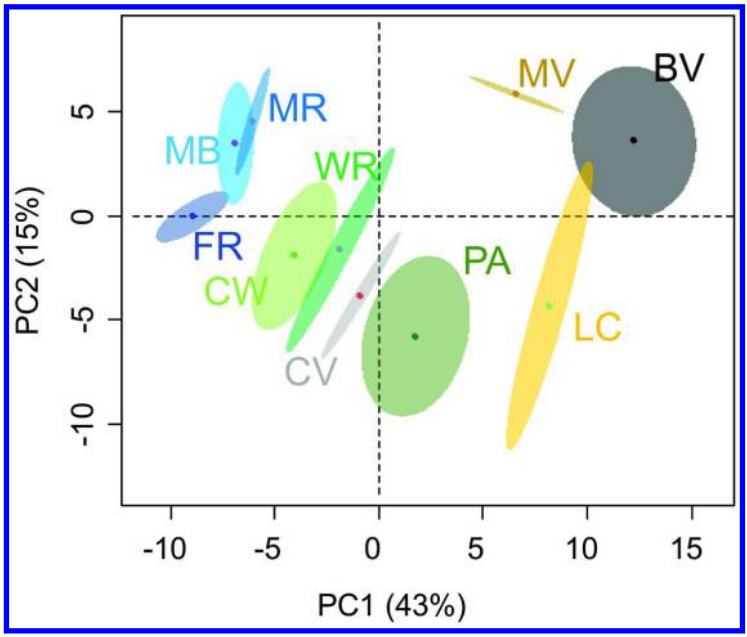

Figure 6. Multiple Factor analysis score plot with partial axes for PC1 and PC2 of mean volatile and sensory profiles for the Cabernet Sauvignon wines from the 10 Australian Geographical Indications.

Argentinian and Californian Malbec Wines

In this study we had no control over the viticultural practices but the wines were made in experimental wineries in Argentina (Catena Institute of Wine) and in California (UC Davis winery) by the same winemaker (Fernando Buscema) using the same protocols (*17*). Wines were made in duplicate lots in Argentina and in triplicate lots in California. Prior to sensory analysis we randomly picked one fermentation replicate for the sensory evaluation but all fermentation replicates were chemically analyzed, at the time of the sensory analyses. Wines

from Argentina were air freighted to Davis, CA after bottling. The grapes were hand harvested at 24 to 25 °Brix in 454 kg uniform lots. In Mendoza, Argentina we selected grapes from twenty six vineyards located in four departments namely Maipù (two), Luján (four), Tupungato (nine) and San Carlos (eleven). In California we received grapes from fifteen vineyards from five counties namely Napa (four), Sonoma (four, where one vineyard was actually located in Lake county on the Sonoma county border and this vineyard is included in the Sonoma county tally), Yolo (three), Lodi (two) and Monterey (two).

The profiles of sixty volatile compounds in the wines were analyzed in triplicate, approximately two months after bottling, using a semi-quantitaive automated HS-SPME GC-MS method combined with synchronous Selected Ion Monitoring (SIM)/scan detection (*18*). Briefly, 10 mL wine, 300 g/L sodium chloride and 50 µg/L 2-undecanone (internal standards) were placed in glass vials with metal crimp caps (Supelco, Bellefonte, PA, U.S.A.). A SPME fiber (2 cm DVB/CAR/PDMS, Supelco) was exposed to the wine headspace for 30 min at 40 °C with agitation. The MSD interface and the inlet temperature was set at 240 °C and the SPME fiber was desorbed with a 20:1 split ratio. The GC column was coated with DB-Wax (polyethylene glycol, 30 m, 0.25 µm I.D., 0.25 µm film thickness, J&W Scientific, Folsom, CA U.S.A.) and a SPME inlet liner (0.7 mm I.D., Supelco) was also used. The oven temperature gradient was 40 °C for 5 min, increased at 3 °C/min to 180 °C, then 30 °C/min to 240 °C which was then held for 10 min. An electronic ionization source was used and the source temperature was 230 °C with an electron energy of -70 eV. A 6890 GC coupled to a 5975 MSD (Agilent Technologies, Santa Clara, CA, U.S.A.) equipped with an MPS2 autosampler (Gerstel, Linthicum, MD, U.S.A.) was used. The instrument was controlled using Maestro (ver. 1.2.3.1, Gerstel) and data was captured using ChemStation software (E.01.01.335, Agilent Technologies).

Sensory descriptive analyses were performed approximately three months after bottling with the twenty six Mendozan wines evaluated in October 2011 and the fifteen Californian wines in March 2012. In Fall 2011 a sensory panel (fifteen subjects) was trained using the consensus method (*9*) and they used sixteen aroma terms (dark fruit, red fruit, dried fruit, floral, fresh green, cooked vegetal, earthy/mushroom, soy, chocolate, wood, sweet spice, black pepper, VA/oxidized, hot, herbal, and anise) and seven taste and mouthfeel (MF) terms (sweet, bitter, acidic, salty, astringent, viscous, and hotMF) to describe the wines. In Winter 2012 a second sensory panel (fourteen subjects) was trained using the consensus method (*7*) and they used seventeen aroma terms (dark fruit, red fruit, dried fruit/oxidized, floral, fresh green, cooked vegetal/cabbage, earthy, soy/meaty/yeasty, chocolate, wood, spice, black pepper, VA/ethyl actate/sulfur dioxide, ethanol, artificial fruit, grapefruit/citrus, and smoke) and six taste and mouthfeel terms (sweet, bitter, sour, salty, astringent and viscous) to describe the wines. See King and coworkers (*17*) for the composition of the reference standards. The wines were evaluated in individual sensory booths (temperature 20 °C) equipped with a computer screen and mouse for data collection using FIZZ (Biosystèmes, Couternon, France) and a continuous unstructured line scale (10 cm). Black tasting glasses (ISO 3591:1977), containing 30 mL aliquots of wine, covered with a plastic lid were labelled with three-digit random codes. Wines

Publication Date (Web): November 24, 2015 | doi: 10.1021/bk-2015-1203.ch007

were served in triplicate over twelve sessions with six or seven wines per session using a randomized complete block design. All samples were expectorated and panelists had an enforced thirty sec break between samples during which time they rinsed their mouths with water and an unsalted water cracker.

Unless otherwise indicated, all analyses were conducted using JMP (ver. 8.0.2, SAS Institute, Cary, NC, U.S.A.). Some multivariate analyses were conducted in either XLSTAT (Addinsoft, New York, NY, U.S.A.) or R-Studio ver. 0.98.507 (http://www.rstudio.com/). Chemical data were analyzed by two-way ANOVA (main effects: region, fermentation replicate) and peaks were quantified relative to the internal standard (2-undecanone) using the peak area of an extracted ion. Significant volatile compounds were used as dependent variables in a PCA with panellipse (SensoMineR, R-Studio) to determine the locations of the regions in multivariate space. The sensory data from the two descriptive analyses were combined using synonymous or shared attributes. The data were standardized to mean zero for each sensory attribute within each descriptive analysis. The combined sensory data were used as dependent variables in a PCA with panellipse (SensoMineR, R-Studio) to determine the locations of the regions in multivariate space. Generalized Procrustes analysis (GPA) using the Gower method was used to compare the means of the combined standardized sensory data to the means of the chemical data.

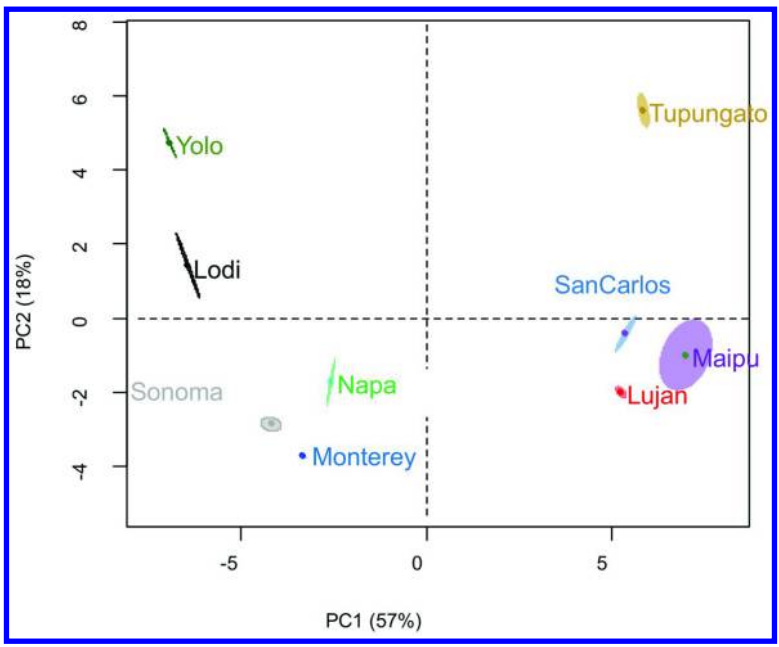

Figure 7. Principal component analysis score plot for PC1 and PC2 of the volatile compounds for the Malbec wines from four departments in Mendoza, Argentina and 5 counties in California, U.S.A.. Ellipses indicate 95% confidence intervals.

Publication Date (Web): November 24, 2015 | doi: 10.1021/bk-2015-1203.ch007

Of the sixty volatile compounds measured by the HS-SPME-GC-MS method forty eight differed significantly across regions. Only one compound (β-ionone) differed across the fermentation replicates indicating that the fermentation replicates did not differ substantially in their composition allowing us to randomly select one fermentation replicate for the sensory descriptive analyses. Figure 7 shows the PCA with 95% confidence ellipses for the Californian counties and the Mendozan departments. The first two dimensions of the PCA explained 75% of the variance. The Argentinean and the Californian regions are very clearly separated from each other and the regions within each country are also clearly separated.

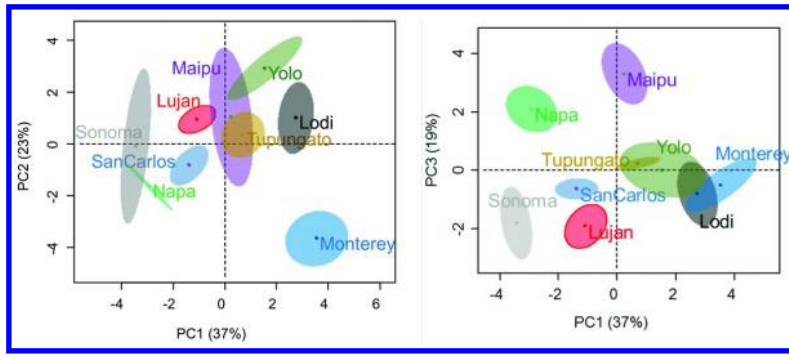

Figure 8. Canonical variate analysis score plots for CV1 and CV2 and for CV1 and CV3 of the sensory attributes for the Malbec wines from four departments in Mendoza, Argentina and five counties in California, U.S.A.. Ellipses indicate 95% confidence intervals.

Based on the ANOVA for regions, fourteen sensory attributes were included in the PCA shown in Figure 8. The first two dimensions explained 60% of the variance and the third dimension an additional 19%. All the regions were clearly separated in the three dimensional space but unlike the volatile data there was not a clear separation by country of origin. The GPA of the chemical and sensory data (Figure 9) explains 76% of the variance and clearly separates not only the Malbec wines from the two countries but also the regions within the countries. The floral sensory attribute was co-located with linalool, β-damascenone, cis-linalool oxide and phenethyl alcohol. The sensory attribute ethanol aroma was located relatively closely to the actual ethanol concentration in the chemical data set. Additionally, the sensory red fruit attribute was collocated to the esters ethyl isovalerate, ethyl butyrate and ethyl 2-methylbutyrate as well as limonene, p-cymene and α-terpinene. On the other hand, the sensory attribute volatile acidity (upper left quadrant) was nowhere near the location of the ethyl acetate compound (lower right quadrant). There were no chemical compounds in close proximity to the astringent attribute, this is not surprising since the chemical profile lacked non-volatile compounds.

Publication Date (Web): November 24, 2015 | doi: 10.1021/bk-2015-1203.ch007

Publication Date (Web): November 24, 2015 | doi: 10.1021/bk-2015-1203.ch007

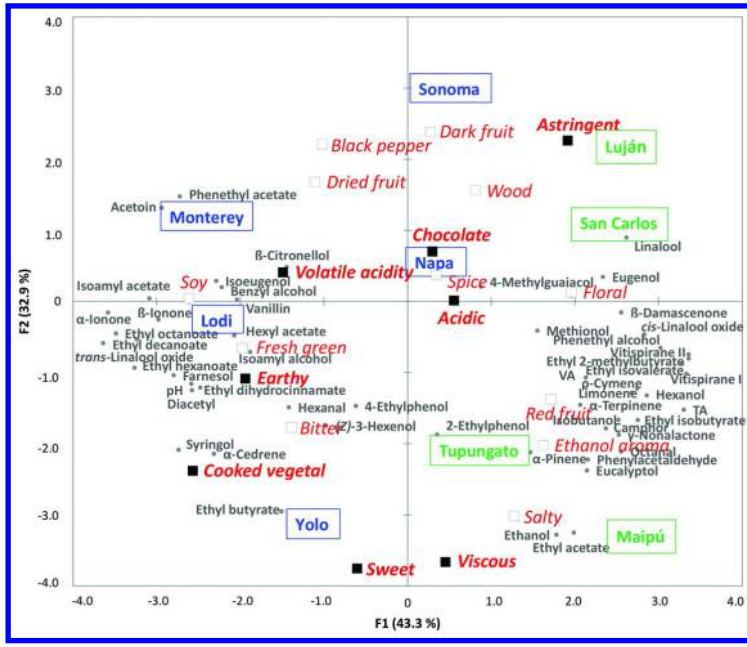

Figure 9. Generalized Procrustes analysis bi-plot of the volatile profiles and sensory attributes for dimensions 1 and 2 for the Malbec wines from four departments in Mendoza, Argentina and five counties in California, U.S.A. (Modified, with permission from Reference (17). Elsevier, 2014)

Conclusions

From these two studies it is clear that regionality is a measureable concept both chemically through the measurement of wine volatile profiles, as well as sensorially through the determination of the sensory attributes that discriminate among the wines. In general, the separation by region is clearer when one either only uses the volatile profile or both the volatile and sensory profiles in the multivariate data analyses. There is still a great deal unknown about regionality and thus this area clearly warrants further study.

References

1. Ramsey, W. In *A Dictionary of Greek and Roman Antiquities*; Smith, W., Ed.; John Murray: London, 1875; pp 1201−1209.
2. Busby, J. *Treatise on the Culture of the Vine and the Art of Making Wine*; B. Howe Government Printer: Sydney, Australia, 1825; pp 23−29.
3. Di Paola-Naranjo, R. D.; Baroni, M. V.; Podio, N. S.; Rubinstein, H. R.; Fabani, M. P.; Badini, R. G.; Inga, M.; Ostera, H. A.; Cagnoni, M.; Gallegos, E.; Gautier, E.; Peral-Garcia, P.; Hoogewerff, J.; Wunderlin, D.

A. Fingerprints for Main Varieties of Argentinean Wines: Terroir Differentiation by Inorganic, Organic, and Stable Isotopic Analyses Coupled to Chemometrics. *J. Agric. Food Chem.* **2011**, *59*, 7854–7865.
4. Reynard, J. S.; Zufferey, V.; Nicol, G. C.; Murisier, F. Vine water status as a parameter of the "terroir" effect under the non-irrigated conditions of the Vaud viticultural area (Switzerland). *J. Int. Sci. Vigne Vin* **2011**, *45*, 139–147.
5. Lopez-Rituerto, E.; Savorani, F.; Avenoza, A.; Busto, J. H.; Peregrina, J. M.; Engelsen, S. B. Investigations of La Rioja Terroir for Wine Production Using H-1 NMR Metabolomics. *J. Agric. Food Chem.* **2012**, *60*, 3452–3461.
6. Cadot, Y.; Caille, S.; Thiollet-Scholtus, M.; Samson, A.; Barbeau, G.; Cheynier, V. Characterisation of typicality for wines related to terroir by conceptual and by perceptual representations. An application to red wines from the Loire Valley. *Food Qual. Pref.* **2012**, *24*, 48–58.
7. Robinson, A. L.; Adams, D. O.; Boss, P. K.; Heymann, H.; Solomon, P. S.; Trengove, R. D. The relationship between sensory attributes and wine composition for Australian Cabernet Sauvignon wines. *Aust. J. Grape Wine Res.* **2011**, *17*, 327–340.
8. Robinson, A. L.; Adams, D. O.; Boss, P. K.; Heymann, H.; Solomon, P. S.; Trengove, R. D. The influence of geographic origin on the sensory characteristics and wine composition of *Vitis vinifera* cv. Cabernet Sauvignon wines from Australia. *Am. J. Enol. Vitic.* **2012**, *63*, 467–476.
9. Heymann, H.; King, E. S.; Hopfer, H. In *Novel Techniques in Sensory Characterization and Consumer Profiling*; Ares, G., Varela, P., Eds.; CRC Press: New York, 2014; pp 9−40.
10. Robinson, A. L.; Boss, P. K.; Heymann, H.; Solomon, P. S.; Trengove, R. D. Development of a sensitive non-targeted method for characterizing the wine volatile profile using headspace solid-phase micro-extraction comprehensive two-dimensional gas chromatography time-of-flight mass spectrometry. *J. Chromatogr. A* **2011**, *1218*, 504–517.
11. Adams, R. P. *Identification of Essential Oil Components by Gas Chromatography/Mass Spectroscopy*, 4th ed.; Allured Publishing Corporation: Carol Stream, IL, 2007.
12. Stein, S. E. Retention Indices. In *NIST Chemistry Webbook, NIST Standard Reference Database Number 69*; Lindstrom, P. J., Mallard, W. G. National Institute of Standards and Technology: Gaitersburg, MD, 2009.
13. Abdi, H. In *Encyclopedia of Measurement and Statistics*; Salkind, N., Ed.; Sage: Thousand Oaks, CA, 2007.
14. Cartier, R.; Rytz, A.; Lecomte, A.; Poblete, F.; Krystlik, J.; Belin, E.; Martin, N. Sorting procedure as an alternative to quantitative descriptive analysis to obtain a product sensory map. *Food Qual. Pref.* **2006**, *17*, 562–571.
15. Nestrud, M. A.; Lawless, H. T. Perceptual mapping of citrus juices using projective mapping and profiling data from culinary professionals and consumers. *Food Qual. Pref.* **2008**, *19*, 431–438.
16. Josse, J.; Pagès, J.; Husson, F. Testing the significance of the RV coefficient. *Comput. Stat. Data Anal.* **2008**, *53*, 82–91.

17. King, E. S.; Stoumen, M.; Buscema, F.; Hjelemeland, A.; Ebeler, S. E.; Heymann, H.; Boulton, R. B. Regional sensory and chemical characteristics of Malbec wines from Mendoza and California. *Food Chem*. **2014**, *143*, 256–267.
18. Hjelmeland, A. K.; King, E. S.; Ebeler, S. E.; Heymann, H. Characterising the chemical and sensory profiles of U.S. Cabernet Sauvignon wines and blends. *Am. J. Enol. Vitic*. **2013**, *64*, 169–179.

Publication Date (Web): November 24, 2015 | doi: 10.1021/bk-2015-1203.ch007

Publication Date (Web): November 24, 2015 | doi: 10.1021/bk-2015-1203.ch008

Chapter 8

Model Study on Changes in Key Aroma Compounds of Dornfelder Red Wine Induced by Treatment with Toasted French Oak Chips (*Q. robur*)

Stephanie Frank, Thomas Koppmann, and Peter Schieberle*

Deutsche Forschungsanstalt für Lebensmittelchemie, Lise-Meitner-Strasse 34, 85354 Freising, Germany
***E-mail Peter.Schieberle@ch.tum.de. Phone +49 8161 71 2932. Fax +49 8161 71 2970.**

A young Dornfelder wine was treated for 15 days with French oak chips, and changes in the overall aroma were evaluated by aroma profiling, the application of an aroma extract dilution analysis followed by quantitative measurements based on stable isotope dilution assays. In particular t*rans*- and *cis*- oak lactone, 4-ethyl-2-methoxyphenol and 2, 6-dimethoxyphenol were not detectable in the untreated wine, while, e.g., vanillin or 2-methoxyphenol were increased. Among the 17 odorants quantitated, vanillin, but also 2,6-dimethoxyphenol, iso-eugenol and both oak lactones increased significantly in the oak treated wine. A sensory experiment, in which the untreated young wine was administered with 13 odorants in the concentrations present in the oaked wine revealed a good agreement of both aroma profiles.

Among color and taste, aroma is an important quality attribute of wine, and thus, in numerous previous studies over 800 volatiles have been considered to contribute to the aroma of different red and white wines (*1*). It is well-accepted in the literature that especially storage in oak barrels has a significant influence on the overall wine aroma (*barrique*-type). But, storage in oak barrels is a time-

In Advances in Wine Research; Ebeler, et al.;
ACS Symposium Series; American Chemical Society: Washington, DC, 2015.

consuming and expensive process, and thus, alternative aging systems have been proposed. One alternative is the use of oak chips leading to the desired *barrique-type* flavor in a faster and cheaper way, and since this practice was approved and allowed by the European Community in 2006, attempts were done to increase knowledge on the differences between aroma compounds present in barrel vs. oak chip aged wines.

The many studies on the influence of barrel aging on wine aroma were previously summarized in a review by Garde-Cerdán and Ancín-Azpilicueta (*2*) also taking storage with oak chips into consideration. However, it becomes clear from a literature survey that only a few studies characterized the odor-active volatiles among the tremendous set of odorless compounds, for example in a study by Díaz-Maroto et al. (*3*), who compared odor-active compounds in untoasted and toasted oak wood by GC-Olfactometry or Culleré et al. (*4*), who reported on the odorants in six different types of wood. However, up to now, no systematic investigation on the key aroma compounds in raw and toasted oak chips has been performed using the Sensomics approach (*5*), except in our recent publication (*6*) in which the key aroma compounds in hydro-alcoholic extracts of oak chips of different toasting degree were compared. In total 39 odorants could be identified, and in the heavily toasted oak chips 14 aroma compounds, particularly vanillin, *trans*-isoeugenol, and 2-methoxyphenol showed very high odor activity values (ratio of concentration to odor threshold). The same concept was previously used by us to characterize the key aroma compounds in a Dornfelder red wine (*7*), and a total of 27 key odorants was quantitated by means of stable isotope dilution assays.

Knowing the key aroma compounds in oak chips as well as in an untreated young Dornfelder red wine, the aim of the present study was to characterize the influence of a treatment with oak chips on the aroma compounds of this wine variety. For this purpose, a young, non-aged Dornfelder wine was stored for 15 days in the presence of French oak chips, and changes in the key odorants were followed by aroma extract dilution analyses and quantitative measurements.

Publication Date (Web): November 24, 2015 | doi: 10.1021/bk-2015-1203.ch008

Experimental Part

Wine and Oak Chips

A young Dornfelder red wine (vintage 2012; not stored in a barrel) was obtained from a winegrower in Saulheim (Rheinhessen, Germany), and was directly used after fermentation for two weeks. Heavily toasted French oak chips (Quercus robur) were purchased from a German wine distributor.

Wine Treatment

Oak chips were ground and soaked in the wine (40 g per liter of wine). The sample was shaken daily and kept for 15 days at room temperature in the dark.

Aroma Profile Analysis

Aroma profile analyses of the wine samples were performed by a trained sensory panel consisting of at least 15 panelists as previously described (*6*). The following aroma descriptors, represented by the compound given in parentheses, were chosen for sensory evaluation, and their intensities were ranked on a seven-point scale from 0 (not perceivable) to 3 (strongly perceivable): flowery, honey-like (2-phenylethanol), smoky (2-methoxyphenol), clove-like (4-allyl-2-methoxyphenol), malty (3-methyl-1-butanol), vanilla-like (vanillin), vinegar-like (acetic acid), cooked apple-like (*β*-damascenone), coconut-like (*cis*-oak lactone), fruity (ethyl 3-methylbutanoate), and woody (powdered oak chips). The judgments of each panelist were averaged.

Publication Date (Web): November 24, 2015 | doi: 10.1021/bk-2015-1203.ch008

Aroma Extract Dilution Analysis and Quantitation by Stable Isotope Dilution Assays

Aroma extract dilution analyses on a distillate isolated by SAFE distillation from the two wine samples, and quantitation of the key odorants by stable isotope dilution assays were carried out as previously described (*6*). In the AEDA experiments, the undiluted sample was evaluated by four panellists to eliminate potential gaps in detecting odor-active areas. The detailed FD-factors were then determined by one panellist. The quantitation was done in three different work-ups of the same sample.

Spiking Experiment

The young Dornfelder wine without added oak chips was spiked with the following 13 odorants: 4-allyl-2-methoxyphenol, 2,6-dimethoxyphenol, 4-ethyl-2-methoxyphenol, 3-ethylphenol, *cis*-isoeugenol, *trans*-isoeugenol, 2-methoxy-phenol, 4-methyl-2-methoxyphenol, *cis*-oak lactone, *trans*-oak lactone, 4-propyl-2-methoxyphenol, sotolon, and vanillin. The amounts of the odorants were adjusted to get identical concentrations to those in the wine stored with oak chips.

Results

Aroma Profile Analysis

First of all aroma profile analyses of both wine samples were performed, and distinct differences in the aroma profiles between the wine stored without chips and with chips were observed (Figure 1). The aroma qualities smoky, clove-like, vanilla-like, coconut-like, and woody were rated higher in the wine stored with oak chips, while smaller changes were noticed for flowery, malty, and cooked apple-like odors. On the other hand, in particular the intensity of the odor impression "fruity" decreased in the oak stored wine.

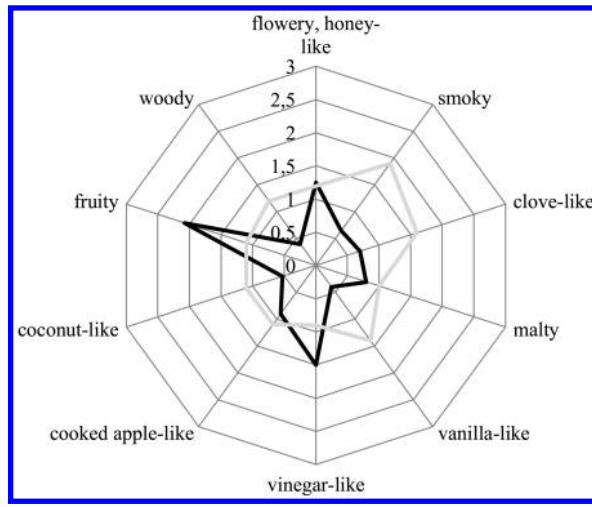

Figure 1. Aroma profile analysis of the young Dornfelder wine stored without (black) and with oak chips (gray).

To elucidate the reasons for these differences on a molecular basis, first a comparative aroma extract dilution analysis (cAEDA) was performed.

Comparative Aroma Extract Dilution Analysis

The cAEDA showed clear differences in the FD-factors for some compounds listed in Table 1. A few odorants were only present in the oak treated wine, e.g., *trans*- and *cis*-oak lactone, 4-ethyl-2-methoxyphenol, and 2, 6-dimethoxyphenol. Further aroma compounds such as vanillin, 4-ally-2-methoxyphenol, and 2-methoxyphenol were increased by the chip treatment and thus, showed higher FD-factors in the wine stored with oak chips. On the other hand, in particular *β*-damascenone was lowered by the oak chip treatment.

Quantitative Measurements

To confirm the results indicated by the aroma extract dilution analyses, 17 odorants, namely 4-allyl-2-methoxyphenol, *β*-damascenone, 2,6-dimethoxyphenol, 4-ethyl-2-methoxyphenol, 2-methoxyphenol, *cis*-oak lactone, *trans*-oak lactone, sotolone, and vanillin) and the further oak related odorants (3-ethylphenol, 4-ethylphenol, *cis*-isoeugenol, *trans*-isoeugenol,

In Advances in Wine Research; Ebeler, et al.;
ACS Symposium Series; American Chemical Society: Washington, DC, 2015.

Publication Date (Web): November 24, 2015 | doi: 10.1021/bk-2015-1203.ch008

4-methyl-2-methoxyphenol, 3-methylphenol, 4-methylphenol, and 4-propyl-2-methoxyphenol) were quantitated in both wines by means of stable isotope dilution assays (Table 2).

Table 1. FD-Factors of Selected Odorants in Dornfelder Young Wine Stored without and with Oak Chips

aroma compound	*FD-factor*	
	without oak chips	*with oak chips*
4-allyl-2-methoxyphenol	128	512
β-damascenone	512	64
2,6-dimethoxyphenol	< 1	128
4-ethyl-2-methoxyphenol	< 1	32
2-methoxyphenol	32	256
cis-oak lactone	< 1	32
trans-oak lactone	< 1	32
sotolon	1024	4096
vanillin	1024	8192

Publication Date (Web): November 24, 2015 | doi: 10.1021/bk-2015-1203.ch008

The concentrations of most compounds were significantly increased in the wine treated with oak chips, in particular vanillin, 2, 6-dimethoxyphenol, *cis*-oak lactone, 4-ethyl-2-methoxyphenol, *trans*-isoeugenol, 4-methyl-2-methoxyphenol, *cis*-isoeugenol, and 4-propyl-2-methoxyphenol. 2-Methoxyphenol, *trans*-oak lactone, 4-allyl-2-methoxyphenol, sotolon, and 3-ethylphenol showed a moderate increase in their concentrations, while 4-methylphenol and 3-methylphenol remained nearly constant. The next step was to confirm that all oak related odorants do contribute to the change in the overall aroma observed for the oaked red wine

Spiking Experiment

For the spiking experiment, the young Dornfelder wine was spiked with 13 odorants showing an increase concentration in the wine treated with oak chips. The added amounts of odorants were chosen in the way that the concentrations in the resulting wine were the same as in the Dornfelder stored with oak chips. To see the change in the overall aroma, aroma profile analyses were performed (Figure 2).

Table 2. Concentrations of 17 Odorants in the Young Dornfelder Red Wine Stored without and with Oak Chips. Selection Was Done in Particular for Compounds Showing Increased/Decreased FD Factors during the AEDA

aroma compound	*concn*[a] *[µg/L] in Dornfelder wine stored*	
	without	*with oak chips*
vanillin	50.0	701.0
2,6-dimethoxyphenol	2.95	104.0
cis-oak lactone	n.d.[b]	27.9
2-methoxyphenol	1.80	16.8
trans-oak lactone	n.d.[b]	6.88
4-ethyl-2-methoxyphenol	0.04	3.06
4-allyl-2-methoxyphenol	5.72	16.5
sotolon	0.99	2.59
β-damascenone	2.14	2.33
trans-isoeugenol	0.40	26.0
4-methyl-2-methoxyphenol	0.23	16.0
cis-isoeugenol	0.11	3.00
4-propyl-2-methoxyphenol	0.02	1.00
3-ethylphenol	0.66	3.15
4-methylphenol	0.47	0.96
3-methylphenol	0.44	0.85
4-ethylphenol	0.26	0.28

[a] calculated as the mean value of at least three different workups; standard deviation ≤ 20 % [b] not detected.

Publication Date (Web): November 24, 2015 | doi: 10.1021/bk-2015-1203.ch008

The aroma profiles of the spiked wine and the wine stored with oak chips stored wine were in quite good agreement. Almost all odor impressions were rated very similar in both samples except the smoky and woody odors, which were perceived more intensely in the spiked wine. The compounds causing these odor attributes are currently under investigation, because these are also present in Whisky and Cognac stored in oak barrels (unpublished results). The results, however, indicate that compounds, such as such as furfural, 5-methylfurfural, and syringaldehyde, which were proposed as important odorants in oak stored wines in the literature, do not contribute to the overall aroma of the spiked Dornfelder wine. On the other hand, *cis*-isoeugenol and *trans*-isoeugenol, which to our knowledge have not been discussed in the literature as being relevant for the oak aroma of wine, clearly contributed to the overall aroma. The data confirm our previous results on the influence of a smaller set of odorants in generating a *barrique-type* aroma (*8*).

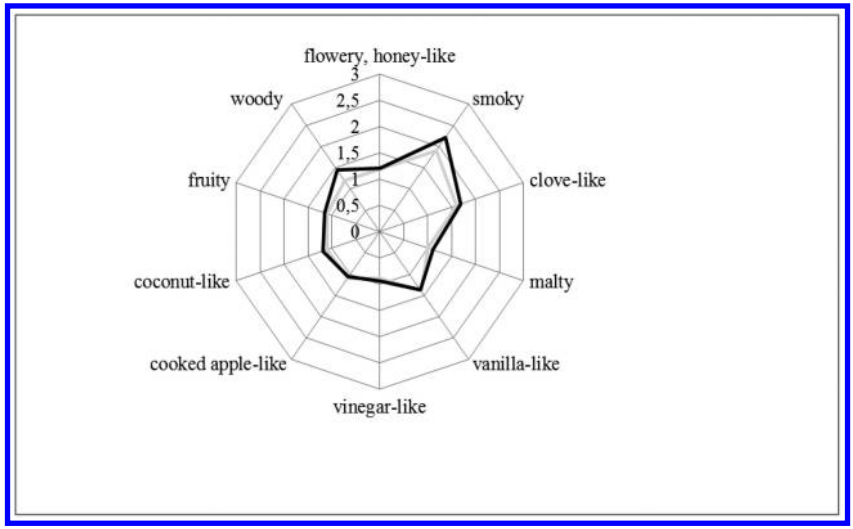

Figure 2. Aroma profile analysis of the spiked Dornfelder wine (grey) and the young wine stored with oak chips (black).

Conclusion

The application of the Sensomics concept on a Dornfelder red wine spiked with oak chips with the respective non-spiked wine of the same batch clearly revealed 13 odorants which were transferred from the oak into the red wine during a 15 days storage. Although all odorants, except the two eugenol isomers, have previously been reported as volatiles in oak wood, this is the first study confirming the contribution of the identified compounds to the aroma differences by sensory experiments. The data are a good basis for further studies on the influence of the signature of the considered set of key odorants on the aroma profiles of different red wines with a pronounced *barrique*-type aroma.

References

1. Nijssen, L. M.; Ingen-Visscher, C. A.; van Donders, J. J. H. *VCF - Volatile compounds in food*; Zeist (The Netherlands): TNO Quality of Life, Version 15.2, 1963-2014 (database).
2. Garde-Cerdán, T.; Ancín-Azpilicueta, C. *Trends Food Sci. Technol.* **2006**, *17*, 438–447.
3. Díaz-Maroto, M. C.; Guchu, E.; Castro-Vázquez, L.; Torres, C. de; Pérez-Coello, M. S. *Flavour Fragrance J.* **2008**, *23*, 93–98.
4. Culleré, L.; de Simón, B. F.; Cadahía, E.; Ferreira, V.; Hernández-Orte, P.; Cacho, J. *LWT−Food Sci. Technol.* **2013**, *53*, 240–248.
5. Schieberle, P. In *Characterization of Food: Emerging Methods*; Goankar, A., Ed.; Elsevier: Amsterdam, Netherlands, 1995; pp 403−431.

Publication Date (Web): November 24, 2015 | doi: 10.1021/bk-2015-1203.ch008

6. Koppmann, T.; Schieberle, P. *J. Agric. Food Chem.* **2015** Submitted for publication.
7. Frank, S.; Wollmann, N.; Schieberle, P.; Hofmann, T. *J. Agric. Food Chem.* **2011**, *59*, 8866–8874.
8. Frank, S.; Schieberle, P. In *Progress in Authentication of Food and Wine*; Ebeler, S. E., Takeoka, G. R., Winterhalter P., Eds.; ACS Symposium Series 1081: American Chemical Society: Washington, DC, 2011; pp 165−173.

Publication Date (Web): November 24, 2015 | doi: 10.1021/bk-2015-1203.ch008

Publication Date (Web): November 24, 2015 | doi: 10.1021/bk-2015-1203.ch009

Chapter 9

Terroir Effects on Grape and Wine Aroma Compounds

M. Herderich,[1,*] S. Barter,[1] C. A. Black,[1] R. Bramley,[2] D. Capone,[1] P. Dry,[1] T. Siebert,[1] and P. Zhang[3]

[1]The Australian Wine Research Institute, Hartley Grove cnr Paratoo Road, Urrbrae, SA 5064, Australia
[2]CSIRO, Waite Campus, PMB 2, Glen Osmond, SA 5064, Australia
[3]Department of Agriculture & Food Systems, University of Melbourne, Parkville, Vic 3010, Australia
E-mail: markus.herderich@awri.com.au.

Terroir is a concept based on the assumption that key wine characteristics can be attributed to a delimited geographical area where grapes and wine have been produced. To explore the concept of terroir, and how terroir may influence wine composition and sensory attributes, we summarise recent studies of the spatial and temporal variability of key wine aroma compounds, 3-mercaptohexanol ('tropical', 'grapefruit' notes), 1,8-cineole ('minty', 'eucalypt' aromas), and rotundone ('peppery', 'spicy' notes). Taken together, these and other studies suggest that environmental and biological interactions together with biotic factors, ie vintage and winemaking procedures, have key roles in shaping wine composition and sensory attributes.

Introduction

According to the International Organisation of Vine and Wine (OIV) vitivinicultural terroir is a holistic concept which refers to an area in which collective knowledge of the interactions between the identifiable physical and biological environment and applied vitivinicultural practices develops, providing distinctive characteristics for the products originating from this area. From a linguistic perspective terroir stems from the word *terra*, or *land*, in Latin. Hence

In Advances in Wine Research; Ebeler, et al.;
ACS Symposium Series; American Chemical Society: Washington, DC, 2015.

it is understandable that at a conceptual level an understanding of terroir may be sought from characterising distinctive geologies, soils and specific minerals present in individual vineyards. However, in the popular wine press and in wine marketing efforts, discussions of the term terroir are further simplified and commonly limited to defining a delimited geographical area with distinct soils as it is thought that soils are responsible for the unique sensory characteristics of wine and provide a key point of differentiation when comparing a wine from a certain terroir to wine from other regions of origin.

All Vineyards Are Located in Unique Sites

All vineyards occupy unique sites, such that substantial differences may exist between vineyards in terms of their geology and soil properties, geomorphology including slope, aspect, and climatic and microclimatic situation. Additional factors that influence terroir are linked to human decisions such as varietal and clonal selection, row orientation, irrigation scheduling and water availability, viticultural practices that influence sun exposure, and harvesting and winemaking practices. With this in mind it is difficult, if not impossible, to explain terroir in terms of a single factor such as geology, soil properties or climate. Scientifically we have a very limited understanding of the relationships between terroir, grape composition and wine sensory properties and have yet to identify many key factors (or combinations of factors) that are responsible for unique sensory characteristics and diversity of styles observed in wine of the same variety.

Minerality

The term 'minerality' is quite commonly used as a taste descriptor for wine; it appears to imply that individual minerals or their water soluble ions can be transported by a vine from its roots to the grape berries where they confer a sensory impact on grapes and/or wine. While wine experts appear to use consistent verbal definitions for 'minerality' a recent study in Chardonnay has demonstrated that 'minerality' is an ill-defined concept from a sensory perspective (*1*).

Indeed there are some inorganic compounds that can have a significant impact on wine flavour; these include sodium and potassium cations (responsible for salty taste) and nitrogen-compounds (as precursors to yeast derived fermentation volatiles). However these are typically linked to viticultural management practices such as irrigation, the salinity of irrigation water and fertiliser use, and their concentrations are further influenced by winemaking practices such as stabilization and ion exchange processes, additives such as diammonium phosphate and processing aids.

In general, the inorganic chemical profile of a grape berry has only a distant and indirect relationship with vineyard geochemistry, concentrations of minerals in wine bear little relationship with geological minerals in vineyard, and so far no evidence supports a direct link between geology, soil composition and presence of soil-derived inorganic compounds and wine flavour (*2*). Instead, the aroma compound benzene methane thiol (*3*), and malic acid, tartaric acid, and titratable acidity (*4*) have been associated with 'minerality' in separate studies.

In Advances in Wine Research; Ebeler, et al.;
ACS Symposium Series; American Chemical Society: Washington, DC, 2015.

Publication Date (Web): November 24, 2015 | doi: 10.1021/bk-2015-1203.ch009

Publication Date (Web): November 24, 2015 | doi: 10.1021/bk-2015-1203.ch009

Environmental and Management Influences on Grape and Wine Composition

A significant amount of research over many years has aimed at characterizing the links between climate, soil and cultivar, grape composition, and sometimes wine composition and sensory. For, example in a study of the influence of climate, soil, and cultivar on terroir (*5*), it was found that the impacts of climate and soil were greater than that of cultivar (Merlot, Cabernet Franc, Cabernet Sauvignon) and that the effects of climate and soil on fruit composition were likely mediated through their influence on vine water status, i.e. a reflection of vine water stress in an un-irrigated vineyard. In another very detailed study, Cortell and Kennedy (*6*) investigated the variations in Pinot Noir growth and resulting fruit and wine phenolic composition. The Pinot Noir study was conducted in a vineyard with vines of the same clone, rootstock and age that had been managed consistently. Again, the authors observed a strong association between soil depth and corresponding water-holding capacity and vine vigor. This was thought to have an indirect effect on bunch sunlight exposure and vine microclimate, leading to the observed variations in grape and wine anthocyanins and tannins. With respect to the variability in key green aromas from 3-isobutyl-2-methoxypyrazine and C_6 compounds, a field study over four years in sixty nine Merlot vineyards in three distinctly different wine grape growing regions within the Central Valley of California demonstrated that seasonal variation was more important than regional variation, and that temperature during spring was related to 'green fruit' aroma compounds at harvest, likely due to its interactions with vine vigor and fruit shading (*7*). Taken together, the studies point out that vine water status and stress, which may vary according to seasonal weather conditions and irrigation practices, are more likely to influence grape and wine composition than soils per se. While all soils are distinct and we in no way suggest that soil physical properties are unimportant, it is much more likely that it is the diversity in weather and climatic conditions, soil fertility and the availability of nutrients, and changes to vineyard management practices that lead to a broad range of wine styles, flavours and unique wines of distinction, rather than the diversity of soils as such. Of course, it is also generally the case that vineyard boundaries do not align with the boundaries between soil types which may create difficulties in the attribution of cause and effect between soil properties and wines.

In an empirical study on the effect of winemaking practices on wine quality in the Bordeaux region, it was shown that technological choices (such as grape varieties, harvesting, and processing) affect wine quality (measured as price at auction) much more than land characteristics and exposure of vineyards (*8*). Similarly, a study of typicality, terroir and sensory properties of red wine from the Loire Valley, demonstrated a disconnect between conceptual typicality (from a wine producers' viewpoint) and perceptual typicality established by sensory testing. In particular, sensory profiles were related to visual descriptors and the influences of oenological factors (i.e. harvest date, winemaking practices) were prevalent, while no direct influence of bed rock type could be observed (*9*).

Finally, results from very detailed research in a Cabernet Sauvignon vineyard in the Murray Valley region into variation in vine vigour, grape yield, vineyard

soils and topography, grape and wine composition and wine sensory attributes demonstrate that it is possible to establish robust relationships between the sites where grapes are grown and the sensory and chemical characteristics of the wines derived from them (*10*). Again, these relationships appear to be based on specific manageable biophysical vineyard attributes which are spatially variable at the within-vineyard scale. The results also pose the question at what scale terroir can be defined in a meaningful way; they further support the view that investigations aiming to establish terroir based on delimited geographical areas at a regional scale are unlikely to provide meaningful explanations for terroir effects; and they identify the need for additional research that goes beyond the presumption (*11*, *12*) that terroir-related wine sensory attributes are predominantly the result of soil physical properties that control wine quality.

Due to this background we have commenced a number of research projects aiming to explore the concept of terroir, and the way terroir may influence wine composition and sensory attributes, through characterising the origin and the spatial and temporal variability of key wine aroma compounds, 3-mercaptohexanol (3-MH; 'tropical', 'grapefruit' notes), 1,8-cineole ('minty', 'eucalypt' aromas), and rotundone ('peppery', 'spicy' notes).

Materials and Methods

Experimental details about grape samples, analysis of 3-MH and its precursors, and experiments studying the effects of transporting and processing have been summarized in (*13–15*). The vineyard and fermentation studies to elucidate the origin of 1,8-cineole in red wine have been summarized in (*16*, *17*).

Experimental details about grape samples, sensory evaluation of 'peppery'aromas in grape homogenates, GC-MS analysis of sesquiterpenes and the untargeted GC-MS metabolomics strategy that led to the identification of the Shiraz grape sesquiterpene, α-ylangene, as marker for 'pepper' aroma have been described in (*18*). The GC-MS-O experiments and sensory studies to identify rotundone as an important impact compound with a strong 'spicy', 'pepper' aroma have been summarised in (*19*) , and the analytical method used to quantify rotundone has been described in (*20*).

Experimental details about the Mount Langi Ghiran vineyard used for the 'pepper-map' study in 2012 and 2013, sampling from 177 georeferenced 'target vines', and GC-MS analysis of rotundone have been described in (*21*). Additional sesquiterpenes and aroma compounds, α-ylangene, α-guaiene, theaspirance, geraniol and β-damascenone were quantified in grape samples from the 2012 vintage as described in (*18*). Three replicate samples were randomly selected from vines within each low, medium and high rotundone zone (*21*). Grape berry subsamples (100 g each) were allowed to partially thaw and then were blended, as described previously (*18*). Aliquots of berry homogenate (5.0 g) and internal standard (α-copaene, 0.1 μg in ethanol, 500 μL) were placed into 20 mL screw cap SPME vials and shaken (22 °C; 24 hr). Then saturated solution of sodium chloride (2.0 mL) was added to each vial and they were analysed by HS-SPME-GC-MS as described for α-ylangene analysis in (*18*) with some adjustments: Each vial and

In Advances in Wine Research; Ebeler, et al.;
ACS Symposium Series; American Chemical Society: Washington, DC, 2015.

Publication Date (Web): November 24, 2015 | doi: 10.1021/bk-2015-1203.ch009

its contents were heated to 45°C and then a polydimethyl-siloxane/divinylbenzene (PDMS/DVB) 65μm SPME fibre was exposed to the headspace for 60 min, with agitation. The MS was operated with simultaneous selected ion monitoring (SIM) and scanning over a mass acquisition range of 35-280 m/z. The method was validated by a series of standard additions of α-copaene (0 to 100 μg/kg; $n = 9 \times 2$) to aliquots of the same blended grapes. The identification of sesquiterpenes was achieved by comparing the mass spectra and retention indicies with the terpenoids library in the MassFinder software (version 4.1). α-Guaiene was the only compound quantified by SIM. The target and qualifier ions were typically m/z 105, 147, 189 and 204 for α-guaiene and 105, 119, 161 and 204 for α-copaene. All compounds were quantified as α-copaene equivalents. Within-vine and within-bunch variability of rotundone was determined as described by Zhang and co-workers (*22*).

Publication Date (Web): November 24, 2015 | doi: 10.1021/bk-2015-1203.ch009

Results and Discussion

Factors Influencing Concentrations of 3-Mercaptohexanol

Varietal thiols such as 3-mercaptohexanol (3-MH) are key odorants in white wine, and together with methoxypyrazines are especially important to the flavour of Sauvignon Blanc. 3-MH has one of the lowest aroma thresholds of any food odorant in the low nanogram per litre range and contributes distinctive 'tropical', 'passion-fruit' flavour to many white wines. However, 3-MH is found only at very low levels in grapes and must (*14*). This is because most 3-MH is formed from odourless, non-volatile precursors (*23*) by the action of C-S-lyases present in yeast or enzyme additions during fermentation. Precursors to 3-MH include the cysteine conjugate Cys-3-MH, and the glutathione analogue Glut-3-MH.

By direct HPLC-MS/MS analysis of both precursors of 3-MH the effect of ripening on the concentration of these compounds in Sauvignon Blanc fruit have been investigated recently. Grapes from five different clones of Sauvignon Blanc vines, all from the same vineyard in the Adelaide Hills, were sampled and analysed for 3-MH precursor levels at approximately 14-day intervals through-out the growing season. The results demonstrated that 3-MH precursor levels were very small at veraison to mid-ripening, then slightly increased pre-harvest, and there was a large increase just prior to commercial harvest with an approximately 10-fold increase in the concentration of both precursors in as little as 14 days. From these results, we can see the importance of fruit ripeness for achieving optimum favour potential while the influence of clone type was relatively small (*14*).

In addition to grape maturity and harvesting decisions, the mode of transportation of machine harvested fruit from the vineyard to the winery has been noticed by some winemakers to result in wines with more tropical aroma compared to fruit processed soon after harvest. To investigate this further, a commercial-scale study was conducted using replicated lots of machine harvested fruit with different additions of sulfur dioxide and ascorbic acid added at the time of harvest. Concentrations of 3-MH precursors were analysed in samples taken

from each of the grape bins at harvest and then again approximately 12 hours later after transportation over approximately 800 km to the winery.

As expected, the antioxidant treatments had a clear visual effect on the must. Regarding the Cys-3-MH concentration there was a very large difference due to the transport, with an approximately 10-fold increase in the concentration of the precursor in the transported fruit. The samples with the lowest precursor concentration within each set were those with the highest addition of sulfur dioxide, likely due to either the SO_2 preventing conjugate formation or interfering with the formation of (*E*)-2-hexenal which is required for the generation of the 3-MH precursor. At concentrations of antioxidants likely to be used in industry, the addition of SO_2 or ascorbate had only a small effect. The precursor Glut-3-MH behaved similarly to the Cys-3-MH, with an approximately two-fold increase observed after transportation (*15*).

In the above examples there are two main factors that have a very large influence on 3-MH precursor concentrations and consequently on the amount of this tropical aroma compound which can be released during winemaking: One is grape ripening and harvest timing; while this could be considered a terroir effect which may reflect impacts of seasonal weather conditions and microclimate on ripening behaviour, the dominant influence of management decisions is quite obvious. Secondly, harvesting choices (hand harvesting vs. machine harvesting), and the way in which grapes are handled prior to fermentation can also have a major effect on 3-MH aroma precursors as berry rupture and length of time through transport of machine harvested fruit gives rise to large increases in thiol precursors. With everything being equal, the distance between a winery and its vineyards could also be seen by some as a spatial effect, although the effects of contact time can be easily modulated through must chilling and/or additions of antioxidants, or increased through extending the standing time of crushed grapes prior to inoculation with yeast and fermentation.

Publication Date (Web): November 24, 2015 | doi: 10.1021/bk-2015-1203.ch009

Factors Responsible for Concentrations of 1,8-Cineole in Red Wine

For some time the origin of ‘eucalypt’ and ‘minty’ aromas in wine had remained a mystery. Some researchers believed that ‘eucalypt’ characters were associated with the proximity of vineyards to *Eucalyptus* trees (*24*) and hence typical expressions of the terroir of some wines; others proposed that there were monoterpenes in grape berries that acted as precursors for the ‘minty’ aroma compound 1,8-cineole (*25*). Further investigations revealed, however, that grape-derived monoterpenes are unable to generate high enough levels of 1,8-cineole to reach sensory threshold concentrations (*16*). These results shifted the focus onto non-grape sources of 1,8-cineole, specifically eucalypt trees that are native to Australia, widely planted throughout the world for providing timber for construction and paper manufacturing, and are known for their essential oils rich in 1,8-cineole.

To find out more about the origin of ‘minty’ aromas in wine, a detailed study investigated the relationship between grape composition and the proximity of vines to *Eucalyptus* trees. The impacts of airborne essential oils, grape leaves,

grape stems and leaves from nearby *Eucalyptus* trees were also included in the investigation (*17*).

Indeed the results demonstrated that the greatest amount of 1,8-cineole was found in wine made from grapes that were closest to the *Eucalyptus* trees. Wine making experiments revealed a continuous increase in the concentration of 1,8-cineole during fermentation that stopped once a wine was drained from skins. This indicated that 1,8-cineole was extracted from the grape skins and/or matter other than grapes (MOG). Somehow unexpectedly, it was not airborne transfer of eucalypt essential oil volatiles that was the main source of 1,8-cineole, but the presence of eucalypt leaves (and to a lesser extent grapevine leaves and stems) in harvested grapes that were the key factors responsible for elevated concentrations of 1,8-cineole in wine. Overall, the closeness of grapevines to *Eucalyptus* trees has a conclusive effect on 1,8-cineole concentrations in wine, and the presence of MOG can significantly influence 1,8-cineole levels. Enhancing or reducing 'minty', 'eucalypt' characters is no longer a case of pure chance or serendipity, as winemakers are in a much stronger position to take greater control of 1,8-cineole and adjust eucalyptus character to create balanced wines that express their terroir, with proximity of vineyards to native or planted eucalypt trees, the species of Eucalypt trees, typical wind direction and harvesting practices being key factors responsible for the unique terroir effects from 1,8-cineole.

Publication Date (Web): November 24, 2015 | doi: 10.1021/bk-2015-1203.ch009

Variability of Rotundone in Cool Climate Shiraz Grapes

Shiraz is one of the most important grape varieties in Australia and accounts for about 40% of all red wine made each year. It is grown across all regions and localities recognised as distinct Australian Geographical Indications. Prominent Australian Shiraz styles include elegant, peppery cool-climate wines (for example from the Adelaide Hills, or the Grampians); more intensely flavoured, spicy and sometimes minty styles of Margaret River, Coonawarra or Clare Valley; sweet chocolaty and ripe-fruited wines (Barossa Valley, McLaren Vale), and leathery and rich wines (Hunter Valley). Despite its importance for the wine industry, information on key aroma compounds of wines made from Shiraz grapes is rather limited. It is known that Shiraz wines do not contain an appreciable concentration of methoxypyrazines yet may be described as 'green', a characteristic that sets this variety apart from some other highly valued red grape varieties, and some Shiraz wines can have sensorially important levels of a distinctive 'spicy'/'pepper' flavour (*26*). Notably, some vineyards consistently produce 'peppery' wines, especially in cooler years, and this can be predicted from analysing the concentration of a sesquiterpene, α-ylangene, as a biomarker in grapes (*18*).

Subsequent studies resulted in the isolation of an aroma fraction from Shiraz grapes, which contained a single component that gave a strong 'peppery' aroma when assessed by GC-MS-O. From the mass spectrum and retention indices for the 'pepper' aroma on three different GC column phases the responsible compound was identified as the sesquiterpene, rotundone, that is found in the skins of Shiraz berries (*19*, *27*). The identity and sensory properties of rotundone could be verified with an authentic reference compound; its low sensory detection

Publication Date (Web): November 24, 2015 | doi: 10.1021/bk-2015-1203.ch009

threshold of 16 ng/L and distinctive 'peppery' aroma are indicative of rotundone's role as an impact aroma compound in wine, and rotundone remains the sole aroma compound identified so far with a 'peppery' aroma in wine (*19*, *28*).

Rotundone typically occurs in grape berries at very low concentrations in the ppt-range and practical, cost effective, sensitive and precise technologies for in-field quantification of rotundone are lacking. Given the notable variability in grape rotundone concentrations between individual vineyards and between growing seasons for the same vineyard a recent study aimed to establish whether rotundone was spatially variable at the within vineyard scale (*21*). Accordingly, the objective was to explore whether the rotundone concentration in the Shiraz berries of a vineyard block known to produce 'peppery' wines was spatially structured or whether grape rotundone concentrations showed a random pattern of variation. For this first study of within-vineyard spatial variability in a grape-derived key aroma compound, grapes were sampled ca. two weeks prior to commercial harvest from 177 georeferenced 'target vines' in a 6.1-ha block planted to Shiraz on own roots at the Mount Langi Ghiran vineyard in the Grampians region of Victoria.

The concentration of rotundone in berries sampled in 2012 from the 177 target vines varied markedly – from 73 to 1082 ng/kg – and the mean and median values of rotundone concentration were 399 and 379 ng/kg, respectively. The resulting high-resolution grape rotundone data were mapped and overlain with other map layers describing variation in soils, topography and vine vigour. Berry rotundone concentration was found to be spatially structured, with higher berry rotundone concentrations occurring in the south and south-eastern parts of the block, while substantially lower values were observed in the north-western parts (Figure 1).

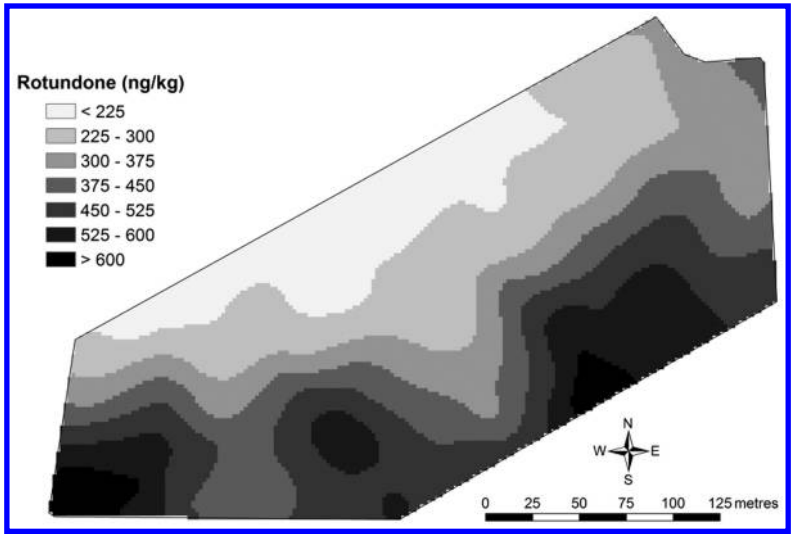

Figure 1. Variation in the rotundone concentration of berries in a 6.1 ha vineyard in the Grampians region, Australia. (data of Scarlett et al. (21))

Publication Date (Web): November 24, 2015 | doi: 10.1021/bk-2015-1203.ch009

The results further suggested that within-vineyard variation in berry rotundone concentration is likely associated with variation in soil properties and topography, with the influences of topography and ambient temperature likely key drivers of rotundone variation (*21*). A similar spatial structure in rotundone concentration could be observed in the 2013 growing season (unpublished data), albeit rotundone was present at much lower concentrations from ca. 6 to 15 ng/kg. The seasonal differences exemplify that aspect and topography may well have an indirect and not necessarily causative effect on grape rotundone concentration. Similarly, ambient temperature alone may not be necessarily sufficient to explain the site-to-site variability in rotundone concentration. Overall, this first study of spatial variability of a key grape and wine aroma compound has established that within-vineyard variation in the concentration of rotundone is not random and is clearly spatially structured; it suggests that the variation in the land underlying the vineyard represents one important variable associated with the presence of rotundone in grapes. While this observation is consistent with the concept of terroir, the large but structured variability within a single vineyard raises questions about the scale at which terroir can be considered a useful construct (*21*, *29*).

In an extension of the work by Scarlett and co-workers (*21*) the distribution was characterised of additional key grape metabolites and aroma compounds in grape samples from low, medium and high rotundone zones of the Mount Langi Ghiran vineyard. For this experiment low, medium and high rotundone zones were identified based on (*21*) and grape samples were taken from randomly selected vines within each zone.

Table 1. Sesquiterpenes and Grape Aroma Compounds in Samples from Low, Medium, and High Rotundone Zones

compound	*concentration (ng/kg)*		
	low (n = 3)	*medium (n = 3)*	*high (n = 3)*
rotundone	82 ± 11	518 ± 10	1,013 ± 63
α-ylangene	5,212 ± 790	20,402 ± 2,162	29,055 ± 7,406
α-guaiene	84 ± 32	364 ± 119	514 ± 177
theaspirane	1,991 ± 71	1,737 ± 153	1,212 ± 90
β-damascenone	1,715 ± 271	2,356 ± 1,005	1,232 ± 366
geraniol	4,539 ± 2,519	3,086 ± 1,158	3,922 ± 789

mean concentration ± standard deviation

The results in Table 1 confirm the significant differences observed by Scarlett and co-workers (*21*) for rotundone in grapes from 2012 across this vineyard, with concentrations ranging from 82 ng/kg in grapes from the low rotundone zone, over 518 ng/kg in grapes from the medium rotundone, to 1013 ng/kg in grapes from

vines located in the high zone. Not surprisingly, the sesquiterpene α-ylangene which has been demonstrated before to represent a very good biomarker for 'pepper' aroma in grapes (*18*), shows a very similar concentration distribution across the low to high rotundone zones. Similarly, the concentration of α-guaiene, which is a likely biochemical precursor to rotundone based on its similar structure and concentration profile, increases in grapes across the three zones approximately six-fold, although only the differences between grapes from the low and high rotundone zones are statistically significant. As expected for aroma compounds formed by other metabolic pathways, no concentration differences but rather large variability between grape samples from individual zones were observed for the monoterpene alcohol geraniol and C_{13}-norisoprenoid β-damascenone. Yet for another C_{13}-norisoprenoid, theaspirane, significant differences were observed between the three zones, with the highest theaspirane concentrations in grapes sampled from the low rotundone zone, and the lowest theaspirane concentration in grapes from the high rotundone zone – i.e. a strikingly inverse relationship compared to the concentration profile observed for rotundone (Table 1).

These results exemplify that the within-vineyard variation in the concentration of a number of grape aroma compounds – not only rotundone - can be clearly spatially structured, and that the spatial structure observed for key grape volatiles is not necessarily limited to metabolites formed by a single biosynthetic pathway. Even from the relatively small number of aroma compounds targeted in this experiment it is evident that for compounds from presumably closely related biosynthetic pathways - such as β-damascenone and theaspirane - distinctive differences in their spatial concentration distributions can be observed.

Notably, no significant differences in commonly used grape compositional parameters, including total soluble solids (TSS), pH, titratable acidity (TA), total phenolics and total anthocyanins were observed among the three zones in 2012 (*22*), indicating that the spatially structured differences in aroma compounds were not related to differences in maturity between grapes from the three zones. Furthermore, this observation suggests that widely used grape quality parameters such as TSS or colour may not necessarily represent suitable proxies for identifying and monitoring the spatial variability in key volatile grape compounds.

To further characterize the variability of rotundone concentration within the Mount Langi Ghiran vineyard, within-vine variability was studied through two approaches (*22*): The influence of row and bunch orientation was examined through comparing rotundone concentrations in grapes from the same vine, but grown on the less exposed south-east or more sun exposed north-west facing side of a vine. Significantly higher rotundone concentrations were observed in shaded bunch sectors and grapes grown on the shaded side of a vine. For example, in the 2013 vintage the rotundone concentrations in grapes from the less exposed south-east facing side of a vine were ca. 50% higher compared to rotundone in grapes grown on the opposite more exposed side. Finally, with-in-bunch variability of rotundone concentration was characterised using grapes from different sectors of individual bunches. In both seasons, the top-back sector at a bunch (2011-12: 493.5 ng/kg, 2012-13: 25.9 ng/kg) had significantly higher concentration of rotundone compared to all other sectors, with grape berries from the bottom-front sector of a bunch consistently having the lowest concentration

Publication Date (Web): November 24, 2015 | doi: 10.1021/bk-2015-1203.ch009

of rotundone (2011-12: 250.2 ng/kg, 2012-13: 15.3 ng/kg). In summary, in this study large differences in rotundone concentration were observed between the two growing seasons (2011-12 and 2012-13), among three vineyard zones, and within individual bunches. The 18-fold variation in rotundone concentration between the two studied seasons was higher than the differences among vineyard zones which one could attribute to terroir effects, hence exemplifying the importance of seasonal weather over site effects. Notably within a season, terroir related variability between the low and medium, or medium and high zones was almost in the same order of magnitude as the differences observed within individual bunch sectors (*22*).

Publication Date (Web): November 24, 2015 | doi: 10.1021/bk-2015-1203.ch009

Key Factors Potentially Explaining the Variability of Rotundone in Grapes

As 'high-rotundone' vineyards are found across regions with rather diverse and distinct geological terroirs it is unlikely that soil chemistry or geology are playing a causative role in rotundone's formation. In addition, the observed seasonal and spatial variability in a key aroma compound between vineyards, within a vineyard, and within grapes from the same vine within a single vineyard raises questions about the scale at which terroir can be considered a useful construct. Instead, the results obtained so far point towards combinations of genetic and environmental factors that result in enhanced rotundone concentrations in grapes.

Arguably, the presence of the sesquiterpene rotundone in specific varieties such as Shiraz or Duras (*30*), while it is absent in other varieties that are planted in the same region and similar iso-climates, points towards a genetic basis for sesquiterpene biosynthesis that is specific for high-rotundone varietals. However, at this stage we cannot fully rule out that rotundone or its putative precursor, α-guaiene, might be formed by other species – i.e. nearby plants, insects or fungi - before being translocated onto grapes. This is because non-vitis biotic sources of key aroma compounds have previously been observed as being responsible for the presence in grapes of the minty monoterpene 1,8-cineole (largely caused by airborne transport of leaves and essential oils of Eucalypt trees (*17*)). Similarly, the presence of Coccinellida species can lead to undesirable alkyl methoxypyrazines in grapes and 'ladybug' taint in wine (*31*).

The observation that specific vineyards within cool climate regions such as Adelaide Hills and Grampians (Australia), or Hawke's Bay (New Zealand), have a historical record of consistently yielding grapes high in 'pepper' aroma and rotundone might also point towards the potential presence of a genetic determinant in the original planting material used for these vineyards. Potentially, mutations leading to SNPs in regulatory or functional elements of sesquiterpene biosynthesis in Shiraz, and/or hitherto unknown epigenetic effects could explain some of the variability in grape rotundone. It is conceivable that the observed spatial structure in grape rotundone concentration within the Mt Langi vineyard could result from epigenetic mechanisms in the vines triggered by the underlying vineyard variability, although such a suggestion would need further investigation to corroborate it. However, the observed differences at a grapevine scale, i.e. the differences between rotundone concentrations of individual grapes within

a bunch and between bunches grown on the same grapevine but on exposed or shaded sides of a row, cannot be explained by genetic effects. Rather, the observed within-vine variability points towards a major role for environmental factors such as light exposure and/or temperature of the bunch zone in regulating the formation of rotundone. Similarly the propensity of 'high-rotundone' Shiraz vineyards to be located across cool-climate regions and the significant seasonal differences in rotundone's concentration point towards weather conditions, especially temperature and perhaps rain or water availability, as playing key roles in influencing the formation of rotundone.

When reconciling environmental factors that may play a key role in the formation of rotundone in grapes and would explain the observed spatial and temporal variability in its concentration, it is important to recognise that biosynthesis of many volatile organic plant metabolites, including sesquiterpenes, can be induced by a herbivore attack (*32*, *33*). For example, herbivores such as light brown apple moth larvae have been demonstrated to cause very high emissions of a range of volatiles including sesquiterpenes, β-caryophyllene, germacrene D and (*E,E*)-α-farnesene from infested apple seedlings (*34*). Similarly, grapevine leaves were reported to release several novel compounds in response to damage by the spider mite *Tetranychus urticae,* including caryophyllene and humulene (*35*). With this in mind it is intriguing to speculate that the presence of rotundone in grapes, or of one of its close precursors such as α-guaiene, could potentially be the consequence of a herbivore attack onto a vine above or below ground. Alternatively, the presence of rotundone could be a consequence of the biological interactions between a grapevine and its associated soil and plant microbiome (*36*) as it has been shown that regional, site-specific, and grape variety factors shape the fungal and bacterial consortia in vineyards and on wine-grape surfaces (*37*, *38*).

As the final step in the formation of rotundone, an allylic oxidation of a sesquiterpene precursor is required. While untargeted and targeted metabolite profiling has identified α-ylangene as the most closely correlated sesquiterpene (*18*), from a structural perspective α-guaiene is most likely the direct precursor to rotundone. Indeed, the oxidation of α-guaiene to rotundone has been shown to occur in presence of the enzyme laccase (*39*), or chemically in the presence of Au/Pd/TiO2-catalysts (*40*) or by autoxidation in air (*41*).

Whether the allylic oxidation of α-guaiene to rotundone in grapes is specifically catalysed by hitherto unknown grapevine enzymes such as P450-oxidases, the consequence of enzymatic reactions by microorganisms on the grape surface, or the result of α-guaiene's chemical degradation in air remains to be established. As higher rotundone concentrations typically can be observed after colder growing seasons, and on the less sunexposed and colder sides of a grapevine and bunch, a biological rather than chemical final oxidation reaction appears to be more likely. An alternative explanation is that the interaction(s) of the grapevine with its biological environment may lead to higher concentrations of direct precursors such as α-guaiene in certain vineyards, vines, bunches and grapes, and that the final concentration of rotundone is limited by the concentration of its precursors and not by the final oxidation step.

Publication Date (Web): November 24, 2015 | doi: 10.1021/bk-2015-1203.ch009

Conclusions

Taken together, these studies into the origin and the spatial and temporal variability of key wine aroma compounds, 3-mercaptohexanol ('tropical', 'grapefruit' notes), 1,8-cineole ('minty', 'eucalypt' aromas), and rotundone ('peppery', 'spicy' notes) suggest that environmental and (potentially) biological factors together with viticultural management and winemaking practices are key to shaping wine flavour chemistry. The large number of possible combinations of these factors and variables would explain the myriad of wines with unique and diverse sensory attributes. Yet it is also clear that a better understanding of terroir, and its role in producing distinctive wines, requires a holistic rather than reductionist approach. While characteristics of the land underlying a vineyard remains one important variable associated with wine composition, both the large plasticity in grape composition that can be attributed to non-land related variables and the large but structured variability within a single vineyard raise questions about the scale at which an area-based definition of terroir can be considered a useful construct (*10*, *21*, *36*).

Publication Date (Web): November 24, 2015 | doi: 10.1021/bk-2015-1203.ch009

Acknowledgments

This work was funded by the Rathbone Wine Group, CSIRO and The Australian Wine Research Institute (AWRI). The work by the AWRI was supported by Australia's grapegrowers and winemakers through their investment bodies, the Grape and Wine Research and Development Corporation (GWRDC) and Australian Grape and Wine Authority (AGWA), with matching funds from the Australian Government. We very much acknowledge the ongoing interest and support by many Australian wine companies and are most grateful to Damien Sheehan and the late Nathan Scarlett (Rathbone Wine Group) for their support, and to Mark Krstic and Leigh Francis (AWRI) for their support and discussions. We acknowledge all former AWRI colleagues and collaborators, who contributed to our research and co-authored publications listed under references.

References

1. Ballester, J.; Mihnea, M.; Peyron, D.; Valentin, D. Exploring minerality of Burgundy Chardonnay wines: A sensory approach with wine experts and trained panelists. *Aust. J. Grape Wine Res.* **2013**, *19*, 140–152.
2. Maltman, A. Minerality in wine: a geological perspective. *J. Wine Res.* **2013**, *24* (3), 169–181.
3. Parr, W. V.; Valentin, D.; Green, J. A.; Dacremont, C. Evaluation of French and New Zealand Sauvignon wines by experienced French wine assessors. *Food Qual. Prefer.* **2010**, *21*, 56–64.
4. Heymann, H.; Hopfer, H.; Bershaw, D. An exploration of the perception of minerality in white wines by projective mapping and descriptive analysis. *J. Sens. Stud.* **2014**, *29*, 1–13.

5. Van Leeuwen, C.; Friant, P.; Choné, X.; Tregoat, O.; Koundouras, S.; Dubourdieu, D. Influence of Climate, Soil, and Cultivar on Terroir. *Am. J. Enol. Vitic.* **2004**, *55* (3), 207–216.
6. Cortell, J. M.; Halbleib, M.; Gallagher, A. V.; Righetti, T. L.; Kennedy, J. A. Influence of Vine Vigor on Grape (Vitis vinifera L. Cv. Pinot Noir) and Wine Proanthocyanidins. *J. Agric. Food Chem.* **2005**, *53*, 5798–5808.
7. Mendez-Costabel, M. P.; Wilkinson, K. L.; Bastian, S. E. P.; McCarthy, M.; Ford, C. M.; Dokoozlian, N. Seasonal and Regional Variation of Green Aroma Compounds in Commercial Vineyards of Vitis Vinifera L. Merlot in California. *Am. J. Enol. Vitic.* **2013**, *64* (4), 430–436.
8. Gergaud, O.; Ginsburgh, V. Natural Endowments, Production Technologies and the Quality of Wines in Bordeaux. Does Terroir Matter? *J. Wine Econ.* **2010**, *5* (1), 3–21.
9. Cadot, Y.; Caillé, S.; Thiollet-Scholtus, M.; Samson, A.; Barbeau, G.; Cheynier, V. Characterisation of typicality for wines related to terroir by conceptual and by perceptual representations. An application to red wines from the Loire Valley. *Food Qual. Prefer.* **2012**, *24*, 48–58.
10. Bramley, R. G. V.; Ouzman, J.; Boss, P. K. Variation in vine vigour, grape yield and vineyard soils and topography as indicators of variation in the chemical composition of grapes, wine and wine sensory attributes. *Aust. J. Grape Wine Res.* **2011**, *17*, 217–229.
11. Seguin, G. Terroirs and pedology of wine growing. *Experientia* **1986**, *42*, 861–873.
12. Van Leeuwen, C.; Tregoat, O.; Choné, X.; Bois, B.; Pernet, D.; Gaudillère, J.-P. Vine water status is a key factor in grape ripening and vintage quality for red Bordeaux wine. How can it be assessed for vineyard management purposes? *J. Int. Sci. Vigne Vin* **2009**, *43*, 121–134.
13. Capone, D. L.; Sefton, M. A.; Hayasaka, Y.; Jeffery, D. W. Analysis of precursors to wine odorant 3-mercaptohexan-1-ol using HPLC–MS/MS: resolution and quantitation of diastereomers of 3-S-cysteinylhexan-1-ol and 3-S-glutathionylhexan-1-ol. *J. Agric. Food Chem.* **2010**, *58*, 1390–1395.
14. Capone, D. L.; Sefton, M. A; Jeffery, D. W. Application of a modified method for 3-mercaptohexan-1-ol determination to investigate the relationship between free thiol and related conjugates in grape juice and wine. *J. Agric. Food Chem.* **2011**, *59*, 4649–4658.
15. Capone, D. L.; Jeffery, D. W. Effects of transporting and processing Sauvignon Blanc grapes on 3-mercaptohexan-1-ol precursor concentrations. *J. Agric. Food Chem.* **2011**, *59*, 4659–4667.
16. Capone, D. L.; van Leeuwen, K.; Taylor, D. K.; Jeffery, D. W.; Pardon, K. H.; Elsey, G. M.; Sefton, M. A. Evolution and occurrence of 1,8-cineole (Eucalyptol) in Australian Wine. *J. Agric. Food Chem.* **2011**, *59*, 953–959.
17. Capone, D. L.; Jeffery, D. W.; Sefton, M. A. Vineyard and fermentation studies to elucidate the origin of 1,8-cineole in Australian red wine. *J. Agric. Food Chem.* **2012**, *60*, 2281–2287.
18. Parker, M.; Pollnitz, A. P.; Cozzolino, D.; Francis, I. L.; Herderich, M. J. Identification and Quantification of a Marker Compound for ‘Pepper’ Aroma and Flavor in Shiraz Grape Berries by Combination of Chemometrics and

Gas Chromatography-Mass Spectrometry. *J. Agric. Food Chem.* **2007**, *55*, 5948–5955.
19. Wood, C.; Siebert, T. E.; Parker, M.; Capone, D. L.; Elsey, G. M.; Pollnitz, A. P.; Eggers, M.; Meier, M.; Vossing, T.; Widder, S.; Krammer, G.; Sefton, M. A.; Herderich, M. J. From Wine to Pepper: Rotundone, an Obscure Sesquiterpene, Is a Potent Spicy Aroma Compound. *J. Agric. Food Chem.* **2008**, *56*, 3738–3744.
20. Siebert, T.; Wood, C.; Elsey, G. M.; Pollnitz, A. P. Determination of Rotundone, the Pepper Aroma Impact Compound, in Grapes and Wine. *J. Agric. Food Chem.* **2008**, *56*, 3745–3748.
21. Scarlett, N. J.; Bramley, R. G. V.; Siebert, T. E. Within-vineyard variation in the 'pepper' compound rotundone is spatially structured and related to variation in the land underlying the vineyard. *Aust. J. Grape Wine Res.* **2014**, *20*, 214–222.
22. Zhang, P.; Barlow, S.; Krstic, M.; Herderich, M.; Fuentes, S.; Howell, K. Within-vineyard, within-vine and within-bunch variability of rotundone concentration in berries of Vitis vinifera L. cv. Shiraz. *J. Agric. Food Chem.* **2015**, *63*, 4276–4283.
23. Tominaga, T.; Peyrot des Gachons, C.; Dubourdieu, D. A New Type of Flavor Precursors in Vitis vinifera L. cv. Sauvignon Blanc: S-Cysteine Conjugates. *J. Agric. Food Chem.* **1998**, *46*, 5215–5219.
24. Herve, E.; Price, S.; Burns, G. In *Proceedings VIIème Symposium International d'Œnologie,* Bordeaux, France, 2010; Lonvaud, A., De Revel, G., Darriet, P., Eds.; Lavoisier: Paris, France; 2003; pp 598−600.
25. Farina, L.; Boido, E.; Carrau, F.; Versini, G.; Dellacassa, E. Terpene compounds as possible precursors of 1,8-Cineole in red grapes and wines. *J. Agric. Food Chem.* **2005**, *53*, 1633–1636.
26. Mayr, C. M.; Geue, J. P.; Holt, H. E.; Pearson, W. P.; Jeffery, D. W.; Francis, I. L. Characterization of the Key Aroma Compounds in Shiraz Wine by Quantitation, Aroma Reconstitution, and Omission Studies. *J. Agric. Food Chem.* **2014**, *62*, 4528–4536.
27. Siebert, T. E.; Solomon, M. R. Rotundone: development in the grape and extraction during fermentation. In *Proceedings of the fourteenth Australian Wine Industry Technical Conference*; Adelaide, South Australia, 2010; Blair, R. J., Lee. T. H., Pretorius, I. S., Eds.; Australian Wine Industry Technical Conference Inc.: Adelaide, SA, Australia; 2011; pp 307–308.
28. Herderich, M. J.; Siebert, T. E.; Parker, M.; Capone, D. L.; Jeffery, D. W.; Osidacz, P.; Francis, I. L. Spice up your life: analysis of key aroma compounds in Shiraz. In *Flavor Chemistry of Wine and Other Alcoholic Beverages;* ACS Symposium Series 1104; Qian, M. C., Shellhammer, T. H., Eds.; American Chemical Society: Washington, DC; 2012; pp 3–13.
29. Bramley, R. Smarter thinking on terroir. *Wine Vitic. J.* **2014** July/August, 53–58.
30. Geffroy, O.; Dufourcq, T.; Carcenac, D.; Siebert, T.; Herderich, M.; Serrano, E. Effect of ripeness and viticultural techniques on the rotundone concentration in red wine made from Vitis vinifera L. cv. Duras. *Aust. J. Grape Wine Res.* **2014**, *20*, 401–408.

Publication Date (Web): November 24, 2015 | doi: 10.1021/bk-2015-1203.ch009

31. Botezatu, A. I.; Kotseridis, Y.; Inglis, D; Pickering, G. J. Occurrence and contribution of alkyl methoxypyrazines in wine tainted by Harmonia axyridis and Coccinella septempunctata. *J. Sci. Food Agric.* **2013**, *93*, 803–810.
32. Takabayashi, J.; Dicke, M.; Posthumus, M. A. Variation in composition of predator attracting allelochemicals emitted by herbivore-infested plants: relative influence of plant and herbivore. *Chemoecology* **1991**, *2*, 1–6.
33. Dicke, M.; Baldwin, I. T. The evolutionary context for herbivore-induced plant volatiles: beyond the 'cry for help'. *Trends Plant Sci.* **2010**, *15* (3), 167–175.
34. Suckling, D. M.; Twidle, A. M.; Gibb, A. R.; Manning, L. M.; Mitchell, V. J.; Sullivan, T. E. S.; Wee, S. L.; El-Sayed, A. M. Volatiles from Apple Trees Infested with Light Brown Apple Moth Larvae Attract the Parasitoid Dolichogenidia tasmanica. *J. Agric. Food Chem.* **2012**, *60*, 9562–9566.
35. Van den Boom, C. E.; Van Beek, T. A.; Posthumus, M. A.; De Groot, A; Dicke, M. Qualitative and quantitative variation among volatile profiles induced by Tetranychus urticae feeding on plants from various families. *J. Chem. Ecol.* **2004**, *30* (1), 69–89.
36. Vaudour, E. The quality of grapes and wine in relation to geography: Notions of terroir at various scales. *J. Wine Res.* **2002**, *13*, 117–141.
37. Bokulich, N. A; Thorngate, J. H.; Richardson, P. M.; Mills, D. A. Microbial biogeography of wine grapes is conditioned by cultivar, vintage, and climate. *Proc. Natl. Acad. Sci. U.S.A.* **2014**, *111*, E139–E148.
38. Zarraonaindia, I.; Owens, S. M.; Weisenhorn, P.; West, K.; Hampton-Marcell, J.; Lax, S.; Bokulich, N. A.; Mills, D. A.; Martin, G.; Taghavi, S.; Van der Lelie, D.; Gilberta, J. A. The Soil Microbiome Influences Grapevine-Associated Microbiota. *mBio* **2015**, *6* (2), e02527–14.
39. Schilling, B.; Granier, T.; Locher, F. 1-Hydroxy-octahydroazulenes as fragrances. Patent WO 2012/001018 A1, January 5, 2012.
40. Tarbit, B.; Hutchings, G. J.; Edwards, J. K.; Miedziak, P. Methods for using allylic oxidation catalysts to perform oxidation reactions. Patent WO 2011/106166 A1, September 1, 2011.
41. Huang, A.-C.; Burrett, S.; Sefton, M. A.; Taylor, D. K. Production of the Pepper Aroma Compound, (−)-Rotundone, by Aerial Oxidation of α-Guaiene. *J. Agric. Food Chem.* **2014**, *62*, 10809–10815.

Publication Date (Web): November 24, 2015 | doi: 10.1021/bk-2015-1203.ch009

Publication Date (Web): November 24, 2015 | doi: 10.1021/bk-2015-1203.ch010

Chapter 10

C_{13}-Norisoprenoids in Grape and Wine Affected by Different Canopy Management

Fang Yuan, Hui Feng, and Michael C. Qian*

Department of Food Science and Technology, Oregon State University, 100 Wiegand Hall, Corvallis, Oregon 97331
***E-mail: Michael.qian@oregonstate.edu.**

High canopy density is common in the cool-climate vinegrowing region of Oregon. Excessive canopy density will produce unbalanced musts, resulting in poor wine quality. Vine growers commonly use vineyard canopy management strategies to regulate vine vigor and improve grape and wine quality. C_{13}-norisoprenoids are found to be very important grape-derived constitutes of many grape varieties and their corresponding wines. This paper introduces the quantification studies on the formation of C_{13}-norisoprenoids during berry development, as well as evaluates the possible impacts of different canopy management (i.e., leaf removal, cover crop and irrigation) on the C_{13}-norisoprenoids and their precursors in grapes. Different viticultural practice could alter C_{13}-norisoprenoid level in grape berries by changing one or more parameters, and affect the C_{13}-norisoprenoid level in corresponding wines.

Introduction

Norisoprenoids are a group of compounds derived from the degradation of carotenoids—a group of tetraterpenoid pigments widely existing in plants. C_{13}-norisoprenoids, with 13 carbon atoms, are among many well-known scent compounds with extremely low sensory thresholds, and are also important sources of grape-derived flavors in wines. The most common C_{13}-norisoprenoids are β-damascenone, β-ionone, 1,1,6-trimethyl-1,2-dihydronaphthalene (TDN), vitispirane, and (E)-1-(2,3,6-trimethylphenyl)buta-1,3-diene (TPB). Their chemical structures are showed in Figure 1.

In Advances in Wine Research; Ebeler, et al.;
ACS Symposium Series; American Chemical Society: Washington, DC, 2015.

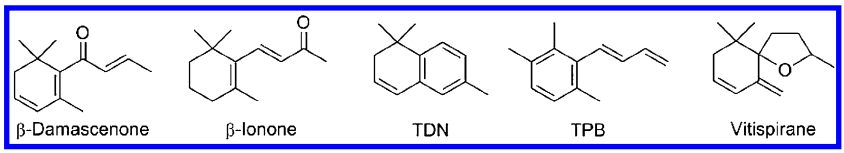

Figure 1. Chemical structures of some important C_{13}-norisoprenoids in grapes.

Publication Date (Web): November 24, 2015 | doi: 10.1021/bk-2015-1203.ch010

β-Damascenone and β-ionone were first reported in wine by Schreier and Drawert (*1*) in 1974. Since β-damascenone and β-ionone are commonly found at levels above their sensory thresholds in wines, they are suggested to be important contributors especially in nonfloral grape varieties such as Merlot, Cabernet Sauvignon and Pinot noir (*2–5*). β-Damascenone smells sweet and honey-like (*6*) with a very low sensory threshold of 2 ng/L in water (*7*) and 50 ng/L in 10% aqueous ethanol respectively (*8*). However, the contribution of β-damascenone to wine aroma is still controversial. The evidence to date indicates that it probably acts as an enhancer of aroma intensity, particularly of fruity-type aromas (*2*, *9–11*), and has the ability to mask the "herbaceous" aroma associated with 2-isobutyl-3-methoxypyrazine (*2*). β-Ionone is often described as violet and raspberry, with a sensory thresholds of 90 ng/L in wine (*8*). TDN has a kerosene-like aromas with sensory threshold of 2 μg/L in both model wine and natural white wines (*12*). Vitispirane has two chiral carbons and thus two pairs of diastereomers (often reported as vitispirane A and vitispirane B). The aroma of the diastereomers was found to be distinctly different; the pair of enantiomers, (2R,5R) and (2S,5S), described as *cis* were fresher and more intense than the *trans* pair, (2S,5R) and (2R,5S). The *cis* pair has an aroma that is comparable to the green odor of chrysanthemum with an additional flowery-fruity wine note. The *trans* pair were characterized by a heavy scent of exotic flowers with an earthy-woody undertone (*13*). The sensory threshold of visispirane has been reported as 800 μg/L (*14*). However, a sensory threshold for each of the stereoisomers of vitispirane has not been reported as yet. Although these two compounds have been detected in many wine varieties, their concentrations are commonly below the sensory threshold, and consequently have no sensory impact (*15*). However, as the wine undergoes bottle aging, TDN and vitispirane concentrations increase and can reach the level above their sensory thresholds, giving the characteristic aroma of aged wine (*16*, *17*), but is also sometimes considered to be detrimental to the wine quality (*12*). Another C_{13}-norisoprenoid, TPB (4-(2,3,6-trimethylphenyl)buta-1,3-diene), were found in wine by Janusz, et al. (*18*) in the year of 2003. It has a pleasant floral aroma at low concentrations but a pungent or chemical odor at high concentrations (*19*). It has been found in several white wine varieties such as Semillon, Chardonnay, and Riesling at levels above its sensory threshold (0.04 μg/L in wine), but not in red wines (*19*).

Formation of C_{13}-Norisoprenoids in Grape Berries

C_{13}-norisoprenoids are present in grape berries partially as the free form, and partially as non-volatile precursors, which could be transformed to the free form by enzyme or acid hydrolysis (*20*). The precursors appear to include glycoconjugates involving different conjugating moieties and also non-glycosidic compounds (carotenoids and its degradation products) (*21*). Several mechanisms of carotenoid degradation into C_{13}-norisoprenoids have been reported, including enzymatic processes, autoxidation and thermal decomposition (*22–24*). In the model system, β-damascenone can be formed directly from neoxanthin (*25*) by peroxyacetic acid oxidation and two-phase thermal degradation without the involvement of enzymatic activity, while β-ionone can be formed as a cleavage product of β-carotene (*23*) and zeaxanthin (*26*).

However, in grapevines, the synthesis pathways are more complicated than the model system because of the enzyme systems involved. Baumes et al. (*27*) investigated the formation pathways of carotenoids to norisoprenoids. They illustrated the formation of C_{13}-norisoprenoids in grape berries as three consecutive steps. The first step was carotenoid degradation catalyzed by oxidases, the degradation product was then modified by oxidases and reductases to form norisoprenoids. Finally, the norisoprenoids were glycosylated by glycosyltransferases. Once formed, these compounds were then subject to further reactions during wine aging (*28*). For the first step, specific tailoring of carotenoids is brought about by enzymatic action of a family of oxidative enzymes cleaving specific double bounds (*29*), which are called carotenoid cleavage dioxygenases (CCDs) by plant researchers. Additional studies have provided evidence supporting generation of C_{13}-norisoprenoids by region-specific enzyme cleavage of carotenoids rather than by non-specific oxidases and/or chemical degradation (*30*, *31*). Among the CCDs, CCD1 was considered to be a prime candidate for enzymatic C_{13} volatile apocartenoid biogenesis. A potential CCD gene (*VvCCD1*) has been identified in *Vitis vinifera* L. in 2005. This gene encoded a functional CCD, which cleaves zeaxanthin symmetrically, yielding 3-hydroxy-β-ionone and a C_{14}-dialdehyde (*30*). There is also evidence that the formation of C_{13}-norisoprenoids is highly associated with *VvCCD1* expression and the gene expression level is variety dependent (*30*). Since the enzymatic systems involved have not yet been fully discovered, the current knowledge still cannot completely explain the biosynthesis pathway of various C_{13}-norisoprenoids formations in grape berries.

Viticultural practices are known to influence secondary metabolites of grape vines. Such practices include regulation of water and nutrient supply, regulation of leaf area to crop ratio, and practices that increase sunlight exposure of leaves and fruits. Relationships between canopy microclimate and secondary metabolites, including aroma and flavor precursors, are not well understood. A single viticultural practice will change several parameters not only at the time the practice are performed but even after, which makes it difficult to determine which factor really impact the final norisoprenoids levels.

Publication Date (Web): November 24, 2015 | doi: 10.1021/bk-2015-1203.ch010

Effect of Canopy Management on C_{13}-Norisoprenoids and Their Precursors in Grape and Wine

Most of the vineyard practices manage the canopy directly or indirectly. Direct practices such as shoot thinning, leaf removal and crop thinning are used to modify the canopy to reach a specific level of shoot density, crop level, or cluster exposure. Indirect vine canopy managements include irrigation, fertilization, and cover crop practice, which can alter vine growth and canopy size through regulation of nutrient and water availability (*31*). Considerable efforts have been made in investigating how a grapevine canopy creates different microclimates that, in turn, affect vine and fruit physiology as well as grape chemical composition, especially the aroma compounds and aroma precursors.

Publication Date (Web): November 24, 2015 | doi: 10.1021/bk-2015-1203.ch010

Leaf Removal

Leaf removal is a canopy management practice that deliberately removes selected leaves around the cluster zones. It has been widely used in coolclimate viticultural regions to improve air circulation, sunlight exposure and to reduce disease pressure (*32–35*). Vine growth and berry development are mainly dependent on leaf photosynthesis, which in turn is markedly affected by sunlight exposure. Sunlight provides energy for photosynthesis and regulates other light-stimulated metabolic processes (*36*). Research has been carried out to study the effect of sunlight exposure on grape quality. It has been reported that grapes from vines grown under low sunlight exposure have delayed ripening, lower soluble solids, lower pH, higher titratable acidity and higher malic acid levels than grapes from unshaded vines (*37–40*).

There have been mixed results regarding leaf removal on grape and wine quality, all confounded by varying experimental settings and other factors. Climate plays a crucial role in affecting the outcome of leaf removal practices. In cool climates, where sunlight and temperature are limiting factors, leaf removal typically has a positive effect by increasing berry sunlight exposure. It has been proposed that sunlight exposure may up-regulate the activity of flavonol synthase (*41*, *42*) and stimulate the activity of the deoxyxylulose-5-phosphate (DXP) pathway that produces monoterpenes and other isoprenoid compounds (*43*). However, in hot climates, berry temperature often increases with concomitant sunlight exposure (*44*), which potentially leads to fruit sunburn and can be detrimental to grape quality (*45*).

Few studies have been done to characterize impacts of leaf removal on C_{13}-norisoprenoids in grapes and wine. Lee, et al. (*46*) compared treatments of no leaf removal to selected leaf removals, focusing on the levels of C_{13}-norisoprenoids in Cabernet Sauvignon grapes. They found that the level of C_{13}-norisoprenoid was not only positively correlated to the degree of leaf removal, but also strongly associated with the number of leaf layers. In addition, their data suggests that individual C_{13}-norisoprenoid responds differently to leaf removal. The highest degree of leaf removal was associated with the highest levels of TDN and vitispirane, while no leaf removal treatment demonstrated the highest β-damascenone level in grapes.

Furthermore, the timing of leaf removal also affects the level of carotenoids as well as C_{13}-norisoprenoids in grapes. It has been shown that leaf removal at 33-day past berry set (PBS) significantly elevated levels of total (free- and bound-form) TDN and vitispirane in mature Riesling grapes compared to the control and other leaf removal treatments (2-day and 68-day PBS). This study also observed an increased zeaxanthin level in Riesling grapes midseason. The lowest level of total β-damascenone was found in grapes with 68-day PBS leaf removal treatment (*47*).

In Oregon, leaf removal is normally performed between fruit set and véraison to increase fruit-zone sunlight exposure, reduce disease incidence without causing fruit sunburn (*31*). In order to better understand the impact of fruit-zone leaf removal practice on Pinot noir grape and wine volatile composition, berry volatile composition was investigated over three growing seasons (2010, 2011, and 2012) in two vineyards located within the Willamette Valley of Oregon, under different levels of leaf removal, including removing 0% (None), 50% and 100% of leaves from the cluster zone at berry pea-size stage, and a current local industry standard treatment (IS). Results revealed that leaf removal practice did not alter vine growth or berry ripening, but the 100% leaf removal increased levels β-damascenone (free- and bound-form) compared to control (none) (Figure 2) and a positive correlation was found between levels of free- and bound-form β-damascenone and sunlight exposure in cluster zone (Figure 3) (*48*).

The increased β-damascenone is presumed to be the result of pre-véraison cluster light environment changes. Temperature might also have an influence on the C_{13}-norisoprenoid content of grapes, but this is difficult to separate from light since sun-exposed berry temperatures will potentially differ from those in the shade. For further understanding, we quantified carotenoid concentrations in the grape samples in the study mentioned above. The carotenoids in Pinot noir berries were extracted by ethyl acetate, and analyzed by HPLC. The results showed that cluster zone leaf removal significantly decreased flavoxanthin content for all the three experimental years (Figure 4). Conversely, increased neochrome *a* content was found at the 50% and 100% leaf removal treatment in year 2011 and 2012, but not in 2010. Decreased β-carotene content in berries was also found in 100% leaf removal treatment in year 2012 but not in the other two years, although a decreasing trend was also observed in 2011. No significant difference in lutein content was observed among the treatments in any of the three years.

There could be several possible explanations for this observation. Since pre-véraison berries are photosynthetically active, higher concentrations of carotenoids and thus higher substrate availabilitycould potentially lead to higher concentrations of C_{13}-norisoprenoid precursors in sun-exposed grapes. Secondly, post-véraison cluster exposure may accelerate carotenoid degradation and C_{13}-norisoprenoid precursor synthesis. A third potential explanation is that sun exposure results in conversion of epoxyxanthophylls (e.g., violaxanthin) to de-epoxidized xanthophylls (e.g., zeaxanthin). Since the putative starting point for the precursors of C_{13}-norisoprenoids may be deepoxidized xanthophylls (*49*), sun exposure may alter the proportion of de-epoxidized vs. epoxidixed forms of xanthophylls, and these different substrates could yield different C_{13}-norisoprenoid precursors post-véraison (*27*). However, a clear correlation has

Publication Date (Web): November 24, 2015 | doi: 10.1021/bk-2015-1203.ch010

not been conclusively demonstrated between a specific carotenoid or carotenoids in grapes and eventual concentrations of TDN or other C_{13}-norisoprenoids in mature fruit. More information is still needed to better understand the effect of leaf removal, sunlight exposure and cluster zone microclimate on carotenoids and C_{13}-norisoprenoid synthesis in grapes.

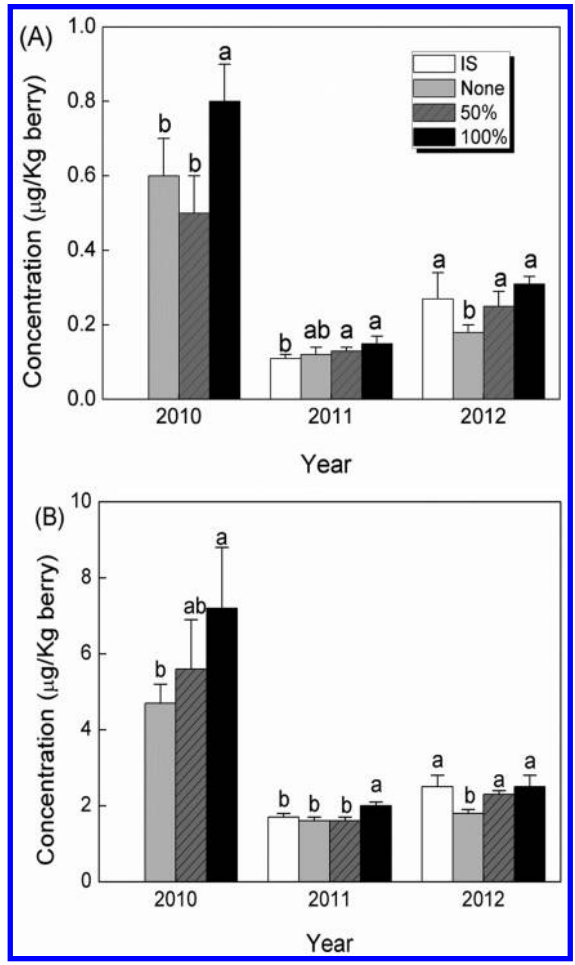

Figure 2. Concentrations of β-damascenone in Pinot noir grape with different vineyard leaf removal treatments from 2010 to 2012. (A) free-form and (B) bound-form. Mean±SD are presented (n=5). Different lowercase letters indicate statistical difference in means between treatments using Tukey HSD mean separation at $p<0.05$. Leaf removal treatments include the following: None (no leaf removal), 100% (all leaves in the cluster zone removed), 50% (half of the leaves in the cluster zone removed) and IS (industry standard where leaves are only removed in the cluster zone on the east side of the canopy. Reproduced with permission from Ref (48). Copyright 2015, ELSEVIER.

Publication Date (Web): November 24, 2015 | doi: 10.1021/bk-2015-1203.ch010

Publication Date (Web): November 24, 2015 | doi: 10.1021/bk-2015-1203.ch010

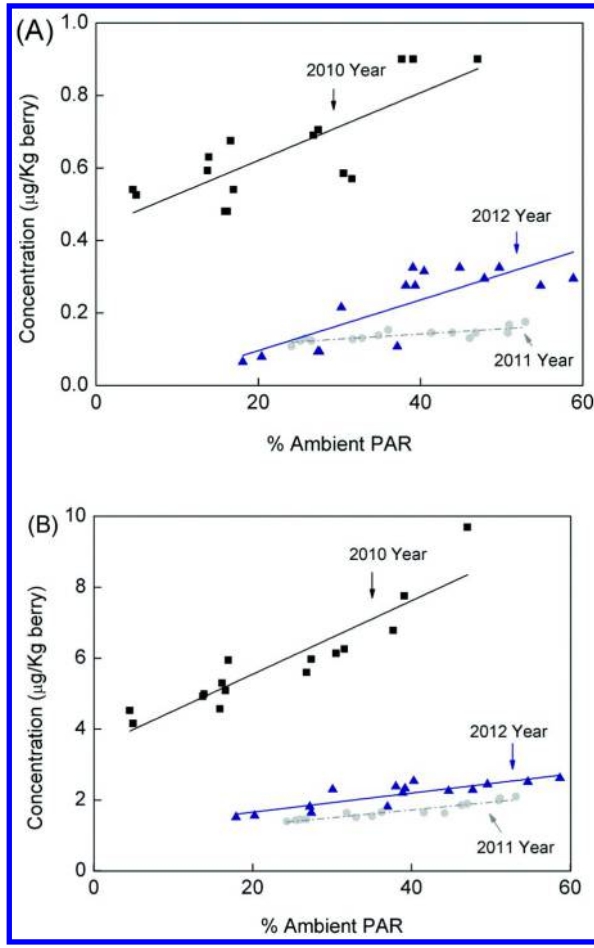

Figure 3. Concentrations of free-form β-damascenone (A) and bound-form β-damascenone (B) in Pinot noir grapes as a function of %ambient photosynthetically active radiation (PAR) of cluster zone from 2010 to 2012. In (A), regression analysis indicated linear relationships demonstrated by the equations as following, in 2010 y=0.0093x+0.4339 (r2=0.6384, p<0.0001), in 2011 y =0.0014x+0.0816 (r2=0.6712, p<0.0001), and in 2012 y =0.007x+0.0377 (r2=0.647, p<0.0001). In (B), regression analysis indicated linear relationships demonstrated by the equations as following, in 2010 y=0.1036x+3.4753 (r2=0.8428, p<0.0001), in 2011 y =0.0218x+0.887 (r2=0.8949, p<0.0001), and in 2012 y =0.0269x+1.1175 (r2=0.735, p<0.0001). Reproduced with permission from Ref (48). Copyright 2015, ELSEVIER.

Publication Date (Web): November 24, 2015 | doi: 10.1021/bk-2015-1203.ch010

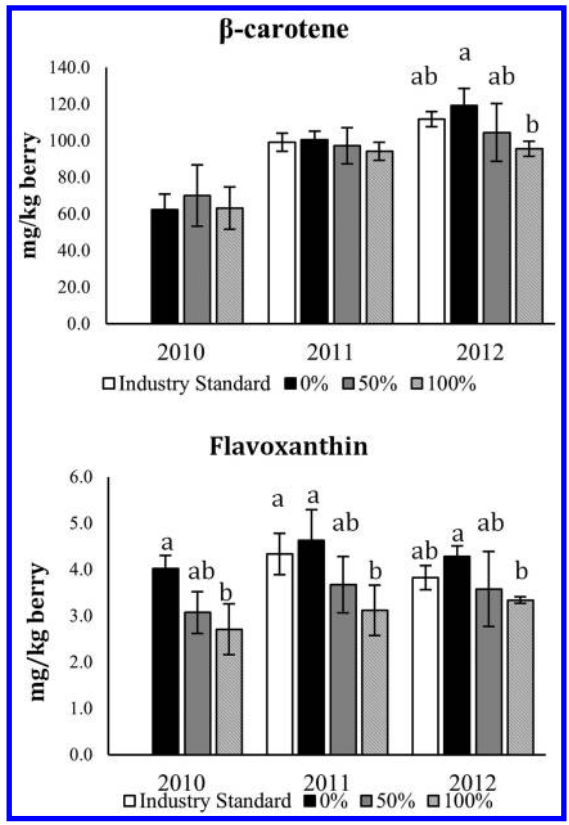

Figure 4. Concentrations of β-carotene and flavoxanthin in Pinot noir grape with different vineyard leaf removal treatments from 2010 to 2012. Mean±SD are presented (n=5). Different lowercase letters indicate statistical difference in means between treatments using Tukey HSD mean separation at p<0.05. Leaf removal treatments include the following: None (no leaf removal), 50% (half of the leaves in the cluster zone removed) and 100% (all leaves in the cluster zone removed).

Cover Crop

Cover crop practice is the vineyard floor management strategy of planting cover crops between vine rows. Growing cover crops in vineyard can help decreases soil erosion (*50*), improves soil structure (*51*, *52*) and suppresses weed growth (*53*). In some coolclimate viticultural regions, deep soil with high soil moisture and nutrient availability commonly leads to significant vine vegetative growth. The use of cover crops practice to control excessive vine vigor could become an effective agronomic tool to control canopy density.

Only a few studies have reported the effect of cover crop management on C_{13}-norisoprenoids compounds, but the results are inconsistent. Xi, et al. (*54*) reported that permanent plantings of alfalfa as a cover crop between the rows led

to the highest β-damascenone and α-ionone in wine compared to clean tillage, while white clover and tall fescue did not affect the C_{13}-norisoprenoids in wine. In Oregon, we conducted a three year study in Pinot noir grape. The grapes were harvested from 2008, 2009 and 2010 at a commercial vineyard located in Dayton, Oregon (45°N, 123°W; Dundee Hills AVA). The climate was characterized as cool with high winter and spring rainfall, which is typical for the climate of much of the grape production region within the Willamette Valley of Oregon. The climate and soil conditions generally resulted in high vegetative growth for vineyards within this region. The vineyard consisted of Pinot noir clone 115 grafted to 101-14 rootstock planted in 1998 to north-south oriented rows with 1.5 m×2.1 m. Vines were cane pruned and trained to a bilateral Guyot system with vertical shoot positioning. The treatments were applied in a completely randomized block design with five field replicates consisting of 16 vines per plot. The areas between vine rows (inter-rows) were managed as follows: 1) grass consisting of hard red fescue (*Festuca rubra spp*.rubra), grown on both sides of the experimental vine rows (Grass); 2) alternating inter-rows with tillage and grass on either side of the vine rows (Alternate); and 3) tillage on both sides of the vine row (Tilled). Tilled areas within the treatments were root-tilled in spring and summer to prevent weed vegetation from establishing. In the Grass treatment, inter-rows were mowed until the grass became quiescent in mid-later summer. The vineyard was managed using regular management practices (e.g., fungicide application, in-row cultivation for weed control, hedging, cluster-zone leaf removal, and cluster thinning). Both free and bound form C_{13}-norisoprenoids in the berries were measured using SBSE-GC-MS method as well as the C_{13}-norisoprenoid concentration in corresponding wines. We found that permanent grass cover lead to a decreased β-damascenone concentration in most of the years (Figure 5A&B) and also decreased levels of β-damascenone in corresponding wines (Figure 5C).

Previous studies have reported that the competition between the cover crop and vine for soil water and nutrients appears to be the principal mechanism behind the reduction in vine vigor (*55–57*). As mentioned previously, increased vine water stress has been reported to increase levels of positive volatile compounds (e.g., bound-form monoterpenes and C_{13}-norisoprenoids) and decrease negative volatile compounds (C_6 compounds and methoxypyrazine) in Cabernet Sauvignon and Merlot grapes, leading to increased fruity aromas in wine (*58–61*). Among nutrients that vines absorb from the soil, nitrogen has a key impact on vine vigor and grape quality. Increased nitrogen stress has been shown to reduce vine vigor, grape yield, berry size and nitrogen levels in grapes, but increase levels of sugar, tannin and anthocyanin in grapes (*62–64*). There is evidence that nitrogen level can also alter the secondary metabolites in grape berries such as C_{13}-norisoprenoids. However, few studies have been available so far about the influence of vine nitrogen status on aromatic compounds or precursors in grape. A study on soil subjected to long-term nitrogen fertilization has revealed that the increase of vine nitrogen level improved Riesling wine quality through the increased β-damascenone concentration (*65*). Besides the direct impact of water and nitrogen on vine growth and berry development, cover crop may also influence grape quality indirectly through the modification of canopy microclimate.

Publication Date (Web): November 24, 2015 | doi: 10.1021/bk-2015-1203.ch010

Publication Date (Web): November 24, 2015 | doi: 10.1021/bk-2015-1203.ch010

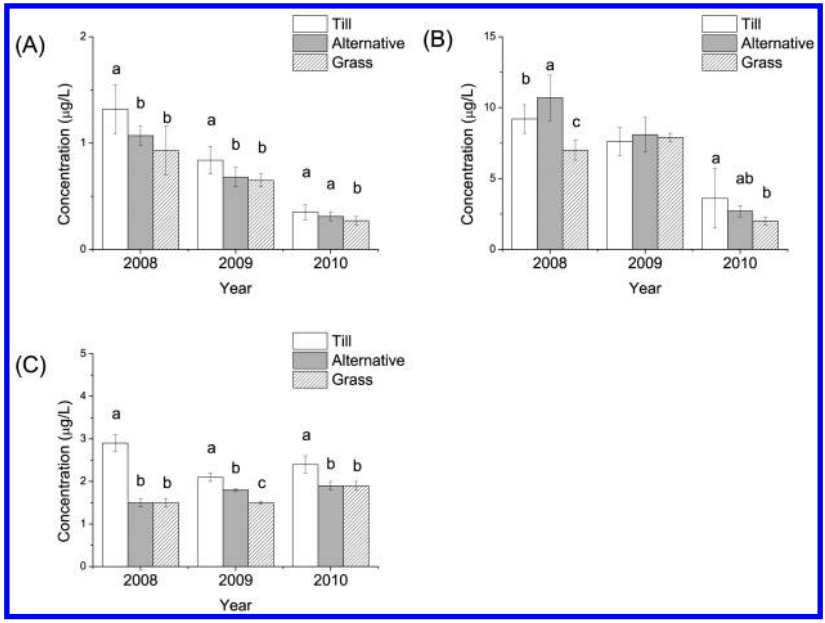

Figure 5. Concentrations of β-damascenone in Oregon Pinot noir grape with different cover crop vineyard floor management from 2010 to 2012. (A) free-form in grape, (B) bound-form in grape and (C) in wine. Mean±SD are presented (n=5). Different lowercase letters indicate statistical difference in means between treatments using Tukey HSD mean separation at $p<0.05$.

Irrigation

It is well known that adequate water is essential to obtain high quality grapes for wine production (*66*, *67*). Previous studies showed that, at critical phenological stages, changes in grapevine water status have direct effects on grape composition and quality by influencing vegetative growth, yield, canopy microclimate, and fruit metabolism (*67*, *68*). These improvements are directly related to wine quality components, such as color, flavor and wine aroma due to an increment of skin to pulp ratio in berries (*69*).

Many studies have shown that water deficiency can increase the C_{13}-norisoprenoid concentrations in grape berries. Qian, et al. (*58*, *59*, *70*) investigated the impact of deficit irrigation during berry development on Merlot wine volatile composition using SBSE-GC-MS technique. The results showed that deficit-irrigated vines had increased the amounts of vitispirane and β-damascenone, while the increase of C_{13}-norisoprenoids in berries were in response to severity of the vine water stress, and an increased level of β-damascenone were also observed in the corresponding wines (*59*). Bindon, et al. (*71*) studied the impact of partial root-zone drying (PRD) on grape volatile composition and showed that in Cabernet Sauvignon grape berries, PRD consistently caused increases in the concentration of hydrolytically released

C_{13}-norisoprenoids in fruit at harvest. The response to PRD was not only independent of water deficit induced changes in berry size but also independent of altered berry surface area to volume ratio. Another research in Agiorgitiko grapes showed a quantitative increase in levels of C_{13}-norisoprenoids in corresponding wines under water deficit in both years (*69*).

The levels of C_{13}-norisoprenoids as a function of irrigation status are assumed to be related to changes in the carotenoid levels. Oliveira et al. reported that carotenoids in berries were lower from irrigated treatment than those found for the nonirrigated treatment, when the vines were grow in low water retention capacity soils. But there is no difference between irrigation and non-irrigation treatments in high water retention capacity soils, indicating that soil was also an important viticultural parameter to take into account in aroma precursor formation (*72*). However, C_{13}-norisoprenoid concentrations were not measured in the berries in this study.

These results imply that water stress can increase C_{13}-norisoprenoids in grape berries, not only by changing the berry size or surface/volume ratio. It is reported that water deficit increased the transcript abundance of CCD gene in grape during berry development (*73*). Meanwhile, water deficit can also reduce shoot growth rate and vine leaf area (*74*), leading to an increase in sunlight penetration to the fruiting zone of the canopy, which may also influence the metabolism of carotenoid degradation and C_{13}-norisoprenoid formation. Since it is hard to separate the light factor, it is still unclear if water deficit have a direct or indirect impact on grape C_{13}-norisoprenoids metabolism.

Publication Date (Web): November 24, 2015 | doi: 10.1021/bk-2015-1203.ch010

Summary

C_{13}-norisoprenoids are important grape-derived aroma compounds in wine, and it remains largely unknown whether they are generated from chemical oxidation, photooxidation or other mechanisms. Viticultural practices could alter C_{13}-norisoprenoid level in grape berries by changing one or more parameters. But there are limited data to illustrate the effect of viticultural practices on grape C_{13}-norisoprenoids. Our review of current research showed that the concentration of C_{13}-norisoprenoids in grape berries could be manipulated by altering levels of water stress, sunlight exposure and nutrient supply by directly or indirectly affecting the biosynthesis of C_{13}-norisoprenoids. More studies are still needed to further understand the mechanisms of these impacts.

References

1. Schreier, P.; Drawert, F. *Eur. Food Res. Technol.* **1974**, *154*, 273–278.
2. Pineau, B.; Barbe, J. C.; Van Leeuwen, C.; Dubourdieu, D. *J. Agric. Food Chem.* **2007**, *55*, 4103–4108.
3. Fang, Y.; Qian, M. *Flavour Fragrance J.* **2005**, *20*, 22–29.
4. Lopez, R.; Ferreira, V.; Hernandez, P.; Cacho, J. F. *J. Sci. Food Agric.* **1999**, *79*, 1461–1467.

5. Gürbüz, O.; Rouseff, J. M.; Rouseff, R. L. *J. Agric. Food Chem.* **2006**, *54*, 3990–3996.
6. Kovats, E. S. *J. Chromatogr.* **1987**, *406*, 185–222.
7. Buttery, R.; Teranishi, R.; Ling, L. *Chem. Ind.* **1988**, *7*, 238–238.
8. Guth, H. *J. Agric. Food Chem.* **1997**, *45*, 3022–3026.
9. Escudero, A.; Campo, E.; Fariña, L.; Cacho, J.; Ferreira, V. *J. Agric. Food Chem.* **2007**, *55*, 4501–4510.
10. Ferreira, V.; Ortín, N.; Escudero, A.; López, R.; Cacho, J. *J. Agric. Food Chem.* **2002**, *50*, 4048–4054.
11. Sefton, M. A.; Skouroumounis, G. K.; Elsey, G. M.; Taylor, D. K. *J. Agric. Food Chem.* **2011**, *59*, 9717–9746.
12. Sacks, G. L.; Gates, M. J.; Ferry, F. X.; Lavin, E. H.; Kurtz, A. J.; Acree, T. E. *J. Agric. Food Chem.* **2012**, *60*, 2998–3004.
13. Schulte-Elte, K. H.; Gautschi, F.; Renold, W.; Hauser, A.; Fankhauser, P.; Limacher, J.; Ohloff, G. *Helv. Chim. Acta.* **1978**, *61*, 1125–1133.
14. Simpson, R. F.; Strauss, C. R.; Williams, P. J. *Chem. Ind.* **1977**, *15*, 663–664.
15. Eggers, N. J.; Bohna, K.; Dooley, B. *Am. J. Enol. Vitic.* **2006**, *57*, 226–232.
16. Marais, J.; Van Wyk, C.; Rapp, A. *S. Afr. J. Enol. Vitic.* **1992**, *13*, 33–44.
17. Winterhalter, P.; Rouseff, R. Carotenoid-derived Aroma Compounds: An Introduction. In *Carotenoid-derived Aroma Compounds*; Winterhalter, P., Rouseff, R., Eds.; ACS Symposium Series 802, American Chemical Society: Washington, DC, 2001; pp 1−17.
18. Janusz, A.; Capone, D. L.; Puglisi, C. J.; Perkins, M. V.; Elsey, G. M.; Sefton, M. A. *J. Agric. Food Chem.* **2003**, *51*, 7759–7763.
19. Cox, A.; Capone, D. L.; Elsey, G. M.; Perkins, M. V.; Sefton, M. A. *J. Agric. Food Chem.* **2005**, *53*, 3584–3591.
20. Williams, P.; Strauss, C.; Wilson, B.; Massy-Westropp, R. *J. Chromatogr. A* **1982**, *235*, 471–480.
21. Winterhalter, P.; Sefton, M.; Williams, P. *Am. J. Enol. Vitic.* **1990**, *41*, 277–283.
22. Mordi, R. C.; Walton, J. C.; Burton, G. W.; Hughes, L.; Ingold, K. U.; Lindsay, D. A. *Tetrahedron Lett.* **1991**, *32*, 4203–4206.
23. Kanasawud, P.; Crouzet, J. C. *J. Agric. Food Chem.* **1990**, *38*, 237–243.
24. Mendes-Pinto, M. M.; Ferreira, A. C. S.; Caris-Veyrat, C.; de Pinho, P. G. *J. Agric. Food Chem.* **2005**, *53*, 10034–10041.
25. Bezman, Y.; Bilkis, I.; Winterhalter, P.; Fleischmann, P.; Rouseff, R. L.; Baldermann, S.; Naim, M. *J. Agric. Food Chem.* **2005**, *53*, 9199–9206.
26. Mathieu, S.; Terrier, N.; Procureur, J.; Bigey, F.; Gunata, Z. *J. Exp. Bot.* **2005**, *56*, 2721–31.
27. Baumes, R.; Wirth, J.; Bureau, S.; Gunata, Y.; Razungles, A. *Anal. Chim. Acta.* **2002**, *458*, 3–14.
28. Loscos, N.; Hernández-Orte, P.; Cacho, J.; Ferreira, V. *Food Chem.* **2010**, *120*, 205–216.
29. Walter, M. H.; Strack, D. *Nat. Prod. Rep.* **2011**, *28*, 663–692.
30. Mathieu, S.; Terrier, N.; Bigey, F.; Günata, Z. *J. Exp. Bot.* **2005**, *56*, 2721–2731.

31. Vance, A. J.; Skinkis, P. *Understanding Vine Balance: An Important Concept in Vineyard Management*; Extension Service, Oregon State University: Corvallis, OR, 2013.
32. Percival, D.; Fisher, K.; Sullivan, J. *J. Agric. Food Chem.* **1994**, *45*, 123–132.
33. English, J.; Thomas, C.; Marois, J.; Gubler, W. *Phytopathology* **1989**, *79*, 395–401.
34. Jackson, D.; Lombard, P. *Am. J. Enol. Vitic.* **1993**, *44*, 409–430.
35. Kliewer, M.; Bledsoe, A. *Symposium on Grapevine Canopy and Vigor Management*, XXII IHC 206; 1986; pp 157−168.
36. Crippen, D. D.; Morrison, J. C. *Am. J. Enol. Vitic.* **1986**, *37*, 235–242.
37. Reynolds, A. G.; Wardle, D. A. *Am. J. Enol. Vitic.* **1989**, *40*, 149–154.
38. Dokoozlian, N.; Kliewer, W. *J. Am. Soc. Hortic. Sci.* **1996**, *121*, 869–874.
39. Keller, M.; Arnink, K. J.; Hrazdina, G. *Am. J. Enol. Vitic.* **1998**, *49*, 333–340.
40. Reynolds, A.; Pool, R.; Matpick, L. *Vitis* **1986**, *25*, 85–95.
41. Downey, M. O.; Harvey, J. S.; Robinson, S. P. *Aust. J. Grape Wine Res.* **2004**, *10*, 55–73.
42. Matus, J. T.; Loyola, R.; Vega, A.; Peña-Neira, A.; Bordeu, E.; Arce-Johnson, P.; Alcalde, J. A. *J. Exp. Bot.* **2009**, *60*, 853–867.
43. Estévez, J. M.; Cantero, A.; Reindl, A.; Reichler, S.; León, P. *J. Biol. Chem.* **2001**, *276*, 22901–22909.
44. Spayd, S. E.; Tarara, J. M.; Mee, D. L.; Ferguson, J. *Am. J. Enol. Vitic.* **2002**, *53*, 171–182.
45. Chorti, E.; Guidoni, S.; Ferrandino, A.; Novello, V. *Am. J. Enol. Vitic.* **2010**, *61*, 23–30.
46. Lee, J.; Skinkis, P. A. *Food Chem.* **2013**, *139*, 893–901.
47. Kwasniewski, M. T.; Vanden Heuvel, J. E.; Pan, B. S.; Sacks, G. L. *J. Agric. Food Chem.* **2010**, *58*, 6841–6849.
48. Feng, H.; Yuan, F.; Skinkis, P. A.; Qian, M. C. *Food Chem.* **2015**, *173*, 414–423.
49. Mendes-Pinto, M. M. *Arch. Biochem. Biophys.* **2009**, *483*, 236–245.
50. Novara, A.; Gristina, L.; Saladino, S.; Santoro, A.; Cerda, A. *Soil Tillage Res.* **2011**, *117*, 140–147.
51. Klik, A.; Rosner, J.; Loiskandl, W. *Soil Water Conserv.* **1998**, *53*, 249–253.
52. Reicosky, D.; Forcella, F. *J. Soil Water Conserv.* **1998**, *53*, 224–229.
53. Steinmaus, S.; Elmore, C.; Smith, R.; Donaldson, D.; Weber, E.; Roncoroni, J.; Miller, P. *Weed Res.* **2008**, *48*, 273–281.
54. Xi, Z; Tao, Y; Zhang, L.; Li, H. *Food Chem.* **2011**, *127*, 516–522.
55. Celette, F.; Findeling, A.; Gary, C. *Eur. J. Agron.* **2009**, *30*, 41–51.
56. Monteiro, A.; Lopes, C. M. *Agric. Ecosyst. Environ.* **2007**, *121*, 336–342.
57. Tesic, D.; Keller, M.; Hutton, R. J. *Am. J. Enol. Vitic.* **2007**, *58*, 1–11.
58. Qian, M. C.; Fang, Y.; Shellie, K. *J. Agric. Food Chem.* **2009**, *57*, 7459–7463.
59. Ou, C.; Du, X.; Shellie, K.; Ross, C.; Qian, M. C. *J. Agric. Food Chem.* **2010**, *58*, 12890–12898.

Publication Date (Web): November 24, 2015 | doi: 10.1021/bk-2015-1203.ch010

60. Sala, C.; Busto, O.; Guasch, J.; Zamora, F. *J. Sci. Food Agric.* **2005**, *85*, 1131–1136.
61. Song, J.; Shellie, K. C.; Wang, H.; Qian, M. C. *Food Chem.* **2012**, *134*, 841–850.
62. Baiano, A.; La Notte, E.; Coletta, A.; Terracone, C.; Antonacci, D. *Am. J. Enol. Vitic.* **2011**, *62*, 57–65.
63. Lee, J.; Steenwerth, K. L. *Sci. Hort.* **2013**, *159*, 128–133.
64. Schreiner, R. P.; Scagel, C. F.; Lee, J. *Am. J. Enol. Vitic.* **2014**, *65*, 43–49.
65. Linsenmeier, A. W.; Lohnertz, O. *S. Afr. J. Enol. Vitic.* **2007**, *28*, 17.
66. Ojeda, H.; Andary, C.; Kraeva, E.; Carbonneau, A.; Deloire, A. *Am. J. Enol. Vitic.* **2002**, *53*, 261–267.
67. Pellegrino, A.; Lebon, E.; Simonneau, T.; Wery, J. *Aust. J. Grape Wine Res.* **2005**, *11*, 306–315.
68. Ezzhaouani, A.; Valancogne, C.; Pieri, P.; Amalak, T.; Gaudillere, J. *J. Int. Sci. Vin.* **2007**, *41*, 131.
69. Koundouras, S.; Marinos, V.; Gkoulioti, A.; Kotseridis, Y.; Van Leeuwen, C. *J. Agric. Food Chem.* **2006**, *54*, 5077–5086.
70. Song, J.; Shellie, K.; Wang, H.; Qian, M. *Food Chem.* **2012**, *134*, 841–50.
71. Bindon, K. A.; Dry, P. R.; Loveys, B. R. *J. Agric. Food Chem.* **2007**, *55*, 4493–4500.
72. Oliveira, C.; Silva Ferreira, A. C.; Mendes Pinto, M.; Hogg, T.; Alves, F.; Guedes de Pinho, P. *J. Agric. Food Chem.* **2003**, *51*, 5967–5971.
73. Deluc, L. G.; Quilici, D. R.; Decendit, A.; Grimplet, J.; Wheatley, M. D.; Schlauch, K. A.; Mérillon, J.-M.; Cushman, J. C.; Cramer, G. R. *BMC Genomics* **2009**, *10*, 212.
74. Dry, P. R.; Loveys, B. R. *Aust. J. Grape Wine Res.* **1998**, *4*, 140–148.

Publication Date (Web): November 24, 2015 | doi: 10.1021/bk-2015-1203.ch010

Publication Date (Web): November 24, 2015 | doi: 10.1021/bk-2015-1203.ch011

Chapter 11

Under-Vine Management To Modulate Wine Chemical Profile

Mark Krasnow,[1] Antony Mavumkal,[2] Tingting Zhang,[3] Petra King,[3] Melissa Annand,[3] Marc Greven,[4] M. Carmo Vasconcelos,[3] Damian Martin,[4] Mandy Herbst-Johnstone,[2] and Bruno Fedrizzi*,[2]

[1]Department of Culinary Science, The Culinary Institute of America, 1946 Campus Drive, Hyde Park, New York, 12538, U.S.A.
[2]Wine Science Programme, School of Chemical Sciences, The University of Auckland, Private Bag 92019, Auckland, New Zealand
[3]Eastern Institute of Technology, School of Viticulture and Winescience, Taradale, Napier, 4142, New Zealand
[4]Plant & Food Research Ltd, Marlborough Wine Research Centre, Blenheim, 85 Budge Street, Blenheim, 7201, New Zealand
***E-mail: b.fedrizzi@auckland.ac.nz.**

Conventional viticulture relies on herbicides to prevent the growth of competing vegetation under the vines. There is a drive within the industry, particularly in New Zealand, to increase sustainability, and therefore nonchemical options to deal with under-vine vegetation would be of great benefit. A very limited number of studies have considered the impact of under-vine management practices on the aroma profiles of wine. The effects of three different under-vine management approaches (mowing, cultivation and herbicide) on vine performance, soil properties and aromas of Sauvignon blanc and Pinot noir grapes and wines were considered in a commercial vineyard in Blenheim, and Merlot and Syrah in the Hawke's Bay, New Zealand. A full factorial randomised block design was developed. Vine performance (i.e.: trunk circumference, leaf area, point quadrat analysis (PQA), midday stem water potential, petiole analysis, and leaf gas-exchange), basic fruit compositional parameters (pH, TSS, TA and berry weights) and wine aroma profile were compared in the 3 treatments.

In Advances in Wine Research; Ebeler, et al.;
ACS Symposium Series; American Chemical Society: Washington, DC, 2015.

There were few differences in vine physiological parameters and canopy measurements. Yield and fruit composition was not significantly affected by the treatments, indicating that ripening was not impaired by the nonchemical options. Wines made from mowed treatments showed lower pyrazine concentrations and lower 3MH and 3MHA concentrations in the Sauvignon blanc wines. These data show that nonchemical methods to control under-vine vegetation are a viable option, as they do not negatively affect the vines and are able to affect the flavor and aroma of the resulting wines.

Publication Date (Web): November 24, 2015 | doi: 10.1021/bk-2015-1203.ch011

About 4.5% of New Zealand's vineyards are currently certified organic, with a goal of 20% by 2020 (*1*), which equates to 5000 hectares yet to be converted. Conversion to organics presents a challenge to viticulturists, as the costs of implementation, disease pressure, and the long-term effects on the productivity of the vineyard have yet to be well established. One of the major challenges to organic viticulture is the management of the space under the vines, as standard mowers and cultivators miss this area.

Conventional viticulture relies on the use of herbicides to keep the undervine region devoid of vegetation that might compete with vines for water or nutrients. This method is rapid and inexpensive, but many growers would prefer to avoid dependence on chemical inputs and grow grapes more sustainably. Additionally, in conventional vineyards, the overuse of herbicides has led to the development of resistance by weed species (*2*, *3*). Recently, there has been a resurgence of organic and biodynamic production approaches worldwide, which do not allow for the use of synthetic herbicides, and therefore require a different strategy to deal with undervine vegetation. There are several nonchemical means to deal with undervine vegetation, including cultivation, mowing, mulches, and flame weeding. Of these, the most commonly used in production vineyards worldwide are undervine cultivation and mowing.

The management of undervine vegetation has direct effects on the vines and the soil, which can have indirect effects on wine quality (*4*, *5*). The growth of the vine canopy is dependent on the availability of water and nutrients (*6*, *7*). The use of herbicides under the vines reduces competition, and therefore can directly affect the growth of the canopy. Canopy characteristics have direct effects on fruit composition and maturity. Inadequate canopy area, and its consequent low levels of photosynthate production, can lead to sluggish ripening. It is generally considered adequate to have 1-1.5 m^2 of exposed canopy per kg of fruit (*8*). Increasing the leaf area/fruit ratio beyond this led to no appreciable increase in sugar accumulation (*8*). The ideal canopy, in addition to having adequate exposed leaf area for ripening, also has 20-40 % canopy gaps allowing for enough photosynthesis to ripen the crop, but also for some airflow and sunlight to reach the developing fruit (*9*).

Publication Date (Web): November 24, 2015 | doi: 10.1021/bk-2015-1203.ch011

Overly dense canopies can create problems for viticulturists. They require more frequent trimming, hedging, and leaf removal, adding to vineyard management costs. Furthermore, the fruit microclimate has effects on the incidence and severity of fungal diseases. Fungal infection can reduce the quality of fruit for winemaking, and in severe cases can render the fruit unusable and valueless. The increased humidity and lack of UV light exposure in dense canopies leads to a microclimate more conducive to the development and spread of fungal diseases, including *Botrytis cinerea* (*10*) and *Erysiphe necator*, the causal agent of powdery mildew (*11*). A dense canopy also reduces antifungal spray penetration, which can exacerbate fungal incidence and severity (*12*, *13*). The negative effects of overly dense canopies are not only due to their promotion of fungal diseases, but also effects on grape and wine composition. Shaded fruit has been shown to have higher concentrations of methoxypyrazines (*14–16*), which lend vegetative aromas and flavors, and at high levels are considered a fault in many wine styles. Fruit exposure induces the synthesis of phenolic compounds (*17–20*), which give red wines their color, bitterness, and astringency. Shading also reduces the synthesis of important aroma and flavor compounds including monoterpenes (*16*, *21–23*) and C13 norisoprenoids (*16*).

Undervine cultivation involves the mounding up of the top 2-3 cm of soil by undercutting with a plow, and then the subsequent "knocking down" of the mound with a rotary hoe. This practice is effective against all types of vegetation, including grasses and broadleaf species, and therefore eliminates any competition with vines, similarly to herbicide application. Cultivation also promotes the mineralization of the green cover and subsequent release of nutrient to soil, making them available for the vine.Undervine mowing involves the use of specialized mowing heads that protrude under the vines, and retract when contact with the vine trunk is made. The vegetation is not killed, and therefore can still compete with vines for water and/or mineral nutrients.

Given the potential effects of competition on grapevine canopy growth and its subsequent effects on fruit, a study to investigate undervine management practices on vine performance and fruit and wine composition is necessary. A three-year trial was established in New Zealand investigating the effects of discontinuation of herbicide treatments under vines and the adoption of cultivation or mowing. The data presented here are from the first two seasons of this trial. The third year of this trial is currently undergoing.

Experimental

Experimental Sites

The trial is being carried out in vineyards on both the North and South Islands of New Zealand. The Sauvignon blanc (SB) and Pinot noir (PN) sites are located in Pernod Ricard's Renwick Vineyard in Marlborough (South Island). The Merlot (ME) site is located in the Te Mata Bullnose Vineyard in the Bridge Pa subregion, and the Syrah (SY) site is located in Elephant Hill's Estate Vineyard in the Te Awanga subregion, both in Hawke's Bay (North Island).

All trial vineyards were established conventionally with the use of herbicide under the vines. In the 2012-13 season, the experimental treatments were imposed, to be maintained for three years. The three treatments were: continued use of herbicide as the control, the implementation of undervine cultivation with a Clemens weeder (FMR group, Germany), and the implementation of undervine mowing with a DuoCut mower (DearTech Limited, New Zealand). In each vineyard, each treatment was replicated 6 times in a randomized block design. Each plot had buffer bays and rows between treatments from which no data were collected (Figure 1).

Publication Date (Web): November 24, 2015 | doi: 10.1021/bk-2015-1203.ch011

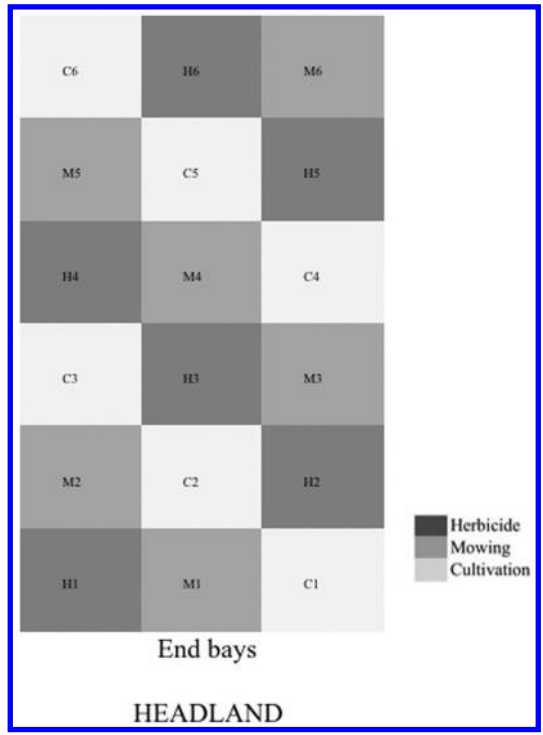

Figure 1. Plot design for all experimental sites. Each column denotes 3 vineyard rows. Each row in this figure denotes a replicate of 3-6 bays. Data was only obtained from vines in the central row and central bays of each replicate. Each replicate is designated by a letter (H=herbicide, C=cultivation, M=mowing) followed by the replicate number (1-6).

For both the ME and SY sites, 4 data vines were chosen from each treatment replicate for water potential, yield measurement, and harvesting for microvinification of experimental wines. For SB, three data vines were chosen, and for PN, 5 data vines were chosen.

Publication Date (Web): November 24, 2015 | doi: 10.1021/bk-2015-1203.ch011

Midday Stem Water Potential

Water status of vines was measured using a pressure chamber (PMS Instrument Company, Albany, OR, USA). Leaves were enclosed in custom built opaquplate reflective aluminized mylar bags, and allowed to equilibrate on the vines for a minimum of 30 min before being measured. Once equilibrated, the leaves were removed from the vine, a straight cut was made with a razor blade near the end of the petiole, and the leaf inserted into the chamber with the cut petiole protruding through the gasket on the lid to the chamber. To obtain tension measurements the chamber was pressurized with nitrogen gas until xylem sap just started to emerge from the cut end of the petiole. All measurements were carried out between 11 AM and 3 PM. Three vines per treatment rep were measured at the Marlborough sites, and 4 vines per treatment replicate were measured in the Hawke's Bay sites. In 2013-14, four vines were measured in all vineyards

Leaf Area

Four shoots from each treatment replicate were randomly sampled and carefully removed from the vines. Shoots were placed into large plastic bags for transport to the laboratory. On occasions where leaf area measurement was not possible on the same day as sampling, the bagged shoots were stored in a 4°C room overnight. On the day of measurement, all leaves were carefully cut from the shoots at the point of petiole attachment to the blade. Leaves were loaded onto a LI-3100 Area Meter (LI-COR Inc., USA), and the total leaf area per shoot was recorded.

Berry Sampling

At approximately two week intervals from veraison onward berries were sampled from data vines. One-hundred forty berries were collected from each replicate. Berries were weighed to determine berry weight for the replicate. Forty-Sixty berries were randomly separated from the sample to be used for analysis of juice total soluble solids (TSS), pH, titratable acidity (TA), and organic acids. The remaining berries were frozen for later GC analysis of methoxypyrazines for ME and SB.

Juice Analysis

The 40-60 berries from each berry sample were crushed in a plastic bag and the juice decanted into 50 mL tubes. The juice was then centrifuged at 4500 rpm for 10 min to pellet any cell material. The supernatant was used for all analyses. Brix was determined using a PAL-1 Digital Hand-held Refractometer (Atago, Japan). In the 2012-13 season TA and pH were measured on 2.5 mL of juice added to 30 mL of water using a Titrator DL50 (Mettler Toledo, USA) for the Marlborough samples and a Metrohm 785 DMP Titrino autotitrator (Metrohm, USA) for the Hawke's Bay samples. In the 2013-14 season all juices were analyzed using a Foss FT2 Winescan (Foss, Denmark).

Yield Measurement

Data vines were harvested as close to commercial harvest as possible. For each data vine, the number of clusters and the total weight of fruit per vine were recorded. Fruit from the same treatment replicate were pooled together for microvinification. For the Marlborough sites, after harvest the fruit was immediately placed into cold storage and shipped under refrigeration to Hawke's Bay.

Microvinification

All experimental wines were made in the research winery of the Eastern Institute of Technology (Napier, New Zealand).

Red wine-fruit was crushed and destemmed using a Pillan crusher-destemmer (Pillan, Italy). Pectinase and SO_2 were added at 1 g/hL and 30 mg/L respectively. Fermentation using EC1118 yeast (Lallemand, Canada) was carried out in a room maintained at 30 °C. Ferments were punched down twice daily until dryness, after which they were pressed with a 20 kg Pillan water bladder press (Pillan, Italy) and inoculated with malo-lactic culture (CHR Hansen Vinflora Oenos, Denmark). Malo-lactic fermentation took about a month to complete for all wines, after which the wines were cold stabilized at -2 °C for a month. After stabilization, wines were warmed to room temperature, racked, coarse filtered, and bottled into 375 mL clear screw cap glass bottles (O-I, New Zealand).

SB-Fruit was crushed and destemmed using a Pillan crusher-destemmer (Pillan, Italy). The crushed fruit was then immediately pressed using a 20 kg capacity water bladder press (Pillan, Italy). Lallzyme HC pectinase (Lallemand, France) was added at 1 g/hL. The juice was allowed to cold settle at -2 °C overnight. The following day, the juice was racked and inoculated with QA23 yeast (Lallemand, France), and placed into a room maintained at 12 °C for fermentation. Once dry, the wine was moved to a -2 °C room for a month for cold stabilization, after which it was warmed to room temperature, racked, coarse filtered, and bottled into 375 mL clear screw cap glass bottles (O-I, New Zealand).

Publication Date (Web): November 24, 2015 | doi: 10.1021/bk-2015-1203.ch011

Skin Extraction

For the red varieties at each sample the skin was removed from 20 berries and placed into a Falcon tube with 20 mL of 50 % methanol in water (v/v). Samples were placed on a shaker at 200 rpm overnight. The following day the methanol was decanted off the skins and used for subsequent spectrophotometric measurements.

Skin Extract and Wine Phenolic Measurements

Skin extracts and red wines were analyzed for anthocyanins, total phenols, and polymeric pigments by the method of Harbertson et al., 2003 (*24*) using a Beckman Coulter DU730 Spectrophotometer.

Publication Date (Web): November 24, 2015 | doi: 10.1021/bk-2015-1203.ch011

Methoxypyrazine HS-SPME and GC-MS Conditions

Approximately 30 SB or ME berries were homogenized to a smooth slurry using a T-25 Ultra-Turrax homogenizer (IKA, USA). Slurries were centrifuged at 6000 rpm to pellet cell material. The supernatant was used for all analyses. If it was not possible to analyze the samples immediately after centrifugation, the supernatant was poured off and frozen at -80 °C for later analysis, which occurred approximately 3 months later.

The method used is based on the one developed by Parr et al. (2007) (*25*) using a novel automated HS-SPME (Head Space Solid-Phase Micro-Extraction) technique for the quantification of the methoxypyrazines in both juice and wine.

For all samples 3 g of sodium chloride was placed into a Agilent 20 mL headspace screw cap vial. For juice analysis 8 mL of the homogenate supernatant was added to the vials. For wine analysis, the wines were diluted 1:5 and 8 mL of this dilution was added to the vials. All samples also had 50 µL of a standard methoxypyrazine mix added prior to analyses (2-methoxy-3-methylpyrazine [50.2 ng/L], 2-isopropyl-3-[$^2H_3$]-methoxypyrazine [40.9 ng/L] and 2-isobutyl-3-[$^2H_3$]-methoxypyrazine [51.0 ng/L]). Finally, the samples were purged with argon, sealed with an Agilent screw cap, and loaded onto the autosampler (Gerstel MultiPurpose Sampler MPS2 tray (VT32-20).

Samples were incubated (40 °C) and agitated (Gerstel Agitator/Stirrer AS) for 5 minutes at 500 rpm. The fibre (2 cm, 23-Gauge, 50/30 µm, DVB/CAR/PDMS fibre for Automated Holder, Gray, Notched, SUPELCO, USA;) was pre-baked out (54 mm penetration) at 250 °C (pressure at 50 kPa, total flow rate of 14.02 mL/min, and a septum purge flow of 2 mL/min) in the front injection port for 5 minutes. Thirty mm of the fibre was exposed into the vial headspace for 40 minutes at 40 °C. The fibre was then transferred to the rear injection port (PTV inlet) of the GC (Agilent 7890A GC System) coupled to the MS (5975C inert XL, USA) where the analytes were injected in splitless mode at 250 °C for 10 minutes (pressure 81.585 kPa, total flow rate of 84.806 mL/min, and a septum purge flow of 3 mL/min). The analytes were separated on a tandem column HP-1ms (30 m, 0.320 mm ID, 0.25 µm film) and HP-INNOWax (30 m, 0.320 mm ID, 0.25 µm film, Agilent, USA), using Helium (flow rate of 1.806 mL/min) as carrier gas. To aid an efficient separation, the analytes were held for a total run time of 38.9 minutes, this included 5 minutes at 60 °C, an increase to 170 °C at a rate of 4 °C/min, and finally 240 °C at a rate of 50 °C/min held for 5 minutes. The interface line was set to 250 °C and the ion source at 230 °C. The electron impact mode was 70 eV and the quadrupole temperature was set at 150 °C. The analytes and internal standards were detected in Selected-Ion Monitoring (SIM) mode.

Sauvignon Blanc Wine Volatile Thiol Analysis

All SB wines were analyzed for 3-mercapto-hexan-1-ol (3MH) and 3-mercapto-hexan-1-ol acetate (3MHA) using the method of Herbst-Johnstone et al., (2013) (*26*).

GC-MS Analysis of Esters, Higher Alcohols, Fatty Acids, C6 Compounds, Terpenes, Norisoprenoids and Cinnamates

All wines were analyzed for a suite of aromatic compounds using a modified method based on that from Jouanneau, S. et al., 2012 (*27*) . Ten mL of wine were used for each analysis.

Statistical Analyses

All data were analyzed for differences among treatments using ANOVA and a Tukey's post hoc test using either SPSS (IBM, USA) or WinSTAT (R. Fitch, USA) software.

Publication Date (Web): November 24, 2015 | doi: 10.1021/bk-2015-1203.ch011

Results

Midday Stem Water Potential

In the 2012-13 season there were few differences found in plant water status between the various treatments (Table 1).

More significant differences were found in the 2013-14 season (Table 1). In ME consistent significant differences were found, with the herbicide treated vines being more supplied with waterthan the cultivation treatments at three of the seven measurement dates. On two of the dates (Nov 18 and Jan 6) the mowing treatments were intermediate between the cultivation and herbicide treatments, while on Jan 16 the mowing treatments were significantly less supplied with water than the herbicide treatments (Table 1). In SY, on both Jan 7 and 15, the cultivated vines were significantly drier than the herbicide vines, with mowing vines intermediate between the two (Table 1). No significant differences were found in the PN at any measurement date and therefore the relevant data were not reported in Table 1.

Leaf Area Per Shoot

Somewhat consistent differences were found in leaf area per shoot in both seasons (Table 2). In ME in 2012-13 ripening season on Dec 4 the herbicide treatment had significantly more leaf area than either of the other two treatments (Table 2). On March 1, the cultivation vines had significantly more leaf area than the mowing treatment, with herbicide treated vines having intermediate values (Table 2). In SY on Dec 4, the herbicide vines had significantly more leaf area than the mowing treatment, with the cultivation treatment intermediate between the two (Table 2).

In 2013-14 in ME the mowing treatment vines had significantly lower leaf area per shoot than the herbicide treatment on the first two measuring dates (Nov 13 and Dec 11). In SY and PN for 2013-2014, leaf area differences were only found at the last measuring date (Feb 3 and Feb 5, respectively) with mowing vines having significantly less leaf area than either of the other two treatments (Table 2). No significant differences were found in the SB at any measurement date and therefore the relevant data were not reported in Table 2.

Table 1. Midday Stem Water Potential (MPa) of Vines during the 2012-13 and 2013-14 Seasons. Different Letters in a Column for Each Variety Indicate Significant Differences at the p=0.05 Level.

Merlot 2012-13

Treatment	11/2/12	11/19/12	11/26/12	12/11/12	12/21/12	1/8/13	1/18/13	1/24/13
Herbicide	-0.36	-0.34	-0.43	-0.35	**-0.45 a**	-0.43	-0.49	-0.76
Mowing	-0.40	-0.33	-0.44	-0.37	**-0.52 b**	-0.46	-0.51	-0.69
Cultivation	-0.40	-0.33	-0.42	-0.37	**-0.52 b**	-0.40	-0.48	-0.70

	1/31/13	2/26/13	3/6/13
Herbicide	-1.08	-0.91	-1.46
Mowing	-1.08	-0.91	-1.40
Cultivation	-1.12	-0.99	-1.50

Sauvignon Blanc 2012-13

Treatment	12/11/12	1/11/13	1/27/13	2/8/13	2/22/13	3/26/13
Herbicide	**-0.50 b**	-0.49	-0.36	**-0.39 a**	-0.53	-0.78
Mowing	**-0.47 ab**	-0.50	-0.40	**-0.48 b**	-0.62	-0.77
Cultivation	**-0.43 a**	-0.52	-0.39	**-0.48 b**	-0.62	-0.83

Merlot 2013-14

Treatment	11/18/13	12/3/2013	12/17/13	1/6/14	1/16/14	1/29/14	2/5/14	2/18/14
Herbicide	**-0.24 a**	-0.21	-0.30	**-0.54 a**	**-0.99 a**	-0.55	-0.65	-1.08
Mowing	**-0.25 ab**	-0.25	-0.38	**-0.62 ab**	**-1.21 b**	-0.56	-0.70	-1.14
Cultivation	**-0.26 b**	-0.23	-0.34	**-0.63 b**	**-1.19 b**	-0.58	-0.72	-1.16

Syrah 2013-14

Treatment	11/8/2013	11/26/13	12/10/13	12/19/13	1/7/14	1/15/14	1/28/14	2/19/14
Herbicide	-0.23	-0.18	-0.18	-0.30	**-0.46 a**	**-0.53 a**	-0.69	-0.64
Mowing	-0.24	-0.19	-0.20	-0.34	**-0.56 ab**	**-0.55 ab**	-0.71	-0.70
Cultivation	-0.23	-0.16	-0.18	-0.29	**-0.61 b**	**-0.63 b**	-0.76	-0.74

	3/10/14	3/18/14
Herbicide	-1.32	-1.05
Mowing	-1.38	-1.05
Cultivation	-1.32	-1.05

Sauvignon Blanc 2013-14

Treatment	12/2/13	12/15/13	12/30/13	1/13/14	1/30/14	2/10/14	2/24/14	3/12/13
Herbicide	-0.23	-0.46	-0.47	-0.29	-0.28	**-0.19 a**	-0.39	-0.23
Mowing	-0.26	-0.45	-0.47	-0.27	-0.30	**-0.26 b**	-0.45	-0.26
Cultivation	-0.20	-0.43	-0.43	-0.33	-0.31	**-0.24 ab**	-0.43	-0.20

Publication Date (Web): November 24, 2015 | doi: 10.1021/bk-2015-1203.ch011

Table 2. Leaf Area Per Shoot (cm^2) during the 2012-13 and 2013-14 Seasons. Different Letters in a Column for Each Variety Indicate Significant Differences at the p=0.05 Level.

Merlot 2012-13				
Treatment	*11/12/2012*	*12/4/2012*	*1/3/2013*	*2/6/2013*
Herbicide	580.5	**1603.6 a**	**2994.1 ab**	3003.4
Mowing	453.6	**1036.4 b**	**2339.4 b**	2164.4
Cultivation	501.6	**1192.8 b**	**3244.9 a**	2574.4
Syrah 2012-13				
Treatment	*11/14/2012*	*12/4/2012*	*12/28/2012*	*1/30/2013*
Herbicide	888.6	**1903.3 a**	3201.6	2708.9
Mowing	694.9	**1395.5 b**	2409.3	2607.9
Cultivation	848.2	**1595.1 ab**	2747.2	2659.6
Merlot 2013-14				
Treatment	*11/13/2013*	*12/11/2013*	*1/9/2014*	*2/11/2014*
Herbicide	**1098.94 a**	**3972.01 a**	4180.54	4364.18
Mowing	**739.04 b**	**2725.53 b**	3448.72	3857.56
Cultivation	**939.55 ab**	**3856.72 a**	4011.96	4689.48
Syrah 2013-14				
Treatment	*11/8/2013*	*12/3/2013*	*1/7/2014*	*2/3/2014*
Herbicide	1009.25	2275.72	3383.22	**4233.86 ab**
Mowing	877.1	1778.99	2949.41	**3165.40 b**
Cultivation	943.14	2398.29	3739.82	**4304.72 a**
Pinot Noir 2013-14				
Treatment	*12/4/2013*	*1/8/2014*	*2/5/2014*	
Herbicide	929.28	1073.67	**1856.91 a**	
Mowing	879.78	950.62	**983.75 b**	
Cultivation	974.84	1196.7	**1553.24 a**	

Publication Date (Web): November 24, 2015 | doi: 10.1021/bk-2015-1203.ch011

Berry Weight

Very consistent differences were found in berry weight in ME in 2012-13, with the mowing treatment always having significantly lower berry weight than either of the other two treatments (Table 3). There were no other significant differences in 2012-13 in any of the other varieties (data not shown).

Table 3. Berry Weight (g) during the 2012-13 and 2013-14 Seasons. Different Letters in a Column for Each Variety Indicate Significant Differences at the p=0.05 Level.

Merlot 2012-13					
Treatment	*2/13/2013*	*2/26/2013*	*3/11/2013*	*3/18/2013*	
Herbicide	**0.97 a**	**1.30 a**	**1.39 a**	**1.44 a**	
Mowing	**0.87 b**	**1.15 b**	**1.21 b**	**1.28 b**	
Cultivation	**0.97 a**	**1.31 a**	**1.40 a**	**1.41 a**	
Merlot 2013-14					
Treatment	*1/30/2014*	*2/11/2014*	*2/24/2014*	*4/03/2014*	
Herbicide	**0.93 a**	**1.29 ab**	**1.38 a**	**1.34 a**	
Mowing	**0.82 b**	**1.18 b**	**1.15 b**	**1.18 b**	
Cultivation	**0.94 a**	**1.32 a**	**1.34 a**	**1.24 ab**	
Syrah 2013-14					
Treatment	*1/28/2014*	*2/12/2014*	*2/25/2014*	*3/10/2014*	*3/20/2014*
Herbicide	**1.04 a**	**1.51 ab**	**1.80 a**	1.90	1.55
Mowing	**0.90 b**	**1.35 b**	**1.58 b**	1.76	1.39
Cultivation	**1.02 a**	**1.53 a**	**1.73 ab**	1.88	1.50
Sauvignon Blanc 2013-14					
Treatment	*2/7/2014*	*2/19/2014*	*3/4/2014*	*3/20/2014*	*4/4/2014*
Herbicide	**1.07 b**	1.60	**1.92 b**	2.03	2.02
Mowing	**1.09 ab**	1.60	**1.89 b**	2.08	1.99
Cultivation	**1.17 a**	1.68	**2.02 a**	2.11	2.13
Pinot Noir 2013-14					
Treatment	*1/29/2014*	*2/11/2014*	*2/25/2014*	*3/10/2014*	*3/27/2014*
Herbicide	0.95	**1.47 a**	1.74	1.82	1.57
Mowing	0.83	**1.30 b**	1.56	1.71	1.47
Cultivation	0.91	**1.44 a**	1.65	1.83	1.54

There were more significant differences in berry weights in 2013-14. ME showed the same trend as in the previous season, with mowing always having the smallest berries (Table 3). In SY the same trend was seen for the first three measuring dates, with berries from the mowing vines having the lightest berries. The trend held for the remainder of the season, but the differences were not statistically significant at the last two measuring dates (Table 3). In SB, the cultivated treatment produced significantly larger berries early in ripening (Table

Publication Date (Web): November 24, 2015 | doi: 10.1021/bk-2015-1203.ch011

3). In PN, differences were only found on a single sampling date (Feb 11), with the mowing treatment berries being significantly smaller than berries from the other two treatments (Table 3). Thereafter this trend held, but differences were not statistically significant (Table 3).

Table 4. Grape Soluble Solids (°Brix) during the 2012-13 and 2013-14 Seasons. Different Letters in a Column for Each Variety Indicate Significant Differences at the p=0.05 Level.

Merlot 2013-14					
Treatment	*1/30/2014*	*2/11/2014*	*2/24/2014*	*5/03/2014*	
Herbicide	**9.6 b**	14.2	19.5	21.4	
Mowing	**10.0 ab**	14.3	19.2	21.0	
Cultivation	**10.7 a**	14.7	19.9	20.8	
Sauvignon Blanc 2013-14					
Treatment	*2/7/2014*	*2/19/2014*	*3/4/2014*	*3/20/2014*	*4/4/2014*
Herbicide	8.1	13.1	16.5	19.3	**21.63 a**
Mowing	8.3	12.8	16.0	19.6	**21.37 a**
Cultivation	8.6	13.2	16.3	18.7	**20.3 b**
Pinot Noir 2013-14					
Treatment	*1/29/2014*	*2/11/2014*	*2/25/2014*	*3/10/2014*	*3/27/2014*
Herbicide	**10.6 a**	**14.5 a**	**18.4 a**	19.9	22.8
Mowing	**10.1 b**	**13.7 b**	**17.6 b**	19.4	22.4
Cultivation	**11.0 a**	**14.6 a**	**18.4 a**	19.7	22.3

Publication Date (Web): November 24, 2015 | doi: 10.1021/bk-2015-1203.ch011

Soluble Solids

In the 2012-13 season there were no differences in soluble solids at any point in the season in any of the varieties (data not shown). In the 2013-14 season there were more significant differences in this parameter. At the first sampling date in ME the cultivation treatment had the highest TSS the herbicide the lowest, and the mowing treatment had intermediate values (Table 4). In SB there was only a difference at harvest, with the cultivation treatment having significantly lower TSS than either of the other two treatments. In PN, the TSS of the mowing treatment was lower than the other treatments for the first three sampling dates, but thereafter there were no differences between any of the treatments through harvest (Table 4). No significant differences were found in the SY at any measurement date and therefore the relevant data were not reported in Table 4.

Table 5. Juice pH during the 2012-13 and 2013-14 Seasons. Different Letters in a Column for Each Variety Indicate Significant Differences at the p=0.05 Level.

Merlot 2012-13							
Treatment	2/13/2013	2/26/2013	3/11/2013	3/18/2013			
Herbicide	**2.71 ab**	3.04	3.23	3.32			
Mowing	**2.67 b**	3.01	3.22	3.32			
Cultivation	**2.74 a**	3.07	3.27	3.30			
Syrah 2012-13							
Treatment	2/14/2013	2/28/2013	3/07/2013	3/12/2013	3/20/2013	3/28/2013	4/02/2013
Herbicide	2.69	**2.84 b**	2.88	3.00	3.14	3.17	3.23
Mowing	2.71	**2.88 a**	2.87	2.99	3.14	3.18	3.22
Cultivation	2.71	**2.84 b**	2.88	2.98	3.15	3.18	3.22
Pinot noir 2012-13							
Treatment	2/14/2013	2/28/2013	3/07/2013	3/12/2013	3/20/2013	3/28/2013	4/02/2013
Herbicide	2.69	**2.84 b**	2.88	3.0000	3.14	3.17	3.23
Mowing	2.71	**2.88 a**	2.87	2.99	3.14	3.18	3.22
Cultivation	2.71	**2.84 b**	2.88	2.98	3.15	3.18	3.22
Merlot 2013-14							
Treatment	1/30/2014	2/11/2014	2/24/2014	5/03/2014			
Herbicide	**2.68 ab**	**2.86 b**	**3.13 ab**	3.20			
Mowing	**2.66 b**	**2.85 b**	**3.08 b**	3.18			
Cultivation	**2.71 a**	**2.92 a**	**3.18 a**	3.18			
Syrah 2013-14							
Treatment	1/28/2014	2/12/2014	2/25/2014	3/10/2014	3/21/2014		
Herbicide	2.60	2.70	2.90	**3.07 a**	3.19		
Mowing	2.60	2.67	2.87	**3.02 b**	3.14		
Cultivation	2.59	2.67	2.85	**3.02 b**	3.18		
Pinot noir 2013-14							
Treatment	1/29/2014	2/11/2014	2/25/2014	3/10/2014	3/27/2014		
Herbicide	2.55	**2.84 a**	**3.03 a**	3.04	3.22		
Mowing	2.48	**2.77 b**	**2.95 b**	3.04	3.17		
Cultivation	2.54	**2.82 a**	**3.01 a**	3.06	3.20		

Juice pH and TA

In the 2012-13 season there were only differences in pH in the first ME ripening sample (2/13/13) and a mid-ripening PN sample (3/20/13). However, in the ME, the mowing treatment had the highest pH, whereas in the PN the mowing treatment had the lowest pH (Table 5). There were more, and more consistent, differences in the 2013-14 season. In ME for every ripening sample, but not at harvest, the mowing treatment had significantly lower pH than the other two

In Advances in Wine Research; Ebeler, et al.;
ACS Symposium Series; American Chemical Society: Washington, DC, 2015.

Publication Date (Web): November 24, 2015 | doi: 10.1021/bk-2015-1203.ch011

treatments (Table 5). In SY, there was a difference near harvest (3/10/14) with the herbicide treatment having higher pH than either of the other two treatments (Table 5). At two sampling dates (2/11/14 and 2/25/14), the mowing treatment in PN had lower pH than either of the other two treatments (Table 5). There were, however no differences in juice pH at harvest between any of the treatments in any of the varieties in either season (Table 5).

Similarly to pH, there were fewer differences in TA in the 2012-13 season than in the 2013-14 season. In 2012-13 the only significant difference in TA was a single sampling date in SB (3/20/14), where the herbicide treatment had significantly higher TA than either of the other two treatments (Table 6). In 2013-14 in ME, early in the season the cultivation treatment had the lowest TA, and the herbicide had the highest. By harvest, the mowing treatment had lower TA than either of the other two treatments, which had similar values (Table 6). In SB, there were no differences during ripening, but at harvest the cultivation treatment had higher TA than either of the other two treatments (Table 6).

Publication Date (Web): November 24, 2015 | doi: 10.1021/bk-2015-1203.ch011

Table 6. Juice TA (g/L) during the 2012-13 and 2013-14 Seasons. Different Letters in a Column for Each Variety Indicate Significant Differences at the p=0.05 Level.

Sauvignon Blanc 2012-13							
Treatment	2/14/2013	2/28/2013	3/07/2013	3/12/2013	3/20/2013	3/28/2013	4/02/2013
Herbicide	36.92	25.17	18.59	17.35	**13.84 a**	13.85	11.51
Mowing	37.74	25.32	19.28	17.43	**12.86 b**	12.35	11.00
Cultivation	37.26	24.80	18.40	16.94	**12.81 b**	12.55	11.04
Pinot Noir 2012-13							
Treatment	2/14/2013	2/28/2013	3/07/2013	3/20/2013	4/02/2013		
Herbicide	19.64	12.05	11.21	**13.84 a**	7.20		
Mowing	18.46	12.42	11.04	**12.86 b**	7.16		
Cultivation	18.86	12.75	11.03	**12.81 b**	7.24		
Merlot 2013-14							
Treatment	1/30/2014	2/11/2014	2/24/2014	3/05/2014			
Herbicide	**28.30 a**	**14.31 a**	9.24	**6.78 a**			
Mowing	**25.90 ab**	**13.76 ab**	8.97	**6.12 b**			
Cultivation	**24.40 b**	**12.51 b**	8.30	**6.72 a**			
Sauvignon blanc 2013-14							
Treatment	2/07/2014	2/19/2014	3/04/2014	3/20/2014	4/04/2014		
Herbicide	37.88	23.58	16.23	12.05	**8.39 b**		
Mowing	37.08	23.52	16.12	12.45	**8.29 b**		
Cultivation	37.02	23.32	15.93	12.07	**9.31 a**		

Table 7. Yeast Available Nitrogen (YAN, mgN/L) for the 2013-14 Growing Season. Different Lower Case Letters in a Column for Each Variety Indicate Significant Differences at the p=0.05 Level.

Merlot					
Treatment	***2/11/2014***	***2/24/2014***	***3/5/2014***		
Herbicide	**167 a**	**174 a**	**151 a**		
Mowing	**133 b**	**124 b**	**109 b**		
Cultivation	**154 ab**	**166 a**	**126 ab**		
Syrah					
Treatment	***2/12/2014***	***2/25/2014***	***3/10/2014***	***3/21/2014***	
Herbicide	**176 a**	**191 a**	**172 a**	**177 a**	
Mowing	**112 b**	**121 b**	**114 b**	**133 b**	
Cultivation	**140 ab**	**159 ab**	**136 ab**	**174 a**	
Sauvignon Blanc					
Treatment	***2/7/2014***	***2/19/2014***	***3/4/2014***	***3/20/2014***	***4/4/2014***
Herbicide	**278 ab**	**187 b**	181	150	180
Mowing	**261 b**	**164 b**	164	141	150
Cultivation	**312 a**	**222 a**	200	172	176
Pinot Noir					
Treatment	***1/29/2014***	***2/11/2014***	***2/25/2014***	***3/10/2014***	***3/27/2014***
Herbicide	**339 a**	**262 a**	**253 a**	223	**242 a**
Mowing	**282 b**	**208 b**	**189 b**	197	**168 b**
Cultivation	**334 a**	**262 a**	**243 a**	242	**210 ab**

Publication Date (Web): November 24, 2015 | doi: 10.1021/bk-2015-1203.ch011

Yeast Available Nitrogen

This parameter was only measured in the 2013-14 season, but showed consistent differences across all varieties. In ME and SY at every sampling date (including harvest), the mowing treatment had the lowest YAN compared with the other two treatments (Table 7). This trend was also seen in PN, with the exception of the sampling date on 3/10/14, where no significant differences were seen (Table 7). In SB, this trend was seen at the first two sampling dates, but thereafter all treatments had similar values (Table 7).

Publication Date (Web): November 24, 2015 | doi: 10.1021/bk-2015-1203.ch011

Table 8. Skin Extract Phenolic Measurements for SY in the 2012-13 Season and ME in the 2013-14 Season. Different Letters in a Column for Each Variety Indicate Significant Differences at the p=0.05 Level.

Syrah 2012-13 Berry skins					
	3/5/2013	*3/25/2013*	***03/28/2013 (Harvest)***		
Treatment	*Anthocyanins (mg/berry Malvidin-3-gluc Equivalents)*	*Anthocyanins (mg/berry Malvidin-3-gluc Equivalents)*	***Anthocyanins (mg/berry Malvidin-3-gluc Equivalents)***	***Tannins (mg/berry Catechin Equivalents)***	***Total Phenolics (mg/berry Catechin Equivalents)***
Herbicide	**1.6 a**	1.5	1.8	0.3	1.6
Mowing	**1.1 b**	1.5	1.6	0.3	1.4
Cultivation	**1.2 ab**	1.3	1.6	0.2	1.4

Merlot 2013-14 Berry skins						
	1/30/2014	*2/11/2014*	*2/24/2014*	***3/5/2014 (Harvest)***		
Treatment	*Anthocyanins (mg/berry Malvidin-3-gluc Equivalents)*	*Anthocyanins (mg/berry Malvidin-3-gluc Equivalents)*	*Anthocyanins (mg/berry Malvidin-3-gluc Equivalents)*	***Anthocyanins (mg/berry Malvidin-3-gluc Equivalents)***	***Tannins (mg/berry Catechin Equivalents)***	***Total Phenolics (mg/berry Catechin Equivalents)***
Herbicide	**0.1 b**	**0.5 b**	0.9	1.6	0.6	2.2
Mowing	**0.1 b**	**0.6 ab**	0.9	1.7	0.6	2.4
Cultivation	**0.2 a**	**0.7 a**	0.9	1.7	0.6	2.4

Publication Date (Web): November 24, 2015 | doi: 10.1021/bk-2015-1203.ch011

Table 9. Bunch Number and Yield Per Vine in 2012-13 and 2013-14 Seasons. Different Letters in a Column for Each Variety Indicate Significant Differences at the p=0.05 Level.

2012-13	***Merlot***		***Syrah***		***Sauvignon Blanc***		***Pinot Noir***	
Treatment	*Bunch number per vine*	*Harvest yield (kg/vine)*	*Bunch number per vine*	*Harvest yield (kg/vine)*	*Bunch number per vine*	*Harvest yield (kg/vine)*	*Bunch number per vine*	*Harvest yield (kg/vine)*
Herbicide	33	**4.90 a**	26	4.07	52	5.56	30	2.86
Mowing	32	**3.91 b**	25	3.88	55	5.76	28	2.44
Cultivation	32	**4.49 ab**	26	4.1	50	5.4	29	2.77
2013-14	***Merlot***		***Syrah***		***Sauvignon Blanc***		***Pinot Noir***	
Treatment	*Bunch number per vine*	*Harvest yield (kg/vine)*	*Bunch number per vine*	*Harvest yield (kg/vine)*	*Bunch number per vine*	*Harvest yield (kg/vine)*	*Bunch number per vine*	*Harvest yield (kg/vine)*
Herbicide	44	**7.02 a**	26	4.20	69	**9.30 b**	38	3.76
Mowing	42	**5.56 b**	25	3.86	70	**9.37 b**	35	3.30
Cultivation	44	**6.54 ab**	25	3.97	73	**11.16 a**	41	3.70

Skin Anthocyanins

In the three red varieties in the 2012-13 season, there was only a difference in total anthocyanins at the first sampling date (3/5/13) in SY (Table 8). In the 2013-14 season, there were differences early in the season in ME, with the Cultivation treatment having more anthocyanins. Throughout the rest of ripening, there were no differences (Table 8). There were no significant differences at any point for either SY or PN in 2013-14 (data not shown).

Bunch Number and Yield Per Vine

There were no significant differences in the number of bunches in any of the varieties in either season (Table 9). In both seasons there was a consistent reduction in yield in ME, with the mowing treatment having the lowest yield, the herbicide having the highest, and the cultivation treatment having intermediate values (Table 9). In the 2013-14 season in SB, the cultivation treatment had higher yield than either of the other two treatments (Table 9).

Wine pH, TA, Tartaric Acid, and Malic Acid

The only difference in basic wine chemistry in the 2012-13 season was that the SY wines from the cultivation treatment had the highest malic acid, the mowing wine showing the lowest, and the herbicide wines having intermediate values (Table 10). In the 2013-14 season differences were only seen in the PN wines, with the mowing treatment having the highest TA and lowest pH, the herbicide wines having the lowest TA and the highest pH, and the cultivation wines intermediate between the two (Table 10).

Wine Total Phenolics, Anthocyanins, Tannins, and Polymeric Pigments

In the 2012-13 season the only significant difference in phenolic profile of the wines was found in ME. The mowing treatment had significantly more total phenolics than either the herbicide or cultivation treatments (Table 11). No significant differences were found for phenolics in any of the red wines from the 2013-14 season (data not shown).

Berry and Wine Methoxypyrazine Content

In the 2012-13 season IBMP was measured in SB berries throughout ripening. Berry IBMP showed the expected decreasing trend from postveraison to harvest (Figure 2). No significant differences were found at any time point. In the same season two sampling dates of ME berries were also tested for IBMP content. No significant differences were found between treatments on either date (data not shown).

Publication Date (Web): November 24, 2015 | doi: 10.1021/bk-2015-1203.ch011

Table 10. Wine pH, TA, Tartaric Acid, and Malic Acid for SY in the 2012-13 Season and PN for the 2013-14 Season. Different Letters in a Column for Each Variety Indicate Significant Differences at the p=0.05 Level.

Syrah 2012-13				
Treatment	*pH*	*TA (g/L)*	*Tartaric acid (g/L)*	*Malic acid (g/L)*
Herbicide	3.49	6.28	2.3	**0.9 ab**
Mowing	3.45	6.28	2.2	**0.8 b**
Cultivation	3.40	6.51	2.6	**1.1 a**
Pinot Noir 2013-14				
Treatment	*pH*	*TA (g/L)*	*Tartaric acid (g/L)*	*Malic acid (g/L)*
Herbicide	**3.65 a**	**5.27 b**	1.00	nd
Mowing	**3.46 b**	**5.72 a**	1.36	nd
Cultivation	**3.50 ab**	**5.62 ab**	1.32	nd

Publication Date (Web): November 24, 2015 | doi: 10.1021/bk-2015-1203.ch011

Table 11. Wine Phenolics for ME from the 2012-13 Season. Different Letters in a Column Indicate Significant Differences at the p=0.05 Level.

Merlot 2012-13				
Treatment	*Total phenols (mg/L Catechin Equivalents)*	*Anthocyanins (mg/L Malvidin-3-gluc Equivalents)*	*Large polymeric pigment (LPP)*	*Small polymeric pigment (SPP)*
Herbicide	**1276 b**	200	0.37	0.43
Mowing	**1527 a**	244	0.34	0.47
Cultivation	**1329 b**	238	0.36	0.47

In the 2013-14 season both ME and SB berries were tested for IBMP at two sampling dates. There were no significant differences in either berry or wine for Merlot (data not ahown). In SB, berries from the mowing treatment always had the lowest amount of IBMP, but these differences were not statistically significant (data not shown).

For SB, wines from the mowing treatment had the lowest amount of IBMP in both seasons. In 2012-13 wines from the herbicide treatment had the highest levels of IBMP, whereas in the 2013-14 the wines from the cultivation treatment had the highest levels of IBMP (Table 12). IPMP was only detected in the 2012-13 SB wines, and no significant differences between treatments were found (Table 12).

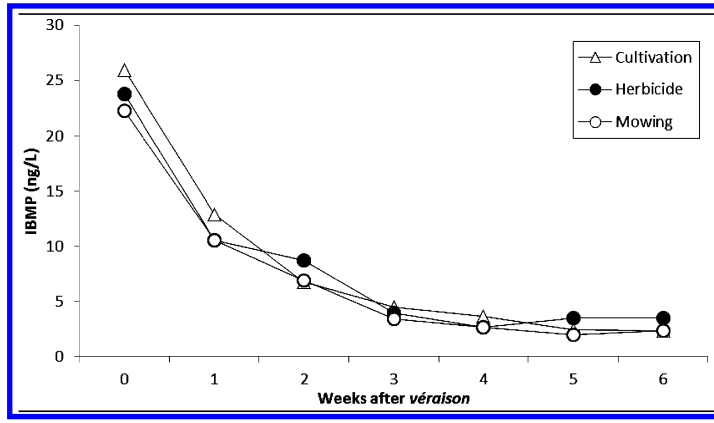

Figure 2. IBMP ripening evolution for Sauvignon blanc in the 2012-13 season.

Publication Date (Web): November 24, 2015 | doi: 10.1021/bk-2015-1203.ch011

Table 12. SB Wine IBMP from 2013 and 2014. Different Letters in a Column Indicate Significant Differences at the p=0.05 Level

Sauvignon blanc 2013		
Treatment	*IBMP (ng/L)*	*IPMP (ng/L)*
Herbicide	**1.2 a**	0.7
Mowing	**0.8 b**	0.7
Cultivation	**0.8 ab**	0.9
Sauvignon blanc 2014		
Treatment	*IBMP (ng/L)*	*IPMP (ng/L)*
Herbicide	**1.9 ab**	nd
Mowing	**1.7 b**	nd
Cultivation	**2.3 a**	nd

Sauvignon Blanc Wine Varietal Thiols

In the SB wines from the 2012-13 season there were no significant differences in 3MH or 3MHA, though there was a trend for the wines from the herbicide vines to have the highest amounts of these varietal compounds (Table 13). There were no thiols detected in the wines from the 2013-14 season (data not shown).

Table 13. Sauvignon Blanc Wine Thiols from 2013 ± SD

Treatment	***3MH (ng/L)***	***3MHA (ng/L)***
Herbicide	920 ± 491	139 ± 74
Mowing	658 ± 173	101 ± 77
Cultivation	540 ± 158	58 ± 46

Wine Esters, Higher Alcohols, Fatty Acids, C6 Compounds, Terpenes, Norisoprenoids, and Cinnamates

In PN wines, significant differences were found in isoamyl acetate and cis-3-hexyl acetate, with the cultivation treatment having higher levels of these esters than either of the other two treatments (Table 14). The only significant difference found in ME wines in 2012-13 was that the herbicide wines had higher amounts of benzyl alcohol than the mowing wines (Table 14). No significant difference in any of the measured cmpounds were found in the SY wines from the 2012-13 season (data not shown).

Publication Date (Web): November 24, 2015 | doi: 10.1021/bk-2015-1203.ch011

Table 14. Aroma Compounds Significantly Different at p=0.05 Level in Wines from the 2012-13 Season

2013 Pinot Noir wine			
	Treatment		
Compound	*Herbicide*	*Mowing*	*Cultivation*
Ethyl hexanoate (µg/L)	**243.6 b**	**252.0 ab**	**290.1 a**
Isoamyl acetate (µg/L)	**207.2 b**	**210.8 b**	**255.8 a**
Hexylacetate (µg/L)	**14.9 b**	**16.0 b**	**26.5 a**
Cis-3-hexenyl acetate (µg/L)	2.1 b	2.1 b	2.2 a
2013 Merlot wine			
	Treatment		
Compound	*Herbicide*	*Mowing*	*Cultivation*
Benzyl alcohol (µg/L)	**327.5 a**	**243.7 b**	**315.0 ab**

More differences were found in the aromatic profile of wines from the 2013-14 season. SB wines from the herbicide treatment had higer levels of ethyl acetate than the other two treatments. Mowing wines had higher levels of isobutanol and ethyl dihydrocinnamate than the other two treatments. Cultvation wines had the highest levels of α-terpineol (Table 15).

Table 15. Aroma Compounds Found to Be Significantly Different at the p=0.05 Level in Wines from the 2013-14 Season

2014 Sauvignon Blanc wine			
	Treatment		
Compound	*Herbicide*	*Mowing*	*Cultivation*
Ethyl acetate (mg/L)	**24.0 a**	**19.7 b**	**19.0 b**
Isobutanol (mg/L)	**38.5 b**	**54.3 a**	**37.4 b**
α-Terpineol (µg/L)	**7.6 b**	**8.1 b**	**13.1 a**
Ethyl dihydrocinnamate (µg/L)	**0.6 b**	**0.8 a**	**0.7 b**
2014 Pinot Noir wine			
	Treatment		
Compound	*Herbicide*	*Mowing*	*Cultivation*
Ethyl isobutyrate (µg/L)	**50.8 b**	**85.4 a**	**65.7 ab**
Ethyl phenylacetate (µg/L)	**2.6 b**	**3.2 a**	**3.1 ab**
β-Phenethyl acetate (µg/L)	**7.9 b**	**10.3 a**	**9.4 ab**
Isobutanol (mg/L)	**41.5 b**	**59.8 a**	**53.9 ab**
Isoamylalcohol (mg/L)	**160.7 b**	**192.6 a**	**182.1 ab**
Phenylethyl alcohol (µg/L)	**22.4 b**	**31.8 a**	**29.1 b**
β-Damascenone (µg/L)	**1.5 b**	**1.8 ab**	**2.3 a**
α-Ionone (µg/L)	**0.2 b**	**0.2 ab**	**0.3 a**
Linalool (µg/L)	**3.0 b**	**4.1 a**	**3.9 ab**
Trans ethyl cinnamate (µg/L)	**0.6 a**	**0.4 b**	**0.5 ab**
2014 Syrah wine			
	Treatment		
Compound	*Herbicide*	*Mowing*	*Cultivation*
Ethyl 2-methyl butanoate (µg/L)	**10.6 ab**	**13.6 a**	**10.1 b**
Isobutyl acetate (µg/L)	**71.8 a**	**65.0 ab**	**57.9 b**
Isoamylalcohol (mg/L)	**209.2 ab**	**232.5 a**	**197.5 b**
Linalool (µg/L)	**7.0 ab**	**7.8 a**	**6.3 b**
β-Citronellol (µg/L)	**17.3 ab**	**19.4 a**	**15.8 b**

Publication Date (Web): November 24, 2015 | doi: 10.1021/bk-2015-1203.ch011

In PN, the mowing treatment led to wines with the highest levels of ethyl isobutyrate, ethyl phenylacetate, β-phenethyl acetate, isobutanol, isoamyl alcohol, phenethyl alcohol, and linalool (Table 15). Wines from the cultivation treatment had the highest amounts of the two norisoprenoids, β-damascenone and α-ionone. Herbicide wines had the highest level of trans ethyl cinnamate (Table 15).

In SY wines, the mowing treatment led to higher amounts of ethyl 2-methyl butanoate, isoamylalcohol, linalool, and β-citronellol (Table 15). Herbicide wines were highest in isobutyl acetate (Table 15).

No significant differences were found in any of the compounds measured by GC-MS in ME wines from 2013-14 (data not shown).

Publication Date (Web): November 24, 2015 | doi: 10.1021/bk-2015-1203.ch011

Discussion

The push to move to more sustainable means of farming grapevines is a stated and noble desire of the New Zealand wine industry. This move to nonchemical means for vineyard operations, however, will only truly gain momentum if it can be shown that switching to them will not negatively affect the health and long-term productivity of the vines. Quality of the fruit must also not suffer due to treatments. It is possible that allowing continued competition from weeds, such as in the mowing treatment in this study, will deplete vine reserves and that differences in canopy growth will become more and more apparent over time. The results from the second year of the study (2013-14) show more significant differences, suggesting that there are carryover effects from year to year. This study was set up to look into the long-term effects of changing management underneath grapevines, and will continue for at least another season. It is possible that over a long period allowing competition underneath the vine may devigorate them to the point where the vineyard is not economically sustainable. While unlikely, this possibility needs to be investigated with multi-season studies such as this one.

The most consistent and significant trends from the different management strategies were in vine physiological performance between the three treatments. Specifically, the vines from the mowing treatments tended to show signs of devigoration in comparison with the other two treatments. Leaf area was generally reduced in mowing treatments (Table 2). Even when differences were not statistically significant the trend for mowed vines to have the smallest canopies still held true in most sites and varieties (data not shown). It has been shown that leaf expansion is one of the first things to be negatively affected by water stress in grapevines (*7*). While the mowing treatment vines vines tended to have the most negative water potentials (Table 1), the observed difference in leaf area cannot easily be explained by water stress because the SWP values obtained in this study generally do not indicate heavily stressed vines, except for some for the measurements near harvest from the ME and SY sites.

In addition to water affecting leaf growth, deficiencies in nitrogen can also reduce canopy growth (*6*). The YAN data obtained in 2013-14 suggests that vines from the mowing treatment were more nitrogen deficient during ripening, as juice from the mowing treatment had consistently lower YAN than the other two treatments (Table 7). When petioles were measured to assess nutrient status

at veraison, however, no significant differences were found (data not shown), suggesting that, at least at veraison, there was not significant nutrient stress induced by any of the treatments. As the leaf area measurements were done prior to and at veraison, it is unlikely that the differences are explained by nitrogen deficiencies.

In ME, there was a consistent trend in both seasons for the berries from the mowing treatment to be smaller than those from either of the other two treatments (Table 3). Again, there is no one variable that can be singled out as having led to this differences, though it must be noted that differences in SWP were found more often in ME than in any of the other varieties (Table 1). Water stress has been shown to lead to smaller berries (Matthews et al., 1987), and even the slight and often non significant differences in SWP might have been enough to have led to the observed differences. It is also possible that there are varietal differences in the response to undervine management, with ME being particularly responsive to undervine competition in terms of both reduced leaf area, and possibly due to this, reduced berry weight. SY berries were also significantly smaller through early ripening in 2013-14, which persisted, though not significantly so, through to harvest (Table 3). A similar trend was seen in PN, with berries from the mowed treatment in the 2012-13 season being similar in weight (data not shown), whereas in the 2013-14 season the mowing berries were lightest at every sampling date, though this difference was only significant on one day (Table 3).

Yield was only negatively affected by mowing in ME. This was the case in both seasons, and was due entirely to smaller berries, as bunch number per vine (Table 9) and berry number per vine (data not shown) were not negatively affected. However, in this vineyard, crop reduction by manually thinning bunches is a normal production practice. It is possible that adoption of mowing in this vineyard could make this expensive and slow pass unnecessary.

In light of some of the physiological and vine performance differences observed in the study, it is important to stress that sugar accumulation was not negatively affected by either of the nonchemical treatments, as evidenced by the similarity in Brix between all treatments. The only exception to this was the cultivation treatment in SB in the 2013-14 season (Table 4), which showed lowest Brix, though this could also be due to the increased yield in this treatment in that season, as the cultivated vines had about 20% more crop than either of the other two treatments (Table 9). No differences were found in Brix between mowing and herbicide treated vines at harvest in either year in any of the varieties, suggesting that while mowing may bring about some physiological and canopy architecture differences in the vines, it does not significantly slow ripening.

There were very few other differences in basic berry chemistry at harvest among the treatments, suggesting that switching from herbicides to mowing or cultivation doesn't negatively affect the basic quality of the fruit produced (Tables 4, 5, 6) although the case may not be the same for wine style. This is good news for organic growers, or those looking to move to organics, as a vineyard wanting to move away from chemical inputs can do so safe in the knowledge that the fruit will likely still come into the winery with similar basic composition to what it had before conversion. The exception to this is the lower YAN induced by mowing (Table 7), though the prefermentation supplementation of juice with nitrogen (such

Publication Date (Web): November 24, 2015 | doi: 10.1021/bk-2015-1203.ch011

as adding diammonium phosphate) is quite common in New Zealand, therefore the risk of stuck or sluggish fermentations is less likely to be an issue.

The finding of significant differences in canopy architecture with no consistent and major significant differences in ripening due to mowing is an important one. Canopies with less leaf area and more canopy gaps (such as in the mowing treatments in this study) have been shown to reduce the incidence of powdery mildew (*12*) and *Botrytis cinerea* infection (*10*). Both seasons of this study have been exceptionally dry, with very little incidence of *Botrytis*, and thus no significant differences in rot incidence or severity have been found (data not shown). However, in a more challenging season with rains near harvest, the more open canopy of the mowing treatment could reduce the negative effect of bunch rot on yield and wine quality. Thus, mowing could be a safety strategy employed by growers against a wet season. Having competing vegetation serves a dual benefit of intercepting some of the rain before it induces excessive vigor in the vines, as well as leading to a canopy more conducive to fruit health and quality. It might also be that canopies from vineyards with undervine mowing, being more open and less conducive to fungal growth, would allow a vineyard manager to get away with fewer, or softer, fungicide sprays during the season, which would further increase the environmental and economic sustainability of the vineyard.

Methoxypyrazines are important impact aroma compounds synthesized in berries of ME and SB (and other related varieties) early in ripening, and degraded after veraison (*28*). They impart distinctive vegetal notes to wines, and especially in red wines, are considered a negative in high concentrations (*29*). The most important member of this family of compounds is 3-isobutyl-2-methoxypyrazine (IBMP), which imparts bell pepper aroma to the wines. In Marlborough SB, however, reasonably high levels of IBMP, as well as the varietal thiols 3-mercapto-hexan-1-ol (3MH), 3-mercapto-hexan-1-ol acetate (3MHA) are part of the preferred style (*25*).

In the 2012-13 season, samples of SB berries were analyzed throughout ripening to quantify the amount of IBMP present. The concentration of IBMP, regardless of treatment, showed the expected trend over ripening, with the concentration of this compound getting lower and lower, especially shortly after veraison (Figure 2). No significant differences were found in IBMP during ripening or at harvest in ME in either season or SB in the 2013-14 season, though there is a trend for the herbicide fruit to have the highest amount of this compound (data not shown). Given the extremely low threshold of these molecules (*29*), these small differences could still be translated into significative sensory changes.

ME wines from 2012-13 mowing treatment had a higher concentration of total phenolics, generally considered positive in red winemaking. Differences in pH, TA, tartaric and malic acids were generally small and nonsignificant (Table 10). There was a difference in malate in 2012-13 in SY wines (Table 10), though there was no difference in malic acid in the fruit at harvest (data not shown), suggesting the differences came about due to differences in the extent of malolactic fermentation, and not due to the fruit itself. There were also differences in PN pH and TA, with the herbicide fruit having higher pH and lower TA (Table 10). While these differences were significant, none of the fruit had composition that would be a worry to winemakers as far as completion of a healthy fermentation.

Publication Date (Web): November 24, 2015 | doi: 10.1021/bk-2015-1203.ch011

Considering the very small effect of treatments on berry ripening and the similarity in basic wine composition parameters, any differences in wine quality brought about by changing undervine management will be in the effect they have on the concentration of aroma and flavor compounds and precursors in the fruit which are subsequently extracted into the wines. The idea that a grower can change the flavor of the wines as the fruit develops by making changes to cultural practices carried out in the vineyard is an attractive one to the industry, and one that would allow more control over the final quality of the product.

The data from this study shows a clear and consistent trend that SB wines from the mowing treatment had the lowest levels of IBMP compared with the other two treatments (Table 12). Interestingly, this trend was not seen in ME (data not shown), despite the fact that ME vines, at least in terms of canopy measurements, were more affected by the treatments than SB (Table 2). This suggests varietal and/or site differences in response to undervine vegetation, even between these related cultivars.

In any case, the suggestion of the data, at least for SB from New Zealand, whose style is predicated on high levels of both IBMP and thiols, is that wine from vineyards that practice undervine mowing will be less typical. That said, there are some growers in New Zealand, especially in regions outside of Marlborough, who would like to differentiate themselves from the "typical" Marlborough SB style (*25*), and the findings of this study show it can be done with a simple change to management. In addition, SB is grown throughout the world, with varied styles and flavor profiles, and therefore a way of reducing IBMP levels in the fruit as it develops can be an important strategy in other growing regions striving for a different flavor spectrum in the wines than those from Marlborough. There were also differences in varietal thiols, though not statistically significant, in the SB wines from the 2012-13 season (Table 13). The repeatability of this difference could not be assessed, as the concentration of thiols in the 2013-14 wines were below the level of detection (data not shown).

In PN wines there were also some difference in ester composition, with wines from the cultivation treatment having higher levels of isoamyl acetate and cis-3-hexenyl acetate (Table 14), which could lend ripe banana and green banana aromas, respectively, to the wines (*30–32*).

More significant differences were found in wine aromatic profile for both SB and PN in the 2013-14 season. Herbicide wines had the highest amount of ethyl acetate, which can impart a general fruit character to the wines. Cultivation wine had higher level of α-terpineol, which lends floral notes to wines. The mowing wines had the highest amounts of isobutanol and ethyl dihydrocinnamate which can impart generic fruity and solvent aromas (Table 15). PN wines showed the most, and most consistent, differences in aroma profile. Wines from the mowing treatment were highest in many compounds, including ethyl isobutyrate, ethyl phenylacetate, β-phenethyl acetate, isobutanol, isoamyl alcohol, phenethyl alcohol, and linalool. These differences suggest that the mowing treatment in 2014 lead to a wine that could potentially be more fruity and floral (*33*). The wines from the cultivation treatment had the highest levels of the two C13 norisoprenoids (β-damascenone and α-ionone), which have been shown to enhance fruity aromas and supress vegetative ones (*34*) and therefore could lead

In Advances in Wine Research; Ebeler, et al.;
ACS Symposium Series; American Chemical Society: Washington, DC, 2015.

Publication Date (Web): November 24, 2015 | doi: 10.1021/bk-2015-1203.ch011

to fruitier wines. The mowing treatment in SY led to wines with higher amounts of ethyl 2-methyl butanoate, isoamylalcohol, linalool, and β-citronellol (Table 15), suggesting this trteatment leads to fruitier and more floral wines. However, sensory analysis would need to be carried out on the wines to show if observable aroma and flavor dfferences were brought about by the differential vineyard management.

Conclusion

Some of the major findings of this study thus far are that very minor differences in water or nutrient status can lead to significant observable differences in vine growth. However, these differences do not greatly affect basic fruit ripening parameters in terms of sugars, acids, and phenolics. The study also clearly shows that there are site and/or variety differences in the response of the vines to undervine manipulations, as no one treatment had the same effect regardless of site and variety. The yield reduction seen in ME could be a positive or a negative depending on the aims of the vineyard. Most interestingly of all, despite only very subtle differences in vine performance and basic fruit composition, there were significant differences in wine aromatic profile, especially for SB. This is exciting news for winegrowers, as undervine management provides additional tools to modify the aromatic composition of the wine as the grapes ripen.

Publication Date (Web): November 24, 2015 | doi: 10.1021/bk-2015-1203.ch011

Acknowledgments

The authos would like to thank New Zealand Winegrowers, Plant and Food Research Ltd and the University of Auckland for funding this project. Karen Ball is sincerely thanked for making the wines for this study.

References

1. New Zealand Winegrowers. *New Zealand Winegrowers Annual Report*; 2012; pp 1−32.
2. Carpenter, D.; Boutin, C. Sublethal effects of the herbicide glufosinate ammonium on crops and wild plants: short-term effects compared to vegetative recovery and plant reproduction. *Ecotoxicology* **2010**, *19*, 1322–1336.
3. Green, J. M. The benefits of herbicide-resistant crops. *Pest Manage. Sci.* **2012**, *68*, 1323–1331.
4. Wheeler, S. J.; Black, A. S.; Pickering, G. J. Vineyard floor management improves wine quality in highly vigorous Vitis vinifera ‘Cabernet Sauvignon’ in New Zealand. *N. Z. J. Crop Hortic. Sci.* **2005**, *33*, 317–328.
5. Palliotti, A.; Cartechini, A.; Petoumenou, D.; Silvestroni, O.; Mattioli, S.; Berrios, J. G. Long-term effects of seeded cover-crop on vegetative characteristics, yield and grape and wine composition of ‘Grechetto’ grapevines in central Italy. *Acta Hortic.* **2007**, *754*, 515–521.

Publication Date (Web): November 24, 2015 | doi: 10.1021/bk-2015-1203.ch011

6. Bell, S.-J.; Robson, A. Effect of nitrogen fertilization on growth, canopy density, and yield of *Vitis vinifera* L. cv. Cabernet Sauvignon. *Am. J. Enol. Vitic.* **1999**, *50*, 351–358.
7. Schultz, H. R.; Matthews, M. A. Growth, osmotic adjustment, and cell-wall mechanics of expanding grape leaves during water deficits. *Crop Sci.* **1993**, *33*, 287–294.
8. Kliewer, W. M.; Dokoozlian, N. K. Leaf area/crop weight ratios of grapevines: Influence on fruit composition and wine quality. *Am. J. Enol. Vitic.* **2005**, *56*, 170–181.
9. Smart, R.; Robinson, M. *Sunlight Into Wine: A Handbook for Winegrape Canopy Management*; Winetitles: Adelaide, Australia, 1991.
10. English, J. T.; Thomas, C. S.; Marois, J. J.; Gubler, W. D. Microclimates of grapevine canopies sssociated with leaf removal and control of *Botrytis* bunch rot. *Phytopathology* **1989**, *79*, 395–401.
11. Keller, M.; Rogiers, S. Y.; Schultz, H. R. Nitrogen and ultraviolet radiation modify grapevines' susceptibility to powdery mildew. *Vitis* **2003**, *42*, 87–94.
12. Austin, C. N.; Grove, G. G.; Meyers, J. M.; Wilcox, W. F. Powdery mildew severity as a function of canopy density: Associated impacts on sunlight penetration and spray coverage. *Am. J. Enol. Vitic.* **2011**, *62*, 23–31.
13. Austin, C. N.; Wilcox, W. F. Effects of fruit-zone leaf removal, training systems, and irrigation on the development of grapevine powdery mildew. *Am. J. Enol. Vitic.* **2011**, *62*, 193–198.
14. Ryona, I.; Pan, B. S.; Intrigliolo, D. S.; Lakso, A. N.; Sacks, G. L. Effects of cluster light exposure on 3-isobutyl-2-methoxypyrazine accumulation and degradation patterns in red wine grapes (*Vitis vinifera* L. Cv. Cabernet Franc). *J. Agric. Food Chem.* **2008**, *56*, 10838–10846.
15. Koch, A.; Ebeler, S. E.; Williams, L. E.; Matthews, M. A. Fruit ripening in *Vitis vinifera*: light intensity before and not during ripening determines the concentration of 2-methoxy-3-isobutylpyrazine in Cabernet Sauvignon berries. *Physiol. Plant.* **2012**, *145*, 275–285.
16. Marais, J.; Haasbroek, P. D.; Calitz, F. Relationship between microclimatic data, aroma component concentrations and wine quality parameters in the prediction of Sauvignon Blanc wine quality. *S. Afr. J. Enol. Vitic.* **2001**, *22*, 22–26.
17. Price, S. F.; Breen, P. J.; Valladao, M.; Watson, B. T. Cluster sun exposure and quercetin in Pinot noir grapes and wine. *Am. J. Enol. Vitic.* **1995**, *46*, 187–194.
18. Dokoozlian, N. K.; Kliewer, W. M. Influence of light on grape berry growth and composition varies during fruit development. *J. Am. Soc. Hortic. Sci.* **1996**, *121*, 869–874.
19. Wicks, A. S.; Kliewer, W. M. Further Investigations into the relationship between anthocyanins, phenolics and soluble carbohydrates in grape berry skins. *Am. J. Enol. Vitic.* **1983**, *34*, 114–116.
20. Chorti, E.; Guidoni, S.; Ferrandino, A.; Novello, V. Effect of different cluster sunlight exposure levels on ripening and anthocyanin accumulation in Nebbiolo grapes. *Am. J. Enol. Vitic.* **2010**, *61*, 23–30.

21. Reynolds, A. G.; Wardle, D. A. Influence of fruit microclimate on monoterpene levels of Gewürztraminer. *Am. J. Enol. Vitic.* **1989**, *40*, 149–154.
22. Reynolds, A. G.; Wardle, D. A. Flavour development in the vineyard: Impact of viticultural practices on grape monoterpenes and their relationship to wine sensory response. *S. Afr. J. Enol. Vitic.* **1997**, *18*, 3–18.
23. Belancic, A.; Agosin, E.; Ibacache, A.; Bordeu, E.; Baumes, R.; Razungles, A.; Bayonove, C. Influence of sun exposure on the aromatic composition of chilean Muscat grape cultivars Moscatel de Alejandría and Moscatel rosada. *Am. J. Enol. Vitic.* **1997**, *48*, 181–186.
24. Harbertson, J. F.; Picciotto, E. A.; Adams, D. O. Measurement of polymeric pigments in grape berry extracts and wines using a protein precipitation assay combined with bisulfite bleaching. *Am. J. Enol. Vitic.* **2003**, *54*, 301–306.
25. Parr, W. V.; Green, J. A.; White, K. G.; Sherlock, R. R. The distinctive flavour of New Zealand Sauvignon blanc: Sensory characterisation by wine professionals. *Food Qual. Prefer.* **2007**, *18*, 849–861.
26. Herbst-Johnstone, M.; Piano, F.; Duhamel, N.; Barker, D.; Fedrizzi, B. Ethyl propiolate derivatisation for the analysis of varietal thiols in wine. *J. Chromatogr., A* **2013**, *1312*, 104–110.
27. Jouanneau, S.; Weaver, R. J.; Nicolau, L.; Herbst-Johnstone, M.; Benkwitz, F.; Kilmartin, P. A. Subregional survey of aroma compounds in Marlborough Sauvignon Blanc wines. *Aust. J. Grape Wine Res.* **2012**, *18*, 329–343.
28. Koch, A.; Doyle, C. L.; Matthews, M. A.; Williams, L. E.; Ebeler, S. E. 2-Methoxy-3-isobutylpyrazine in grape berries and its dependence on genotype. *Phytochemistry* **2010**, *71*, 2190–2198.
29. Roujou de Boubée, D.; Van Leeuwen, C.; Dubourdieu, D. Organoleptic impact of 2-Methoxy-3-isobutylpyrazine on red Bordeaux and Loire wines. Effect of environmental conditions on concentrations in grapes during ripening. *J. Agric. Food Chem.* **2000**, *48*, 4830–4834.
30. Lopez, R.; Ferreira, V.; Hernandez, P.; Cacho, J. F. Identification of impact odorants of young red wines made with Merlot, Cabernet Sauvignon and Grenache grape varieties: a comparative study. *J. Sci. Food Agric.* **1999**, *79*, 1461–1467.
31. Aznar, M.; Lopez, R.; Cacho, J. F.; Ferreira, V. Identification and quantification of impact odorants of aged red wines from Rioja. GC−Olfactometry, quantitative GC-MS, and odor evaluation of HPLC fractions. *J. Agric. Food Chem.* **2001**, *49*, 2924–2929.
32. Escudero, A.; Campo, E.; Farina, L.; Cacho, J.; Ferreira, V. Analytical characterization of the aroma of five premium red wines. Insights into the role of odor families and the concept of fruitiness of wines. *J. Agric. Food Chem.* **2007**, *55*, 4501–4510.
33. Campo, E.; Ferreira, V.; Escudero, A.; Cacho, J. Prediction of the wine sensory properties related to grape variety from dynamic-headspace gas chromatography−olfactometry data. *J. Agric. Food Chem.* **2005**, *53*, 5682–5690.
34. Hein, K.; Ebeler, S. E.; Heymann, H. Perception of fruity and vegetative aromas in red wine. *J. Sens. Stud.* **2009**, *24*, 441–455.

Publication Date (Web): November 24, 2015 | doi: 10.1021/bk-2015-1203.ch011

Publication Date (Web): November 24, 2015 | doi: 10.1021/bk-2015-1203.ch012

Chapter 12

Induction of de Novo Mono- and Sesquiterpene Biosynthesis by Methyl Jasmonate in Grape Berry Exocarp

B. May and M. Wüst*

Institute of Nutrition and Food Sciences, Chair of Bioanalytics/Food Chemistry, Rheinische Friedrich-Wilhelms-Universität Bonn, Endenicher Allee 11-13, 53115 Bonn, Germany
***E-mail: matthias.wuest@uni-bonn.de.**

Methyl jasmonate (MeJ) induced biosynthesis of volatile organic compounds (VOCs) was observed in a time-course experiment with grape berries of *Vitis vinifera* cv. Lemberger. A rapid emission of linalool within 2-6 hours after application of the elicitor was observed, followed by the emission of additional monoterpenes, indole and homo- as well as sesquiterpenes within 36 hours. The parallel application of [5,5-$^2H_2$]-1-deoxy-D-xylulose (d_2-DOX) confirmed the rapid de novo synthesis of the induced terpenes, especially linalool. Indole and the dehydroterpene cosmene were detected for the first time as defense related volatiles in grape berries.

Methyl jasmonate (MeJ) is frequently used as an elicitor to study plant defense mechanisms. Even though the jasmonate (JA)-amino acid conjugate jasmonoyl-L-isoleucine (JA-Ile) is the underlying phytohormone (*1*), the application of the exogenous methyl ester induces defense mechanisms already known from plant-pathogen-interactions. Both, plant-pathogen-interaction as well as the use of exogenous elicitors can provoke a multitude of responses. Direct defense strategies include the synthesis of antimicrobial phytoalexins, such as stilbenes, or the synthesis of pathogenesis related proteins, e.g. defensin. Indirect defense strategies include the emission of volatile organic compounds (VOCs) (*2*). As VOCs they facilitate the short and long distance plant interaction

In Advances in Wine Research; Ebeler, et al.;
ACS Symposium Series; American Chemical Society: Washington, DC, 2015.

(*3*) or the ability to attract carnivorous insects (*4*). These VOCs include mono-, homo- and sesquiterpenes, as well as green leaf volatiles (GLVs) and compounds of the shikimate pathway (e.g. indole, methyl salicylate) (*2*). The induced mechanism is aligned to the pathogen but depends also on the affected plant species (*5*, *6*). Normally, the response to an attack is a complex interaction of different phytohormones or hormone-like compounds with synergistic or antagonistic effects (*7*). Furthermore, a plant is often exposed to several vermin and the induced mechanism due to this multiple attack may differ (*8*). The use of exogenous elicitors like MeJ, but also benzothiadiazole or abscisic acid provides a simplified model to study these complex interactions in plants. The emission of different VOCs had been shown for pest infested grape vine leaves (*9*), MeJ treated leaves (*10*) and grape cell cultures (*11*). An increased resistance of *Vitis vinifera* against different pathogens, e.g. *Botrytis cinerea*, *Plasmopara viticola* or *Erysiphe necator*, was observed for several elicitors (*12–14*), associated with an accumulation of bioactive phytochemicals, e.g. stilbenes and proanthocyanidins in grape berry skins (*15*). Beside these effects, the influence on primary wine aroma compounds is of particular interest. A change in volatile composition, in particular terpenes, norisoprenoids, acetals, alcohols and esters, in wine made from elicitor treated grapes was already demonstrated (*16*, *17*).

In this study we investigated the time-course of the emission of VOCs from detached grape berries after induction by methyl jasmonate. The parallel application of [5,5-$^2H_2$]-1-deoxy-D-xylulose (d_2-DOX) allowed us to verify whether the emitted terpenes were synthesized *de novo* or released from bound, constitutively formed and stored precursors, e.g. from glycosidically bound terpenols. d_2-DOX was used as a probe to detect a *de novo*-terpene biosynthesis, because previous studies demonstrated the incorporation of d_2-DOX into mono-, sesqui- and diterpenes *via* the methylerythritol phosphate (MEP) pathway in grape berry exocarp (*18*).

Experimental

Material

Berries of the variety Lemberger were collected at two stages of ripening (t_1: August 30, 2012, 10.2 brix and t_2 September 29, 2012, 17.1 brix). The material was obtained from the Institute of Crop Science and Resource Conservation (INRES) of the University of Bonn.

Experimental Setting

10 µL of an aqueous solution of MeJA (0.1 %) was injected through the receptacle into the pulp of intact grape berries. The injected solution at sampling stage t_1 contained also 1 % d_2-DOX (synthesized according to Meyer et al., 2004 (*19*)). After injection, four berries were immediately transferred into a 20 mL headspace vial and the volatiles were sampled as described below by HS-SPME-GC-MS. All measurements at the two described sampling stages were performed

Publication Date (Web): November 24, 2015 | doi: 10.1021/bk-2015-1203.ch012

in duplicate (total measurements: n=4). For Figures 2 and 4 the time course for typical experiments are shown (n=1) for clarity reasons. In Figure 3 the mean value for each data point is displayed together with its standard deviation for all measurements (n=4; see above) for selected volatiles. Absolute emission in this case was normalized to 1 to illustrate the average temporal development. In a parallel setting, water was administered as control at each sampling stage. The time-course measurements were performed using an autosampler over a period of 65 hours after injection of the elicitor. Each sample was measured every 2-3 hours, while the control sample was measured every 5 hours. Samples were kept at room temperature during the whole time-course study.

Publication Date (Web): November 24, 2015 | doi: 10.1021/bk-2015-1203.ch012

Analysis

VOCs analysis was performed by HS-SPME-GC-MS. A 85 µm polyacrylate fiber, from Supelco (Bellefonte, PA, USA) was used for solid phase microextraction (SPME). The extraction was performed at room temperature for 20 minutes. Subsequently, the analytes were thermally desorbed in the GC-injection port. GC-MS-analysis was performed using a Varian 450 GC coupled to a Varian 240 MS ion trap mass spectrometer (Palo Alto, CA, United States). The injection port was set to 220 °C. Splitless injection was used and the split valve was opened after 3 min. Separation was achieved using a DB5 column (Varian, length 30 m, 0.25 mm i.d., film thickness = 0.25 µm). The carrier gas (helium, 5.0) was set to 1 mL/min (constant flow). The column temperature program started at 35°C for 3 min, and was increased to 250°C at a rate of 5°C/min. The transfer line temperature was set to 260°C, the ion source to 150°C. An internal EI-ionization (70 eV) was performed and mass spectra were recorded in the range of m/z 35-350 (full scan), at a scan rate of 0.64 sec/scan. Compounds were identified by comparison of the retention times and mass spectra with standard substances or by comparing their mass spectra and Kovats retention indices using the Massfinder® library (Hochmuth Scientific Consulting, Hamburg, Germany). Incorporation rates were calculated by dividing the peak area of the labeled compound by the peak area of the genuine compound multiplied by 100%.

Results and Discussion

The application of MeJ enhanced the emission of several terpenes, namely monoterpenes (e.g. linalool, *(E)*-β-ocimene), the homoterpene 4,8-dimethylnona-1,3,7-triene (DMNT) and sesquiterpenes (e.g. *(E,E)*-α-farnesene, nerolidol) as well as indole and *(E,E)*-2,6-dimethyl-1,3,5,7-octatetraen (cosmene) (Figure 1). Most of the induced volatiles were previously reported as herbivore induced plant volatiles emitted by green leaves. Their release was demonstrated for MeJ treated grapevine leaves (*10*), beetle-damaged grapevine leaves (*9*), as well as for several other plant-pathogen combinations (*6*, *20*).

Publication Date (Web): November 24, 2015 | doi: 10.1021/bk-2015-1203.ch012

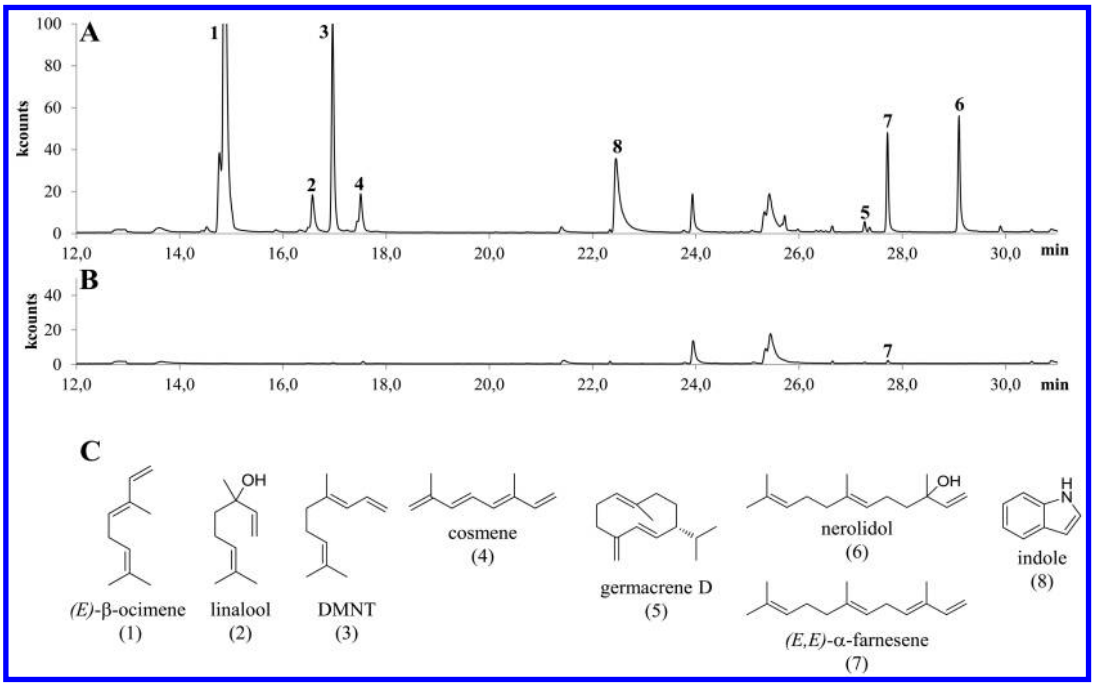

Figure 1. Total ion chromatogram of volatiles of grape berries measured by HS-SPME-GC-MS, 36 hours after application of methyljasmonate (A) and water as control (B); chemical structures of most abundant compounds are given below (C).

Publication Date (Web): November 24, 2015 | doi: 10.1021/bk-2015-1203.ch012

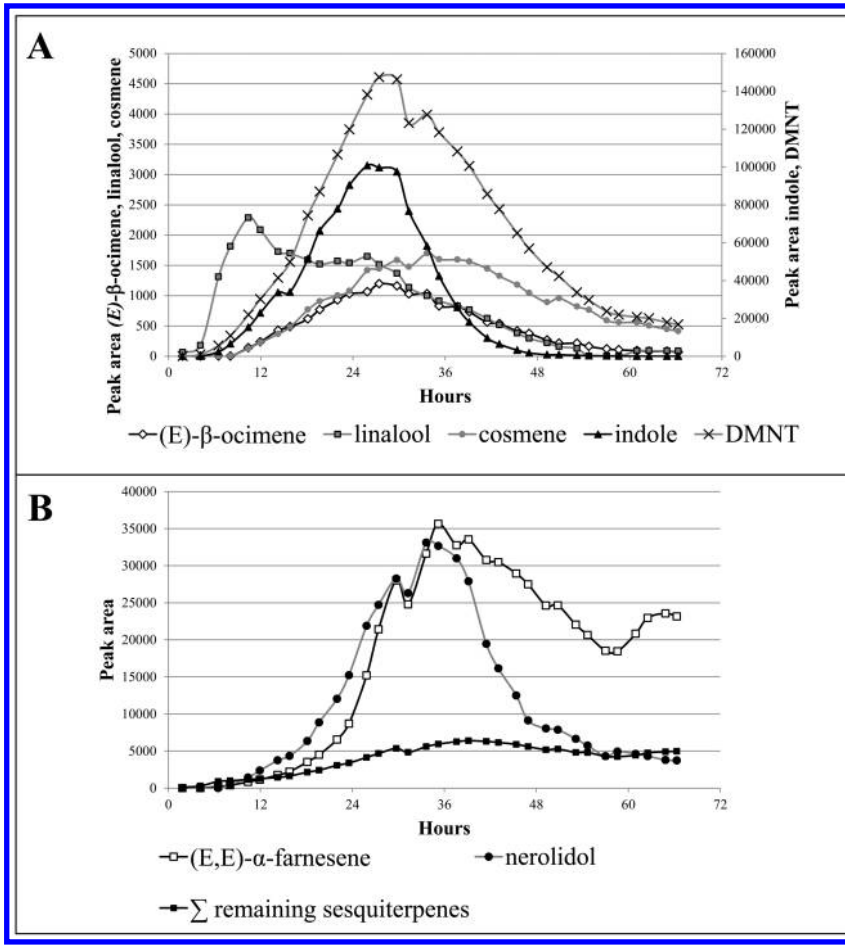

Figure 2. Time-course of VOC emission after methyl jasmonate application (August 30, 2012) shown for a typical experiment (n=1). The peak areas are based on the ion traces given in Table 1 for the genuine compounds.

The applied experimental setting allowed us to obtain a detailed insight in the temporal dynamics of VOC release (Figure 2). The depicted data belong to the early stage of berry development (August 30, 2012). All four time-course studies showed comparable temporal pattern in volatile release (Figure 3) after MeJ application, even though the absolute amount of induced volatiles varied within the four measurements (e.g. twofold observed for *(E)*-β-ocimene and up to 35-fold observed for nerolidol). Volatile emission was 10-100 times higher after MeJ application compared to the control samples (water application). Some induced volatiles (e.g. linalool, nerolidol, DMNT) were not observed in the control samples. Linalool was the first VOC whose emission from grape berry exocarp was enhanced after MeJ application. Its release started 2-6 hours after application and reached its maximum after 12 hours. Afterwards, the emission

declined slowly and ceased between 45-60 hours after application. In contrast, the induced emission of the monoterpene *(E)*-β-ocimene was slower and reached its maximum about 24 hours after application of MeJ. The clearly different emission pattern of the two monoterpenes raises the question whether the hydroxylated terpene linalool is quickly released from stored precursors, e.g. glycosides, or whether its enhanced emission is a result of the quick up-regulation of the corresponding linalool synthase. The simultaneous application of d_2-DOX results in a clearly detectable deuterium incorporation already 5 hours after elicitation (Figure 4A), which demonstrates a rapid activation of a de novo synthesis of linalool. However, a participation of stored precursors cannot be excluded. Ion traces used for the calculation of the incorporation rates are given in Table 1. The extreme velocity of plant defense reactions was already demonstrated for *Arabidopsis thaliana*, where 5 minutes after wounding the JA-Ile level increased in the affected tissues (*21*).

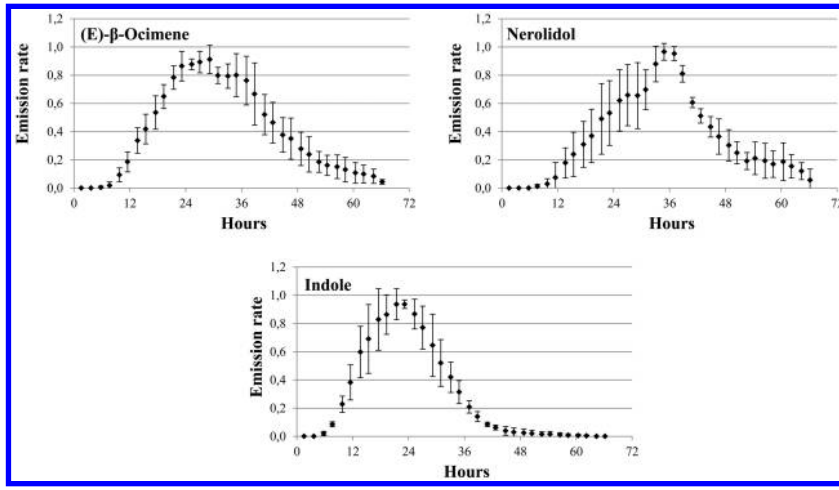

Figure 3. Variability of the time dependent VOC emission after methyl jasmonate application (n=4). Absolute emission was normalized to 1 to illustrate the average temporal development.

Only limited data is available for the induced emission of the dehydroterpene cosmene. Although it has been detected in essential oils (*22*) as well as in a few studies as volatile after pest infestation (*23*), it is reported to be highly unstable (*24*) and its origin remained unknown. Some studies suggest that it might be a degradation product from *(E)*-β-ocimene formed during sample preparation (*5*). However, a HS-SPME-GC-MS measurement of an aqueous solution of *(E)*-β-ocimene yielded in no detectable amounts of cosmene (data not shown). Furthermore, in our time course study cosmene showed an emission profile that was clearly different from the emission profile of ocimene, which demonstrates that cosmene is indeed an inducible monoterpene.

Publication Date (Web): November 24, 2015 | doi: 10.1021/bk-2015-1203.ch012

Indole, which belongs to the phenylpropanoid aromatic compounds, showed an emission profile similar to *(E)*-β-ocimene. Amongst others, indole is detected in the volatile blend of beetle infested grapevine leaves (*9*). However, to the best of our knowledge, this is the first time that the induced emission of indole is demonstrated in grape berries. In maize, for example, indole is generated by the degradation of indole-3-glycerol phosphate. Studies demonstrated that the enzyme indole-3-glycerol phosphate lyase (IGL), which catalyzes its formation, can be activated by volicitin, a fatty acid derivate from regurgitates of the armyworm (*25*).

Publication Date (Web): November 24, 2015 | doi: 10.1021/bk-2015-1203.ch012

Table 1. Ion Traces (m/z) Used for Data Evaluation and Calculation of the Incorporation Rates

No.	*Name*	*Quantifier ions*		*Deuterium incorporation (x)*
		Genuine (d_0)	*Labelled (d_x)*	
1	*(E)*-β-ocimene[a]	136	140	d_4
2	linalool[a]	121	124[c]	d_4
3	DMNT[b]	69	71	d_2/d_3[d]
4	cosmene[b]	134	137	d_3
5	germacrene D[a]	161	163/165/167	d_2/d_4/d_6
6	nerolidol[a]	161	163	d_2
7	*(E,E)*-α-farnesene[a]	93[e]	-	-
8	indole[b]	117[f]	-	-

[a] Identified using standard substances. [b] Identified by mass spectrum and kovats index. [c] Loss of deuterium due to fragmentation. [d] Exact degree of deuterium labeling cannot be determined. [e] Deuterium incorporation was not calculated for *(E,E)*-α-farnesene due to its non-characteristic fragmentation pattern. [f] Not of isoprenoid origin.

While the emission of all monoterpenes, DMNT, cosmene and indole declined after 36 hours after elicitation, the emission rates of the sesquiterpenes remained elevated during the entire observation period, except for the sesquiterpene nerolidol, which also declined after 36 hours (Figure 2B). The increased emission of all sesquiterpenes may be caused by a general up- regulation of specific genes of the MEP- and MVA-pathway.

Surprisingly, only up to 4% of d_2-nerolidol was detectable, after application of d_2-DOX (Figure 4B) even though our previous studies revealed that both, the MEP- and MVA-pathway, can be utilized for sesquiterpene biosynthesis (*18*). The incorporation of two deuterium atoms into nerolidol results from the incorporation of only one C5-isoprenoid building block generated from d_2-DOX and two genuine, nonlabelled, isoprenoid building blocks.

Publication Date (Web): November 24, 2015 | doi: 10.1021/bk-2015-1203.ch012

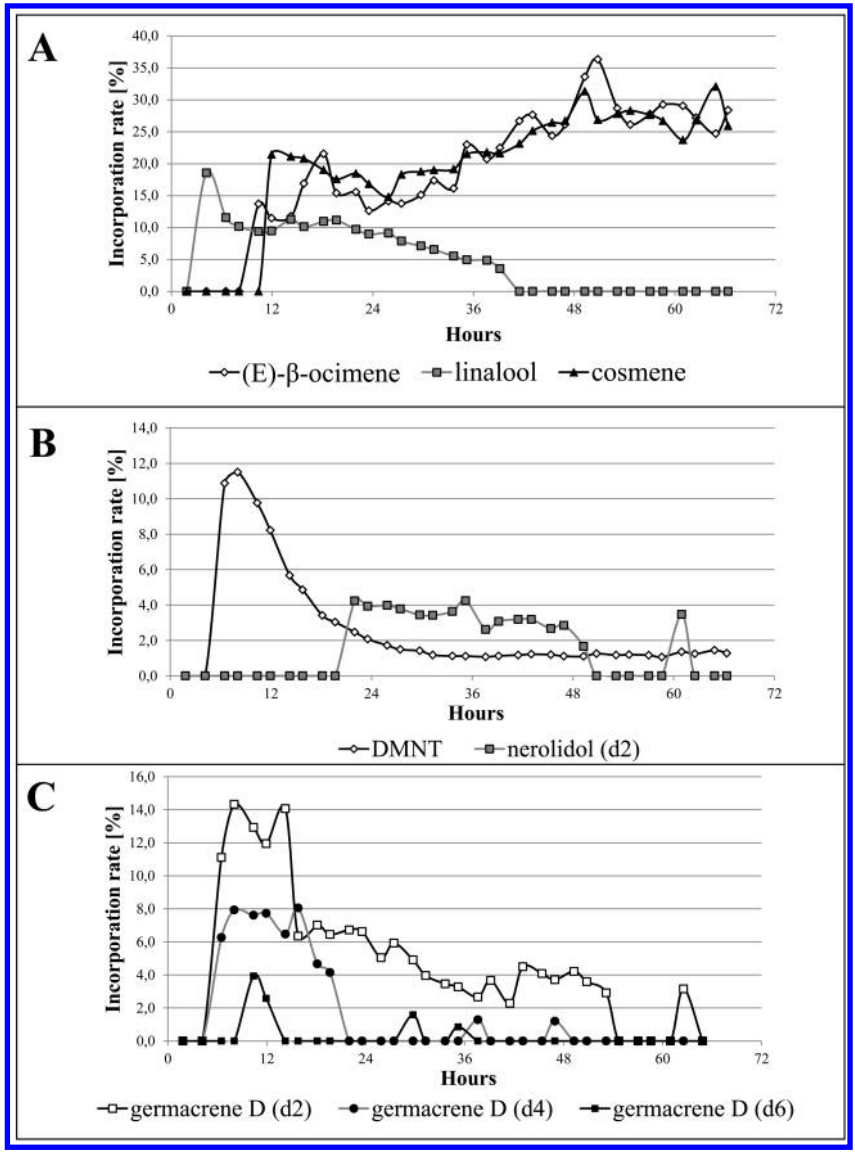

Figure 4. Incorporation rates during the time-course studies after application of d_2-DOX and MeJ at time zero. Table 1 informs about corresponding ion traces used for the calculation of the deuterium labeling degree. For clarity reasons volatiles were grouped in sections A-C.

A poor incorporation was detected for germacrene D, too (Figure 4C). The highest incorporation rate of labelled d_2-DOX into germacrene D was detected between 5-15 hours after application. At this time, the emission rate of sesquiterpenes was still low, and increased later on. Hence, an enhanced supply of genuine isoprenoid intermediates via the

MVA-pathway might be the reason for the low incorporation of d_2-DOX into sesquiterpenes. Onofrio et al. (2009) already demonstrated the up-regulation of 3-hydroxy-3-methylglutaryl-CoA synthase, mevalonate-5-pyrophosphate decarboxylase and 3-hydroxy-3-methylglutaryl-CoA reductase of the MVA-pathway after incubation of grape cell cultures with MeJ and JA (*11*).

The deuterium labelling degree of DMNT, which is generated in a cytochrome P450-mediated oxidative degradation reaction of the sesquiterpene nerolidol (*26*), should correspond to the labelling degree of its precursor nerolidol. The lower incorporation rate of DMNT compared to nerolidol in the time range from 20-50 hours can be explained by the loss of deuterium due to the oxidative cleavage reaction. However, the considerably higher labelling of DMNT between 5-15 hours after application of labeled d_2-DOX might be explained by the oxidative degradation of *de novo* synthesized, labelled nerolidol. The similar time-course of the incorporation rates of germacrene D and the sesquiterpene derived DMNT support this assumption.

Publication Date (Web): November 24, 2015 | doi: 10.1021/bk-2015-1203.ch012

Conclusions

The results demonstrate a rapid activation of the *de novo* synthesis of terpenes in the grape berry exocarp by MeJ. The distinct emission profiles of linalool and nerolidol underline the special role of both compounds. Recently, the induced synthesis and the antimicrobial activity of nerolidol were demonstrated for callus and grape cell cultures inoculated with *Phaecremonium parasiticum* (*27*). Studies using *Arabidopsis thaliana* confirmed the repellent effect of linalool on aphids (*28*). However, an investigation of gene expression levels or inhibition experiments could provide further information about the involvement of the constitutive and induced biosynthesis of VOCs in grape berry defense mechanisms.

The VOCs analyzed in this study belong to so called airborne signals. Until now, much less is known about the effect of elicitors on the increased accumulation of wine aroma compounds. The investigation of wines and grapes, treated with MeJ during ripening, already demonstrated an enhanced accumulation of volatile compounds (*16*). MeJA caused a significant increase of monoterpenes, such as linalool, and sesquiterpenes (nerolidol and farnesol) in the final wine. These results compare well with ours and demonstrate that defense related reactions of the grape berry might influence the final wine flavor in a perceivable manner.

References

1. Melotto, M.; Mecey, C.; Niu, Y.; Chung, H. S.; Katsir, L.; Yao, J.; Zeng, W.; Thines, B.; Staswick, P.; Browse, J.; Howe, G. A.; He, S. Y. A critical role of two positively charged amino acids in the Jas motif of Arabidopsis JAZ proteins in mediating coronatine- and jasmonoyl isoleucine-dependent interactions with the COI1 F-box protein. *Plant J.* **2008**, *55*, 979–988.

2. Schulze, B.; Kost, C.; Arimura, G.-I.; Boland, W. Duftstoffe: Die Sprache der Pflanzen. Signalrezeption, Biosynthese und Ökologie. *Chem. Unserer Zeit* **2006**, *40*, 366–377.
3. Heil, M.; Karban, R. Explaining evolution of plant communication by airborne signals. *Trends Ecol. Evol.* **2010**, *25*, 137–144.
4. Hilker, M.; Kobs, C.; Varama, M.; Schrank, K. Insect egg deposition induces Pinus sylvestris to attract egg parasitoids. *J. Exp. Biol.* **2002**, *205*, 455–461.
5. Leitner, M.; Boland, W.; Mithöfer, A. Direct and indirect defences induced by piercing-sucking and chewing herbivores in Medicago truncatula. *New Phytol.* **2005**, *167*, 597–606.
6. Bartram, S.; Jux, A.; Gleixner, G.; Boland, W. Dynamic pathway allocation in early terpenoid biosynthesis of stress-induced lima bean leaves. *Phytochemistry* **2006**, *67*, 1661–1672.
7. Beckers, G. J. M.; Spoel, S. H. Fine-Tuning Plant Defence Signalling: Salicylate versus Jasmonate. *Plant Biol.* **2006**, *8*, 1–10.
8. Dicke, M.; van Loon, J. J. A. L.; Soler, R. Chemical complexity of volatiles from plants induced by multiple attack. *Nat. Chem. Biol.* **2009**, *5*, 317–324.
9. Loughrin, J. H.; Potter, D. A.; Hamilton-Kemp, T. R.; Byers, M. E. Diurnal emission of volatile compounds by Japanese beetle-damaged grape leaves. *Phytochemistry* **1997**, *45*, 919–923.
10. Hampel, D.; Mosandl, A.; Wüst, M. Induction of de Novo Volatile Terpene Biosynthesis via Cytosolic and Plastidial Pathways by Methyl Jasmonate in Foliage of Vitis vinifera L. *J. Agric. Food Chem.* **2005**, *53*, 2652–2657.
11. Onofrio, C. D.; Cox, A.; Davies, C.; Boss, P. K. Induction of secondary metabolism in grape cell cultures by jasmonates. *Funct. Plant Biol.* **2009**, *36*, 323–338.
12. Iriti, M.; Rossoni, M.; Borgo, M.; Faoro, F. Benzothiadiazole Enhances Resveratrol and Anthocyanin Biosynthesis in Grapevine, Meanwhile Improving Resistance to Botrytis cinerea. *J. Agric. Food Chem.* **2004**, *52*, 4406–4413.
13. Aziz, A.; Poinssot, B.; Daire, X.; Adrian, M.; Bézier, A.; Lambert, B.; Joubert, J.-M.; Pugin, A. Laminarin Elicits Defense Responses in Grapevine and Induces Protection Against Botrytis cinerea and Plasmopara viticola. *Mol. Plant-Microbe Interact.* **2003**, *16*, 1118–1128.
14. Belhadj, A.; Saigne, C.; Telef, N.; Cluzet, S.; Bouscaut, J.; Corio-Costet, M.-F.; Mérillon, J.-M. Methyl Jasmonate Induces Defense Responses in Grapevine and Triggers Protection against Erysiphe necator. *J. Agric. Food Chem.* **2006**, *54*, 9119–9125.
15. Iriti, M.; Rossoni, M.; Borgo, M.; Ferrara, L.; Faoro, F. Induction of Resistance to Gray Mold with Benzothiadiazole Modifies Amino Acid Profile and Increases Proanthocyanidins in Grape: Primary versus Secondary Metabolism. *J. Agric. Food Chem.* **2005**, *53*, 9133–9139.
16. Gomez-Plaza, E.; Mestre-Ortuno, L.; Ruiz-Garcia, Y.; Fernandez-Fernandez, J. I.; Lopez-Roca, J. M. Effect of Benzothiadiazole and Methyl Jasmonate on the Volatile Compound Composition of Vitis vinifera L. Monastrell Grapes and Wines. *Am. J. Enol. Vitic.* **2012**, *63*, 394–401.

Publication Date (Web): November 24, 2015 | doi: 10.1021/bk-2015-1203.ch012

17. Vitalini, S.; Ruggiero, A.; Rapparini, F.; Neri, L.; Tonni, M.; Iriti, M. The application of chitosan and benzothiadiazole in vineyard (Vitis vinifera L. cv Groppello Gentile) changes the aromatic profile and sensory attributes of wine. *Food Chem.* **2014**, *162*, 192–205.
18. May, B.; Lange, B. M.; Wüst, M. Biosynthesis of sesquiterpenes in grape berry exocarp of Vitis vinifera L.: Evidence for a transport of farnesyl diphosphate precursors from plastids to the cytosol. *Phytochemistry* **2013**, *95*, 135–144.
19. Meyer, O.; Hoeffler, J.-F.; Grosdemange-Billiard, C.; Rohmer, M. Practical synthesis of 1-deoxy-d-xylulose and 1-deoxy-d-xylulose 5-phosphate allowing deuterium labelling. *Tetrahedron* **2004**, *60*, 12153–12162.
20. Suckling, D. M.; Twidle, A. M.; Gibb, A. R.; Manning, L. M.; Mitchell, V. J.; Sullivan, T. E. S.; Wee, S. L.; El-Sayed, A. M. Volatiles from Apple Trees Infested with Light Brown Apple Moth Larvae Attract the Parasitoid Dolichogenidia tasmanica. *J. Agric. Food Chem.* **2012**, *60*, 9562–9566.
21. Glauser, G.; Grata, E.; Dubugnon, L.; Rudaz, S.; Farmer, E. E.; Wolfender, J.-L. Spatial and Temporal Dynamics of Jasmonate Synthesis and Accumulation in Arabidopsis in Response to Wounding. *J. Biol. Chem.* **2008**, *283*, 16400–16407.
22. Tian, J.; Zeng, X.; Zhang, S.; Wang, Y.; Zhang, P.; Lü, A.; Peng, X. Regional variation in components and antioxidant and antifungal activities of Perilla frutescens essential oils in China. *Ind. Crops Prod.* **2014**, *59*, 69–79.
23. Quaglia, M.; Fabrizi, M.; Zazzerini, A.; Zadra, C. Role of pathogen-induced volatiles in the Nicotiana tabacum–Golovinomyces cichoracearum interaction. *Plant Physiol. Biochem.* **2012**, *52*, 9–20.
24. Christensen, L. P.; Lam, J.; Thomasen, T. A chalcone and other constituents of bidens tripartitus. *Phytochemistry* **1990**, *29*, 3155–3156.
25. Frey, M.; Stettner, C.; Pare, P. W.; Schmelz, E. A.; Tumlinson, J. H.; Gierl, A. An herbivore elicitor activates the gene for indole emission in maize. *Proc. Natl. Acad. Sci. U.S.A.* **2000**, *97*, 14801–14806.
26. Lee, S.; Badieyan, S.; Bevan, D. R.; Herde, M.; Gatz, C.; Tholl, D. Herbivore-induced and floral homoterpene volatiles are biosynthesized by a single P450 enzyme (CYP82G1) in Arabidopsis. *Proc. Natl. Acad. Sci. U.S.A.* **2010**, *107*, 21205–21210.
27. Escoriaza, G.; Sansberro, P.; García-Lampasona, S.; Gatica, M.; Bottini, R.; Piccoli, P. In vitro cultures of Vitis vinifera L. cv. Chardonnay synthesize the phytoalexin nerolidol upon infection by Phaeoacremonium parasiticum. *Phytopathol. Mediterr.* **2013**, *52*, 289–297.
28. Aharoni, A.; Giri, A. P.; Deuerlein, S.; Griepink, F.; de Kogel, W. J.; Verstappen, F. W. A.; Verhoeven, H. A.; Jongsma, M. A.; Schwab, W.; Bouwmeester, H. J. Terpenoid Metabolism in Wild-Type and Transgenic Arabidopsis Plants. *Plant Cell* **2003**, *15*, 2866–2884.

Publication Date (Web): November 24, 2015 | doi: 10.1021/bk-2015-1203.ch012

Publication Date (Web): November 24, 2015 | doi: 10.1021/bk-2015-1203.ch013

Chapter 13

Critical Oxygen Levels Affecting Wine Aroma: Relevant Sensory Attributes, Related Aroma Compounds, and Possible Mechanisms

Maurizio Ugliano,* Stéphanie Bégrand, Jean-Baptiste Diéval, and Stéphane Vidal

Nomacorc France, Av. Yves Cazeaux, Rodilhan 30230, France
***E-mail: m.ugliano@nomacorc.be.**

The importance of post-bottling oxygen to wine aroma development has been demonstrated. However, from a practical point of view, the degrees of oxygen exposures needed to induce significant aroma modification remain to be established. In addition, certain styles of wine are more responsive to oxygen than others, possibly reflecting the key role of specific aroma compounds with lower/higher oxygen sensitivity in their sensory profile. In this study, 36 wines from different grape varieties were submitted to sensory descriptive analyses. The wines were in an age bracket of 9-19 months (whites), 5-11 months (rosé), 12-48 months (reds). Each wine had received at least two different oxygen exposure levels by means of different closures, with some wines tasted at different time points. In total, 96 wines were tasted. When considering only the contribution of closure-derived oxygen, aroma intensity, fruity attributes, and reduction were in white wines the sensory descriptors mostly affected by oxygen. In the case of rosé wines, oxygen appeared to influence mainly aroma intensity and red fruit attributes, whereas for red wines red fruits, cooked fruits, spices and gamey were mostly affected. Analyses conducted on selected wines indicated that esters, largely associated with wine fruity aromas were not affected by oxygen. Conversely, the fruit-enhancer ß-damascenone increased with higher oxygen exposure, while fruity thiols such as 3-sulfanylhexanol (3SH) decreased. H_2S and methyl mercaptan were mostly implicated

In Advances in Wine Research; Ebeler, et al.;
ACS Symposium Series; American Chemical Society: Washington, DC, 2015.

with reduction attribute, and they might negatively affect expression of fruity attributes. The possible mechanisms implicated in the response of these compounds to oxygen are discussed.

Introduction

In recent years, a number of different studies have shown that the type of closure, in particular its ability to allow a certain degree of oxygen exposure in the bottle, plays a crucial role in the chemical and sensory evolution of the wine during bottle maturation (reviewed in (*1*)). Overall, the conclusions of these studies support the anecdotal observation that, in order for bottle aging to contribute positively to wine quality, a certain degree of oxygen exposure is required. Nevertheless, several aspects remain to be clarified. First, in view of the great variety of wine styles produced in different parts of the world, the type of aroma attributes that can be effectively modulated by oxygen needs to be better characterized. This appears crucial in order to provide practical information as to which wine styles can be more effectively modulated by informed closure selection. Second, while extreme oxygen exposure levels (e.g. too little or too much) during bottle maturation can result in oxidative off-odors such as reduction or oxidation, the outcomes of intermediate oxygen levels, which are most common in today industry, are not well described. Among these, some studies indicate that the fruity attributes of wine can be affected by closure-derived oxygen, but the trends observed seem to be inconsistent. In fact, while some authors indicated increased fruit expression at lower oxygen, other data show the opposite (*2–4*). In addition, the chemical compounds and transformations implicated in the sensory changes associated with the mild levels of oxygen exposure found during bottle maturation need to be clarified.

In this study, the sensory changes associated with bottle maturation under closures allowing different oxygen exposure levels have been studied for 126 wines. The purpose was to evaluate which aroma attributes were more frequently associated with changes in oxygen exposure, as well as to characterize the oxygen levels at which these changes might occur. The mechanisms underlying oxygen interactions with different wine aroma compounds potentially implicated in these changes are also discussed.

Materials and Methods

Wines were collected in the period 2011-2014 from different commercial and experimental cellars located in various European winemaking regions. Preliminary assessments were carried out to ensure adequate bottling conditions at each cellar. Thirty-six wine types from different grape varieties were bottled, using at least two different Nomacorc Select series closures allowing defined oxygen ingress values (Table 1). Oxygen ingres values of individual closure types were measured as described by Dieval et al. (*5*). At the moment of tasting, the wines were in an age bracket of 9-19 months (whites), 5-11 months (rosé), 12-48

Publication Date (Web): November 24, 2015 | doi: 10.1021/bk-2015-1203.ch013

months (reds). Within single wines, the difference in oxygen exposure created by the different closures was in the range of 0.5-1.2 mg (whites), 0.4-1.2 mg (rosé), and 0.6-1.4 mg (reds). A total of 126 wines were submitted to sensory analysis, including 28 white wines, 47 rose' wines and 51 red wines.

Table 1. Oxygeningress (mg of O_2) of the Different Closures Used in the Study at Different Times of Bottle Aging

	Closure			
	Select 700	**Select 500**	**Select 300**	**Select 100**
3 Months	1.72	1.54	1.35	0.37
6 Months	2.29	2.06	1.79	0.64
1 Year	3.4	3.0	2.4	1.2
After 1st year	2.1 mg/ yr	1.7 mg /yr	1.1 mg/yr	1.1 mg/yr

Sensory analysis was carried out at *In Senso Veritas* (Beaune, France), by a panel of 16 trained panelists. Evaluations were performed under white light, at room temperature, at isolated tables. The wines were evaluated on pre-defined attributes (11 for white wines, 12 for rose wines and 10 for red wines), rating each attribute on a 7 points continuous scale (from 0 to 6). Reference standards were provided for each one of the aroma attributes tested as indicated in Table 2. Wines were served in blind, with a random 3 digit code. Each panelist had a randomized order of presentation in order to avoid effects of order. Panelist performance was assessed using FIZZ software.

For the sensory analysis data, analysis of variance (ANOVA) was carried out to assess the effect of oxygen exposure on individual aroma descriptors. Within each wine type, the number of times a single descriptor showed significant differences at $p<0.05$ was divided by the number of total tastings conducted, in order to obtain the percentage of tastings in which that specific descriptor was significantly affected by oxygen exposure.

Analyses of volatile compounds were carried out as described elsewhere. Fermentation esters, 3SH, H_2S and MeSH were measured following the procedures described by Ugliano et al. (*6*). Analysis of phenylacetaldehyde was carried out as described by Culleré et al. (*7*). *ß*-Damascenone was analyzed by a stable isotope dilution assay, as described by Kotseridis et al (*8*). Measurement of oxygen ingress for the different closures used was carried out as described by Dieval et al. (*5*). Not in all cases chemical analyses were done at the same time as sensory evaluation of the wines. Statistical analyses were carried out using XLStat (AddinSoft, Paris, France).

Publication Date (Web): November 24, 2015 | doi: 10.1021/bk-2015-1203.ch013

Table 2. Reference Standards Used for Sensory Analysis

Red fruits	A mix of cassis, strawberry, raspberry, and myrtle juice
Exotic fruit	Passion fruit and mango juice
Citrus	A mix of lemon, orange and grapefruit juice
Cooked fruits	A mix of red fruits and apricot jam
Floral	A mix of rose and violet extracts
Empyreumatic	Grilled bread
Fermentative	Butter
Vegetal	Fresh green capsicum
Reduction	A solution of methyl mercaptan
Oxidation	Tawny port
Mineral	Struck match

Publication Date (Web): November 24, 2015 | doi: 10.1021/bk-2015-1203.ch013

Results and Discussion

Influence of Oxygen Exposure on Wine Sensory Characteristics and Contribution of Individual Sensory Attributes

Figure 1a-c summarizes the results concerning the influence of oxygen exposure on the 3 set of wines tested, expressed as percentage rate of statistically significant differences observed across the entire number of tastings.

In the case of white wines, the descriptor *white fruit* was most frequently associated with statistically differences (67 %) followed by *aromatic intensity*, *citrus*, and *reductive*, all showing a 42 % rate of statistically significant differences. The attributes *exotic fruits*, *dry fruit*s, *floral*, and *vegetal* contributed less to the differences observed (33 %). Finally, the rate of significant differences of the attributes empyreumatic, mineral, and oxidized was in no case greater than 25 %. It is important to emphasize that the type of wines tested can greatly influence the type of descriptors that are mostly contributing to the observed differences. In this sense, the results in Figure 1 should be regarded as a global overview of the potential of oxygen to influence wine aroma attributes, which could be different for another set of wines. Nevertheless, the range of attributes used in this study was sufficiently broad to cover the aroma characteristics more often used in wine sensory assessment, the only exclusion being oak-related attributes, which were not used here. Also worth mentioning that the differences in oxygen exposures created by the different closures were relatively small, with a maximum of 1.4 mg of oxygen for the wines submitted to longer aging. Such range of oxygen exposures is fairly common in commercial bottled wines, for example it was recently reported that natural cork closures from the same batch can deliver between 0.8 mg and 3.5 mg of oxygen during one year of bottle storage (*9*, *10*).

Common aroma attributes related to fruity descriptors were among the most responsive to oxygen, in particular white fruit and citrus. Other authors have also observed an influence of closure type on citrus attributes of white wine (*11*), as well as for pear and peach attributes (*12*). The observation of a relatively high contribution of *reductive* to the differences induced in white wine by post-bottling oxygen is also in agreement with previous observations (*13*).

Publication Date (Web): November 24, 2015 | doi: 10.1021/bk-2015-1203.ch013

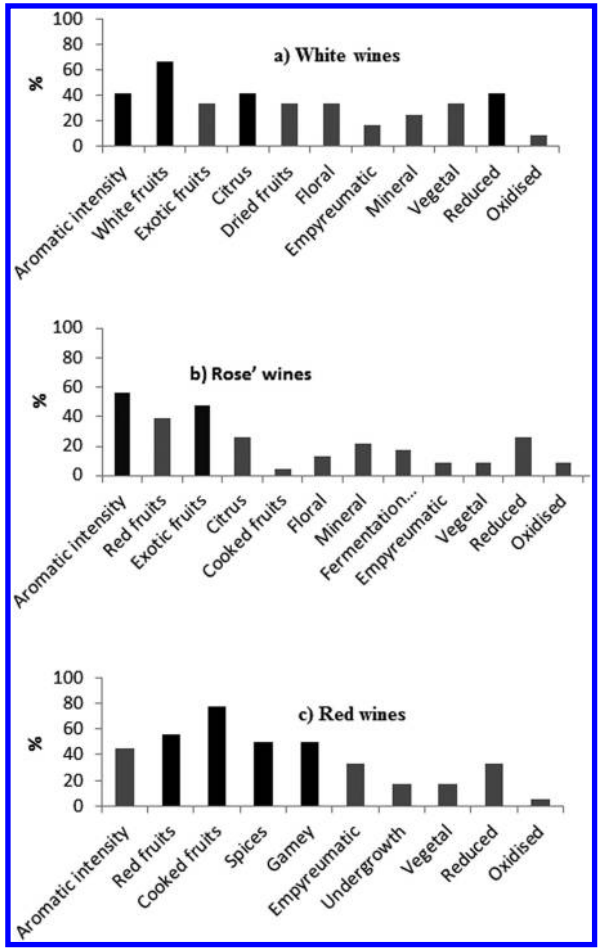

Figure 1. a-c. Contribution of individual sensory attributes to the differences observed, expressed as the percentage of times that the attribute was found significantly different across all the tasting for that wine category (white, left top; red, left bottom, rosé, right). Black bars highlight the most frequent attributes for each category.

The results obtained for rosé wines are also shown in Figure 1, indicating a predominant contribution of *aroma intensity*, *red fruit*, and *exotic fruit*, all at least at 39% of rate of significant differences. Given that rosé wines from Provence were mostly used in the study, it is not surprising to see a high incidence of attributes such as *red fruit* and *exotic fruit*, which are typical of rosé wines from this region (*14*). The observation that these attributes can be modulated by post-bottling oxygen exposure suggest that closure selection could be an important packaging decision for this type of wine.

In the case of red wines, a broader range of aroma attributes contributed to the aroma differences observed, including *aroma intensity*, *red fruit*, *cooked fruit, spicy, animal*, all with rates higher than 40%, with *empyreumatic* and *reduction* also contributing with rates of 33 %. The influence of post-bottling oxygen on animal and red fruit attribute have been previously reported in a study on Grenache wines, but the data provided herein indicate that this trend is likely to occur in other wines too. In particular, we observed here a high rate of contribution for the attribute *cooked fruit*, which has been indicated as primary sensory attribute of certain wine styles such as Californian Cabernet Sauvignon, Spanish Tempranillo or Australian Shiraz (*15*, *16*).

Publication Date (Web): November 24, 2015 | doi: 10.1021/bk-2015-1203.ch013

Key Compounds and Related Chemical Pathways Contributing to Oxygen Influence on Wine Aroma Characteristics

Among the sensory attributes that were mostly related to oxygen exposure, fruit aromas were in all cases contributing to a large extent to the differences observed. However, the data in Figure 1 do not allow to specifically describe the influence of oxygen on wine fruity attributes, namely the possibility of increasing or decreasing the expression of fruity aroma characteristic in a given wine. As an example, further detail on this is provided in Figure 2, highlighting the complex relationship between wine oxygen exposure and wine fruity attributes. Indeed, while in Wine 1 increased exposure to oxygen resulted in more intense *red fruit* and *exotic fruit* attributes, in the case of Wine 2 increased oxygen gave less intense *exotic fruit* attributes. Throughout the course of this survey, such differences in response have been observed often, suggesting that the outcomes of oxygen exposure on wine fruity attributes are strongly wine dependent.

Previous work indicated that fruity attributes of wine are primarily linked to a relatively small range of aroma compounds including fermentation-derived esters, norisoprenoids such as ß-damascenone, and volatile sulfur compounds such as 3-sulfanylhexanol (3SH), 4-sulfanyl-4-mercaptopentanone (4SMP), and dimethyl sulfide (DMS), the latter when present in concentrations around 20-60 µg/L. Analysis of fermentation derived esters in wines stored under closures allowing different degrees of oxygen exposure showed that these compounds are not influenced by oxygen (Figure 3), at least over the range of mild oxidative conditions that can be obtained by the use of different wine closures. Likewise, DMS was not affected by closure derived oxygen (Figure 4). Conversely, losses of thiol compounds such as 3SH were observed when wine was exposed to increasing concentrations of oxygen, as it can be observed in Figure 4. Loss of volatile thiols under conditions of increased oxygen exposure is essentially due to the nucleophilic addition of thiols on the quinones arising from the oxidation of wine ortho-diphenol compounds (Figure 4) (*17*, *18*). Additional mechanisms such as quenching by hydroxyethyl radical is also possible, although recent studies indicated a secondary contribution of this to wine thiol loss in the presence of oxygen (*19*). The observations collected on esters and thiols indicate that the loss of fruity attributes observed in certain wines upon exposure to oxygen should be primarily due to degradation of volatile thiols but not of fermentation-derived esters.

Publication Date (Web): November 24, 2015 | doi: 10.1021/bk-2015-1203.ch013

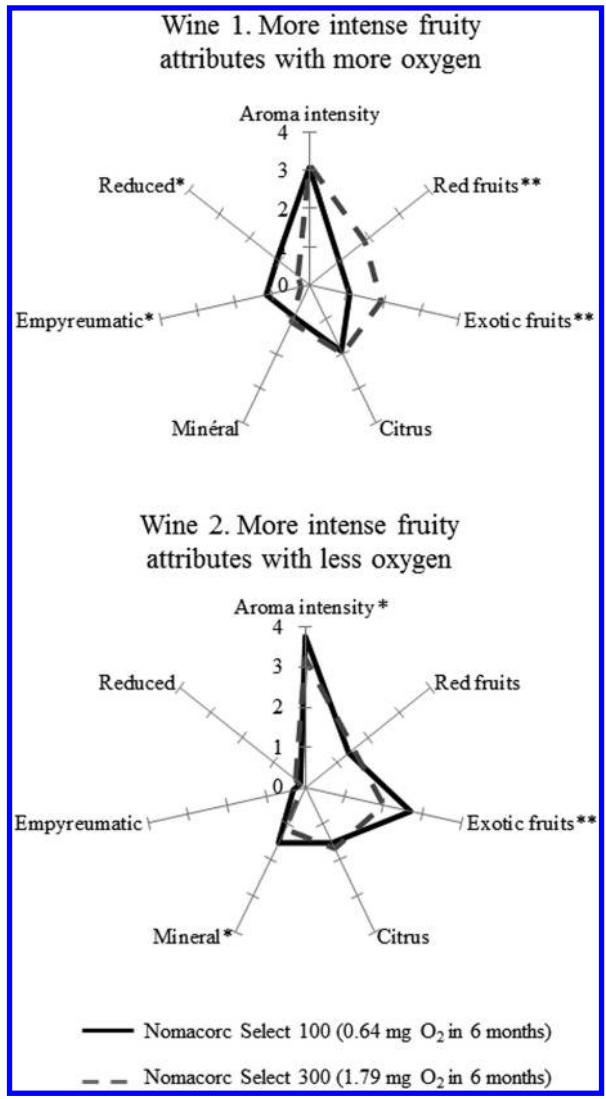

*Figure 2. Response of two different rosé wines to two closures allowing different degrees of oxygen exposure. Asterisks denote, within each wine, statistically significant difference at * 10 % and ** 5 %.*

On the opposite end, we did observe wines where increased in-bottle exposure to oxygen resulted in improved expression of fruity attributes, as previously shown in Figure 2. During a study on rosé wines, analysis of the potent fruity aroma compound β-damascenone provided some interesting insights in this phenomenon. It was indeed observed that increased oxygen exposure

resulted in increased ß-damascenone concentrations, with an extra 1.2 mg of oxygen during 12 months roughly doubling β-damascenone concentration (Figure 5). ß-damascenone is known to be derived from the acid catalyzed hydrolysis of different free and glycosylated norisoprenoid precursors, a process that should not be directly affected by oxygen. Some authors have shown that ß-damascenone can react with different wine nucleophiles, including SO_2 and thiols, accounting for significant losses of ß-damascenone in the first months of bottle storage (*20*). This could explain the higher ß-damascenone concentrations observed in wines stored with closures allowing more oxygen in the bottle, given that both thiols and SO_2 would be consumed to a greater extent under conditions of higher oxygen exposure. In addition, because of its carbonyl moiety, ß-damascenone can also form reversible adducts with SO_2. Increased loss of free SO_2 due to higher oxygen exposure could then result in increased release of ß-damascenone from such sulfite adducts. The latter hypothesis would imply that, in addition to the well-known pool of free and glycosylated norisoprenoidic precursors, another type of precursors, namely sulfite adducts, exists in wine, which could be harnessed though oxygen exposure. This hypothesis would certainly deserve further investigation.

Publication Date (Web): November 24, 2015 | doi: 10.1021/bk-2015-1203.ch013

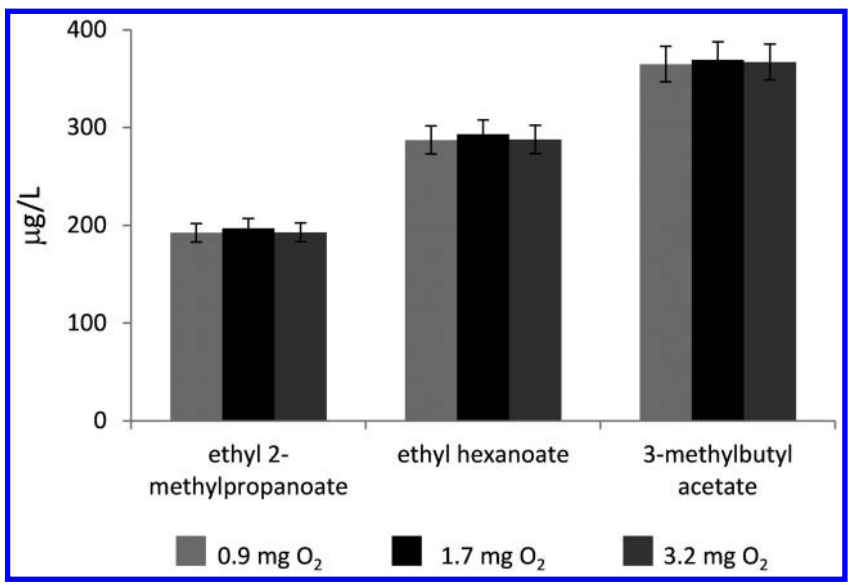

Figure 3. Influence of oxygen on ester concentrations in red wine after 12 months of bottle storage.

Publication Date (Web): November 24, 2015 | doi: 10.1021/bk-2015-1203.ch013

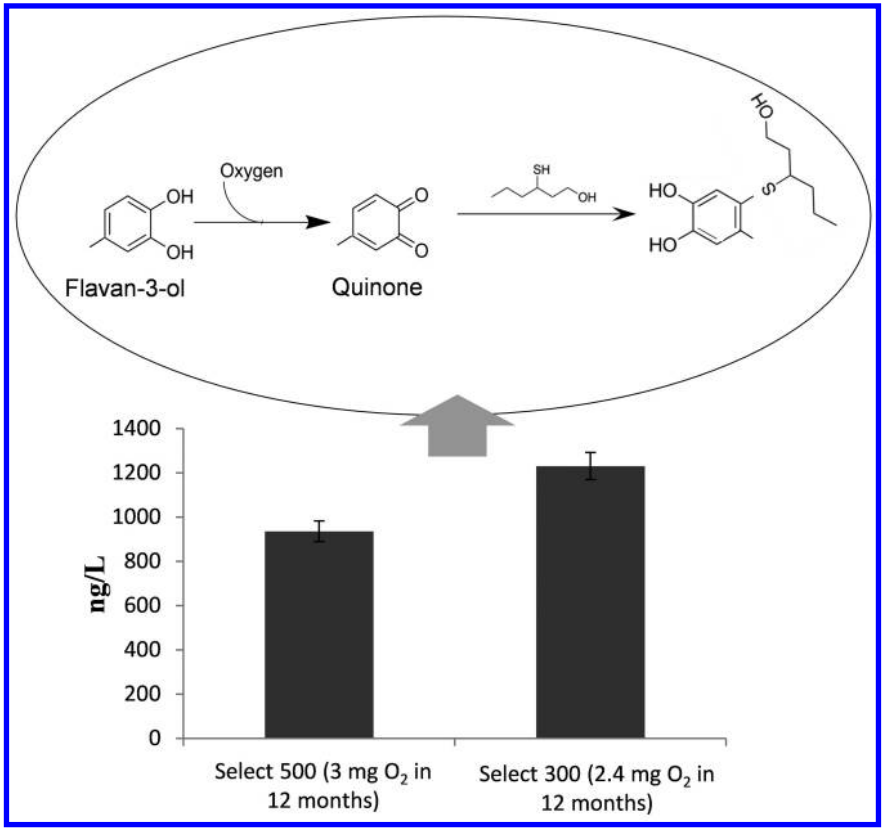

Figure 4. 3SH concentration in red wine after 12 months of bottle storage with closures allowing different degrees of oxygen exposure, with related chemical mechanism.

Oxygen-driven variations in ß-damascenone concentrations could also contribute to relatively high rate of significance for the attribute cooked fruit/jam in red wines, especially in combination with variations in phenyl-acetaldehyde content (*7*, *21*). We observed increased concentrations of phenylacetaldehyde in conjunction with closures allowing higher oxygen exposure (data not shown).

Reduction was another sensory attribute displaying relatively high contribution to significant differences. In all cases where a significant difference in reductive attributes was observed, wines exposed to increased oxygen were characterized by less intense reductive notes. Factors affecting occurrence of reductive attributes in bottle aged wines have been recently reviewed (*1*). The

compounds H_2S and methyl mercaptan (MeSH) have been identified as primary contributors to reductive attributes in wine (*22*, *23*). In our assessment of the influence of closure-derived oxygen on the accumulation of these compounds during wine bottle aging, we have seen a clear influence of oxygen on their post-bottling evolution, as it can be seen in Figure 6 for MeSH. Similar to the case of 3SH, H_2S and MeSH can act as nucleophiles and therefore react with the quinones arising from the oxidation of wine catechols (Figure 6). Because of its low steric hindrance, reaction of H_2S with quinones has been shown to be faster than in the case of 3SH (*18*). These observations suggest that removal of reductive compounds by means of closure selection can he achieved with minor consequences for 'positive' aroma compounds such as 3SH, as recently discussed (*10*).

Publication Date (Web): November 24, 2015 | doi: 10.1021/bk-2015-1203.ch013

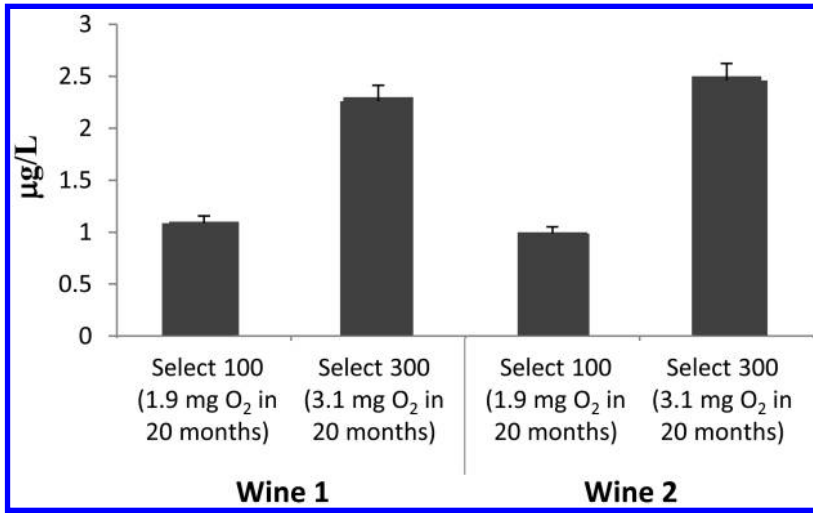

Figure 5. ß-Damascenone concentration in two rosé wines after 20 months of bottle storage with closures allowing different degrees of oxygen exposure.

In conclusion, this study confirmed the primary influence of closure-derived oxygen on the aroma characteristics of wine, allowing to characterize the main sensory attributes responsible for significant differences in wines stored under closures with different oxygen ingress properties. Fruit attributes were the main contributors to the differences existing, including white fruit, exotic fruit, dry fruit and citrus (white wine), red fruit, exotic fruit and citrus (rosé wine), red fruit and cooked fruit (red wine). Reductive aroma attribute also contributed significantly to the differences observed.

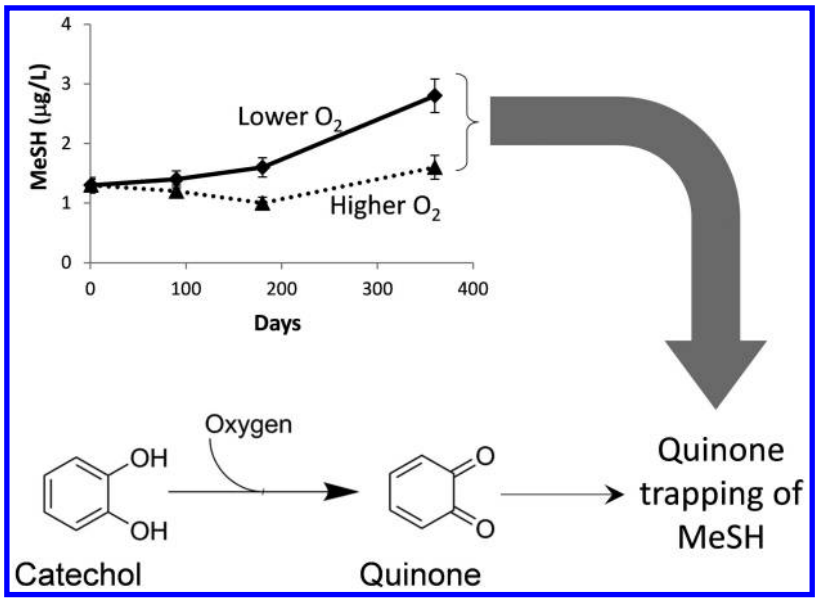

Figure 6. Evolution of MeSH during bottle aging with two different degrees of oxygen exposure and quinone trapping effect accounting for lower MeSH levels with higher oxygen exposure.

Publication Date (Web): November 24, 2015 | doi: 10.1021/bk-2015-1203.ch013

Different aroma compounds and chemical mechanism potentially implicated in these differences were discussed. No change in fermentation-derived esters was observed in response to varying levels of oxygen exposure. On the contrary, loss of varietal polyfunctional thiols associated with nucleophilic attack on oxidized ortho-diphenols may be responsible for the decrease of fruity attributes observed in certain wines upon exposure to oxygen. The case of wines where increased oxygen exposure resulted in improved expression of fruit attributes appears more complex. A positive influence of oxygen exposure on wine ß-damascenone content has been observed, potentially contributing to increased intensity of fruit attributes. We speculate that this effect is mediated by SO_2 which can either degrade ß-damascenone through nucleophilic attack or reversibly bind it. As for reductive attributes, the reductive sulfur compounds H_2S and MeSH were shown to be highly responsive to oxygen exposure, typically decreasing at increased oxygen levels. Nucleophilic attack on oxidized ortho-diphenols may be responsible for this behavior, with a mechanism similar to the one occurring for polyfunctional thiols.

Publication Date (Web): November 24, 2015 | doi: 10.1021/bk-2015-1203.ch013

References

1. Ugliano, M. *J. Agric. Food Chem.* **2013**, *61*, 6125–6136.
2. Caillé, S.; Samson, A.; Wirth, J.; Dieval, J.-B.; Vidal, S.; Cheynier, V. *Anal. Chim. Acta* **2010**, *660*, 35–42.
3. Wirth, J.; Morel-Salmi, C.; Souquet, J.M.; Dieval, J.B.; Aagaard, O.; Vidal, S.; Fulcrand, H.; Cheynier, V. *Food Chem.* **2010**, *123*, 107–116.
4. Hopfer, H.; Buffon, P.; Ebeler, S.E.; Heymann, H. *J. Agric. Food Chem.* **2013**, *61*, 3320–3334.
5. Dieval, J-B.; Vidal, S.; Aagaard, O. *Packag. Technol. Sci.* **2011**, *24*, 375–385.
6. Ugliano, M.; Kwiatkowski, M.; Vidal, S.; Capone, D.; Siebert, T.; Dieval, JB.; Aagaard, O.; Waters, E.J. *J. Agric. Food Chem.* **2011**, *59*, 2564–2572.
7. Culleré, L.; Cacho, J.; Ferreira, V. *J. Agric. Food Chem.* **2007**, *55*, 876–888.
8. Kosteridis, Y.; Baumes, R.; Skouroumounis, G. K. M. A. *J. Chromatogr. A* **1998**, *824*, 71–78.
9. Oliveira, V.; Lopes, P.; Cabral, P.; Pereira, H. *Am. J. Enol. Vitic.* **2013**, *64*, 395–399.
10. Ugliano, M.; Dieval, J-B.; Vidal, S. *Practical Winery Vineyard.* **2014** Jan, 4–8.
11. Skouroumounis, G.K.; Kwiatkowski, M.J.; Francis, I.L.; Oakey, H.; Capone, D.L.; Duncan, B.; Sefton, M.A.; Waters, E.J. *Aust. J. Grape Wine Res.* **2005**, *11*, 369–384.
12. Dimkou, E.; Ugliano, M.; Dieval, J-B.; Vidal, S.; Jung, R. *Am. J. Enol. Vitic.* **2013**, *64*, 325–332.
13. Dimkou, E.; Ugliano, M.; Dieval, J-B.; Vidal, S.; Aagard, O.; Rauhut, D.; Jung, R. *Am. J. Enol. Vitic.* **2011**, *62*, 261–269.
14. Masson, G.; Schneider, R. *Am. J. Enol. Vitic.* **2009**, *60*, 116–122.
15. Lattey, K.; Bramley, B.; Francis, I.L. *Austr. J. Grape Wine Res.* **2010**, *16*, 189–200.
16. Hjelmeland, A.; King, E.S.; Ebeler, S.E.; Heymann, H. *Am. J. Enol. Vitic.* **2013**, *64*, 169–179.
17. Laurie, F.; Zúñiga, M.C.; Carrasco-Sánchez, V.; Santos, L.; Cañete, A.; Olea-Azar, C.; Ugliano, M.; Agosin, E. *Food Chem.* **2012**, *131*, 1510–1516.
18. Nikolantonaki, M.; Waterhouse, A.L.W. *J. Agric. Food Chem.* **2012**, *60*, 8484–8491.
19. Kreitman, G.Y.; Laurie, F.; Elias, R. *J. Agric. Food Chem.* **2013**, *61*, 685–692.
20. Daniel, M.A.; Elsey, G.M.; Capone, D.L.; Perkins, M.V.; Sefton, M.A. *J. Agric. Food Chem.* **2004**, *52*, 8127–8131.
21. Ferreira, V.; Fernandez-Zubrano, P.; Escudero, A.; San Juan, F.; Saenz Navajas, M.P.; Campo, E.; Cacho, J. In *Proceedings of the 16th International Symposium of Enology*; Fischer, U., Ed.; Meininger, Neustadt, 2011.
22. Ugliano, M.; Dieval, J.B.; Siebert, T.E.; Kwiatkowski, M.; Aagaard, O.; Vidal, S.; Waters, E.J. *J. Agric. Food Chem.* **2012**, *60*, 8561–8570.
23. O'Brien, V.; Francis, L.; Osidacz, P. *Wine Ind. J.* **2009**, *24*, 48–54.

Publication Date (Web): November 24, 2015 | doi: 10.1021/bk-2015-1203.ch014

Chapter 14

Influence of Antioxidant Additions at Harvest on Sauvignon Blanc Wine Aroma

P. A. Kilmartin,* O. Makhotkina, L. D. Araujo, and J. A. Homer

Wine Science Programme, School of Chemical Sciences, The University of Auckland, Private Bag 92019, Auckland, New Zealand
***E-mail: p.kilmartin@auckland.ac.nz.**

The varietal thiols 3-mercaptohexanol (3MH) and 3-mercaptohexyl acetate (3MHA) contribute tropical fruit aromas to Sauvignon blanc wines. These thiols increase in levels following machine harvesting, whereas other aroma compounds are less affected by harvesting procedures. In a series of harvesting trials, grapes from Marlborough, New Zealand were fermented in triplicate 750 mL bottles at 15 °C. In one trial, different SO_2 additions were made at harvest, and the highest concentrations of 3MH and 3MHA were found in wines for a 120 ppm SO_2 addition. Increases in 3MH and 3MHA were also seen when a 30 ppm SO_2 addition was supplemented with 100 ppm of ascorbic acid or glutathione. Finally, 50 ppm SO_2 additions were made at different times up to two hours after harvest, and there was a gradual lowering in wine 3MH and 3MHA for a later sulfite application. Antioxidant additions at harvest can be used to lessen the effects of juice oxidation and maximise levels of thiols in the wine, to suit the requirements of the target wine style.

Introduction

Sauvignon blanc is the main wine variety for the New Zealand industry and constitutes over 70% of exported wines, with the majority coming from the Marlborough grape-growing region. A number of styles of Sauvignon blanc wine are produced in New Zealand, and the major Marlborough style combines intense passionfruit/ tropical aromas with prominent fresh-green characters (*1*).

In Advances in Wine Research; Ebeler, et al.;
ACS Symposium Series; American Chemical Society: Washington, DC, 2015.

Aroma compounds that contribute to the fruity aromas include the varietal thiols, particularly 3-mercaptohexanol (3MH) and 3-mercaptohexyl acetate (3MHA) (*2*), along with several esters. Green and grassy aromas have their origin in various compounds, including methoxypyrazines, C_6-alcohols and the varietal thiols themselves (*3*, *4*). Many of these compounds are found at levels well above their perception thresholds in Marlborough wines (*5*).

The importance of 3MHA, the acetate ester of 3MH, and other fruity esters in defining Sauvignon blanc wine styles, has been illustrated through changes in commercial wines with time and in temperature storage trials (*6*, *7*). The hydrolysis of these esters (*8*), is the major factor in changes in the aroma profiles of the New Zealand wines during the first 1-2 years in the bottle, ahead of issues to do with wine oxidation and closure type, which affect 3MH levels and wine aroma profiles in the longer term. The importance of 3MHA to the wine aroma profile will be illustrated in this report through sensory panel descriptive analysis and associated aroma compound concentrations for two typical Marlborough Sauvignon blanc wines of different ages.

The wide-spread use of machine harvesting in Marlborough has been identified as a factor leading to increased levels of C_6 alcohols, 3MH and 3MHA in Sauvignon blanc wines from the region (*9*). At the same time, juices more advanced in oxidation, leading to a higher 420 nm absorbance, were associated with lower 3MH and 3MHA concentrations in the finished wines (*10*). The importance of oxidative and antioxidant elements in the juice were further highlighted by the recent demonstration of the role for H_2S during the early stages of fermentation in the formation of 3MH from C_6 compound precursors (*11*). In this context the influence of antioxidant additions at harvest has been pursued through a series of harvesting trials undertaken in Marlborough, and key findings from these trials in relation to impacts upon 3MH and 3MHA formation, and levels of C_6 compounds in the finished wines, are reported here.

Experimental

Sensory Panel

The sensory panel consisted of thirteen postgraduate Wine Science students who completed training in descriptive anlaysis for the aromas of Sauvignon blanc wines during 11 two hour sessions over a three week period in August 2013. The reference standards were based upon those developed at the Plant and Food Sensory and Consumer Science facility and used to profile Sauvignon blanc wines in earlier trials (*3*, *7*, *12*). The naming of reference standards was established by the panelists themselves (Table 1), and this produced similar terms to those reported in previous publications, but differed in some instances. For example, the present panel named the reference containing hexanol as “Pina colada”, whereas “Bourbon” has been used previously. The “Floral” descriptor was based upon phenylethyl acetate, while the “Fruit salad + cream” was based upon three ethyl esters. The panelists were trained to rank the aroma descriptors by smell only on an unstructured 150 mm line scale ranging from “absent” (0) to “extreme” (150).

In Advances in Wine Research; Ebeler, et al.;
ACS Symposium Series; American Chemical Society: Washington, DC, 2015.

Publication Date (Web): November 24, 2015 | doi: 10.1021/bk-2015-1203.ch014

Table 1. Sensory Descriptors and Their Associated Reference Standards

Descriptor	*Reference standard*
Tropical Passionfruit	2,000 ng/L 3MHA in diluted base wine
Stalky	2,000 ng/L 3MH in diluted base wine
Apple lolly Banana	2.4 µL isoamyl acetate, 0.5 µL hexyl acetate in 100 mL $CuSO_4$ treated based wine
Fruit salad + cream	402 µL ethyl butanoate stock (1.7 µL ethyl butanoate/10 mL water) + 1.2 mL ethyl octanoate stock (1.73 µL ethyl octanoate/10 mL water) + 7.56 µL ethyl hexanoate stock (15.74 g ethyl hexanoate/1 L ethanol) in 99 mL $CuSO_4$ treated diluted base wine
Floral	36.6 µL phenylethyl acetate in 100 mL $CuSO_4$ treated diluted base wine
Capsicum	1 mL MIBP (2-methoxy-3-isobutylpyrazine) stock (6 µL MIBP/100 mL water) in 99 mL $CuSO_4$ treated diluted base wine + 5 µL (Z)-3-hexenol
Asparagus	2.5 mL Watties® canned asparagus juice + 2.5 mL cooked pea juice in 95 mL diluted base wine
Musty flinty	12.4 µL BMT stock (8 µL BMT (benzene methane thiol)/ 1 L water) in 100 mL diluted base wine
Cat's pee	1000 ng/L 4MMP (4-mercapto-4-methylpentan-2-one) in diluted base wine
Grass	28,800 ng/L (Z)-2-hexenol in diluted base wine
Spicy citrus	30 g 'Yen Ben' lemon plus 15 g "bear' lime soaked in diluted base wine for 30 min
Pina Colada	50 mL hexanol stock (10 µL hexanol/ 300 mL water) in 50 mL diluted base wine
Fruity flowers	40 mL Golden Circle® Mango juice plus 40 mL Golden Circle Golden Pash drink
Apple	70 g 'Sciros'/Pacific Rose™ apple peeled soaked in diluted base wine for 30 min

Publication Date (Web): November 24, 2015 | doi: 10.1021/bk-2015-1203.ch014

For data collection, 20 mL wine samples were presented in standard XL5 wine glasses with lids to the panelists in triplicate. The glasses were labelled with three digit codes and served at room temperature (c. 20 °C). A total of 16 Sauvignon blanc wines of different ages and geographic origin were presented to the panel across five days of data collection. The results for two Marlborough wines from the same company are presented here, one from the 2010 vintage and thus three years old at the time of sensory profiling, and the other just released from the 2013 vintage.

Aroma Chemical Analyses

The wines presented to the sensory panel, and the wines obtained from the harvesting trials described below, were analysed for concentrations of varietal thiols, C_6 compounds, wine esters, higher alcohols and terpenes, using GC-MS procedures outlined in recent publications (*5*, *9*, *13*, *14*).

Harvesting Trials

Sauvignon blanc grapes were sourced from vineyards in the Marlborough grape growing region in April in each of three years. The trials were undertaken in 2011 at three sites (*13*), in 2012 at three sites (*14*), and at two further sites in the Wairau Valley area of Marlborough in 2013. In each case 50 to 100 kg of the mix of grapes and juice that come from machine harvesting were collected in a large picking bin. The grapes and juices were well mixed and then 10.0 kg lots were transferred using a 2 L scoop into a series of plastic buckets. At this point the antioxidant additions were made, consisting of sufite additions at 0, 30, 60, 120 and 300 mg/kg (ppm) of SO_2 in the first 2011 trial; 30 ppm of SO_2 on its own or in conjunction with either 100 ppm ascorbic acid or 100 ppm glutathione in the 2012 trial. In the final 2013 trial, additions of either 50 ppm SO_2 alone or with 100 ppm ascorbic acid, were made at the following time points after the buckets were filled: 0, 15, 45, 75 and 120 min. At the time of antioxidant additions the grapes and juices were stirred and lids applied to the buckets before transfer for pressing for 10 min at 1 to 3 bar using an 80 L hydro press into 5 L plastic bottles (*13*, *14*), either after refrigerated transport to Auckland (2011), or at a local winery in Marlborough (2012 and 2013), after which the pressed juices were transported to Auckland.

After cold settling 700 mL of juice was transferred to 750 mL green wine bottles in triplicate, and inoculated with 0.2 g/L EC1118 yeast (Lalvin, Lallemand, Montreal, Canada). A 100 µL plastic pipette tip filled with glass wool was inserted into a rubber stopper on each bottle to released CO_2 during fermentation in a 15 °C temperature controlled room. The fermentations were considered complete once the weight remained unchanged for five days, and at this point samples were frozen at -18 °C for later analyses for aroma compounds by GC-MS.

Results and Discussion

Aroma Chemistry and Sensory Profiling of Two Wines

The sensory profile and selected results of chemical analyses for two Marborough Sauvignon blanc wines are presented to illustrate the importance of certain compounds, including the varietal thiols, to the aroma profile. The 2013 wine was marked by high concentrations of 3MH, 3MHA and other acetate esters, along with levels of phenylethyl alcohol and β-damascenone that were well above their respective preception thresholds (Table 2), typical of many young Marlborough Sauvignon blanc wines (*3*, *5*). The presence of these aroma compounds matches the high scores given to this wine of 55 for the sensory

In Advances in Wine Research; Ebeler, et al.;
ACS Symposium Series; American Chemical Society: Washington, DC, 2015.

Publication Date (Web): November 24, 2015 | doi: 10.1021/bk-2015-1203.ch014

attribute “Tropical Passionfruit” (Figure 1), for which 3MHA was the reference standard (Table 1), and 38 for “Stalky”, where 3MH was the reference. The moderate score of 26 for “Apple lolly Banana”, based upon a mixed hexyl acetate and isoamyl acetate standard, “Floral” at 21, and “Fruity flowers” at 35, can be linked to the esters, phenylethyl alcohol and β-damascenone present.

Publication Date (Web): November 24, 2015 | doi: 10.1021/bk-2015-1203.ch014

Table 2. Aroma Compound Concentrations in Two Marlborough Sauvignon Blanc Wines from the Same Company

Aroma compound	*2010 wine*	*2013 wine*	*Perception Threhold*[a]
3MHA (ng/L)	22	954	4
3MH (ng/L)	3,480	3,914	60
Isoamyl acetate (μg/L	346	6,044	160
Hexyl acetate (μg/L)	68	647	400
Ethyl hexanoate (μg/L)	837	899	45
Phenylethyl alcohol (μg/L)	7,555	71,259	14,000
Hexanol (μg/L)	2,515	2,478	1,100
Dimethyl sulfide (μg/L)	170	39	25
β-damascenone (μg/L)	0.5	3.3	0.14
Linaool (μg/L)	2.8	11.5	25

[a] Perception threshold values from (*3*, *5*) and references cited therein.

By contrast, the 2010 wine contained a similar high level of 3MH, and about the same amounts of hexanol and ethyl hexanoate (Table 2), but much lower concentrations of 3MHA and the other acetate esters, which are known to hydrolyse with time (*6*, *8*). The level of dimethyl sulfide was over 4 times higher in the 2010 wine compared to the 2013 wine. Both β-damascenone and linalool were present at lower levels in the older wine, although the latter compound was present below perception threshold in both wines. These trends were reflected in the similar sensory scores given to the two wines for the descriptors “Stalky” and “Pina Colada”, the latter based upon a hexanol reference standard (Figure 1). It can be noted here that other wines profiled in the trial, including those from made from hand-picked grapes or produced overseas, had lower 3MH concentrations and a lower “stalky” sensory rating.

Publication Date (Web): November 24, 2015 | doi: 10.1021/bk-2015-1203.ch014

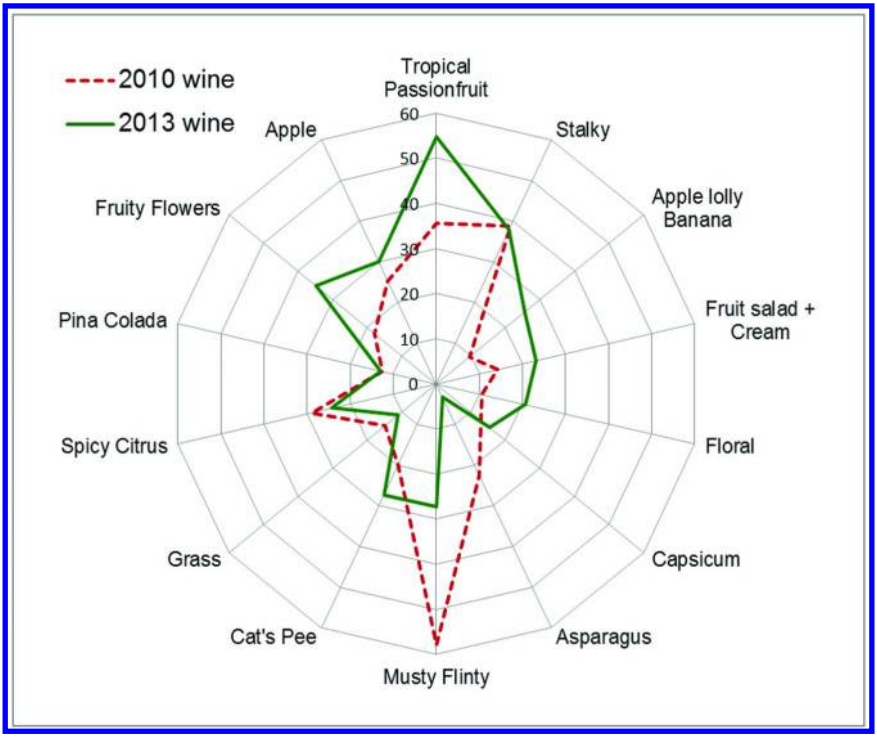

Figure 1. Spider plot for two Marlborough Sauvignon blanc wines profiled by a sensory panel trained in descriptive analysis in 2013.

A much higher value of 58 for "Musty Flinty" with the 2010 wine matches the higher content of dimethyl sulfide and a lowering of some fruity esters that may otherwise mask this attribute. The ester-related descriptors of "Tropical Passionfruit" and "Apple lolly Banana" were both lower with the 2010 wine, which can be linked to the lower concentrations of the acetate esters, including 3MHA. In the case of 3MHA, the data presented in an earlier survey of 50 Sauvignon blanc wines showed a high correlation of 3MHA with tropical and passionfruit descriptors (*12*), and it was found that when 3MHA was present at levels above 200 ng/L, the "sweet-sweaty-passionfruit" descriptor was consistently above 60, and when the concentration of 3MHA exceeded 500 ng/L, the panel rated this descriptor with a value greater than 65. This behavior is typical of a compound that acts as a genuine impact compound at higher concentrations, and as a "major contributor" to the aroma profile at moderate concentrations (*15*). These sensory results underscore the importance of the varietal thiols 3MH and 3MHA to the aroma profile of young Sauvignon blanc wines.

Publication Date (Web): November 24, 2015 | doi: 10.1021/bk-2015-1203.ch014

2011 Harvesting Trial

Particular attention was paid to levels of 3MH and 3MHA in the harvesting trials with antioxidant additions, owing to effects that juice oxidative conditions can have on their formation indicated previously (*9*, *10*), and their important contribution to wine sensory profiles. There was a major impact of SO_2 on the formation of 3MH and 3MHA in the wines, and maximum levels were seen with 120 ppm sulfite additions (Figure 2). It was only at this level of sulfting that measurable free SO_2 was maintained in all of the juices during transport and pressing prior to fermentation, matched by 420 nm absorbance values less than 0.1 units (*13*). By contrast juices to which either 0 or 30 ppm SO_2 had been added at harvest had no measurable free SO_2, and the concentration of the polyphenol caftaric acid declined to a low level; the 420 nm absorbance ranged from 0.16 to 0.63 units, and the juices were evidently browner and more oxidized in character. At the other extreme, a 300 ppm SO_2 addition maintained the same high level of 3MH in the wines from all three vineyard sites, even though the fermentation was delayed by 12-13 days and some residual sugar remained at the end of fermentation (*13*). However, for 3MHA, the concentration with a 300 ppm SO_2 addition was not so high, and a similar decline was seen with the other acetate esters, pointing to some adverse effects on yeast acetylation processes.

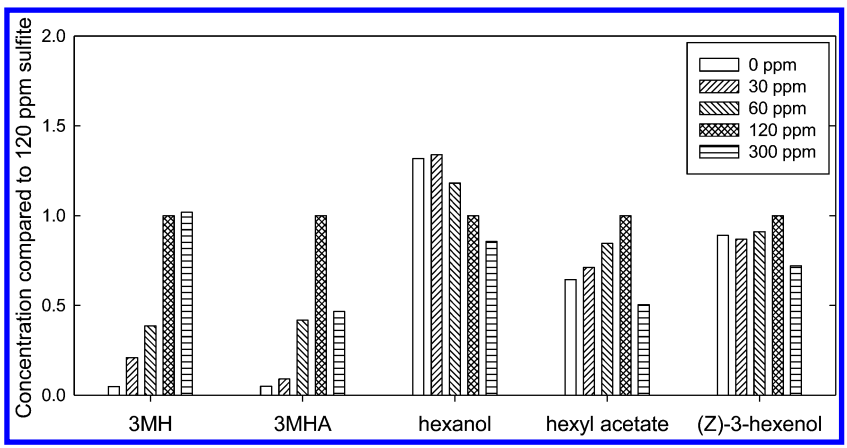

Figure 2. Relative concentrations of the varietal thiols 3MH and 3MHA and selected C_6 compounds following different sulfite additions at harvest. The data presented are the averages for three vineyard sites.

The C_6 compounds in the wines were also monitored, being the other group of compounds that were particularly affected by the method of harvesting in a previous trial, with lower levels seen in wines made from hand-picked grapes (*9*, *10*). With no added sulfites, the level of hexanol was at a maximum, and then declined by up to 30% as the higher SO_2 applications were made (Figure 2). The initial C_6 compound formation could be greater when fewer antioxidants are present allowing lipoxygenase enzymes act more readily on unsaturated fatty acid substrates (*16*). By constrast the formation of hexyl acetate was up to 30% higher

as more SO_2 was added, with the exception of the high 300 ppm SO_2 addition. The concentration of the grassy (Z)-3-hexenol was largely independent of added SO_2, as were the concentrations of most other aroma compounds.

2012 Harvesting Trial

A common winemaking practice in countries such as New Zealand is to include ascorbic acid alongside SO_2, for protection of grape juice and wine against oxidation. There is also growing interest in the antioxidant properties of glutathione, naturally present in the grape but not yet an allowed wine additive. Given the delays in fermentations that can arise with higher sulfite applications, and to avoid excessive levels for health reasons, a second trial was conducted in which 100 ppm ascorbic acid or glutathione was added to machine harvested grapes at harvest, alongside a moderate 30 ppm SO_2 application (*14*).

A number of effects on the wine aroma compounds were noted, with a near doubling in both 3MH and 3MHA when either ascorbic acid or glutathione was added as a supplement to SO_2 (Figure 3). With the inclusion of extra glutathione, more of a further varietal thiol, 4-mercapto-4-methylpentan-2-one (4MMP), was generated, suggesting the formation of a glutathione-conjugate precursor for this thiol. Most other aroma compounds were unaffected, except a small decrease in some C_6 compounds and acetate esters when ascorbic acid was included (*14*).

Amongst the roles that the antioxidant additives can play in the juices are direct scavenging of oxygen with ascorbic acid, and enzyme inhibition of polyphenol oxidases to lessen quinone formation, at least in the case of SO_2 (13). All three antioxidant compounds could remove oxidized polyphenol quinones that would otherwise react with H_2S and limit its availability to react with C_6 compounds to form 3MH and 3MHA (*11*, *17*). Removal of quinones also lessens their reaction with 3MH (*18*) once it is formed during fermentation.

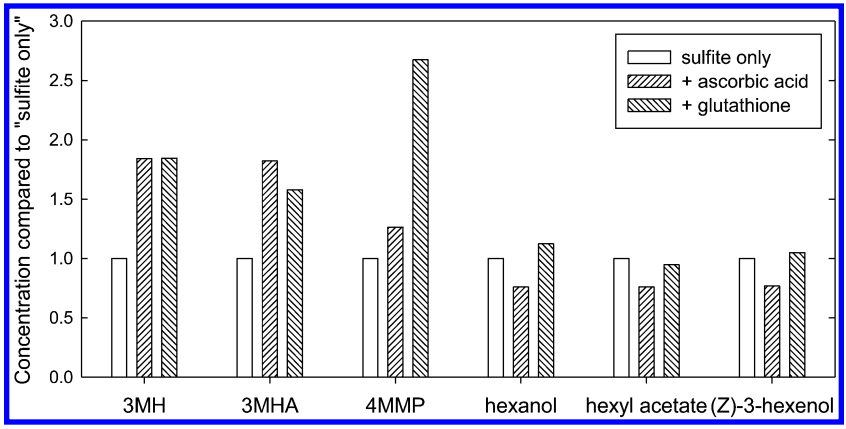

Figure 3. Relative concentrations of the varietal thiols 3MH and 3MHA and selected C_6 compounds following a sulfite addition of 30 ppm in each case, and with a further 100 ppm ascrobic acid or glutathione in certain treatments. The data presented are the averages for three vineyard sites.

In Advances in Wine Research; Ebeler, et al.;
ACS Symposium Series; American Chemical Society: Washington, DC, 2015.

Publication Date (Web): November 24, 2015 | doi: 10.1021/bk-2015-1203.ch014

Publication Date (Web): November 24, 2015 | doi: 10.1021/bk-2015-1203.ch014

2013 Harvesting Trial

The timing of the antioxidant addtions in the period following mechanical harvesting was also examined in a trial undertaken in 2013. There was some suggestion that a delay in the application of the antioxidants could provide more time for lipoxygenase activity and the formation of C_6 compounds that could ultimately be transformed into 3MH and 3MHA during fermentation (*11*). However, a gradual decease in wine 3MH and 3MHA content was instead observed as the additions were made between 0 and 120 minutes after the grapes and juice were collected in the trial buckets, and little change to the wine C_6 compounds (Figure 4). There was thus benefits in the earlier application of the antioxidants to achieve a higher thiol wine. It remains unclear how much C_6 compound formation could be affected by added antioxidants in the 10-15 min directly following mechanical harvesting and before the buckets could be filled.

With these two juices, there was no consistent increase in 3MH when 100 ppm ascorbic acid was included alongside 50 ppm of SO_2, which likely provided adequate antioxidant protection on its own. Included in this trial were some further hand-picked samples for comparison purposes, and lower levels of 3MH, 3MHA and the C_6 alcohols were again observed (Figure 4), with particularly low levels of the grassy compound (Z)-3-hexenol.

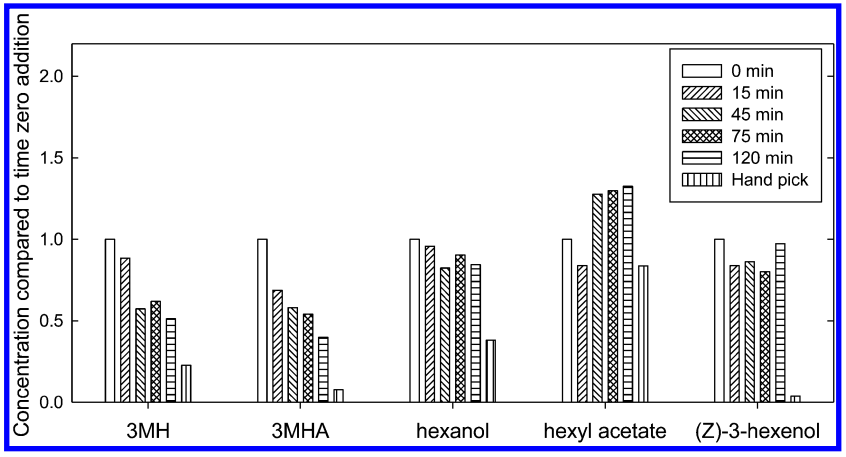

Figure 4. Relative concentrations of the varietal thiols 3MH and 3MHA and selected C_6 compounds following a sulfite addition of 50 ppm, with and without ascorbic acid at 100 ppm, at various time points. The data presented are the averages for two vineyard sites and the two antioxidant treatments.

In Advances in Wine Research; Ebeler, et al.;
ACS Symposium Series; American Chemical Society: Washington, DC, 2015.

Concluding Remarks

As a result of a series of harvesting trails undertaken with Sauvignon blanc in Marlborough, we now have a greater appreciation of the impact that adequate and timely sulfite and ascorbic acid additions can have on ultimate wine aroma composition. The findings provide tools to winemakers as they make decisions regarding the style of wine they would like to produce.

The variable thiol potential of Sauvignon blanc juices, and their oxidative status, raises the need for more immediate monitoring of sulfite levels and juice browning during harvesting, the transport of juice and juice pressing. This could lead to a "precision harvesting" approach (*13*), where sulfite and ascorbic acid additions are made tailored to the needs of a particular juice, to ensure adequate antioxidant protection but avoid excessive applications.

Acknowledgments

The authors greatfully thank Villa Maria New Zealand and Constellation New Zealand for the supply of grapes, along with Mandy Herbst-Johnstone, Gerard Logan, Rebecca Deed and Bruno Fedrizzi at the University of Auckland for assistance with grape collection, sensory panel training and instrumental analyses.

References

1. Benkwitz, F.; Tominaga, T.; Kilmartin, P. A.; Lund, C.; Wohlers, M.; Nicolau, L. *Am. J. Enol. Vitic.* **2012**, *63*, 62–72.
2. Tominaga, T.; Niclass, Y.; Frérot, E.; Dubourdieu, D. *J. Agric. Food Chem.* **2006**, *54*, 251–7255.
3. Benkwitz, F.; Nicolau, L.; Lund, C.; Beresford, M.; Wohlers, M.; Kilmartin, P. A. *J. Agric. Food Chem.* **2012**, *60*, 6293–6302.
4. King, E. S.; Osidacz, P.; Curtin, C.; Bastian, S. E. P.; Francis, I. L. *Aust. J. Grape Wine Res.* **2011**, *17*, 169–180.
5. Jouanneau, S.; Weaver, R. J.; Nicolau, L.; Herbst-Johnstone, M.; Benkwitz, F.; Kilmartin, P. A. *Aust. J. Grape Wine Res.* **2012**, *18*, 329–343.
6. Herbst-Johnstone, M.; Nicolau, L.; Kilmartin, P. A. *Am. J. Enol. Vitic.* **2011**, *62*, 495–502.
7. Makhotkina, O.; Pineau, B.; Kilmartin, P. A. *Aust. J. Grape Wine Res.* **2012**, *18*, 91–99.
8. Makhotkina, O.; Kilmartin, P. A. *Food Chem.* **2012**, *135*, 486–493.
9. Herbst-Johnstone, M.; Araujo, L. D.; Allen, T. A.; Logan, G.; Nicolau, L.; Kilmartin, P. A. *Acta Hortic.* **2013**, *978*, 179–186.
10. Allen, T.; Herbst-Johnstone, M.; Girault, M.; Butler, P.; Logan, G.; Jouanneau, S.; Nicolau, L.; Kilmartin, P. A. *J. Agric. Food Chem.* **2011**, *59*, 10641–10650.
11. Harsch, M. J.; Benkwitz, F.; Frost, A.; Colonna-Ceccaldi, B.; Gardner, R. C.; Salmon, J. M. *J. Agric. Food Chem.* **2013**, *61*, 3703–3713.

12. Lund, C. M.; Benkwitz, F.; Thompson, M. K.; Wohler, M. W.; Triggs, C. M.; Gardner, R. C.; Heymann, H. G.; Nicolau, L. *Am. J. Enol. Vitic.* **2009**, *60*, 1–12.
13. Makhotkina, O.; Herbst-Johnstone, M.; Logan, G.; Du Toit, W.; Kilmartin, P. A. *Am. J. Enol. Vitic.* **2013**, *64*, 203–213.
14. Makhotkina, O.; Araujo, L. D.; Olejar, K.; Herbst-Johnstone, M.; Fedrizzi, B.; Kilmartin, P. A. *Am. J. Enol. Vitic.* **2014**, *65*, 388–393.
15. Ferreira V. In *Managing Wine Quality*; Reynolds, A. G., Ed.; Woodhead Publishing Ltd: Oxford, 2010; Vol. 1, pp 3−28.
16. Joslin, W. S.; Ough, C. S. *Am. J. Enol. Vitic.* **1978**, *29*, 11–17.
17. Schneider, R.; Charrier, F.; Razungles, A.; Baumes, R. *Anal. Chim. Acta* **2006**, *563*, 58–64.
18. Blanchard, L.; Darriet, P.; Dubourdieu, D. *Am. J. Enol. Vitic.* **2004**, *55*, 115–120.

Publication Date (Web): November 24, 2015 | doi: 10.1021/bk-2015-1203.ch014

Publication Date (Web): November 24, 2015 | doi: 10.1021/bk-2015-1203.ch015

Chapter 15

New Insights into Intrinsic and Extrinsic Factors Triggering Premature Aging in White Wines

Alexandre Pons,[*,1,2,3] Maria Nikolantonaki,[1,2,5] Valérie Lavigne,[1,2,3] Kentaro Shinoda,[4] Denis Dubourdieu,[2,3] and Philippe Darriet[2,3]

[1]Seguin-Moreau, Z.I. Merpins, BP 94, 16103 Cognac, France
[2]Université de Bordeaux, ISVV, EA4577 Œnologie, F-33140 Villenave d'Ornon, France
[3]INRA, ISVV, USC 1366 Œnologie, F-33140 Villenave d'Ornon, France
[4]Suntory Wine International Limited, 2-3-3 Daiba, Minato-ku, Tokyo 135-8631, Japan
[5]Current address: Université de Bourgogne, Institut Universitaire de la Vigne et du Vin, Jules Guyot, UMR A 02.102 PAM AgroSup Dijon/, F-21078 Dijon France
[*]E-mail: alexandre.pons@u-bordeaux.fr.

Two grape antioxidants, ascorbic acid and glutathione, and a flavan-3-ol, catechin, were analyzed and related to the production or depletion of volatile compounds (phenylacetaldehyde, methional, and sotolon) that act as markers of premature aging in dry white wines. This research assessed the impact of adding ascorbic acid (AA, 80 mg/L) and glutathione (GSH, 10 mg/L) to a Sauvignon Blanc wine sealed with two closures with different permeability to oxygen on wine flavor development over 10 years' bottle storage. A decrease in AA was correlated with the closure's oxygen permeability, while GSH depletion (90 % in 12 months) was associated with the dissolved oxygen content at bottling. Sensory analysis revealed significant differences in the development of wine oxidation flavors, correlated with the closure, as well as AA and GSH content. Wines spiked with AA and GSH at bottling were preferred by panelists to controls, without GSH. The sensory data were in complete agreement with analytical results,

In Advances in Wine Research; Ebeler, et al.;
ACS Symposium Series; American Chemical Society: Washington, DC, 2015.

showing that these wines had the lowest sotolon content. We also demonstrated that, on the basis of analyzing the oxidation markers (sotolon, methional, and phenylacetaldehyde), high catechin levels in white wines contributed to their formation in a temperature-dependent manner.

Introduction

Aging potential is one of the important features for high quality white wines. One particularity of these wines is that they conserve the flavor nuances of young wines while developing specific varietal aromas. However, this ideal aging does not occur in every wine. Premature aging is a well-known phenomenon in white wines (*1–3*), revealed by oxidative aroma degradation, leading to a rapid loss of their varietal qualities (*4*): both the formation of off-flavors and the loss of floral and fruity notes (*5*, *6*).

Prematurely-aged white wines develop several aromatic nuances reminiscent of honey, beeswax, and cooked vegetables and the volatile compounds associated with these odors have now been identified. Two of them, methional and phenylacetaldehyde, reminiscent of boiled potatoes and old rose, have detection thresholds of 0.5 and 1 µg/L, respectively, in wine model solution (*7*). These compounds, known as Strecker aldehydes, are formed by several pathways. The first involves the degradation of amino acids with dicarbonyl compounds (*8*). Generally, in wine chemistry, all dicarbonyls are potential substrates for this reaction. Indeed, phenolic compounds that have oxidized to *ortho*-quinones may be involved in the reactions that form these volatile compounds, via the Strecker reaction (*9*). This suggested mechanism has been demonstrated in synthetic solutions (*10*) but its contribution in wine was downplayed in a recent publication (*11*). Nikolantonaki and Waterhouse (*12*) explained this result by determining low first-order reaction rates between *ortho*-quinones and amino acids in a wine-like solution, thus suggesting the secondary importance of this pathway in Strecker aldehyde formation.

These carbonyls have been found to be related to the wine content in combined SO_2, suggesting that a significant part of the aldehydes could be present in wine under the form of SO_2 adduct (*13*). So, these carbonyls might be released from trapped forms upon depletion of SO_2 during oxidation phenomenon. The last potential precursors are alcohols, methionol and phenylethanol, who are able to be converted in there aldehydes forms via Fenton reactions during wine oxidation (*13*, *14*).

Sotolon (4,5-dimethyl-3-hydroxy-2(5)H-furanone) is a chiral volatile lactone with an intense curry odor (*15*). The chemical mechanism responsible for sotolon formation in wine involves oxygen, which explains the high sotolon content (100-1000 µg/L) found in wine aged under oxidation conditions, e.g.: *vin jaune* from the Jura (*16*), port, and *vins doux naturels* (French fortified wines) (*17*), which contributes to their quality and typicality. On the contrary, its presence in wines made traditionally under reductive conditions is considered an off-flavor.

Publication Date (Web): November 24, 2015 | doi: 10.1021/bk-2015-1203.ch015

The presence of yeast lees and sulfur dioxide during barrel aging minimize the attenuation of Sauvignon Blanc varietal aromas, as well as preventing sotolon formation (*15*).

More recently, several authors determined the contribution of sotolon to the oxidation aromas of prematurely-aged dry white wines (*1*, *2*). The highest level measured in these dry wines was 15-20 µg/L. Chemical deamination of threonine to 2-ketobutyric acid, followed by aldol condensation with acetaldehyde, led to the formation of racemic sotolon. 2-ketobutyric acid was also identified as a product of the oxidative degradation of ascorbic acid (*18*).

Ascorbic acid is a natural antioxidant found in small quantities in grapes. It disappears rapidly when the must first comes into contact with oxygen and during alcoholic fermentation. Wine generally does not contain any (*19*). Ascorbic acid was authorized many years ago as an antioxidant for wine in most countries. Its use does not raise any health-related objections. It is now used in most winegrowing countries at a maximum concentration of 150 mg/l, always in association with sulfur dioxide. The recommended concentrations are between 50 and 100 mg/l, as higher concentrations may affect wine flavor (*20*). The addition of ascorbic acid to prevent or delay the development of oxidative flavor in white wine continues to be a matter of debate in the literature. The advantages and disadvantages of this enological practice have been reviewed many times in the past (*21*, *22*). Indeed, ascorbic acid is considered a powerful antioxidant which may also act as a pro-oxidant in specific cases, depending on its concentration and some physicochemical parameters (*i.e.* dissolved oxygen and temperature).

According to several studies, the major advantage of using ascorbic acid was its rapid elimination of oxygen dissolved at bottling (*23*, *24*) and its capacity to decrease the redox potential of wines (*25*). According to a study by Bauereinfeind (*26*), ascorbic acid addition may be favorable to wine aroma, taste, and clarity. Many years later, Peng (*21*), cited no protection from browning in wines containing ascorbic acid and sulfur dioxide during bottle storage. More recently, Skouroumounis (*27*) used sensory analysis to determine that adding ascorbic acid to Chardonnay and Riesling wines was never detrimental but could, in some cases, protect them from oxidative spoilage.

As early as 1966, Ribéreau-Gayon emphasized in the Handbook of Enology that "ascorbic acid, associated with sulfur dioxide, is able to protect the wine from gentle aeration but it does not work against strong oxidation" (*19*). This observation was in agreement with Bradshaw (*28*) study, who demonstrated that ascorbic acid had a concentration-dependent pro-oxidant effect in model solution. According to our recent study, ascorbic acid under oxidative conditions was associated with sotolon formation via the formation of 2-ketobutyric acid and its reaction with acetaldehyde (*18*).

Another natural antioxidant found in grapes but also in wines has drawn attention to researchers since the role of glutathione (GSH) has been considered in preventing must browning (*29*). More recently, it has been reported that this compound exerts a protective effect on certain wine aromas in Sauvignon Blanc wines (*1*). In this study, Lavigne showed that spiking with GSH (10 mg/L) at bottling had positive effects on wine color and varietal aroma; by preventing the degradation of varietal thiols, and sotolon formation, as well as decreasing

Publication Date (Web): November 24, 2015 | doi: 10.1021/bk-2015-1203.ch015

the intensity of yellow color after 3 years' bottle storage. Very recently, Herbst (*30*) showed that adding sulfur dioxide and glutathione slowed the decrease in 3-mercaptohexan-1-ol and 3-mercaptohexyl acetate over a 4-week period. This phenomenon was more pronounced in the case of low oxygen exposure during bottling and bottle aging (*31*). This behavior of thiols was recently explained in a study on the reactivity of these compounds with (+) catechin and (-) epicatechin, naturally found in white wines (*32*). GSH is found at high levels in young white wines compared to volatile thiols (mg/L *vs.* ng/L) and may act as a radical or quinone trap, thus protecting the volatile thiols.

Over the past fifteen years, the influence of closures on the color and flavor of white wines has been explored in several studies, using a variety of closures and storage conditions (*33–36*). It is well known that the rate of ingress of oxygen into the bottle through the closure and closure-bottle interface affect the quality of aging. As recently discussed, high oxygen permeability of closures is probably responsible for the high levels of dissolved oxygen found in prematurely-aged white wines (*15*). The choice of wine closure type is therefore likely to have a considerable impact on the extent of wine oxidation (*36*). For example, Brajkovich (*37*), corroborated this observation, concluding that the use of screw caps stabilized the varietal flavor of Sauvignon wines (3-SH, 4-MSP) over a two-year period. Moreover, based on these results and for the reasons cited previously, we hypothesized that the ability of ascorbic acid to prevent white wine from oxidative mechanisms was associated with the closure oxygen transfer rate (OTR).

The aim of this study was to investigate the effect of adding ascorbic acid, alone or with glutathione, on a Sauvignon Blanc wine, according to the oxygen permeability of two closures, based on analytical and sensory approaches. The goal of the first part of our investigation was a better understanding of the organoleptic impact of adding ascorbic acid and GSH and their influence on sotolon formation according to closure OTR. The second section focused on the impact of (+)-catechin on the oxidative evolution of white wines.

Materials and Methods

Ascorbic Acid and GSH Spike in Trials

In cooperation with a winery, ascorbic acid was added to a Sauvignon Blanc wine bottled on a large scale under commercial conditions at the CVBG bottling facility, using two closures with very different oxygen permeabilities. Wines were produced from Sauvignon Blanc grapes in the Bordeaux appellation during the 2003 vintage. Standard winemaking procedure for white wines was applied, avoiding all contact with wood (*38*). A single batch was divided between two 50 HL stainless steel vats. Free sulfur dioxide was adjusted (30 mg/L) and ascorbic acid was added (80 mg/L) to the wines in vat, two days prior to bottling. GSH was added manually to each bottle, just before filling. The overall experimental design is presented in Table 1. 750 mL green bottles were from Saint-Gobain Emballage (Cognac, France). The head space of the bottles was saturated with CO_2 before sealing. Bottles were inverted for one hour after bottling. The main oenological

Publication Date (Web): November 24, 2015 | doi: 10.1021/bk-2015-1203.ch015

parameters of the white wine are presented in Table 2. The wines were bottled at a single fill height of 10 mm, using either natural cork (Amorim, 44x24 mm, super grade) with on average, a lower oxygen permeability or a synthetic stopper (supremcorq, 36x21 mm) with tenfold higher oxygen permeability.

Table 1. Experimental Design

	AA addition (80 mg/L)	*GSH addition (10 mg/L)*	*Type of closure*	
			Cork (Low OTR)	*Synthetic (High OTR)*
2003 dry white Bordeaux	No	No	Lw-O_2	Hi-O_2
	Yes	No	Lw-O_2 AA	Hi-O_2 AA
		Yes	Lw-O_2 AA GSH	Hi-O_2 AA GSH

Publication Date (Web): November 24, 2015 | doi: 10.1021/bk-2015-1203.ch015

Flavan-3-ols Spike in Trials

The experiment was carried out using a Sauvignon Blanc wine from the Bordeaux area (Entre Deux Mers, 2009 vintage). The wine's analytical parameters were as follows: pH 3.4, 12.4% alcohol (v/v), 0.3 g/L volatile acidity (eq. sulfuric acid), 3.4 g/L titratable acidity (eq. sulfuric acid), 21.0 mg/L free sulfur dioxide, 48.0 mg/L total sulfur dioxide, 7 mg/L reduced glutathione, 6.1 mg/L (+)-catechin, and 3.4 mg/L (-)-epicatechin. Wines were spiked with 50 mg/L catechin. All wines were transferred to inert vials closed with silicone septum and crimped with aluminum caps. Wines were stored in a thermostat-controlled room at 20°C or 37°C for 12 months.

Oxygen Permeability Assay

This assay was performed in collaboration with LNE laboratory (Trappe, France). The methodology was consistent with ASTM D 3985 and ISO 15105-2:2003 standard applied to oxygen permeability of plastic films. Oxygen transmission rates were tested using an Oxtran 100 coulometer (Modem Controls Inc., Mineapolis). The samples were conditioned for one month to remove residual oxygen in cork cells prior to testing.

Dissolved Oxygen Assay

DO was measured in 10 bottles of each condition a few minutes after bottling, using an Orbisphere 31120, according to (*15*). Each measurement was performed in duplicate.

Table 2. Main Enological Parameters of the Dry Bordeaux White Wine Studied Just after Bottling

Enological Parameters		*Value (SD)*
Ethanol (% vol.)		12.8
AV (g/L H_2SO_4)		0.24
pH		3.3 (0.02)
AT (g/L H_2SO_4)		3.2 (0.2)
free SO_2 (mg/L) *		27 (1)
total SO_2 (mg/L) *		50 (2)
Ascorbic acid (mg/L) *	Without	nd
	With	79.8 (6.2)
Glutathione (mg/L) *	Without	1.9 (0.3)
	With	11.2 (0.9)
Sotolon (µg/L)		nd
Dissolved oxygen	Without AA	1.28 (0.13)
(mg/L)**	With AA	1.35 (0.18)

SD: standard deviation; nd: not detected; * average of 3 samples; ** average of 15 samples.

Publication Date (Web): November 24, 2015 | doi: 10.1021/bk-2015-1203.ch015

Sotolon, Phenylacetaldehyde, and Methional Analysis

The content of the wines was determined, using 3-octanol as an internal standard, as previously described (*15*).

HPLC-FLP Flavan-3-ols Analysis

A Dionex Ultimate 3000 with a ternary pump (RS) and an autosampler (WPS-3000RS) were coupled to a fluorimetric detector (FLD-3100). A Chromeleon was used for acquisition, solvent delivery, and detection. Chromatograms corresponding to excitation at 275 nm and emission at 320 nm in the fluorescence detector were used to detect and quantify the various compounds (*39*). Separation was performed on a reversed-phase Beckman Coulter Ultrasphere ODS C18 (250 mm × 4.6 mm, 5 μm). A binary solvent was run at a flow rate of 0.7 mL/min employing (A) 5% aqueous trifluoroacetic

acid (0.1%) and (B) acetonitrile (65%) trifluoroacetic acid (0.1%). Elution was performed with a gradient: 0-30 min from 15 to 35% solvent B, 30-35 min from 35 to 100% B. The wine injection volume was 10 μL. Each sample was injected three times.

Glutathione and Ascorbic Acid Analysis

The reduced glutathione was quantified as described by Lavigne (*40*) whereas the ascorbic acid assay was performed as described previously by Pons (*18*).

Sensory Analysis

Approximately 30 mL wine was presented in black glasses corresponding to AFNOR (Association Française des Normes) standards. Indeed, the glasses were chosen to avoid any potential bias among the panel due to visual cues, due to the risk that wines presented in standard, clear glasses would score higher on attributes such as "oxidized". The sensory panel, which was similar throughout the experiment, consisted of 15 tasters from ISVV staff with extensive experience in white wine tasting, aged from 25 to 50. Before each session, wines from three replicates of each treatment were blended. Basic analyses (free SO_2, DO) were carried out to ensure that the white wines were in a similar oxidation state.

The impact of adding ascorbic acid and glutathione on wine aroma was evaluated by triangular tests in individual booths at controlled room temperature (20°C). Sensory analysis consisted of presenting three samples, two identical and one different, to a large number of judges (forced-choice method). The sensory recognition test was accompanied by a question regarding the taster's preference. Once the tasters had determined which sample was different, they were asked to give their preference. Results of tasters who failed in the triangular test were not included in the preference test results. In our experiment, we considered that the sample was preferred when at least 80 % of the panel preferred the sample identified during the triangular test.

Moreover, after 120 months, during the last sensory analysis session, the intensity of oxidized flavors in the six conditions was also assessed. Panelists scored the "oxidized" attribute on a scale of 0 to 5, where 0 indicated the wine was not oxidized and 5 corresponded to an intense oxidized flavor. Wines presenting trichloroanisole (TCA) taint were not analyzed.

Results

Oxygen Permeability Assay

For many years in the wine industry, closure quality was mainly assessed by its mechanical properties. Nowadays, closure oxygen permeability is considered a key factor in wine quality during storage. Many studies have investigated this process in recent years, producing different oxygen permeability data, leading to contrasting conclusions. Indeed, the oxygen permeability of a stopper is linked

Publication Date (Web): November 24, 2015 | doi: 10.1021/bk-2015-1203.ch015

to its macroporous structure (*41*, *42*) or the existence of a preferential cork-glass interface route for cork stoppers (*43*), and probably both. Direct measurements of oxygen permeability of the stopper using various methods are presented in Table 3. Several studies have determined that the steady state of diffusion is reached after 1 month storage, when the air trapped in the cork cells has been completely expulsed and consumed by the wine (*44*, *45*). For this reason, the oxygen permeability assay was performed one month after bottling. The oxygen permeability measurements obtained in this study were similar to those found elsewhere: the synthetic stopper used was 10 times more permeable than natural cork, which had a value close to the coulometer detection limit. Consequently, oxygen permeability was probably over-estimated at 30 µL/month.

Publication Date (Web): November 24, 2015 | doi: 10.1021/bk-2015-1203.ch015

Table 3. Examples of Oxygen Permeability of Natural and Synthetic Corks from Several Studies

References	*OTR (µL/months)*	
	Natural Cork (min-max)[1]	*Synthetic stopper (min-max)*[1]
Personal results	30 <	300
(*45*)	52 - 200	400
(*46*)	15 - 240	60 - 1150
(*47*)	3.8 - 2600	/
(*44*)	< 70	/

[1] if data available.

It is interesting to note that oxygen permeability is not a recent concern. Ribéreau-Gayon was the first to measure the oxygen ingress in wine bottles in 1933. This colorimetric method over 75 years' old, based on the oxidation of sodium hydrosulfate by oxygen in the presence of indigo carmine, was recently successfully adapted by Lopes (*48*) to measure oxygen ingress with several different stoppers. This study revealed that the oxygen permeability of synthetic closures was systematically higher than that of natural cork. More generally, the results obtained several authors (*46*, *47*) highlighted the large oxygen permeability range of natural cork.

Average dissolved oxygen concentrations assayed in wines during the two days of bottling were low and similar. Indeed, according to Vidal (*49*), it is not unusual to input up to 4 mg/L oxygen during industrial bottling. Samples corresponding to each treatment were analyzed in a steady state.

Publication Date (Web): November 24, 2015 | doi: 10.1021/bk-2015-1203.ch015

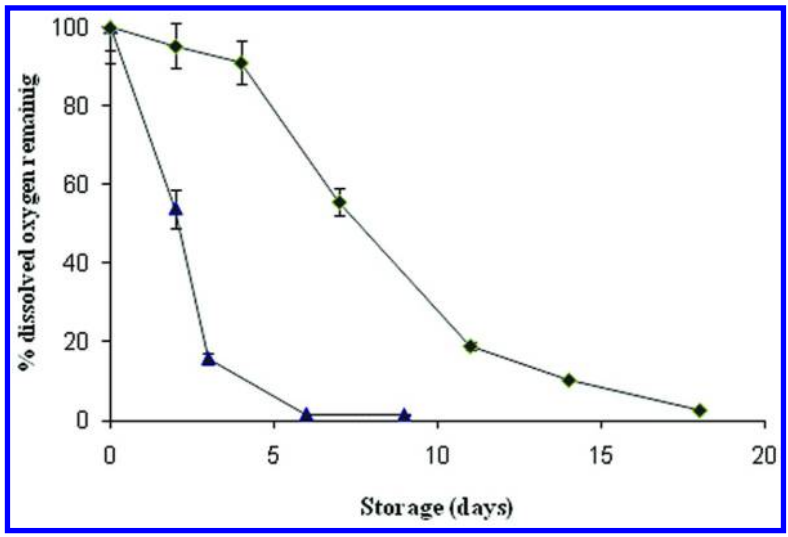

Figure 1. Evolution of dissolved oxygen in a dry, white Bordeaux wine spiked or not with ascorbic acid (80 mg/L) at bottling (condition ♦ without ascorbic acid; ▲with ascorbic acid). n=3.

Dissolved Oxygen

Dissolved oxygen concentrations were monitored by an electrochemical probe during the first few days after bottling. Figure 1 shows that the consumption of approximately 1.3 mg/L dissolved oxygen took 6 days in the presence of 80 mg/L ascorbic acid, whereas, in the absence of ascorbic acid, 16 days were required for concentrations to drop below 30 µg/L. Under our experimental conditions, this dissolved oxygen level reached in a few days corresponded to the average dissolved oxygen concentrations found in certain wines after 6 months' aging. One month later (T0), the dissolved oxygen level in the wines was very low; almost 98 % of the dissolved oxygen at bottling had been consumed. The average dissolved oxygen concentration was 20 µg/L and no differences were observed according to the treatments or the type of closure.

Ascorbic Acid and GSH Evolution

Ascorbic acid is not very stable in wine and easily oxidizes into dehydroascorbate. This instability is well known to be influenced by the synergistic effect of molecular oxygen and catalytic metal ions (such as iron and copper), inducing radical chain oxidation reactions. The effect of closure OTR and GSH supplementation on ascorbic acid concentrations in dry white wines during 10 years' storage is shown in Figure 2. Half of the samples spiked with ascorbic acid were also spiked with GSH (10 mg/L).

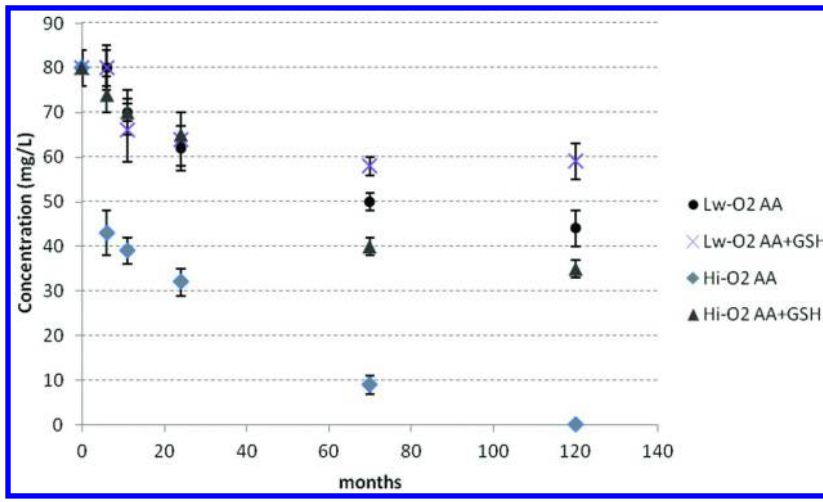

Figure 2. Changes in ascorbic acid concentration (AA) in a dry white wine during aging in bottles sealed with low-OTR (Lw-O_2) and high-OTR (Hi-O_2) closures, with or without GSH supplementation (10 mg/L) at bottling. (n=3).

Six months after bottling, the ascorbic acid concentrations were significantly different between the two sealing systems. Indeed, the concentration was stable with the Lw-O_2 closure (Lw-O_2), but had dropped to 43 mg/l with the Hi-O_2 closure (50 % loss). Surprisingly, when GSH was added in the Hi-O_2-AA condition, ascorbic acid levels remained approximately stable over the same period. However, beyond six months, a slow decrease in ascorbic acid concentrations was observed in all conditions.

After 24 months' storage, the decrease in ascorbic acid content was similar for low- and high-OTR closures spiked with GSH, reaching more than 20 % for theses modalities, whereas a 59% loss was measured for the high OTR closure (Hi-O_2 AA) non-spiked with GSH. These results illustrated that ascorbic acid loss was strongly linked to the oxygen permeability of the closures. As ascorbic acid is well known as a strong oxygen scavenger, its decrease during aging was associated with different molecular oxygen levels in bottled dry white wines. Moreover, it was observed for the first time that GSH addition apparently protected ascorbic acid during bottle-aging. This finding was confirmed at 70 months. According to several tests, GSH and AA have similar antioxidant properties (*50*), so it is not surprising to observe that GSH addition protect AA during bottle aging. At the end of the experiment (120 months), a 25 % loss was observed for the Lw-O_2 AA+GSH condition, 45 % for Lw-O_2 AA, 57 % for Hi-O_2 AA+GSH, and, finally, a 100 % loss for the Hi-O_2 condition.

Publication Date (Web): November 24, 2015 | doi: 10.1021/bk-2015-1203.ch015

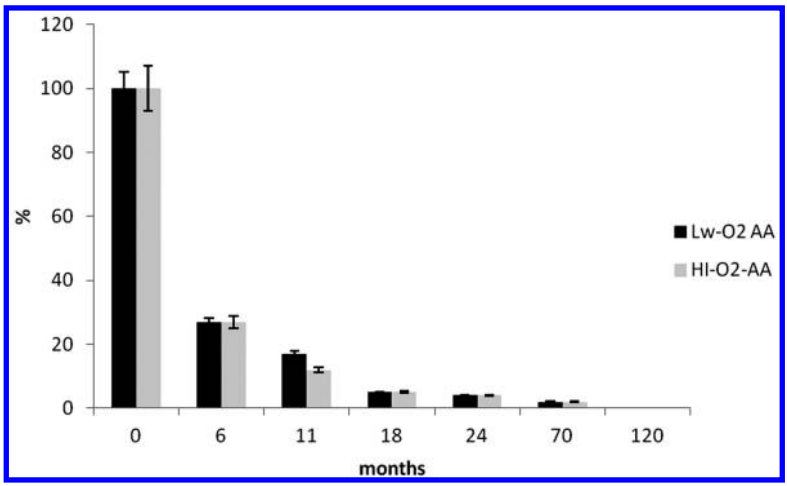

Figure 3. Changes in GSH evolution in a bottled dry white wine according to closure permeability (n=3).

Figure 3 shows variations in GSH concentrations in wines sealed with natural and synthetic stoppers during 120 months' bottle storage. GSH was more unstable than ascorbic acid in dry white wines during bottle-aging. Indeed, six and 11 months after bottling, GSH loss reached 75 % and 85 % respectively. Beyond two years' storage, only traces of GSH were detected in all wine samples. Surprisingly, this evolution was similar for both closures independently of their OTR level. This finding may be explained by the similar oxygen levels (~1.3 mg/L) introduced at bottling for both closures.

Sotolon Evolution

Ascorbic Addition Effect

It was recently demonstrated that the oxidation of ascorbic acid in model wine solution was likely to produce non-negligible amounts of sotolon (*18*). Consequently, in this experiment, it was hypothesized that the concomitant presence of dissolved oxygen and ascorbic acid was likely to promote sotolon formation during aging in bottles sealed with a high-OTR closure.

Sotolon was not detected in the young dry white wine just after bottling or during the first year of storage with natural cork or synthetic closures (Figure 4). At 18 and 24 months, bottles supplemented with ascorbic acid and sealed with synthetic closures (Hi-O_2) had the highest sotolon content, Bottles with synthetic closures non-spiked with ascorbic acid contained the second highest levels. Wine in bottles sealed with natural corks tended to be protected from sotolon formation compared to synthetic closures. This effect was particularly marked at 24 months, when the sotolon content of the wine supplemented with AA and sealed with a synthetic closure exceeded its perception threshold (2 µg/L). Of course, the

Publication Date (Web): November 24, 2015 | doi: 10.1021/bk-2015-1203.ch015

concentrations were low, but this rapid sotolon production in a wine with a permeable closure (300 µL O_2/month), in the presence of ascorbic acid spiked at 80 mg/L, was a significant finding. However, it is noteworthy that, at 24 and 70 months, the sotolon increase was always similar in the both conditions (Hi-O_2 / Hi-O_2 AA), i.e. sotolon formation was not exacerbated in the wine spiked with ascorbic acid.

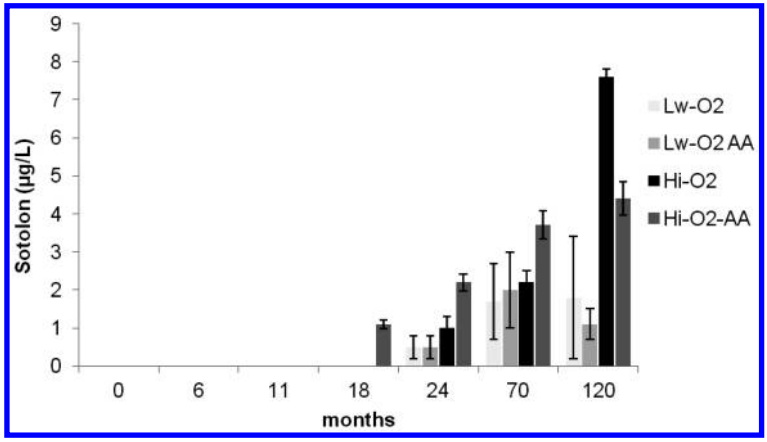

Figure 4. Sotolon evolution during bottle aging with or without ascorbic acid supplementation, according to oxygen permeability of cork stoppers. (n=3)

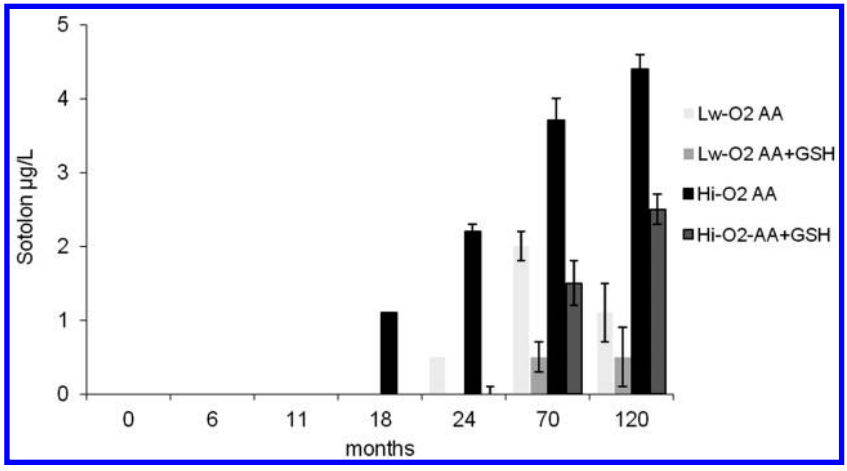

Figure 5. Sotolon evolution during bottle aging with ascorbic acid or ascorbic acid and glutathione supplementation, according to the oxygen permeability of cork stoppers. (n=3)

In Advances in Wine Research; Ebeler, et al.;
ACS Symposium Series; American Chemical Society: Washington, DC, 2015.

Publication Date (Web): November 24, 2015 | doi: 10.1021/bk-2015-1203.ch015

At 10 years, average sotolon concentrations in wines sealed with cork closure were low (≤ 1.5 µg/L) but with considerable variability, probably due to the heterogeneous permeability of cork stoppers (*45*, *47*). Surprisingly, the highest level (7.5 µg/L) in bottles with synthetic closure was found in non-spiked wines (Hi-O2). This analysis indicated a clear impact on the non-protected wine (i.e. by adding ascorbic acid) in the Hi-O2 sample. Finally, two trends were observed in wine sealed with synthetic closures: a late, exponential evolution of sotolon when no ascorbic acid was added at bottling (Hi-O2), contrasted with a premature formation of sotolon, with a slow, linear evolution when the wine was spiked with ascorbic acid at bottling (Hi-O2 AA).

Publication Date (Web): November 24, 2015 | doi: 10.1021/bk-2015-1203.ch015

GSH Addition

Figure 5 shows sotolon evolution in wines supplemented with ascorbic acid (80 mg/L) and spiked or not with GSH (10 mg/L). The trends exhibited by these data were similar to those obtained previously for wines spiked or not with ascorbic acid (Figure 4): a slow increase in sotolon formation during aging in all conditions. However, while sotolon was detected at 18 months in the Hi-O_2 AA condition, 70 months were necessary to reach a similar level in the same condition spiked with GSH (Hi-O_2 AA+GSH). This phenomenon was also observed in the dry white wine sealed with cork (Lw-O_2), where concentrations below 1 µg/L were assayed in the Lw-O_2 AA+GSH condition at 120 months. Generally, at 120 months, wines supplemented with ascorbic acid and spiked with GSH at bottling had a lower sotolon content than those supplemented with ascorbic acid alone. These results are consistent with those of Lavigne (*51*), who demonstrated that adding 10 mg/L GSH at bottling delayed sotolon formation in a Sauvignon Blanc white wine after 3 years' aging. These new data revealed that that, even though the wine was protected from oxidation at bottling by adding ascorbic acid, supplementation with GSH delayed the formation of sotolon during bottle aging.

Sensory Analysis

Effect of Ascorbic Acid Supplementation

During the experiment, wine samples were evaluated by a trained panel of 15 subjects. First, the flavors of the wines sealed with natural cork and synthetic closure with or without added ascorbic acid were assessed by a triangular test (Table 4). After six months' storage, data analysis did not reveal any significant differences between conditions supplemented with ascorbic acid or not, or those with low- (cork) or high-OTR (synthetic) closures.

After 12 months' storage, no difference was observed between the wines sealed with natural corks and spiked or not with ascorbic acid at bottling. On the contrary, a marked difference ($p<0.05$) was already observed between the wines spiked or not with ascorbic acid, sealed with synthetic closures. After two years' storage, significant differences ($p<0.01$) emerged between natural cork and the synthetic closures. The stability of these perceived differences was confirmed

during the rest of the experiment. Results of the preference test revealed that the wines spiked with ascorbic acid were systematically preferred by the panel (when they were able to differentiate between the control wine and the one spiked with ascorbic acid). The choice of wine closure type is, therefore, likely to have a considerable impact on the extent of wine oxidation. Moreover, sensory effects related to ascorbic acid addition were detected earlier when wines were aged in bottles with a high rather than low-OTR closures.

Publication Date (Web): November 24, 2015 | doi: 10.1021/bk-2015-1203.ch015

Table 4. Results of Triangular and Preference Tests for Ascorbic Acid Addition (AA, 80 mg/L) for High- (Hi O_2) and Low-Oxygen (Lw O_2) Permeability Closures during Aging[1]

	Aging time (months)						
	6	*11*	*18*	*24*	*40*	*70*	*120*
Hi O_2	Ns[2]	AA**	AA*	AA*	AA*	AA*	AA*
Lw O_2	Ns	Ns	Ns	AA*	AA*	AA*	AA*

[1] three bottles were blended and used for the assessment. [2] for triangular test, ns: not significant; * significant at $p<0.05$; ** significant at $p<0.01$.

Effect of GSH Supplementation

The sensory impact of adding GSH to wines spiked with ascorbic acid at bottling was evaluated (Table 5). In the high-OTR condition (Hi-O_2), significant differences ($p<0.01$) were observed between wines spiked or not with GSH 18 months after bottling: the wine spiked with GSH was preferred by the jury. Thirty-two months later, significant differences were observed for low-OTR closures (Lw O_2). As in the case of ascorbic acid (Table 4), the jury's preference also remained stable throughout bottle aging. Similar, delayed trends were observed when wines spiked with ascorbic acid and supplemented with GSH were compared to those spiked with ascorbic acid only.

Finally, after 120 months' aging, to conclude on the impact of these two antioxidants on wine aging, the intensity of oxidation flavor was compared for all the conditions (Table 6). The Friedman test used for statistical analysis was significant at 0.1 %, which meant that tasters were able to differentiate between wines according to the intensity of their oxidation flavors. The highest score was obtained for Hi-O_2, followed by Hi-O_2 AA, Hi-O_2 AA+GSH, Lw-O_2, Lw-O_2 AA, and Lw-O_2 AA+GSH. The wine spiked with ascorbic acid and GSH at bottling and sealed with a low-OTR closure was perceived as the least oxidized, with very little aging flavor, 120 months after bottling.

Table 5. Results of Triangular and Preference Tests for GSH Addition (10 mg/L) to Wines Spiked with Ascorbic Acid (AA, 80 mg/L) for High- (Hi O_2) and Low-Oxygen (Lw O_2) Permeability Closures during Aging[1]

	Aging time (months)						
	6	*11*	*18*	*24*	*40*	*70*	*120*
Hi O_2 AA	ns[2]	ns	GSH*	GSH*	GSH*	GSH**	GSH**
Lw O_2 AA	ns	ns	ns	ns	GSH*	GSH*	GSH**

[1] three bottles were blended and used for the assessment. [2] for triangular test, ns: not significant; * significant at $p<0.05$; ** significant at $p<0.01$

Publication Date (Web): November 24, 2015 | doi: 10.1021/bk-2015-1203.ch015

Table 6. Intensity of Oxidation Flavors Following GSH (10 mg/L) and Ascorbic Acid (80 mg/L) Supplementation in Wines Sealed with High- (Hi O_2) and Low-Oxygen (Lw O_2) Permeability Closures, 120 Months after Bottling[1]

	Hi O_2			*Lw O_2*		
	Control	*AA*	*AA+GSH*	*Control*	*AA*	*AA+GSH*
Sum of oxidation scores[1]	75 a	56 b	41 c	33 d	13 e	8 f

[1] Values with the same letter (a-f) were not significantly different by Friedman rank sum for analysis of ranked data at $p < 0.01$

Impact of Flavan-3-ols on Strecker Aldehyde and Sotolon Formation

In 1974, Wildenradt & Singleton were the first to explore the chemical oxidation mechanism leading to the formation of volatile compounds in wine. More precisely, they demonstrated that the oxidation of ethanol to acetaldehyde required the presence of polyphenols and further proposed two specific steps (*5*) . Sotolon and acetaldehyde formation has also been reported in wine stored under oxidation conditions. The identification of an aldol reaction between acetaldehyde and α-ketobutyric acid as a possible sotolon formation pathway (*18*) led us to hypothesize that the oxidation of phenolic compounds also contributed to sotolon formation during bottle aging, via the production of acetaldehyde. The major aim of this study was to investigate the impact of phenolic compounds on the acceleration of negative wine aroma development particularly focusing on the role played by Strecker aldehydes and sotolon.

In order to assess the impact of flavan-3-ols (catechin and epicatechin) on phenylacetaldehyde, methional, and sotolon formation, 54 Sauvignon Blanc wine samples from three wineries in the Bordeaux area (two from the Pessac-Leognan appellation (PLI, PLII) and one from the Medoc appellation (M)) were analyzed over 18 consecutive vintages (1992 to 2009) in 2010.

The pattern of phenylacetaldehyde, methional, and sotolon production and flavan-ol evolution related to wine oxidation during bottle aging was revealed in the principal component analysis shown in Figure 6 and Figure 7. The results indicated that the carbonyl compounds, sotolon, and flavan-3-ols assessed had positive loadings on the PC1, which assesses wines according to their capacity to produce these aroma compounds upon oxidation. Moreover, estimation of the Pearson Kendall correlation coefficient, sotolon ($r = 0.578$, $p < 0.01$) and methional ($r = 0.209$, $p < 0.05$) were also shown to be positively correlated with the wines' flavan-3-ol content. Also, methional ($r = 0, 440$, $p < 0.01$) and sotolon ($r = 0.517$, $p < 0.01$) were significantly correlated with wine age. However, phenylacetaldehyde content was not correlated, indicating that it had a different formation pattern in wine under oxidation conditions, dependent on its *in situ* precursor content.

Publication Date (Web): November 24, 2015 | doi: 10.1021/bk-2015-1203.ch015

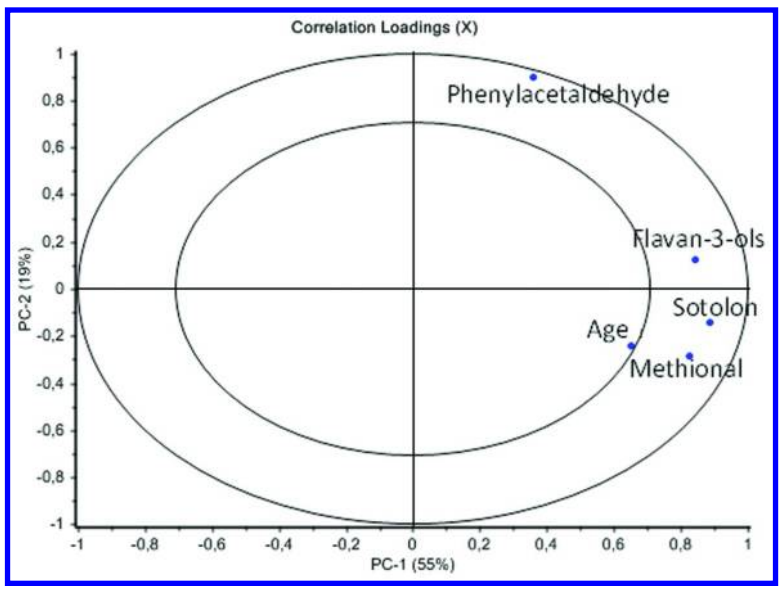

Figure 6. PCA showing the projection of variables.

In Advances in Wine Research; Ebeler, et al.;
ACS Symposium Series; American Chemical Society: Washington, DC, 2015.

Publication Date (Web): November 24, 2015 | doi: 10.1021/bk-2015-1203.ch015

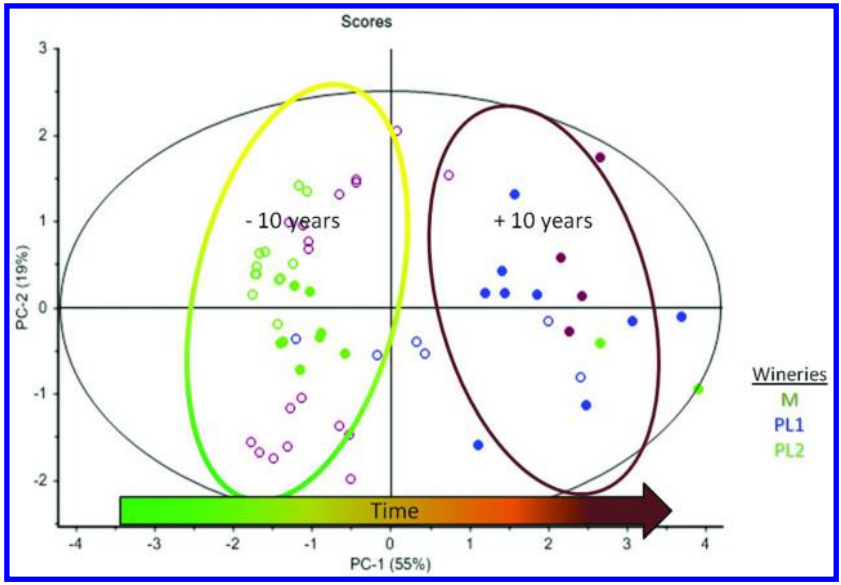

Figure 7. Plot of PCA scores derived from analyses of phenylacetaldehyde, methional, sotolon, flavan-3-ols, and vintage data from 54 Sauvignon Blanc wine samples [Wine samples from three wineries in the Bordeaux area (PLI, PLII, M) over 18 consecutive vintages (1992 to 2009)].

The second component of the PCA separated wines from different wineries according to their vintage. Taking into account the presence of two clearly identified groups of samples, the plot reveals that the wines on the left, under 10 years' old, had retained their freshness, while wines over 10 years' old had already developed oxidative aromas, which undoubtedly caused them to lose their varietal character. It was possible to discriminate among the wine samples over 10 years' old by distribution according their origin (winery). Indeed, PL II wines containing less than 3 mg/L flavan-3-ols (data not shown) had undergone prolonged oxidative bottling-aging without any noticeable formation of aldehydes or sotolon. However, samples on the right of the diagram, such as M and PLI, rapidly developed oxidation-related aroma compounds.

Impact of Catechin Supplementation on the Formation of Phenylacetaldehyde, Methional, and Sotolon According to Temperature

The wine used for this experiment was a dry Sauvignon Blanc from Bordeaux (France, 2009 vintage), kept under high oxygen exposure conditions (4 mg/L dissolved oxygen) at two different temperatures (20°C and 37°C) for 12 months. Catechin (C) (50 mg/L) was added to assess its impact on the production of these aroma compounds. Phenylacetaldehyde, methional and sotolon, as well as (+)-catechin were assayed in each wine. The change in 420 nm absorbance was also monitored to measure oxidative color change during the experiment.

Publication Date (Web): November 24, 2015 | doi: 10.1021/bk-2015-1203.ch015

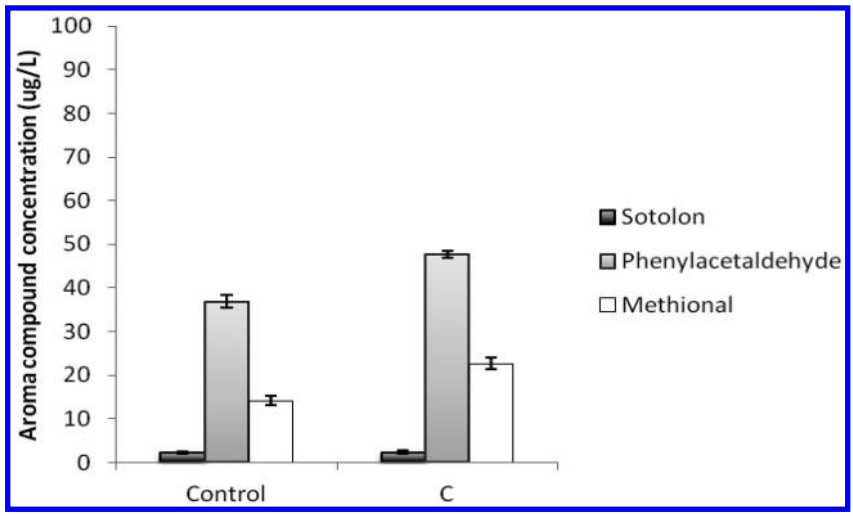

Figure 8. Concentrations of phenylacetaldehyde, methional, and sotolon in white wine, spiked or not with 50mg/L catechin (C) after 12 months' storage at 20°C.

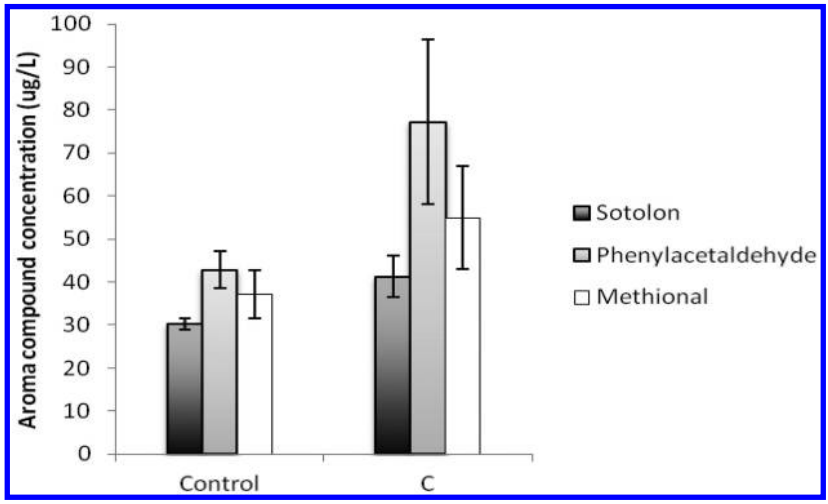

Figure 9. Concentrations of phenylacetaldehyde, methional, and sotolon in dry white wine, spiked with 50 mg/L catechin (C) after 12 months' storage at 37°C.

Within 8 months' storage, C concentrations decreased to 15 mg/L and 6 mg/L in samples stored at 20°C and 37°C, respectively (data not shown). At 20°C, after 12 months' storage, phenylacetaldehyde and methional were highest in the C sample (Figure 8) and lowest in the control, albeit with a non-significant difference for sotolon. In the equivalent samples stored at 37°C (Figure 9) the concentrations of all tested aroma compounds in all samples were higher than at 20°C, reaching levels above their perception thresholds. At 37°C, C contained

the highest concentrations of phenylacetaldehyde, methional, and exhibited a dominant effect on increasing DO_{420} absorbance units compare to control (Figure 10). These results showed that, in oxygenated white wine at high temperatures, phenylacetaldehyde, methional, and sotolon could be generated in excess from the presence of C. In this case, it is likely that depletion of C promoted the formation of some oxidation products (such as acetaldehyde and quinones) that induced the formation of aldehydes and sotolon in a temperature-dependant manner.

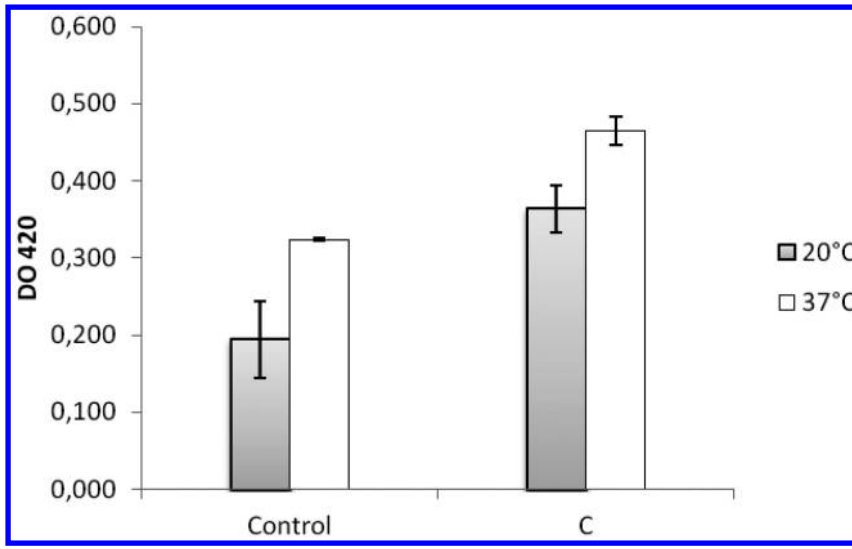

Figure 10. Absorbance units at 420 nm of dry white wine, spiked with 50 mg/L catechin (C) after 12 months' storage at 20 and 37 °C.

Conclusion

Oxidative spoilage of white wines during aging in bottle is influenced by their intrinsic composition, known as "aging potential" i.e. the occurrence of antioxidant, and triggered by oxygen ingress, dependent on closure permeability. The results obtained in this study demonstrated that, under the aging conditions tested, similar to those found in a cellar, simultaneous addition at bottling of the natural antioxidants ascorbic acid and glutathione provides effective protection from flavor deterioration and sotolon formation. Not only was glutathione able to delay the degradation of ascorbic acid but also the formation of sotolon and oxidation flavors throughout 10 years℉ aging. This effect was independent of closure permeability. This study emphasized once again that the choice of closure is a crucial parameter in managing the bottle aging of white wine. It was also demonstrated that under the experimental conditions of the study, an initial average OTR, estimate at 30 µL/month, lower than the OTR of the synthetic closure (300

Publication Date (Web): November 24, 2015 | doi: 10.1021/bk-2015-1203.ch015

μL/month) induced a one year delay in the oxidation of a Sauvignon Blanc wine. We also demonstrated that, based on the analysis of oxidation markers, high (+)-catechin concentration in dry white wines promoted their premature aging in a storage-temperature dependent manner.

Ascorbic acid addition is permitted in wines but GSH supplementation is not legal. Consequently, the overall results highlight the fact that preservation of the GSH potential of grapes during winemaking is a crucial parameter for ensuring the aging potential of a white wine.

References

1. Lavigne-Cruège, V.; Dubourdieu, D. Role of glutathione on development of aroma defects in dry white wines. In *13th International Enology Symposium*; International Association of Enology: Montpellier, France, 2002.
2. Escudero, A.; Cacho, J.; Ferreira, V. Isolation and identification of odorants generated in wine during its oxidation: a gas chromatography-olfactometric study. *Eur. Food Res. Technol.* **2000**, *211*, 105–110.
3. Silva Ferreira, A. C.; Hogg, T.; Guedes de Pinho, P. Identification of key odorants related to the typical aroma of oxidation-spoiled white wines. *J. Agric. Food Chem.* **2003**, *51*, 1377–1381.
4. Singleton, V. L.; Trousdale, E.; Zaya, J. Oxidation of Wines. I. Young White Wines Periodically Exposed to Air. *Am. J. Enol. Vitic.* **1979**, *30* (1), 49–54.
5. Wildenradt, H. L.; Singleton, V. L. The production of aldehydes as a result of oxidation of polyphenolic compounds and its relation to wine aging. *Am. J. Enol. Vitic.* **1974**, *25* (2), 119–126.
6. Escudero, A.; Cacho, J.; Ferreira, V. Isolation and identification of odorants generated in wine during its oxidation: A gas chromatography-olfactometric study. *Eur. Food Res. Technol.* **2000**, *211* (2), 105–110.
7. Culleré, L.; Cacho, J.; Ferreira, V. An assessment of the role played by some oxidation-related aldehydes in wine aroma. *J. Agric. Food Chem.* **2007**, *55* (3), 876–881.
8. Yaylayan, V. A. Recent advances in the chemistry of Strecker degradation and amadori rearrangement: Implications to aroma and color formation. *Food Sci. Technol. Res.* **2003**, *9* (1), 1–6.
9. Mathew, A. G.; Parpia, H. A. B. Food browning as a polyphenol reaction. *Adv. Food Res.* **1971**, *19*, 75–135.
10. Rizzi, G. P. Formation of strecker aldehydes from polyphenol-derived quinones and α-amino acids in a nonenzymic model system. *J. Agric. Food Chem.* **2006**, *54* (5), 1893–1897.
11. Grant-Preece, P.; et al. Sensorially important aldehyde production from amino acids in model wine systems: Impact of ascorbic acid, erythorbic acid, glutathione and sulphur dioxide. *Food Chem.* **2013**, *141* (1), 304–312.
12. Nikolantonaki, M.; Waterhouse, A. L. A Method To Quantify Quinone Reaction Rates with Wine Relevant Nucleophiles: A Key to the Understanding of Oxidative Loss of Varietal Thiols. *J. Agric. Food Chem.* **2012**, *60* (34), 8484–8491.

Publication Date (Web): November 24, 2015 | doi: 10.1021/bk-2015-1203.ch015

13. Ferreira, V.; et al. Key changes in wine aroma active compounds during bottle storage of spanish red wines under different oxygen levels. *J. Agric. Food Chem.* **2014**, *62* (41), 10015–27.
14. Danilewicz, J. C. Review of reaction mechanisms of oxygen and proposed intermediate reduction products in wine: central role of iron and copper. *Am. J. Enol. Vitic.* **2003**, *54*, 73–85.
15. Lavigne, V.; et al. Changes in the sotolon content of dry white wines during barrel and bottle aging. *J. Agric. Food Chem.* **2008**, *56* (8), 2688–2693.
16. Pham, T. T.; et al. Optimal conditions for the formation of sotolon from alpha-ketobutyric acid in the french "Vin Jaune". *J. Agric. Food Chem.* **1995**, *43*, 2616–2619.
17. Cutzach, I.; Chatonnet, P.; Dubourdieu, D. Rôle du sotolon dans l'arôme des vins doux naturels, influence des conditions d'élevage et de vieillissement. *J. Int. Sci. Vigne Vin* **1998**, *32* (4), 223–233.
18. Pons, A.; et al. Identification of a sotolon pathway in dry white wines. *J. Agric. Food Chem.* **2010**, *58*, 7273–7279.
19. Ribereau-Gayon, P. *Traité d'Oenologie. Tome 1: Microbiologie du Vin, Vinifications*; Dunod: Paris,1998.
20. Ribereau-Gayon, P. *Traité d'Oenologie. Tome 2: Chimie du vin, stabilisation et traitements*; Dunod: Paris,1998.
21. Peng, Z.; et al. The effect of ascorbic acid on oxidative browning of white wines and model wines. *Aust. J. Grape Wine Res.* **1998**, *4*, 127–135.
22. Bradshaw, M. P.; et al. Defining the ascorbic acid crossover from anti-oxidant to pro-oxidant in a model wine matrix containing (+)-catechin. *J. Agric. Food Chem.* **2003**, *51*, 4126–4132.
23. Napier, C. E. The antioxydant properties of ascorbic acid and its use for improving the shelf-life of beer. In *Wallestein Laboratory Communications*; Wallerstein Laboratories: New York, 1956, p 193−206.
24. Cort, W. M. Antioxidant properties of ascorbic acid in foods. In *Ascorbic Acid: Chemistry, Metabolism, and Uses*; Seib, P. A., Tolbert, B. M., Eds.; American Chemical Society: Washington, DC, 1982; p 533−550.
25. Peynaud, E. Utilisation des propriétés réductrices de l'acide ascorbique dans le traitement des vins. *C. R. Acad. Agric. Fr.* **1961**, *47*, 67–70.
26. Bauernfeind, J. C.; Pinkert, D. M. Food processing with added ascorbic acid. *Adv. Food Res.* **1970**, *18*, 219–315.
27. Skouroumounis, G. K.; et al. The influence of ascorbic acid on the composition, colour and flavour properties of a Riesling and a wooded Chardonnay wine during five years' storage. *Aust. J. Grape Wine Res.* **2005**, *11* (3), 355–368.
28. Bradshaw, M. P.; et al. Defining the ascorbic acid crossover from anti-oxidant to pro-oxidant in a model wine matrix containing (+)-catechin. *J. Agric. Food Chem.* **2003**, *51* (14), 4126–4132.
29. Singleton, V. L.; et al. Caftaric acid disappearance and conversion to products of enzymatic oxidation in grape must and wine. *Am. J. Enol. Vitic.* **1985**, *36*, 50–56.

Publication Date (Web): November 24, 2015 | doi: 10.1021/bk-2015-1203.ch015

30. Herbst-Johnstone, M.; Nicolau, L.; Kilmartin, P. A. Stability of Varietal Thiols in Commercial Sauvignon blanc Wines. *Am. J. Enol. Vitic.*. **2011**, *62* (4), 495–502.
31. Ugliano, M.; et al. Evolution of 3-mercaptohexanol, hydrogen sulfide, and methyl mercaptan during bottle storage of sauvignon blanc wines. Effect of glutathione, copper, oxygen exposure, and closure-derived oxygen. *J. Agric. Food Chem.* **2011**, *59*, 2564–2572.
32. Nikolantonaki, M.; et al. Reactivity of volatile thiols with polyphenols in a wine-model medium: Impact of oxygen, iron, and sulfur dioxide. *Anal. Chim. Acta* **2010**, *660* (1-2), 102–109.
33. Francis, L.; et al. The AWRI closure trial: sensory evaluation data 36 months after bottling. *Aust. N. Z. Grapegrower Winemaker* **2003**, *475*, 59–64.
34. Waters, E. J.; et al. The role of corks in oxidative spoilage of white wines. *Aust. J. Grape Wine Res.* **1996**, *2*, 191–197.
35. Caloghiris, M.; Waters, E. J.; Williams, P. J. An industrial trial provides further evidence for the role of corks in oxidative spoilage of bottled wines. *Aust. J. Grape Wine Res.* **1997**, *3*, 9–17.
36. Godden, P.; et al. Wine bottle closures: physical characteristics and effect on composition and sensory properties of a Semillon wine. 1.Performance up to 20 months post-bottling. *Aust. J. Grape Wine Res* **2001**, *7*, 64–105.
37. Brajkovich, M.; et al. Effect of screwcap and cork closures on SO2 levels and aromas in a Sauvignon Blanc wine. *J. Agric. Food Chem.* **2005**, *53* (26), 10006–10011.
38. Ribereau-Gayon, P. *Traité d'Oenologie*; Dunod: Paris, 1998; Vol. 2.
39. Carando, S.; Teissedre, P. L.; Cabanis, J. C. HPLC coupled with fluorescence detection for the determination of procyanidins in white wines. *Chromatographia* **1999**, *50* (3-4), 253–254.
40. Lavigne, V.; Pons, A.; Dubourdieu, D. Assay of glutathione in must and wines using capillary electrophoresis and laser-induced fluorescence detection: Changes in concentration in dry white wines during alcoholic fermentation and aging. *J. Chromatogr. A* **2007**, *1139* (1), 130–135.
41. Riboulet, J. M.; Alegoet, C. Le liège. In *Aspects pratiques du bouchage des vins*; Bourgone Publication: La Chapelle-de-deGuinchay- France, 1986.
42. Casey, J. A. Closures for wine bottles - a user's point of view. *Aust. Grapegrower Winemaker* **1989**, *4*, 99–107.
43. Lopes, P.; et al. Main Routes of Oxygen Ingress through Different Closures into Wine Bottles. *J. Agric. Food Chem.* **2007**, *55* (13), 5167–5170.
44. Ribereau-Gayon, J. Dissolution d'oxygène dans les vins. In *Contribution à l'étude des oxidations et réductions dans les vins*; Delmas, Ed.; Bordeaux, 1933.
45. Lopez, P. L'etude des phénomènes oxydatifs pendant le vieillissement des vins en bouteille. Role de l'obturateur. In *Faculté d'Oenologie*; Ségalen, Victor, Ed.; Bordeaux 2: Bordeaux, 2005 p. 211.
46. Squarzoni, M.; Limbo, S.; Piergiovanni, L. Proprietà barriera all'ossigeno di differenti tipologie di tappi per vino. *Ind. Bevande* **2004**, *33*, 113–116.
47. Sanchez, J.; Aracil, J. M. Gaseous permeability of different obturators. *Bull. l'O.I.V.* **1998**, *71*, 279–283.

48. Lopes, P.; Saucier, C.; Glories, Y. Nondestructive colorimetric method to determine the oxygen diffusion rate through closures used in winemaking. *J. Agric. Food Chem.* **2005**, *53* (18), 6967–6973.
49. Vidal, J. C.; Boulet, J. C.; Moutonet, M. Les apports d'oxygène au cours des traitements des vins. Bilan des observations sur sites. *Rev. Française d'œnologie* **2004**, *205*, 25–33.
50. Tabart, J.; et al. Comparative antioxidant capacities of phenolic compounds measured by various tests. *Food Chem.* **2009**, *113* (4), 1226–1233.
51. Lavigne, V. Role du glutathion sur l'évolution aromatique défectueuse des vins blancs secs au cours de l'élevage et de la conservation en bouteilles. In *VII^eme Symposium International d'Oenologie*; Bordeaux: 2003.

Publication Date (Web): November 24, 2015 | doi: 10.1021/bk-2015-1203.ch015

Publication Date (Web): November 24, 2015 | doi: 10.1021/bk-2015-1203.ch016

Chapter 16

Evolution of Anthocyanin-Derived Compounds during Micro-Oxygenation of Red Wines with Different Anthocyanin-Flavanol Ratios

Dominik Durner,[*,1,2] Patrick Nickolaus,[1] Fabian Weber,[3] Hai-Linh Trieu,[1] and Ulrich Fischer[1]

[1]Dienstleistungszentrum Ländlicher Raum Rheinpfalz, Competence Center for Wine Research, Breitenweg 71, D-67435 Neustadt/Weinstrasse, Germany
[2]Hochschule Kaiserslautern, Department of Applied Logistics and Polymer Sciences, Carl-Schurz-Strasse 10, D-66953 Pirmasens, Germany
[3]Institute of Nutritional and Food Sciences, Chair of Food Technology and Food Biotechnology, University of Bonn, Römerstrasse 164, D-53117 Bonn, Germany
[*]E-mail: dominik.durner@dlr.rlp.de.

The continuous addition of oxygen, referred to as micro-oxygenation (MOX), is a technique mimicking the slow oxygen ingress taking place in barrel ageing. The objective of this study was to monitor the concentration changes in anthocyanin-derived compounds during MOX and to draw conclusions on the polymerization processes of anthocyanins and flavanols in red wine. A 2013 Pinot noir was treated with MOX applying different oxygen dosages. The flavanol-to-anthocyanin ratio was changed prior to MOX by the addition of a commercial tannin preparation. Color intensity, acetaldehyde, and polymeric pigments were monitored during MOX and compared with concentration changes of ethylidene-bridged anthocyanin-flavanol adducts and vitisin B. Photometric analysis revealed a continuous increase in color intensity. More oxygen and a higher flavanol-to-anthocyanin ratio synergistically amplified the increase in color. MOX was also associated with an accumulation of acetaldehyde. While acetaldehyde was noticeably affected by the amount of oxygen applied, an altered flavanol-to-anthocyanin ratio

In Advances in Wine Research; Ebeler, et al.;
ACS Symposium Series; American Chemical Society: Washington, DC, 2015.

had no significant influence on its accumulation. Anthocyanin and flavanol concentrations decreased due to MOX. This observation was accompanied by an increase in polymeric pigments, explaining the enhanced color intensity. Higher flavanol-to-anthocyanin ratio amplified the formation of large polymeric pigments in particular. MOX increased concentrations in vitisin B (+4 mg/L), ethylidene-bridged malvidin-3-glucoside-(epi)catechin dimer (+10 mg/L), and double ethylidene-bridged (epi)catechin-malvidin-3-glucoside-(epi)catechin trimer (+6 mg/L). Different to color and polymeric pigments, vitisin B and ethylidene-bridged dimers reached a constant concentration and decreased after turning off MOX suggesting that these compounds are intermediates in polymerization reactions. In contrast, the concentration of the double ethylidene-bridged trimers increased linearly showing that trimers are formed out of dimers. While higher flavanol-to-anthocyanin ratio amplified the increase in ethylidene-bridged trimers, vitisin B and dimers were not affected. Hence, a higher flavanol-to-anthocyanin ratio is thought to particularly promote the formation of large(r) polymeric pigments.

Publication Date (Web): November 24, 2015 | doi: 10.1021/bk-2015-1203.ch016

Introduction

Many studies examining oxygen-induced changes in red wines have claimed that small amounts of oxygen promoted balanced tannicity (*1–4*), enhanced fruit aroma (*4*, *5*), and improved color (*6–9*). On the other hand, oxygen can also cause detrimental changes in red wines such as browning, lighter color, oxidized aroma, and dry tannins (*2*, *4*, *10*, *11*). Reactions triggered by oxygen in red wine include the oxidation of phenolics with vicinal hydroxyl groups yielding highly reactive quinones and hydrogen peroxide (*12–14*), the oxidation of ethanol to acetaldehyde (*12*, *15*), and the formation of anthocyanin derivatives, polymeric pigments, and other polymerized polyphenols (*16–19*). Knowledge of these compounds, their reactions, and their sensory impact on red wine has increased over the last decades. It is therefore feasible to monitor reaction processes that allow controlling oxygen-induced reactions during red winemaking.

Since its commercial release in 1996, micro-oxygenation (MOX) has become a common practice and is now used worldwide. Although many articles have been written on reaction products occurring upon MOX, only a few scientific studies addressed the necessity to monitor and to control the oxygen-induced changes during the MOX process or proposed analytical parameters for that purpose. Carlton, et al. (*20*) suggested to monitor the acetaldehyde concentration by means of a HS-SPME-GC technique as an effective method for determining the endpoint for the MOX process. More recently, several researchers focused on the monitoring of dissolved oxygen (DO) concentrations during MOX (*21–25*) because DO indicates the balance between the consumption and dissolution of

oxygen in wine. There is no doubt that acetaldehyde and DO recordings are useful to control the MOX process. However, the limitations of these methods should be considered as well. Both DO and acetaldehyde only consider initial reactants of oxidation reactions in red wine. The objectives of MOX to improve color and/or to soften green astringency are not regarded by these measures.

Color and astringency of red wines are driven by phenolic substances, which are extracted during winemaking and modified during wine elaboration and aging. Among these phenolic substances, anthocyanins and the flavanols (+)-catechin and (-)-epicatechin are of special interest, because these are the most abundant in red wines, can be easily evaluated by HPLC-DAD analysis, and are highly reactive upon exposure to oxygen. Via the oxygen-induced formation of acetaldehyde, anthocyanins and flavanols can react to compounds such as ethylidene-bridged anthocyanin-flavanol-adducts (*26–28*) and – without the participation of flavanols – to ethylidene-bridged anthocyanin dimers (*29*) or vitisin B (*30*, *31*) and – without the contribution of anthocyanins – to ethylidene-bridged flavanol dimers (*32*, *33*). As a result, the concentrations of anthocyanins and flavanols decrease during MOX (*6*, *8*, *9*). Fulcrand, et al. (*34*) emphasized that the ratio of flavanols to anthocyanins is of prime importance for phenolic composition changes, because both compounds compete as nucleophilic species in acetaldehyde-induced reactions. It would therefore be conceivable that a relatively high concentration in anthocyanins (A >> F) entails a vast increase in anthocyanin derivatives such as ethylidene-bridged anthocyanin dimers or vitisin B (Figure 1). A more balanced ratio between anthocyanins and flavanols (A ≈ F) should yield more ethylidene-bridged anthocyanin-flavanol dimers. An excess in flavanols (F >> A) could lead to the formation of ethylidene-bridged oligomers with a higher proportion of flavanols incorporated.

Ethylidene-bridged anthocyanin-flavanol adducts are known to shift wine color to purple hue, enhance color intensity, and increase the resistance to sulphite bleaching and pH changes. However, experiments in model solutions showed that these pigments are not stable over time (*35*, *36*). Interestingly, the color of micro-oxygenated wines was reported to be stable for at least 20 months (*37*), raising the question whether ethylidene-bridged anthocyanin-flavanol dimers can be responsible for oxygen-induced color changes or not.

Vitisin B is generally described as a highly stable pigment although results from Morata, et al. (*38*) suggest that concentrations may decrease over time. The pyranoanthocyanin is an orange pigment (*34*) and may cause browning in red wines (*39*). Other compounds responsible for unpleasant color changes due to MOX have not been described yet. However, it is feasible that MOX can also lead to less-colored compounds.

The oro-sensory characteristics of polymeric pigments and proanthocyanidins have been thoroughly investigated by different authors. The astringency is reported to increase with the degree of polymerization of proanthocyanidins (*40–42*). The bitterness decreases with an increasing molecular weight of proanthocyanidins (*43*). More recent findings showed that astringency does not only depend on the degree of polymerization but also on the composition of the polymers. Vidal et al. (*44*) assumed that adducts between proanthocyanidins and anthocyanins are less astringent than pure proanthocyanidins. Accordingly,

Publication Date (Web): November 24, 2015 | doi: 10.1021/bk-2015-1203.ch016

the authors concluded that the attenuation and smoothing of the mouth-feel may be explained by polymerization processes between proanthocyanidins and anthocyanins. More recently Weber, et al. (*45*) showed that a high degree of anthocyanins incorporated in polymeric pigments is responsible for a balanced mouth-feel and less unripe astringency perception.

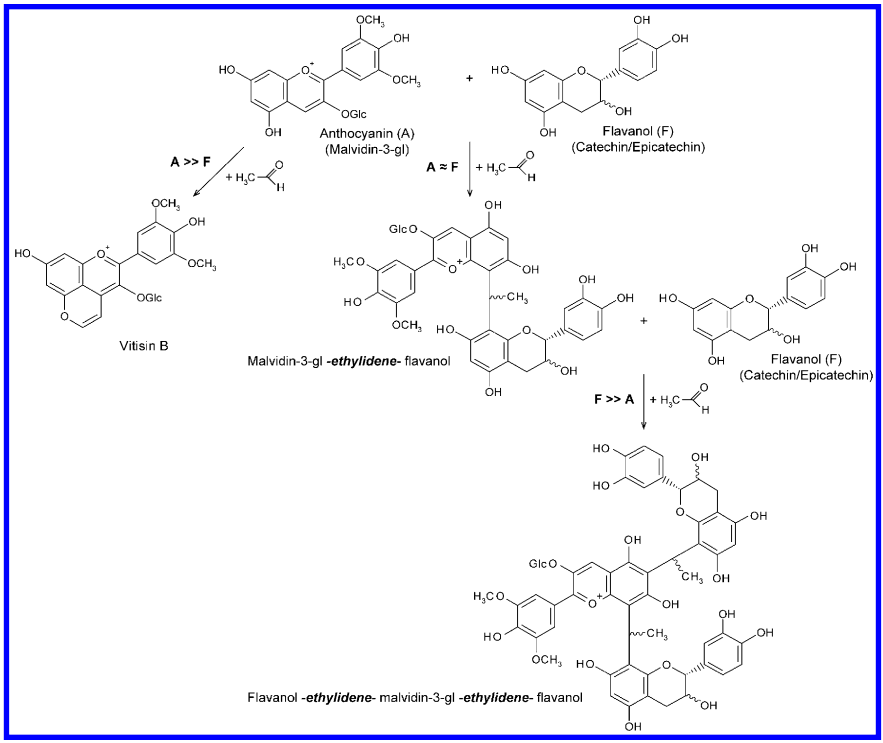

Figure 1. Acetaldehyd induced formation of anthocyanin derivatives depending on the relative proportion of anthocyanins (A) and flavanols (F).

From a winemaker's perspective, it is desirable to promote deeply colored and palatable anthocyanin-flavanol adducts instead of vitisin B or other weakly colored pigments or harsh tannins. Besides aforementioned chemical theory (*34*) there is only few empirical knowledge about the relation between the flavanol-to-anthocyanin ratio, the amount of oxygen, and the formation of pigments contributing to a stable color and a soft mouth-feel. In this study, a 2013 Pinot noir wine was treated with 10 or 20 mg O_2/L/month for 12 weeks after malolactic fermentation or elaborated without MOX becoming the control wine. Before alcoholic fermentation, an aliquot of the Pinot noir must was supplemented with commercial grape seed tannins approaching a different flavanol-to-anthocyanin ratio. The tannin wine was also treated with 10 mg O_2/L/month for 12 weeks after malolactic fermentation or left untreated becoming the tannin control wine. Process-related analysis of color, acetaldehyde, and

Publication Date (Web): November 24, 2015 | doi: 10.1021/bk-2015-1203.ch016

polymeric pigments was used to control the efficacy of MOX. Monitoring of different anthocyanin-derived compounds allowed to identify primary and secondary reaction products, to make considerations about the stability of anthocyan-flavanol adducts and vitisin B, and to understand polymerization processes resulting in anthocyan-flavanol adducts with multiple ethylidene bridges.

Materials and Methods

Winemaking

Vitis vinifera L. cv. Pinot noir, clone Mariafeld, grapes were harvested from a vineyard in Oberderdingen (Württemberg, Germany) on 12 Oct in 2013. Prior to alcoholic fermentation, de-stemmed and crushed grapes were heated to 82 °C for 2 min and cooled down to 40°C for depectinization using 30 µL/L pectinase (Trenolin Frio DF, Erbsloeh, Geisenheim, Germany). After 13.5 h, grapes were pressed and the juice was clarified using a separator. An aliquot of the clarified juice was supplemented with 200 mg/L grape seed tannins (UVATANN ST, Ever Intec, Pramaggiore, Italy). Both, tannin supplemented and regular musts were inoculated with 200 mg/L of the hydrated Mycoferm Cru 05 yeast strain according to manufacturer's instructions (Ever Intec, Pramaggiore, Italy). After two days, the two batches were inoculated with the Extremo IT14 strain (Ever Intec, Pramaggiore, Italy) to initiate malolactic fermentation (MLF). During alcoholic fermentation and simultaneous MLF, tannin supplemented and regular wines were kept at 20 °C.

Micro-Oxygenation

Fourteen days after completion of MLF, the two wines were racked off the solids omitting sulphite addition, were subdivided into portions of 100 L, and transferred to sealable stainless steel tanks with a diameter of 200 mm and a height of 3200 mm for MOX experiments. Reception tanks and pipelines were flushed with nitrogen before filling to remove atmospheric oxygen. Two different MOX treatments with oxygen dosages of 10 and 20 mg O_2/L/month were started for a period of 12 weeks at a constant temperature of 15 °C in duplicate. Oxygen delivery was conducted using food grade oxygen (BIOGON O E948, Linde Gas, Pullach, Germany), a VinO_2 MOX system (Ever Intec, Pramaggiore, Italy), and ceramic diffusers with a pore size of 0.4 µm (Thonhauser, Perchtolsdorf, Austria). The diffusers were suspended approximately 200 mm above the bottom of the tanks. Besides MOX treatments, control batches of the same two wines were stored without oxygen addition for the same time period at the same temperature in duplicate (→ "control" and "tannin control"). Regardless of the treatment applied, all batches were elaborated in identical tanks. Upon completion of MOX, all experimental batches were sulphited by consecutive additions of SO_2 in order to achieve a stable level of 35 mg/L free SO_2.

Publication Date (Web): November 24, 2015 | doi: 10.1021/bk-2015-1203.ch016

Publication Date (Web): November 24, 2015 | doi: 10.1021/bk-2015-1203.ch016

Chemicals

Acetaldehyde (99.5 %), (+)-catechin hydrate (98 %), (-)-epicatechin (90 %), formic acid (LC-MS grade), glyoxal (40 %, w/v) phosphoric acid (85 %) and potassium dihydrogen phosphate (HPLC grade) were purchased from Sigma-Aldrich (Taufkirchen, Germany). Acetonitrile (gradient grade), ethanol (p.a.), potassium iodide (p.a.), sodium hydroxide pellets (p.a.) and sulfuric acid (95-98 %) were purchased from Applichem (Darmstadt, Germany). Iodide/Iodate concentrate for 1L standard solution (1/128 M) was purchased from Merck Chemicals (Darmstadt, Germany). Malvidin-3-glucoside chloride (85 %) and cyanidin-3-rutinoside chloride (97 %) were purchased from Phytoplan (Heidelberg, Germany). The ethylidene-bridged cyanidin-3-glucoside-catechin dimer and the double ethylidene-bridged catechin-cyanidin-3-glucoside-catechin trimer were synthesized by the Institute of Food Chemistry, Technische Universität Braunschweig as previously described (*35*). Deionized water was purified to HPLC grade using a Millipore Milli-Q water purification system (Bedford, MA).

Chemical Analyses

Titratable acidity (TA), malic acid, pH, volatile acidity (VA), reducing sugar, and ethanol were determined using Fourier transform mid-infrared (FT-MIR) spectroscopy including the appropriate calibration method for red wine (Foss WineScan FT120 Basic, Hillerød, Denmark). Free and total SO_2 were analyzed by redox titration with iodide/iodate using an automatic titrator T50 with voltammetric indication (Mettler Toledo, Gießen, Germany). For measuring free SO_2, 2.5 mL of potassium iodide (10 %, w/v) and 5 mL sulfuric acid (5 N) were added to 25 mL of the sample and titrated with iodide/iodate solution (3.91 mmol/L). Total SO_2 content was determined by adding 10 mL sodium hydroxide solution (2 N) to 25 mL of the sample. After 10 min incubation time, the sample was neutralized with 5 mL of sulfuric acid and titrated as described above. Reductone content was analyzed as described for free SO_2 after addition of 5 mL glyoxal to 25 mL sample and after incubation for 5 min. Reductone content was subtracted from free and total SO_2 values.

Acetaldehyde was analyzed by means of HS-GC/FID using a CE Instruments GC 8000 Top (Wigan, UK). The carrier gas was supplied through the headspace (HS) sampler by connecting the PerkinElmer TurboMatrix HS 40 Trap (Waltham, MA) directly to the GC. To obtain vapor-liquid phase equilibrium, 10 ml of the sample was filled in a 22.5 ml vial pre-flushed with argon and heated to 45 °C for 50 min. The needle and the transfer line temperature of the HS sampler were set to 115 °C. The injection time was 1.2 s. The separation was carried out by using serially coupled columns: 10 m polar phase CP-Sil-19 CB with 0.53 mm ID and 2.00 µm FT and 30 m apolar phase DB-1 with 0.53 mm ID and 3.00 µm FT (both Agilent Technologies, Santa Clara, CA). Nitrogen was used as carrier gas at a pressure of 25 kPa. The injector temperature was set to 150 °C and the FID to 220 °C. The following GC oven temperature program was used: 32 °C for 5 min, 40 °C/min to 200 °C, hold for 5 min. The calibration curve was established

by adding different amounts of acetaldehyde to one random sample per sampling series. The obtained standard addition plot was applied to the rest of the samples.

Color density, calculated as the sum of absorbance at 620, 520, and 420 nm (*46*), was measured by a Cary 100 double-beam spectrophotometer (Varian, Palo Alto, CA). Large polymeric pigments (LPP), small polymeric pigments (SPP), and tannin concentrations were analyzed by means of the Harbertson-Adams Assay as described by Harbertson, et al. (*47*) and Harbertson, et al. (*48*).

Anthocyanins and the flavanols (+)-catechin and (-)-epicatechin (in the following referred to as flavanols) were quantified by HPLC-DAD using a PU-2080 Plus Intelligent HPLC Pump, a DG-2080-53 3-Line Degasser, a LG-2080-02 Ternary Gradient Unit, a AS-2057 Plus Intelligent Sampler, a CO-2060 Plus Intelligent Column Oven, and a MD-2010 Plus Multiwavelength Detector (Jasco, Groß-Umstadt, Germany). The column was a Gemini NX-C18, 250 x 4.6 mm, 5 µm, 110 Å (Phenomenex, Aschaffenburg, Germany) equipped with a guard column of the same material and kept at 40 °C. For preparation of eluents phosphate buffer was used: 1.36 g (10 mmol) KH_2PO_4 in Milli-Q water, pH adjusted to 1.5 by phosphoric acid. The two eluents were composed as follows: Eluent A: 95 % phosphate buffer, 5 % acetonitrile; Eluent B: 50 % phosphate buffer, 50 % acetonitrile. The following binary gradient was used with a flow rate of 1.2 mL/min: 0 min: 100 % A; 12 min: 88 % A; 12-18 min: 88 % A; 37.5 min: 49 % A; 38 min: 25 % A; 38-41 min: 25 % A; 42 min: 100 % A; 42-43 min: 100 % A. The injection volume was 20 µL. The detection wavelengths were 520 nm for anthocyanins and 280 nm for the flavanols (+)-catechin and (-)-epicatechin. Anthocyanins were quantified using malvidin-3-glucoside, flavanols were quantified using (+)-catechin and (-)-epicatechin as external standards prepared in ethanol/water (12/88, v/v). Five working standards per compound were prepared by diluting primary standards using the same solvent.

Publication Date (Web): November 24, 2015 | doi: 10.1021/bk-2015-1203.ch016

LC-Q-ToF-MS Analyses

A 6530 Accurate-Mass QToF LC/MS (Agilent, Santa Clara, CA) with electrospray ionization (ESI) was connected to a 1260 UHPLC station (Agilent, Waldbronn, Germany). The column was a Kinetex RP-18 endcapped 150 × 2.1 mm, 2.6 µm, 100 Å (Phenomenex, Aschaffenburg, Germany) which was kept at 40 °C. The following binary gradient was used with a flow rate of 0.4 mL/min: 0-2 min: 100 % A; 18 min: 30 % A; 22 min: 0 % A; 22-23 min: 0 % A; 24-31 min: 100 % A, with eluent A being water/acetonitrile/formic acid (93/5/2, v/v/v) and eluent B being water/acetonitrile/formic acid (5/93/2, v/v/v). Mass spectrometry data was acquired in the positive ionization mode. The nebulizer was set to 35 psig. The gas temperature was 320 °C, the gas flow was adjusted to 8 L/min. The sheath gas temperature was kept at 380 °C, the sheath gas flow was 11 L/min. The capillary and fragmentor voltage were maintained at 3000 and 170 V, respectively. Before injection, each sample was spiked with 1 ppb cyanidin-3-rutinoside (IStd). Vitisin B was quantified using malvidin-3-glucoside as an external standard. Four isomers of the ethylidene-bridged malvidin-3-glucoside-(epi)catechin dimer were quantified

using the ethylidene-bridged cyanidin-3-glucoside-catechin dimer. Four isomers of the double ethylidene-bridged (epi)catechin-malvidin-3-glucoside-(epi)catechin trimer were quantified using the double ethylidene-bridged catechin-cyanidin-3-glucoside-catechin trimer. All standards were prepared in ethanol/water (12/88, v/v). Five working standards per compound were used to establish calibration curves. The quantification was conducted using the quasi molecular ions [M+H$^+$] in MS mode. All compounds named above were identified using exact masses of molecular ions and fragmentation patterns. As an example for the identification procedure, the fragmentation spectrum of the trimer is shown in Figure 2. The quasi molecular ion at m/z=1125.3196 [M+H$^+$] is cleaved into three fragment ions. The first at m/z=835.2432 [M+H$^+$-290] results from the elimination of a (epi)catechin unit; the second at m/z=545.1656 [M+H$^+$-290-290] from both (epi)catechin units; and the third at m/z=383.1114 [M+H$^+$-290-290-162] from both (epi)catechin units and the glucose moiety from the malvidin-3-glucoside.

Publication Date (Web): November 24, 2015 | doi: 10.1021/bk-2015-1203.ch016

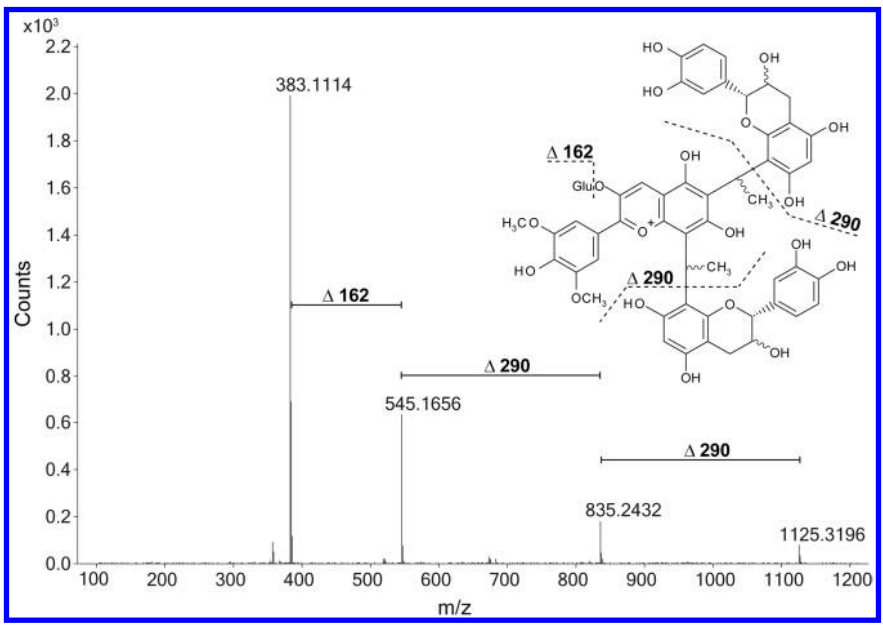

Figure 2. Fragmentation pattern of the double ethylidene-bridged (epi)catechin-malvidin-3-glucosid-(epi)catechin trimer in wine treated with 20 mg O2/L/months.

Statistical Analyses

Data was processed using one-way ANOVA. The least significant difference (LSD) test was used to determine statistically different values at a significance level of $p < 0.05$. Statistical analyses were performed using XLSTAT (version 2011.4.04, Addinsoft, Paris, France).

Results and Discussion

Chemical Composition of the Wine before and after MOX

Prior to MOX, the wine composition was ethanol, 12.5 % vol.; reducing sugar, < 1 g/L; pH, 3.7; titratable acidity, 4.8 g tartaric acid equivalents/L; malic acid, < 0.1 g/L; and volatile acidity, 0.55 g/L. The anthocyanin concentration was 135 g/L (Table 1). The addition of 200 mg/L condensed tannins caused a significant increase of 43 mg/L in tannin concentration and 15 mg/L in flavanol concentration. Accordingly, the flavanol-to-anthocyanin ratio was 25 % higher in the tannin supplemented wine.

After 12 weeks MOX, anthocyanin concentration decreased 13 % in the control wine, 21 % in the wine treated with 10 mg O_2/L/months, and 40 % in the wine treated with 20 mg O_2/L/months (Table 1). Flavanols showed a decrease of 17 % in the control wine, 24 % in the wine treated with 10 mg O_2/L/months, and 36 % in the wine treated with 20 mg O_2/L/months. In tannin supplemented wines, anthocyanins decreased 15 % in tannin control wine and 28 % in wine treated with 10 mg O_2/L/months. The flavanols (+)-catechin and (-)-epicatechin declined 22 % in the tannin control wine and 26 % in the wine treated with 10 mg O_2/L/months. The decrease in anthocyanins and flavanols is well described in literature and indicates polymerization and derivatization reactions of polyphenols (*6*, *8*, *9*). In fact, the formation of polymeric pigments was significantly amplified by MOX. While the control wine showed 41 % higher readings in polymeric pigments after 12 weeks, the MOX treated wines showed an increase of 76 % and 157 % for the oxygen dosages 10 mg O_2/L/months and 20 mg O_2/L/months. The tannin supplemented wine yielded 87 % more polymeric pigments after 12 weeks MOX with 10 mg O_2/L/months. Thus, tannin supplementation may be regarded as an accelerating factor for the MOX induced formation of polymeric pigments. A similar observation has been recently made by Oberholster, et al. (*49*) who concluded that the synergistic effect between MOX and tannin addition is a result of an increased acetaldehyde formation. Similar to polymeric pigments, tannin concentrations were higher in MOX treated wines suggesting that oxygen promoted the formation of tannic structures from low molecular weight flavonoids which was also observed by Del Carmen Llaudy, Canals, Gonzalez-Manzano, Canals, Santos-Buelga and Zamora (*3*). As MOX is often discussed in the context of a higher SO_2 demand in wines, the SO_2 concentrations were determined after bottling. Free SO_2 concentrations were similar in all treatments ranging from 34 to 38 mg/L. Total SO_2 showed no significant differences either, except for the wine treated with 20 mg O_2/L/month (Table 1). However, 109 mg/L total SO_2 may be still tolerable as the value is not atypical for commercial red wines.

Publication Date (Web): November 24, 2015 | doi: 10.1021/bk-2015-1203.ch016

Publication Date (Web): November 24, 2015 | doi: 10.1021/bk-2015-1203.ch016

Table 1. Impact of Tannin Addition and Oxygen Dosage on the Chemical Composition of the Wine before and after MOX

	Tannin addition[b] (mg/L)	*Oxygen dosage[c] (mg/L/month)*	*Anthocyanins (mg/L Mv-3-gl eq.)*	*Flavanols[d] (mg/L Catechin eq.)*	*Flavanol/ anthocyanin-ratio (w/w)*	*Polymeric Pigments (AU)*	*Tannins (mg/L Catechin eq.)*	*Free SO_2[e] (mg/L)*	*Total SO_2[e] (mg/L)*
Pre MOX	0		135 a	78 b	0.58	0.49 de	131 f		
	200		130 a	93 a	0.71	0.53 d	174 c		
Post MOX	0	0	117 b	65 cde	0.55	0.69 c	136 f	34 a	84 b
	0	10	107 c	59 ef	0.55	0.84 b	143 e	34 a	81 b
	0	20	81 e	50 fg	0.62	1.26 a	161 d	37 a	109 a
	200	0	111 bc	73 bc	0.66	0.76 bc	189 b	38 a	79 b
	200	10	94 d	69 cd	0.74	1.00 ab	203 a	34 a	86 b
p value[a]			*0.0074*	*0.0381*		*0.0244*	*0.0002*	*0.7301*	*0.0347*

[a] One-way ANOVA to compare data; n = 2: values sharing the same letter within a column are not significantly different at $p \geq 0.05$. [b] Tannin addition before alcoholic fermentation. [c] MOX treatment for 12 weeks. [d] Sum of (+)-catechin and (-)-epicatechin. [e] Free and total SO_2 were analyzed 4 weeks after completion of MOX.

Publication Date (Web): November 24, 2015 | doi: 10.1021/bk-2015-1203.ch016

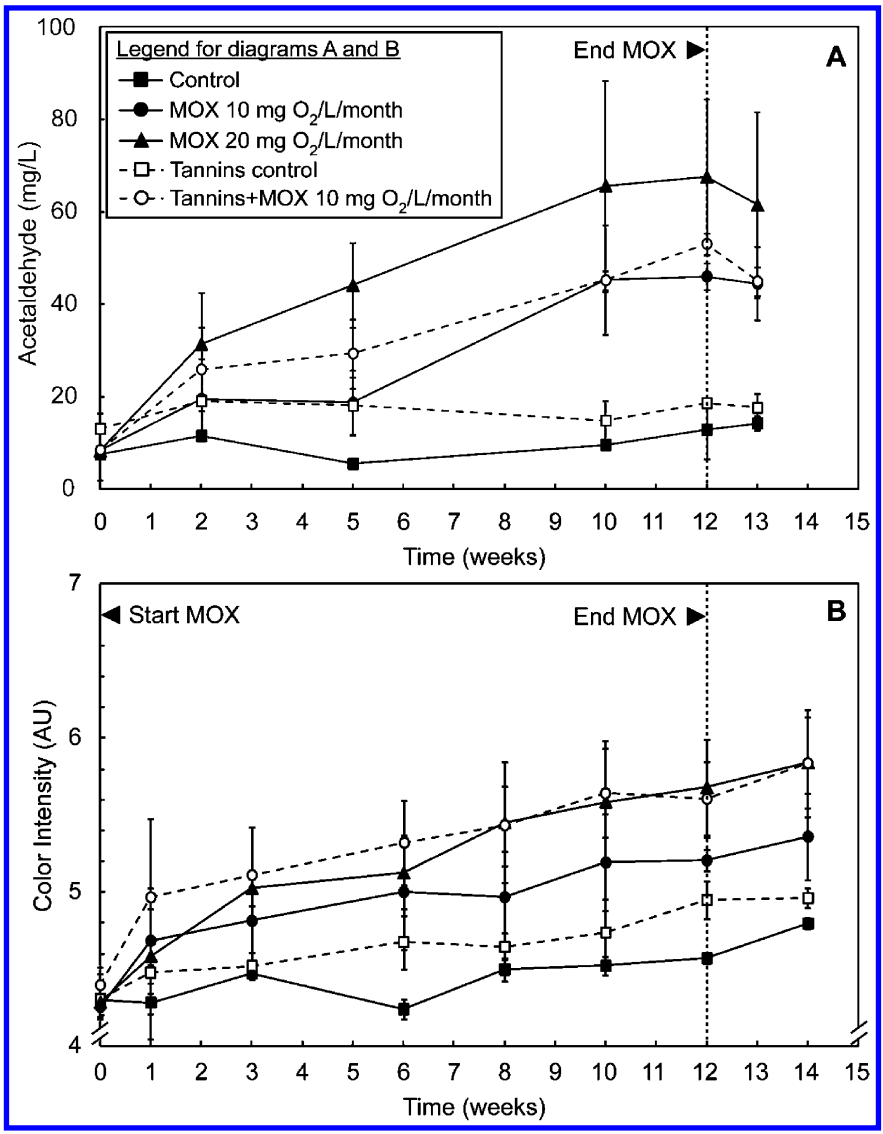

Figure 3. Evolution of color density (A) and acetaldehyde (B) during MOX with different oxygen dosage rates for wines with and without tannin supplementation.

Monitoring Acetaldehyde and Wine Color during MOX

As an intermediate product, acetaldehyde plays a major role during MOX as it is able to link certain flavanoid structures with each other. Liu and Pilone (*50*) reported that red wines contain 30 mg/L acetaldehyde on average. It can contribute to fruity aromas in red wine at low levels. At higher concentrations the wine aroma is considered a defect and is reminiscent of rotten apples. The sensory threshold of

acetaldehyde in wine ranges between 100-125 mg/L (*50*) and therefore any strong accumulation of acetaldehyde is supposed to determine the endpoint of MOX (*20*). Monitoring acetaldehyde in our study revealed increasing concentrations during 12 weeks MOX for the wine which was treated with 20 mg O_2/L/month (Figure 3 A). After 10 weeks, the concentration leveled off at 65 mg/L suggesting a state of equilibrium between formation and consumption of acetaldehyde. The low MOX dosage caused a slower and later increase in acetaldehyde finally reaching a concentration of 45 mg/L. After turning off MOX, acetaldehyde concentrations began to decrease. This observation suggests that the wine was capable to utilize excessive acetaldehyde. Therefore, the application of MOX must be regarded with a follow-up time which should be kept to reduce the acetaldehyde before SO_2 addition. Tannin addition caused slightly higher acetaldehyde concentrations for both, control and MOX treated wine. However, no synergistic effect was found between tannin addition and MOX treatment (Figure 3 A).

Monitoring color intensity revealed a steady increase throughout 12 weeks MOX for wines with and without tannin addition (Figure 3 B). While the color intensity in the control wine remained unchanged during the first six weeks, wines treated with MOX immediately inclined in color. At completion of MOX, the color intensity was increased by 10 % in the control wine, by 23 % in the wine which was treated with 10 mg O_2/L/month, and by 36 % in the wine which received twice the amount of oxygen. Accordingly, the color gain was 13 % per 10 mg O_2/L/month for three months. Tannin addition caused higher color intensity for both, control and micro-oxygenated wine. Particularly the micro-oxygenated wine showed a strong color increase: In fact, MOX with 10 mg O_2/L/month in tannin supplemented wines yielded similar color intensity as 20 mg O_2/L/month without tannin addition.

The amplification effect in color, observed for wines supplemented with tannins, is most likely due to a better utilization of the oxygen provided. Hypothetically, a higher tannin concentration could increase the formation of acetaldehyde via the Fenton reaction. And eventually, a higher acetaldehyde concentration may increase the yield of ethylidene-bridged anthocyanin-flavanol-adducts. However, tannin supplementation plus MOX yielded no higher acetaldehyde concentrations and can therefore not explain the observed amplification in wine color.

Evolution of Polymeric Pigments, Ethylidene-Bridged Anthocyanin-Flavanol-Adducts, and Vitisin B

The evolution of polymeric pigments is shown in Figure 4 A and B. Both, SPP and LPP increased throughout the observation period for treated and untreated wines. The formation of polymeric pigments was faster when MOX was applied, which has been indicated several times before (*6*, *51*, *52*). In the last third of the experiment, different oxygen dosages could be distinguished from each other by means of SPP and LPP demonstrating that the method is capable to control oxygen-induced changes. Tannin addition caused higher values for both, SPP and LPP. While SPP were only slightly influenced, LPP readings were much higher upon MOX. Since polymeric tannins may be regarded as direct educts in reactions

Publication Date (Web): November 24, 2015 | doi: 10.1021/bk-2015-1203.ch016

with anthocyanins such as monomeric flavanols, a higher tannin concentration in the wine may have directely accelerated the oxygen-induced formation of LPP. The delayed increase of LPP may also allow the presumption that LPP were formed out of SPP in an ongoing polymerization process. Monomeric flavanols, which are increased by 20 % in the wine after adding the tannin preparation (Table 1), would, therefore, be responsible for a step-by-step growth of SPP eventually turing into LPP.

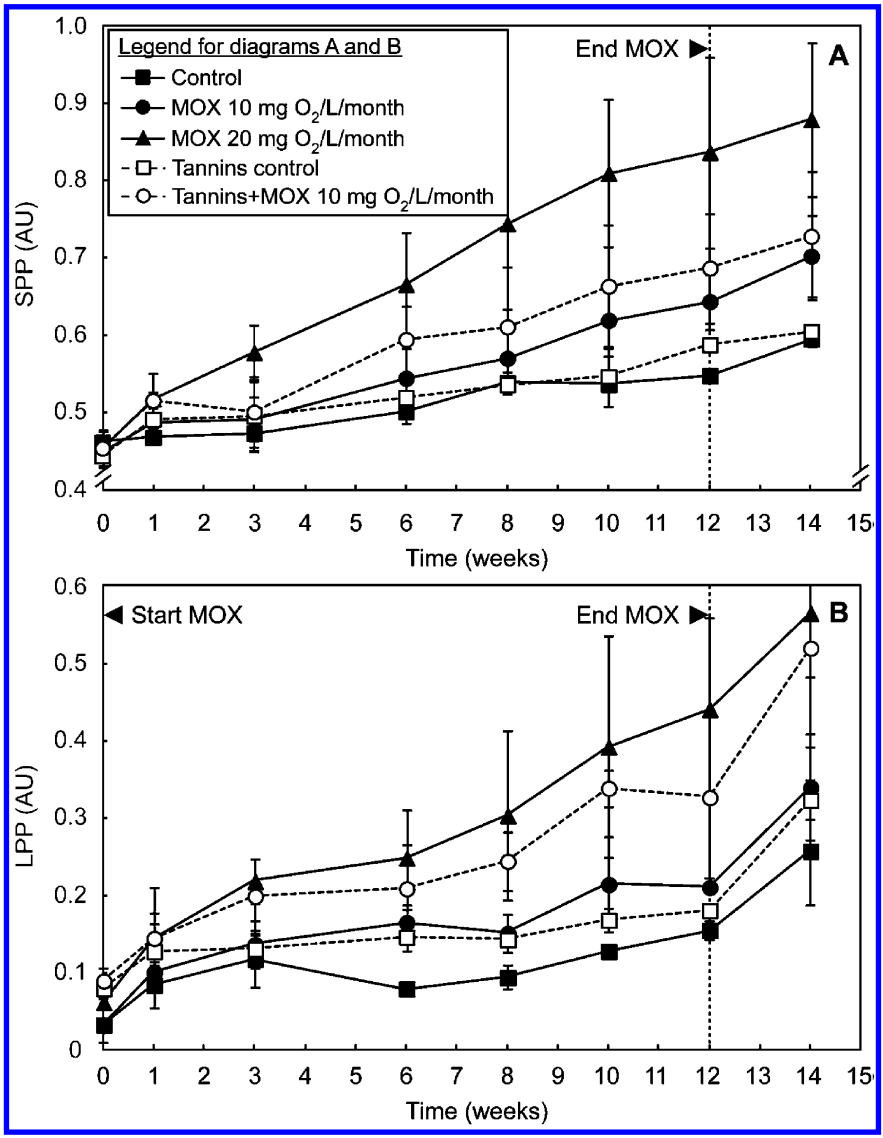

Figure 4. Evolution of Small Polymeric Pigments (A) and Large Polymeric Pigments (B) during MOX with different oxygen dosage rates for wines with and without tannin supplementation.

In Advances in Wine Research; Ebeler, et al.;
ACS Symposium Series; American Chemical Society: Washington, DC, 2015.

Publication Date (Web): November 24, 2015 | doi: 10.1021/bk-2015-1203.ch016

Monitoring vitsin B during the 14 weeks of observation revealed no changes for the untreated wine; the concentration was stable at 1.5 mg/L (Figure 5 A). The application of 10 mg O_2/L/months caused a continuous incline in vitisin B concentration finally reaching 4.5 mg/L. In contrast, an oxygen dosage of 20 mg O_2/L/months induced a steeper increase in vitisin B until week 4 reaching a concentration of 6.5 mg/L. From this point of time, vitisin B remained stable until the end of MOX after 12 weeks. After termination of oxygen supply, MOX treated wines showed decreasing vitisin B concentrations indicating that this compound is not stable, which is in good accordance with the findings of Morata, Calderón, González, Gómez-Cordovés and Suárez (*38*). Assuming that vitisin B is not subject to cleavage, the observed decrease in vitisin B concentration after MOX is attributed to polymerization reactions. Possible reaction products are directly linked vitisin B-flavanol adducts possessing the identical structure of vinylflavanol-pyranoanthocyanins (*53*) but formed by different reaction pathway. Furthermore it might be assumed that vitisin B acts as the anthocyanin moiety in ethylidene-bridged anthocyanin-flavanol adducts. Tannin addition showed, as expected, no effect on vitisin B concentration, neither in control nor in MOX treated wines.

The evolution of the ethylidene-bridged malvidin-3-glucoside-(epi)catechin dimer, which was quantified by the use of the isolated analytical standard, is shown in Figure 5 B. The control wine exhibited constant concentrations of around 7 mg/L during the 14 weeks of observation. MOX increased dimer concentrations within the first 4 weeks. Subsequently, the ethylidene-bridged dimer remained nearly stable exhibiting a steady state. The application of 10 mg O_2/L/months led to a maximum dimer concentration of 14 mg/L, the application of 20 mg O_2/L/months to 17 mg/L. After termination of MOX, the concentration of the ethylidene-bridged dimer started to decrease. The formation rate of the dimer was much faster compared to vitisin B, as well as the degradation rate after termination of oxygen supply. This suggests that the ethylidene-bridged dimer is (1) favored in oxygenation regimes and is (2) less stable (in the sense of consecutive reactions/further polymerization) than vitisin B. The dimer can be regarded as an intermediate because of the above described steady state and the degradation after MOX.

Tannin addition before alcoholic fermentation caused higher concentrations of the dimer prior to MOX ranging around 11 mg/L (Figure 5 B). The higher flavanol content due to tannin addition (Table 1) may have enhanced the production of ethylidene-bridged compounds already during alcoholic fermentation where acetaldehyde is released by the yeast. Interestingly, the MOX effect was quite similar for wines with and without tannin supplementation: the difference between “tannins control” and “tannins + 10 mg O_2/L/month” was not higher than the difference between “control” and “10 mg O_2/L/month”. This means that the initial concentration of flavanols (+)-catechin and (-)-epicatechin had no impact on the oxygen-induced formation of the ethylidene-bridged malvidin-3-glucoside-(epi)catechin dimer. At first sight, a higher educt concentration may be expected to increase product concentration. However, the assumption made above, describing the dimer as an intermediate in a

Publication Date (Web): November 24, 2015 | doi: 10.1021/bk-2015-1203.ch016

polymerization process, may explain why an altered educt concentration has no (or only minor) impact on product concentration.

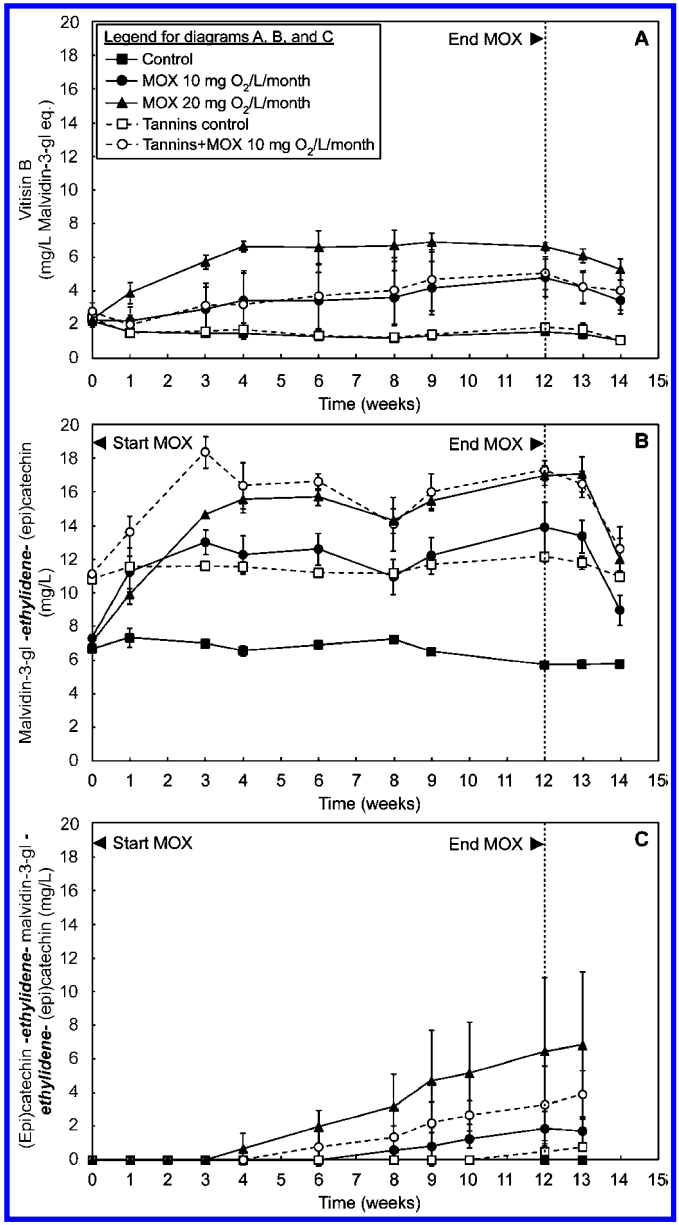

Figure 5. Evolution of vitisin B (A), ethylidene-bridged malvidin-3-glucoside-flavanol dimer (B), and double ethylidene-bridged flavanol-malvidin-3-glucoside-flavanol trimer (C) during MOX with different oxygen dosage rates for wines with and without tannin supplementation.

In Advances in Wine Research; Ebeler, et al.;
ACS Symposium Series; American Chemical Society: Washington, DC, 2015.

Publication Date (Web): November 24, 2015 | doi: 10.1021/bk-2015-1203.ch016

The concentration of the trimer, consisting of two (epi)catechin units, two ethylidene bridges and one anthocyanin unit, is shown in Figure 5 C. While the trimer was not found in the control wine during the 14 weeks of observation, its concentration started to increase linearly after 4 weeks MOX in the wine treated with 20 mg O_2/L/month and after 8 weeks in the wine treated with 10 mg O_2/L/month. At termination of oxygen supply, the concentrations of the double ethylidene-bridged (epi)catechin-malvidin-3-glucoside-(epi)catechin trimer were 7 mg/L and 2 mg/L for the high and low oxygen dosage. Within the observation period of 13 weeks, the formation rate of the trimer was not decelerated indicating a high stability compared to the dimer. As this trimer can only be formed in a subsequent reaction out of the ethylidene-bridged malvidin-3-glucoside-flavanol dimer, the increase of the trimer (1) explains the instability of dimer and (2) demonstrates on a molecular level that the formation of polymeric pigments from monomeric anthocyanins is a polymerization process in the sense of repetitive reactions.

A higher flavanol concentration due to the addition of tannins resulted in a faster increase of the trimer, which is again different to what was observed for the dimer earlier. Weber (*54*) recently made similar observations in a model wine with acetaldehyde, where higher initial flavanol concentrations did not change concentrations in ethylidene-bridged anthocyanin-flavanol dimers, but eventually increased the concentrations of trimers, tetramers, and pentamers with multiple ethylidene bridges. The observations made by Weber (*54*) and the findings presented in this study indicate that ethylidene-bridged anthocyanin-flavanol adducts can increase in size by means of the formation of further ethylidene bridges, but these are apparently not as favored as the formation of the first ethylidene bridge between two flavanoid molecules.

Figure 6A shows the molar loss in malvidin-3-glucoside and flavanols (sum of (+)-catechin and (-)-catechin) after 12 weeks MOX for all five treatments. The control wine exhibited a decline of 24 µM malvidin-3-glucoside and 42 µM flavanols. This finding indicates a higher reactivity of flavanols compared to malvidin-3-glucoside under non-oxidative conditions. The application of MOX caused a greater loss in both compounds, which has already been shown in Table 1 for total anthocyanins and flavanols on the basis of mass concentrations. Interestingly, with an increasing amount of oxygen, the molar loss of malvidin-3-glucoside and flavanols came into line, finally accounting for almost the same value when 20 mg O_2/L/month were applied. This can be explained by the vitisin B formation, which only occurred when MOX was applied (Figure 6 B). Of course, vitisin B may not be the only reason; oxygen could have also triggered the formation of polymeric species with a higher proportion of anthocyanins incorporated. The addition of tannins caused a larger drop in malvidin-3-glucoside and flavanols compared to the control wine (Figure 6 A). Again, the loss in flavanols was twice as much compared to malvidin-3-glucoside after 12 weeks. Ethylidene-bridged compounds (Figure 6 B) were slightly increased in the tannin control wine, which may be explained by the slightly higher acetaldehyde concentrations (Figure 3 A). This observation is also associated with higher readings in SPP and LPP (Figure 4 A and B). Analogous to the non-tannin wine, MOX caused a greater loss in malvidin-3-glucoside and flavanols (Figure

Publication Date (Web): November 24, 2015 | doi: 10.1021/bk-2015-1203.ch016

6 A); malvidin-3-glucoside was again disproportionally affected. The data in Figure 6 B reveals that vitisin B formation was not influenced by tannin addition. Looking at the ethylidene-bridged compounds, MOX in tannin wines caused a similar molar increase compared to non-tannin wines when 10 mg O_2/L/month were applied. However, trimer formation was greater at the expense of dimer formation suggesting that tannin addition promoted the -induced polymerization process. This observation is consistent with the findings earlier showing higher LPP readings in tannin wines upon MOX.

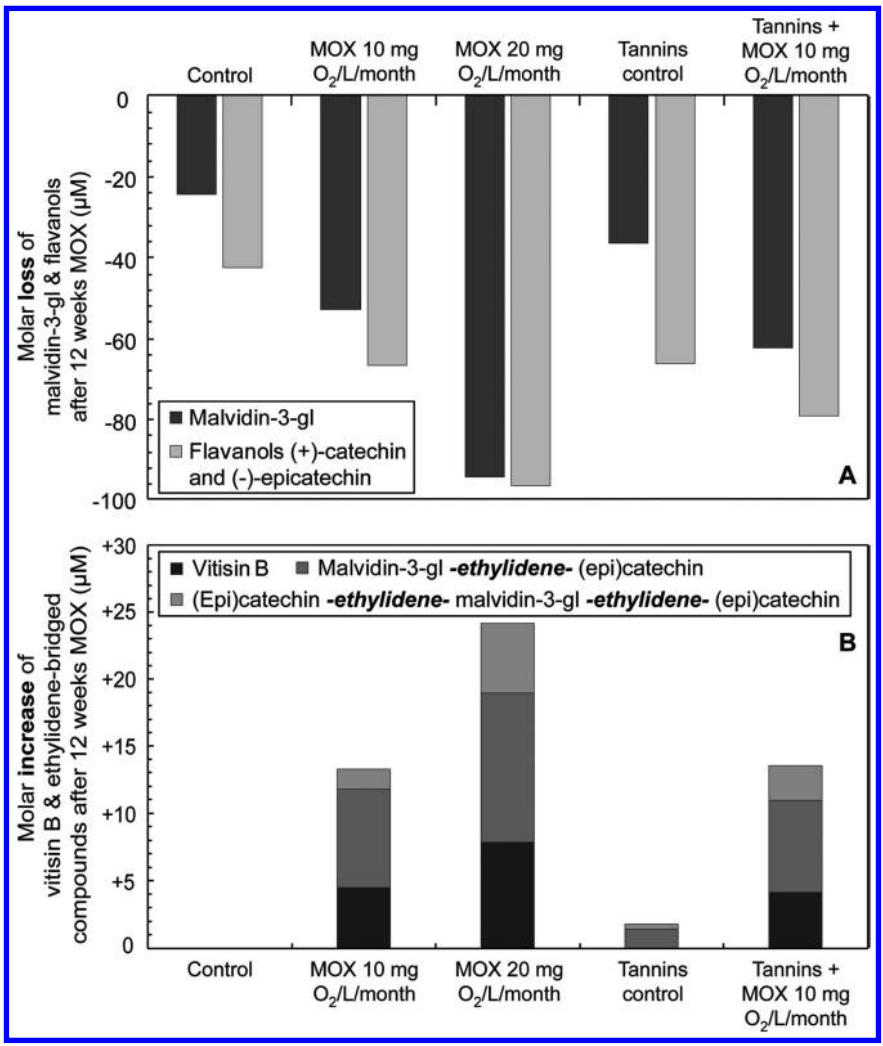

Figure 6. Molar loss of malvidin-3-glucoside and flavanols (A) and molar increase of vitisin B, ethylidenebridged malvidin-3-glucoside-flavanol dimer, and double ethylidene-bridged flavanol-malvidin-3-glucosideflavanol trimer (B) after 12 weeks MOX with different oxygen dosage rates for wines with and without tannin supplementation.

Publication Date (Web): November 24, 2015 | doi: 10.1021/bk-2015-1203.ch016

Publication Date (Web): November 24, 2015 | doi: 10.1021/bk-2015-1203.ch016

Table 2. Influence of MOX, Tannin Addition, and a Combined Application on Color, Educts, and Products Resulting from Oxygen Induced Reactions

	Micro-oxygenation	*Tannin addition*	*Synergistic effect*
Color	++	+	++
SPP	++	0	+
LPP	++	+	++
Acetaldehyde	+++	+	0
Anthocyanins	---	-	0
Flavanols	--	-	0
Ethylidene-bridged anthocyanin-flavanol dimer	++	++	0
Double ethylidene-bridged anthocyanin-flavanol trimer	++	+	+
Vitisin B	+	0	0

+++ strong increase; ++ increase; + slight increase; 0 no effect;--- strong decrease; -- decrease; -slight decrease.

Conclusions

The application of MOX significantly increased the color intensity of the treated Pinot noir wine. This increase was strongly dependent on the oxygen dosage applied. Although tannin addition without MOX had little impact on wine color, the combination of MOX and tannin addition revealed a strong synergistic effect (Table 2). Besides color increase, polymeric pigments were formed upon MOX. Compared to SPP, LPP formation was delayed suggesting that LPP are formed out of SPP. A changed flavanol-to-anthocyanin ratio due to tannin addition amplified the oxygen-induced formation of polymeric pigments, in particular the formation of LPP.

MOX was also accompanied with an alarming increase in acetaldehyde concentrations. However, after turning off MOX, acetaldehyde began to decrease immediately, recommending a follow-up time to be kept after MOX in order to reduce the SO_2 demand. Although tannin addition caused slightly higher acetaldehyde levels, tannin supplementation plus MOX did not amplify the acetaldehyde content in the wine (Table 2).

Anthocyanin and flavanol concentrations were decreased upon MOX treatment; anthocyanins were affected stronger than flavanols. Vice versa, MOX triggered the formation of ethylidene-bridged anthocyanin-flavanol oligomers as well as the formation of vitisin B (Table 2). The ethylidene-bridged malvidin-3-glucoside-(epi)catechin dimer and vitisin B quickly reached a constant concentration during MOX and decreased after stopping MOX. These findings clearly indicate that the ethylidene-bridged dimer and vitisin B are only intermediates in an ongoing polymerization process. In contrast, the concentration of the double ethylidene-bridged trimer increased linearly suggesting that trimers are formed in a subsequent reaction out of dimers. The oxygen-induced formation of the ethylidene-bridge dimer and vitisin B was quite similar for wines with and without tannin supplementation. However, the trimer formation in tannin wines was greater compared to non-tannin wines (Table 2) suggesting that tannin addition, and accordingly a higher flavanol-to-anthocyanin ratio, promotes oxygen-induced polymerization processes leading to adducts of high molecular weight.

Publication Date (Web): November 24, 2015 | doi: 10.1021/bk-2015-1203.ch016

Acknowledgments

This research project is supported by the German Ministry of Economics and Energy (via AiF) and the FEI (Forschungskreis der Ernährungsindustrie e.V., Bonn) in cooperation with the German Winegrowers' Association (DWV), project AiF 17719 N. The authors thank the Württembergische Weingärtner-Zentralgenossenschaft e. G. for donating the wines for this study. Ever Intec is acknowledged for providing enological supplies and the MOX equipment. The authors express gratitude to Hans-Georg Schmarr from the Competence Center for Wine Research for his expert advice in GC. Furthermore, the authors thank Florian Schraut from the Competence Center for Wine Research for his support in winemaking. We thank Peter Winterhalter from the Institute

Publication Date (Web): November 24, 2015 | doi: 10.1021/bk-2015-1203.ch016

of Food Chemistry at TU Braunschweig for providing the ethylidene-bridged compounds for quantification.

References

1. Loch, R. *Uses of Gases in Winemaking Conference*, Adelaide, Australia; Allen, M., Bell, S., Rowe, N., Wall, G., Eds.; Australian Society of Viticulture and Oenology: Adelaide, Australia, 2002; pp 45−53.
2. Parish, M.; Wollan, D.; Paul, R. *Aust N. Z. Grapegrower Winemaker* **2000**, *438A*, 47–50.
3. Del Carmen Llaudy, M.; Canals, R.; Gonzalez-Manzano, S.; Canals, J. M.; Santos-Buelga, C.; Zamora, F. *J. Agric. Food Chem.* **2006**, *54* (12), 4246–4252.
4. Durner, D.; Weber, F.; Neddermeyer, J.; Koopmann, K.; Winterhalter, P.; Fischer, U. *Am. J. Enol. Vitic.* **2010**, *61* (4), 474–485.
5. Cejudo-Bastante, M. J.; Hermosín-Gutiérrez, I.; Pérez-Coello, M. S. *J. Agric. Food Chem.* **2012**, *60* (23), 5962–5973.
6. Cano-Lopez, M.; Pardo-Minguez, F.; Lopez-Roca, J. M.; Gomez-Plaza, E. *Am. J. Enol. Vitic.* **2006**, *57* (3), 325–331.
7. Cano-Lopez, M.; Pardo-Minguez, F.; Lopez-Roca, J. M.; Gomez-Plaza, E. *Eur. Food Res. Technol.* **2007**, *225* (1), 127–132.
8. Cano-Lopez, M.; Pardo-Mínguez, F.; Schmauch, G.; Saucier, C.; Teissedre, P.-L.; Lopez-Roca, J. M.; Gomez-Plaza, E. *J. Agric. Food Chem.* **2008**, *56* (14), 5932–5941.
9. De Beer, D.; Joubert, E.; Marais, J.; Manley, M. *S. Afr. J. Enol. Vitic.* **2008**, *29* (1), 13–25.
10. Paul, R. *der Uses of Gases in Winemaking Conference*, Adelaide, Australia; Allen, M., Bell, S., Rowe, N., Wall, G., Eds.; Australian Society of Viticulture and Oenology: Adelaide, Australia, 2002; pp 18−22.
11. Lemaire, T. *La micro-oxygénation des vins*; Ecole Nationale Superieure Agronomique: Montpellier, France, 1995.
12. Danilewicz, J. C. *Am. J. Enol. Vitic.* **2003**, *54* (2), 73–85.
13. Wildenradt, H. L.; Singleton, V. L. *Am. J. Enol. Vitic.* **1974**, *25* (2), 119–126.
14. Waterhouse, A. L.; Laurie, V. F. *Am. J. Enol. Vitic.* **2006**, *57* (3), 306–313.
15. Fenton, H. J. H. *J. Chem. Soc., Trans.* **1894**, *65*, 899–910.
16. Cheynier, V.; Atanasova, V.; Fulcrand, H.; Mazauric, J.-P.; Moutounet, M. *der Uses of Gases in Winemaking Conference*, Adelaide, Australia; Allen, M., Bell, S., Rowe, N., Wall, G., Eds.; Australian Society of Viticulture and Oenology: Adelaide, Australia, 2002; pp 23−27.
17. Vernhet, A.; Dubascoux, S.; Cabane, B.; Fulcrand, H.; Dubreucq, E.; Poncet-Legrand, C. *Anal. Bioanal. Chem.* **2011**, *401* (5), 1559–1569.
18. Salas, E.; Fulcrand, H.; Meudec, E.; Cheynier, V. *J. Agric. Food Chem.* **2003**, *51* (27), 7951–7961.
19. Cruz, L.; Mateus, N.; de Freitas, V. *Rapid Commun. Mass Spectrom.* **2012**, *26* (18), 2123–2130.

20. Carlton, W. K.; Gump, B.; Fugelsang, K.; Hasson, A. S. *J. Agric. Food Chem.* **2007**, *55* (14), 5620–5625.
21. Durner, D.; Ganss, S.; Fischer, U. *Am. J. Enol. Vitic.* **2010**, *61* (4), 465–473.
22. Laurie, V. F.; Law, R.; Joslin, W. S.; Waterhouse, A. L. *Am. J. Enol. Vitic.* **2008**, *59* (2), 215–219.
23. Nevares, I.; Del Alamo, M. *Anal. Chim. Acta* **2008**, *621* (1), 68–78.
24. Nevares, I.; Del Alamo, M.; Carcel, L.; Crespo, R.; Martin, C.; Gallego, L. *Food Bioprocess Technol.* **2008**, *2* (3), 328–336.
25. Nevares, I.; del Alamo, M.; Gonzalez-Muñoz, C. *Anal. Chim. Acta* **2010**, *660* (1-2), 232–239.
26. Escribano-Bailon, T.; Dangles, O.; Brouillard, R. *Phytochemistry* **1996**, *41* (6), 1583–1592.
27. Es-Safi, N. E.; Fulcrand, H.; Cheynier, V.; Moutounet, M. *J. Agric. Food Chem.* **1999**, *47* (5), 2096–2102.
28. Timberlake, C. F.; Bridle, P. *Am. J. Enol. Vitic.* **1976**, *27* (3), 97–105.
29. Atanasova, V.; Fulcrand, H.; Cheynier, V.; Moutounet, M. *Anal. Chim. Acta* **2002**, *458* (1), 15–27.
30. Bakker, J.; Timberlake, C. F. *J. Agric. Food Chem.* **1997**, *45* (1), 35–43.
31. Fulcrand, H.; Benabdeljalil, C.; Rigaud, J.; Cheynier, V.; Moutounet, M. *Phytochemistry* **1998**, *47* (7), 1401–1407.
32. Drinkine, J.; Glories, Y.; Saucier, C. *J. Agric. Food Chem.* **2005**, *53* (19), 7552–7558.
33. Es-Safi, N. E.; Fulcrand, H.; Cheynier, V.; Moutounet, M. *J. Agric. Food Chem.* **1999**, *47* (5), 2088–2095.
34. Fulcrand, H.; Atanasova, V.; Salas, E.; Cheynier, V. The fate of anthocyanins in wine: Are there determining factors? In *Red Wine Color. Revealing the mysteries*; Waterhouse, A. L., Kennedy, J. A., Eds.; ACS Symposium Series Vol. 886; American Chemical Society: Washington, DC, 2004; pp 68−88.
35. Weber, F.; Winterhalter, P. *Food Res. Int.* **2014**, *65*, 69–76.
36. Escribano-Bailon, T.; Alvarez-Garcia, M.; Rivas-Gonzalo, J. C.; Heredia, F. J.; Santos-Buelga, C. *J. Agric. Food Chem.* **2001**, *49* (3), 1213–1217.
37. González-del Pozo, A.; Arozarena, Í.; Noriega, M.-J.; Navarro, M.; Casp, A. *Eur. Food Res. Technol.* **2010**, *231* (4), 589–601.
38. Morata, A.; Calderón, F.; González, M. C.; Gómez-Cordovés, M. C.; Suárez, J. A. *Food Chem.* **2007**, *100* (3), 1144–1152.
39. Rentzsch, M.; Weber, F.; Durner, D.; Fischer, U.; Winterhalter, P. *Eur. Food Res. Technol.* **2009**, *229* (4), 689–696.
40. Goldstein, J. L.; Swain, T. *Phytochemistry* **1963**, *2*, 371–383.
41. Lea, A. G. H.; Arnold, G. M. *J. Sci. Food Agric.* **1978**, *29* (5), 478–483.
42. Vidal, S.; Francis, L.; Guyot, S.; Marnet, N.; Kwiatkowski, M.; Gawel, R.; Cheynier, V.; Waters, E. J. *J. Sci. Food Agric.* **2003**, *83* (6), 564–573.
43. Noble, A. C. Astringency and Bitterness of Flavonoid Phenols. In *Chemistry of Taste*; ACS Symposium Series 825; American Chemical Society: Washington, DC, 2002; pp 192−201.
44. Vidal, S.; Francis, L.; Noble, A.; Kwiatkowski, M.; Cheynier, V.; Waters, E. *Anal. Chim. Acta* **2004**, *513* (1), 57–65.

45. Weber, F.; Greve, K.; Durner, D.; Fischer, U.; Winterhalter, P. *Am. J. Enol. Vitic.* **2013**, *64* (1), 15–25.
46. Glories, Y. *Connaiss. Vigne Vin* **1984**, *18*, 195–217.
47. Harbertson, J. F.; Kennedy, J. A.; Adams, D. O. *Am. J. Enol. Vitic.* **2002**, *53* (1), 54–59.
48. Harbertson, J. F.; Picciotto, E. A.; Adams, D. O. *Am. J. Enol. Vitic.* **2003**, *54* (4), 301–306.
49. Oberholster, A.; Elmendorf, B. L.; Lerno, L. A.; King, E. S.; Heymann, H.; Brenneman, C. E.; Boulton, R. B. *Food Chem.* **2015**, *173* (0), 1250–1258.
50. Liu, S.-Q.; Pilone, G. J. *Int. J. Food Sci. Technol.* **2000**, *35* (1), 49–61.
51. Du Toit, W. J.; Lisjak, K.; Marais, J.; Du Toit, M. *S. Afr. J. Enol. Vitic.* **2006**, *27* (1), 57–67.
52. Perez-Magarino, S.; Sanchez-Iglesias, M.; Ortega-Heras, M.; Gonzalez-Huerta, C.; Gonzalez-Sanjose, M. L. *Food Chem.* **2007**, *101* (3), 881–893.
53. Francia-Aricha, E. M.; Guerra, M. T.; Rivas-Gonzalo, J. C.; Santos-Buelga, C. *J. Agric. Food Chem.* **1997**, *45* (6), 2262–2266.
54. Weber, F. Untersuchung von polymeren Polyphenolen in Rotwein. Dissertation, Technische Universität Braunschweig, Cuvillier Verlag, Göttingen, 2012.

Publication Date (Web): November 24, 2015 | doi: 10.1021/bk-2015-1203.ch016

Publication Date (Web): November 24, 2015 | doi: 10.1021/bk-2015-1203.ch017

Chapter 17

New Insights into the Chemistry Involved in Aroma Development during Wine Bottle Aging: Slow Redox Processes and Chemical Equilibrium Shifts

V. Ferreira,* M. Bueno, and E. Franco-Luesma

Laboratory for Flavor Analysis and Enology,
Aragón Institute of Engineering Research (I3A)
Analytical Chemistry, Faculty of Sciences, University of Zaragoza,
50009, Zaragoza, Spain
***E-mail: vferre@unizar.es.**

This chapter summarizes some recent findings about the occurrence and formation of oxidation and reduction related off-odors during wine aging in the bottle. Concerning oxidation, different wines are able to produce -per the same amount of consumed oxygen-, quite different amounts of oxygen-related carbonyls. Those diverse carbonyl formation rates are related to wine metal content (iron, copper and manganese) and also to the wine content of precursor amino acids. With a new analytical strategy for measuring bonded and free forms of carbonyls, it is demonstrated that part of the oxidation-related aldehydes are already present in the wine in the form of bisulfite-complexes, so that part of the increase in carbonyl levels noted upon wine aging in the bottle, is just the simple consequence of the reversion of the bisulfite complex upon oxidation of sulfite to sulfate. A similar analytical strategy for measuring free and bonded forms of hydrogen sulfide and small mercaptans has revealed that the storage of wine under strict anaerobic conditions creates eventually the conditions –lowering wine redox potential- under which odorless mercaptan species are transformed into odor-active forms. Only in some whites and rosé wines, a slight "de novo" formation of mercaptans has been

In Advances in Wine Research; Ebeler, et al.;
ACS Symposium Series; American Chemical Society: Washington, DC, 2015.

observed, suggesting that in reds, formation of mercaptans is more the consequence of the reduction of some unknown form of metal cation complexed to the previously existent mercaptan than the direct reduction of sulfur itself.

Introduction

The best wines require time for being ready to be consumed. Time is basically required for stabilizing the color and the wine macromolecular structure, and also for lowering astringency and for general flavor development. The second essential component in many of those changes is oxygen, whose presence may be crucial for color stabilization, for lowering astringency and for limiting the production of reduced off-flavors (*1*, *2*). But oxygen can also have nasty consequences on wine quality by oxidizing polyfunctional mercaptans (*3*, *4*), by producing oxidation related aldehydes (*5*, *6*) and by forming brown pigments (*7*). Therefore, a crucial question in winemaking is to predict the best combination of time and oxygen for reaching the best results for each specific wine. Even if science has significantly progressed in recent years, this question does not have today a straightforward answer because of the many open questions regarding the chemical basis of astringency, the chemical definition of wine aroma development and maturation and the chemical processes involved in the formation of oxidation and reduction related aroma compounds.

Nevertheless, even if defining the chemical composition of the perfect wine is today not possible, it seems feasible to define in chemical terms the problems that limit what can be acceptable; i.e., to define the problems linked to aroma reduction and to aroma oxidation which most likely will demark the points of too much or too less oxygen points from which the wine will be no longer valuable (*8*). Since our main concern is about wines which most often are not rich in polyfunctional mercaptans, we have exclusively focused on the production of reductive aroma, particularly SH_2, dimethyl sulfide (DMS) and Methanethiol (MeSH) and of oxidation-related aldehydes. Our main aims have been to establish the links between the wine chemical composition and its natural tendency to form oxidation-related aldehydes upon wine oxidation, to form or to eliminate reductive aroma compounds and to understand the equilibria in which both aldehydes and reduction related compounds are involved and which could have relevance in aroma maturation.

Experimental Setup

In order to gain knowledge on these issues, three independent aging experiments have been carried out and two new analytical strategies have been developed. The two analytical strategies have been published recently and details can be found in the corresponding references (*9*, *10*).

In the first experiment 16 different Spanish red wines were stored at 25ºC for 6 months under different oxygen regimes, ranging from 0 to 56 mg/L. The levels of oxygen exposure were just indirectly controlled by bottling the wine in

In Advances in Wine Research; Ebeler, et al.;
ACS Symposium Series; American Chemical Society: Washington, DC, 2015.

Publication Date (Web): November 24, 2015 | doi: 10.1021/bk-2015-1203.ch017

special vials with three barriers (internal and external septa plus and additional plastic film with certified oxygen permeability), of which the most internal one (internal septa) was pierced at different levels, as detailed in reference (*11*). For each one of the wines, 17 different specimens were therefore produced, and these were characterized in terms of oxidation and reduction related aroma compounds. Original samples were characterized in terms of mineral content, polyphenols, amino acids, antioxidant and aroma composition.

The second experiment was an accelerated oxidation experiment in which 24 previously well chemically characterized wines were subjected to a forced oxidation procedure. Wines were saturated with oxygen, kept in clear bottles with oxygen sensors provided by Nomacorc, and when the dissolved oxygen level of the wine dropped to 1 ppm, or after 7 days, a sample was taken to analyze free aldehydes, SO_2 and color parameters, and the wine was resaturated with air again, repeating the whole process along 5 cycles.

In the third experiment, the same 24 wines were stored in complete anoxia for 3 weeks at 50ºC. Samples were taken after 1.5, 5, 10 and 21 days, for the analysis of free and total VSCs, redox potential and color parameters.

Publication Date (Web): November 24, 2015 | doi: 10.1021/bk-2015-1203.ch017

Results and Discussion

Aldehyde Formation Rates (AFRs)

The same wine stored 6 months at 25ºC under different levels of oxygen became oxidized to different extents and produced different levels of oxidation related aldehydes. When the amount of aldehydes, formed by each one of the 17 specimens derived from a particular wine after the 6 months of storage are plotted versus the amount of oxygen taken by that specimen, what we observe are plots like the one for methional shown in Figure 1.

The Figure reveal that the amount of aldehyde found in the wine is directly related to the oxygen consumed by the wine and that the proportionality constants are strongly dependent on the wine. In the examples given in the Figure, one of the wines formed in average 1.2 ppb of methional for each mg/L of oxygen taken, while the second one, formed just 0.028 ppb of the aldehyde per mg/L of oxygen consumed.

The slopes of the least square regression lines, as shown in the figure, are the average methional formation rates. As the linear pattern was observed in most wines and for most aldehydes, it was possible to use linear regression analysis to calculate those slopes which represent the average amount of aldehyde that a wine forms per mg/L of oxygen consumed or "aldehyde formation rate" AFR (*11*). Mimimum and maxima AFRs for all of the determined carbonyls and for the 16 different wines considered in the study are summarized in Table 1. The table reveals the existence of important differences in AFRs between samples. For instance, in the case of methional, the sample forming the most formed 1.57 ppb per mg/L of O_2 consumed, while the sample forming the least just formed 0.028 ppb per mg/L of O_2 consumed, i.e., the methional AFR of the former is 57 times faster than that of the latter.

Publication Date (Web): November 24, 2015 | doi: 10.1021/bk-2015-1203.ch017

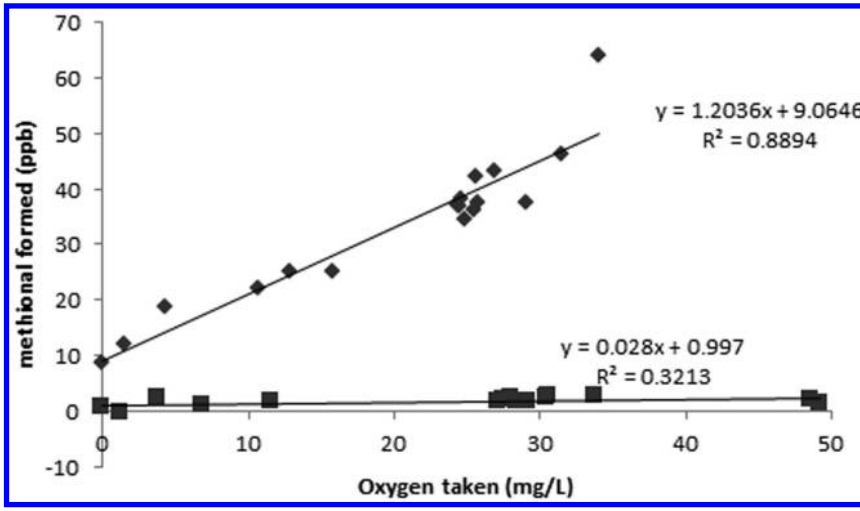

Figure 1. Determination of methional formation rates in two different wines.

Another relevant observation is about the potential sensory effect of the aldehyde formed upon oxidation on wine aroma. This can be estimated with the help of the last column in Table 1, which gives the increase in Odor Activity Value of the carbonyl for the wine which formed it fastest after consumption of 25 mg/L of Oxygen. As seen in the table, methional, phenylacetaldehyde, 2- methylpropanal and 3 -methylbutanal are potentially the most important carbonyls formed upon wine oxidation, in agreement with previous reports (*12*, *13*). 1-octen-3-one can also be formed in aromatically relevant amounts, but that happened only in a single wine, which formed this molecule 600 times faster than the slowest wine.

In the particular case of Strecker aldehydes, AFRs were found to be significantly and positively correlated to some wine components:

1. The corresponding amino acids and not the corresponding alcohols
2. The wine level of combined SO_2 and of Zn

And negatively correlated to the wine content in:

1. The wine level of Free SO_2
2. Wine levels of pyranoanthocyanin pigments and total flavonols

In some of the cases good PLS models could be built relating the AFR with the wine initial composition. The Correlation Loadings of the best model found for the particular case of methional are given in Figure 2. The model has a satisfactory prediction power, with a Mean Root Square prediction Error (MRSE) for methional AFR of 0.15 ppb per mg/L of Oxygen measured by cross-validation. The model confirms what the univariated correlations had shown about the major

Publication Date (Web): November 24, 2015 | doi: 10.1021/bk-2015-1203.ch017

importance of combined SO_2 and methionine levels on the methional formation rate, but also suggests that the AFR is the consequence of complex interactions between wine cations and wine phenolics.

Table 1. Formation of Aldehydes upon Wine Storage under Different Oxygen Regimes. Maxima and Minima AFRs and Potential Sensory Significance of the Maxima AFR.

	Aldehyde formation rate (ppb per mg/L O_2)		*Max OAV prod. rate (per 25 mg/L O_2)*
	minimum	***maximum***	
methional	0.028	1.57	78.5
phenylacetaldehyde	0.34	2.49	62.3
2-methylpropanal	0.13	2.72	11.3
2-methylbutanal	0.14	1.58	2.5
3-methylbutanal	0.14	3.88	21.1
E-2-hexenal	0.000	0.004	0.0
E-2-heptenal	0.000	0.002	0.0
E-2-octenal	0.000	0.007	0.1
E-2-nonenal	0.000	0.019	0.8
1-octen-3-one	0.000	0.009	15.1
benzaldehyde	0.19	8.56	0.1
vanillin	0.51	17.6	2.2

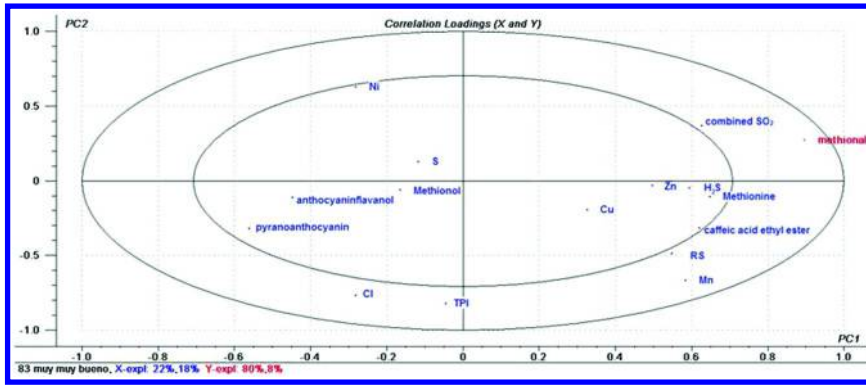

Figure 2. Correlation Loadings of the best PLS model explaining the methional formation rate of red wines from the wine.

In Advances in Wine Research; Ebeler, et al.;
ACS Symposium Series; American Chemical Society: Washington, DC, 2015.

Publication Date (Web): November 24, 2015 | doi: 10.1021/bk-2015-1203.ch017

Release of Aldehydes from SO_2 Complexes or De Novo Formation?

The observed correlations between AFCs and the wine level in combined SO_2, which extended to nearly all the studied aldehydes, made us think that part of the measured increments in aldehydes were the simple consequence of the previous existence of aldehyde-bisulfite combinations (hydroxyalquilsulphonic acids or colloquially bisulfite adducts) from which the aldehydes were released after the SO_2 was depleted by oxidation, as recently suggested by Grant-Preece et al. (*14*). In order to address this question, a novel analytical method able to measure free forms of wine carbonyls and to provide an estimation of the total amounts of aldehyde (total=free + bonded forms), has been developed (10). With such a new analytical tool we have been able to estimate the apparent aldehyde-bisulfite adduct formation constants, finding values that confirm that the most important oxidation related aldehydes, such as methional, phenylacetaldehyde and 3-methylbutanal are strongly complexed with SO_2 (more than 90%) at the normal free SO_2 levels found in wine.

In fact, results obtained with such a method applied to the study of 24 different wines (16 reds, 8 whites or rosés) have shown that some wines contain large amounts of oxidation-related aldehydes in bonded non-volatile and odorless forms. Table 2 gives an example of those findings, showing the free and total amounts of relevant wine aldehydes found in the wines with maximum proportions of bonded forms.

Table 2. Measured Free and Estimated Total Amounts of Oxidation-Related Aldehydes Found in the Wines Showing Maxima Proportions of Bonded Forms

	Free (ppb)	*total (ppb estimated)*	*% bonded*
methional	**4.8**	**53**	91%
phenylacetaldehyde	**8**	**130**	94%
2-methylbutanal	**1.5**	**8.5**	82%
isovaleraldehyde	**4**	**116**	97%
isobutyraldehyde	**6**	**30**	80%
diacetyl (ppm)	**4.0**	**14.7**	73%

As can be seen and taking methional as example, one of the red wines contained 4.8 ppb of free methional, which is a reasonable amount for a red wine. However, the same wine contained 53 ppb of methional in bonded form. From the sensory point of view, this is more than enough to make the aroma of that wine to become oxidized if such a pool would be released into free forms. The aroma perception would shift from a fresh fruit note (at low levels of free methional) to raisin notes (at high levels of methional) typically found in oxidized wines (*15*).

Publication Date (Web): November 24, 2015 | doi: 10.1021/bk-2015-1203.ch017

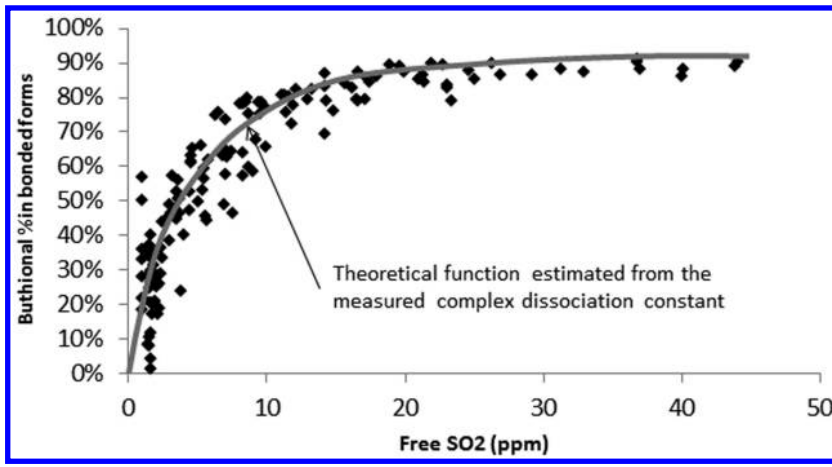

Figure 3. Percent of added methylthiobuthional in bonded forms as a function of wine free SO_2 content.

The next key question is whether such bonded forms could be effectively released during wine oxidation. This has been studied in an accelerated oxidation experiment in which 24 Spanish wines were subjected to 5 cycles of oxygen saturation/consumption. At the beginning of the experiment, the wines were spiked with the surrogates used in the analytical method. Such surrogates are aldehydes non-naturally occurring in wine with SO_2 bonding properties very similar to those of wine natural aldehydes. For instance, for methional (methylthio-propanal), the surrogated used was methylthio-butanal or buthional (*10*). The plot shown in Figure 3 shows the proportion of bonded buthional of the 120 wines (24 different wines x 5 different oxidation states) as a function of the wine content of free SO_2. The plot confirms that buthional is effectively released from the SO_2 complex (the % in bonded forms decrease) as the wine is oxidized, and that the proportion of bonded forms can be closely predicted from the buthional-SO_2 adduct apparent formation constant and the wine level in free SO_2.

The amount of total aldehyde present in the original wine before the oxidation, information that the developed procedure can provide, makes it possible to interpret what is really happening to aldehydes in wine during oxidation. This is shown with the help of Figure 4. The figure shows the evolution of free methional of one particular wine during the oxidation experiment as a function of the measured free SO_2 level of the wine (main solid line). As can be seen in the figure, the free methional levels increase continuously as the oxidation progresses (as the level of free SO_2 becomes smaller), in accordance with previous results (see for instance Figure 1). The level of total methional estimated in the original wine is represented by the large dot and the dotted straight line at 48 ppb. With such a total value and the apparent formation constant of the methional-SO_2 adduct it is possible to calculate the expected level of free methional associated to a particular free SO_2 concentration. Such expected levels, labeled as "estimated" in the Figure, were totally coincident to measured levels until a free SO_2 level

of around 3 ppm. Below that point, the measured free levels of methional are consistently above those estimated, strongly suggesting that at those low levels of free SO_2, de novo formation of methional from methionine or methionol is actively taking place.

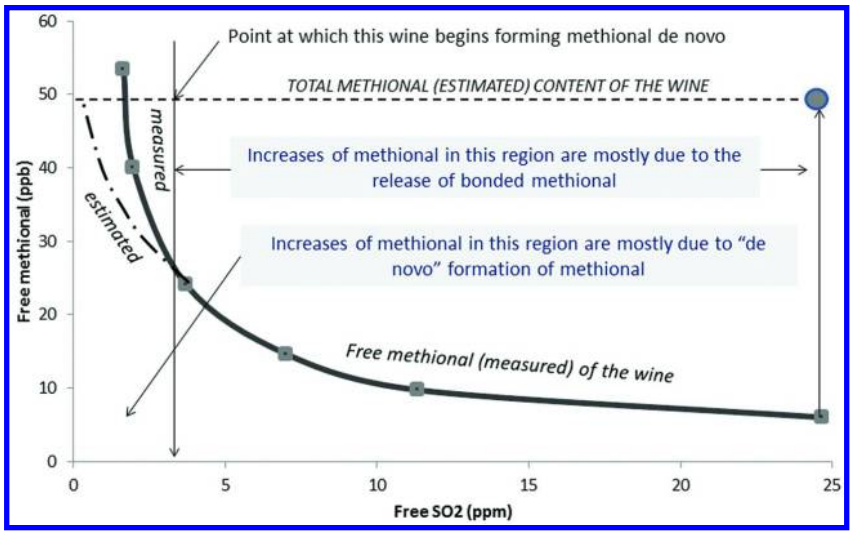

Figure 4. Evolution of free methional levels of a red wine along its accelerated oxidation as a function of its free SO_2 content. The dotted line labeled as "estimated" corresponds to the calculated release of methional from the SO_2-methional adduct originally present in the wine.

In other words, this result demonstrates that wine can contain a large pool of oxidation-related aldehydes under non-volatile odorless forms which could eventually explain the development of oxidation-related aroma nuances without the need for a "de novo" formation of the aldehydes.

Formation and Degradation of Mercaptans

Coming back to the first experiment, the levels of the three measured VSCs (SH_2, MeSH and DMS) in each one of the 17 specimens produced from each wine sample were plotted versus the level of oxygen consumed by the specimen along its storage under a specific oxygen regime, as exemplified in Figure 5 for the case of SH_2. The plot reveals the existence of a negative linear correlation between the levels of VSC (SH_2 in the figure) and the levels of oxygen consumed by the specimen. The slopes define in these cases the depletion rates of each one of the VSCs in each one of the 16 studied red wines (*11*). In the case shown in the figure,

In Advances in Wine Research; Ebeler, et al.;
ACS Symposium Series; American Chemical Society: Washington, DC, 2015.

Publication Date (Web): November 24, 2015 | doi: 10.1021/bk-2015-1203.ch017

the slope of the regression line indicates that the SH_2 degradation rate of such wine was 0.53 ppb of SH_2 per each mg/L of oxygen consumed. It should be remarked that the method used for the analysis of VSCs was specifically designed to avoid matrix effects by weakening intermolecular interactions between the analytes and the matrix elements (*16*), so that it gives an estimation of both free and bonded forms of VSCs (*9*).

Two different types of patterns emerge out of the data. In the case of hydrogen sulfide, in all the cases there was a clear decrement in the levels of this molecule with respect to the levels of the original wines. Such decrements were proportional to the level of oxygen taken by the wine. In the cases of methanethiol and DMS, in some wines the levels of these molecules in the specimens exposed to very little amounts of oxygen in the 6 month storage period were higher than those of the original wines.

Publication Date (Web): November 24, 2015 | doi: 10.1021/bk-2015-1203.ch017

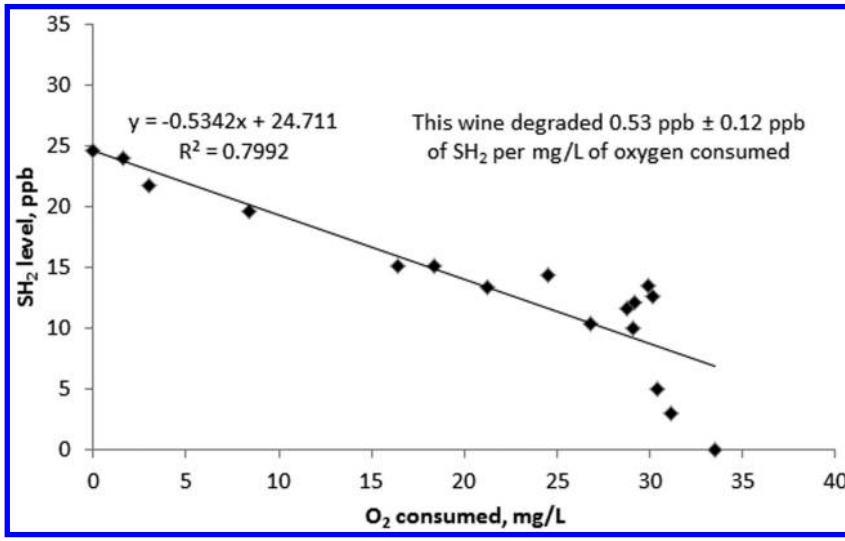

Figure 5. Determination of SH_2 depletion rate in one red wine.

Hydrogen sulfide degradation rates ranged from 0.23 to 2.3 µg/L per mg/L O_2 consumed, and such degradation rates were strongly correlated to the initial level of hydrogen sulfide (r = -0.99), as shown in Figure 6. Such strong linear dependence basically suggests that the oxidation kinetics of this molecule follow a second order kinetic model, according to which oxidation rate would be proportional to both the concentration of initial product (SH_2) and of a reactant (a wine quinone, hydrogen peroxide or other reactive oxygen species), being the kinetic constant very similar in all the wines. This finding is consistent with the highest reaction rates between SH_2 and quinones as recently measured (*17*).

Degradation rates are also correlated to Copper ($r = -0.85$, $p < 0.0001$) and Iron ($r = -0.60$; $p < 0.05$) levels. This observation could be, however, biased by the fact that the three wines with highest levels of Cu, contained also highest levels of SH_2. The inexistence of SH_2 accumulation may suggest that there are no specific precursors for this molecule able to increase the total levels of SH_2 in red wine, which is what we measured in the present work.

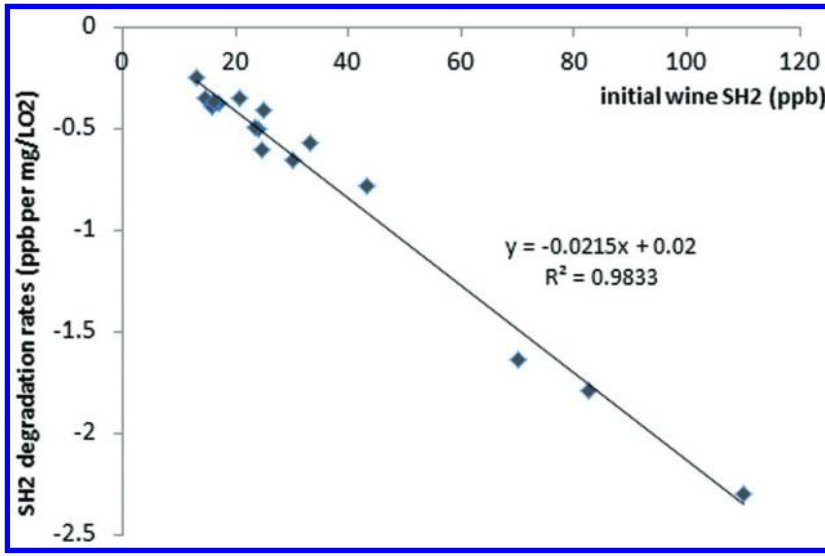

Figure 6. Relationship between the SH_2 degradation rates measured in 16 wines and their initial content of (total) SH_2.

In the cases of MeSH and DMS significant accumulations of these molecules, with respect to the levels measured in the original wines, were found in the specimens stored 6 months under very little contact with oxygen. The effect of oxidation in these two cases was similar to that observed for SH_2, and the levels of both molecules decreased proportionally to the amount of oxygen taken.

In the case of MeSH a tiny but neat and significant increment on the levels of this molecule was measured in 12 out of the 16 wines. The highest increment measured was 6.9 ppb after 6 months of storage. Remarkably, MeSH increments were positively correlated to the wine levels in Methionine ($r = 0.53$, $p < 0.05$), which could be a specific precursor for MeSH, as recently demonstrated for soy proteins (*18*). Formation rates were also related to total proanthocyanidin levels ($r = 0.60$, $p < 0.05$) and negatively correlated to the wine content in resveratrol (-0.58, $p < 0.05$) and Aluminium ($r = -0.59$, $p < 0.05$).

Methanethiol levels also decreased with oxidation. As no disulfide was detected in this study, the main degradation route should be the reaction of the mercaptan with a quinone produced through oxidation (*17*). As MeSH levels were very low, degradation rates were also low and difficult to measure with sufficient precision to extract clear conclusions. However, a trend similar to that observed for SH_2 showing a linear relationship between MeSH degradation

Publication Date (Web): November 24, 2015 | doi: 10.1021/bk-2015-1203.ch017

rates and MeSH initial level was observed in this case. Notwithstanding this, degradation rates are related to wine content in Copper ($r = -0.59$, $p < 0.05$), Iron ($r = -0.67$, $p < 0.01$) and Manganese ($r = -0.67$, $p < 0.01$).

Mercaptans Also Form Stable Complexes in Wine

The fact that we could not observe any increase in SH_2 in the wines stored without contact with oxygen was unexpected and in clear contrast with published data and with our own personal experience. This made us think that maybe the apparent contradiction was caused by the nature of the analytical method used in such study, which as previously explained, was designed to avoid matrix effects. The hypothesis is that mercaptans in wine are present under the form of stable complexes mostly with metals cations, and that those complexes could be broken or reverted in anoxic conditions which would lead to the development of reductive character. If the analytical method breaks such complexes, what it measures is total forms and hence, such a method is unable to see changes affecting the distribution of mercaptans between free and complexed forms.

Then a simple gentle headspace method has been developed in order to be sure to measure just free forms (*9*). The method is fairly sensitive, linear and repetitive, but as expected suffers from matrix effects, which simply shows that these compounds exert strong interactions with some wine components.

As an example Table 3 shows the recoveries of different VSCs added to two different wines, showing quite different patterns with regards to the ability of each wine to trap mercaptans. While the first wine does not seem to have much ability to trap them, the second one had a huge ability. Significantly, none of them was able to trap tioethers, suggesting that the interaction was specific to the SH group.

Table 3. Recoveries of VSCs Added to Two Different Wines Using a Headspace Analytical Method (*9*). Recovery of 100 Means That the Headspace Signal Is the Same than That Found on a Synthetic Wine.

Recovery (%)	*SH_2*	*MeSH*	*EtSH*	*DMS*	*DES*	*PrSH*	*Tiophene*
Wine 2	108	101	105	128	119	94.6	109
Wine 3	0.00	61.7	69.3	94.2	125	73.9	115

Table 4 gives the native content of free and complexed SH_2 of the two previous wines. The free level of SH_2 was measured with the headspace method (*9*), while the total level was determined with the old method involving a strong sample pretreatment (*16*). The results confirm that both wines contain important amounts of "trapped or concealed" SH_2. As seen in the table, wine 3 which was previously identified in Table 3 as the one having a strong ability to trap mercaptans, already contains a large pool of concealed SH_2, more than enough to cause a strong reduction off-odor, but the concentration of this SH_2 in the headspace is so tiny, that no smell is being perceived.

In Advances in Wine Research; Ebeler, et al.;
ACS Symposium Series; American Chemical Society: Washington, DC, 2015.

Publication Date (Web): November 24, 2015 | doi: 10.1021/bk-2015-1203.ch017

Table 4. Free and Total Levels of SH_2 Measured in Two Wines by Using Two Independent Analytical Methods (*9*, *16*)

	free	*total*	*% Complexed*
Wine 2	1.16	37.9	96.9
Wine 3	0.34	105	99.7

Publication Date (Web): November 24, 2015 | doi: 10.1021/bk-2015-1203.ch017

Three major questions remain then to be answered: First, under what forms are SH_2 and the other mercaptans trapped in the wines; second, whether those trapped forms could somehow be released back into the headspace as free odorous forms; and third, when and why this may happen.

Different experiments have been carried out in order to get some clues about these questions. In a first experiment, synthetic hydroalcoholic solutions containing VSCs and small amounts (0.5 ppm) of different metal cations were analyzed by both analytical methods. Results for the free forms of SH_2 are summarized in figure 7, which gives the headspace concentrations of hydroalcoholic solutions containing different metal cations and 30 ppb of SH_2 monitored along different days. As can be seen, SH_2 is completely absent from the beginning in the headspace of solutions containing Cu^{2+}, decreases slowly in those solutions containing Fe^{2+} and Zn^{2+}, and remains stable in the headspaces of solutions containing Fe^{3+} or Mn^{2+}. These results clearly indicate that these two last cations cannot bind SH_2 under those conditions, while Cu^{2+} is particularly effective. This is not surprising, and it is the reason why this cation is often used in winemaking to remove the excesses of SH_2 eventually produced in some fermentations.

However, the generally accepted thinking that Cu^{2+} removes completely SH_2 by forming a stable solid precipitate is strongly questioned by the results obtained when the Copper-SH_2 solutions were analyzed with the method for total forms, since the method recovered most of the signal of SH_2 (*9*).

Even in the samples that were analyzed 6 days after the SH_2 was added to the synthetic wine containing Copper, the recovery of SH_2 with the method for total forms was above 75%. What this result strongly indicates, is that SH_2 is not forming a stable irreversible precipitate with Cu^{2+}, but rather a soluble complex that remains in the solution and that can be relatively easily broken, suggesting that there is a reversible chemical process. In fact, in the method for total forms the sample is just strongly diluted in a brine and the headspace further preconcentrated in a SPME fiber. Such dilution seems to be enough to revert the equilibrium from the complex to the free volatile form of SH_2. In other words, these results strongly suggest that SH_2 (and the other mercaptans) can be present as nonvolatile complex forms with Cu^{2+} and secondarily with Fe^{2+} and Zn^{2+}, and that those complex forms are reversible.

Publication Date (Web): November 24, 2015 | doi: 10.1021/bk-2015-1203.ch017

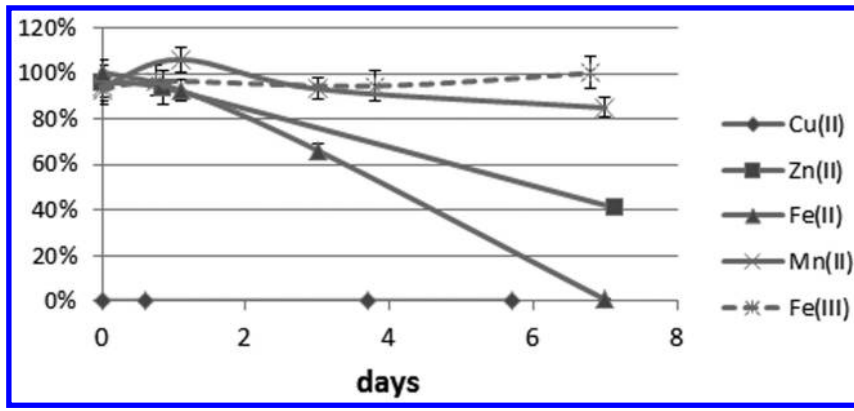

Figure 7. SH_2 headspace levels contained in hydroalcoholic solutions containing 0.5 ppm of one cation and 30 ppb of SH_2. 100% is the signal measured in a solution without metals.

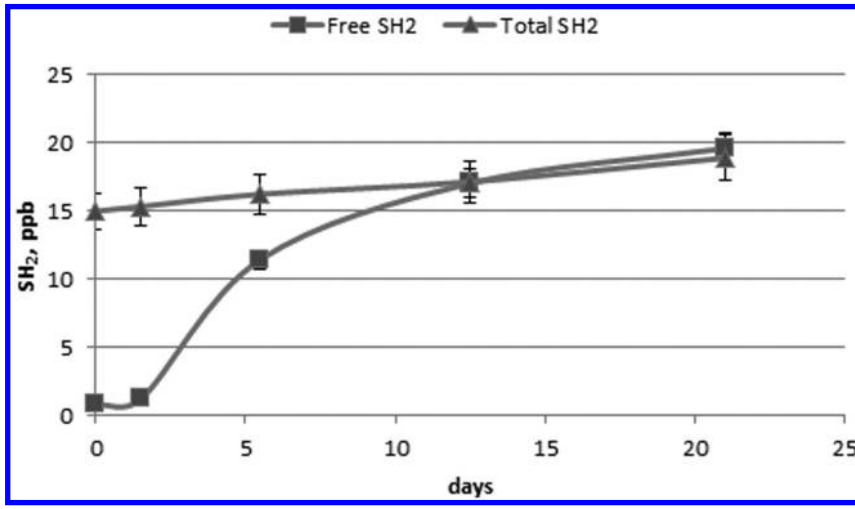

Figure 8. Evolution of free and total SH_2 levels of one red wine during an accelerated reductive storage in complete anoxia at 50ºC.

Finally, and in order to get an initial answer about the possibility that SH_2 can be formed back from complexed forms during reductive storage of wine, different red wines have been stored for a period under strict anoxia at 50ºC. Results are illustrated for one of the wines in Figure 8. The figure shows the evolution of free and total forms of SH_2 during the storage of the wine in reductive conditions. As can be seen, while the level of total SH_2 increased just slightly, the levels of free SH_2 increased to a point in which the levels of free forms equaled the levels of total forms, suggesting that most of the observed increase of free SH_2 is in fact a simple release of bonded forms.

During the storage in an anoxic environment, the redox potential (measured only after wine O_2 level dropped to 0) of that particular wine decreased by -38mV, becoming more reductive. This was a general trend, and redox potential of red wines decreased on average -25 mV. Moreover, the increases in free SH_2 observed during the reductive storage were proportional to the decrease of the redox potential, which may support the hypothesis that the increases of SH_2 and other mercaptans during reductive aging are at least in part caused by the release of complexed forms by the chemical reduction of Cu^{2+} to Cu^{o} producing complex cleavage. These results do not support the current belief that reduction problems related to the use of Cu^{2+} are primarily caused by the reduction of disulfides previously formed by the oxidation of mercaptans catalyzed by the Cu^{2+} added during copper finning. While such a possibility cannot be excluded, the results presented here would support that the small amounts of Cu^{2+} naturally present or further added to wine may in fact act as SH_2 and mercaptan "containers" from which these molecules could be released during reduction.

Publication Date (Web): November 24, 2015 | doi: 10.1021/bk-2015-1203.ch017

Acknowledgments

This work has been funded by the Spanish Ministry of Economy and Competitiveness (Project AGL2010 230183)

References

1. Gambuti, A.; Rinaldi, A.; Ugliano, M.; Moio, L. Evolution of Phenolic Compounds and Astringency during Aging of Red Wine: Effect of Oxygen Exposure before and after Bottling. *J. Agric. Food Chem.* **2013**, *61*, 1618–1627.
2. Ugliano, M. Oxygen Contribution to Wine Aroma Evolution during Bottle Aging. *J. Agric. Food Chem.* **2013**, *61*, 6125–6136.
3. Blanchard, L.; Darriet, P.; Dubourdieu, D. Reactivity of 3-mercaptohexanol in red wine: Impact of oxygen, phenolic fractions, and sulfur dioxide. *Am. J. Enol. Vitic.* **2004**, *55*, 115–120.
4. Herbst-Johnstone, M.; Nicolau, L.; Kilmartin, P. A. Stability of Varietal Thiols in Commercial Sauvignon blanc Wines. *Am. J. Enol. Vitic.* **2011**, *62*, 495–502.
5. Escudero, A.; Asensio, E.; Cacho, J.; Ferreira, V. Sensory and chemical changes of young white wines stored under oxygen. An assessment of the role played by aldehydes and some other important odorants. *Food Chem.* **2002**, *77*, 325–331.
6. Ferreira, A. C. S.; Oliveira, C.; Hogg, T.; de Pinho, P. G. Relationship between Potentiometric Measurements, Sensorial Analysis, and Some Substances Responsible for Aroma Degradation of White Wines. *J. Agric. Food Chem.* **2003**, *51*, 4668–4672.
7. Singleton, V. L.; Kramling, T. E. Browning of white wines and an accelerated test for browning capacity. *Am. J. Enol. Vitic.* **1976**, *27*, 157–160.

8. Ugliano, M.; Kwiatkowski, M. J.; Travis, B.; Francis, I. L.; Waters, E. J.; Herderich, M. J.; Pretorius, I. S. Post-bottling management of oxygen to reduce off-flavour formation and optimise wine style. *Aust. N. Z. Wine Ind. J.* **2009**, *24*, 24–28.
9. Franco-Luesma, E; Ferreira, V. Quantitative analysis of free and bonded forms of Volatile Sulfur Compouds (VSCs) in wine. Basic methodologies and evidences showing the existence of reversible cation-complexed forms. *J. Chromatgr., A* **2014**, *1389*, 8–15.
10. Bueno, M.; Zapata, J.; Ferreira, V. Simultaneous determination of free and bonded forms of odor-active carbonyls in wine using a headspace solid phase microextraction strategy. *J. Chromatogr., A* **2014**, *1369*, 33–42.
11. Ferreira, V.; Bueno, M.; Franco-Luesma, E.; Cullere, L.; Fernandez-Zurbano, P. Key Changes in Wine Aroma Active Compounds during Bottle Storage of Spanish Red Wines under Different Oxygen Levels. *J. Agric. Food Chem.* **2014**, *62*, 10015–10027.
12. Cullere, L.; Cacho, J.; Ferreira, V. An Assessment of the Role Played by Some Oxidation-Related Aldehydes in Wine Aroma. *J. Agric. Food Chem.* **2007**, *55*, 876–881.
13. Ferreira, A. C. S.; Hogg, T.; de Pinho, P. G. Identification of Key Odorants Related to the Typical Aroma of Oxidation-Spoiled White Wines. *J. Agric. Food Chem.* **2003**, *51*, 1377–1381.
14. Grant-Preece, P.; Fang, H. J.; Schmidtke, L. M.; Clark, A. C. Sensorially important aldehyde production from amino acids in model wine systems: Impact of ascorbic acid, erythorbic acid, glutathione and sulphur dioxide. *Food Chem.* **2013**, *141*, 304–312.
15. San-Juan, F.; Ferreira, V.; Cacho, J.; Escudero, A. Quality and Aromatic Sensory Descriptors (Mainly Fresh and Dry Fruit Character) of Spanish Red Wines can be Predicted from their Aroma-Active Chemical Composition. *J. Agric. Food Chem.* **2012**, *59*, 7916–7924.
16. Lopez, R.; Lapena, A. C.; Cacho, J.; Ferreira, V. Quantitative determination of wine highly volatile sulfur compounds by using automated headspace solid-phase microextraction and gas chromatography-pulsed flame photometric detection - Critical study and optimization of a new procedure. *J. Chromatogr. A* **2007**, *1143*, 8–15.
17. Nikolantonaki, M.; Waterhouse, A. L. Method To Quantify Quinone Reaction Rates with Wine Relevant Nucleophiles: A Key to the Understanding of Oxidative Loss of Varietal Thiols. *J. Agric. Food Chem.* **2012**, *60*, 8484–8491.
18. Landaud, S.; Helinck, S.; Bonnarme, P. Formation of volatile sulfur compounds and metabolism of methionine and other sulfur compounds in fermented food. *Appl. Microbiol. Biotechnol.* **2008**, *77*, 1191–1205.

Publication Date (Web): November 24, 2015 | doi: 10.1021/bk-2015-1203.ch017

Publication Date (Web): November 24, 2015 | doi: 10.1021/bk-2015-1203.ch018

Chapter 18

Quinone Reactions in Wine Oxidation

Andrew L. Waterhouse*,[1] and Maria Nikolantonaki[2]

[1]Department of Viticulture and Enology, University of California, Davis, California 95616, U.S.A.
[2]Institut Universitaire de la Vigne et du Vin, Jules Guyot, UMR A 02.102 PAM AgroSup Dijon/Université de Bourgogne, Rue Claude Ladrey, BP 27877, 21078 Dijon Cedex, France
***E-mail: alwaterhouse@ucdavis.edu.**

Wine oxidation chemistry involves two major steps as first described by Singleton. The formation of quinones from phenolics followed by the creation of acetaldehyde from ethanol. Quinones react with several wine nucleophiles including thiols and the tannin phloroglucinol group. The quinones can also react with SO_2 and ascorbic acid as antioxidants. Reactions with aromatic varietal thiols results in the loss of fruity aromas, and phenolics can produce brown products, both oxidative degradation of the wine. However, SO_2, ascorbic acid and glutathione all react very quickly with quinones and thus can be protective antioxidants by intercepting the quinone, avoiding oxidative degradation reactions. Competitive reaction kinetics may provide predictive tools for managing wine oxidation.

Introduction

The preservation of wine, as with most foods, is limited largely by its oxidation. The earliest specific report on this question was by Pasteur, who showed, comparing the addition of inert gas and oxygen to wine in hermetically sealed glass ampules, that the oxygen-treated wine aged much more quickly, and that the control showed no noticeable changes Figure 1. In fact, Pasteur attributed all aging to oxidation (*1*), although it is now clear that other non-oxidation related reactions do occur on aging, such as ester equilibration and glycoside hydrolysis.

In Advances in Wine Research; Ebeler, et al.;
ACS Symposium Series; American Chemical Society: Washington, DC, 2015.

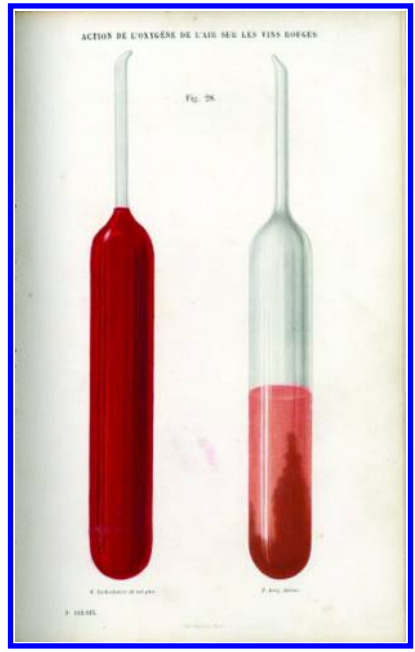

Figure 1. Image from Pasteur's experiment. See Reference (1).

Others have commented on the effect of oxidation as well. In the first US published book on wine, Rixford states, "In a few instances, where the wines are strong enough to bear it, aging may be hastened by some exposure to the air, but great care must be taken that they are not left too long under its influence or disorganization many ensue (*2*)." In an important technology reference text from the 1970's Amerine et al stated that "The principal changes in flavor and bouquet during aging in the wood are generally believed to be due to slow oxidation (*3*)." Numerous other sources comment on the significance of oxidation to the stability, flavor and color of wine. It would be of great value to winemakers to be able to more precisely predict the wine's capacity to resist oxidation and/or to benefit from it. Such predictions will be based on understanding the oxidation pathways as well as the relative reaction rates of the key reactions. This report describes our understanding of one of those pathways as well as how that understanding arose.

Early Studies

Perhaps the first mechanistic pathway of the chemical reactions involved in wine oxidation was defined by Vernon Singleton, Figure 2. In a paper that linked the production of the well known oxidation product, acetaldehyde to the oxidation of phenolic substances, Wildenradt and Singleton proposed that the first reaction of oxygen was with phenolic substrates, and these initial products lead to the subsequent reactions. Specifically they suggest that it is catechols

Publication Date (Web): November 24, 2015 | doi: 10.1021/bk-2015-1203.ch018

that are oxidized to quinones, with hydrogen peroxide being the other product of the reaction. They then show hydrogen peroxide reacting with ethanol to yield acetaldehyde. Their data was strengthened by conducting reactions with propanol, with the corresponding 3-carbon aldehyde, propanal, as the product (*4*).

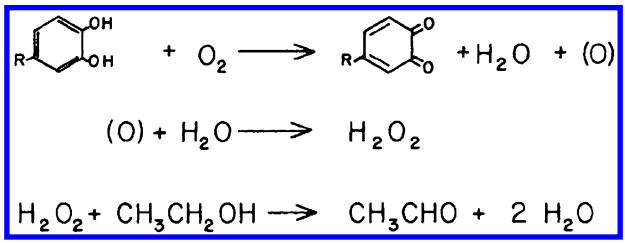

Figure 2. Formation of quinone in wine oxidation as proposed by Wildenradt and Singleton, 1974 (4). Reprinted by permission of AJEV.

One very important step in the Singleton mechanism was the identification of the phenolic oxidation product, the quinone. Singleton referred to this as coupled oxidation, and in subsequent papers recognized that the quinone was a reactive species. There were two proposed fates for the quinone that appeared in these later reports. The first expectation was that the quinone would be the precursor to browning, as it was pigmented, and the second was reaction with an abundant sulfur nucleophile, glutathione (GSH).

Browning was and continues to be a major issue in wine and food preservation with entire symposia devoted to the subject (*5*). The extent of white wine oxidation can be quantified by measuring the "darkening" of the wine, and the amount of brown color can be directly related to chemical measures of oxidation as well as the appearance of oxidized flavors as observed by a sensory panel (*6*). The specific chemical reactions that lead to browning have been linked to quinones, but the pathway and products are complex (*7*) and only some of the brown pigments are known (*8*). The latter are derived not directly from quinone products but from electrophilic oxidation products of organic acids.

Singleton first reported that caftaric acid was susceptible to oxidation during juice processing, and that a product was being formed in proportion to the losses of caftaric acid (*9*). He subsequently reported the first specific product of oxidation catalyzed quinone reaction in a 1985 report that showed reaction with GSH (*10*). The pathway was proposed to involve enzymatic polyphenol oxidase (PPO) oxidation of the caftaric acid, followed by reaction with the sulfur nucleophile, Figure 4. This product is found in most commercial wines, a consequence of must oxidation during crushing, and reaction with naturally occurring GSH. The observation of this product is not surprising in light of the fact that GSH is the most abundant thiol in grape juice, and is thus most readily available to react with the quinone. Its concentration in juices is reported in the range of 50-320 μM (*11*), much higher than cysteine, reported at 8-60 μM (*12*), and orders of magnitude higher than the volatile thiols, at about 2-20 nM.

Publication Date (Web): November 24, 2015 | doi: 10.1021/bk-2015-1203.ch018

Publication Date (Web): November 24, 2015 | doi: 10.1021/bk-2015-1203.ch018

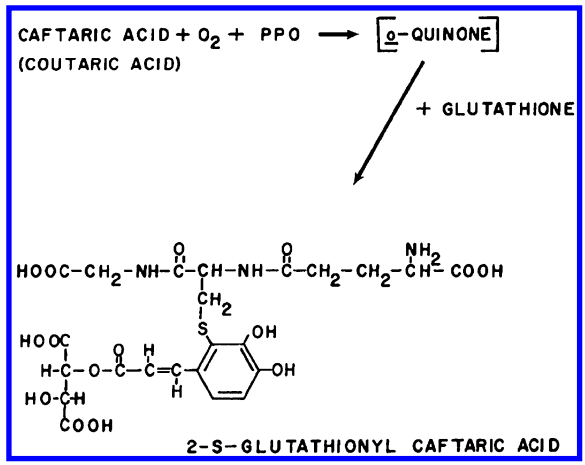

Figure 3. Quinone product with GSH, from Singleton et al 1985 (10). Reprinted by permission of AJEV.

As a consequence of these reactions, the presence of thiols prevents the formation of brown products. Juice browning appears to involve hydroxycinnamates, as these are major substrates of enzymatic oxidation via PPO and related enzymes. However, the formation of the hydroxycinnamate quinones leads to dimeric products (Figure 4), and these products are not colored (*13*).

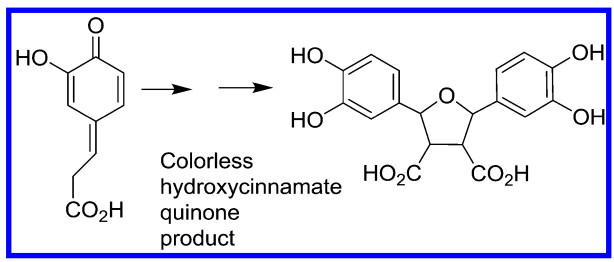

Figure 4. Quinone dimerization as reported by Fulcrand et al (13).

Instead, browning is correlated to flavan-3-ol content (*14*), which under enzymatic oxidation conditions are oxidized by the hydroxycinnamate quinones in a coupled redox reaction. The coupled oxidation leads to quinones of the flavan-3-ols, such as catechin, epicatechin and other monomers, as well as oligomers and condensed tannins. Some specific reactions of flavan-3-ol quinones have been shown to yield products which have color and potentially contribute to browning of wine and the many other flavanol-containing products that turn brown, such as apples, tea, cocoa, etc. The mechanism of product formation involves coupling between a quinone and the nucleophilic A-ring of another flavanol, followed by repeated re-oxidation of the product to an electrophilic quinone and new bond formation and re-oxidation. The product shown (Figure 5) has color due to the large number of conjugated double bonds.

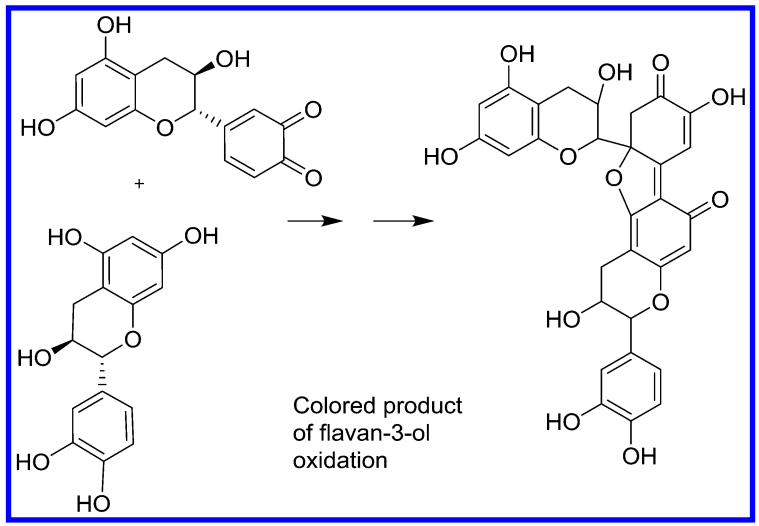

Figure 5. Pigmented products of flavan-3-ols as described by Cheynier et al (14).

Browning is also suppressed by sulfur dioxide, with early studies reporting that sulfite reacted with the quinone and reduced the production of melanins (*15*). Chemical studies of p-quinone demonstrated early on that at low pH sulfite both reduces and adds to quinones, leading largely to the hydroquinone, but also 20-30% of the sulfonate addition products depending on the concentration of the sulfite, while at higher pH, only the addition reaction is observed (*16*). Recent studies with an *o*-quinone, more relevant to food and wine, showed largely the same results, with the majority of the *o*-quinone being reduced to the catechol, and a fraction being converted to the sulfonate (Figure 6). (*17*).

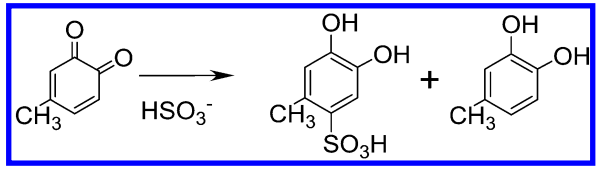

Figure 6. Competitive reactions of o-quinone with sulfite, from (17).

Later Studies

Quinones also react quickly with ascorbic acid, and this can be a very protective antioxidant reaction under circumstances where ascorbate is added to wine. The small amount found in grapes is lost during the fermentation process. Some winemakers add ascorbate at bottling as a preservative. The first demonstration of ascorbate reacting with *ortho*-quinones under wine conditions

was reported recently (*18*). The only product of the reaction is the formation of the reduced quinone, or hydroquinone. In the example from Nikolantonaki (*18*), the quinone was reduced to the catechol (Figure 7).

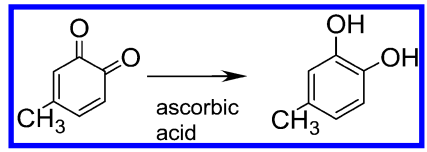

Figure 7. Reduction of ortho-quinone to catechol.

Publication Date (Web): November 24, 2015 | doi: 10.1021/bk-2015-1203.ch018

The relative effectiveness of any particular antioxidant must be evaluated in comparison with a reference reaction. In the case of quinone reactions in wine, a key effect of oxidation on flavor is the loss of the desirable aromatic thiols that provide some wines with distinctive varietal character. For instance, Sauvignon blanc and related varieties rely on the presence of 3-mercaptohexanol (3-MH) as an impact compounds that provides a grapefruit/citrus aroma. This compound is of particular importance to cool-climate Sauvignon blanc such as the wines from New Zealand (*19*). So, in evaluating the protective effect of antioxidants, it would be useful to evaluate the relative reaction rates of candidate nucleophiles/reducing agents. Possible reactions based on the known nucleophiles discussed above are shown in Figure 8.

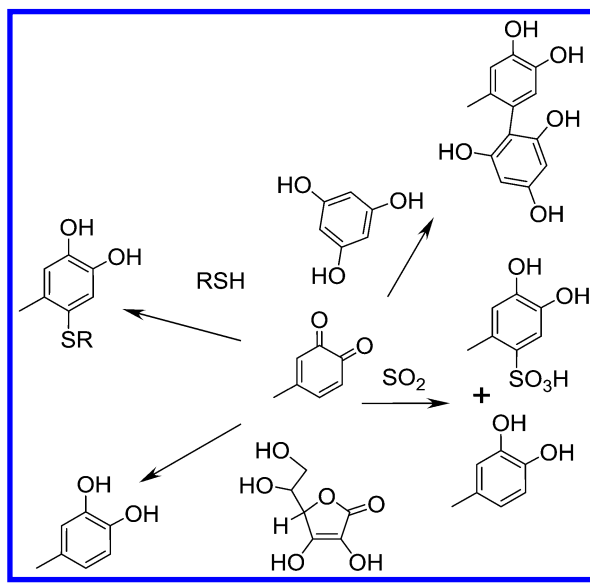

Figure 8. Alternate pathways for reactions of quinones with known nucleophilic functional groups and reactants.

A study of the reactions of the quinone of 4-methyl catechol showed the reaction rates of a few key nucleophile and reducing agents (*18*). After normalizing the rates in of the reactions, all conducted at equimolar concentrations, in terms of 3-mercaptohexanol (3-MH), it is notable that the antioxidants, SO_2, ascorbate and GSH, have much higher rates, approximately 6+ times greater. Phloroglucinol has a much slower rate, and the amino acids do not appear to react with the quinone. The consequence of these differing rates is that the antioxidants should all provide excellent protection against oxidation, even with relatively low concentrations. This would be expected as the actual concentration of 3-MH is typically a few µg/L, compared to several to many mg/L for any of the antioxidants. Thus, with a much lower concentration and a slower rate of reaction, 3-MH should be well protected even with "low" levels of antioxidants.

Publication Date (Web): November 24, 2015 | doi: 10.1021/bk-2015-1203.ch018

Table 1. Relative Reaction Rates of Nucleophiles and Reducing Agents with 4-Methylcatechol (*18*)

Compound	*Relative Rate*
Methionine	0.003
Phenyl alanine	0.009
Phloroglucinol	0.110
4-methyl-4-sulfanylpentan-2-one	0.100
3 Mercaptohexanol	1.000
2-furanmethanethiol	1.440
Sulfur Dioxide	5.800
Ascorbic Acid	6.000
Glutathione	6.600
Hydrogen Sulfide	7.200

Winemakers often oxygenate fermenting wines when a "reduced" aroma is detected. Most likely this reduced aroma is the result of the yeast producing hydrogen sulfide. As can be seen from the table, in the presence of quinones produced by oxidation, hydrogen sulfide will react with the quinone very quickly, possibly explaining the effectiveness of oxygen entrainment during fermentation at removing this off-aroma.

To confirm these rates under competitive conditions, Nikolantonaki et al looked at reactions between the ortho-quinone of 4-methycatechol using multiple nucleophiles (*20*). The reactions were conducted with iso-molar concentrations of each nucleophile, and then the product ratios were determined by LC analysis of the products. In addition, all the products with each nucleophile were identified

by isolation and NMR spectral analysis of each component. Thus it was possible to determine the outcome of the reactions, comparing the product ratios against the relative reaction rates measured previously. In both cases, approximately 1 mM quinone reacted with 4 mM of each nucleophile.

Viewing the data in Figure 9, one notes that when SO_2 and ascorbic acid are combined, the fraction of the sulfonate is very small. This suggests that ascorbic acid might react somewhat more quickly than SO_2, and that the difference is likely to be more than the 3% observed in the rate measurement experiment listed in Table 1. Comparing SO_2 and GSH, it appears that the GSH might react more slowly than SO_2, though by a small difference, and not more quickly as reported in Table 1. Also, comparing ascorbic acid and GSH, it appears that the ascorbate is the faster reactant. The competition reactions suggest a reactivity ranking of ascorbate > SO_2 > GSH. However, the rate differences between them are fairly small and perhaps of minor significance compared to the differences in concentration that are typically encountered.

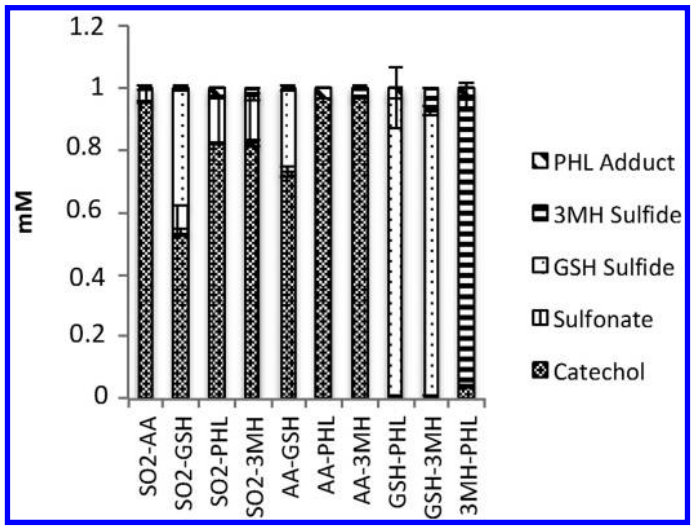

Figure 9. Products obtained with nucleophile pairs. AA = ascorbic acid, GSH = glutathione, PHL = phloroglucinol, 3MH = 3 mercaptohexanol. Data from (20).

As phloroglucinol has a slow reaction rate, its fractional amount in any of the competition reactions is expected to be fairly small, especially when compared with ascorbate, SO_2 or GSH. The ratio of the reaction rates between these antioxidants and phloroglucinol is about 60-1; for instance phloroglucinol's rate is 1.5% of ascorbic acid. In the competitive reaction scenarios, the amount of phloroglucinol observed is about 3% of those antioxidants, exceptionally close to a prediction based on relative rates. When compared to 3-MH, the amount of phlorglucinol is also about 3%, lower than would be expected with the lower reaction rate of 3-MH.

In Advances in Wine Research; Ebeler, et al.;
ACS Symposium Series; American Chemical Society: Washington, DC, 2015.

Publication Date (Web): November 24, 2015 | doi: 10.1021/bk-2015-1203.ch018

Due to this low reaction rate of phloroglucinol, it would appear that condensed tannins and related flavan-3-ols would not be suitable substances to prevent the loss of thiol aroma substances from reactions with quinone. Phloroglucinol is a model for the A-ring functional group of the flavan-3-ols. However, despite the low reaction rate, tannins may still be protective because the concentration of tannin is very high in red wines. With amounts over 2 grams per liter in some wines, the concentration of phloroglucinol functional groups is in the range of 5-7 mM. The concentration of 3-MH is highly variable but a level of 1.4 μg/L would be a quite noticable level, and that would equate to 10 nM. Thus in red wine, the effective concentration of the tannins would be about 500,000 times that of the thiols. So, even with a reaction rate that is only one tenth that of 3-MH, the very high concentration of tannin should make these compounds very effective at scavenging quinone electrophiles, and preventing the loss of thiols. And, of course, red wines are well known to be much more resistant to oxidative change compared to white wines.

The relative product rations of 3-MH compared to the antioxidants is small, perhaps smaller than might be expected, especially with ascorbate, where there is only about 3.5% of the 3-MH product. This is a favorable result if ascorbate is expected to react quickly with quinones under oxidative conditions, preventing the reaction of 3-MH, thus preserving the citrus aroma of the 3-MH from oxidative degradation. Similarly, GSH and SO_2 competitive reactions were quite fast by comparison with 3-MH, also suggesting these would be very effective preservatives for thiol based aromas.

The reactions in model systems therefore predict that the substances traditionally used for the protection of wines from oxidation appear to be very protective. The next step is to study these reactions in actual wines in order to test whether or not the protective effects might be compromised by anything present in wine. It is known that sulfur dioxide binds to carbonyl compounds, but it is not known how much this might diminish it protective effect.

To conclude, the first stage of wine oxidation involves the formation of quinones from wine phenolics. These reactive *ortho*-quinones are one means by which oxidation reactions affect wine flavor by forming covalent products with varietal aromatic thiols, reducing fruity character. Other nucleophiles and reducing agents can protects against this loss by reacting with the quinones instead of the varietal thiols. In the near future it may be possible to predict the capacity of these antioxidants to protect the wine based on known reaction kinetics and factors that may alter the effective reaction rates.

References

1. Pasteur, M. L. *Etudes sur le vin*, 2nd ed.; Librairie F. Savy: Paris, 1875; 544 pages.
2. Rixford, E. *The Wine Press and the Cellar*; Robert Mondavi Institute: Davis, CA, 2008; 244 pages.
3. Amerine, M. A., Berg, H. W., and Cruess, W. *The Technology of Wine Making*, 3rd ed.; AVI: Westport, CT, 1972. pages.

Publication Date (Web): November 24, 2015 | doi: 10.1021/bk-2015-1203.ch018

4. Wildenradt, H. L.; Singleton, V. L. The production of aldehydes as a result of oxidation of polyphenolic compounds and its relation to wine aging. *Am. J. Enol. Vitic.* **1974**, *25*, 119–126.
5. *Enzymatic Browning and Its Prevention*; Lee, C. Y., Whitaker, J. R., Eds.; ACS Symposium Series 600; American Chemical Society: Washington, DC, 1995.
6. Skouroumounis, G. K.; Kwiatkowski, M.; Sefton, M. A.; Gawel, R.; Waters, E. J. In situ measurement of white wine absorbance in clear and in coloured bottles using a modified laboratory spectrophotometer. *Austr. J. Grape Wine Res.* **2003**, *9*, 138–147.
7. Cheynier, V.; Basire, N.; Rigaud, J. Mechanism of Trans-Caffeoyltartaric Acid and Catechin Oxidation in Model Solutions Containing Grape Polyphenoloxidase. *J. Agric. Food Chem.* **1989**, *37*, 1069–1071.
8. Es-Safi, N. E.; Le Guerneve, C.; Cheynier, V.; Moutounet, M. New Phenolic Compounds Formed by Evolution of (+)-Catechin and Glyoxylic Acid in Hydroalcoholic Solution and Their Implication in Color Changes of Grape-Derived Foods. *J. Agric. Food Chem.* **2000**, *48*, 4233–4240.
9. Singleton, V. L.; Zaya, J.; Trousdale, E.; Salgues, M. Caftaric acid in grapes and conversion to a reaction product during processing. *Vitis* **1984**, *23*, 113–120.
10. Singleton, V. L.; Salgues, M.; Zaya, J.; Trousdale, E. Caftaric acid disappearance and conversion to products of enzymic oxidation in grape must and wine. *Am. J. Enol. Vitic.* **1985**, *36*, 50–56.
11. Cheynier, V.; Souquet, J. M.; Moutounet, M. Glutathione content and glutathione to hydroxycinnamic acid ratio in vitis vinifera grapes and musts. *Am. J. Enol. Vitic.* **1989**, *40*, 320–324.
12. Bell, S. J.; Henschke, P. A. Implications of nitrogen nutrition for grapes, fermentation and wine. *Austr. J. Grape Wine Res.* **2005**, *11*, 242–295.
13. Fulcrand, H.; Cheminat, A.; Brouillard, R.; Cheynier, V. Characterization of compounds obtained by chemical oxidation of caffeic acid in acidic conditions. *Phytochemistry* **1994**, *35*, 499–505.
14. Cheynier, V.; Rigaud, J.; Souquet, J. M.; Barillere, J. M.; Moutounet, M. Effect of Pomace contact and Hyperoxidation on the Phenolic composition and quality of grenache and chardonnay wines. *Am. J. Enol. Vitic.* **1989**, *40*, 36–42.
15. Embs, R. J.; Markakis, P. Mechanism of Sulfite Inhibition of Browning Caused by Polyphenol Oxidase. *J. Food Sci.* **1965**, *30*, 753&.
16. Luvalle, J. E. The Reaction of Quinone and Sulfite .1. Intermediates. *J. Am. Chem. Soc.* **1952**, *74*, 2970–2977.
17. Danilewicz, J. C.; Seccombe, J. T.; Whelan, J. Mechanism of interaction of polyphenols, oxygen, and sulfur dioxide in model wine and wine. *Am. J. Enol. Vitic.* **2008**, *59*, 128–136.
18. Nikolantonaki, M.; Waterhouse, A. L. A Method To Quantify Quinone Reaction Rates with Wine Relevant Nucleophiles: A Key to the Understanding of Oxidative Loss of Varietal Thiols. *J. Agric. Food Chem.* **2012**, *60*, 8484–8491.

19. Benkwitz, F.; Tominaga, T.; Kilmartin, P. A.; Lund, C.; Wohlers, M.; Nicolau, L. Identifying the Chemical Composition Related to the Distinct Aroma Characteristics of New Zealand Sauvignon blanc Wines. *Am. J. Enol. Vitic.* **2012**, *63*, 62–72.
20. Nikolantonaki, M.; Magiatis, P.; Waterhouse, A. L. Measuring protection of aromatic wine thiols from oxidation by competitive reactions vs wine preservatives with ortho-quinones. *Food Chem.* **2014**, *163*, 61–67.

Publication Date (Web): November 24, 2015 | doi: 10.1021/bk-2015-1203.ch018

Publication Date (Web): November 24, 2015 | doi: 10.1021/bk-2015-1203.ch019

Chapter 19

Photodegradation of Organic Acids in a Model Wine System Containing Iron

P. Grant-Preece,[1,*] C. Barril,[1] L. M. Schmidtke,[1] G. R. Scollary,[1,2] and A. C. Clark[1]

[1]National Wine and Grape Industry Centre, School of Agricultural and Wine Sciences, Charles Sturt University, Locked Bag 588, Wagga Wagga, 2678, NSW, Australia
[2]School of Chemistry, The University of Melbourne, 3010, VIC, Australia
[*]E-mail: pgrant-preece@csu.edu.au.

UV-visible light has previously been shown to greatly accelerate the degradation of tartaric acid in model wine solutions containing iron, resulting in the production of glyoxylic acid. In this study, model wine solutions containing tartaric acid, malic acid, succinic acid, citric acid or lactic acid, as well as iron, were exposed to light at wavelengths above 300 nm or stored in darkness. All the organic acids were partially degraded in the samples exposed to light, but were stable in the samples stored in darkness. The photodegradation products identified using ion-exclusion liquid chromatography with diode array and mass spectrometry detection included a number of aldehydes and ketones. Glyoxylic acid and 2,3-dioxopropanoic acid were derived from tartaric acid, 3-oxopropanoic acid from malic acid and succinic acid, 1,3-acetonedicarboxylic acid and acetoacetic acid from citric acid and acetaldehyde from lactic acid. Possible pathways for the formation of these compounds are discussed. In addition, the potential implications of these reactions in white wine are described.

In Advances in Wine Research; Ebeler, et al.;
ACS Symposium Series; American Chemical Society: Washington, DC, 2015.

Publication Date (Web): November 24, 2015 | doi: 10.1021/bk-2015-1203.ch019

Introduction

Oxidation processes allowed to occur under controlled conditions can improve the sensory properties of red wines (*1*); however, these reactions generally do not improve white wines (*2*). On the contrary, in white wines, they can cause detrimental changes such as off-odor production and brown coloration. Oxygen has a triplet ground state, while organic compounds have singlet ground states, and the direct reaction between oxygen and organic compounds in their ground states is therefore spin-forbidden. Hence, triplet oxygen must be activated in order to react with organic compounds, and in wine, this is achieved by transition metal ions such as iron and copper. The reduced metal can activate oxygen by donating a single electron. The oxygen radical intermediate, possibly in the form of a metal complex (*3*), is further reduced to hydrogen peroxide, which is itself reduced by iron(II) or copper(I) in the Fenton reaction (*4*). Tartaric acid and other organic acids in wine have an important role in this process. At wine pH, these acids exist as a mixture of the carboxylic acid and carboxylate anion forms. Carboxylate anions have a high charge density and generally bind more strongly to iron(III) than to iron(II). Polycarboxylate anions can act as polydentate ligands and therefore may form more stable complexes with iron(III) than monocarboxylate anions. The formation of iron(III) complexes in wine is thought to shift the iron(III)/iron(II) equilibrium to favor the iron(III) form, which in turn promotes the reduction of oxygen and its derivatives by iron(II) (*3*). Furthermore, studies in model wine solutions suggest that the rate of oxidation is dependent on the relative proportions of iron(II) and iron(III) (*3*). When iron(II) (10 mg/L) and copper(II) (0.6 mg/L) were added to an air-saturated model wine solution containing tartaric acid, oxygen was initially consumed at a relatively rapid rate, with the simultaneous oxidation of iron(II) to iron(III). The rate of oxygen consumption decreased and appeared to become insignificant when about 2 mg/L of oxygen had been consumed, and the iron(II):iron(III) ratio was close to 1:5. The addition of iron(II) to the model wine solution without copper(II) resulted in a slower rate of oxygen consumption (*3*).

The Fenton reaction plays a key role in the oxidation of the major organic compounds in wine. The hydroxyl radical has been suggested to react with wine components at rates that are almost proportional to their concentrations (*5*) and to react with organic compounds primarily via hydrogen atom abstraction and addition to unsaturated carbon-carbon bonds (*6*). Ethanol in wine is oxidized by the hydroxyl radical to the 1-hydroxyethyl radical (*7*), which is further oxidized to acetaldehyde (*8*). Tartaric acid is degraded in model wine solutions containing iron, resulting in the production of glyoxylic acid, which can then react with flavan-3-ols, phenolic compounds derived from grape skins and seeds, to form yellow-colored xanthylium cations (*9*, *10*). There is evidence that this is initiated via the oxidation of tartaric acid by the hydroxyl radical, leading to the formation of hydroxyoxaloacetic acid, which would be in equilibrium with dihydroxyfumaric acid (*11*) (Figure 1). It is possible that tartaric acid could be oxidized to the extent observed in model wine solutions despite the large excess of ethanol because tartrate anions can interact with iron(II). Sulfur dioxide, the main preservative added to wine, reacts irreversibly with hydrogen peroxide to form sulfuric acid, and thus can limit the Fenton reaction (*12*). However,

hydrogen sulfite, the dominant form of sulfur dioxide in wine, reacts reversibly with carbonyl compounds to form addition products (*13*) and this decreases the amount of free sulfur dioxide able to scavenge hydrogen peroxide.

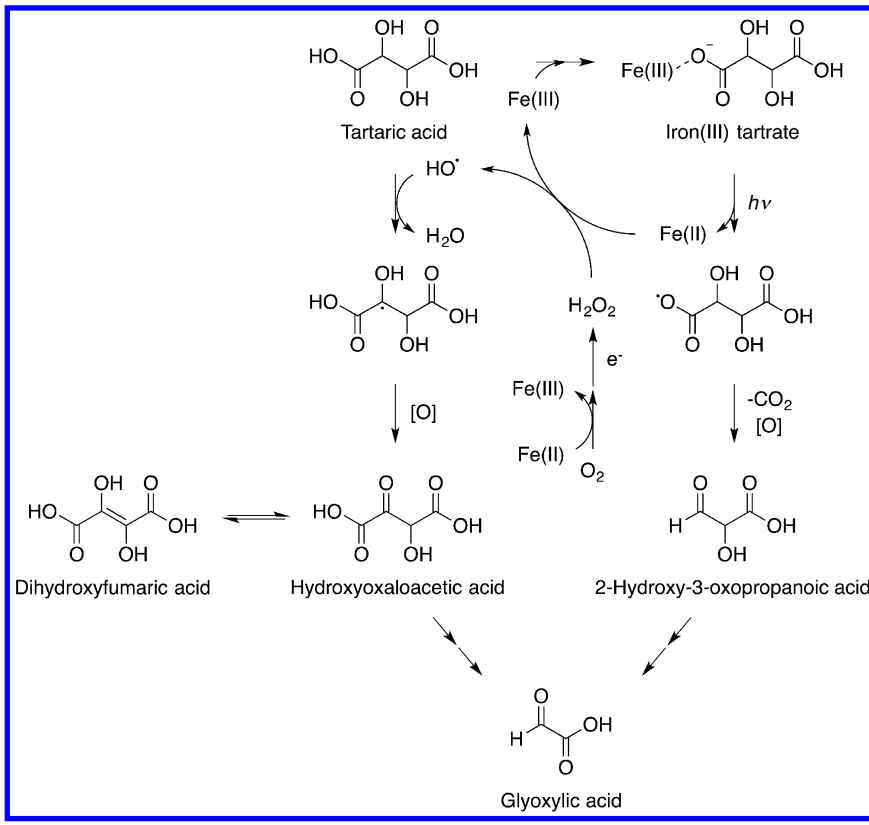

Figure 1. Pathways for the degradation of tartaric acid in wine, resulting in the production of glyoxylic acid (11, 14).

Bottled white wine is exposed to UV-visible light in different situations. For example, in the retail industry, bottles are often chilled in fridges in close proximity to artificial light sources such as fluorescent tubes, or stored at room temperature under these light sources. All glass wine bottles absorb wavelengths below 300 nm and the light that reaches the wine depends on the properties of the glass (*15*). Light has been found to induce a number of changes in white wine that are associated with a decrease in wine quality. Light can induce off-odors in bottled white wine in a relatively short period of time (*16*) and there is evidence that in many white wines (*17*), this is a consequence of the photosensitized oxidation of wine components such as sulfur-containing amino acids by riboflavin (*18*). Furthermore, light has been shown to bleach the color of white wine (*19*) and promote brown coloration (*20*) under different conditions, and to accelerate the uptake of oxygen by different wines (*2*, *21*) as well as the loss of sulfur dioxide (*22*).

Publication Date (Web): November 24, 2015 | doi: 10.1021/bk-2015-1203.ch019

Publication Date (Web): November 24, 2015 | doi: 10.1021/bk-2015-1203.ch019

Light has also been shown to greatly accelerate the oxidation of tartaric acid in model wine solutions containing iron. Tartaric acid was partially degraded in a model wine solution containing iron (10 ± 5 μg/L) exposed to sunlight, resulting in the formation of glyoxylic acid and formic acid, while it was stable in samples stored in darkness (*14*). Model wine solutions containing tartaric acid and iron have an absorption peak with a maximum around 340 nm, tailing into the visible region, associated with iron(III) tartrate (*3*, *15*). Studies on light-induced degradation of iron(III) carboxylate complexes suggest that this peak most likely corresponds to the ligand-to-metal charge transfer (LMCT) transition of iron(III) tartrate (*23*). The absorption of wavelengths within the LMCT band elicits partial electron transfer from the carboxylate ligand to iron(III), and in the resulting excited state, the complex can degrade to form iron(II) and an oxidized carboxylate radical. For α-hydroxy carboxylic acids, the carboxylate radical is further degraded via decarboxylation and oxidation to form an aldehyde or a ketone (*24*).

In the model wine solutions exposed to light, the authors proposed that tartaric acid was degraded to form glyoxylic acid as a result of the photodegradation of iron(III) tartrate and the Fenton reaction (*14*) (Figure 1). While the Fenton reaction alone would appear to favor the oxidation of ethanol in preference to tartaric acid, the evidence suggests that the light-induced degradation of iron(III) tartrate will considerably increase the oxidation of the organic acid. Iron and exposure to wavelengths below 520 nm were critical for the production of glyoxylic acid in the model wine system during short-term storage, suggesting that the degradation of tartaric acid was initiated by the photodegradation of iron(III) tartrate (*15*). It was also shown that the production of glyoxylic acid under these conditions was dependent on the oxygen concentration, with less of the compound being formed in samples that received limited exposure to air or had a low initial oxygen concentration (*14*, *15*). Furthermore, acetaldehyde was detected in model wine samples exposed to sunlight, but not in samples stored in darkness or in samples without tartaric acid exposed to light (*14*). Acetaldehyde was suggested to arise as a result of the oxidation of ethanol by the hydroxyl radical, implying that the photodegradation of iron(III) tartrate could accelerate the production of hydrogen peroxide from oxygen as well as the Fenton reaction, by increasing the proportion of iron in the form of iron(II) (Figure 1). The light-induced degradation of iron(III) complexes including iron(III) carboxylate complexes and the associated thermal reactions that occur in the presence of oxygen have been studied in detail in natural water (*25*) and wastewater (*26*) systems. However, it appears that with the exception of the model wine studies described here, very little work has been done to assess their role in the light-induced deterioration of foods and beverages.

The aim of this study was to determine whether some of the other major organic acids in wine, namely malic acid, succinic acid, citric acid and lactic acid, are degraded in a model wine system containing iron upon exposure to UV-visible light above 300 nm, and to identify the products using ion-exclusion liquid chromatography with diode array and mass spectrometry detection. In acidic aqueous solutions, these organic acids and/or structurally related acids are known to form iron(III) complexes that absorb light in the region above 300 nm (*23*, *27*). In addition, numerous studies have demonstrated that carboxylic acids

are degraded in aqueous systems containing iron and oxygen upon exposure to light (*24*). In the work described here, 12% (v/v) aqueous ethanol solutions of the individual acids at 18 mmol/L and at wine-like concentrations were prepared. The pH was adjusted to 3.2 and iron(II) was added at 5 mg/L, a concentration within the range typically observed in white wines (*28*). The solutions were bubbled with oxygen to promote the oxidation process, and then exposed to wavelengths above 300 nm or left in darkness at 15 °C.

Materials and Methods

General

Glass and plastic items were soaked in 10% (v/v) nitric acid for at least 12 hours and then rinsed thoroughly with Milli-Q water. All of the solutions were prepared using Milli-Q water. L-Tartaric acid (99.5%), glyoxylic acid monohydrate (98%), fumaric acid (neat), pyruvic acid (98%), 3-hydroxypropanoic acid (30%) and 1,3-acetonedicarboxylic acid (98.7%) were obtained from Sigma-Aldrich (USA). Malonic acid (neat) was obtained from Supelco (USA). L-(–)-Malic acid (≥ 99%), succinic acid (≥ 99.5%), anhydrous citric acid (≥ 99.5%), formic acid (98%), ethyl acetoacetate (≥ 99.0%) and acetaldehyde (≥ 99.5%) were obtained from Fluka (Switzerland). Tartronic acid (98%) was obtained from ABCR GmbH & Co (Germany). Lactic acid (88% w/w) and sodium hydroxide (1 mol/L) were obtained from Chem-supply (Australia). Oxalic acid (≥ 99.5%), sulfuric acid (98%) and orthophosphoric acid (85%) were obtained from Ajax Chemicals (Australia). Nitric acid (67 – 70%) was obtained from BDH Chemicals (Australia). Iron(II) sulfate heptahydrate (≥ 99.0%) was obtained from Biolab (Australia).

Model Wine Solutions

Solutions of the individual organic acids at 18 mmol/L, corresponding to 2.70 g/L tartaric acid, 2.41 g/L malic acid, 2.13 g/L succinic acid, 3.46 g/L citric acid and 1.62 g/L lactic acid, were prepared in 12% (v/v) aqueous ethanol. In wine, tartaric acid and malic acid are typically present at similar concentrations, however the concentrations of succinic acid, citric acid and lactic acid are generally closer to 0.8 g/L, 0.5 g/L and 0.2 g/L respectively (*29*), hence, additional solutions of these acids at the wine-like concentrations were also prepared. The pH was adjusted to 3.2 ± 0.1 through the addition of 1 mol/L sodium hydroxide or 0.5% (v/v) sulfuric acid. Aliquots (10 mL) of each solution were added to three separate 20 mL scintillation vials. An iron(II) stock solution was prepared by dissolving iron(II) sulfate heptahydrate in water acidified to pH 3.1 ± 0.1 and then purged with nitrogen gas. The 10 mL samples were treated one at a time, in a randomized order, as described below. Immediately before storage, 100 µL of the iron(II) stock solution was added to give an iron concentration equal to 5 mg/L (0.090 mmol/L) and then oxygen gas was bubbled through the solution for 5 min. Based on trial experiments conducted using the tartaric acid-based model wine solution, in which the oxygen concentration was measured using a PreSens Fibox 3 LCD trace v7

Publication Date (Web): November 24, 2015 | doi: 10.1021/bk-2015-1203.ch019

oxygen meter and pre-calibrated PSt3 oxygen sensor, the oxygen concentration was 33 ± 2 mg/L. The trial experiments showed that the photodegradation products were formed at higher concentrations in samples bubbled with oxygen than in air-saturated samples, and the former was thus adopted in order to generate sufficient amounts of the products for direct detection. Sulfur dioxide was not added to the solutions as it most likely would have supressed the oxidation process and also complicated the identification of any carbonyl compounds by reacting with these species to form adducts.

Storage Conditions

After preparation of a model wine solution as outlined above, 3 mL aliquots of the solution were added to two standard 3 mL quartz cuvettes, which were sealed with Teflon stoppers to prevent the escape and/or ingress of oxygen during the storage time. The sample to be exposed to light was placed in a temperature-controlled cuvette holder, with a 2.1 cm^2 elliptical window, which was positioned 28.8 cm from a 300 W xenon arc lamp (Cermax LX300F, Perkin Elmer). The light emitted by the lamp was passed through a heat-absorbing glass filter (FSQ-KG5, Newport). The lamp had a spectral distribution similar to that of sunlight and the filter transmitted wavelengths between approximately 300 and 860 nm. The average intensity of the light in the range 400 – 700 nm that reached the cuvette was 16200 μmol/m^2/s. The cuvette holder, lamp and filter were assembled in a custom-made box with a lid and a shutter, which allowed samples to be initially stored without exposure to light. The sample to be stored in darkness was wrapped in aluminum foil and placed in an incubator (see below). Both samples were initially left in darkness for 30 min to allow the temperature to equilibrate. At the end of this time, the sample in the irradiation set-up was exposed to light for one hour, while the other sample remained in darkness for the same period of time. The temperature of the sample in the irradiation set-up was 13 ± 0.5 °C at the end of the temperature equilibration time. It increased to 15 ± 0.5 °C within the first 10 min of exposure to the lamp and remained at this temperature for the rest of the storage time. The temperature of the dark sample was 15 ± 0.5 °C at the end of the temperature equilibration time and remained at this value for the duration of the experiment.

Liquid Chromatography with Diode Array Detection (LC-DAD)

LC-DAD analysis was conducted using a Waters 2690 Separation Module and a Waters 2996 diode array detector, run by Empower 3 software (Waters). The method was similar to that used previously to quantify the major organic acids and sugars in wine and must (*30*). Two 300 × 7.8 mm Aminex HPX-87H cation exchange columns (Bio-Rad Laboratories, Australia), with a guard column of the same material, were connected in series. The columns were maintained at 60 °C, the injection volume was 10 μL, the isocratic mobile phase was 0.065% (v/v) phosphoric acid in water and the flow rate was 0.7 mL/min. The organic acids were detected at 210 nm and all of the photodegradation products were also detected at 210 nm, except for acetaldehyde, which was detected at 278

Publication Date (Web): November 24, 2015 | doi: 10.1021/bk-2015-1203.ch019

nm. Tartaric acid, malic acid, succinic acid, citric acid, fumaric acid, pyruvic acid, glyoxylic acid and acetaldehyde were quantified using external calibration graphs. All of the photodegradation products were identified by comparison with commercial standards, except for 2,3-dioxopropanoic acid and 3-oxopropanoic acid, which were identified by LC-DAD-MS and accurate mass LC-MS (see below). Acetoacetic acid was prepared from ethyl acetoacetate as described previously (*31*).

Liquid Chromatography with Diode Array and Mass Spectrometry Detection (LC-DAD-MS)

LC-DAD-MS analysis was performed using an Agilent 6410 Triple Quadrupole LC-MS instrument with an electrospray ionization (ESI) source and an Agilent 1200 Series LC system equipped with a diode array detector, run by MassHunter Workstation software for Triple Quad B.03.01 (Agilent). The conditions were the same as above, except the mobile phase was 10 mmol/L formic acid in water and the 0.7 mL/min flow was split after the diode array detector at a ratio of 1:3 (MS:waste), such that the flow to the MS detector was about 0.18 mL/min. The MS detector was operated in both the negative and positive ion modes, scanning in the region *m/z* 55 – 400, with a fragmentor voltage of 30 V. The gas temperature was 325 °C, the gas flow was 8 L/min, the nebulizer pressure was 40 psi and the capillary voltage was 4000 V.

Accurate Mass LC-MS

Accurate mass LC-MS analysis was performed using an Agilent 6530 Quadrupole-Time of Flight (Q-TOF) Accurate Mass LC-MS instrument with an ESI source and an Agilent 1290 Infinity LC system, run by MassHunter Workstation software for 6500 series Q-TOF B.05.01 (Agilent). The LC conditions were the same as those used in the LC-DAD-MS method, except the injection volume was 3 μL. The MS detector was operated in extended dynamic range (2 GHz) mode and in both the negative and positive ion modes, scanning in the range *m/z* 70 – 1700. The nozzle voltage was 1000 V, the fragmentor voltage was 30 V, the skimmer 1 voltage was 65 V and the octopole RF peak voltage was 750 V. The gas temperature, gas flow, nebulizer pressure and capillary voltage were the same as those used in the LC-DAD-MS method. The sheath gas temperature was 350 °C and the sheath gas flow was 11 L/min. The internal reference ions for mass calibration in the negative ion mode were *m/z* 112.985587 and 1033.988109, and in the positive ion mode were *m/z* 121.050873 and 922.009798.

Results and Discussion

Degradation of the Organic Acids

Upon exposure to light at wavelengths above 300 nm, all of the organic acids were partially degraded in the model wine system; however, they were

In Advances in Wine Research; Ebeler, et al.;
ACS Symposium Series; American Chemical Society: Washington, DC, 2015.

Publication Date (Web): November 24, 2015 | doi: 10.1021/bk-2015-1203.ch019

stable in the samples stored in darkness. In the equimolar solutions (18 mmol/L), the concentration of tartaric acid, malic acid, succinic acid and citric acid decreased by 5 – 6%. Interestingly, the concentration of succinic acid decreased by around the same absolute amount in the wine-like concentration and the 18 mmol/L solutions exposed to light, and this was also the case for the citric acid solutions exposed to light (Table 1). Although malic acid co-eluted with one of its photodegradation products using the 0.065% (v/v) phosphoric acid in water mobile phase, the compounds were separated using 10 mmol/L formic acid in water. In the 210 nm chromatogram obtained using the LC-DAD-MS method, the peak area of malonic acid was about 0.5% that of malic acid. Hence, the error in the measured concentration of malic acid in the irradiated samples associated with the co-elution of malic acid and malonic acid was considered to be negligible.

Publication Date (Web): November 24, 2015 | doi: 10.1021/bk-2015-1203.ch019

Table 1. Concentrations of Tartaric Acid, Malic Acid, Succinic Acid and Citric Acid, and Lactic Acid Monomer Peak Areas, before Storage and after Irradiation or Storage in Darkness

Solution	*Initial*	*Irradiated*[2]	*Dark*[3]
Tartaric acid (18 mmol/L)	2.76 ± 0.05	2.60 ± 0.09	2.78 ± 0.06
Malic acid (18 mmol/L)	2.46 ± 0.02	2.32 ± 0.05	2.48 ± 0.05
Succinic acid (18 mmol/L)	2.20 ± 0.02	2.08 ± 0.07	2.19 ± 0.01
Citric acid (18 mmol/L)	3.51 ± 0.07	3.31 ± 0.02	3.53 ± 0.03
Lactic acid (18 mmol/L)[1]	7.5 ± 0.1	6.8 ± 0.2	7.48 ± 0.03
Succinic acid (6.8 mmol/L)	0.84 ± 0.03	0.73 ± 0.02	0.84 ± 0.01
Citric (2.6 mmol/L)	0.51 ± 0.02	0.27 ± 0.01	0.51 ± 0.01
Lactic acid (2.2 mmol/L)[1]	0.9 ± 0.1	0.18 ± 0.07	0.18 ± 0.07

Values are the average of three replicates ± 95% confidence limits. For all of the organic acids except lactic acid (see below), values are concentrations in g/L. [1] The concentration of lactic acid was not determined and reasons for this are given in the text. Values are lactic acid monomer peak areas ($\times 10^5$). [2] In all cases, the value for the solution exposed to light was significantly lower than the initial value. [3] In all cases, the value for the solution stored in darkness was not significantly different from the initial value.

Lactic acid was present as a mixture of the acid and various oligomers derived through the intermolecular esterification of the acid. The peak attributed to the lactic acid monomer and those attributed to the oligomers were identified by LC-DAD-MS (data not shown). The different lactic acid species were only partially separated using the methods described herein and it is possible that their distribution may have changed during the course of the experiment due to ester hydrolysis. Nevertheless, a comparison between the total ion and the 210 nm chromatograms of the lactic acid solutions stored under the different conditions,

obtained using the LC-DAD-MS method, indicated that the lactic acid oligomers were present at similar levels in these solutions, while the amount of the lactic acid monomer was lower in the irradiated samples than in the dark samples. The area of the lactic acid monomer peak in the LC-DAD chromatograms extracted at 210 nm decreased significantly in both the wine-like concentration and the 18 mmol/L lactic acid solutions upon exposure to light, while it remained unchanged during storage in darkness (Table 1). The peak area values suggest that the lactic acid monomer decreased by the same absolute amount in the wine-like concentration and the 18 mmol/L lactic acid samples exposed to light.

The organic acids were degraded in the model wine solutions exposed to light as a result of photochemical reactions. Previous studies in model wine solutions (*14*, *15*) and in aqueous solutions containing an organic acid and iron (*24*) suggest that the organic acids were degraded largely due to the light-induced degradation of the corresponding iron(III) carboxylate complexes. In the present study, some of the iron(II) added to the solutions may have been oxidized to iron(III), with the amount of iron(III) generated depending on the concentration of the organic acid, its ability to deprotonate and the affinity of the carboxylate anions for iron(III) (*3*). It should be noted that the iron(III) monohydroxy complex ($Fe(III)(OH)(H_2O)_5^{2+}$), the main monomeric iron(III) complex in aqueous solutions at pH 2.5 – 5, has an absorption maximum at 300 nm and can degrade upon exposure to UV radiation to form iron(II) and a hydroxyl radical (*32*). Hence, this reaction may have contributed to the degradation of the organic acids in the solutions exposed to light. However, it is expected that in the model wine solutions the majority of the iron(III) present would be coordinated by carboxylate anions. Furthermore, it has been shown that glyoxylic acid was formed in a model wine solution containing tartaric acid and iron exposed to wavelengths between 400 and 520 nm, and under these conditions only iron(III) tartrate could have degraded, leading to the formation of glyoxylic acid (*15*).

Contaminant organic acids were identified in some of the model wine solutions. Fumaric acid (11.5 μmol/L) was detected in the 18 mmol/L malic acid solution, and pyruvic acid (4.9 and 50.0 μmol/L, respectively) was detected in the wine-like concentration and the 18 mmol/L lactic acid solutions. Interestingly, pyruvic acid was completely degraded in the lactic acid solutions exposed to light, and fumaric acid was almost completely degraded in the malic acid solution exposed to light, while both acids were stable in the solutions stored in darkness. Malonic acid was detected in the 18 mmol/L citric acid solution, however it was stable under both storage conditions and possible reasons for this difference are discussed below.

Photodegradation Products

Glyoxylic acid, oxalic acid, formic acid and tartronic acid were detected in the irradiated tartaric acid solution, in agreement with previous studies (*14*, *15*). The 210 nm chromatogram of this solution also had a peak immediately before the peak corresponding to tartaric acid (peak 2, Figure 2). The mass spectrum of this compound, acquired in the negative ion mode, showed the most intense peak at *m/z* 101, and a peak indicative of the decarboxylation of the *m/z* 101 ion. It also

Publication Date (Web): November 24, 2015 | doi: 10.1021/bk-2015-1203.ch019

exhibited peaks corresponding to the hydrate and dihydrate of the *m/z* 101 ion, and the adducts of the species and its hydrated forms (Figure 3). The mass spectrum is similar to that of glyoxylic acid (*33*), the main differences being the ability of the unknown compound to undergo hydration at two positions, and the apparent mass of the unknown compound, which was 28 mass units greater than that of glyoxylic acid, suggesting that it had additional carbon and oxygen atoms. The proposed molecular formula was confirmed by accurate mass LC-MS analysis (Table 2). The data are consistent with 2,3-dioxopropanoic acid (Figure 4). This compound is a reported product of the oxidation of succinic acid in an aqueous system (*34*).

Publication Date (Web): November 24, 2015 | doi: 10.1021/bk-2015-1203.ch019

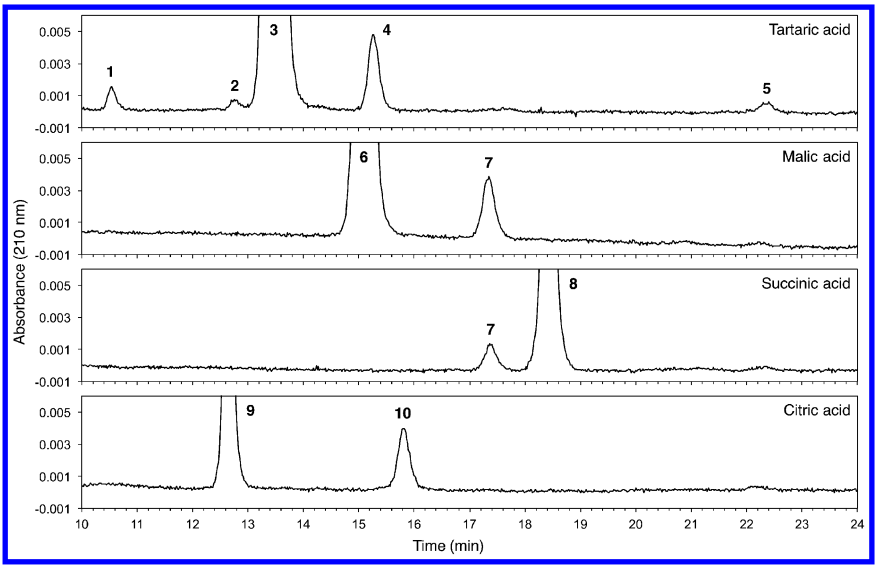

Figure 2. LC-DAD chromatograms extracted at 210 nm of the wine-like concentration tartaric acid, malic acid, succinic acid and citric acid solutions exposed to light. The peaks were assigned as follows; ***1*** *oxalic acid;* ***2*** *2,3-dioxopropanoic acid;* ***3*** *tartaric acid;* ***4*** *glyoxylic acid;* ***5*** *formic acid;* ***6*** *malic acid; 7 3-oxopropanoic acid;* ***8*** *succinic acid;* ***9*** *citric acid;* ***10*** *1,3-acetonedicarboxylic acid.*

The photodegradation of iron(III) tartrate would lead to the generation of a carboxylate radical, which can undergo decarboxylation and oxidation to form 2-hydroxy-3-oxopropanoic acid (Figure 4). Carboxylic acids that have a β carbonyl group can undergo thermal decarboxylation. Hence, 2-hydroxy-3-oxopropanoic acid could degrade in this manner to form glycolaldehyde, which could then be oxidized to form a variety of two carbon products including glyoxylic acid. Alternatively, 2-hydroxy-3-oxopropanoic acid could be oxidized, thereby generating 2,3-dioxopropanoic acid via the oxidation

of the alcohol group, while the oxidation of the aldehyde would give tartronic acid (Figure 4). 2,3-Dioxopropanoic acid could then degrade via decarboxylation and oxidation to form glyoxylic acid (Figure 4), which could in turn be oxidized to form oxalic acid. The concentration of glyoxylic acid in the tartaric acid solution exposed to light was 1.45 ± 0.30 mmol/L. This was more than four times greater than the amount detected in a similar model wine solution that was exposed to light emitted by a xenon arc lamp, filtered using glass that transmitted 300 – 400 nm or 400 – 520 nm radiation, for 30 min (*15*). It has been shown that the production of glyoxylic acid in model wine solutions containing tartaric acid and iron exposed to light is limited by the amount of oxygen present (*14*, *15*), therefore, in this experiment, it is likely that the high oxygen concentration contributed to the greater yield of glyoxylic acid.

Publication Date (Web): November 24, 2015 | doi: 10.1021/bk-2015-1203.ch019

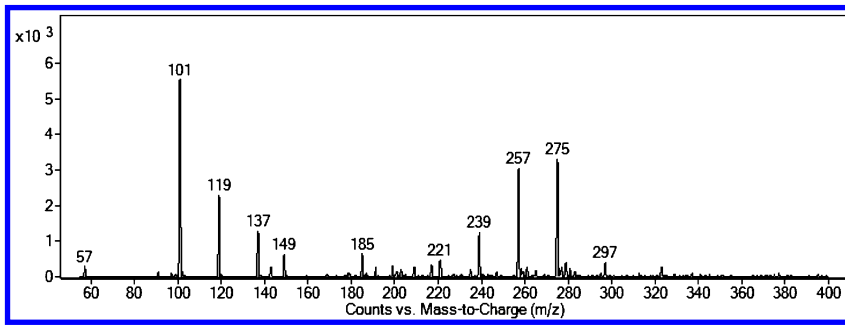

Figure 3. Mass spectrum of the compound corresponding to peak 2 in Figure 2. The spectrum was obtained using the LC-DAD-MS method, in the negative ion mode. The compound was identified as 2,3-dioxopropanoic acid.

Oxalic acid was detected in the tartaric acid solution stored in darkness, and the area of the oxalic acid peak was about 15% of the area of this peak in the irradiated solution. In the solution stored in darkness, glyoxylic acid was not detected using the LC-DAD method, however it was detected using the LC-DAD-MS method. These compounds were not observed in an air-saturated model wine solution containing tartaric acid and a trace amount of iron stored in darkness for 10 days (*14*), or in samples with 5 mg/L iron stored in darkness for 30 min (*15*). Factors that may have contributed to the oxidation of tartaric acid in the dark samples in the present study include the presence of iron, initially in the form of iron(II), at 5 mg/L, the higher oxygen concentration, and the one-hour storage time, which was preceded by a 30 min temperature equilibration time. Initially, oxygen would have been reduced by iron(II) at a moderate rate, resulting in the production of hydrogen peroxide, and oxygen consumption would have slowed as iron(III) accumulated (*3*). Hydroxyl radicals generated by the Fenton reaction can oxidize tartaric acid, leading to the formation of hydroxyoxaloacetic acid and/or its tautomers (*11*). Hydroxyoxaloacetic acid could degrade via decarboxylation

to form hydroxypyruvic acid, a tautomer of 2-hydroxy-3-oxopropanoic acid (Figure 4). The presence of oxalic acid and glyoxylic acid in the tartaric acid samples stored in darkness suggests that the Fenton reaction also contributed to the degradation of tartaric acid in the samples exposed to light. This mechanism would have occurred in both the samples exposed to light and those stored in darkness, however the associated loss of tartaric acid may have been greater in the samples exposed to light due to the continual conversion of iron(III) to iron(II) via iron(III) complex photodegradation (Figure 1).

Publication Date (Web): November 24, 2015 | doi: 10.1021/bk-2015-1203.ch019

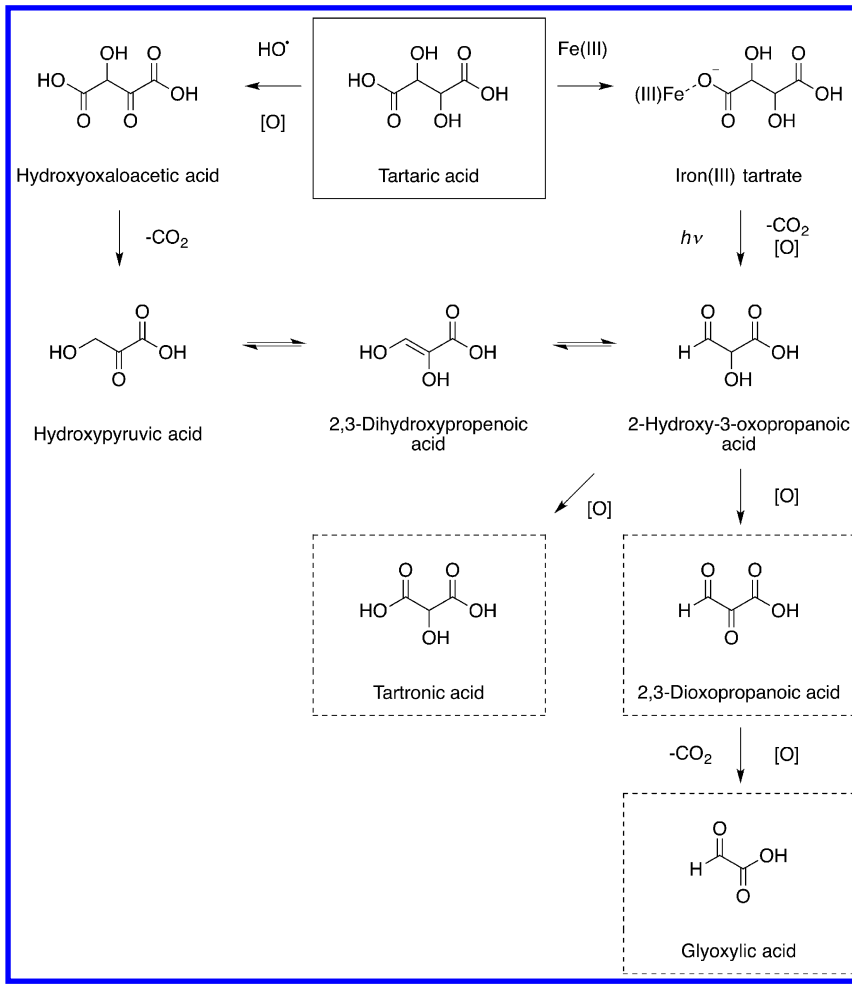

Figure 4. Proposed pathways for the degradation of tartaric acid in the model wine system. Compounds identified in the samples exposed to light are in dashed boxes.

Publication Date (Web): November 24, 2015 | doi: 10.1021/bk-2015-1203.ch019

Table 2. Photodegradation Products of the Organic Acids Identified by LC-DAD and MS

Proposed compound	*Formula*	*MS polarity*	*Selected ions (m/z)*[1]	*Exact mass (m/z)*[2]	*UV maxima (nm)*[3]
Oxalic acid	$C_2H_2O_4$	Negative	89	ND	ND
Tartronic acid	$C_3H_4O_5$	Negative	75, 119	ND	ND
2,3-Dioxopropanoic acid	$C_3H_2O_4$	Negative	57, 101, 119, 137[4]	100.9884	ND
Glyoxylic acid	$C_2H_2O_3$	Negative	73, 91, 147, 165	72.9938	207
Malonic acid	$C_3H_4O_4$	Negative	59, 103	103.0038	ND
3-Oxopropanoic acid	$C_3H_4O_3$	Negative	87, 105	87.0093	231
3-Hydroxypropanoic acid	$C_3H_6O_3$	Negative	89	89.0248	ND
1,3-Acetonedicarboxylic acid	$C_5H_6O_5$	Positive	129, 147	147.0287	242
Acetoacetic acid	$C_4H_6O_3$	Positive	85, 103	103.0397	ND

ND Not determined. All of the compounds, except for 2,3-dioxopropanoic acid and 3-oxopropanoic acid, were also identified by comparison with commercial standards. [1] Ions in the mass spectrum obtained using the LC-DAD-MS method relevant to the assignment. [2] For all of the compounds for which an accurate mass was obtained, the mass was within ± 10 ppm of the theoretical mass of the proposed compound. [3] UV absorption maxima were only recorded for compounds that had a maximum absorbance > 0.002. [4] Refer to Figure 3 for the mass spectrum of the compound identified as 2,3-dioxopropanoic acid.

Acetaldehyde was detected in most of the irradiated samples using the LC-DAD method, though in many of these samples it was only marginally above the limit of quantification (0.16 mmol/L). The absence of acetaldehyde in some of the irradiated samples may have been due to the loss of the compound before analysis, as it is relatively volatile. Acetaldehyde was not detected in any of the samples stored in darkness. The light-induced production of acetaldehyde was previously observed in a model wine solution containing tartaric acid and iron, and in this system, acetaldehyde was suggested to arise from ethanol as a consequence of the Fenton reaction. In addition, the formation of acetaldehyde was shown to be dependent on the presence of tartaric acid, as it was not detected in a tartrate-free aqueous ethanol solution at pH 3.2 exposed to sunlight (*14*). This suggests that the light-induced degradation of iron(III) carboxylate complexes to form iron(II) and an oxidized carboxylate radical, could in turn accelerate oxygen consumption, as well as the Fenton reaction, resulting in the more rapid oxidation of ethanol to acetaldehyde.

Malic acid was degraded in the model wine solution exposed to light to form malonic acid and a second compound, corresponding to peak 7 in Figure 2. The mass spectrum of this compound, acquired in the negative ion mode, showed ions with *m/z* 87 and 105, the latter ion consistent with the hydration of the *m/z* 87 ion. The exact mass indicated that the molecular formula was $C_3H_4O_3$ (Table 2). This suggested that the compound could be 3-oxopropanoic acid or pyruvic acid (2-oxopropanoic acid), although pyruvic acid had a different retention time to that of peak 7, and it was thus concluded that the compound was 3-oxopropanoic acid. This compound is the product of the light-induced degradation of iron(III) malate, followed by the decarboxylation and oxidation of the oxidized malate radical (Figure 5). The compound corresponding to peak 7 had an absorption maximum at around 230 nm, consistent with the conjugated enol form of 3-oxopropanoic acid. Malonic acid could then be derived from 3-oxopropanoic acid through the oxidation of the aldehyde group (Figure 5).

3-Oxopropanoic acid was also identified as the major initial product of the photodegradation of malic acid in an aqueous solution using titanium dioxide as an oxidation catalyst (*35*). Malonic acid was observed in this system (*35*) and was also shown to be the major primary product of the degradation of malic acid in an acidic aqueous solution containing iron exposed to wavelengths above 290 nm (*36*). These studies also provided evidence for a minor pathway involving the reaction of malic acid with the hydroxyl radical, resulting in the production of tartaric acid, which then degraded to form glyoxylic acid. In the present study, tartaric acid was not detected in the irradiated malic acid samples. Glyoxylic acid co-eluted with malic acid (Figure 2) in both mobile phases used here, and thus evidence for its formation could not be obtained. This limitation could be overcome in future studies by using a method involving the derivatisation of the carbonyl compounds prior to analysis.

Publication Date (Web): November 24, 2015 | doi: 10.1021/bk-2015-1203.ch019

Publication Date (Web): November 24, 2015 | doi: 10.1021/bk-2015-1203.ch019

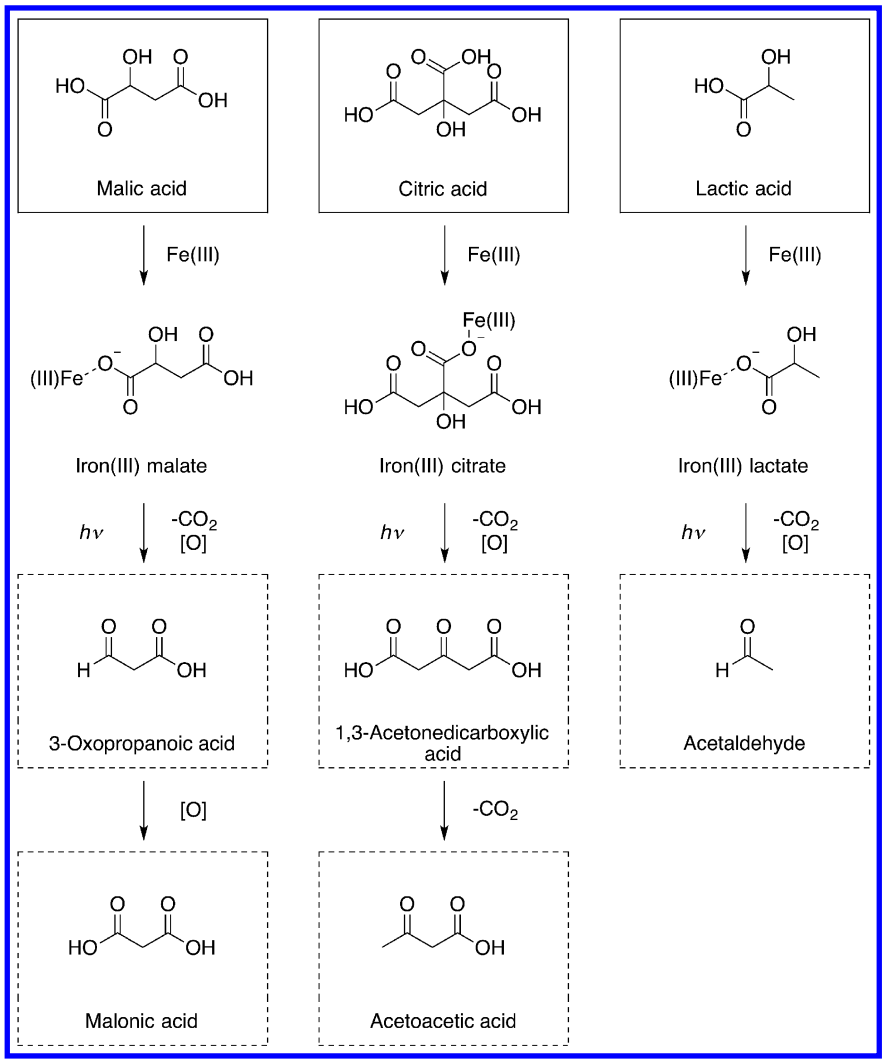

Figure 5. Proposed pathways for the photodegradation of malic acid, citric acid and lactic acid in the model wine system. Compounds identified in the samples exposed to light are in dashed boxes.

3-Oxopropanoic acid was also detected in the irradiated succinic acid solutions (Figure 2), along with 3-hydroxypropanoic acid. Similar amounts of these compounds were detected in the solutions at the wine-like concentration and at 18 mmol/L after exposure to light, consistent with the equivalent loss of succinic acid in these solutions. Succinic acid differs from the other organic acids in that it does not have an α-hydroxyl group that can be converted to a carbonyl group following the photochemical oxidation of the carboxylate anion by iron(III) (*37*). 3-Oxopropanoic acid was tentatively identified as the major initial product of the oxidation of succinic acid in an aqueous system containing titanium dioxide

exposed to near UV radiation (*38*). The authors proposed that succinic acid was degraded through the oxidation of the carboxylate anion and the loss of carbon dioxide to form an alkyl radical, which then reacted with oxygen to generate an alkylperoxyl radical. This pathway may have occurred in the model wine solutions exposed to light as a result of the light-induced degradation of iron(III) succinate (Figure 6). Primary alkylperoxyl radicals may undergo intermolecular reactions to form an aldehyde and an alcohol (*39*) or two molar equivalents of the aldehyde (*40*) (reactions 1 and 2, Figure 7). Primary alkylperoxyl radicals can also give rise to alkoxyl radicals (reactions 3 – 5, Figure 7), which can then be oxidized or reduced to generate the same compounds (*34*, *38*) (reactions 6 and 7, Figure 7). These reactions may have contributed to the formation of 3-oxopropanoic acid and 3-hydroxypropanoic acid in the succinic acid model wine solutions exposed to light (Figure 6).

Citric acid was degraded in the model wine solutions exposed to light to form 1,3-acetonedicarboxylic acid and acetoacetic acid. As was the case for succinic acid, approximately the same amounts of the citric acid degradation products were detected in the wine-like concentration and the 18 mmol/L solutions exposed to light. 1,3-Acetonedicarboxylic acid and acetoacetic acid, in addition to acetone, are the major reported products of the degradation of citric acid in aqueous solutions containing iron and oxygen exposed to light (*31*, *37*). The proposed pathway for the degradation of citric acid under these conditions involves light-induced charge transfer from the central carboxylate group to iron(III) resulting in the production of 1,3-acetonedicarboxylic acid. This compound is unstable and degrades via decarboxylation to form acetoacetic acid (Figure 5) and acetone. However, acetone was not detected in the irradiated citric acid-based model wine solutions using the methods described.

The concentration of acetaldehyde in the irradiated wine-like concentration lactic acid sample was 1.4 ± 0.1 mmol/L and the concentration in the irradiated 18 mmol/L lactic acid sample did not differ significantly, while the greatest amount of acetaldehyde observed in the samples of the other organic acids exposed to light was 0.36 mmol/L. Acetaldehyde is the expected product of the photodegradation of iron(III) lactate, and the further degradation of the oxidized lactate radical (Figure 5), and has been reported to be a product of the photodegradation of lactic acid in aqueous solutions containing iron (*24*). Given that the area of the acetaldehyde peak in the lactic acid solutions was four times greater than that of the largest acetaldehyde peak observed in the samples of the other organic acids exposed to light, it appears that only a small proportion of the acetaldehyde detected in the lactic acid solutions was derived from ethanol.

For succinic acid, citric acid and the lactic acid monomer, the equivalent loss of the acid in the wine-like concentration and 18 mmol/L solutions exposed to light suggests that the concentration of the acid only had a minor impact on the processes that resulted in its degradation. Another possibility is that the degradation of the acid may have been limited by the amount of oxygen present, since if oxygen was depleted this could affect the oxidation of iron(II) to iron(III) and therefore the amount of iron(III) available to form carboxylate complexes. The photodegradation of iron(III) carboxylate complexes could increase the proportion of iron(II) in solution and thus overcome the observed inhibitory

Publication Date (Web): November 24, 2015 | doi: 10.1021/bk-2015-1203.ch019

effect of iron(III) accumulation on oxygen consumption in model wine systems (*3*). Furthermore, the radicals generated as a result of the photodegradation of these complexes could also contribute to the reduction of oxygen. If the oxygen in these samples was largely consumed before the end of the storage time, this would have limited the oxidation of iron(II) to iron(III) and therefore limited the formation of iron(III) carboxylate complexes. This could be investigated by monitoring the organic acid, iron(II)/iron(III) and oxygen concentrations during exposure to light.

Publication Date (Web): November 24, 2015 | doi: 10.1021/bk-2015-1203.ch019

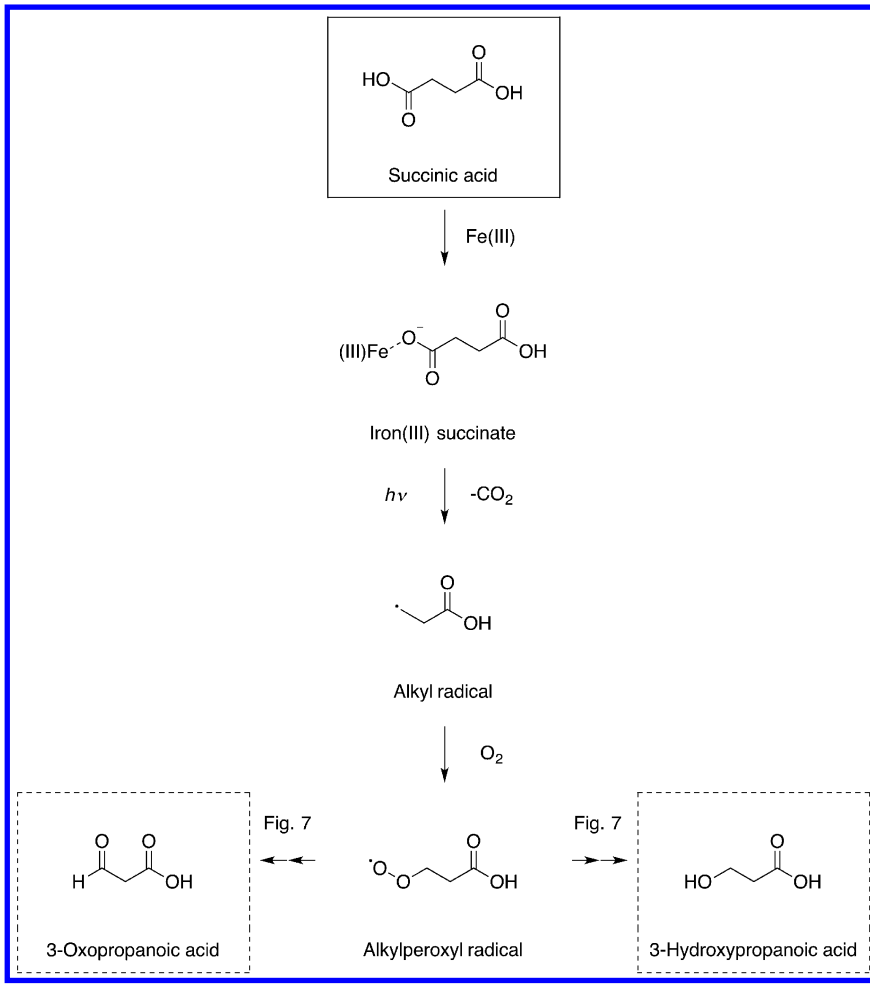

Figure 6. Proposed pathways for the photodegradation of succinic acid in the model wine system. Compounds identified in the samples exposed to light are in dashed boxes. Reactions of alkylperoxyl radicals that could contribute to the formation of the products are listed in Figure 7.

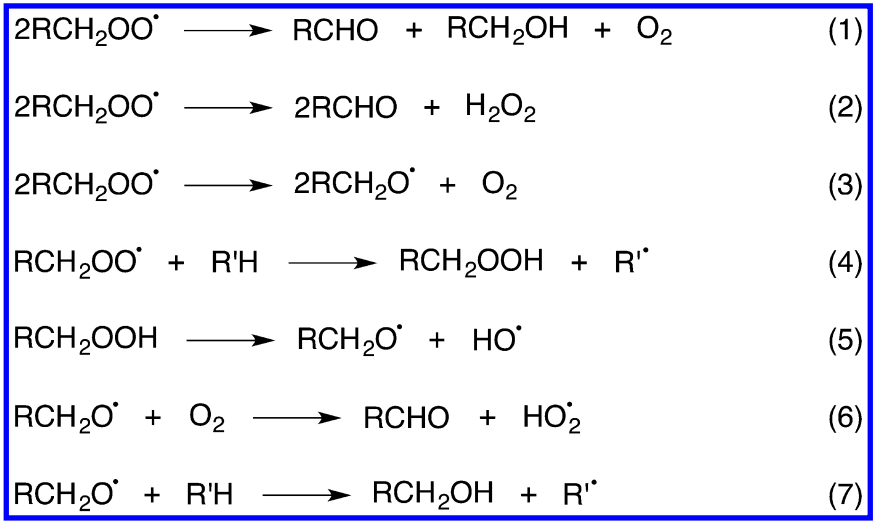

Figure 7. Reactions of primary alkylperoxyl radicals ($RCH_2COO\cdot$) and alkoxyl radicals ($RCH_2CO\cdot$) resulting in the formation of aldehyde and alcohol products (34, 38–40).

Publication Date (Web): November 24, 2015 | doi: 10.1021/bk-2015-1203.ch019

Fumaric acid, an impurity in the malic acid solution, and pyruvic acid, an impurity in the lactic acid solutions, were extensively degraded in the samples exposed to light, whereas malonic acid, an impurity in the 18 mmol/L citric acid solution, was stable under these conditions. Fumaric acid has a carbon-carbon double bond while pyruvic acid is known to exist in its enol form in wine conditions (*41*). Studies in model wine solutions containing hydroxycinammic acids, phenolic compounds that have an unsaturated carboxylic acid substituent, have provided evidence that the double bond is attacked by various radicals that could be generated as a result of oxidation processes in wine. The radicals that attacked the double bond included the carbon-centered 1-hydroxyethyl radical (*42*) and the sulfur-centered glutathiyl radical (*43*). Hence, in the present study, the reaction of radicals such as the 1-hydroxyethyl radical with unsaturated organic acids such as fumaric acid and the enol form of pyruvic acid may have contributed to their degradation.

Possible Implications in White Wine

It is important to note the similarities and differences between the light exposure conditions used in this study and the conditions under which bottled wine is commonly exposed to light in the wine industry. In this work, the samples were exposed to UV-visible light at wavelengths that are known to pass through glass wine bottles (> 300 nm). In addition the samples were stored at a temperature (15 °C) that is within the range typically used for wine storage. On the other hand, the samples had a much higher initial oxygen concentration than

would be expected in bottled wine (i.e. 33 ± 2 mg/L in comparison to less than a few mg/L). Furthermore, the measured intensity of the light (400 – 700 nm) that reached the samples was on average 16200 μmol/m^2/s. In contrast, the intensity of two 36 W Phillips cool daylight fluorescent tubes measured at a distance equal to 5 cm from the tubes was 150 μmol/m^2/s, and it is expected that this would be close to the light intensity inside illuminated fridges used in bottle shops. Other major differences include the small volume of sample that was exposed to light and the absence of sulfur dioxide, phenolic compounds and other compounds that could influence the outcome in wine. The light exposure conditions used in the present study were chosen as they allowed the organic acids to be degraded to such an extent that the products could be directly detected and identified.

The results of this study suggest that exposing bottled white wine to light could induce the degradation of tartaric acid, malic acid, succinic acid, citric acid and lactic acid, resulting in the production of a variety of aldehydes and ketones, though further work is required under more typical wine storage conditions. Glyoxylic acid can induce the polymerization of flavan-3-ols, leading to the formation of yellow pigments (*9*, *10*), and both glyoxylic acid and acetaldehyde can bind sulfur dioxide, thereby decreasing the amount of sulfur dioxide available to protect the wine from spoilage. The other carbonyl compounds identified in this study could also potentially react with sulfur dioxide and flavan-3-ols. It appears that the organic acids in white wine could be degraded upon exposure to light due to the photodegradation of the corresponding iron(III) carboxylate complexes to form iron(II) and an oxidized carboxylate radical. As well as initiating the degradation of organic acids, this reaction could accelerate oxygen consumption, leading to the production of hydrogen peroxide and the loss of sulfur dioxide, and therefore could influence the shelf life of the wine.

Publication Date (Web): November 24, 2015 | doi: 10.1021/bk-2015-1203.ch019

Conclusion

UV-visible light at wavelengths above 300 nm induced the partial degradation of tartaric acid, malic acid, succinic acid, citric acid and lactic acid in a model wine system containing iron and oxygen, while the organic acids were stable in samples stored in darkness. The photodegradation products identified using LC-DAD, LC-DAD-MS and/or accurate mass LC-MS included a number of aldehydes and ketones. Glyoxylic acid and 2,3-dioxopropanoic acid were derived from tartaric acid, 3-oxopropanoic acid from malic acid and succinic acid, 1,3-acetonedicarboxylic acid and acetoacetic acid from citric acid and acetaldehyde from lactic acid. Acetaldehyde was also detected in most of the other organic acid samples exposed to light, though at lower levels than those observed in the irradiated lactic acid solutions, but was not detected in any of the samples stored in darkness. It is probable that the organic acids were degraded in the irradiated solutions as a result of the photodegradation of the corresponding iron(III) carboxylate complexes. This reaction could potentially contribute to the consumption of oxygen and sulfur dioxide, as well as the sensory changes, in bottled white wine exposed to light.

Publication Date (Web): November 24, 2015 | doi: 10.1021/bk-2015-1203.ch019

Acknowledgments

This work was supported by a National Wine and Grape Industry Centre (NWGIC) funded PhD scholarship (P G-P). The NWGIC is a research center within Charles Sturt University in alliance with the Department of Primary Industries NSW and the NSW Wine Industry Association.

References

1. Schmidtke, L. M.; Clark, A. C.; Scollary, G. R. Micro-oxygenation of red wine: Techniques, applications, and outcomes. *Crit. Rev. Food Sci. Nutr.* **2011**, *51*, 115–131.
2. Singleton, V. L. Oxygen with phenols and related reactions in musts, wines, and model systems: Observations and practical implications. *Am. J. Enol. Vitic.* **1987**, *38*, 69–77.
3. Danilewicz, J. C. Reactions involving iron in mediating catechol oxidation in model wine. *Am. J. Enol. Vitic.* **2013**, *64*, 316–324.
4. Danilewicz, J. C. Review of reaction mechanisms of oxygen and proposed intermediate reduction products in wine: Central role of iron and copper. *Am. J. Enol. Vitic.* **2003**, *54*, 73–85.
5. Waterhouse, A. L.; Laurie, V. F. Oxidation of wine phenolics: A critical evaluation and hypotheses. *Am. J. Enol. Vitic.* **2006**, *57*, 306–313.
6. Buxton, G. V.; Greenstock, C. L.; Helman, W. P.; Ross, A. B. Critical review of rate constants for rections of hydrated electrons, hydrogen atoms and hydroxyl radicals in aqueous solution. *J. Phys. Chem. Ref. Data* **1988**, *17*, 513–851.
7. Elias, R. J.; Andersen, M. L.; Skibsted, L. H.; Waterhouse, A. L. Identification of Free Radical Intermediates in Oxidized Wine Using Electron Paramagnetic Resonance Spin Trapping. *J. Agric. Food. Chem.* **2009**, *57*, 4359–4365.
8. Wildenradt, H. L.; Singleton, V. L. The production of aldehydes as a result of oxidation of polyphenolic compounds and its relation to wine aging. *Am. J. Enol. Vitic.* **1974**, *25*, 119–126.
9. Fulcrand, H.; Cheynier, V.; Oszmianski, J.; Moutounet, M. An oxidized tartaric acid residue as a new bridge potentially competing with acetaldehyde in flavan-3-ol condensation. *Phytochemistry* **1997**, *46*, 223–227.
10. Es-Safi, N. E.; Guernevé, C.; Fulcrand, H.; Cheynier, V.; Moutounet, M. Xanthylium salts formation involved in wine colour changes. *Int. J. Food Sci. Tech.* **2000**, *35*, 63–74.
11. Clark, A. C. The production of yellow pigments from (+)-catechin and dihydroxyfumaric acid in a model wine system. *Eur. Food Res. Technol.* **2008**, *226*, 925–931.
12. Boulton, R. B.; Singleton, V. L.; Bisson, L. F.; Kunkee, R. E. *Principles and Practices of Winemaking*; Chapman & Hall: New York, 1996.
13. Bradshaw, M. P.; Barril, C.; Clark, A. C.; Prenzler, P. D.; Scollary, G. R. Ascorbic acid: A review of its chemistry and reactivity in relation to a wine environment. *Crit. Rev. Food Sci. Nutr.* **2011**, *51*, 479–498.

14. Clark, A. C.; Prenzler, P. D.; Scollary, G. R. Impact of the condition of storage of tartaric acid solutions on the production and stability of glyoxylic acid. *Food Chem.* **2007**, *102*, 905–916.
15. Clark, A. C.; Dias, D. A.; Smith, T. A.; Ghiggino, K. P.; Scollary, G. R. Iron(III) Tartrate as a Potential Precursor of Light Induced Oxidative Degradation of White Wine: Studies in a Model Wine System. *J. Agric. Food. Chem.* **2011**, *59*, 3575–3581.
16. Dozon, N. M.; Noble, A. C. Sensory study of the effect of fluorescent light on a sparkling wine and its base wine. *Am. J. Enol. Vitic.* **1989**, *40*, 265–271.
17. Mattivi, F.; Monetti, A.; Vrhovšek, U.; Tonon, D.; Andrés-Lacueva, C. High-performance liquid chromatographic determination of the riboflavin concentration in white wines for predicting their resistance to light. *J. Chromatogr. A* **2000**, *888*, 121–127.
18. Maujean, A.; Seguin, N. Contribution a l'étude des goûts de lumière dans les vins de Champagne 3 Les réactions photochimiques responsables des goûts de lumière dans le vin de Champagne. *Sci. Aliments* **1983**, *3*, 589–601.
19. Sato, S.; Nakamura, K.; Tadenuma, M.; Motegi, K. Effects of light rays on the colour of alcoholic beverages. *Nihon Jozo Kyokai Zasshi* **1970**, *65*, 433–438.
20. Dias, D. A.; Smith, T. A.; Ghiggino, K. P.; Scollary, G. R. The role of light, temperature and wine bottle colour on pigment enhancement in white wine. *Food Chem.* **2012**, *135*, 2934–2941.
21. Rossi, J. A.; Singleton, V. L. Contributions of grape phenols to oxygen absorption and browning of wines. *Am. J. Enol. Vitic.* **1966**, *17*, 231–239.
22. Blake, A.; Kotseridis, Y.; Brindle, I. D.; Inglis, D.; Pickering, G. J. Effect of light and temperature on 3-alkyl-2-methoxypyrazine concentration and other impact odourants of Riesling and Cabernet Franc wine during bottle ageing. *Food Chem.* **2010**, *119*, 935–944.
23. Pozdnyakov, I. P.; Kolomeets, A. V.; Plyusnin, V. F.; Melnikov, A. A.; Kompanets, V. O.; Chekalin, S. V.; Tkachenko, N.; Lemmetyinen, H. Photophysics of Fe(III)-tartrate and Fe(III)-citrate complexes in aqueous solutions. *Chem. Phys. Lett.* **2012**, *530*, 45–48.
24. Balzani, V.; Carassiti, V. In *Photochemistry of Coordination Compounds*; Academic Press: New York, 1970; pp 172−174.
25. Zuo, Y.; Hoigné, J. Formation of hydrogen peroxide and depletion of oxalic acid in atmospheric water by photolysis of iron(III)-oxalato complexes. *Environ. Sci. Technol.* **1992**, *26*, 1014–1022.
26. Pignatello, J. J.; Oliveros, E.; MacKay, A. Advanced oxidation processes for organic contaminant destruction based on the Fenton reaction and related chemistry. *Crit. Rev. Environ. Sci. Technol.* **2006**, *36*, 1–84.
27. Glebov, E. M.; Pozdnyakov, I. P.; Grivin, V. P.; Plyusnin, V. F.; Zhang, X.; Wu, F.; Deng, N. Intermediates in photochemistry of Fe(III) complexes with carboxylic acids in aqueous solutions. *Photochem. Photobiol. Sci.* **2011**, *10*, 425–430.
28. Paneque, P.; Álvarez-Sotomayor, M. T.; Clavijo, A.; Gómez, I. A. Metal content in southern Spain wines and their classification according to origin and ageing. *Microchem. J.* **2010**, *94*, 175–179.

29. Fowles, G. W. A. Acids in grapes and wines: A review. *J. Wine Res.* **1992**, *3*, 25–41.
30. Frayne, R. F. Direct analysis of the major organic components in grape must and wine using high performance liquid chromatography. *Am. J. Enol. Vitic.* **1986**, *37*, 281–287.
31. Frahn, J. L. The photochemical decomposition of the citrate-ferric iron complexes: A study of the reaction products by paper ionoporesis. *Aust. J. Chem.* **1958**, *11*, 399–405.
32. Faust, B. C.; Hoigné, J. Photolysis of Fe(III)-hydroxy complexes as sources of OH radicals in clouds, fog and rain. *Atmos. Environ., Part A* **1990**, *24*, 79–89.
33. Clark, A. C.; Scollary, G. R. Influence of light exposure, ethanol and copper (II) on the formation of a precursor for xanthylium cations from tartaric acid. *Aust. J. Grape Wine Res.* **2003**, *9*, 64–71.
34. Chan, M. N.; Zhang, H.; Goldstein, A. H.; Wilson, K. R. Role of Water and Phase in the Heterogeneous Oxidation of Solid and Aqueous Succinic Acid Aerosol by Hydroxyl Radicals. *J. Phys. Chem. C* **2014**, *118*, 28978–28992.
35. Herrmann, J. M.; Tahiri, H.; Guillard, C.; Pichat, P. Photocatalytic degradation of aqueous hydroxy-butandioic acid (malic acid) in contact with powdered and supported titania in water. *Catal. Today* **1999**, *54*, 131–141.
36. Franch, M. I.; Ayllón, J. A.; Peral, J.; Domènech, X. Fe(III) photocatalyzed degradation of low chain carboxylic acids: Implications of the iron salt. *Appl. Catal., B* **2004**, *50*, 89–99.
37. Abrahamson, H. B.; Rezvani, A. B.; Brushmiller, J. G. Photochemical and spectroscopic studies of complexes of iron(III) with citric acid and other carboxylic acids. *Inorg. Chim. Acta* **1994**, *226*, 117–127.
38. Irawaty, W.; Friedmann, D.; Scott, J.; Pichat, P.; Amal, R. Photocatalysis in TiO_2 aqueous suspension: Effects of mono- or di-hydroxyl substitution of butanedioic acid on the disappearance and mineralisation rates. *Catal. Today* **2011**, *178*, 51–57.
39. Russell, G. A. Deuterium-Isotope Effects in the Autoxidation of Aralkyl Hydrocarbons. Mechanism of the Interaction of Peroxy Radicals. *J. Am. Chem. Soc.* **1957**, *79*, 3871–3877.
40. Bennett, J. E.; Summers, R. Product studies of the mutual termination reactions of sec-alkylperoxy radicals: Evidence for non-cyclic termination. *Can. J. Chem.* **1974**, *52*, 1377–1379.
41. Fulcrand, H.; Benabdeljalil, C.; Rigaud, J.; Cheynier, V.; Moutounet, M. A new class of wine pigments generated by reaction between pyruvic acid and grape anthocyanins. *Phytochemistry* **1998**, *47*, 1401–1407.
42. Gislason, N. E.; Currie, B. L.; Waterhouse, A. L. Novel Antioxidant Reactions of Cinnamates in Wine. *J. Agric. Food. Chem.* **2011**, *59*, 6221–6226.
43. Bouzanquet, Q.; Barril, C.; Clark, A. C.; Dias, D. A.; Scollary, G. R. A Novel Glutathione-Hydroxycinnamic Acid Product Generated in Oxidative Wine Conditions. *J. Agric. Food. Chem.* **2012**, *60*, 12186–12195.

Publication Date (Web): November 24, 2015 | doi: 10.1021/bk-2015-1203.ch019

Publication Date (Web): November 24, 2015 | doi: 10.1021/bk-2015-1203.ch020

Chapter 20

Oxidation Signature of Grape Must and Wine by Linear Sweep Voltammetry Using Disposable Carbon Electrodes

Maurizio Ugliano,* Jérémie Wirth, Stéphanie Bégrand, Jean-Baptiste Dieval, and Stéphane Vidal

Nomacorc France, Av. Yves Cazeaux, Rodilhan, 30230, France
***E-mail: m.ugliano@nomacorc.be.**

Linear sweep voltammetry (LSV) coupled with antioxidant sensing carbon paste disposable electrodes was used for the characterization of grape and wine oxidation. Four white grapes musts were submitted to controlled oxidation (eg. con-sumption of sequential oxygen saturations), and their oxida-tion patterns obtained by voltammetric analysis. Musts exhibiting higher current in the 0-600 mV region of the voltammograms were characterized by higher oxygen con-sumption rates, indicating greater ability to combine oxygen. Various changes in the voltammograms were observed with oxidation, in particular in the regions around 580 and 850 mV, allowing to obtain for each must a specific oxidation signature. In one case, in spite of oxygen being consumed, no change in must voltammetric profile occurred. Oxidation signatures of different white wines were also obtained, showing characteristics which were in some cases similar to the oxidation signature of reference wine phenolic com-pounds. The LSV setup developed allowed rapid monitoring of the changes in grape and wine phenolics during oxidation.

In Advances in Wine Research; Ebeler, et al.;
ACS Symposium Series; American Chemical Society: Washington, DC, 2015.

Publication Date (Web): November 24, 2015 | doi: 10.1021/bk-2015-1203.ch020

Introduction

During the last two decades, a number of studies have demonstrated that, at different steps of the winemaking process, oxygen exposure can result in chemical modifications that are of primary importance to composition, sensory quality and shelf-life of the finished wine (*1–6*).

The mechanisms by which oxygen can impact wine composition and quality revolve around the oxidation of phenolic compounds (*1–3*). In grape must, this is taking place primarily through an enzymatic mechanism involving the action of grape polyphenol oxidase (*1*, *2*), while in finished wines phenolic oxidation is purely chemical, with oxygen being 'activated' by the catalytic action of copper and iron (*7–9*). In addition to the direct consequences for wine phenolic composition, these oxidation reactions can have a number of implications for wine aroma composition and perceived quality. For example, under certain (hitherto unclarified) circumstances, oxidation of grape must can result in increased content of precursors to volatile thiols that could then be liberated during winemaking (*10*, *11*). Exposure to small doses of oxygen during wine cellar and bottle storage can also prevent excessive accumulation of low molecular weight sulfur compounds responsible for wine reductive off-odors (*5*, *6*).

While all these possibilities have been thoroughly documented by a number of studies, today's wineries have limited tools to characterize grapes and wines with regard to their ability to react with oxygen and the potential consequences of these reactions. The work of Kilmartin indicated that cyclic voltammetry at a glassy carbon electrode can be used to generate reactive oxidized phenolics (eg. quinones) and study their interactions with the wine environment (*12–14*). Martins et al. (*15*) also suggested that this technique can be used in the practical management of wine oxidation. Nevertheless, electrode fouling by wine phenolics requires tedious electrode cleaning procedures, limiting practical application of voltammetric techniques in the wine industry. This limitation can be by-passed by the use of disposable screen printed electrodes which are becoming available on the market. The antioxidant sensing capacity of carbon paste electrodes has been recently demonstrated (*16*, *17*), although they have not been thoroughly applied to the study of must and wine properties.

In this study, we have used a simple voltammetric approach such as linear sweep voltammetry combined with antioxidant sensing screen printed electrodes for the study of white grape must and wine oxidation.

Materials and Methods

Voltammetry: Electrode strips were prepared by screen-printing. Working and counter electrodes were made with carbon ink (Electra Polymer & Chemicals Ltd., Roughway Mill, Dunk Green, UK) while the reference electrode was made using an Ag/AgCl ink (Ercon, Wareham, MA, USA). The electrode area was defined by printing an insulating layer. Electrochemical measurements were performed using a commercial potentiostat (Nomacorc, Zebulon, NC). For each measurements, one drop of sample (50 µL) was deposited on the electrode strip. Linear sweep voltammograms were recorded from 0 V to 1.2 V with a scan rate

of 100 mV/s under ambient conditions. For each measurement a fresh electrode was employed. All measurements were performed in duplicate, with no prior dilution of the sample. Preliminary experimetns indicated that sample dilution did not improve quality of the results, as reported by others for glassy carbon electrodes (*12*).

Must oxidation experiment: Grape samples of Viognier, Chardonnay, Riesling, and Grenache blanc were obtained in the 2013 vintage. Grapes were crushed using a small fruit crusher, and the juice obtained was used for the oxidation experiments. Three mL of juice were placed in a 5 mL vial fitted with an oxygen sensor (Pst5, Presens, Regensburg, Germany) and rapidly brought to a dissolved oxygen content of 8 mg/L by vigorous shaking. The vials were then placed on a SDR sensor dish reader (Presens, Regensburg, Germany) for continuous measurement of oxygen consumption. When the first dose of oxygen was consumed, a small volume was taken for chemical and voltammetric analyses, and then the dissolved oxygen was brought up again to 8 mg/L. This sequence of operations was repeated for a total of three consecutive oxygen consumptions, after which the experiment was stopped. Four experimental replicates were carried out for each grape variety, with analyses carried out in duplicate.

Wine oxidation experiment: Commercial wines were purchased at local outlets. The set of wines studied included Picpoul, Viognier, Cotes du Rhone (a blend of Grenache blanc, Marsanne, and Roussanne) Pinot Gris, Vermentino, Muscadet. One sample per wine type was studied. All wines were from 2012 vintage, and were made with a single grape variety, excluding the Cots du Rhone, which was a blend including Grenache, Roussanne and Viognier. Wines were added with 5 mg/L of oxygen and stored for 3 months along with a reference sample that had not received any oxygen. At the end of the storage period, dissolved oxygen was measured (< 0.2 mg/L in all cases), and both wine and controls where submitted to voltammetric analyses after pH adjustment to 3.4. Additional samples were prepared by adding to the Cotes du Rhone catechin, SO_2, phloroglucinol, caffeic acid or ascorbic acid to a final concen-tration of 0.4 mM or commercial enological tannins to a final concentration of 200 mg/L.These samples were oxidized and analyzed in the same conditions as the wines.

Publication Date (Web): November 24, 2015 | doi: 10.1021/bk-2015-1203.ch020

Results and Discussion

Oxygen Consumption by Different Musts

Must obtained from the four different grapes were saturated with air and oxygen evolution was constantly monitored during three consecutive oxidation cycles. Figure 1 show a summary of oxygen consumption speed for the four musts, calculated for the first 3 minutes of each saturation. Looking at consumption of the first oxygen saturation, Riesling was the fastest consuming grape, followed by Chardonnay and Grenache. In comparison, consumption of oxygen by Viognier was much slower. While this overall picture did not change with the following saturations, differences were observed within each grape with regard to changes in oxygen consumption speed following each oxygen saturation. Indeed, in the case of Riesling and Grenache, there was virtually no difference between the speed of

consumption observed for the first two oxygen saturations, probably indicating the fact that in these grapes the initial concentration of oxidizable substrates was not a limiting factor. Conversely, in the case of both Chardonnay and Viognier, upon the second oxygen saturation a noteworthy decrease in oxygen consumption speed was already observed, probably reflecting limited substrate availability.

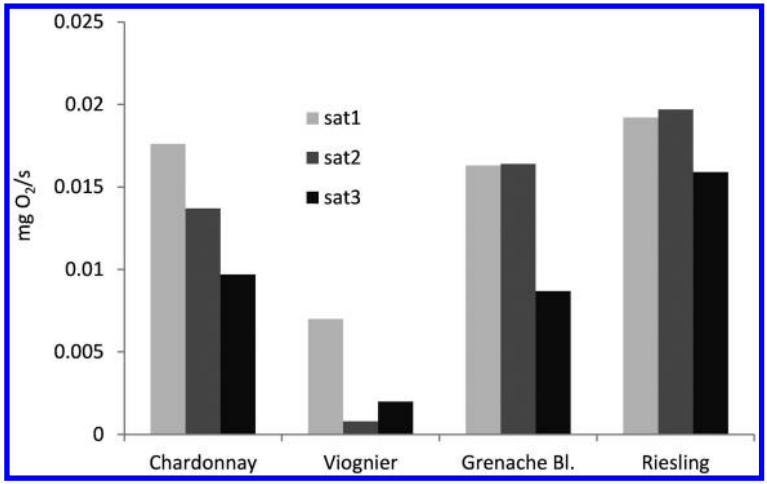

Figure 1. Speed of oxygen consumption of the four must during three consecutive oxygen consumption cycles (sat1-3).

Publication Date (Web): November 24, 2015 | doi: 10.1021/bk-2015-1203.ch020

Must Voltammetric Analyses

The voltammograms of the four grape musts during the oxidation experiment are shown in Figure 2. Electrochemical profiles before oxygen consumption were characterized by a first broad wave at approximately 520 mV, corresponding to the most readily oxidizable compounds, including catechins and hydroxycinnamic acids (*12*). Riesling must exhibited higher current in this region, followed by Grenache. Chardonnay and Viognier showed similar current values in this region, which were much lower than those observed for the other two grapes. A second wave was observed around 780 mV, which according to reported oxidation potentials should be linked to the oxidation of vanillic and coumaric acids, as well as to catechin A ring. Again, higher current was observed in this region for

Riesling, followed by Grenache. Peak current was lower and similar for Viognier and Chardonnay, although for Viognier this wave was less pronounced and not immediately followed by a trough, as was the case for the other grapes.

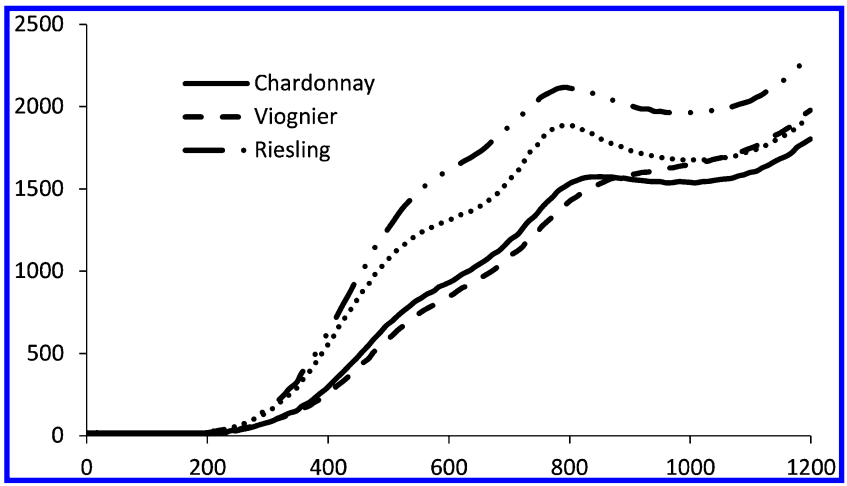

Figure 2. Linear sweep voltammograms of the four grape musts.

Publication Date (Web): November 24, 2015 | doi: 10.1021/bk-2015-1203.ch020

Various modifications were observed in the voltammetric profiles when the four musts were submitted to oxidation, and these were generally must dependent. With the exception of Viognier, a major drop in the charge passed across the entire potential range was observed (Figure 3), in line with the fact that oxygen consumption results in the oxidation of different phenolic compounds, in particular catechins and hydroxycinnamic acids. The progressive depletion of oxidizable substrates induced by sequential must oxidation was clearly visible in the voltammetric profiles obtained after each oxidation step. The wave around 520 mV progressively disappeared, while the one around 780 mV not only decreased in intensity, but was shifted towards less positive potentials. The latter observation is indicating probably oxidation-induced modifications in the pool of compound accounting for the initial wave. The only exception to this general trend was seen for Viognier, for which the voltammetric profiles appeared to be only marginally influenced by the three consecutive oxidation steps.

Publication Date (Web): November 24, 2015 | doi: 10.1021/bk-2015-1203.ch020

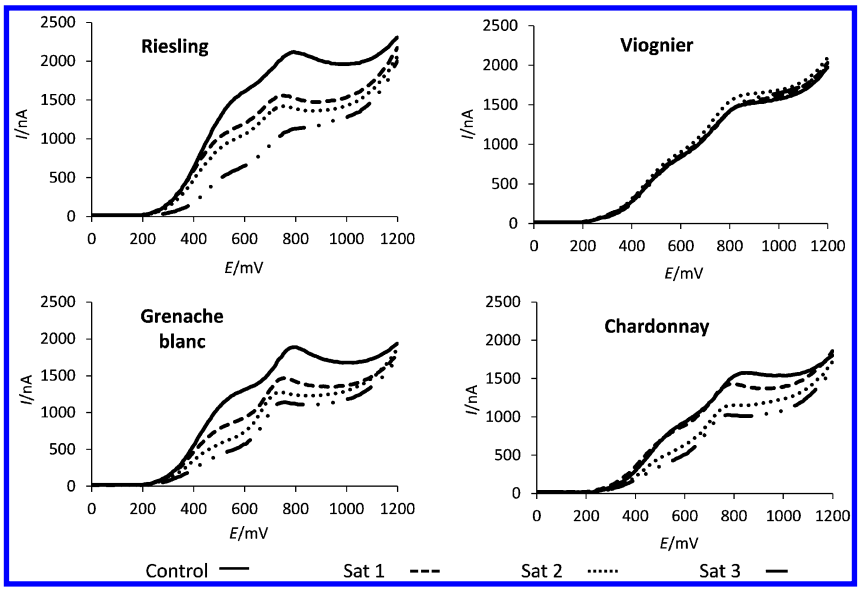

Figure 3. Linear sweep voltammograms of the four different musts at the beginning of the oxidation experiment and after consumption of three sequential oxygen saturations (Sat 1-3).

The plots in Figure 4, obtained by subtraction of the initial voltammograms minus the one obtained after the first and third saturation (and therefore accounting for a total consumed oxygen of 8 and 24 mg/L respectively), provide an effective representation of modifications induced by the sequential oxidation steps. This can be considered a sort of 'oxidation signature' of the different musts. In the case of Riesling, first saturation resulted in significant current loss around 580 mV, with a second major loss observed around 850 mV. Further oxygen supplementation up to third saturation increased in particular signal loss around 580 mV. When Grenache and Chardonnay were submitted to sequential oxidations, peaks of current loss were observed again around 580 mV and 850 mV, resulting in a characteristic two peaks profile with the two peaks showing similar extent of signal loss. The case of Viognier was substantially different, as oxidation did not bring major changes in the voltammograms. Interestingly, Viognier was also the grape exhibiting the slowest oxygen consumption rates. Slow oxygen consumption by grape must might be linked to an imbalance in glutathione (GSH) and caftaric acid concentrations, two main substrates involved in must oxidative reactions. For example, when excess GSH is present, all caftaric is converted to grape reaction product, and this will be not oxidized further, with stalling oxygen consumption and little additional oxidation of must phenolics (*2*, *17*). Caftaric acid and grape reaction products have been reported to have similar oxidation potentials (*14*), which might explain why in the case of Viognier we did not observe any change of voltammetric profile after the various oxidation steps.

Publication Date (Web): November 24, 2015 | doi: 10.1021/bk-2015-1203.ch020

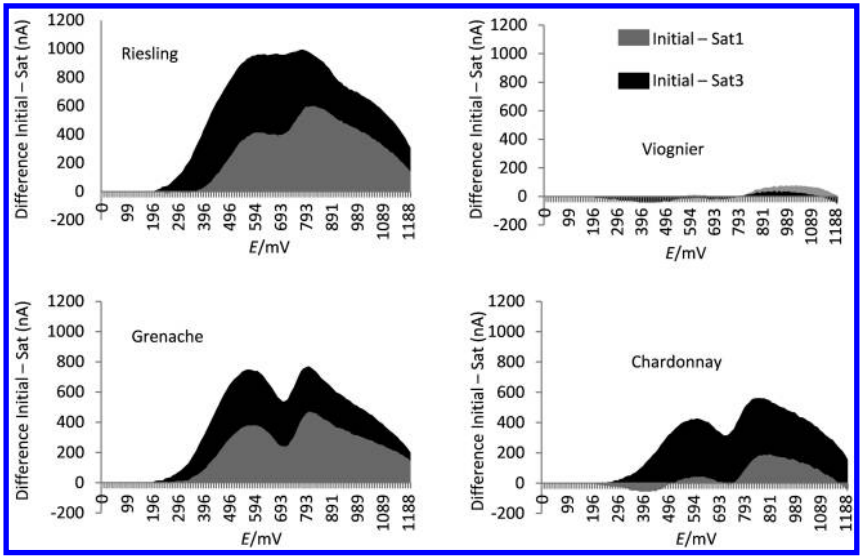

Figure 4. Oxidation signatures of the four grape musts for consumption of one (Initial – Sat1) or three (Initial – Sat3) oxygen saturations.

Wine Oxidation Study

The evolution of commercial wines and reference wine antioxidants during consumption of 5 mg/L of dissolved oxygen was studied by voltammetry using carbon paste electrodes. Figure 5 shows an example of the oxidation signature obtained by subtraction of the voltammogram of the control wine minus the one obtained after oxidation, for three of the wines studied and for the reference wine spiked with caffeic acid. Generally speaking, these oxidation sigantures are reporesentative of the different changes taking place in winr composition upond consumption of oxygen. Further studies are needed to better characterize these changes, although they are expected to include loss of strong nucleophiles such as free SO_2 and ascorbic acid (if present). Nevertheless, the variations observed across the set of wines studies indicate that other modifications are also captured by these fingerprints, and that they are to some extent wine specific. For example, oxidation of the Vermentino sample resulted in lower charge passed across the entire scan range. Differences were detectable since about 250 mV, indicating substantial presence of readily oxidizable substrates which were depleted with oxidation. A different profile was observed for the Pinot Gris, for which signal loss in the region 200-500 mV was less than half then for Vermentino, suggesting lower content of readily oxidizable substrates. The Muscadet wine was characterized by a different oxidation signature, with a virtually flat signal until 550 mV, followed by substantial signal loss peaking around 900 mV. After

1000 mV, negative values were obtained for Muscadet, indicating that compounds with oxidation potentials in this region were actually formed during oxidative storage of this wine. Similar features were observed for the oxidation of the reference wine added with caffeic acid, suggesting that the oxidation fingerprint of this wine was strongly influenced by caffeic acid.

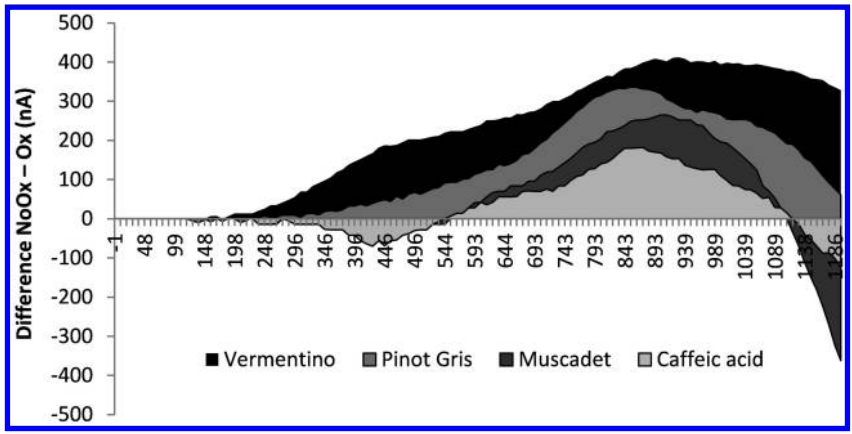

Figure 5. Oxidation signatures of three commercial white wines and of reference wine added with caffeic acid.

To further explore the contribution of individual wine constituents to the oxidation fingerprints observed, a Principal component analysis (PCA) of the oxidation signatures of the different wines and reference compounds was carried out. The results are shown in Figure 6. Similarities were observed in the signatures of original wines and those of the reference white wine spiked with different compounds. For example Vermentino displayed a signature similar to that of ascorbic acid, while Pinot Gris' signature had features similar to those of catechin. Muscadet grouped with SO_2 and caffeic acid. However, for wines such as Cotes du Rhone, Picpoul and Viognier no grouping with reference compounds was observed, probably indicating complex modifications that could not be related to the oxidation of single molecules as reference. In spite of the fact that oxidation of reference compounds was carried out in a real wine matrix, this observation suggests the need for further work on the oxidation of mixtures of different molecules, in order to effectively characterize and classify a broader range of wine oxidation fingerprints.

In Advances in Wine Research; Ebeler, et al.;
ACS Symposium Series; American Chemical Society: Washington, DC, 2015.

Publication Date (Web): November 24, 2015 | doi: 10.1021/bk-2015-1203.ch020

Publication Date (Web): November 24, 2015 | doi: 10.1021/bk-2015-1203.ch020

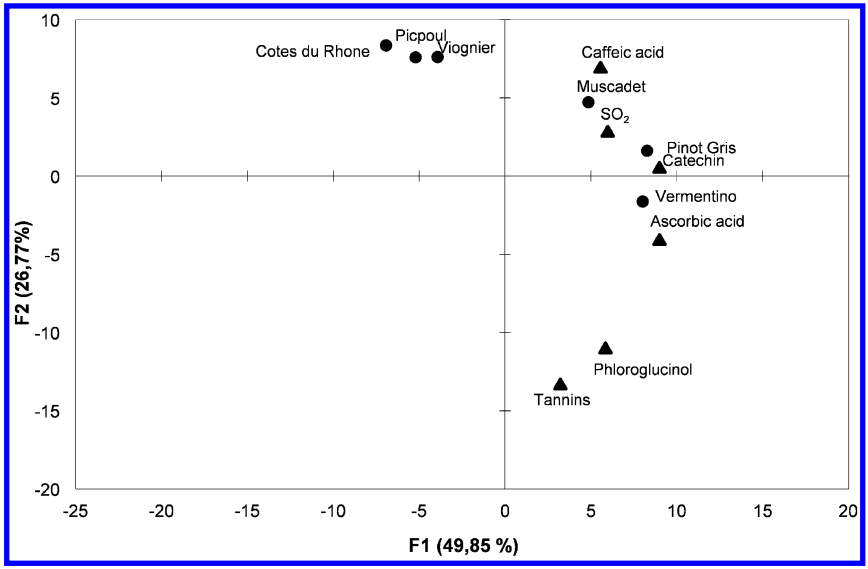

Figure 6. Principal component analysis of the oxidation signatures of different commercial white wines and reference wine antioxidants.

In conclusion, linear sweep voltammetry with disposable screen printed electrodes provided a useful mean to characterize oxidation patterns of musts, wines and reference wine components. Unique oxidation signatures were obtained for each matrix, reflecting the different transformations induced in the wine by oxidation. The simplicity of the technique allows for use in the winery to monitor antioxidants evolution during winemaking. The possibility of classifying wines against reference wine antioxidants was also shown, opening up new possibilities with respect to classification and prediction of wine response to oxygen.

References

1. Singleton, V. L. Oxygen with phenols and related reactions in musts, wines and model systems: Observations and practical implications. *Am. J. Enol. Vitic.* **1987**, *38*, 69–77.
2. Cheynier, V.; Fulcrand, H.; Guyot, S.; Oszmianski, J.; Moutounet, M. Reactions of Enzymically Generated Quinones in Relation to Browning in Grape Musts and Wines. In *Enzymatic Browning and its Prevention*; Lee, C. Y., Whitaker, J. R., Eds.; ACS Symposium Series 600; American Chemical Society: Washington, DC, 1995; pp 130−143.
3. Ugliano, M. Oxygen Contribution to Wine Aroma Evolution during Bottle Aging. *J. Agric. Food Chem* **2013**, *61*, 6125–6136.
4. Caillé, S.; Samson, A.; Wirth, ; J., ; Diéval, J.-B.; Vidal, S.; Cheynier, V. Sensory characteristics changes of red Grenache wines submitted to different oxygen exposures pre and post bottling. *Anal. Chim. Acta* **2010**, *660*, 35–42.

5. Ugliano, M.; Kwiatkowski, M.; Vidal, S.; Capone, D.; Siebert, T.; Dieval, J.-B.; Aagaard, O.; Waters, E. J. Evolution of 3-Mercaptohexanol, Hydrogen Sulfide, and Methyl Mercaptan during Bottle Storage of Sauvignon Blanc Wines. Effect of Glutathione, Copper, Oxygen Exposure, and Closure-Derived Oxygen. *J. Agric. Food Chem.* **2011**, *59*, 2564–2572.
6. Ugliano, M.; Dieval, J.-B.; Siebert, T. E.; Kwiatkowski, M.; Aagaard, O.; Vidal, S.; Waters, E. J. Oxygen Consumption and Development of Volatile Sulfur Compounds during Bottle Aging of Two Shiraz Wines. Influence of Pre- and Postbottling Controlled Oxygen Exposure. *J. Agric. Food Chem.* **2012**, *60*, 8561–8570.
7. Waterhouse, W. L.; Laurie, V. F. Oxidation of wine phenolics: a critical evaluation and hypotheses. *Am. J. Enol. Vitic.* **2006**, *57*, 306–331.
8. Danilewicz, J. C. Interaction of sulfur dioxide, polyphenols, and oxygen in a wine-model system: central role of iron and copper. *Am. J. Enol. Vitic.* **2007**, *58*, 53–60.
9. Danilewicz, J. C.; Seccombe, J. T.; Whelan, J. Mechanism of interaction of polyphenols, oxygen, and sulfur dioxide in model wine and wine. *Am. J. Enol. Vitic.* **2008**, *59*, 128–136.
10. Roland, A.; Vialaret, J.; Razungles, A.; Rigou, P.; Schneider, R. Evolution of S-Cysteinylated and S-Glutathionylated Thiol Precursors during Oxidation of Melon B. and Sauvignon Blanc Musts. *J. Agric. Food Chem.* **2010**, *58*, 4406–4413.
11. Larcher, R.; Nicolini, G.; Tonidandel, L.; Roman Villegas, T.; Malacarne, M.; Fedrizzi, B. Influence of oxygen availability during skin-contact maceration on the formation of precursors of 3-mercaptohexan-1-ol in Müller-Thurgau and Sauvignon Blanc grapes. *Aust. J. Grape Wine Res.* **2013**, *19*, 342–348.
12. Kilmartin, P. A.; Zou, H.; Waterhouse, A. L. A Cyclic Voltammetry Method Suitable for Characterizing Antioxidant Properties of Wine and Wine Phenolics. *J. Agric. Food Chem.* **2001**, *49*, 1957–1965.
13. Kilmartin, P. A.; Zou, H.; Waterhouse, A. L. Correlation of wine phenolic composition versus cyclic voltammetry response. *Am. J. Enol. Vitic.* **2002**, *53*, 294–302.
14. Makhotkina, O.; Kilmartin, P. A. Uncovering the influence of antioxidants on polyphenol oxidation in wines using an electrochemical method: Cyclic voltammetry. *J. Electroanal. Chem.* **2009**, *633*, 165–174.
15. Martins, R. C.; Oliveira, R.; Bento, F.; Geraldo, D.; Lopes, V. V.; Guedes de Pinho, P.; Oliveira, C. M.; Silva Ferreira, A. C. Oxidation Management of White Wines Using Cyclic Voltammetry and Multivariate Process Monitoring. *J. Agric. Food Chem.* **2008**, *56*, 12092–12098.
16. Tacchini, P.; Lesch, A.; Neequaye, A.; Lagger, G.; Liu, J.; Cortés-Salazar, F.; Giraud, H. Electrochemical pseudo-titration of water-soluble antioxidants. *Electroanalysis* **2013**, *25*, 922–930.
17. Apetrei, C.; Apetrei, I. M.; De Saja, J. A.; Rodriguez-Mendez, M. L. Carbon paste electrodes made from different carbonaceous materials: application in the study of antioxidants. *Sensors* **2011**, *11*, 1328–1344.

Publication Date (Web): November 24, 2015 | doi: 10.1021/bk-2015-1203.ch021

Chapter 21

Bioactives from Side Streams of Wine Processing

P. Winterhalter, Stefanie Kuhnert, and Philipp Ewald**

Institute of Food Chemistry, Technische Universität Braunschweig, Schleinitzstrasse 20, 38106 Braunschweig, Germany
***E-mail: p.winterhalter@tu-bs.de.**

Large amounts of waste streams are produced in viticulture and vinification. They consist *inter alia* of vine prunings, grape stalks, pomace, grape seeds and yeast lees. All of these side streams contain important functional polyphenols with diverse biological activities (e.g. antioxidant, anticancer, antimutagenic). This chapter will present novel approaches for the exploitation of under-utilized processing wastes and by-products of the wine industry by converting them into value-added products relevant to market demands. Examples will include the use of membrane technologies for the recovery of pure anthocyanin fractions, a novel rapid characterization of grape seed extracts on a diol HPLC phase, depolymerization of polymeric proanthocyanidins in order to enhance their bioavailability, and the search for bioactive oligomeric stilbenoids in vine prunings.

The world grape production in 2011 was 69 million tons including approximately 22 million tons of table grapes (*1*). Of the remaining 47 million tons used in wine making, one can estimate that roughly 9 million tons of grape pomace are obtained as by-product (*2*). Grape pomace consists mainly of skins, seeds and stalks and is used for the production of ethanol, tartaric and citric acid, grape seed oil, protein, dietary fiber, and polyphenols (*3*–*5*). Whereas red grape skins mainly contain anthocyanins which can be used as natural food colorants, grape seeds are rich in proanthocyanidins. The latter are increasingly used in functional food, dietary supplements and cosmetics due to their strong antioxidant

In Advances in Wine Research; Ebeler, et al.;
ACS Symposium Series; American Chemical Society: Washington, DC, 2015.

effects. In the following strategies for the fractionation of the complex mixture of polyphenols in grape pomace will be presented. Moreover, the use of vine prunings as a rich source of resveratrol and oligomeric resveratrol derivatives will be demonstrated.

Fractionation of Polyphenols From Grape Pomace

Solvent extraction is frequently used to recover polyphenols from the solid matrix grape pomace. As solvents water and ethanol are widely applied often in combination with acids (e.g. citric acid) and SO_2 ((*6*) and refs cited therein). Alternatively, extraction with subcritical water or subcritical sulfured water has been described (*7*). In order to enhance extraction yield, enzyme-treatment (pectinolytic and cellulytic enzymes) and pulsed-electric field treatment or high hydrostatic pressure have been applied (*8*, *9*). After the extraction process crude phenolic extracts are obtained which are commercialized as food colorants or due to their antioxidant activities as nutraceuticals (red and white grape extracts). Our attempt was a further fractionation of these crude extracts by application of membrane technology (membrane adsorber Sartobind S) in combination with liquid-liquid extraction (ethyl acetate). This approach allows the separation of the crude extracts into the following three groups of polyphenols: anthocyanins, color-less copigments (e.g. flavonols, flavanols, cinnamates, stilbenes) and polymers.

In a first step the crude phenolic extracts are applied onto an Amberlite XAD-7 resin (Sigma, St. Louis, MO). The column is washed with water and the polyphenols are eluted with methanol/acetic acid (19:1, v/v) (*10*, *11*). After evaporation of the solvents and freeze-drying, the phenolic mixture is redissolved in ethanol/acetic acid (19:1, v/v) and pumped through the membrane adsorber Sartobind S 75 (Sartorius Stedim Biotech, Göttingen, Germany). The adsorber consists of a stabilized cellulose membrane with negatively charged sulfonic acid groups. Under acidic conditions only the positively charged flavylium cations are retarded (*retentate fraction*) on the membrane surface and the other phenolic compounds pass the adsorber unretained (*permeate fraction*). After rinsing of the adsorber with ethanol/acetic acid (19:1, v/v), elution of anthocyanins is performed with a mixture of 1 M aqueous NaCl solution/methanol (50:50, v/v). In this way, a pure anthocyanin fraction free of copigments can be obtained. This method has first been developed for bilberry anthocyanins and later been adapted to anthocyanins from grape pomace (*12*). Depending on the size of the membrane adsorber cartridge, separation in the 10 g to one kg-scale can be carried out.

From the permeate fraction which contains the copigments and polymeric phenolics, the low-molecular phenolic constituents are easily liquid-liquid extracted with ethyl acetate. In this way, three clearly separated fractions, i.e. anthocyanins, copigments, and polymers, are obtained. Whereas anthocyanins and copigments can be directly used for nutraceutical or pharmaceutical purposes, the polymer fraction may require a further treatment, e.g. an acid-catalyzed depolymerization (see below) in order to increase its bioavailability (*13*). In case an isolation of individual phenolic constituents of the different fractions

Publication Date (Web): November 24, 2015 | doi: 10.1021/bk-2015-1203.ch021

is required, application of the support-free technique of countercurrent chromatography (CCC) is recommended. This all-liquid chromatographic technique is especially suited for polar constituents and its versatility and preparative capabilities are well documented (*14*). First separations of anthocyanins have already been reported in the year 2000 (*10*, *15*). In the meantime novel instrumentation has been developed enabling separations in the 100 g to kg scale (*16*). Whereas anthocyanins and copigments are easily separated by CCC, fractionation of the intact polymers requires alternative techniques, such as size-exclusion chromatography or centrifugal precipitation chromatography (for details cf. (*17*)).

Publication Date (Web): November 24, 2015 | doi: 10.1021/bk-2015-1203.ch021

Rapid Characterization of Proanthocyanidins in Grape Seed Extracts

A large proportion of grape pomace consists of grape seeds (approx. 200 kg per ton of pomace). Grape seeds contain a valuable vegetable oil (approx.15-20%) rich in linoleic acid which is widely used for cosmetics and culinary applications. In addition grape seeds contain high amounts of proanthocyanidins (4-6%). Phenolic grape seed extracts (GSE) are important dietary supplements with an average market share of 150 tons per year.

So far characterization of GSE is mainly made by spectrophotometric assays, namely the vanillin (*18*) as well as the acid butanol assay (*19*). Although widely applied, both methods are not considered to be appropriate for the determination of the content of oligmeric proanthocyanidins, for details cf. (*20*, *21*). For this reason we attempted to establish a more reliable determination of the proanthocyanidin (PA) content of GSE and developed a novel HPLC method for PA analysis using a diol stationary phase (MonoChrom diol column, Agilent, Waldbronn, Germany). As can be seen from Figure 1 the analysis is completed within 32 min and allows a differentiation of bioavailable short chain PA and non-bioavailable polymeric forms. The latter elute together in a quantifiable peak at the end of the chromatographic run. Authentic references are used for the the quantification of the individual groups of oligomers (dimers, galloylated dimers, trimers, tetramers, and pentamers). The newly developed HPLC method enables a verification of the labeling of the PA content in nutraceuticals (Figure 2). In several cases considerable deviations from the labeled PA value have been detected.

Depolymerization of Polymeric Proanthocyanidins

Bioavailability of proanthocyanidins is restricted to oligomers with up to three flavan-3-ol units. In order to convert the polymeric PA into bioavailable ones, an acid-catalyzed depolymerization process has to be applied. Generally, there are two possibilities. The first one uses a random cleavage of the flavan-3-ol chain under acidic conditions and gives rise to short chain cleavage products. The second approach uses a more controlled degradation, the so-called semisynthesis (*13*) (cf. Figure 3).

Publication Date (Web): November 24, 2015 | doi: 10.1021/bk-2015-1203.ch021

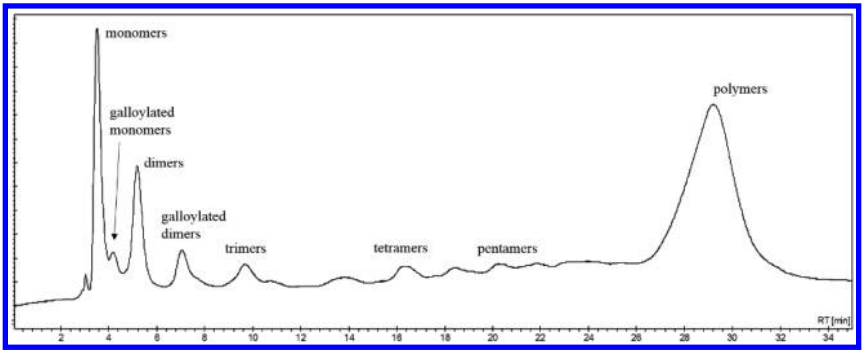

Figure 1. Chromatogram of the HPLC separation of a grape seed extract on a diol stationary phase.

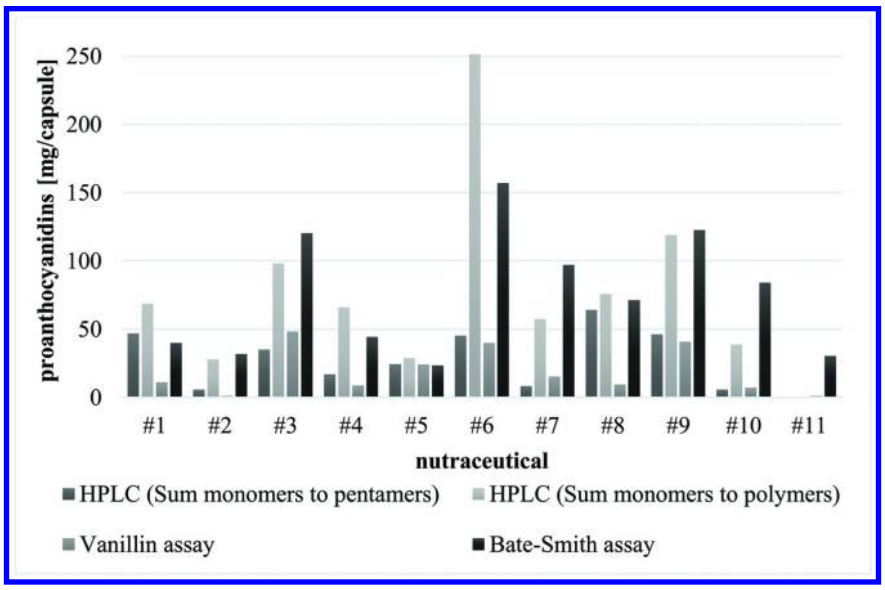

Figure 2. Results of the analysis of commercial nutraceuticals and comparison of the newly developed HPLC method with spectrophotometric assays, i.e. vanillin assay (18) and the acid butanol (Bate-Smith) assay (19).

Publication Date (Web): November 24, 2015 | doi: 10.1021/bk-2015-1203.ch021

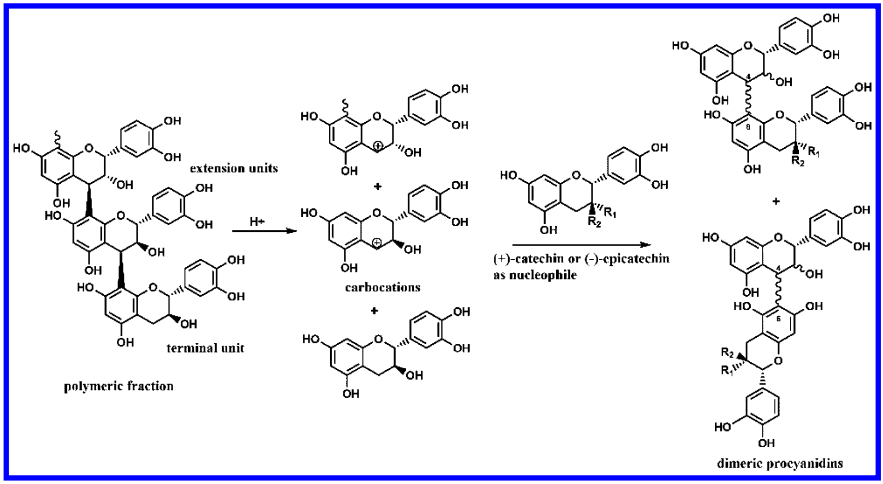

Figure 3. Mechanism of the directed depolymerization of polymeric PA.

For this purpose the GSE polymers are enriched by a simple cleanup step using solvent precipitation. The PA extract is dissolved in ethanol and increasing amounts of *n*-hexane as a nonpolar solvent are added. The precipitate obtained (polymeric PA) is then treated with 1 N methanolic HCl. During this process the interflavanoid linkage of polymeric PA is cleaved by releasing the flavan-3-ol moieties of the extension unit as carbocation together with an uncharged terminal unit. The liberated carbocation can immediately react with in excess added nucleophiles, such as (+)-catechin or (−)-epicatechin, giving rise to the formation of dimeric procyanidins. During this process the polymeric procyanidins are depolymerized and bioavailable dimeric procyanidins are formed. Depending on the nucleophiles chosen, the reaction products can be tailored in a simple way. Isolation of the dimeric reaction products is then performed by preparative countercurrent chromatography (*13*, *22*).

Oligomeric Resveratrol Derivatives from Vine Prunings

Vine pruning production is up to 5 tons per hectare and year. Traditional use is for compost or charcoal production, only in recent years vine shoots have been recognized as an important source of resveratrol derivatives (*23*). Resveratrol as a phytoalexin is known to occur in free and glycosidically bound form in the skins of grapes in amounts up to 50 mg/kg. The same is true for grape pomace. Resveratrol is known to exhibit a broad range of biological effects that include antioxidant and anticancer activity and it apparently also increases stress resistance and lifespan (*24*).

Vine shoots or canes which are obtained during the annual pruning of grape vine contain in addition to *trans*-resveratrol also high levels of resveratrol oligomers consisting of two to eight stilbene units. The main oligomer is the dimer *trans*-ε-viniferin (cf. Figure 4) .

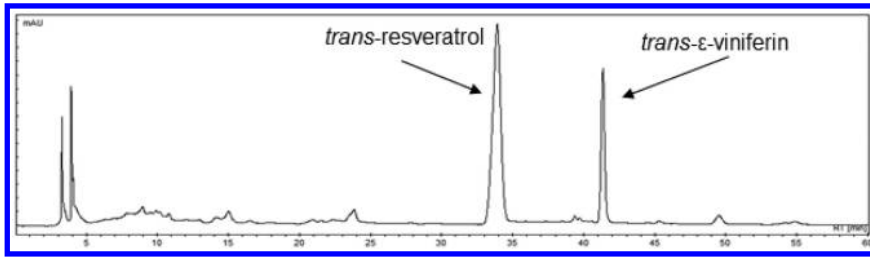

Figure 4. HPLC chromatogram of the stilbenes in vine shoots. Example: Spätburgunder (Column: Kromasil 100-5; C18; 5 µm; 250 mm × 4,6 mm i.d.).

Publication Date (Web): November 24, 2015 | doi: 10.1021/bk-2015-1203.ch021

The yield of resveratrol derivatives extracted from vine prunings can be as high as 7 g/kg dry weight and it has been estimated that the commercial value of these stilbene derivatives is around 2000-3000 US$ per kg (*25*, *26*). In contrast to resveratrol, the biological effects of the oligomers have hardly been studied. We therefore performed an activity-guided isolation of stilbenes from the commercially available vine shoot extract Vineatrol®30. This is a standardized product with a total stilbene content of >30%. For the fractionation the preparative all-liquid chromatographic technique of low-speed rotary countercurrent chromatography has been applied and the separated fractions were submitted to *in-vitro* testing using the following cell lines: A-431 (human epidermoid carcinoma), LNCaP (human prostatic adenocarcinoma), SW 480 and HT-29 (colorectal adenocarcinoma), MCF-7 (human breast adenocarcinoma), HepG2 (human liver hepatocellular carcinoma) (*27*, *28*). The chemical structures of some of the active compounds identified are depicted in Figure 5.

In Table 1 the IC_{50}-values for *trans*-resveratrol, hopeaphenol and r-2-viniferin are shown. Importantly, hopeaphenol and r-2-viniferin inhibited the growth of human tumor cell lines more strongly than resveratrol itself. In a recent study, hopeaphenol and r-2-viniferin were furthermore found to inhibit the growth of a canine glioblastoma cell line and a canine histiocytic sarcoma cell line (*29*).

Today there are quite a few data available concerning the stilbene content of vine prunings throughout the world. Recent publications indicated that the stilbene levels in vine prunings strongly depend on postharvest storage conditions. After a storage period of approximately 6 months highest stilbene concentrations were observed (*30*, *31*). Interestingly there was so far no information about stilbene levels in vine shoots from Germany available. We therefore analyzed the stilbene profile of eight grape vine varieties. The shoots were obtained during pruning season 2013 and stored for 6 months at room temperature protected from light exposure. Prior to analysis the vine shoots were lyophilized, ground and extracted with ethanol/water (80:20, v/v) with the assistance of ultrasonication as described in (*26*). HPLC analysis was performed on a Kromasil 100-5; C18; 5 µm column (250 mm × 4.6 mm i.d.; Eka Chemicals AB, Bohus, Sweden). We found *trans*-resveratrol and *trans*-ε-viniferin to be the major stilbenes beside minor amounts of e.g. ampelopsin A, hopeaphenol, r-viniferin, r-2-viniferin and miyabenol C (Figure 6).

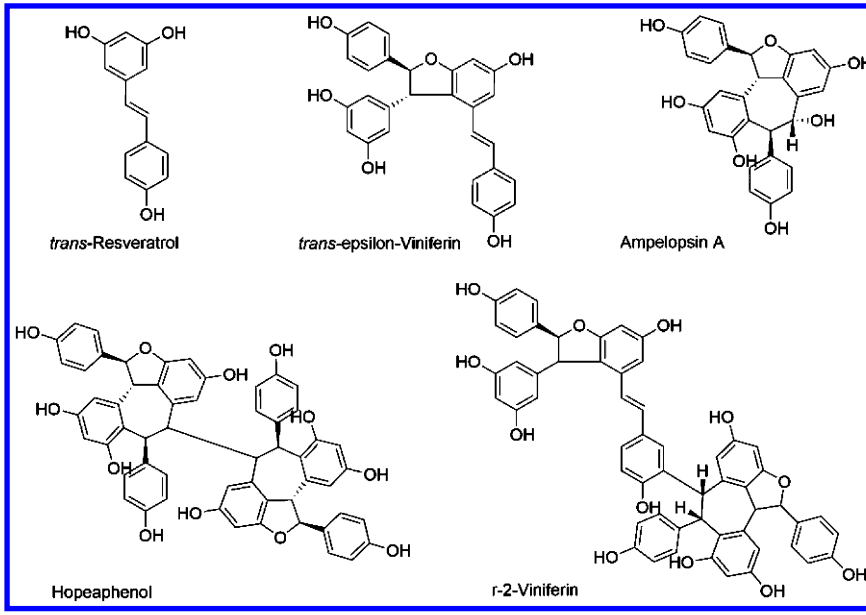

Figure 5. Chemical structures of stilbene derivatives from vine prunings exhibiting anti-proliferative effects.

Publication Date (Web): November 24, 2015 | doi: 10.1021/bk-2015-1203.ch021

Table 1. IC_{50}-values for *trans*-Resveratrol, Hopeaphenol and r-2-Viniferin in Human Tumor Cell Lines

	IC_{50}-Values (μM)					
	A431	***LNCaP***	***SW480***	***HT-29***	***MCF7***	***HepG2***
Resveratrol	20	5	25	20	27	10
Hopeaphenol	4.3	2	4.5	0.8	4.3	3.8
r-2-Viniferin	4.7	4	5	2.7	2	1.4

Publication Date (Web): November 24, 2015 | doi: 10.1021/bk-2015-1203.ch021

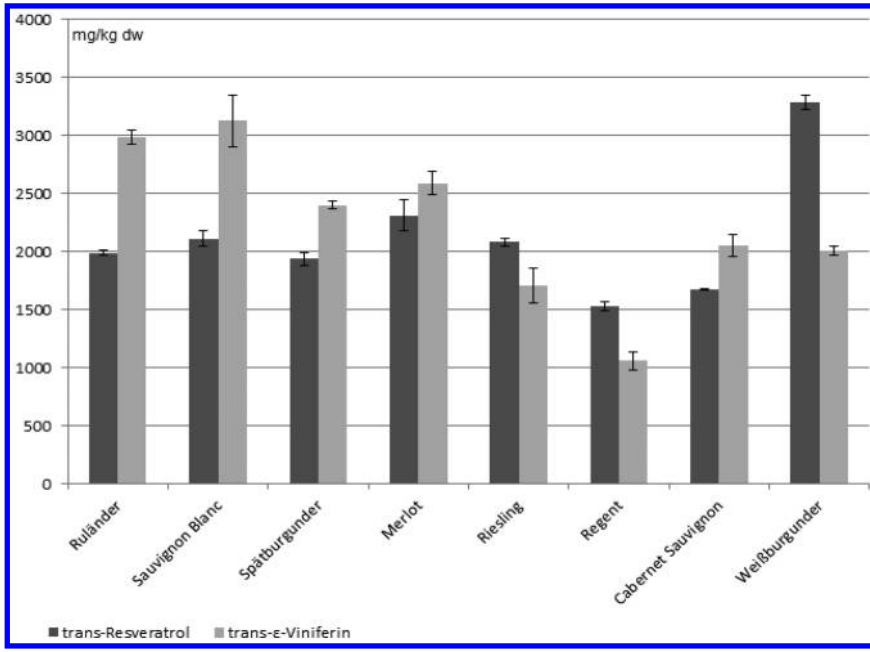

Figure 6. trans-Resveratrol and trans-ε-viniferin content in prunings from Germany 2013.

The content of *trans*-resveratrol ranged between approx. 1500 and 3300 mg/kg dw. While the lowest content was observed for the variety "*Regent"* which is known to exhibit resistance against fungal diseases, the highest content was found in the variety "*Weißburgunder*". The content of *trans*-ε-viniferin was in a similar range (approx. 1000 – 3100 mg/kg dw). Again, the variety "*Regent*" was found to possess the lowest amount, whereas the variety "Sauvignon Blanc" exhibited the largest amount of the dimeric stilbene.

References

1. *Statistical report on world vitiviniculture 2012*; International Organisation of Vine and Wine, 2012.
2. Schieber, A.; Stinzing, F. C.; Carle, R. *Trends Food Sci. Technol.* **2001**, *12*, 401–413.
3. Hang, Y. D. *Process Biochem.* **1988**, *23*, 2–4.
4. Shrikhande, A. J. *Food Res. Int.* **2000**, *33*, 469–474.
5. Ju, J.; Ahmedna, M. *Int. J. Food Sci. Technol.* **2013**, *48*, 221–237.
6. Brazinha, C.; Cadima, M.; Crespo, J. G. *J. Food Sci.* **2014**, *79*, E1142–E1149.
7. Yu, Z. Y.; Howard, L. R. *J. Food Sci.* **2005**, *70*, S270–S276.

8. Kammerer, D.; Claus, A.; Schieber, A.; Carle, R. *J. Food Sci.* **2005**, *70*, C157–C163.
9. Corrales, M.; Toepfl, S.; Butz, P.; Knorr, D.; Tauscher, B. *Innovative Food Sci. Emerg. Technol.* **2008**, *9*, 85–91.
10. Degenhardt, A.; Knapp, H.; Winterhalter, P. *J. Agric. Food Chem.* **2000**, *48*, 338–343.
11. Schwarz, M.; Hillebrand, S.; Habben, S.; Degenhardt, A.; Winterhalter, P. *Biochem. Eng. J.* **2003**, *14*, 179–189.
12. Juadjur, A.; Winterhalter, P. *J. Agric. Food Chem.* **2012**, *60*, 2427–2433.
13. Köhler, N.; Wray, V.; Winterhalter, P. *J. Agric. Food Chem.* **2008**, *56*, 5374–5385.
14. Winterhalter, P. *Am. J. Enol. Vitic.* **2009**, *60*, 123–129.
15. Degenhardt, A.; Knapp, H.; Winterhalter, P. *Vitis* **2000**, *39*, 43–44.
16. Köhler, N.; Chou, E.; Ito, Y.; Winterhalter, P. *J. Liq. Chromatogr. Relat. Technol.* **2004**, *27*, 2547–2560.
17. Degenhardt, A.; Engelhardt, U. H.; Winterhalter, P.; Ito, Y. *J. Agric. Food Chem.* **2001**, *49*, 1730–1736.
18. Sun, B.; Ricardo-da-Silva, J. M.; Spranger, I. *J. Agric. Food Chem.* **1998**, *46*, 4267–4274.
19. Porter, L. J.; Hrstich, L. N.; Chan, B. G. *Phytochemistry* **1986**, *25*, 223–230.
20. The Grape Seed Method Evaluation Committee (2001). *Grape Seed Extract White Paper*; Under the Auspices of NNFA ComPli.
21. Kuhnert, S.; Lehmann, L.; Winterhalter, P. *J. Funct. Foods* **2015**, *15*, 225–232.
22. Esatbeyoglu, T.; Wray, V.; Winterhalter, P. *J. Agric. Food Chem.* **2010**, *58*, 7820–7830.
23. Billard, C.; Izard, J.-C.; Roman, V.; Kern, C.; Mathiot, C.; Mentz, F.; Kolb, J.-P. *Leuk. Lymphoma* **2002**, *43*, 1991–2002.
24. Baur, J. A.; Sinclair, D. A. *Nat. Rev. Drug Discovery* **2006**, *5*, 493–506.
25. Rayne, S.; Karacabey, E.; Mazza, G. *Ind. Crops Prod.* **2008**, *27*, 335–340.
26. Vergara, C.; von Baer, D.; Mardones, C.; Wilkens, A.; Wernekinck, K.; Damm, A.; Macke, S.; Gorena, T.; Winterhalter, P. *J. Agric. Food Chem.* **2012**, *60*, 929–933.
27. Macke, S.; Jerz, G.; Empl, M. T.; Steinberg, P.; Winterhalter, P. *J. Agric. Food Chem.* **2012**, *60*, 11919–11927.
28. Steinberg, P. *Ernährungs Umschau* **2011**, *58*, 366–371.
29. Empl, M. T.; Macke, S.; Winterhalter, P.; Puff, C.; Lapp, S.; Stoica, G.; Baumgärtner, W.; Steinberg, P. *Vet. Comp. Oncol.* **2014**, *12*, 149–159.
30. Houillé, B.; Besseau, S.; Courdavault, V.; Oudin, A.; Glévarec, G.; Delanoue, G.; Guérin, L.; Simkin, A. J.; Papon, N.; Clastre, M.; Giglioli-Guivarc'h, N.; Lanoue, A. *J. Agric. Food Chem.* **2015**, *63*, 1631–1638.
31. Gorena, T.; Saez, V.; Mardones, C.; Vergara, C.; Winterhalter, P.; von Baer, D. *Food Chem.* **2014**, *155*, 256–263.

Publication Date (Web): November 24, 2015 | doi: 10.1021/bk-2015-1203.ch021

Publication Date (Web): November 24, 2015 | doi: 10.1021/bk-2015-1203.ch022

Chapter 22

Evaluation of the Potential of Grape Canes as a Source of Bioactive Stilbenoids

Tamara Gorena, Claudia Mardones, Carola Vergara, Vania Saez, and Dietrich von Baer*

Departamento de Análisis Instrumental, Facultad de Farmacia, Universidad de Concepción, Barrio Universitario s/n, Concepción, Chile
***E-mail: dvonbaer@udec.cl.**

The health-promoting properties of stilbenoids have been widely documented. In plants, stilbenoids form part of a complex defense mechanism, playing an important role in the response to biotic and abiotic stress in grape vines. The health benefits of (*E*)-resveratrol have been used to promote moderate wine consumption. However, wine contains only 0.4–8.1 $mg \cdot L^{-1}$ of (*E*)-resveratrol. Approaches to increase these levels in grape vines involved subjecting the vines to different growing conditions, and irradiating grapes with UV-C light. These methods increased the stilbenoid levels in grapes; however, the levels were still much lower compared to grape canes obtained after pruning the vineyard. In grape canes, the (*E*)-resveratrol concentration can reach up to 5959 $mg \cdot kg^{-1}$ DW. In *Vitis vinifera* canes stored for some months after pruning, the concentration of (*E*)-resveratrol increased five-fold (based on dry matter). The mechanism of this increase is still unknown, but indeed it has a significant impact on the potential of grape canes as a source of stilbenoids. Cane-management after pruning has a greater influence on this potential than the grape variety or other factors.

In Advances in Wine Research; Ebeler, et al.;
ACS Symposium Series; American Chemical Society: Washington, DC, 2015.

Publication Date (Web): November 24, 2015 | doi: 10.1021/bk-2015-1203.ch022

Introduction

The grape is a crop widely distributed in different areas of the world, occupying approximately 7.5 million hectares (ha). To optimize the quality of grapes, certain viticultural practices must be utilized, such as pruning some months after grape harvest. This process influences the shape and size of the vine and the balance between vegetative growth and the yield and the quality of grape production (*1*). The grape canes, which are the lignified material generated by pruning, represent a mass of more than 1 ton·ha^{-1}·year^{-1}. Usually, grape canes are chopped and incorporated into the soil as fertilizer or are burned. However, such agricultural waste has great economic potential as a source of phytochemicals (especially stilbenoids) with high added value.

In several studies of grape canes, the presence of phenylpropanoids that include hydroxycinnamic acid derivatives (coumaric, caffeic, and ferulic), flavonoids such as catechin and epicatechin, and stilbenoids such as (*E*)-resveratrol and its derivatives (i.e., (*E*)-ε-viniferin, (*E*)-piceatannol, (*E*)-piceid), and other dimers, trimers, and tetramers (*2*–*5*) have been reported. Furthermore, carbohydrates and minerals such as K, P, Ca, Fe, Mg, and Zn have been detected in grape cane (*6*).

Stilbenoids in *Vitis vinifera*

Stilbenoids are phenolic compounds derived from the phenylpropanoid pathway, present in a large number of plant families (*7*–*9*), including *Vitaceae*. The biosynthesis of (*E*)-resveratrol involves four main enzymes: phenylalanine ammonia lyase (PAL), cinnamate 4-hydroxylase (C4H), 4-coumarate:CoA ligase (4CL), and resveratrol synthase, also known as stilbene synthase (STS). Only the plants with the STS enzyme can synthesize resveratrol, for which *p*-coumaryl CoA and malonyl CoA are required. In the grape vine, different stilbenoids are formed from (*E*)-resveratrol. The (*E*)-resveratrol molecule may undergo a number of modifications, including photoisomerization, glycosylation, and oligomerization to form compounds such as (*Z*)-resveratrol, (*E*)- and (*Z*)-piceids, and (*E*)-ε-viniferin, respectively (*7*).

Stilbenoids play an essential role in the plant defense mechanism. In the case of *Vitis*, stilbenoid synthesis is differentiated, depending on the organ of production (*10*, *11*). Stilbenoids can act as primary or secondary action barriers against pathogen attack and against different types of stress to which the plant may be exposed. Wang *et al*. (*10*) reported that stilbenoids in *Vitis* spp. accumulate in branches, canes, auxiliary buds, and roots, whereas leaves, which are more exposed to environmental stress, have a low concentration of these compounds; the highest concentration of (*E*)-resveratrol was found in branches, specifically in phloem tissue, and the lowest concentration was found in leaves (*10*). However, the concentration of the STS enzyme was highest in the leaves (almost twice that in the stem). These findings suggest a differential response of the plant to stress. The stilbenoid induction capacity is higher in leaves to provide enhanced protection, given their higher exposure to the environment and resulting susceptibility to attack by pests and diseases. Furthermore, Keller *et al*.

(*12*) showed that secondary metabolite formation is decreased by leaf removal. A similar event occurs in the inflorescence, where the stilbenoid concentration can be significantly low in whole berries while being high in the skin, but disappearing in the pulp and seeds (*13*, *14*).

Table 1. Resveratrol Levels in *Vitis vinifera*

Source	*Concentration (E)-resveratrol*[a]	*Reference*
Grapes	0.06–33.5 mg kg^{-1} FW	(*15–17*)
Wine	0.1–14.3 mg L^{-1}	(*18–21*)
Grape Skin	0.24–366 mg kg^{-1} DW	(*22–25*)
Pomace	6.00–53.21 mg kg^{-1} DW	(*22*, *26*)
Grape seeds	14.2–588 mg kg^{-1} DW	(*23*, *27*, *27*)
Leaves	0.12–71.5 mg kg^{-1} FW	(*25*, *28*, *29*)
Grape Cane	190–6533 mg kg^{-1} DW	(*2–5*, *30*)

[a] FW: fresh weight; DW: dry weight.

Publication Date (Web): November 24, 2015 | doi: 10.1021/bk-2015-1203.ch022

As shown in Table 1 (*15–30*), grape canes are an important source of *(E)*-resveratrol. The concentration of *(E)*-resveratrol in this underexploited residue obtained during annual vine pruning is 50–100 times greater than in grapes and wine. High levels of other phenolic compounds have been detected in other winemaking byproducts, whereas the stilbenoid content was lower.

In grape vines, several factors induce response-mediated stilbenoid accumulation in different plant organs. The factors affecting the metabolite contents in berries have been extensively studied. Agronomic factors such as irrigation (*31*) and nitrogen fertilization can increase the concentration of these compounds (*13*). Pathogens (*32*, *33*), short-wave ultraviolet light (*34–38*), ozone, ethylene (*39*), and storage time (*13*) may also have a similar effect.

In grape berries, resveratrol is stored primarily in the skin and to a minor extent in the seeds. Accumulation of resveratrol in red cultivars is higher than in white congeners (*34*). Genetic factors that codify aspects such as the number of enzymes related to the synthesis and degradation of these metabolites (*7*) can influence the contents of this secondary metabolite in the plant. During ripening, a negative correlation between the maturity of grapes and the ability to induce resveratrol synthesis has been observed (*37*).

The resveratrol content in wines depends primarily on the grape variety and winemaking practices employed (*34*). In order to improve the concentration of these compounds in wine and methyl jasmonate, grape berries have been irradiated with short wavelength UV light (*36–38*).

The presence of resveratrol in lignified grape tissue is well established (*40*). However, there is little information about what influences the accumulation of stilbenoids in grape canes. Recent studies show that grape canes from *Vitis vinifera* are a promising source of (*E*)-resveratrol and other stilbenoids (*41*) and have significant economic potential because of their high concentration of phytochemicals (*4*, *6*). Stilbenoids have generated increasing interest because of their diverse beneficial effects on human health, which have been extensively studied (*32*, *42–45*). In parallel, other authors have evaluated the potential of stilbenoids as a part of the defense mechanism of the plant (*46–48*). Furthermore, stilbenoids in conjunction with other phenolic compounds present in grape cane have more recently been evaluated as grape biostimulants and/or foliar fertilizers (*49*).

Publication Date (Web): November 24, 2015 | doi: 10.1021/bk-2015-1203.ch022

Stilbenoids in Grape Cane

Eleven stilbenoids were detected in canes of *Vitis vinifera* cv. Pinot Noir collected in southern Chile, 8 of which were identified (*5*). The structures of these compounds are shown in Figure 1. The unidentified compounds correspond to two dimers and one trimer. In most of the samples collected in the aforementioned study, the predominant stilbenoid was (*E*)-resveratrol, followed by (*E*)-ε-viniferin, while (*E*)-piceatannol, hopeaphenol, and vitisin A were only detected in some samples. In most cases, (*E*)-piceid, vitisin B, dimers, and trimers were only present at concentrations below the limit of quantification.

Factors that Induce Accumulation of Stilbenoids in *Vitis*

The stilbenoid concentration in *Vitis vinifera* canes varies by cultivar (*5*, *30*, *41*) and the phytosanitary conditions of the grape vines (*50*, *51*). Furthermore, stilbenoids play an important role in the defense mechanism of plants, particularly in the complex response against various biotic or abiotic stress (*15*, *20*, *52*); thus, environmental factors (by way of elicitors) may also induce stilbenoid biosynthesis (*15*).

The evaluation of elicitors of stilbenoids in grape canes conducted by Tang *et al*. (*11*) demonstrated an increase in the concentration of resveratrol in roots, stems, leaves, and ribs of young plants irradiated with short-wavelength UV light. Two points of maximal (*E*)-resveratrol concentrations were thus induced in stems at 16 and at 24 h post irradiation, with a return to the basal concentration at 64 h post irradiation. They also observed an increase in the concentration of the STS enzyme, which is distributed mainly in the cell wall, and is found in lower concentrations in the cytoplasm, chloroplast, and nucleus of cells in the stem. Amalfitano *et al*. (*51*) studied the stilbenoid profiles in wood naturally infected by a fungal complex and found an increase in the level of stilbenoids (mainly viniferins) in attacked wood that was thought to enhance the resistance to fungal invasion.

Publication Date (Web): November 24, 2015 | doi: 10.1021/bk-2015-1203.ch022

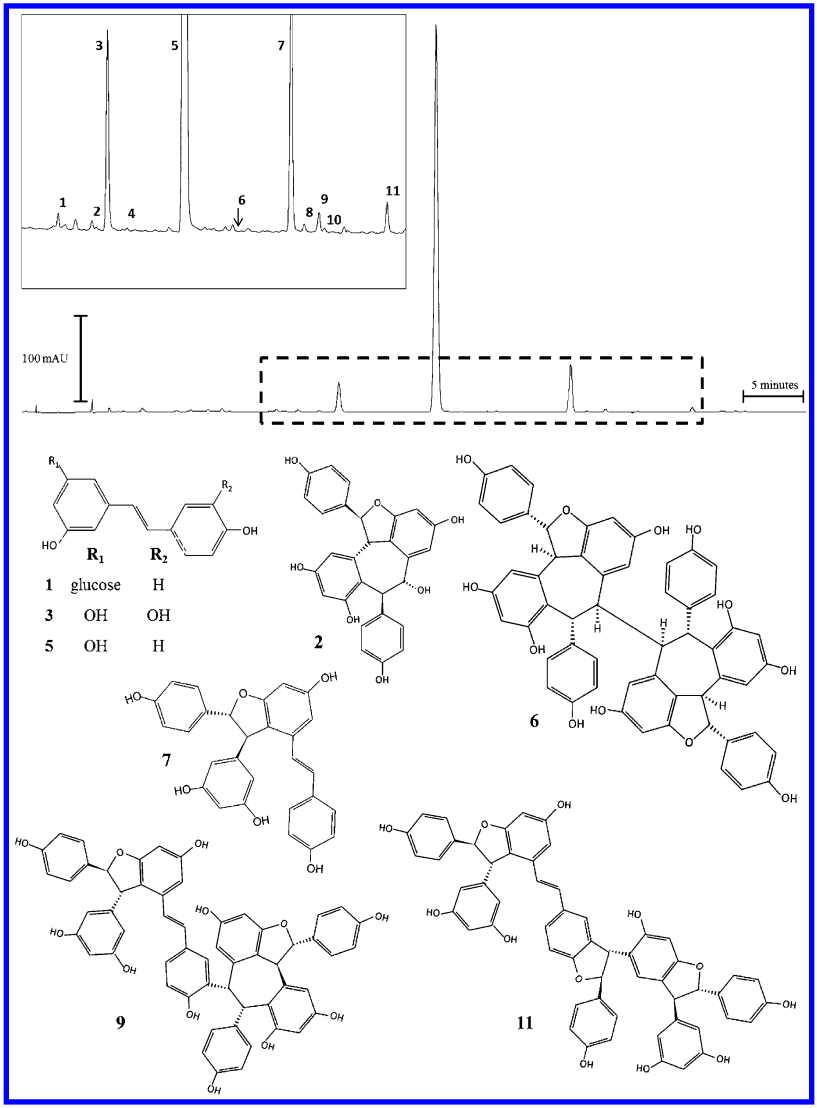

Figure 1. HPLC–DAD chromatogram of Pinot Noir cane extract (λ = 306 nm) and structures of detected stilbenoids: 1: (E)-piceid; 2: ampelopsin A; 3: (E)-piceatannol; 5: (E)-resveratrol; 6: hopeaphenol; 7: (E)-ε-viniferin; 9: vitisin A; 11: vitisin B; 4 and 10: unidentified dimers; 8: unidentified trimer. (Reproduced with permission from Reference (41). Copyright 2014 Elsevier Ltd.)

Effect of Cultivar on Stilbenoid Levels

Different stilbenoid levels have been reported in *Vitis vinifera* canes. Vergara *et al*. (*5*) were the first to evaluate the stilbenoid concentration in grape canes of the main wine cultivars of southern Chile Subsequently, Lambert *et al*. (*30*) evaluated

In Advances in Wine Research; Ebeler, et al.;
ACS Symposium Series; American Chemical Society: Washington, DC, 2015.

different cultivars of *Vitis vinifera* canes of economic importance in France. Recently, Gorena *et al*. (*41*) studied the stilbenoid concentration in cultivars found in Central-South Chile. The stilbenoid level in grape canes depends on the cultivar. In all of these publications, Pinot Noir and Gewürztraminer canes were consistently found to be the cultivars with the highest stilbenoid concentration.

Table 2 summarizes the stilbenoid concentration in different *Vitis vinifera* cultivars from the main publications over the last 8 years. (*E*)-resveratrol concentrations of 4250 mg kg^{-1} dry weight (DW) were reported for the Pinot Noir cultivar in Canada (*2*), very similar to the levels reported by Vergara *et al*. (*5*) for the same cultivar in southern Chile, with 5590–868 mg·kg^{-1} DW (*E*)-resveratrol and (*E*)-ε-viniferin, respectively. Concentrations of up to 6533 mg·kg^{-1} DW of (*E*)-resveratrol were also obtained for Gewürztraminer canes in the aforementioned study. The lowest levels of (*E*)-resveratrol in grape canes were reported in different species of *Vitis* from China by Zhang et al. (*53*), with concentrations between 570 and 1751 mg·kg^{-1} fresh weight (FW). Piñero *et al*. (*54*) found low levels of (*E*)-resveratrol in the red grape stem stripping residue, ranging from undetected levels in Cabernet Sauvignon, Merlot, and Petit Verdot to 135 mg·kg^{-1} DW (DW) in Tintorera after irradiation with UV light. In hybrid cultivars from Estonia, Püssa *et al*. (*3*) reported levels in the range of 1100–3200 mg·kg^{-1} DW of (*E*)-resveratrol and between 700 and 1700 mg·kg^{-1} DW of (*E*)-ε-viniferin.

The effect of latitude in the extensive wine growing area of Chile (between the Limarí and Bio-Bio valleys) on the stilbenoid content of Pinot Noir canes was evaluated (*55*) for grape canes after post-pruning storage for 3 months. No clear increasing or decreasing trend in the stilbenoid content was observed as a function of latitude.

Worldwide, grapes occupy 7.5 million hectares of agricultural land. Considering a grape cane yield of at least one ton·ha^{-1}·$year^{-1}$, the potential worldwide production of grape canes is 7.5 million tons grape canes per year. Considering only the surface planted with grapes for winemaking and not including table grapes, on the basis of at least 1 kg·ton^{-1}, the potential annual production of stilbenoids in the world could reach 7500 tons per year and that of Chile 128 tons.

Various analytical factors can also contribute to differences in the stilbenoid concentration of grape canes. These include the extraction conditions, such as different solvents and proportions (*4*), in addition to the quantification method. Quantitation has been conducted by external calibration using (*E*)-resveratrol as described by several authors (*2*, *3*, *5*, *41–46*, *56*), where all concentrations were expressed as (*E*)-resveratrol equivalents. Quantitation may also be performed with respect to purified non-commercial standards, as described by Pawlus *et al*. (*57*) and Lambert *et al*. (*30*) Another important factor to consider during extraction is the photochemical isomerization of (*E*)-resveratrol to the (*Z*)-isomer. Vian *et al*. (*58*) showed that 80–90% of (*E*)-resveratrol in solution is transformed to (*Z*)-resveratrol upon exposure to daylight for 1 h.

Publication Date (Web): November 24, 2015 | doi: 10.1021/bk-2015-1203.ch022

Table 2. Stilbenoid Levels in Lignified Material of Grape Vines

Plant Material	*Cultivar (cv)*	*Stilbene Concentration*[a]	*Reference*
Terminal parts of lignified stems	Different *Vitis* from Estonia	(*E*)-resveratrol 1100–3200 mg kg^{-1} DW (*E*)-ε-viniferin 700–1700 mg kg^{-1} DW	(*3*)
Grape canes	Pinot Noir	(*E*)-resveratrol 3320 mg kg^{-1} DW (*E*)-ε-viniferin 1300 mg kg^{-1} DW	(*4*)
Grape canes	Pinot Noir	(*E*)-resveratrol 4060 mg kg^{-1} DW (*E*)-ε-viniferin 1087 mg kg^{-1} DW	(*2*)
Stem	Cabernet Sauvignon	(*E*)-resveratrol 16.5 mg kg^{-1} FW	(*10*)
Grape canes (pruning waste)	Different cv *V. vinifera*, *V. labrusca* and hybrids (118 cv)	In cultivars of *V. vinifera*: (*E*)-resveratrol 570 to 1751 mg kg^{-1} FW	(*53*)
Grape canes (pruning waste)	10 cv of table grapes (white and red)	(*E*)-resveratrol 0.95 – 3.94 μg 100 g^{-1} DW	(*6*)
Grape canes (pruning waste)	Pinot Noir	(*E*)-resveratrol 3400 mg kg^{-1} DW (*E*)-ε-viniferin 1650 mg kg^{-1} DW	(*59*)
Grape canes (pruning waste)	Pinot Noir	(*E*)-resveratrol 446–6533 mg kg^{-1} DW (*E*)-ε-viniferin 75–868 mg kg^{-1} MS	(*5*)
Grape canes	Cabernet Sauvignon	(*E*)-resveratrol 1621 mg kg^{-1} DW; (*E*)-ε-viniferin 2585 mg kg^{-1} DW	(*57*)
Grape canes	Different cv *V. vinifera* (8 red and 8 white)	(*E*)-resveratrol 190–1526 mg kg^{-1} DW (*E*)-ε-viniferin 967–3737 mg kg^{-1} DW	(*30*)
Grape canes (pruning waste)	Different cv *V. vinifera*	(*E*)-resveratrol 1360–5959 mg kg^{-1} DW; (*E*)-ε-viniferin 94–656 mg kg^{-1} DW	(*41*)

[a] FW: fresh weight; DW: dry weight.

Effect of Post-Pruning Storage on Stilbenoid Levels

The period of storage of the grape canes seems to be the most important trigger for increasing the stilbenoid levels, particularly that of (*E*)-resveratrol. Aaviksaar *et al*. (*56*) first reported augmentation of the stilbenoid concentration in canes of hybrid *Vitis vinifera* cultivars from Estonia based on comparison of samples stored for durations of one and two months.

In Advances in Wine Research; Ebeler, et al.;
ACS Symposium Series; American Chemical Society: Washington, DC, 2015.

Publication Date (Web): November 24, 2015 | doi: 10.1021/bk-2015-1203.ch022

Publication Date (Web): November 24, 2015 | doi: 10.1021/bk-2015-1203.ch022

The presence of resveratrol in lignified grape tissue (*40*) is well established. However, there is little available information regarding stilbenoids in fresh canes collected directly from grape vines. Studies by Gorena *et al.* (*41*) showed that (*E*)-ε-viniferin was the predominant stilbenoid in fresh canes collected successively from Pinot Noir grape vines between 20 and 120 days after grape harvest and processed immediately after collection. The concentrations of (*E*)-resveratrol and (*E*)-ε-viniferin were 87–223 mg·kg^{-1} DW and 430–611 mg·kg^{-1} DW, respectively.

In a similar experiment with fresh Cabernet Sauvignon canes (Figure 2), collected directly from grape vines at different time periods before and after commercial pruning and processed immediately after collection, the concentration of (*E*)-ε-viniferin was 284–345 mg·kg^{-1} DW and that of (*E*)-resveratrol was 53–129 mg·kg^{-1} DW (*56*). The concentrations of minor stilbenoids such as (*E*)-piceid, (*E*)-piceatannol, vitisin A, and vitisin B were below the limit of quantification and hopeaphenol was found only in low concentrations (39–50 mg·kg^{-1} DW) in all samples analyzed. As in the case of Pinot Noir canes, the major stilbenoid in fresh canes was (*E*)-ε-viniferin.

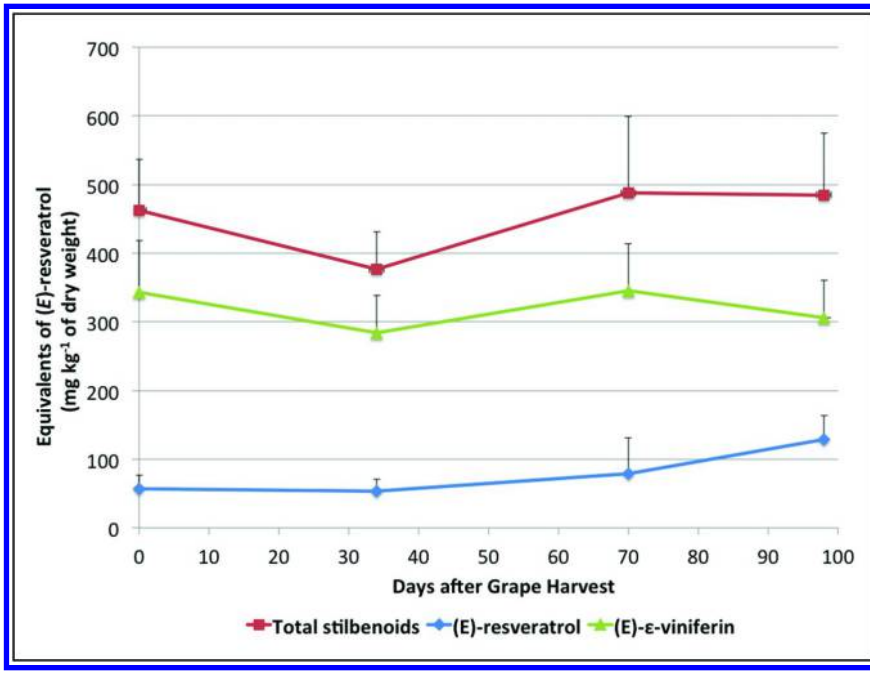

Figure 2. Concentration of the main stilbenoids in canes freshly cut from intact Cabernet Sauvignon vines. The samples were immediately processed without storage.

The concentrations of (*E*)-resveratrol in freshly cut and immediately processed Pinot Noir and Cabernet Sauvignon canes were significantly lower than that of canes stored for some months before analysis (*5*, *41*, *55*). This observation indicates that cutting and/or loss of water are prerequisites for increasing the

stilbenoid content of grape canes, mainly the *E*-resveratrol levels. These factors either trigger the biosynthesis of stilbenoids or promote their liberation during wood ageing, as discussed in the context of the following experiments.

Post-pruning storage is the major factor influencing the stilbenoid levels (mainly (*E*)-resveratrol) in grape canes. Vergara *et al*. (*5*) reported a 35% increase of the (*E*)-resveratrol level of pruned canes after 2-month storage. In subsequent studies, Gorena *et al.* (*41*) evaluated the stilbenoid concentrations in Pinot Noir canes stored at room temperature for a period of up to 8 months after pruning. Figure 3 highlights the different trends observed for both major stilbenoids during storage. The concentration of (*E*)-resveratrol increased significantly up to the second month, declined to some extent in the third month, and then remained nearly constant. In contrast, the level of (*E*)-ε-viniferin did not vary significantly during the entire period. At the end of the assay, the concentrations of other minor stilbenoids such as (*E*)-piceatannol, hopeaphenol, vitisin A, and vitisin B increased slightly (*55*). The total stilbenoid concentration increased significantly after 2 months, reaching 4777 mg·kg^{-1} DW, and subsequently decreased up to the fifth month. This was followed by another increase, reaching a concentration of 4443 mg·kg^{-1} DW after the eighth month.

Publication Date (Web): November 24, 2015 | doi: 10.1021/bk-2015-1203.ch022

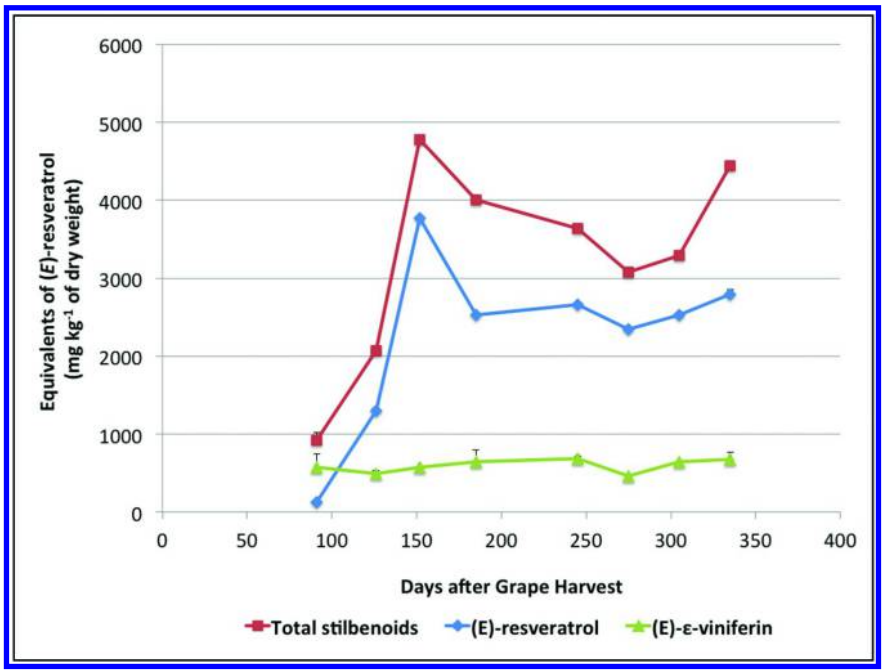

Figure 3. Concentration of the main stilbenoids in Pinot Noir canes collected after commercial pruning and storage at room temperature. (Reproduced with permission from Reference (41). Copyright 2014 Elsevier Ltd.)

Publication Date (Web): November 24, 2015 | doi: 10.1021/bk-2015-1203.ch022

A similar trend was observed for Cabernet Sauvignon canes collected during commercial pruning in 2012 and analyzed after different periods of post-pruning storage at room temperature for a period of up to 7 months (*55*), as shown in Figure 4. With increasing storage time, the concentration of stilbenoids in the grape cane increased. Peak concentrations were observed after 2 and 7 months storage, where respective total stilbenoid concentrations of 4402 mg·kg^{-1} DW and 4456 mg·kg^{-1} DW were observed.

Similar to the trend observed for Pinot Noir canes, the increase in the total stilbenoid concentration of Cabernet Sauvignon canes during storage was derived primarily from augmented (*E*)-resveratrol levels, where (*E*)-resveratrol became the major stilbenoid after the first month, reaching a concentration of 3642 mg·kg^{-1} after 2 months.

A non-significant increase in the concentration of (*E*)-ε-viniferin (from 278 to 356 mg·kg^{-1}) was observed in these samples during the storage period. (*E*)-Piceatannol and hopeaphenol were found in low concentrations in all analyzed samples. Only traces of the minor stilbenoids (i.e., (*E*)-piceid, vitisin A, and vitisin B) were detected.

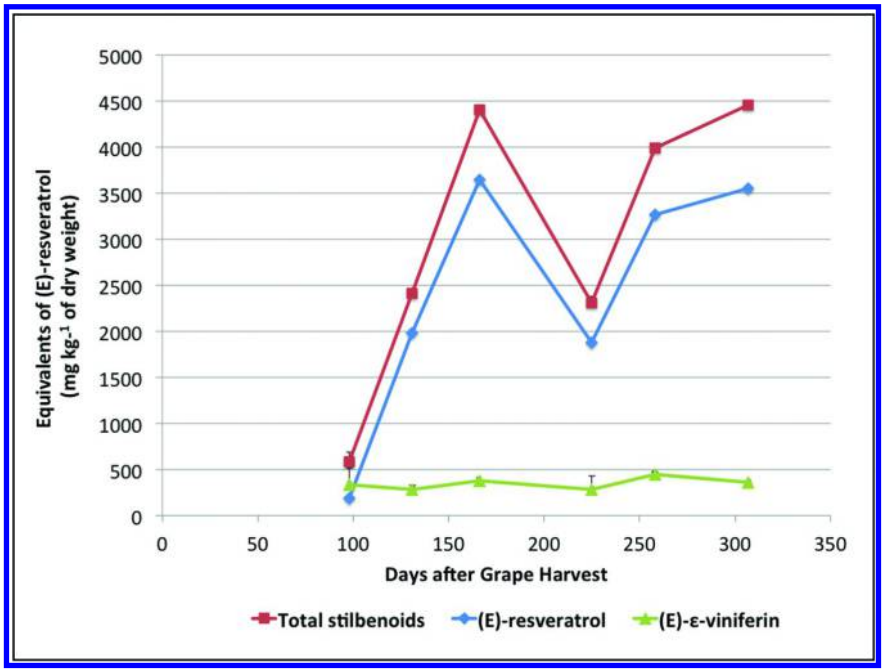

Figure 4. Concentration of the main stilbenoids of Cabernet Sauvignon canes collected after commercial pruning and storage at room temperature.

These results indicate that post-pruning storage is a key requirement for further increasing the concentration of stilbenoids in grape canes, especially the concentration of (*E*)-resveratrol. The large increase in the stilbenoid levels of

intact grape canes during storage, which did not occur in milled canes, indicates clearly that this increase requires the presence of intact cells and also does not occur if the canes are kept frozen or are freeze-dried (*41*).

Gorena *et al*. (*41*) compared the stilbenoid levels of Pinot Noir cane samples obtained from vineyards in different areas of the Bio-Bio Region in South Chile after 2 and 6 months of storage subsequent to commercial pruning (Figure 5). Significant increases in the total stilbenoid levels of four- to seven-fold were observed for all Pinot Noir samples. Differences in the stilbenoid profiles of samples stored for 2 and 6 months were also observed, given that traces of (*E*)-vitisin B were only detected in the 6-month samples, again demonstrating that post-pruning storage significantly influences the stilbenoid concentration in grape canes.

Publication Date (Web): November 24, 2015 | doi: 10.1021/bk-2015-1203.ch022

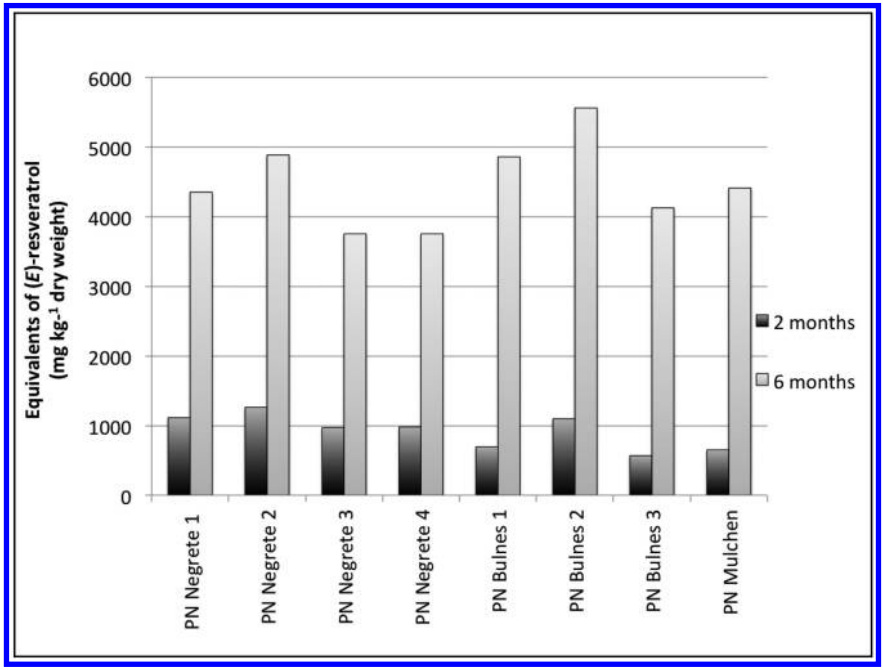

Figure 5. Total stilbenoid concentration in Pinot Noir canes 2 and 6 months after post-pruning storage at room temperature. (Reproduced with permission from Reference (41). Copyright 2014 Elsevier Ltd.)

Hart (*60*) observed that the increase in the stilbenoid content was primarily observed in dying wood, and that the stilbenoid concentration in healthy wood was much lower. However, as alluded to earlier, an increase in the viniferins was thought to enhance the resistance to fungal invasion in wood (*51*), whereas in healthy canes stored after pruning at room temperature over some months,

the (*E*)-resveratrol levels increased significantly and the level of (*E*)-viniferin was not significantly affected (*41*, *55*). This can be attributed to activation of the biosynthesis of stilbenoids in the canes during storage, probably induced by the loss of water during cane storage. Another possible alternative is that (*E*)-resveratrol remains bound to other components in the fresh cane, and is thus less easily extracted. During cane ageing, stilbenoids may be gradually released thereby becoming more extractable. For determination of whether either or both of these mechanisms causes the significant increase of stilbenoids (mainly (*E*)-resveratrol) during cane storage, additional research and experimental evidence is required.

However, it is evident that cane storage over some months at room temperature enhances the stilbenoid levels in grape canes to a great extent, improving their potential as a source of these bioactive compounds.

Publication Date (Web): November 24, 2015 | doi: 10.1021/bk-2015-1203.ch022

Conclusions

Grape canes stored at room temperature for a few months after pruning are a promising source of (*E*)-resveratrol and other bioactive stilbenoids. The stilbenoid concentrations in this underexploited viticulture residue are 50–100-fold higher than in grapes and wine and are also higher than in other winemaking byproducts. Considering the area of agricultural land occupied by grapes worldwide, the global potential of stilbenoids that can be obtained from grape canes could reach 7500 tons and 128 tons per year worldwide and in Chile, respectively.

The canes of certain grape cultivars, like Pinot Noir and Gewürztraminer, have higher stilbenoid levels than other varieties. However, these levels are mainly influenced by post-pruning storage at room temperature. The observed 5–7-fold increase of stilbenoids, and (*E*)-resveratrol in particular, is triggered by pruning. This is not observed if canes are cut fresh from the vine or if the pruned grape canes are stored frozen, powdered, or lyophilized. These observations indicate that intact cells and certain temperatures are necessary for increasing the stilbenoid content of grape canes. However, the mechanism by which the increase in the stilbenoid levels occurs still remains unknown. It is proposed that the increase in the stilbenoid level may be derived from biosynthesis during storage of pruned canes or to stilbenoid liberation during ageing of canes, where stilbenoids in fresh canes remain bound to other cane components. Irrespective of the mechanism, it is evident that cane storage over a few months at room temperature enhances the stilbenoid levels in grape canes to a great extent, improving their potential as a source of these bioactive compounds.

Acknowledgments

FONDECYT (Chile), Grant 1110767, CONICYT Insertion in Academia Grant 79112036, CONICYT Doctoral Fellowship, and CONICYT Basal Grant PFB-27.

References

1. Gil, G.; Pszolkowski, P. *Viticultura. Fundamentos para optimizar producción y calidad*; Universidad Católica de Chile: Santiago, Chile, 2007; Vol. 1, pp 1−535.
2. Karacabey, E.; Mazza, G. Optimization of Solid−Liquid Extraction of Resveratrol and Other Phenolic Compounds from Milled Grape Canes (*Vitis vinifera*). *J. Agric. Food Chem.* **2008**, *56*, 6318–6325.
3. Püssa, T.; Floren, J.; Kuldkepp, P.; Raal, A. Survey of Grapevine *Vitis vinifera* Stem Polyphenols by Liquid Chromatography-Diode Array Detection-Tandem Mass Spectrometry. *J. Agric. Food Chem.* **2006**, *54*, 7488–7494.
4. Rayne, S.; Karacabey, E.; Mazza, G. Grape cane waste as a source of *trans*-resveratrol and *trans*-viniferin: High-value phytochemicals with medicinal and anti-phytopathogenic applications. *Ind. Crops Prod.* **2008**, *27*, 335–340.
5. Vergara, C.; von Baer, D.; Mardones, C.; Wilkens, A.; Wernekinck, K.; Damm, A.; Macke, S.; Gorena, T.; Winterhalter, P. Stilbene Levels in Grape Cane of Different Cultivars in Southern Chile: Determination by HPLC-DAD-MS/MS method. *J. Agric. Food Chem.* **2012**, *60*, 929–933.
6. Çetin, E.; Altinöz, D.; Tarçan, E.; Baydar, N. Chemical composition of grape canes. *Ind. Crops Prod.* **2011**, *34*, 994–998.
7. Chong, J.; Poutaraud, A.; Hugueney, P. Review: Metabolism and roles of stilbenes in plants. *Plant Sci.* **2009**, *177*, 143–155.
8. Counet, C.; Callemien, D.; Collin, S. Chocolate and cocoa: New sources of *trans*-resveratrol and *trans*-piceid. *Food Chem.* **2006**, *98*, 649–657.
9. Yu, C.; Springob, K.; Schmidt, J.; Nicholson, R.; Chu, I.; Kin Yip, W.; Lo, C. A stilbene synthase gene (*SbSTS1*) is involved in host and nonhost defense responses in sorghum. *Plant Physiol.* **2005**, *138*, 393–401.
10. Wang, W.; Tang, K.; Yang, H.; Wen, P.; Zhang, P.; Wang, H.; Huang, W. Distribution of resveratrol and stilbene synthase in young grape plants (*Vitis vinifera* L. cv. Cabernet Sauvignon) and the effect of UV-C on its accumulation. *Plant Physiol. Biochem.* **2010**, *48*, 142–152.
11. Tang, K.; Fang, F.; Yang, H.; Huang W. Effect of UV-C irradiation on stilbene synthase localization in young grape plants. *Russ. J. Plant Physiol.* **2011**, *58*, 603–614.
12. Keller, M.; Steel, C.; Creasy, G. Stilbene accumulation in grapevine tissues: Developmental and environmental effects. *Acta Hortic.* **2000**, *514*, 275–286.
13. Cavaliere, C.; Foglia, P.; Marini, F.; Samperi, R.; Antonacci, D.; Laganà, A. The interactive effects of irrigation, nitrogen fertilization rate, delayed harvest and storage on the polyphenol content in red grape (*Vitis vinifera*) berries: A factorial experimental design. *Food Chem.* **2010**, *122*, 1176–1184.
14. Fornara, V.; Onelli, E.; Sparvoli, F.; Rossoni, M.; Aina, R.; Marino, G.; Citterio, S. Localization of stilbene synthase in *Vitis vinifera* L. during berry development. *Protoplasma* **2008**, *233*, 83–93.
15. Bavaresco, L.; Pezzutto, S.; Gatti, M.; Mattivi, F. Role of the variety and some environmental factors on grape stilbenes. *Vitis* **2007**, *46*, 57–61.

16. Gatto, P.; Vrhovsek, U.; Muth, J.; Segala, C.; Romualdi, C.; Fontana, P.; Pruefer, D.; Stefanini, M.; Moser, C.; Mattivi, F.; Velasco, R. Ripening and Genotype Control Stilbene Accumulation in Healthy Grapes. *J. Agric. Food Chem.* **2008**, *56*, 11773–11785.
17. Bachteler, K.; Riedel, M.; Tisch, C.; Merkt, N.; Amann, R.; Wünsche, J. Influence of berry shrivel on concentrations of resveratrol, catechin, epicatechin and ε-viniferin in berries of *Vitis vinifera* L. cultivars 'Zweigelt', 'Pinot Blanc' and 'Pinot Gris'. *Eur. J. Hort. Sci.* **2013**, *78*, 49–55.
18. Mark, L.; Nikfardjam, M. S.; Avar, P.; Ohmacht, R. A validated HPLC method for the quantitative analysis of *trans*-resveratrol and *trans*-piceid in Hungarian wines. *J. Chromatogr. Sci.* **2005**, *43*, 445–449.
19. Boutegrabet, L.; Fekete, A.; Hertkorn, N.; Papastamoulis, Y.; Waffo-Téguo, P.; Mérillon, J.; Jeandet, P.; Gougeon, R.; Schmitt-Kopplin, P. Determination of stilbene derivatives in Burgundy red wines by ultra-high-pressure liquid chromatography. *Anal. Bioanal. Chem.* **2011**, *401*, 1513–1521.
20. Bavaresco, L.; Mattivi, F.; De Rosso, M.; Flamini, R. Effects of elicitors, viticultural factors, and enological practices on resveratrol and stilbenes in grapevine and wine. *Mini Rev. Med. Chem.* **2012**, *12*, 1366–1381.
21. Fernández-Marín, M.; Puertas, B.; Guerrero, R.; García-Parrilla, M.; Cantos-Villar, E. Preharvest methyl jasmonate and postharvest UVC treatments: Increasing stilbenes in wine. *J. Food Sci.* **2014**, *79*, C310–C317.
22. Careri, M.; Corradini, C.; Elviri, L.; Nicoletti, I.; Zagnoni, I. Direct HPLC Analysis of Quercetin and *trans*-resveratrol in Red Wine, Grape, and Winemaking Byproducts. *J. Agric. Food Chem.* **2003**, *51*, 5226–5231.
23. Kammerer, D.; Claus, A.; Carle, R.; Schieber, A. Polyphenol Screening of Pomace from Red and White Grape Varieties (*Vitis vinifera* L.) by HPLC-DAD-MS/MS. *J. Agric. Food Chem.* **2004**, *52*, 4360–4367.
24. Katalinić, V.; Možina, S.; Skroza, D.; Generalić, I.; Abramovič, H.; Miloš, M.; Ljubenkov, I.; Piskernik, S.; Pezo, I.; Terpinc, P.; Boban, M. Polyphenolic profile, antioxidant properties and antimicrobial activity of grape skin extracts of 14 *Vitis vinifera* varieties grown in Dalmatia (Croatia). *Food Chem.* **2010**, *119*, 715–723.
25. Wang, L.; Xu, M.; Liu, C.; Wang, J.; Xi, H.; Wu, B.; Loescher, W.; Duan, W.; Fan, P.; Li, S. Resveratrols in grape berry skins and leaves in *Vitis* germplasm. *PLoS One* **2013**, *8*, e61642.
26. Ector, B. J.; Magee, J. B.; Hegwood, C. P.; Coign, M. J. Resveratrol concentration in muscadine berries, juice, pomace, purees, seeds, and wines. *Am. J. Enol. Vitic.* **1996**, *47*, 57–62.
27. Casazza, A.; Aliakbarian, B.; Mantegna, S.; Cravotto, G.; Perego, P. Extraction of phenolics from *Vitis vinifera* wastes using non-conventional techniques. *J. Food Eng.* **2010**, *100*, 50–55.
28. Vrhovsek, U.; Malacarne, G.; Masuero, D.; Zulini, L.; Guella, G.; Stefanini, M.; Velasco, R.; Mattivi, F. Profiling and accurate quantification of *trans*- resveratrol, *trans*-piceid, *trans*-pterostilbene and 11 viniferins induced by *Plasmopara viticola* in partially resistant grapevine leaves. *Aust. J. Grape Wine Res.* **2012**, *18*, 11–19.

29. Liu, C.; Wang, L.; Wang, J.; Wu, B.; Liu, W.; Fan, P.; Liang, Z.; Li, S. Resveratrols in *Vitis* berry skins and leaves: Their extraction and analysis by HPLC. *Food Chem.* **2013**, *136*, 643–649.
30. Lambert, C.; Richard, T.; Renouf, E.; Bisson, J.; Waffo-Téguo, P.; Bordenave, L.; Ollat, N.; Mérillon, J.; Cluzet, S. Comparative Analyses of Stilbenoids in Canes of Major *Vitis vinifera* L. Cultivars. *J. Agric. Food Chem.* **2013**, *61*, 11392–11399.
31. Deluc, L.; Decendit, A.; Papastamoulis, Y.; Mérillon, J.; Cushman, J.; Cramer, G. Water Deficit Increases Stilbene Metabolism in Cabernet Sauvignon Berries. *J. Agric. Food Chem.* **2011**, *59*, 289–297.
32. Aggarwal, B.; Bhardwaj, A.; Aggarwal, R.; Seeram, N.; Shishodia, S.; Takada, Y. Review: Role of resveratrol in prevention and therapy of cancer: Preclinical and clinical studies. *Anticancer Res.* **2004**, *24*, 2783–2840.
33. Pezet, R.; Gindro, K.; Viret, O.; Spring, J. Glycosylation and oxidative dimerization of resveratrol are respectively associated to sensitivity and resistance of grapevine cultivars to downy mildew. *Physiol. Mol. Plant Pathol.* **2004**, *65*, 297–303.
34. Cantos, E.; Espín, J.; Tomás-Barberan, F. Postharvest Stilbene-Enrichment of Red and White Table Grape Varieties Using UV-C Irradiation Pulses. *J. Agric. Food Chem.* **2002**, *50*, 6322–6329.
35. González-Barrio, R.; Beltrán, D.; Cantos, E.; Gil, M.; Espín, J.; Tomás-Barberán, F. Comparison of Ozone and UV-C Treatments on the Postharvest Stilbenoid Monomer, Dimer, and Trimer Induction in var. 'Superior' White Table Grapes. *J. Agric. Food Chem.* **2006**, *54*, 4222–4228.
36. Guerrero, R.; Puertas, B.; Jiménez, M.; Cacho, J.; Cantos-Villar, E. Monitoring the process to obtain red wine enriched in resveratrol and piceatannol without quality loss. *Food Chem.* **2010**, *122*, 195–202.
37. Guerrero, R.; Puertas, B.; Fernández, M.; Palma, M.; Cantos-Villar, E. Induction of stilbenes in grapes by UV-C: Comparison of different subspecies of *Vitis*. *Innovative Food Sci. Emerging Technol.* **2010**, *11*, 231–238.
38. Guerrero, R.; Puertas, B.; Fernández, M.; Piñeiro, Z.; Cantos-Villar, E. UVC-treated skin-contact effect on both white wine quality and resveratrol content. *Food Res. Int.* **2010**, *43*, 2179–2185.
39. Grimmig, B.; Schubert, R.; Fischer, R.; Hain, R.; Schreier, P. H.; Betz, C.; Langebartels, C.; Ernst, D.; Sandermann, H. Ozone- and ethylene-induced regulation of a grapevine resveratrol synthase promoter in transgenic tobacco. *Acta Physiol. Plant.* **1997**, *19*, 467–474.
40. Langcake, P.; Pryce, R. The production of resveratrol by *Vitis vinifera* and other members of the Vitaceae as a response to infection or injury. *Physiol. Plant Pathol.* **1976**, *9*, 77–86.
41. Gorena, T.; Saez, V.; Mardones, C.; Vergara, C.; Winterhalter, P.; von Baer, D. Influence of post-pruning storage on stilbenoid levels in *Vitis vinifera* L. canes. *Food Chem.* **2014**, *155*, 256–263.
42. Baur, J. A.; Pearson, K. J.; Price, N. L.; Jamieson, H. A.; Lerin, C.; Kalra, A.; Prabhu, V. V.; Allard, J. S.; Lopez- Lluch, G.; Lewis, K.; Pistell, P. J.; Poosala, S.; Becker, K. G.; Boss, O.; Gwinn, D.; Wang, M.; Ramaswamy, S.;

Fishbein, K. W.; Spencer, R. G.; Lakatta, E. G.; Le Couteur, D.; Shaw, R. J.; Navas, P.; Puigserver, P.; Ingram, D. K.; de Cabo, R.; Sinclair, D. A. Resveratrol improves health and survival of mice on a high-calorie diet. *Nature* **2006**, *444*, 337–342.
43. Baur, J. A.; Sinclair, D. A. Therapeutic potential of resveratrol: The *in vivo* evidence. *Nat Rev. Drug Discovery* **2006**, *5*, 493–506.
44. Bishayee, A. Cancer prevention and treatment with resveratrol: From rodent studies to clinical trials. *Cancer Prev. Res.* **2009**, *2*, 409–418.
45. Borriello, A.; Cucciolla, V.; Della Ragione, F.; Galletti, P. Dietary polyphenols: Focus on resveratrol, a promising agent in the prevention of cardiovascular diseases and control of glucose homeostasis. *Nutr. Metab. Cardiovasc. Dis.* **2010**, *20*, 618–625.
46. Adrian, M.; Jeandet, P.; Douillet-Breuil, A. C.; Tesson, L.; Bessis, R. Stilbene Content of Mature *Vitis vinifera* Berries in Response to UV-C Elicitation. *J. Agric. Food Chem.* **2000**, *48*, 6103–6105.
47. Alonso-Villaverde, V.; Voinesco, F.; Viret, O.; Spring, J. L.; Gindro, K. The effectiveness of stilbenes in resistant Vitaceae: Ultrastructural and biochemical events during *Plasmopara viticola* infection process. *Plant Physiol. Biochem.* **2011**, *49*, 265–274.
48. Legay, G.; Marouf, E.; Berger, D.; Neuhaus, J. M.; Mauch-Mani, B.; Slaughter, A. Identification of genes expressed during the compatible interaction of grapevine with *Plasmopara viticola* through suppression subtractive hybridization (SSH). *Eur. J. Plant Pathol.* **2011**, *129*, 281–301.
49. Sánchez-Gómez, R.; Zalacain, A.; Alonso, G.; Salinas, R. Vine-Shoot Waste Aqueous Extracts for Re-use in Agriculture Obtained by Different Extraction Techniques: Phenolic, Volatile, and Mineral Compounds. *J. Agric. Food Chem.* **2014**, *62*, 10861–10872.
50. Lambert, C.; Bisson, J.; Waffo-Téguo, P.; Papastamoulis, Y.; Richard, T.; Corio-Costet, M.; Mérillon, J.; Cluzet, S. Phenolics and Their Antifungal Role in Grapevine Wood Decay: Focus on the Botryosphaeriaceae Family. *J. Agric. Food Chem.* **2012**, *60*, 11859–11868.
51. Amalfitano, C.; Agrelli, D.; Arrigo, A.; Mugnai, L.; Surico, G.; Evidente, A. Stilbene polyphenols in the brown red wood of *Vitis vinifera* cv. Sangiovese affected by "esca proper". *Phytopathol. Mediterr.* **2011**, *50*, S224–S235.
52. Mattivi, F.; Vrhovsek, U.; Malacarne, G.; Masuero, D.; Zulini, L.; Stefanini, M.; Moser, C.; Velasco, R.; Guella, G. Profiling of Resveratrol Oligomers, Important Stress Metabolites, Accumulating in the Leaves of Hybrid *Vitis vinifera* (Merzling x Teroldego) Genotypes Infected with *Plasmopara viticola*. *J. Agric. Food Chem.* **2011**, *59*, 5364–5375.
53. Zhang, A.; Fang, Y.; Li, X.; Meng, J.; Wang, H.; Li, H.; Zhang, Z.; Guo, Z. Occurrence and estimation of *trans*-resveratrol in one-year-old canes from seven major Chinese grape producing regions. *Molecules* **2011**, *16*, 2846–2861.
54. Piñero, Z.; Guerrero, M.; Fernández-Marin, M.; Cantos-Villar, E.; Palma, M. Ultrasound-Assisted Extraction of Stilbenoids from Grape Stems. *J. Agric. Food Chem.* **2013**, *61*, 12549–12556.

Publication Date (Web): November 24, 2015 | doi: 10.1021/bk-2015-1203.ch022

55. Gorena, T. Efecto del cultivar y de diferentes prácticas agronómicas sobre el potencial de los sarmientos de Vitis vinifera *como fuente de estilbenos*. Ph.D. Thesis, Universidad de Concepción, Concepción, 2014.
56. Aaviksaar, A.; Haga, M.; Püssa, T.; Roasto, M.; Tsoupras, G. Purification of resveratrol from vine stems. *Proc. Est. Acad. Sci., Chem*. **2003**, *52*, 155–164.
57. Pawlus, A.; Sahli, R.; Bisson, J.; Rivière, C.; Delaunay, J.; Richard, T.; Gomès, E.; Bordenave, L.; Waffo-Téguo, P.; Mérillon, J. Stilbenoid Profiles of Canes from *Vitis* and *Muscadinia* Species. *J. Agric. Food Chem*. **2013**, *61*, 501–511.
58. Vian, M.; Tomao, V.; Gallet, S.; Coulomb, P.; Lacombe, J. Simple and rapid method for *cis*- and *trans*-resveratrol and piceid isomers determination in wine by high-performance liquid chromatography using Chromolith columns. *J. Chromatogr. A*. **2005**, *1085*, 224–229.
59. Karacabey, E.; Mazza, G.; Bayındırlı, L.; Artık, N. Extraction of bioactive compounds from milled grape canes (*Vitis vinifera*) using a pressurized low-polarity water extractor. *Food Bioprocess Technol*. **2012**, *5*, 359–371.
60. Hart, J. Role of phytostilbenes in decay and disease resistance. *Ann. Rev. Phytopathol*. **1981**, *19*, 437–458.

Publication Date (Web): November 24, 2015 | doi: 10.1021/bk-2015-1203.ch022

Publication Date (Web): November 24, 2015 | doi: 10.1021/bk-2015-1203.ch023

Chapter 23

Objective Chemical Measures of Grape Quality

Michael Cleary,* Huihui Chong, Nona Ebisuda, Nick Dokoozlian, Natalia Loscos, Bruce Pan, David Santino, Qiang Sui, and Cynthia Yonker

E. & J. Gallo Winery, P.O. Box 1130, Modesto, California 95353
***E-mail: Mike.cleary@ejgallo.com.**

Nine classes of molecules have been identified in dark grape varieties to measure chemical quality; total anthocyanins, Yeast Assimilable Nitrogen (YAN) compounds, 3-isobutyl-2-methoxypyrazine, C_6 alcohols/aldehydes, hydrolytically-released β-damascenone, malic acid, pH, polymeric tannins, and skin tannins. These attributes can be used to identify regional differences within a single variety of grapes. In addition, different grape varieties exhibit unique chemical distributions among these nine classes of molecules.

Introduction

Historically, the value of California wine grapes has been determined by the region in which they are grown. However, research in grape composition and wine sensory indicate that differences in grape quality and resulting wines can sometimes vary as much within a region as across regions, raising the need to elucidate grape quality irrespective of regional biases. Cultural vineyard practices, soil types, micro-climates, and harvest timing, are just a few examples of factors that can influence the chemical make-up and thus the quality of the grapes and respective wines. The use of objective measures of grape quality is the first step in building a foundation to better understand the relationships between vineyard environment, grape, and ultimately, wine quality.

In Advances in Wine Research; Ebeler, et al.;
ACS Symposium Series; American Chemical Society: Washington, DC, 2015.

A universal definition of grape chemical quality has always been elusive. It is known that many grape components contribute to wine quality. One logical place to begin to develop a definition of grape chemical quality is to consider the components that constitute wine consumption. The process of experiencing wine can be divided into four steps of evaluation and description:

- Sight
- Smell
- Taste
- Touch

Sight is the first impression one obtains from a wine. One observes the color and clarity of the wine. The second impression is smell. One is taught to swirl the wine in a glass to release the aromas, hold the glass up to one's nose, and inhale. Next, one takes the wine into their mouth and tastes. At the same time as one tastes the wine, there is the sensation of how it "feels" in the mouth. From this wine consumption process, a classification of the components of Chemical Grape and Wine Quality can be defined by the following:

- Color
- Aroma
- Taste
- Mouthfeel

These proposed attributes of Chemical Grape and Wine Quality can be traced to certain classes of molecules intrinsic to grapes. This is shown in the following Table 1.

Several studies have been conducted to evaluate relationships between single chemical attributes and wine scores in Australian Shiraz. Francis et al. (*1*) conducted studies that demonstrated the positive relationship between high berry color and high wine score for Shiraz vineyards in the Riverland region. Ristic et al. (*2*) conducted a study that showed a positive relationship between wine quality score and bound β-damascenone in the berries. In the same study, Ristic et al. demonstrated a positive relationship with skin tannins and wine quality scores.

In a study by Ugliano et al. (*3*), the YAN concentration in grape juice significantly affected the aroma of the resulting wine. YAN is identified as the concentration of primary amino acids and ammonia. High juice YAN concentrations (>350 mg/L) led to increased formation of ethyl acetate and acetic acid in the resulting wine. Methoxypyrazines, compounds with the odor of "bell pepper", can negatively impact aroma for many red wines, such as Cabernet Sauvignon and Merlot. Maga (*4*) reported that Methoxypyrazine contributed leafy aroma to red wine at 2 ng/L. Chapman et al. (*5*) demonstrated a significant correlation between Methoxypyrazine concentrations, in the range 0 to 10 ng/L, and sensory ratings of bell pepper aroma in Cabernet Sauvignon wine. Degradation of polyunsaturated fatty acids occurs when the cell structure

Publication Date (Web): November 24, 2015 | doi: 10.1021/bk-2015-1203.ch023

of grape berries are disrupted, leading to the formation of C_6 compounds (*6*), which augment "green" and "grassy" perception in grapes. Malic acid, beyond contributing acidity to grapes, serves as a marker of grape maturity as it has been demonstrated to decreases as berries ripen (*7*).

Table 1. Classes of Molecules Responsible for Grape Quality Attributes

Grape Quality Attribute	*Class of Molecules*
Color	Anthocyanins, Pigmented Polymers
Aroma	Alcohols, Aldehydes, Esters, Ketones, Terpenes, Norisoprenoids, Nitrogen Heterocyclics
Taste	Sweet - Sugars
	Sour - Acids
	Bitter Amino Acids
	Salty Potassium, Sodium
Mouthfeel	Polymeric Tannins, Skin Tannins, Polysaccharides, Organic Acids

Publication Date (Web): November 24, 2015 | doi: 10.1021/bk-2015-1203.ch023

Analytical Methodologies

Twenty clusters of grapes were completely homogenized to prepare total anthocyanins, 3-isobutyl-2-methoxypyrazine, C_6 alcohols/aldehydes, hydrolytically-released β-damascenone, polymeric tannins, and skin tannins samples for instrumental analysis. Whole grape homogenization was chosen as the sample preparation technique to accommodate the high sample throughput requirements of the laboratory. Juice from twenty clusters of grapes was used to prepare samples for YAN compounds, malic acid, and pH measurements.

Total Anthocyanins were measured using the visible spectroscopy method published by Iland et al. (*8*). Hydrolytically released β-damascenone, 3-isobutyl-2-methoxypyrazine, and C_6 alcohols/aldehydes were analyzed using the Headspace Gas Chromatography/Mass Spectrometry method proposed by Lee and Noble (*9*). Polymeric Tannins and Skin Tannins were characterized using High Performance Liquid Chromatography employing a method described by Peng et al. with slight variations (*10*). The chromatography peaks from Flavonols were employed as markers for Skin Tannins. YAN compounds, malic acid, and pH concentrations were determined using Fourier Transform Infrared Spectroscopy. FTIR calibration curves were developed for each of these attributes using standard primary analytical methodologies.

Analytical methods validation format employed two analysts using two different instruments on two separate days. The precision for each attribute, presented as % Relative Standard Deviation, is shown in Table 2.

Table 2. Analytical Method Precision for Each Chemical Attribute

Chemical Attribute	*Precision (% RSD)*
Total Anthocyanins	2.9
3-Isobutyl-2-methoxypyrazine	3.2
C_6 alcohols/aldehydes	11
Hydrolytically-released β-damascenone	2.1
Polymeric Tannins	5.0
Skin Tannins	4.9
YAN	7.2
Malic Acid	4.5
pH	1.2

Publication Date (Web): November 24, 2015 | doi: 10.1021/bk-2015-1203.ch023

Validation of Important Grape Attributes for Wine Quality

How grape chemical quality is measured objectively to assist streaming and harvest decisions requires a careful assessment of grape maturity on a yearly basis. It is not unusual for a single vineyard to be streamed to different wine programs in different years. Ideally, each vineyard should be monitored several times between veraison and harvest. These multiple analyses per vineyard will support the winemakers' harvest date decisions as they observe the chemical changes during fruit maturation. A final analysis taken close to harvest can support the winemakers wine program streaming decisions. This harvest analysis can also be used to establish chemical grape composition targets for various wine programs. Meaningful data requires proper vineyard sampling techniques (Krstic (*11*)), prompt sample transportation to the laboratory, consistent analytical sample preparation, precise, rapid instrumentation, and timely reporting of results to the viticulturalists and winemakers. In order for the Chemistry data to have credibility with the viticulturalists and winemakers, small scale fermentations at each sampling time need to be produced and sensorally evaluated. The logistics to coordinate all of these activities and the staff required to successfully accomplish a grape assessment program should not be overlooked. Grape chemical quality from a single vineyard is greatly influenced by unique weather conditions every season. Therefore, several years of analyses are required to establish growing region averages.

From 2008 – 2013, grapes from thirty Merlot vineyards and forty Cabernet Sauvignon vineyards from all of the major California winegrowing regions were chemically characterized weekly from 19° Brix until two weeks post commercial harvest. From this data, varietal and regional trends could be identified. At or near the date of commercial harvest, sufficient grapes were collected to conduct 10 gallon fermentations. These fermentations employed identical, standard winemaking practices. No oak was added and no Malolactic fermentation was

conducted such that each fermentation represented only the attributes provided by the grapes. The resulting wines from these fermentations were evaluated by winemakers. The winemakers evaluated the wines for aroma, color, and mouthfeel on a 5 point scale. In addition, they were asked to rank each wine based on a price point scale.

Figure 1 below shows the correlation between grape color and winemakers evaluation of color for nine Central Valley Cabernet Sauvignon wines. Color was measured as Total Anthocyanins. In general wines with higher color, both chemically and visually, were ranked into higher price points. It is accepted that color is not the only criteria for quality when winemakers evaluate wines.

Publication Date (Web): November 24, 2015 | doi: 10.1021/bk-2015-1203.ch023

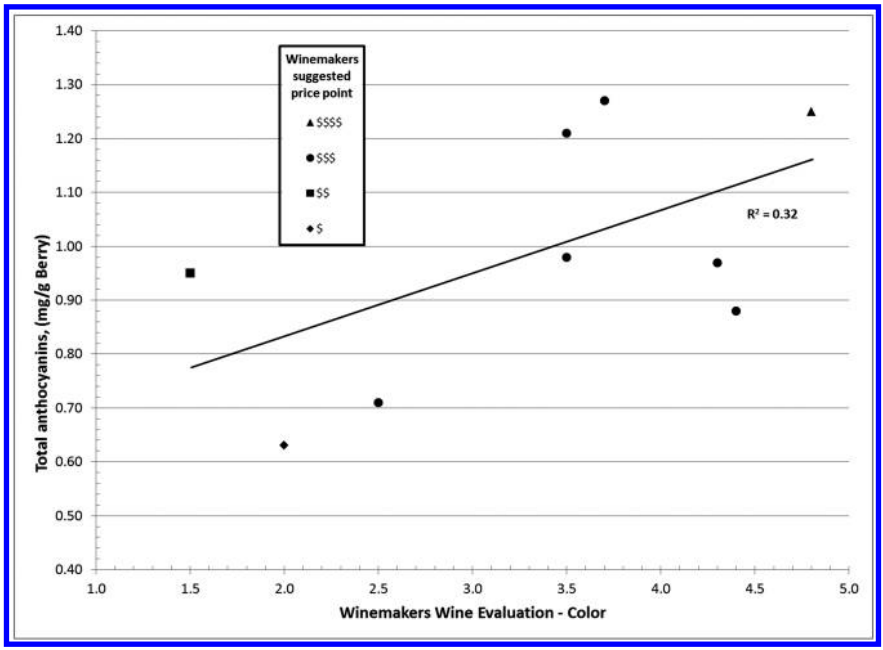

Figure 1. Grape total anthocyanins (mg/g berry) color compared to wine color evaluation.

Figure 2 shows the comparison between grape C_6 aldehydes and alcohols content and winemakers' evaluation of "green" aroma for 15 North Coast Cabernet Sauvignon wines. The wines with lower levels of C_6 aldehydes and alcohols in their grapes are more preferred than those wines with higher levels of C_6 aldehydes and alcohols. As with color, the lack of "green" aroma is not the only measure of winemaker quality.

Publication Date (Web): November 24, 2015 | doi: 10.1021/bk-2015-1203.ch023

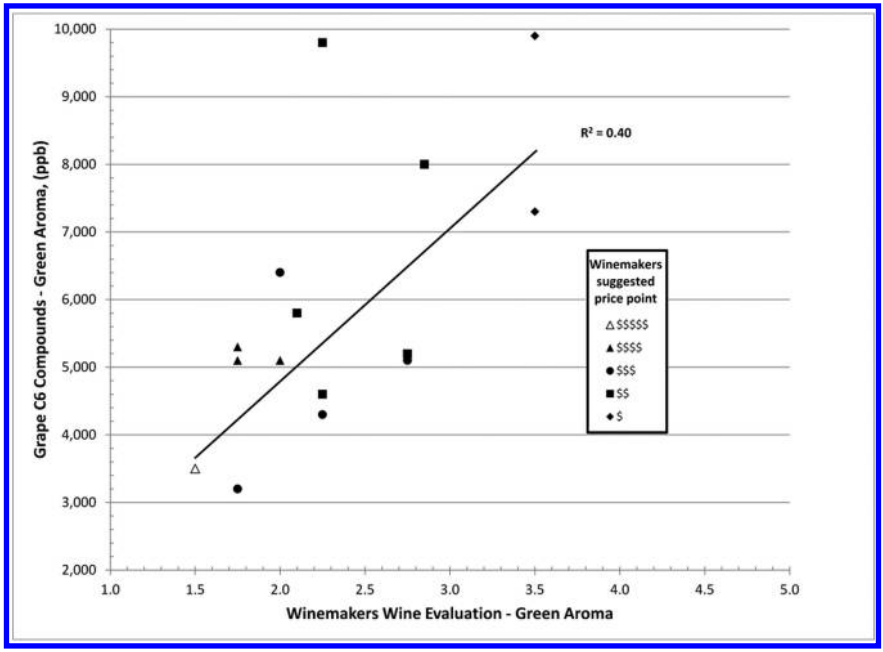

Figure 2. Grape C6 aldehydes and alcohols content compared to wine "green" aroma evaluation.

In Figure 3, malic acid and 3-isobutyl-2-methoxypyrazine contents in the grapes were combined with the C_6 aldehydes and alcohols contents in the grapes for comparison with winemakers' evaluation of "green" aroma in 11 Central Valley Merlot wines. The wines with lower levels of C_6 aldehydes/alcohols, malic acid and 3-isobutyl-2-methoxypyrazine in their grapes are more preferred than those wines with higher levels of these compounds. Combining multiple attributes gave a stronger correlation than using individual attributes.

Publication Date (Web): November 24, 2015 | doi: 10.1021/bk-2015-1203.ch023

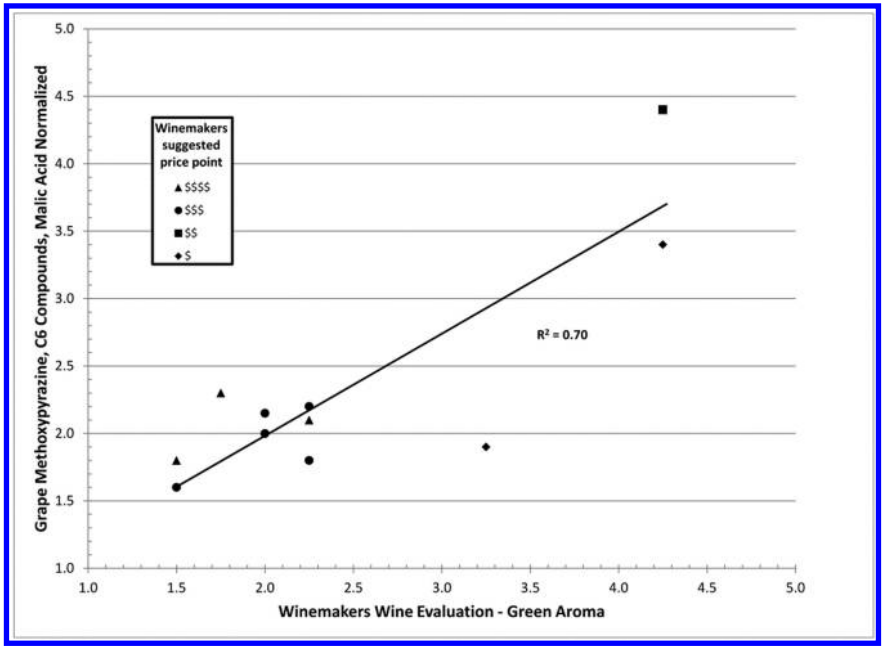

Figure 3. Grape C_6 aldehydes/alcohols, malic acid, and 3-isobutyl-2-methoxypyrazine content compared to wine "green" aroma evaluation.

Figure 4 shows the comparison between grape Polymeric Tannins, Skin Tannins, Total Anthocyanins, and Brix content with winemakers' evaluation of mouthfeel for 16 North Coast Cabernet Sauvignon wines. The wines with higher levels of these grape components are more preferred than those wines with lower levels. Again the combination of multiple attributes gave a stronger correlation than single attributes.

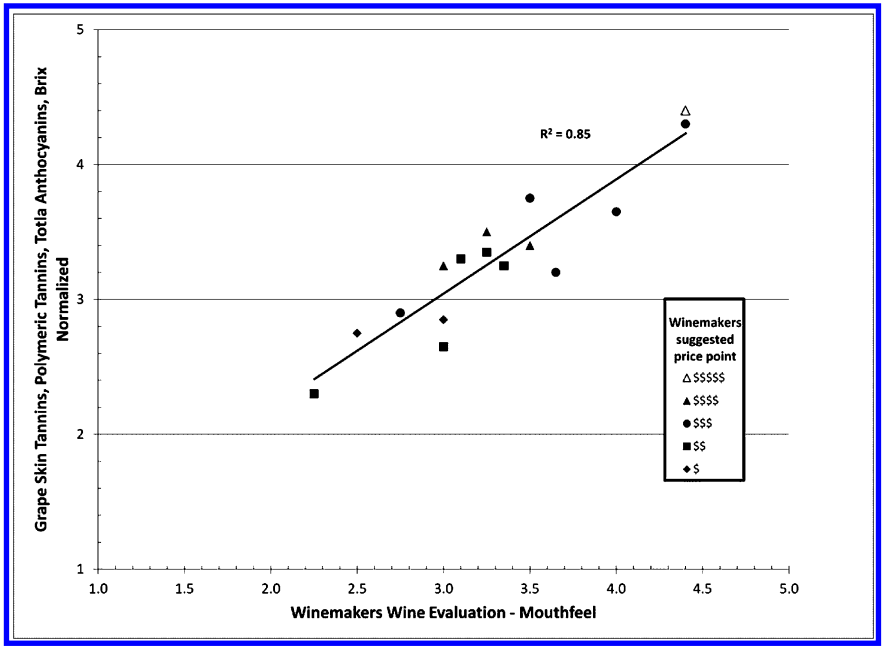

Figure 4. Grape Skin Tannins, Polymeric Tannins, Total Anthocyanins, and Brix content, compared to wine mouthfeel evaluation.

Publication Date (Web): November 24, 2015 | doi: 10.1021/bk-2015-1203.ch023

Combining the previous work from the researchers outlined above with the grape chemistry versus winemaker tastings data presented here, nine classes of molecules have been identified in dark grape varieties to measure chemical quality; total anthocyanins, YAN, 3-isobutyl-2-methoxypyrazine, C_6 alcohols/aldehydes, hydrolytically-released β-damascenone, malic acid, pH, polymeric tannins, and skin tannins.

Growing Region Variation in Chemical Quality Attributes for California Cabernet Sauvignon Grapes

Grapes from a total of 1,949 Cabernet Sauvignon vineyards from the major wine growing regions of California were chemically characterized at commercial harvest during the years 2008 to 2013. The nine classes of molecules which have been identified in dark grape varieties to measure chemical quality; total anthocyanins, YAN, 3-isobutyl-2-methoxypyrazine, C_6 alcohols/aldehydes, hydrolytically-released β-damascenone, malic acid, pH, polymeric tannins, and skin tannins were quantified. The results of this study are shown in the PCA plot in Figure 5.

Publication Date (Web): November 24, 2015 | doi: 10.1021/bk-2015-1203.ch023

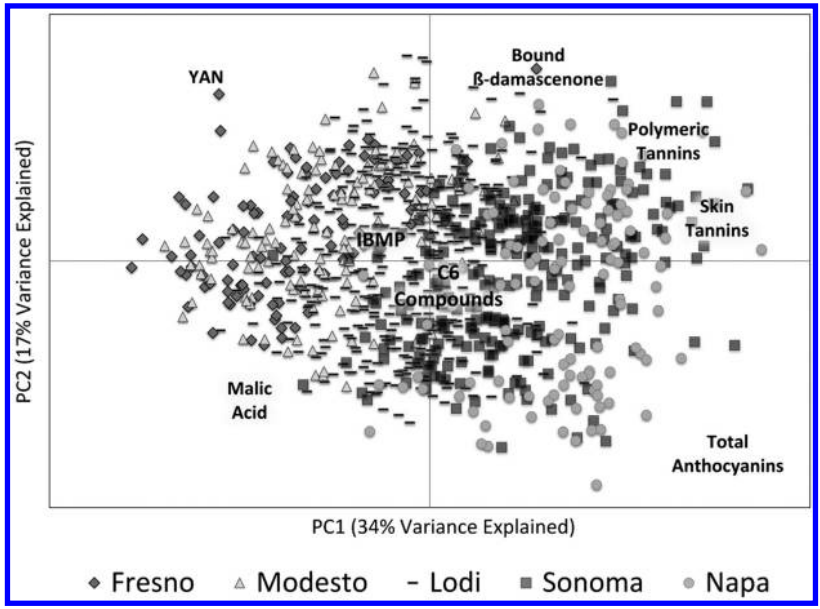

Figure 5. Chemical characterizations of Cabernet Sauvignon grapes from vineyards across California's major wine growing regions.

The PC1 axis is essentially an axis of quality. The positive chemical attributes consisting of total anthocyanins, hydrolytically-released β-damascenone, polymeric tannins, and skin tannins appear farther to the right of the origin than the negative chemical attributes YAN, 3-isobutyl-2-methoxypyrazine, C_6 alcohols/aldehydes, and malic acid. There is also a trend between chemical attributes and vineyard location. In general, the vineyards in the Napa and Sonoma regions have higher concentrations of the positive attributes and the vineyards in the Fresno and Modesto regions have higher amounts of the negative attributes. This chemical relationship is consistent with the generally accepted wine industry judgment that better wines are produced from grapes in the Napa and Sonoma regions than are produced from grapes in the Fresno and Modesto regions. However, it is very apparent from the PCA plot that location by itself is not a measure of grape quality. There are Lodi vineyards that have similar chemical quality attributes to vineyards in Napa and Sonoma. In addition, there are Napa and Sonoma vineyards that have chemical quality attributes that are more similar to those in the Modesto and Lodi regions.

These objective chemical measures of grape quality provide a means to establish regional differences. Additionally, year to year variations within a region and a single vineyard can be monitored. Three hundred eighty-nine Cabernet Sauvignon vineyards in 2013 from the major winegrowing regions of California were chemical characterized at commercial harvest. Table 3 shows the average values of the nine chemical attributes by region.

Publication Date (Web): November 24, 2015 | doi: 10.1021/bk-2015-1203.ch023

Table 3. 2013 California Cabernet Sauvignon Vineyards Average Chemical Quality Attributes by Growing Region

Growing Region	*Color*	*Positive Aroma*	*Negative Aroma*			*Positive Mouthfeel*		*Taste*	
	Total Anthocyanins (mg/g Berry)	*Beta-Damascenone (µg/L)*	*Methoxy Pyrazine (ng/L)*	*C6 Compounds (µg/L)*	*YAN (mg/L)*	*Polymeric Tannins (mg/L)*	*Skin Tannins (mg/L)*	*Malic Acid (mg/L)*	*pH*
Mendocino	**1.69**	**38**	**4**	**3,102**	**77**	**3,223**	**103**	**1,447**	**3.57**
Napa	**1.88**	**55**	**1**	**3,217**	**112**	**3,309**	**142**	**1,108**	**3.60**
Sonoma	**1.80**	**53**	**4**	**2,371**	**111**	**3,378**	**130**	**1,653**	**3.68**
Central Coast	**1.39**	**52**	**1**	**2,622**	**140**	**3,420**	**133**	**1,195**	**3.66**
Lodi	**1.05**	**47**	**2**	**3,597**	**165**	**2,342**	**100**	**1,600**	**3.63**
Modesto	**0.87**	**46**	**2**	**3,364**	**168**	**2,418**	**87**	**1,867**	**3.73**
Fresno	**0.74**	**44**	**2**	**3,445**	**143**	**1,755**	**57**	**1,868**	**3.94**

Color as measured by Total Anthocyanins shows clear increasing trend from Fresno to Napa. This trend is consistent with established viticulture practices and typical weather conditions. Similar, although not as consistent trends are observed for the positive mouthfeel chemical attributes Polymeric Tannins and Skin Tannins. Additionally, the data discloses that Central Coast, Napa, and Sonoma vineyards on average contain grapes with higher amounts of hydrolytically-released β-damascenone than grapes from vineyards in the Central Valley (Fresno, Modesto, and Lodi). The negative chemical attributes YAN, C_6 alcohols/aldehydes, and malic acid are in general lower in grapes from Central Coast, Napa and Sonoma vineyards than grapes from vineyards in the Central Valley. As shown in the above PCA plot, the data in Table 3 is consistent with the generally accepted wine industry judgment that better wines are produced from grapes in the Napa and Sonoma regions than are produced from grapes in the Central Valley regions.

Publication Date (Web): November 24, 2015 | doi: 10.1021/bk-2015-1203.ch023

Table 4. Number of 2013 Central Valley Vineyards within a Variety Characterized for Chemical Quality Attributes

Grape Variety	*Number of Vineyards*
Alicante Bouschet	7
Cabernet Sauvignon	153
Malbec	21
Merlot	105
Petit Verdot	16
Petite Sirah	39
Pinot Noir	60
Ruby Cabernet	18
Syrah	34
Tannat	2
Tempranillo	5
Zinfandel	143

Publication Date (Web): November 24, 2015 | doi: 10.1021/bk-2015-1203.ch023

Table 5. 2013 Central Valley Vineyards Average Chemical Quality Attributes by Variety

Variety	*Color*	*Positive Aroma*	*Negative Aroma*			*Positive Mouthfeel*		*Taste*	
	Total Anthocyanins (mg/g Berry)	*Beta-Damascenone (µg/L)*	*Methoxy Pyrazine (ng/L)*	*C6 Compounds (µg/L)*	*YAN (mg/L)*	*Polymeric Tannins (mg/L)*	*Skin Tannins (mg/L)*	*Malic Acid (mg/L)*	*pH*
Alicante Bouschet	**2.18**	**24**	**0**	**3,521**	**216**	**2,194**	**60**	**1,817**	**3.74**
Cabernet Sauvignon	**0.97**	**47**	**2**	**3,334**	**163**	**2,366**	**63**	**1,699**	**3.70**
Malbec	**1.57**	**43**	**0**	**4,452**	**184**	**2,978**	**38**	**1,799**	**3.98**
Merlot	**0.84**	**28**	**7**	**2,642**	**143**	**2,482**	**70**	**1,065**	**3.75**
Petit Verdot	**1.51**	**41**	**1**	**3,069**	**173**	**2,609**	**31**	**2,351**	**3.66**
Petite Sirah	**2.01**	**51**	**1**	**6,322**	**234**	**2,712**	**42**	**1,575**	**3.73**
Pinot Noir	**0.66**	**42**	**0**	**4,722**	**252**	**2,600**	**67**	**1,821**	**3.53**
Ruby Cabernet	**1.20**	**64**	**6**	**2,998**	**186**	**2,306**	**50**	**2,557**	**3.86**
Syrah	**1.12**	**41**	**0**	**5,977**	**169**	**2,407**	**86**	**1,362**	**3.95**
Tannat	**2.03**	**43**	**0**	**4,290**	**153**	**3,946**	**24**	**1,973**	**3.57**
Tempranillo	**0.85**	**41**	**0**	**4,253**	**182**	**2,602**	**48**	**1,391**	**3.83**
Zinfandel	**1.01**	**34**	**0**	**3,165**	**227**	**1,947**	**40**	**2,070**	**3.64**

Varietal Variation in Chemical Quality Attributes for Central Valley Grapes

The literature cited in this chapter and the data presented have focused on Cabernet Sauvignon, Merlot, and Shiraz varieties. The same chemical quality attributes characterized for these varieties of grapes can be applicable to other red grape varieties. Therefore in 2013, Central Valley vineyards including 12 different varieties of grapes were characterized for chemical quality attributes. Table 4 lists the number of vineyards from each variety that was characterized.

Table 5 shows the average results of the chemical quality attributes analyses for the 12 Central Valley grape varieties identified in Table 4.

The different grape varieties have unique chemical fingerprints using the nine classes of molecules as shown in Table 5. These chemical fingerprints are consistent with the established varietal tasting differences associated with wines made from the various grape varieties. Alicante Bouschet, Petite Sirah, and Tannat are known to have high color. Pinot Noir has low color compared to the other varieties. Ruby Cabernet and Petite Sirah wines are known for having dark fruit aroma. Unfortunately, Ruby Cabernet wine is also known for high vegetal aroma. As presented in Figure 3, this can be correlated with high concentrations of 3-isobutyl-2-methoxypyrazine and malic acid. Table 5 shows Ruby Cabernet grapes to have high levels of both of these classes of molecules. Merlot wine can have a serious issue with bell pepper or vegetal aroma and Merlot grapes have the highest average concentration of 3-isobutyl-2-methoxypyrazine among the varieties shown in Table 5. Tannat grapes have been given their name due to a high level of tannins. Of all the grape varieties characterized, Tannat has a significantly higher level of Polymeric Tannins than the other varieties. Many wine experts will state the mouthfeel of Syrah in such terms as velvety, silky, weighty, or chewy. Hufnagel and Hofmann (*12*, *13*) have published two papers identifying Flavonols as tannin compounds that have velvety/silky astringent mouthfeel and Table 5 shows Syrah to have the highest level of Skin Tannins.

Publication Date (Web): November 24, 2015 | doi: 10.1021/bk-2015-1203.ch023

Conclusions

Nine classes of molecules have been identified in dark grape varieties to measure chemical quality; total anthocyanins, YAN, 3-isobutyl-2-methoxypyrazine, C_6 alcohols/aldehydes, hydrolytically-released β-damascenone, malic acid, pH, polymeric tannins, and skin tannins. These attributes can be used to identify regional differences within a single variety of grapes. In addition, different grape varieties have unique chemical fingerprints using the nine classes of molecules. These measures of grape chemical attributes will permit the objective comparison of regional and varietal grape quality from year to year at the individual vineyard level. Vintage to vintage variations can be observed in these nine attributes. However, the overall regional and varietal trends are maintained. These objective chemical measures of grape quality will permit the monitoring of grape quality improvements through the use of advanced viticulture practices such as deficit irrigation and mechanical pruning. In the future it could augment weight and Brix as the measures to pay growers.

Publication Date (Web): November 24, 2015 | doi: 10.1021/bk-2015-1203.ch023

References

1. Francis, I. L.; Iland, P. G.; Cynkar, W. U.; Kwiatkowski, M.; Williams, P. J.; Armstrong, H. D.; Bottling, D. G.; Gawel, R.; Ryan, C. Assessing wine quality with the G-G assay. *Proceedings of the 10th Australian Wine Industry Technical Conference*, August 2−5, 1998; Australian Wine Industry Technical Conference Inc.: Adelaide, SA, 1999; pp 104−108.
2. Ristic, R.; Bindon, K.; Francis, I. L.; Herderich, M. J.; Iland, P. G. Flavonoids and C_{13}-norisoprenoids in *Vitis vinifera* L. cv. Shiraz: relationships between grape and wine composition, wine colour and wine sensory properties. *Aust. J. Grape Wine Res.* **2010**, *16*, 369–388.
3. Ugliano, M.; Henschke, P. A.; Herderich, M. J.; Pretoriuo, I. S. Nitrogen management is critical for wine flavor and style. *Wine Industry J.* **2007**, *22*, 24–30.
4. Maga, J. A. Sensory and stability properties of added methoxypyrazines to model and authentic wines. *Proceedings of the 6th International Flavour Conference*, July 5−7, 1989, Rethymnon, Crete; Elsevier, New York, 1989; pp 61−70.
5. Chapman, D. W.; Thorngate, J. H.; Matthews, M. A.; Guinard, J.-X.; Ebeler, S. Yield effects on 2-methoxy-3-isobutylpyrazine concentration in Cabernet Sauvignon using a solid phase microextraction gas chromatography/mass spectrometry method. *J. Agric. Food Chem.* **2004**, *52*, 5431–5435.
6. Hatanaka, A. The biogeneration of green odour by green leaves. *Phytochemistry*. **1993**, *34*, 1201–1218.
7. Lamikanra, O.; Inyang, I. D.; Leong, S. Distribution and effect of grape maturity on organic acid content of red muscadine grapes. *J. Agric. Food Chem.* **1995**, *43*, 3026–3028.
8. Iland, P. *Techniques for chemical analysis and quality monitoring during winemaking*; Patrick Iland Wine Promotions: Cambelltown, Australia, 2000; pp 78−79.
9. Lee, S-J.; Noble, A. C. Characterization of Odor-Active Compounds in Californian Chardonnay Wines Using GC-Olfactometry and GC-Mass Spectrometry. *J. Agric. Food Chem.* **2003**, *51*, 8036–8044.
10. Peng, Z.; Hayasaka, Y.; Iland, P. G.; Sefton, M.; Hoj, P.; Waters, E. J. Quantitative Analysis of Polymeric Procyanidins (Tannins) from Grape (*Vitis vinifera*) Seeds by Reverse Phase High-Performance Liquid Chromatography. *J. Agric. Food Chem.* **2001**, *49*, 26–31.
11. Krstic, M.; Moulds, G.; Panagiotopoulos, B.; West, S. *Growing quality grapes to winery specifications; quality measurement and management options for grapegrowers*; Winetitles: Adelaide, Australia, 2003.
12. Hufnagel, J. C.; Hofmann, T. Orosensory-Directed Identification of Astringent Mouthfeel and Bitter-Tasting Compounds in Red Wine. *J. Agric. Food Chem.* **2008**, *56*, 1376–1386.
13. Hufnagel, J. C.; Hofmann, T. Quantitative Reconstruction of the Nonvolatile Sensometabolome of a Red Wine. *J. Agric. Food Chem.* **2008**, *56*, 9190–9199.

Publication Date (Web): November 24, 2015 | doi: 10.1021/bk-2015-1203.ch024

Chapter 24

Paired Potassium-Based Buffers for Sanitizing Winery Equipment and the Carbon, Nitrogen, Sodium, and Phosphorus Footprints of Winery Cleaning Practices

Roger Boulton*

Department of Viticulture and Enology, University of California, One Shields Ave, Davis, California 95616, U.S.A.
***E-mail: rbboulton@ucdavis.edu.**

There is a need for the adoption of green chemistries for the sanitizing solutions in food, pharmaceutical and fermented beverage facilities such as breweries and wineries. One approach is the application of equimolar, potassium-based, inorganic buffers that separately keep the pH outside of the range in which known pathogens can survive but when mixed for discharge they provide a neutral, dilute solution of potassium monohydrogen sulfate. This buffer system, coupled with 10 g/L hydrogen peroxide, provides the same reduction in viable bacteria as 10 mg/L free chlorine. The solutions have no biological or chemical oxygen demands to be treated before discharge. The choice of monovalent salts enables the recovery and reuse of both buffers using nanofiltration membranes and eliminates the carbon, nitrogen, sodium and phosphorus footprints associated with existing cleaning solutions.

The selection of sanitizing buffers needs to consider the effectiveness of the solutions in disinfection, possible worker exposure, compatibility with the materials with which it will be in contact and the environmental impact of all components when discharged.

In Advances in Wine Research; Ebeler, et al.;
ACS Symposium Series; American Chemical Society: Washington, DC, 2015.

Publication Date (Web): November 24, 2015 | doi: 10.1021/bk-2015-1203.ch024

Historically, wine fermentors and storage vessels were made from either wood, stone, clay or cement. Cleaning practices ranged from a water rinse, the burning of sulfur wicks for the generation of sulfur dioxide to simply refilling with the vessel with another wine. The introduction of stainless steel vessels into the dairy, brewing and wine industries occurred at about the same time as the introduction of sodium hydroxide and hypochlorite solutions for sanitation, often with trisodium phosphate as a detergent and citric acid for the low pH finishing solution. The awareness of stress-corrosion cracking in some types of stainless steel in contact with chloride ions at neutral pH led to the practice of using a mildly acidic solution for the final rinse. The use of either 2 or 3 sanitizing solutions based on these chemistries continued to be a widespread practice in clean-in-place systems. The main alternative application of steam and/or high temperature water for sanitation but can have other undesirable outcomes due to protein denaturation and surface fouling due to colloidal matter.

As information about the occurrence of chloramines in food related facilities began to accumulate and with the discovery of chlorinated phenols (*1*), in particular the identification trichloroanisole (TCA), a phase out of chlorinated cleaning chemistry, especially in wineries, occurred. The movement away from hypochlorite has led to the adoption of ozone, chlorine dioxide and other halide derivatives each with their advantages and disadvantages. While the disinfection power was often equivalent or superior to hypochlorite in terms of contact time required, they were also more hazardous and in the case of ozone and chlorine dioxide needing safety clothing and masks and considerable training of the production teams using them. The discovery of bromine analogs of TCA and their related odor contributions made the use the bromides limited and short lived.

Today many facilities have moved to non-halide cleaning methods using a high pH NaOH solution with trisodium phosphate (TSP), and a low pH finishing rinse with peroxyacetate or peroxycarbonate. Other approaches use ozonated water at ambient temperatures, while significant use of hot water in conjunction with one of these regiments remains. The use of steam and hot water while it remains the most widely practiced method of sanitizing bottling lines, in most milk and beverage facilities, is energy intensive and carries a carbon footprint when hydrocarbon fuels are employed.

Sustainable Sanitation Practice Considerations

With the evolving awareness of carbon, energy and water footprints in the food and beverage industries and the extensive use of water for cleaning process equipment, it is reasonable to reconsider the chemical footprints of the cleaning and sanitation solutions, the temperature and time basis for their use, their contribution to the chemical and biological oxygen demand of spent solutions and the sodium, nitrate, phosphate and chloride released into the soil and surface and groundwater environments due to these practices. Ideally, disinfection agents and buffer solutions will have no hazardous vapors and will be effective in dilute rather than concentrated solutions. The choice of inorganic chemistries would

be favored so that there are not added contributions to the biological oxygen demand (BOD) and the chemical oxygen demand (COD) of treatment systems and not contribute further to carbon dioxide or methane (GHG) emissions. The inorganic components should also be compatible with soil and groundwater environments and not contribute to the nitrate levels of ground water. An additional consideration might be for the solutions to be captured, recovered and reused, requiring the buffers to be chosen for their suitability for separation on membrane systems, either so that the water is recovered or that both the water and the buffer components are recovered and reused.

Publication Date (Web): November 24, 2015 | doi: 10.1021/bk-2015-1203.ch024

The Reference Organism

Choosing a rigorous cleaning approach will begin by choosing a reference organism. In drinking water standards throughout the world this has been *Escherichia coli*, while in food toxicity is considered it is often *Staphylococcus aureus.* In the wine domain where no known pathogens survive, the yeast families of *Saccharomyces* and *Brettanomyces,* and the bacteria families of *Oenococcus, Acetobacter, Pediococcus* and *Lactobacillus* would be of particular interest. Unfortunately there is virtually no useful information regarding disinfection models and related survival data for these organisms. In order to investigate the potential of some alternative green cleaning chemistries we have chosen *E. coli* as the reference organism.

The Disinfection Time Course

The FDA criterion for the destruction of pathogens such as *Listeria* and *Clostridium* species evaluates conditions that lead to a 6-decade reduction in cooked food. Both the ASTM and AOAC standard methods for disinfection assessment use a 5-decade reduction in the viable counts as the basis for comparisons. While there are a number of agencies that regulate microbial inactivation practices in the food and pharmaceutical industries, the US wine industry is regulated by the TTB, and at present no official standards and no reference organisms for equipment sanitization exist. The green chemistry cleaning solutions presented have been chosen to be applicable for brewery and dairy sanitizing purposes as well. The 5-decade reduction in viable cells has been used as the standard performance when comparing alternative disinfection conditions. This basis enables various combinations of composition, temperature, pH and contact time to be evaluated. As a reference for disinfection with time, water containing 5 mg/L of free chlorine would cause a 5-decade reduction in viable cells of in approximately 20 minutes. In terms of cleaning cycles, solutions contact times of 20, 30 and 60 minutes, corresponding to 1,200, 1,800 and 3,600 seconds are of particular interest since they represent acceptable contact times in automated recirculation cleaning systems.

The Hot Water Option

The simplest disinfection can be obtained using water at various temperatures. The equations developed by others (*2*) enable the survival of *E. coli* to be estimated at various temperatures. The time required for a 5-decade reduction in viable cells ranges from 10 seconds at 70º C (158º F) to 3,000 seconds at 50º C (122º F) as shown in Figure 1.

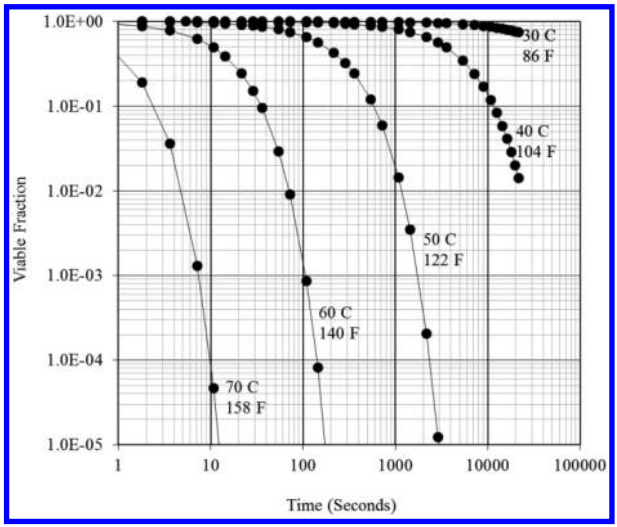

Figure 1. Survival of E. coli at temperatures between 30 and 70º C at pH = 7.0.

Publication Date (Web): November 24, 2015 | doi: 10.1021/bk-2015-1203.ch024

Hot Water and pH of 2.0 and 12.0

The hot water example can be extended by considering the survival curves for acidified water at pH=2.0, where the times range from 7 seconds at 70º C (158º F) to 1,800 seconds at 50º C (122º F) as shown in Figure 2, typically providing the same disinfection in 30% less time. The advantage of using a low pH buffer is that no pathogen can survive at this pH, even at ambient temperatures. This can be extended to pH of 12 where the effect is even greater and at another solution condition at which no known pathogen can survive. At this pH, only 2 seconds at 70º C (158º F) or 400 seconds at 50º C (122º F) is required for the 5 decade reduction as shown in Figure 3.

Publication Date (Web): November 24, 2015 | doi: 10.1021/bk-2015-1203.ch024

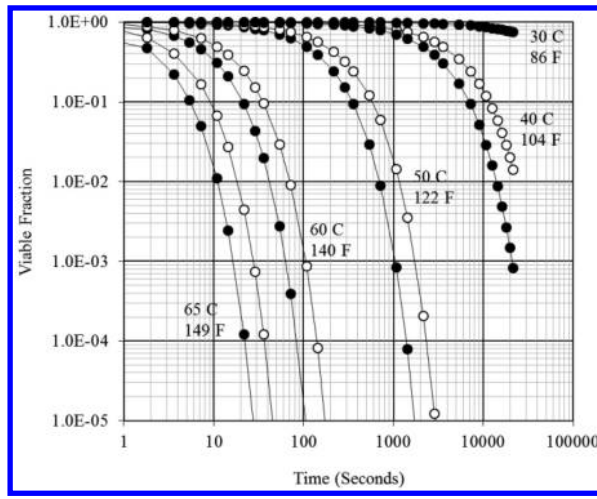

Figure 2. Survival of E. coli at temperatures between 30 and 70° C, pH = 2.0 (●) and 7.0 (○).

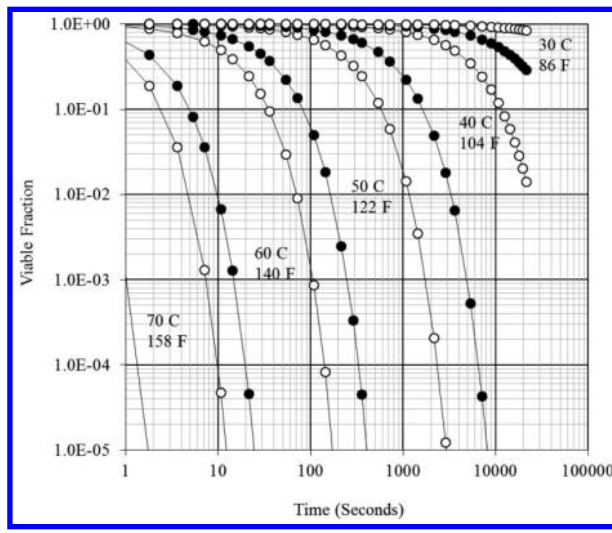

Figure 3. Survival of E. coli at temperatures between 30 and 70° C, pH = 7.0 (○) and 12.0 (●).

The hot water option is undermined by the decline in solution temperature due to heat losses during the cleaning cycle and while this can be compensated for on a site specific basis, the performance of alternative buffer solutions at ambient temperature will result in a more general and reproducible cleaning regime.

Low pH Hydrogen Peroxide Solutions

The disinfection power of various hydrogen peroxide solutions at pH 7.0 and 20º C can be evaluated using the modified series model (*3*) and the survival curves are shown in Figure 4. Concentrations of 1, 10 and 100 g/L require times of 4,200, 9,000 and 18,000 seconds to achieve the 5-decade reduction in viable cells. However, the application of hydrogen peroxide in a buffered solution at pH 2.3 has been shown to result in 5-decade reduction of *E. coli* in 2000 seconds (*4*), with the disinfection curve, based on their reported data is shown in Figure 5. This study also reported similar disinfection rates for *Staphylococcus aureus*, *Bacillus subtilis* and a number of other bacteria in acidified hydrogen peroxide solutions at pH values of 2.3 and 3.3. This has been summarized using the same disinfection model and the data is replotted as the 5 decade reduction times in Figure 6.

Publication Date (Web): November 24, 2015 | doi: 10.1021/bk-2015-1203.ch024

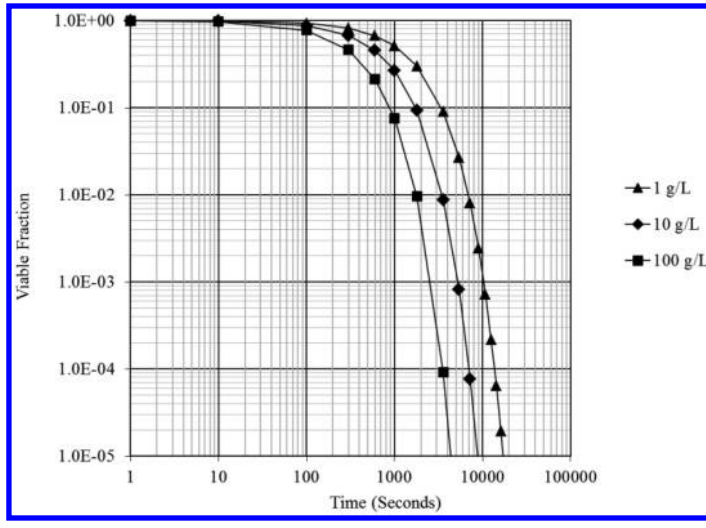

Figure 4. Survival of E. coli at concentrations between 1 g/L and 10 g/L Hydrogen Peroxide in 20º C Water, pH = 7.0.

Publication Date (Web): November 24, 2015 | doi: 10.1021/bk-2015-1203.ch024

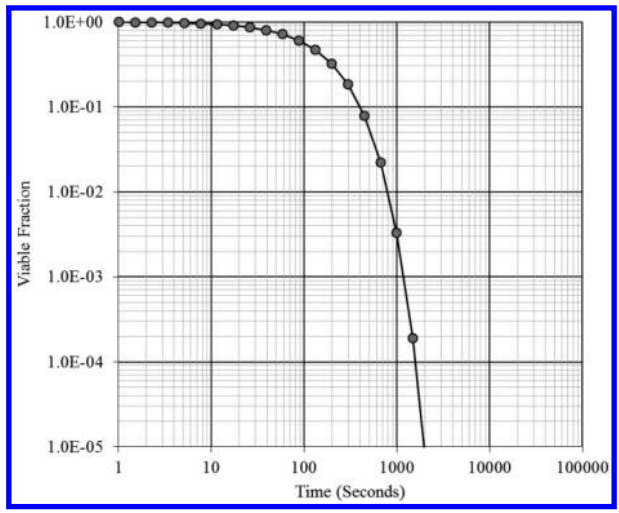

Figure 5. Survival of E. coli at 10 g/L Hydrogen Peroxide at 20° C and pH = 2.3.

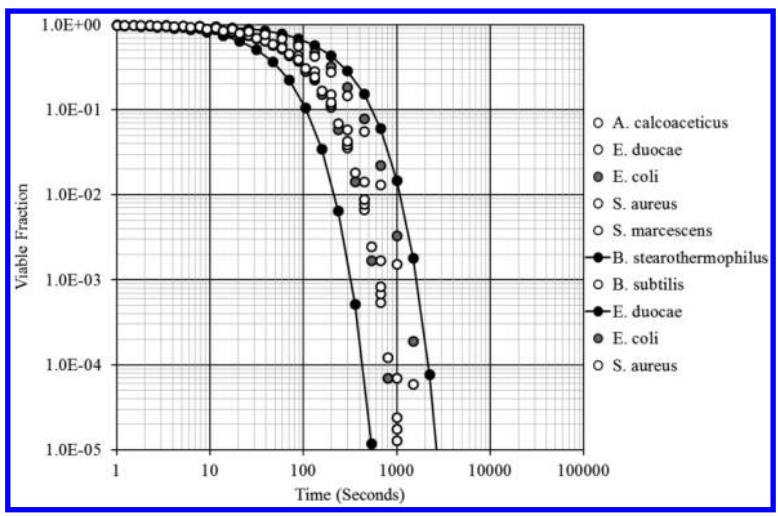

Figure 6. Survival of several organisms at 10 g/L Hydrogen Peroxide at 20° C at pH = 2.3, shortest times and pH = 3.3, longest times.

The challenge is now to develop a pair of buffer solutions that support acceptable sanitizing pH ranges for hydrogen peroxide, be capable of providing a defined reduction in viable cells and ideally be used at ambient temperatures.

The Potassium Buffer Solutions with Hydrogen Peroxide

If the high pH solution is made from 20 mM KOH, pH=11.5, (1.1g/L) and the low pH solution from 20 mM $KHSO_4$, pH=2.5, (2.7g/L), these matched buffers would become 20 mM K_2SO_4 at pH 7.0 on mixing. The interest in using buffered hydrogen peroxide solutions stems from the H_2O_2 entity being available at both pH conditions (completely at pH=2.5 and approximately 50% at pH=11.5) and the possibility of achieving similar disinfection rates to free chlorine at ambient temperatures.

An additional consideration was development of more sustainable practices in terms of their water and chemistry footprints. The possibility of choosing solutions which could be recovered to a significant extent by membranes was included and the elimination of buffers which contained sodium (from sodium hydroxide and trisodium phosphate), nitrogen as nitrate (from aerobic degradation of organic nitrogen) and phosphate (from trisodium phosphate). The recovery and reuse approach has the potential to reduce the discharge to only potassium sulfate at levels commonly found in natural ground waters. The elimination of the contributions to the sodium, nitrogen and phosphate footprints is driven by their negative impact when released onto soils or into groundwater. The elimination of organic buffers ensures no contribution to either the BOD or the COD of the spent cleaning solutions streams or to the carbon footprint due the release of carbon dioxide from aerobic degradation.

Publication Date (Web): November 24, 2015 | doi: 10.1021/bk-2015-1203.ch024

Buffer Requirements, Cation and Anion Choices

The pH range for the growth and survival of known pathogens is 4.0 to 10.0 and while there are a number of inorganic salts that could be used to achieve pH conditions outside of this range, the consideration of not using nitrate, phosphate or chloride for environmental discharge reasons and the wish to have only monovalent anions led to the choice of a monohydrogen sulfate anion buffer for the low pH (2.5) and an equimolar hydroxide anion buffer for the high pH (11.5).

The preferred cations should also be monovalent so that recovery of both cations and anions can be performed using a nanofilter that provides rejection of multivalent ions and neutral molecular species with a molecular weight of more than 150. This leads to either sodium or potassium salt buffers. The further consideration of cation exchange preference in clay soils suggests that potassium is a less impactful choice since it leads to significantly less swelling and fracturing when compared to sodium and even calcium and magnesium (*5*).

The Clean-In-Place and Cleaning Solution Recovery

The movement towards more sustainable practices must address both water usage and discharge chemistry onto sites due to processes. The adoption of clean-in-place technologies while aimed at more consistent cleaning and automated operations, often after the workday ends, will now be an essential part of the adoption of a solution recovery and re-use program. This approach will lead to immediate reduction in both the water and chemical footprints of the facility.

The choice of a matched pair of monovalent inorganic buffers, based on potassium rather than sodium, is aimed at being able to recover as much as 90% of each solution on nanofilter membranes with a MWCO of 150. At the same time, the major organic solutes from the juice or wine on the equipment surface (tartaric and malic acids, sugars and all phenolics and proteins) will be concentrated into the 10% retentate stream, making it more suitable for anaerobic digestion in a biodigestor. The long-term accumulation of smaller molecules such as glycerol, lactic and ethanol in the recovered solutions can be managed by capturing most of them in the initial water rinse and using reverse osmosis rather than nanofilter membranes to recover the rinse water.

Publication Date (Web): November 24, 2015 | doi: 10.1021/bk-2015-1203.ch024

Next Steps

The path forward calls for the development of disinfection models for the survival of wine organisms and the adoption of an n-decade reduction standard for winery equipment cleaning practices. With this information the effectiveness of various composition-temperature-contact time schemes can be compared and more optimal conditions established. The performance of alternative nanofilter and reverse osmosis membranes under these conditions, their cleaning and economic lifetime need to be investigated. In the sustainability world, the effective footprints of water, energy and major chemical components will need to be verified and a life-cycle analysis performed.

Closure

The development of paired potassium-based cleaning solutions that can perform effective sanitation at ambient temperature is presented. Using *E. coli* as the reference organism, the application of 300 mM hydrogen peroxide, at pH 2.5, can provide a 5-decade reduction in viable cells. The selected equimolar potassium-based buffers at pH 2.5 and 11.5 are designed to permit recovery of as much as 90% of both cleaning solutions by nanofilter membranes. The selected buffers eliminate any contribution to the BOD and COD of the spent solutions and the discharge of sodium, nitrates, chlorides and phosphates onto soils and into surface or ground waters.

References

1. Buser, H. R.; Zanier, C.; Tanner, H. *J. Agric. Food Chem.* **1982**, *30*, 359–382.
2. Cerf, O.; Davey, K. R.; Sadoudi, A. K. *Food Res. Int.* **1996**, *29*, 219–226.
3. Labas, M. D.; Zalazar, C. S.; Brandi, B. R.; Cassano, A. E. *Biochem. Eng. J.* **2008**, *38*, 78–87.
4. Mazzola, P. G.; Penna, T. C. V.; Martins, A. M. S. *BMC Infect. Dis.* **2003**, *34*, 24–34.
5. Robbins, C. W.; Carter, D. L. *Irrig. Sci.* **1983**, *4*, 95–102.

Subject Index

In Advances in Wine Research; Ebeler, et al.;
ACS Symposium Series; American Chemical Society: Washington, DC, 2015.

Publication Date (Web): November 24, 2015 | doi: 10.1021/bk-2015-1203.ix002

D

G

Publication Date (Web): November 24, 2015 | doi: 10.1021/bk-2015-1203.ix002

H

L

M

In Advances in Wine Research; Ebeler, et al.;
ACS Symposium Series; American Chemical Society: Washington, DC, 2015.

O

Q

R

In Advances in Wine Research; Ebeler, et al.;
ACS Symposium Series; American Chemical Society: Washington, DC, 2015.

Publication Date (Web): November 24, 2015 | doi: 10.1021/bk-2015-1203.ix002

S

T

W

In Advances in Wine Research; Ebeler, et al.;
ACS Symposium Series; American Chemical Society: Washington, DC, 2015.

Publication Date (Web): November 24, 2015 | doi: 10.1021/bk-2015-1203.ix002

Publication Date (Web): November 24, 2015 | doi: 10.1021/bk-2015-1203.ix002